UNIVERSIDAD COMPLUTENSE DE MADRID

FACULTAD DE CIENCIAS BIOLÓGICAS

Departamento de Microbiología III

TESIS DOCTORAL

Filogeografía y biología de líquenes Antártidos

MEMORIA PARA OPTAR AL GRADO DE DOCTOR

PRESENTADA POR

Isaac Garrido Benavent

Directores

Asunción de los Ríos Murillo

Sergio Pérez Ortega

Madrid, 2017

UNIVERSIDAD COMPLUTENSE MADRID

FACULTAD DE CIENCIAS BIOLÓGICAS

DEPARTAMENTO DE MICROBIOLOGÍA III

FILOGEOGRAFÍA Y BIOLOGÍA DE LÍQUENES ANTÁRTICOS

TESIS DOCTORAL

ISAAC GARRIDO BENAVENT

Madrid, 2017

Dirigida por

DRA. ASUNCIÓN DE LOS RÍOS MURILLO

DR. SERGIO PÉREZ ORTEGA

UNIVERSIDAD
COMPLUTENSE
MADRID

Facultad de Ciencias Biológicas
Departamento de Microbiología III

FILOGEOGRAFÍA Y BIOLOGÍA DE LÍQUENES ANTÁRTICOS

TESIS DOCTORAL

ISAAC GARRIDO BENAVENT

Madrid, 2017

Dirigida por

DRA. ASUNCIÓN DE LOS RÍOS MURILLO

DR. SERGIO PÉREZ ORTEGA

FILOGEOGRAFÍA Y BIOLOGÍA DE LÍQUENES ANTÁRTICOS

TESIS DOCTORAL

ISAAC GARRIDO BENAVENT

MUSEO NACIONAL DE CIENCIAS NATURALES-CSIC

MADRID, 2017

Dirigida por

DRA. ASUNCIÓN DE LOS RÍOS MURILLO

MUSEO NACIONAL DE CIENCIAS NATURALES-CSIC

DR. SERGIO PÉREZ ORTEGA

REAL JARDÍN BOTÁNICO-CSIC

Doña Asunción de los Ríos Murillo, Doctora en Ciencias Biológicas y Científico Titular del Museo Nacional de Ciencias Naturales (CSIC), y Don Sergio Pérez Ortega, Doctor en Ciencias Biológicas y contratado Ramón y Cajal en el Real Jardín Botánico (CSIC) de Madrid informan que:

La memoria titulada "Filogeografía y biología de líquenes antárticos" que presenta Isaac Garrido Benavent, Licenciado en Biología, para optar al Grado de Doctor, ha sido realizada en el Departamento de Biogeoquímica y Ecología Microbiana del Museo Nacional de Ciencias Naturales (CSIC) bajo su dirección, reuniendo todas las condiciones exigidas a los trabajos de tesis doctoral.

Madrid, 2017

Fdo.: Asunción de los Ríos Murillo

Fdo.: Sergio Pérez Ortega

La presente Tesis Doctoral ha sido financiada por una beca predoctoral de Formación de Profesorado Universitario (FPU) con referencia AP2012-3556 del Ministerio de Educación, Cultura y Deporte, y por los Proyectos Nacionales CTM2012-38222-C02-02 y CTM2015-64728-C2-2-R.

Als meus pares, Mª Àngels i Ricardo

A Nàdia, per tot!!

Als meus uelos,

gent de poble, llauradors i humils,

segur que n'estaríeu orgullosos!

A todas las muestras de líquenes usadas

para elaborar esta tesis y a los organismos

cuya supervivencia dependía de las mismas,

por haberles privado de su libertad

Agradecimientos

En primer lugar quisiera agradecer a mis directores de tesis, Asun y Sergio, por haberme brindado la oportunidad de desarrollar mi doctorado bajo su tutela. Para mí ha sido un placer compartir todos estos años y momentos con vosotros, y en especial quiero agradeceros toda vuestra ayuda en la etapa final de la tesis. He aprendido mucho a vuestro lado, tanto en lo personal como en lo profesional. Considero que el mérito de esta tesis y de mi formación como doctor es vuestro también. ¡Gracias!

En segundo lugar, es para mí un orgullo haber podido hacer la tesis en una institución tan emblemática como el Museo Nacional de Ciencias Naturales, del CSIC. Gracias a la gente que me acogió y me ayudó en todos los trámites. En especial, quería agradecer al Departamento de Biogeoquímica y Ecología Microbiana y, en particular, al Grupo de Ecología Microbiana y Geomicrobiología, que me han ofrecido un despacho y un sinfín de equipos con los que trabajar, como los microscopios.

A Carmen y Jacek, por vuestra ayuda, consejos y buenos momentos. Y a los otros compañeros que han integrado el grupo de investigación en estos cuatro años: Virginia, Miguel Ángel, Cristina, Lorena, Rocío y Rudi. También a los compañeros del ICA, en particular a Leti y Mikel, con quienes he compartido risas y buenos momentos. A Jae Eun So (Korea del Sur) por la cesión de fotos. ¡Suerte en vuestro futuro investigador!

A Fernando, por los buenos momentos en Graz, consejos y sabiduría. ¡Gracias!

Quería también agradecer a todas las personas que han recolectado muestras de líquenes que han sido usadas en esta tesis. Como haría falta más de una página para nombrarlas, remito al lector a cada uno de los capítulos. ¡Gracias!, Thank you!, Danke schön, Tak!, Gràcies! No obstante, quiero mostrar mi especial agradecimiento a Leo G. Sancho y Ulrik Søchting por la notable contribución que han hecho en esta tesis por lo que se refiere a la recogida de muestras, en especial, de la Antártida, a los proyectos CTM2009-12838-C04 y CTM2012-38222-C02, y a los Programas Antárticos de España y Nueva Zelanda. También a los investigadores del Institute of Plant Sciences (Graz).

Als meus pares i a tota la meua família, en especial als uelos, per tot el temps que no he pogut estar amb vosaltres des que "me'n vaig anar a València a estudiar". Han sigut molts anys de "pegar bacs", d'entrar a casa, estar un parell de dies, i tornar-me'n a anar ben lluny. Almenys espere que aquesta tesi demostre que he fet tot el possible per no perdre el temps i fer honor a la vostra confiança! Espere tornar prompte prop de casa!

A Nàdia, per estar amb mi en els mals i bons moments d'aquesta tesi. Per estar compartint amb mi una vida a Madrid que fa anys ni ens haguérem imaginat. Aquesta tesi també és teua, que ho sàpigues! També a la teua família, pel seu recolzament emocional durant tots aquests darrers anys. Gràcies a tots!

Madrid, Abril 2017

TABLA DE CONTENIDO

SUMMARY

PHYLOGEOGRAPHY AND BIOLOGY OF ANTARCTIC LICHENS

Introduction

Lichens constitute the most conspicuous and diverse group of macroorganisms inhabiting Antarctic terrestrial ecosystems. After approximately two centuries of lichenological research in Antarctica, the study of the diversity of its lichen biota has recently gained momentum, thanks to the application of new DNA-based techniques. Current estimates of the number of lichen-forming fungi fairly exceed 500 species (Øvstedal & Lewis Smith 2011). Despite the abundance of Antarctic lichens, little is known about their origin. The number of Antarctic species showing a bipolar or amphitropical distribution corresponds to *c*. 40% of the total diversity, whereas *c*. 30% are endemic to this continent (Øvstedal & Lewis Smith 2001). Most authors during the XX century assumed that endemic Antarctic species would have a relict origin, dating to before the Pleistocene, whereas extant populations of bipolar and cosmopolitan species would originate from a more recent colonisation (e. g. Lamb 1948, 1970; Dodge 1964; Seppelt 1995).

Aim

The scope of this doctoral thesis is to improve the knowledge of the diversity of the Antarctic lichen biota and their origin through phylogeographical studies dealing with either endemic or bipolar Antarctic species.

Methods

The diversity of the Antarctic lichen biota was examined by means of an integrative taxonomy approach that combines traditional methods focused on the study of morphological, anatomical, chemical and ecological characters with newly developed methods that use DNA sequences to infer phylogenetic relationships among taxa. To investigate the origin of the lichen biota, three Antarctic lichens showing a bipolar distribution were selected: *Mastodia tessellata* (*Verrucariaceae*, Ascomycota), *Pseudephebe pubescens* and *P. minuscula* (*Parmeliaceae*, Ascomycota). A phylogeographical approach based on an extensive sampling of individuals in both hemispheres and molecular datasets combining sequences from several loci was then implemented in order to (1) investigate intraspecific variability and genetic structure in myco- and photobiont populations, (2) infer a temporal framework for the diversification and spatial evolution of lineages, and (3) compare different biogeographic hypotheses.

Results

New taxa of lichenized and lichenicolous fungi are described based on collections made in Antarctica. In the family *Teloschistaceae* (Ascomycota), the endemic genera *Charcotiana* and *Amundsenia*, and species *C. antarctica*, *A. austrocontinentalis* and *Shackletonia cryodesertorum*, are reported as new to science. Additionally, a new genus and species of lichenicolous fungus, *Austrostigmidium mastodiae* (*Capnodiales*, Ascomycota) are described from Antarctica and Tierra del Fuego (southern Chile) growing on *Mastodia tessellata* thalli.

The occurrence of cryptic speciation was revealed in the bipolar species studied using a DNA-based species delimitation approach Thus, *Mastodia tessellata* was shown to include two genetically independent myco- and photobiont species. *Mastodia* sp. 1 associated with *Prasiola borealis* (*Trebouxiophyceae*, Chlorophyta) in Antarctica, Tierra del Fuego and North America (bipolar distribution), whereas *Mastodia* sp. 2 and *Prasiola* sp. are apparently Antarctic-endemic. Species in *Pseudephebe* were shown to be cryptic due to extreme phenotypic plasticity. By using an extensive sampling of individuals and the sequencing of different loci, the known geographic distribution of the morphologically variable and amphitropical species *P. minuscula* was extended to Antarctica, New Zealand, the Andes and China. Moreover, the geographical restriction of *P. pubescens* to the European continent was confirmed, and evidence for the existence of a third, undescribed taxon in Alaska (USA), morphologically and genetically close to *P. pubescens*, was provided.

A Miocene to Plio/Pleistocene divergence for symbionts in *Mastodia tessellata* s.l. (*Mastodia* sp.1 and *Mastodia* sp. 2; *Prasiola borealis* and *Prasiola* sp.) was revealed through the phylogeographical analyses. In addition, higher levels of intraspecific variability of the bipolar *Mastodia* sp. 1 and *Prasiola borealis* were found in Tierra del Fuego as compared to North America populations. On the other hand, the three phylogenetic *Pseudephebe* species could have diverged between the Miocene and Pliocene, but the highest genetic diversity of the amphitropical species *P. minuscula* was found in the Northern Hemisphere. The Maritime Antarctic populations of *P. minuscula* were genetically close to those of Tierra del Fuego, whereas populations from the Transantarctic Mountains (Continental Antarctica) showed a close connexion with the Arctic ones. Furthermore, the acquisition of a bipolar distribution in *Mastodia* sp. 1, *Prasiola borealis* and *Pseudephebe minuscula* was estimated to have occurred during the Pleistocene. In contrast, divergence time estimates for the Antarctic endemic species *Shackletonia cryodesertorum* placed its origin between the Oligocene and Miocene.

Discussion and Conclusions

The use of an integrative taxonomy approach coupled with DNA-based species delimitation methods have allowed description of three genera and four species new to science, while also revealing cryptic lineages in Antarctic lichenized fungi and algae. These results indicate that the diversity of the Antarctic lichen biota is far from resolved.

The temporal framework set up for the origin of the Antarctic species of lichenized fungi and algae studied in this thesis supports the idea that endemic taxa are old, dating back to pre-Pleistocene times, whereas amphitropical species are more recent colonisers, their populations establishing in relatively recent times (Pleistocene or later).

The combined effect of geographic distance between Antarctica and South America, the intensification of the Antarctic Circumpolar Current and the re-establishment of the Antarctic ice sheets since the middle Miocene may have promoted vicariant speciation in symbionts of *Mastodia tessellata* s.l. in the Southern Hemisphere.

Contrasting evidence provided in this thesis points towards a mixed spatial origin for amphitropical distributions in lichens, with austral species such as *Mastodia* sp. 1 and *Prasiola borealis* migrating jointly to the Northern Hemisphere by direct long-distance dispersal, whereas other species such as the boreal *Pseudephebe minuscula* may have migrated southwards through “mountain-hopping” along the American Cordilleras and/or by direct long-distance dispersal.

RESUMEN

FILOGEOGRAFÍA Y BIOLOGÍA DE LÍQUENES ANTÁRTICOS

Introducción

Los líquenes son los organismos macroscópicos dominantes en los ecosistemas terrestres de la Antártida. Con casi dos siglos de historia, el estudio de la biota liquénica antártica ha sufrido un nuevo impulso con la irrupción de las técnicas basadas en el ADN, lo que ha permitido incrementar las estimas de hongos liquenizados en la Antártida por encima de las 500 especies (Øvstedal y Lewis Smith 2011). Pese a su abundancia, poco se sabe aún sobre su origen. Alrededor de un 40% de las especies muestra un patrón de distribución bipolar o anfitropical, mientras que un 30% son endemismos antárticos (Øvstedal y Lewis Smith 2001). Durante el siglo XX, la mayoría de autores aceptaron un origen temporal dual, por el que las especies endémicas tendrían un origen relicto, anterior al Pleistoceno, y las especies bipolares (y cosmopolitas) habrían colonizado la Antártida en tiempos más recientes (p. ej. Lamb 1948, 1970; Dodge 1964; Seppelt 1995).

Objetivos

La presente tesis doctoral tiene como objetivo principal contribuir al conocimiento de la diversidad liquénica en la Antártida y a dilucidar su origen, enfocándose en estudios filogeográficos de especies endémicas y de especies con distribución bipolar.

Metodología

La estrategia empleada aúna métodos propios de la sistemática tradicional de líquenes (morfología, anatomía, química y ecología) y aproximaciones basadas en datos moleculares (ADN), lo que en conjunto configura una taxonomía integradora. Para indagar en el origen de la biota liquénica antártica se han escogido tres líquenes con distribución bipolar (*Mastodia tessellata*, *Pseudephebe pubescens* y *P. minuscula*) y empleado análisis propios de la filogeografía basados en un muestreo extenso de individuos en ambos hemisferios y secuenciación de varios *loci*. En particular, se analiza la diversidad intraespecífica y la estructura genética de las poblaciones de mico- y fotobiontes, se estiman marcos temporales para la evolución espacial de los linajes y se construyen y comparan diferentes hipótesis biogeográficas.

Resultados

Se han descrito nuevos taxones de hongos liquenizados y liquenícolas a partir de diversas colecciones antárticas. Para la familia *Teloschistaceae* (Ascomycota) se proponen los nuevos géneros *Charcotiana* y *Amundsenia*, y las especies *C. antarctica*, *A. austrocontinentalis* y *Shackletonia cryodesertorum*, todos representantes endémicos de la biota antártica. Por otra parte, se describe el género de hongos liquenícolas *Austrostigmidium* (*Capnodiales*, Ascomycota), y la especie *A. mastodiae*, presente en talos del liquen *Mastodia tessellata* (*Verrucariaceae*, Ascomycota) en varias localidades de la Antártida Marítima y Tierra del Fuego (sur de Chile).

Además se ha revelado la existencia de especiación críptica en los taxones con distribución bipolar estudiados a través de la metodología de delimitación de especies implementada en esta tesis. Así, bajo el nombre de *Mastodia tessellata* se incluyen dos especies genéticamente diferenciadas de micobionte y fotobionte. *Mastodia* sp. 1 y *Prasiola borealis* (*Trebouxiophyceae*, Chlorophyta) están asociadas en la Antártida, Tierra del Fuego y Norteamérica (distribución bipolar), mientras que *Mastodia* sp. 2 y *Prasiola* sp. se asocian de forma restringida en el continente antártico (endemismos). También se demuestra que las especies de *Pseudephebe* (*Parmeliaceae*, Ascomycota) son crípticas dado el elevado grado de plasticidad fenotípica. Gracias a la secuenciación de diversos marcadores genéticos de un gran número de individuos, se amplía la distribución geográfica de la especie morfológicamente variable y anfitropical *P. minuscula* a la Antártida, Nueva Zelanda, los Andes y China. Además, se confirma el rango de distribución restringido al continente europeo de *P. pubescens*, y la presencia de un tercer taxón, no descrito, morfológica y genéticamente próximo al anterior en Alaska (EEUU).

Los estudios filogeográficos de los dos simbiontes de *Mastodia tessellata* s.l. revelan que la divergencia entre *Mastodia* sp. 1 y *Mastodia* sp. 2, y entre *Prasiola borealis* y *Prasiola* sp. ocurrió entre el Mioceno y el Plio/Pleistoceno, y que los niveles de diversidad genética intraespecífica en las especies bipolares *Mastodia* sp. 1 y *Prasiola borealis* son mayores en las poblaciones de Tierra del Fuego que en Norteamérica. Por otra parte, las tres especies filogenéticas de *Pseudephebe* se ha estimado que divergieron también entre el Mioceno y Plioceno, pero la mayor diversidad genética de la especie anfitropical *P. minuscula* se encuentra en el Hemisferio Norte. Las poblaciones de la Antártida Marítima de esta especie están genéticamente emparentadas con las de Tierra del Fuego, mientras que las de las Montañas Transantárticas (Antártida Continental) muestran afinidades con poblaciones del Ártico. Asimismo, la adquisición de una distribución bipolar en *Mastodia* sp. 1, *Prasiola borealis* y *Pseudephebe minuscula* ocurrió en el Pleistoceno. En contraposición, las estimas de tiempo de divergencia para la nueva especie endémica de la Antártida *Shackletonia cryodesertorum* sitúan su origen entre el Oligoceno y Mioceno.

Discusión y Conclusiones

Los estudios de diversidad de hongos y algas liquenizados antárticos basados en una taxonomía integradora y en la delimitación de especies con datos de ADN han permitido describir tres nuevos géneros y cuatro especies, e identificar potenciales linajes crípticos lo que en conjunto apunta a que todavía queda mucha diversidad por descubrir dentro de la biota liquénica antártica.

Los análisis filogeográficos y, en particular, las estimas de divergencia entre las diferentes especies de mico- y fotobiontes estudiadas en la presente tesis, confirman un origen temporal dual de la biota liquénica antártica, siendo los taxones endémicos más antiguos (pre-pleistocénicos), y los de distribución anfitropical datando de tiempos más recientes (a partir del Pleistoceno).

Se aportan evidencias de especiación por vicariancia en los simbiontes de *Mastodia tessellata* s.l. en el hemisferio austral, probablemente debido a un efecto combinado de la separación geográfica entre Antártida y Suramérica, la intensificación de la Corriente Circumpolar Antártica y el restablecimiento de las masas de hielo antárticas desde mediados del Mioceno.

Según los resultados de esta tesis, queda patente que el origen de la distribución anfitropical en líquenes no es único, existiendo especies australes como *Mastodia* sp. 1 y *Prasiola borealis* que probablemente migraron al Hemisferio Norte conjuntamente y de manera directa, mientras que otras especies como *Pseudephebe minuscula*, de origen boreal, habrían migrado en sentido reverso, norte-sur, por "*mountain-hopping*" a través de las principales cordilleras americanas y/o por dispersión a larga distancia directa entre ambos hemisferios.

INTRODUCCIÓN

"*Consider the Lichen. Lichens are just about the hardiest visible organisms on Earth, but the least ambitious*". – Bill Bryson

1. Los líquenes

1.1. La simbiosis liquénica

El origen del concepto de simbiosis (del griego: *syn* = junto, *bio* = vida) se remonta al siglo XIX, cuando de Bary (1878), en su obra "*Ueber Symbiose*", se refirió por primera vez a las asociaciones físicas íntimas y perdurables entre diferentes organismos. Entre otros tipos de interacciones simbióticas, éstas pueden tener un carácter mutualista, cuando los dos simbiontes, huésped y hospedador, se benefician mutuamente de la relación, o antagonista, cuando uno de los simbiontes prospera en detrimento del otro. Ejemplos de ambos casos existen en todo el espectro del árbol de la vida, y son especialmente comunes entre eucariotas heterótrofos, como los hongos, y autótrofos, como las plantas, algas y cianobacterias.

Los líquenes representan uno de los ejemplos más paradigmáticos de simbiosis entre organismos pertenecientes a grupos taxonómicos dispares. Tradicionalmente han sido definidos como una asociación mutualista estable, ecológicamente obligada, entre un hongo, el habitante externo o micobionte, y una población interna de un organismo fotosintético unicelular o filamentoso, o fotobionte, que puede ser un alga (ficobionte) y/o una cianobacteria (cianobionte) (Hawksworth y Honegger 1994). En algunos líquenes, el fotobionte primario es un alga verde, y el secundario una cianobacteria localizada en estructuras particulares que reciben el nombre de cefalodios (Friedl y Büdel 2008). Por el contrario, en algunos cianolíquenes se ha demostrado la coexistencia de algas verdes y cianobacterias, y su contribución por igual a la función fotosintética (Henskens et al. 2012). Otros trabajos han probado que algunos hongos liquenizados se asocian con diferentes fotobiontes en las distintas etapas del ciclo vital del liquen (Friedl 1987). El hongo liquenizado obtiene carbohidratos y otros nutrientes del fotobionte, incluso nitrógeno cuando el fotobionte es una cianobacteria fijadora de nitrógeno. Por su parte, la población de fotobiontes vive protegida por las células fúngicas del exceso de radiación lumínica, de cambios abruptos de temperatura y de la desecación. Aparte de la visión clásica de la simbiosis liquénica entendida como un mutualismo, algunos autores han propuesto la idea de un parasitismo controlado, mediante el cual el hongo parasitaria a las algas, afectando a su crecimiento y metabolismo, pero sin llegar a destruirlas ("helotismo", Schwendener 1869), mientras que otros opinan que los hongos puedan actuar como "agricultores de algas" (Goward 1994, pág. 14; Sanders 2001; Lücking et al. 2009). Asimismo, existen ejemplos atípicos de asociaciones liquénicas, como las que establecen especies en los géneros de hongos *Collemopsidium* (Kohlmeyer et al. 2004), *Racodium* y *Cystocoleus* (Muggia et al. 2008) con diferentes tipos de fotobionte, y muy especialmente la asociación entre el hongo *Mastodia tessellata* y el género de algas trebouxiofíceas *Prasiola* (Kohlmeyer et al. 2004; Pérez-Ortega et al. 2010). Esta última asociación simboliza uno de los pocos ejemplos de alga macroscópica (foliosa) liquenizada que constituye el habitante externo (Figura 1) y, además, demuestra la complejidad de las relaciones simbióticas, ya que esta asociación no se podría describir en términos de parasitismo, mutualismo o saprofitismo, si no que más bien representa un equilibrio dinámico en el que el

fotobionte, ante ciertas condiciones bióticas y abióticas, puede "escapar" de la interacción con el micobionte (Pérez-Ortega et al. 2010).

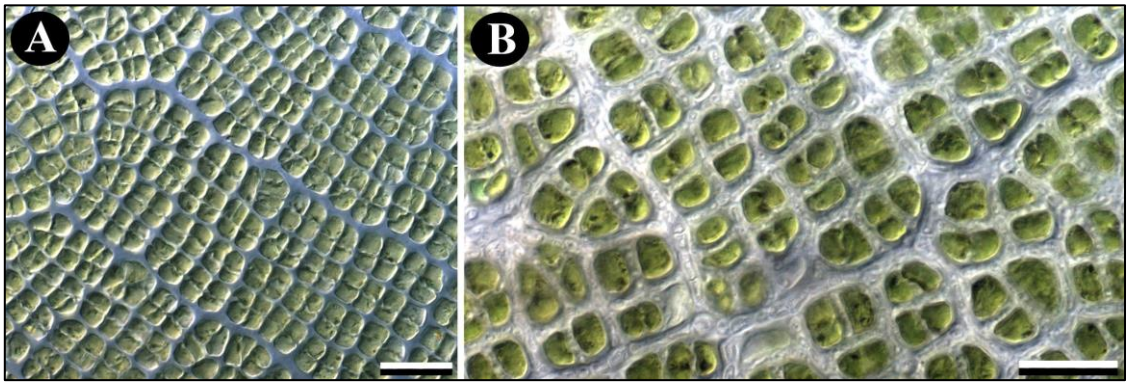

Figura 1. (A) Talo de *Prasiola* no liquenizado y (B) liquenizado por el hongo *Mastodia tessellata*. En (B) se observa un mayor grado de segregación de las células algales como consecuencia de la interacción con las hifas fúngicas. Éstas ocupan todo el espacio intercelular. Escalas: 20 μm. (Fotografías de microscopía óptica: IGB).

1.2. El talo liquénico

El resultado fenotípico de la liquenización es el talo liquénico. El micobionte es capaz de diferenciar plecténquimas (falsos tejidos) o hasta verdaderos parénquimas (Sanders y de los Ríos 2017) con funciones muy especializadas, llegando a alcanzar el 50–90% de la biomasa total del talo (Honegger 2012). A nivel anatómico, los talos liquénicos se agrupan en dos grandes tipos: los homómeros, en los cuales las hifas del micobionte y las células de los fotobiontes se distribuyen de manera homogénea por todo el volumen del talo; o heterómeros, cuando presentan una estratificación interna en la distribución de ambos simbiontes. En este último caso, se suele diferenciar una capa superior fúngica, o córtex, de grosor variable y en donde se pueden acumular algunas sustancias relacionadas con la protección del aparato fotosintético del fotobionte y contra el consumo por animales herbívoros, como el ácido úsnico, la atranorina y la parietina (Rundel 1978; Lawrey 1986; Asplund y Wardle 2013). Inmediatamente inferior al córtex se sitúa la capa de fotobiontes ("capa algal"), en la que coexisten ambos simbiontes y en donde se establecen los contactos físicos entre ellos. Seguidamente aparece la médula, un estrato fúngico formado por hifas laxamente entremezcladas que ocupan el mayor volumen del talo al mismo tiempo que dejan espacios libres para facilitar la aireación del mismo. Es también en la médula donde se acumulan la mayor parte de sustancias liquénicas en forma de cristales incrustados en las paredes hifales. Estos compuestos derivan del metabolismo secundario de los micobiontes y protegen al talo frente a las infecciones de microorganismos, la radiación y la oxidación (Lawrey 1986). Además, estas sustancias son importantes moduladores de las relaciones hídricas de los talos dada su naturaleza hidrófoba, evitando que la médula se sature de agua, y por tanto facilitando el intercambio gaseoso necesario para la fotosíntesis (Souza-Egipsy et al. 2000). Finalmente, algunos líquenes pueden

desarrollar un córtex inferior que suele estar en contacto con el sustrato y que puede participar en la retención capilar de agua extratalina (Nash 2008).

A nivel macroscópico, los talos liquénicos se clasifican según la forma de crecimiento o arquitectura. Se establecen varias categorías principales, o biotipos, entre los que destacan el crustáceo, foliáceo y fruticuloso (Nash 2008; Honegger 2012). Los talos crustáceos están en contacto estrecho con el sustrato, ya sea rocoso o vegetal (madera, hojas, briófitos, etc.), por medio de la médula o de un hipotalo, y no se pueden separar del mismo sin destruirlos. Los foliáceos tienen forma laminar, presentan una organización dorsiventral y el córtex inferior generalmente diferenciado, y están parcialmente adheridos al sustrato, de manera que se pueden separar del mismo sin destruirse. Finalmente, los talos fruticulosos tienen el aspecto de pequeños arbustos, colgantes o erectos, más o menos alargados y se adhieren al sustrato mediante regiones discretas, como discos de fijación o hapterios. Existen también biotipos mixtos, configurados por una parte basal crustácea y una parte erecta, fruticulosa, que recibe el nombre de podecio (de aspecto ramificado) o escifo (en forma de trompeta).

Los micobiontes desarrollan estructuras destinadas a la reproducción, ya sea ésta sexual o vegetativa. En el primer caso, la producción de esporas meióticas en ascos (ascósporas) o en basidios (basidiósporas) se produce en estructuras fúngicas especializadas denominadas ascomas, cuando los micobiontes son ascomicetos, o basidiomas, cuando son basidiomicetos. La reproducción vegetativa se acomete mediante la formación de propágulos que incluyen células de ambos simbiontes, como los soredios e isidios. Los primeros son grupos de células del fotobionte envueltos por una red laxa de hifas. Éstos se desarrollan en áreas especializadas, los soralios, situadas en la superficie o en la región marginal del talo. Los isidios se caracterizan por presentar una capa externa atribuible a un córtex talino típico y por ser generalmente de mayor tamaño que los soredios. Además, son propágulos que se forman en la superficie de los talos y que se desprenden con facilidad ante cualquier perturbación física (p. ej. viento, caída de una gota de agua, pisada de un animal). Un tercer mecanismo de reproducción vegetativa sería la fragmentación de los talos liquénicos. Igualmente, el micobionte puede reproducirse de manera asexual mediante la producción de pequeñas esporas mitóticas, denominadas conidios. En general, la reproducción mediante meiósporas o mitósporas tiene la desventaja de que las hifas deben encontrar en el medio las células del fotobionte adecuado para establecer de nuevo la simbiosis. No obstante, ante la ausencia de fotobiontes compatibles, los hongos pueden llegar a establecer asociaciones menos íntimas con otras algas (Ott 1987) o incluso comportarse como saprófitos (Lawrey 1984, pág. 407; Wedin et al. 2004).

La notable complejidad y diversidad morfológica y funcional de los talos liquénicos proporciona, además, una gran variedad de servicios en el ecosistema. En este sentido, Ellis (2012) y Asplund y Wardle (2016) revisaron el papel que tienen los líquenes en diferentes ambientes terrestres y forestales. Gracias a la información compilada, estos trabajos pusieron de relieve la destacada repercusión que los diferentes biotipos liquénicos, el tipo de fotobionte, o incluso la pigmentación de los talos y la

naturaleza de las sustancias liquénicas que contienen, pueden tener sobre aspectos ecológicos tan importantes como la descomposición, la acumulación y el reciclado de agua y nutrientes (C y N), el ensamblaje de comunidades de invertebrados, la abundancia de microorganismos, el crecimiento de las plantas, así como la erosión de sustratos rocosos (Figura 2). Asimismo, gracias a su longevidad y a su capacidad de crecer continuamente durante décadas, incluso siglos, los líquenes son usados como bioindicadores para la monitorización del impacto de la polución del aire, edad de los bosques, calidad del suelo y cambio climático (McCune 2000).

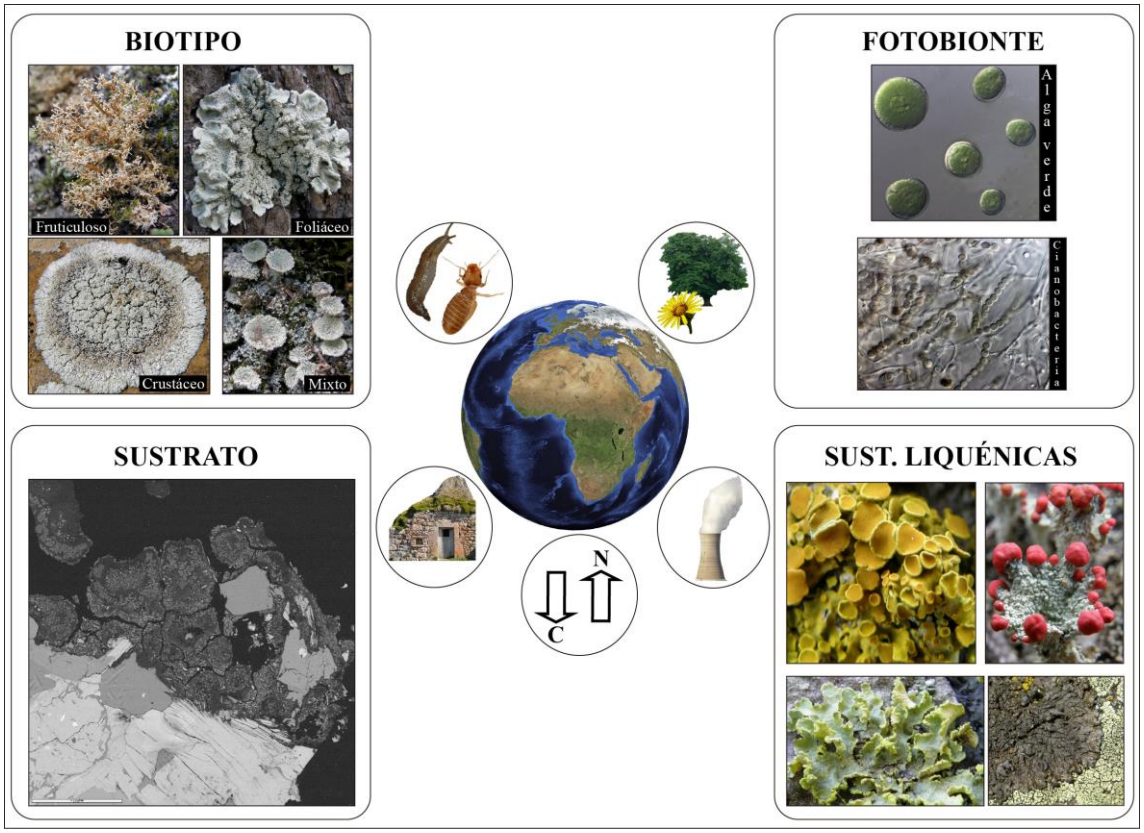

Figura 2. Esquema ilustrativo de algunas propiedades de los talos liquénicos (biotipo, fotobionte asociado, relaciones con el sustrato y presencia de sustancias liquénicas) que ofrecen servicios ecosistémicos y de bioindicación. Se muestran los cuatro grandes biotipos liquénicos (fruticuloso, foliáceo, crustáceo y mixto), los dos tipos mayoritarios de fotobionte (alga verde y cianobacteria), el crecimiento epilítico de un talo liquénico con efecto erosivo sobre la roca, así como talos liquénicos de varias especies cuya pigmentación es un buen indicador del tipo de sustancias liquénicas que contienen (Fotografías macroscópicas y de microscopía óptica: IGB; microscopía electrónica: AdR; montaje: IGB).

1.3. Diversidad de micobiontes y fotobiontes

Aunque en la actualidad no existe una cifra oficial del número de hongos liquenizados a nivel global, se estima que ésta ronda entre las 17.000 y 20.000 especies (Kirk et al. 2008; Feuerer y Hawksworth 2007; Honegger 2012). Si se considera que el número de especies descritas de hongos es de unas 80.000, ello supone que cerca del

20% del total de especies fúngicas han adoptado la simbiosis liquénica como estrategia de vida. Actualmente, más del 90% de hongos liquenizados pertenecen a la división Ascomycota; sin embargo, el número de basidiomicetos liquenizados está siendo actualmente revisado mediante aproximaciones moleculares, revelando niveles insospechados de diversidad específica (Lücking et al. 2014, 2016). Los fotobiontes liquénicos son menos conocidos a nivel taxonómico que sus aliados fúngicos. Más de 40 géneros de fotobiontes han sido documentados, destacando los géneros de microalgas verdes *Trebouxia*, *Asterochloris*, *Coccomyxa*, *Dictyochloropsis* (clase *Trebouxiophyceae*) y *Trentepohlia* (clase *Ulvophyceae*), y los de cianobacterias *Nostoc*, *Scytonema*, *Stigonema* y *Gloeocapsa* (Tschermak-Woess 1988; Friedl y Büdel 2008; Thüs et al. 2011). Aunque tradicionalmente la liquenización ha sido entendida como la asociación entre una única especie de hongo y otra de alga (y/o una cianobacteria), diferentes estudios basados en técnicas de microscopía y biología molecular han demostrado la presencia de varios genotipos del micobionte o incluso de especies compatibles de fotobionte en un mismo talo liquénico (Hawksworth 1988; Murtagh et al. 2000; Casano et al. 2011; Muggia et al. 2014b; Catalá et al. 2016).

La asociación simbiótica entre hongos y fotobiontes muestra patrones opuestos según el nivel filogenético al que se examine. Por ejemplo, una de las familias de ascomicetos liquenizados más diversa, *Parmeliaceae* (más de 2.500 especies), se asocia estrictamente con algas del género *Trebouxia* (Leavitt et al. 2015c). De la misma manera, el orden *Peltigerales* (Ascomycota) se asocia primaria o secundariamente con el género de cianobacterias *Nostoc* (Rikkinen 2013; Zúñiga et al. 2017), mientras que los órdenes tropicales *Arthoniales* y *Ostropales* liquenizan preferiblemente con algas del orden *Trentepohliales* (Nelsen et al. 2011). Estas interacciones más o menos estrictas se mantienen a distintas escalas geográficas, al menos, a nivel supraespecífico (Fernández-Mendoza et al. 2011; Magain et al. 2016). En contraposición, los miembros de la familia *Verrucariaceae* interaccionan con al menos siete géneros de fotobiontes pertenecientes a tres filos distintos (Thüs et al. 2011).

1.4. El talo liquénico como consorcio microbiano

El desarrollo de nuevas técnicas de microscopía y biología molecular también ha permitido reconocer la existencia de otros linajes de procariotas y eucariotas (microbioma) cohabitando en los talos liquénicos, lo que demuestra que los líquenes deben ser más bien considerados como pequeños ecosistemas, muy complejos y con autonomía morfológica (Chapman y Margulis 1998; Honegger 2012). Así, se conocen hongos endoliquénicos, una buena parte de los cuales son imperceptibles a nivel macroscópico y suelen ser asintomáticos (Arnold et al. 2009a; U'Ren et al. 2010, 2012), mientras que otros suelen formar estructuras de reproducción reconocibles a simple vista, en cuyo caso se denominan hongos liquenícolas. Estos últimos constituyen un grupo filogenéticamente diverso, con más de 1.800 especies descritas, y muestran diferentes grados de especificidad con los líquenes, pudiendo actuar como parásitos, saprófitos, o simples comensales (de los Ríos y Grube 2000; Lawrey y Diederich 2003, 2016). Sin embargo, al igual que ocurre en los hongos endófitos, el estilo de vida de los

hongos endoliquénicos puede cambiar a lo largo de su ciclo vital desde un parasitismo a un mutualismo (Rodríguez y Redman 2008). Por otra parte, Spribille et al. (2016) han evidenciado la presencia de levaduras de basidiomicetes embebidas en el córtex de ciertos líquenes, cuya abundancia parece estar relacionada con variaciones en el fenotipo liquénico. Asimismo, diferentes técnicas "ómicas" han puesto de relevancia el papel que juegan varios grupos de bacterias en el aprovisionamiento de nutrientes y protección contra factores de estrés bióticos y abióticos en la asociación liquénica (Hodkinson y Lutzoni 2009; referencias en Grube et al. 2015).

1.5. Taxonomía y sistemática de hongos y algas liquenizados

Puesto que el hongo contribuye mayormente al fenotipo liquénico, los líquenes han sido identificados tradicional y erróneamente con el nombre científico del micobionte. En realidad, tanto los hongos como las algas liquenizadas siguen su respectiva nomenclatura botánica, sujeta a las normas del Código Internacional de Nomenclatura Botánica para algas, hongos y plantas. Es decir, los líquenes no poseen un nombre científico *per se*.

Durante más de un siglo, la sistemática de hongos liquenizados estuvo basada en la comparación de caracteres morfológicos, químicos y ecológicos. No obstante, la taxonomía de las especies es complicada en muchos grupos de hongos liquenizados debido al escaso número de caracteres observables (Printzen 2009). Además existen los problemas de convergencia morfológica entre grupos dispares (Crespo et al. 2010a; Amo de Paz et al. 2012). Por otro lado, una situación común a la mayoría de estudios es la presencia de especies crípticas, es decir, dos o más linajes distintos a nivel de especie que habían sido incluidos erróneamente bajo el mismo epíteto (Bickford et al. 2007; Crespo y Pérez-Ortega 2009; Crespo y Lumbsch 2010).

Por su parte, la sistemática de algas y cianobacterias liquenizadas es incluso más compleja puesto que estos grupos de organismos muestran un elevado grado de homoplasia morfológica a la vez que plasticidad fenotípica a diferentes niveles filogenéticos (Fraser et al. 2009a; Škaloud y Rindi 2013; Verbruggen 2014). La correcta identificación de estos fotobiontes requiere de su aislamiento y cultivo en medios específicos para determinar si son uni- o pluricelulares y el tipo y grado de ramificación de los filamentos (cianobacterias, Friedl y Büdel 2008) así como la morfología plastidial y la ultrastructura de los pirenoides (microalgas, Friedl 1989; Friedl y Büdel 2008). En algas verdes, además, existe la problemática del uso de diferentes criterios taxonómicos para la delimitación de especies en distintos linajes, lo que complica aún más el avance del conocimiento de la diversidad en este grupo, que actualmente cuenta con más de 4.500 especies descritas (Guiry 2012; Leliaert et al. 2014).

Con la aparición de las técnicas de biología molecular y el establecimiento de un marco filogenético para la comparación de especies basado en secuencias de ADN, la taxonomía de muchos grupos de mico- y fotobiontes, que hasta el momento había sido difícil de abordar mediante datos morfológicos, está siendo finalmente resuelta (Moya et al. 2015; Mark et al. 2016; Pérez-Ortega et al. 2016; Škaloud et al. 2016). En la

actualidad se propone una taxonomía integradora basada en completar la información aportada por los caracteres tradicionales (morfológicos, químicos y ecológicos) con los caracteres genéticos generando una aproximación holística a la delimitación de especies (Dayrat 2005; Will et al. 2005; Padial et al. 2010). El análisis de los datos genéticos también se ha sofisticado considerablemente en las dos últimas décadas con la profusión de algoritmos para la delimitación de especies (p. ej. GMYC, Pons et al. 2006; ABGD, Puillandre et al. 2012; PTP, Zhang et al. 2013), y las aproximaciones derivadas de la genética de poblaciones y la teoría de la coalescencia (BP&P, Yang y Rannala 2010; BFD, Grummer et al. 2014). Todos estos avances están permitiendo delimitar y describir fehacientemente la diversidad de hongos y fotobiontes involucrados en simbiosis liquénicas (p. ej. Leavitt et al. 2016c). La correcta documentación de esta biodiversidad es esencial como base para estudios más avanzados sobre conservación de las especies y ecosistemas así como aquellos enfocados a la biogeografía (Wiens 2007).

1.6. Biogeografía y filogeografía de líquenes

Los líquenes están presentes en la mayoría de ecosistemas terrestres del planeta, cubriendo alrededor del 8% de la superficie terrestre (Nash 2008). Gracias a su naturaleza poiquilohídrica y a las propiedades emergentes que resultan de la asociación simbiótica, los líquenes sobreviven en ambientes en donde otros organismos, como las plantas, no son capaces de hacerlo. Por ejemplo, en hábitats sometidos a temperaturas extremas, como desiertos cálidos (Namib, Lalley y Viles 2005) y fríos (Valles Secos de McMurdo en la Antártida, Øvstedal y Lewis Smith 2001; Figura 3) y las gélidas cumbres de hasta 7.400 m en el Himalaya (Hertel 1977), y en ambientes donde los organismos soportan un elevado estrés salino, como es el caso de las zonas intermareales de la mayoría de océanos (p. ej. Pérez-Ortega et al. 2016). La singular biología y ecología de estos microsistemas simbióticos los ha convertido, desde los inicios de la liquenología, en el objetivo perfecto para dilucidar los mecanismos responsables de la distribución geográfica que ocupan.

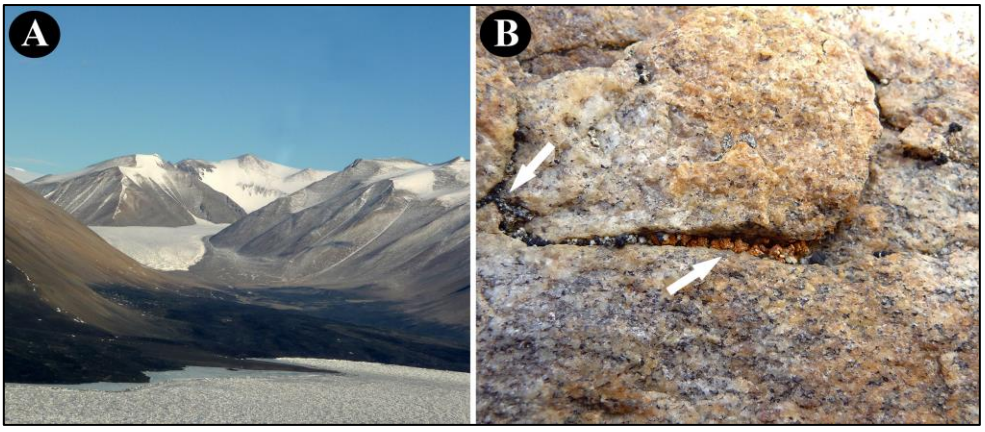

Figura 3. Los Valles Secos de McMurdo en la Antártida Continental. (A) Vista aérea de uno de los valles. (B) Varios líquenes crustáceos creciendo en las grietas de la roca granítica (flechas). (Fotografías: AdR).

El estudio de los patrones de distribución de los hongos liquenizados se ha abordado al menos desde tres puntos de vista distintos dentro de la liquenología. En primer lugar, se han compilado y comparado listados de especies a nivel mundial para delimitar regiones biogeográficas e inferir relaciones de similitud entre ellas (Lücking 2003; Martínez et al. 2003; Feuerer y Hawksworth 2007). Este tipo de trabajo representa la herencia de la fanerogamia (Spribille 2011), puesto que es de esperar que los patrones de distribución observados actualmente para los líquenes hayan sido determinados por los mismos mecanismos que causaron la distribución de otros organismos (p. ej. plantas vasculares), como las cambios climáticos del Pleistoceno, la fragmentación de masas continentales, el desarrollo de cordilleras montañosas, etc. (Fernández-Mendoza 2013). De hecho, existen numerosos ejemplos de patrones de distribución geográfica que son equiparables entre líquenes, plantas y briófitos, como es el caso de la distribución anfitropical o bipolar (p. ej. Du Rietz 1940; Raven 1963; Moore y Chater 1971; Galloway y Aptroot 1995; Wen y Ickert-Bond 2009), la circumpolar y la disyunta en el hemisferio austral (p. ej. Hooker 1853; Walker 1985; Galloway 1991; Sanmartín y Ronquist 2004; Winkworth et al. 2015) o la disyunción entre el este de Norteamérica y este de Asia (la disyunción Asa Gray, Wen 1999; Galloway 2008).

En segundo lugar, la presencia de rangos de distribución singulares en ciertas especies de hongos liquenizados ha despertado un notable interés por conocer la historia evolutiva de estas especies. Por ejemplo, especies muy conocidas y casi cosmopolitas como *Parmelia saxatilis*; (Crespo et al. 2002) o con un centro de distribución eminentemente europeo-macaronésico típico de *Parmelina carporrhizans* (Alors et al. 2017); los disyuntos entre ambos hemisferios (p. ej. *Cetraria aculeata*; ver resumen de Printzen et al. 2013) o dentro de un mismo hemisferio (p. ej. *Cavernularia hultenii*; Printzen et al. 2003); y, finalmente, distribuciones anómalas como la presentada por *Staurolemma omphalarioides*, con localidades disyuntas mediterráneas y nórdicas (Bendiksby et al. 2014). El desarrollo de nuevos análisis basados en datos de ADN así como el número cada vez mayor de marcadores genéticos disponibles (obtenidos a menor coste) está permitiendo descubrir las historias evolutivas y los eventos que han originado estos rangos de distribución mediante análisis filogeográficos (Printzen 2008; Werth 2010, 2011). La filogeografría estudia la distribución espacial de los linajes genéticos, especialmente la que incumbe a especies individuales y a las estrechamente emparentadas (Avise 2000). La geografía tiene un impacto profundo en la estructuración de las poblaciones y en la diversificación de los linajes, y es por ello que esta disciplina tiende puentes entre la genética de poblaciones, enfocada en los análisis microevolutivos, y la filogenética, que atiende aspectos de la macroevolución. En la última década, han florecido los estudios filogeográficos en líquenes que, además, han permitido testar hipótesis de flujo génico y su direccionalidad entre distintas poblaciones (Buschbom 2007; Geml et al. 2010; Fernández-Mendoza et al. 2011; Fernández-Mendoza y Printzen 2013; Sork y Werth 2014). En este contexto filogeográfico, el macroliquen amenazado *Lobaria pulmonaria* ha recibido especial atención en diferentes trabajos recientes llevados a cabo en un ámbito continental,

regional o local (p. ej. Zoller et al. 1999; Walser et al. 2005; Scheidegger et al. 2012; Widmer et al. 2012; Nadyeina et al. 2014; Otálora et al. 2015). Estos últimos trabajos se ubican en la genética del paisaje (del inglés "*landscape genetics*"), un campo interdisciplinar que integra estudios de genética de poblaciones y ecología de paisaje. En *L. pulmonaria*, dichos trabajos han tratado de examinar la distribución geográfica de linajes y la diversidad genética para relacionarla con factores locales de microclima, el estado de conservación del hábitat, o con diferentes tipos de interacciones bióticas (p. ej. Zoller et al. 1999; Walser et al. 2005; Scheidegger et al. 2012; Otálora et al. 2015). Por otro lado, el análisis de datos genéticos ha permitido en numerosas ocasiones demostrar que especies de hongos liquenizados que se pensaba poseían una amplia distribución, en realidad corresponden a diferentes taxones (p. ej. Crespo et al. 2010a; Divakar et al. 2010; Spribille et al. 2011; Amo de Paz et al. 2012).

El tercer y último aspecto abordado en la biogeografía de líquenes ha sido la comparación de los patrones filogeográficos de mico- y fotobiontes. A escala regional, se ha evaluado el efecto que puede ejercer sobre dichos patrones el tipo de multiplicación (sexual o vegetativo) de los talos liquénicos (p. ej. Werth y Sork 2010; Wornik y Grube 2010; Fernández-Mendoza et al. 2011; Dal Grande et al. 2012) así como las discontinuidades ecológicas y geográficas (Widmer et al. 2012; Chen et al. 2016). Chen et al. (2016) demostraron incluso que dentro de regiones geográfica y climáticamente diferentes la historia de flujo génico puede ser diferente para ambos simbiontes. Otros estudios, además, han usado aproximaciones de la genética de poblaciones para constatar que, dado que la distribución geográfica de los fotobiontes se ve afectada por las condiciones ambientales (Peksa y Škaloud 2011), algunas especies de hongos liquenizados con amplia distribución mundial son capaces de establecer relaciones simbióticas con diferentes fotobiontes, posiblemente mejor adaptados a nivel local (Blaha et al. 2006; Fernández-Mendoza et al. 2011). Asimismo, la asociación diferencial a fotobiontes ha sido postulada como mecanismo promotor de especiación ecológica en micobiontes (Ortiz-Álvarez et al. 2015). Pese a todos estos avances conceptuales, poco se sabe del origen propiamente dicho de los patrones de distribución geográficos de los fotobiontes. Uno de los motivos más evidentes es la imposibilidad de rastrear e incorporar a los análisis linajes de fotobiontes típicos que forman poblaciones de vida libre (i.e. no están asociados con ningún hongo, aunque puedan estar coexistiendo en los mismos microhábitats). De hecho, existen evidencias de fotobiontes de vida libre (p. ej. Tschermak-Woess 1988; Mukhtar et al. 1994; Sanders 2005), incluso en ambientes climáticamente adversos como los Valles Secos de McMurdo de la Antártida (Yung et al. 2014). Otra razón sería la existencia de diferentes linajes, incluso especies, cohabitando el mismo talo liquénico (p. ej. Casano et al. 2011), que pueden presentar diferentes historias evolutivas, lo cual distorsionaría la interpretación de los patrones filogeográficos resultantes. Sin embargo, existen unos pocos ejemplos paradigmáticos de hongos liquenizados asociados a un único fotobionte a lo largo de todo su rango de distribución, como es el caso del liquen *Mastodia tessellata*. En esta situación, resultaría más factible la comparación de la historia evolutiva de ambos simbiontes tanto bajo un marco espacial como temporal.

2. Los líquenes en la Antártida

2.1. La Antártida

De acuerdo al Tratado Antártico de 1959, la Antártida se define como todas las tierras y masas de hielo localizadas al sur del paralelo 60º S. Su superficie es cercana a los 14 millones de kilómetros cuadrados, y abarca todo el continente antártico, que contiene el Polo Sur, así como las Islas Shetland del Sur, por el oeste, y las Islas Orcadas del Sur, por el norte (Figura 4). Diversas variables climáticas y bióticas han sido usadas tradicionalmente para dividir el continente antártico y archipiélagos circundantes en dos zonas: la Antártida Marítima y la Antártida Continental (p. ej. Lewis Smith 1984; Seppelt et al. 1995; Peat et al. 2007). La primera sería considerada como un semi-desierto, más húmedo a menor latitud, e incluiría las Islas Sandwich, Orcadas y Shetland del Sur, Bouvetøya, y la vertiente occidental de la Península Antártica hasta los 72º S aproximadamente. Por su parte, la Antártida Continental englobaría la vertiente oriental de la Península Antártica per debajo de los 63º S más el resto del continente antártico. La masa continental más cercana a la Antártida es el sur del continente americano, situado a unos 900 km a través del Paso de Drake, el cual conecta Tierra del Fuego con la Península Antártica (Figura 4). El Océano Antártico, u Océano Austral, rodea al continente y se extiende desde sus costas hasta el paralelo 55º S, el límite convencional con los océanos Atlántico, Pacífico e Índico. La posición actual de la Antártida en el globo terrestre representa el resultado de millones de años de aislamiento desde el inicio de la fragmentación de Gondwana (Scotese 2001).

Desde el Mesozoico, sin embargo, la Antártida y su océano han sufrido grandes cambios geológicos, oceanográficos y climáticos (Feakins et al. 2012; Scher et al. 2015; Lear y Lunt 2016). En la actualidad, sólo un 0.5% del territorio antártico está desprovisto de hielo y es susceptible de ser colonizado por organismos, como es el caso de las regiones costeras y, más al interior, *nunataks* y desiertos polares como los Valles Secos de McMurdo (Peat et al. 2007; Hawes 2015). Las condiciones climáticas actuales están consideradas como las más extremas de todo el planeta para la vida. A destacar, las bajas temperaturas, la aridez, la elevada radiación y los fuertes vientos (Convey et al. 2008). Como ejemplo, la precipitación anual es de alrededor de 200 mm en las zonas costeras, siendo mucho menor hacia el interior del continente. Asimismo, se ha registrado la temperatura más baja de la Tierra (-89.2º C, estación Vostok el 21 de Julio de 1983) y se estima que podrían llegar incluso a -96º C (Turner et al. 2009), mientras que la temperatura media en el periodo más frío del año ronda los -63º C. Aunque la nieve y el hielo pueden conferir protección frente a temperaturas extremas y a la abrasión por el viento, estos dos factores también limitan los periodos de actividad biológica que, aunque dependen de la latitud y las condiciones microclimáticas, en general son cortos, comparados a los de otros biomas terrestres (Kappen 2000; Green et al. 2007; Pointing et al. 2015). Los vientos catabáticos también pueden provocar alteraciones en la temperatura media anual en localidades tan inhóspitas como los Valles Secos de McMurdo (Nylen et al. 2004) así como influenciar sobre los patrones de dispersión de organismos dentro de la Antártida y entre ésta y regiones circundantes

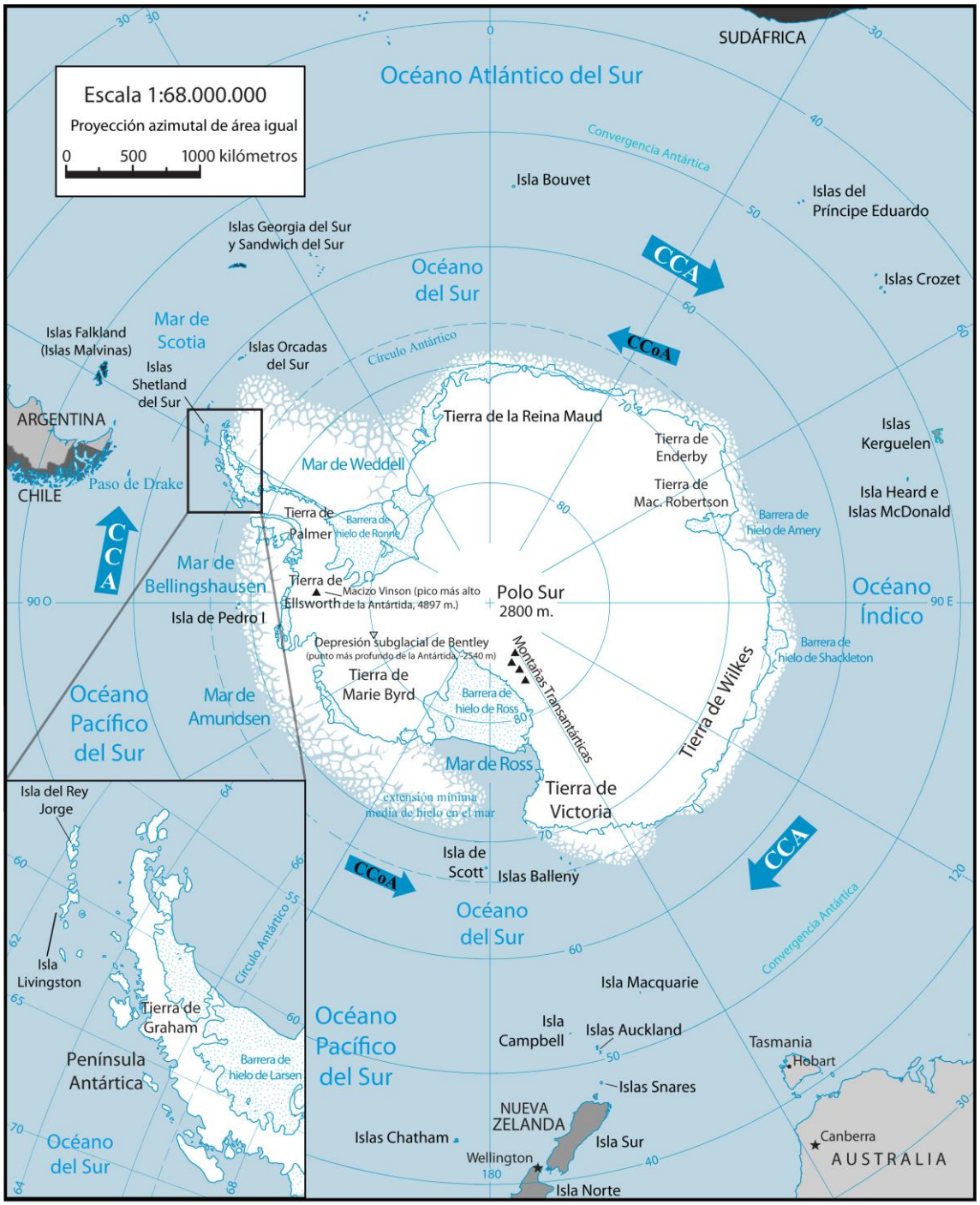

Figura 4. Situación de la Antártida en el Océano Austral. Se incluye también la posición de los archipiélagos subantárticos, las regiones más australes de Suramérica, África y Oceanía, y un detalle de la Península Antártica. El sentido del flujo de la Corriente Circumpolar Antártica (CCA) y la Corriente Costera Antártica (CCoA) está indicado con flechas. (Montaje: IGB).

(Pearce et al. 2009; Hawes 2015; Bowman y Deming 2017). A estas condiciones climáticas también se les debe sumar la baja disponibilidad de nutrientes (oligotrofia) en muchos ambientes antárticos. De hecho, los suelos en zonas libres de hielo presentan un desarrollo pobre, son inestables y están muy influenciados por los ciclos de

congelación-descongelación (p. ej. Blume et al. 2002). Además, estos mismos ciclos, asociados a la formación y desaparición de masas de hielo, han tenido un fuerte impacto sobre los ecosistemas terrestres y acuáticos antárticos, que de manera periódica, y en el mejor de los casos, cambiaban de situación geográfica o, en otros, desaparecían en su totalidad (ver Convey et al. 2008).

Las características del Océano Antártico han ido cambiando desde su configuración inicial. Por ejemplo, la separación de la Antártida de Suramérica, que tuvo lugar entre el Eoceno y Oligoceno (hace entre 45 y 30 Millones de Años, MA) significó, a su vez, el inicio de la Corriente Circumpolar Antártica (CCA), cuyo flujo actual supera los 173 x 10^6 m^3 seg^{-1} en el Paso de Drake (Donohue et al. 2016). Esta corriente oceanográfica fluye principalmente de oeste a este y queda delimitada por el Frente Polar Antártico y el Subantártico (Figura 4). Paralela a la CCA y con sentido opuesto, de este a oeste, fluye la Corriente Costera Antártica (CCoA), con un flujo estacionalmente variable (Kim et al. 2016). En el Mioceno, hace unos 14 MA, el restablecimiento de la placa de hielo antártica oriental propició la intensificación de la CCA (Dalziel et al. 2013). Durante el Cuaternario, la alternancia entre periodos glaciares e interglaciares es posible que no sólo haya afectado al propio continente y a sus costas, sino también a las características de la CCA. Diferentes estudios han recalcado que tanto la distancia geográfica que separa la Antártida del resto de masas continentales como la CCA han tenido y tienen una fuerte influencia sobre la biogeografía antártica. Por ejemplo, se sospecha que la CCA ha actuado como barrera para el flujo génico en algunas especies, mientras que para otras ha constituido un importante vector de transporte (González-Wevar et al. 2012; Moon et al. 2017).

2.2. Vegetación y gradientes bióticos

Las condiciones abióticas que ofrece la Antártida en la actualidad dificultan el asentamiento de vegetales, principalmente de plantas vasculares, de las cuales se conocen dos únicas especies autóctonas que están presentes sólo en la Antártida Marítima: *Deschampsia antarctica* y *Colobanthus quitensis*. Sin embargo, algunos hábitats terrestres y subacuáticos antárticos, pese a ser hostiles para la vida, permiten el asentamiento de variadas comunidades de criptógamas (briófitos, hongos –levaduras negras y liquenizados–, cianobacterias y algas verdes). Así, primero Seppelt (1995) para la región Antártica en general, y después Peat et al. (2007) para la Península Antártica, constataron un gradiente de diversidad, con menos especies de briófitos y hongos liquenizados según aumentaba la latitud. De la misma manera, Green et al. (2007) recalcaron la existencia de un gradiente de cobertura vegetal (especialmente de criptógamas) que reflejaba una reducción paulatina en la extensión desde latitudes al norte del continente antártico hasta localidades cercanas al Polo Sur. Además, los trabajos de Lewis Smith (1984) y Peat et al. (2007) fueron congruentes en sugerir la existencia de dos regiones fitogeográficas principales en la Antártida. De acuerdo con el segundo trabajo, más reciente, la Antártida Marítima sería diferente de la Antártida Continental. La primera se caracterizaría por la presencia de paisajes dominados por las criptógamas (Figura 5) y pequeñas parcelas con las dos fanerógamas autóctonas,

mientras que en la segunda las fanerógamas estarían ausentes y existirían comunidades menos biodiversas de criptógamas, particularmente de briófitos (Peat et al. 2007). Unas de las localidades de la Antártida Continental que ejemplifica con mayor claridad lo adversas que son las condiciones para la vida son los Valles Secos de McMurdo, situados al sur de la Tierra de Victoria. Según Marchant y Head (2007) esta región antártica es la zona del planeta Tierra con condiciones climáticas y relieve más similares a las de Marte. En conjunto, constituyen un desierto frío hiperárido, con temperaturas mínimas, fuerza del viento y sequedad extremas, y con agua líquida prácticamente inexistente dado que la nieve no se derrite, si no que se sublima. En estas condiciones, sólo algunos pocos microorganismos y las criptógamas prosperan (Pointing et al. 2009; Green et al. 2011b; Pérez-Ortega et al. 2012a; de los Ríos et al. 2014).

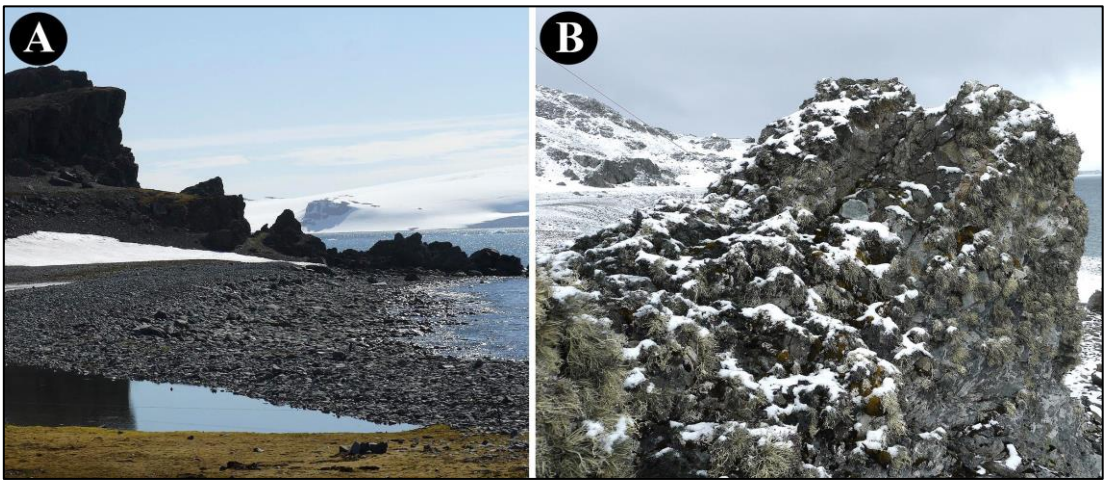

Figura 5. (A) Costa de la Isla Livingston, en la Antártida Marítima. (B) Roca cubierta por talos fruticulosos del género de hongos liquenizado *Neuropogon*. (Fotografías: AdR).

2.3. La liquenología en la Antártida

La cita más antigua de líquenes recolectados en la Antártida corresponde a J. Torrey (1823) y se basa en muestras recogidas por expediciones que tenían como objetivo la caza de focas (1820–1821). Posteriormente, serían el naturalista americano J. Eights, en 1830, y el eminente botánico británico J. D. Hooker, en la década de 1840, quienes visitaron el territorio antártico, recolectando líquenes en las Islas Shetland del Sur y en pequeñas islas alrededor de la Tierra de Graham. A finales del siglo XIX, una expedición belga a la costa oeste de la Tierra de Graham muestreó alrededor de 50 líquenes diferentes, de los cuales más de 20 especies de hongos liquenizados fueron descritas como nuevas para la ciencia por Vainio (1903), como por ejemplo *Acarospora macrocyclos*, *Buellia anisomera* y *Pertusaria corallophora* (Figura 6). Otros liquenólogos y micólogos eminentes, como O. V. Darbishire, T. M. Fries, E. A. Zahlbruckner y M. l'Abbé Hue participaron de la descripción de las colecciones de líquenes efectuadas en los primeros años del siglo XX (para más detalles, ver Lamb 1948). Pero no es hasta mediados del siglo entrante cuando se incrementa el interés por el conocimiento de la biota liquénica antártica. Durante este periodo florecen los

trabajos taxonómicos, sobre todo gracias al esfuerzo de I. M. Lamb y D. C. Lindsay, quienes revisaron de manera detallada colecciones de líquenes depositadas en varios herbarios de las principales instituciones europeas (Øvstedal y Lewis Smith 2001). Asimismo, Dodge (1973) publicó la obra posiblemente más controvertida sobre líquenes antárticos en la que, según Castello y Nimis (1995), llegó a describir varias veces el mismo hongo liquenizado con distintos nombres, lo que conllevó al incremento desmesurado del número de especies antárticas endémicas. Como ejemplo, estos últimos autores descubrieron que Dodge habría descrito una especie relativamente común, *Physcia caesia*, como nueva para la ciencia hasta 12 veces en cinco géneros diferentes, y *Xanthoria elegans* hasta 8 veces también en cinco géneros distintos. Hertel (1988) estimaría con posterioridad que aproximadamente el 80% de las especies descritas como nuevas por Dodge resultarían ser sinónimas de otras ya publicadas. Más adelante, a finales del siglo XX e inicios del presente siglo, se elaboran los primeros trabajos especializados en grupos de líquenes así como revisiones y catalogaciones florísticas (p. ej. Hertel 1984; Hale 1987; Castello y Nimis 1995; Øvstedal y Lewis Smith 2001; Olech 2004). La escasez de colecciones así como la complejidad en la identificación y descripción morfológica de los líquenes antárticos fue resaltada por Lindsay (1977) y Hertel (1988). Este último autor también señaló, primero, la falta de monografías adecuadas (particularmente de líquenes crustáceos) y la no disponibilidad de material tipo para muchas de las colecciones; y segundo, el elevado grado de modificación morfológica de los talos liquénicos antárticos inducida por las condiciones ambientales extremas. Esto último se une al hecho de que muchos especímenes antárticos carecen de estructuras de reproducción sexual, carácter de máxima importancia para la sistemática y taxonomía de hongos liquenizados (Pérez-Ortega et al. 2012a).

Otro campo de estudio muy relevante de la liquenología antártica desde mediados del siglo XX ha sido la ecofisiología. Tanto el micobionte como el fotobionte que, en conjunto, configuran el talo liquénico, son poiquilohidros, es decir, sólo están activos metabólica y fotosintéticamente en estado hidratado (Green y Lange 1995; Kappen y Valladares 2007). Esta y otras particularidades fisiológicas, como la capacidad del córtex talino de reflejar y absorber la radiación lumínica y los mecanismos de fotoprotección de los fotobiontes en estado liquenizado, constituyen algunas de las razones del éxito de los líquenes en la supervivencia en el continente Antártico (Kappen 2000; Schlensog et al. 2003; Sadowsky y Ott 2016). Así, muestran una gran tolerancia al estrés derivado de las bajas temperaturas y a la elevada radiación lumínica, además de conseguir ser fotosintéticamente activos a temperaturas subóptimas y captar vapor de agua proveniente de la nieve (Kappen et al. 1981; Schroeter et al. 1994; Kappen 2000). Por otro lado, los líquenes que viven en ambientes climáticos extremos como los desiertos, zonas alpinas, y el Ártico y la Antártida suelen contar con cortos periodos de tiempo para realizar las funciones metabólicas y crecer (Kappen 1988, 1993). Ello puede explicar, en parte, la asunción general de que los líquenes son muy longevos, especialmente en zonas como la Antártida, con talos que pueden tener una edad mesurable en décadas, e incluso centurias o milenios (ver Nash 2008). En la Antártida,

Sancho et al. (2007) mostraron la existencia de un gradiente latitudinal por el que las tasas de crecimiento de los talos liquénicos disminuían hasta en dos órdenes de magnitud cuando se comparaban localidades situadas en la Antártida Marítima y la Continental. En conjunto, los gradientes observados de diversidad, cobertura y tasa de crecimiento de hongos liquenizados entre los extremos norte y sur del continente antártico han sido relacionados con factores abióticos. Así, en la Antártida Marítima, estos gradientes se explicarían por cambios en la temperatura media anual, mientras que el efecto combinado de la disponibilidad de luz, agua y la temperatura sería el de mayor peso en la Antártida Continental (Green et al. 2011a; Colesie et al. 2014). Raggio et al. (2016) sugirieron que los líquenes crustáceos presentan estrategias adicionales para mejorar su hidratación que explicarían su mayor abundancia en regiones tan extremas como los Valles Secos de McMurdo.

2.4. Diversidad de hongos liquenizados

Los líquenes constituyen el elemento más conspicuo no sólo de los paisajes rocosos alpinos, sino también de los polares (Seppelt 1995; Kappen 2000). Uno de los primeros compendios de líquenes antárticos fue elaborado por Dodge (1973), con un total de 415 especies de hongos liquenizados, el 44.6% de las cuales fueron descritas como nuevas para la ciencia. Estas cifras fueron inicialmente discutidas por Hertel (1988) y Galloway (1991) quienes, desconfiando del trabajo taxonómico de Dodge, estimaron la riqueza de hongos liquenizados en unas 160–200 especies. Más adelante, revisiones críticas del material disponible de Dodge efectuadas por Castello y Nimis (1995) confirmaron que sólo un 20% de las nuevas especies propuestas por dicho autor eran válidas. Fruto de estas investigaciones iniciales, Castello y Nimis (1997) publicaron el primer sumario de la biota liquénica antártica, con un total de 260 especies de hongos liquenizados. Pero ya es en el nuevo siglo cuando aparece el primer tratado pormenorizado sobre diversidad y ecología de hongos liquenizados antárticos, elaborado por Øvstedal y Lewis Smith (2001). Estos autores sitúan dicha diversidad en más de 350 especies en toda la región antártica. La región peninsular, con más de 264 taxones, superaba el número de especies existentes en el resto del continente, que ascendía a 90 (ver Castello y Nimis 1997; Peat et al. 2007). Este contraste entre localidades de la Antártida Marítima y Continental queda bien representado en algunos géneros de hongos liquenizados como *Caloplaca* s.l. (Søchting y Olech 1995; Søchting et al. 2004). Sin embargo, Øvstedal y Lewis Smith (2001) admitieron que estas cifras podrían ser muy inexactas, debido a un desconocimiento general de la biota liquénica provocado por un muestreo parcial, por la subestimación de la variabilidad fenotípica de muchos líquenes, así como por el estado morfológicamente alterado y estéril que muestran la mayoría de talos liquénicos a elevadas latitudes, como ya habían apuntado anteriormente otros autores (Lindsay 1977; Hertel 1988; Castello y Nimis 1997). Además, se ha observado por microscopía electrónica de barrido que los hongos liquenizados y fotobiontes antárticos ocupan frecuentemente posiciones endolíticas, por lo que pueden pasar desapercibidos (de los Ríos et al. 2014). De hecho, desde finales del siglo XX, diferentes estudios han documentado valores relativamente bajos de

taxones en localidades situadas a elevadas latitudes. Así, 7 especies de hongos liquenizados se citaron en las formaciones de areniscas de Beacon, en los Valles Secos de McMurdo (Hale 1987), 27 en la Tierra de Wilkes, a 66º S (Lewis Smith 1988), 22 en el Altiplano Kar (76º S) en el sur de la Tierra de Victoria (Seppelt et al. 1995), 29 en la Bahía Botany, a 77º S (Seppelt et al. 2010) y 30 en el Monte Kyffin, a 84º S cerca del glaciar Beardmore (Green et al. 2011b). El valor más elevado de riqueza se corresponde con las 59 especies citadas en la Bahía Terra Nova y alrededores (Castello 2010) y en el Cabo Hallett, a 72º S (Green et al. 2015). Por su parte, las islas Shetland del Sur y Orcadas del Sur contendrían, según las valoraciones de Øvstedal y Lewis Smith (2001), alrededor de 220 especies de hongos liquenizados. En las primeras, Søchting et al. (2004) documentaron unos años después 187 especies de hongos liquenizados únicamente de la Península Hurd, que ocupa un área de 3 km^2 en la Isla Livingston. Finalmente, en la última revisión de la biota liquénica antártica realizada por Øvstedal y Lewis Smith (2011), en donde incluyen también líquenes de las Islas Georgias del Sur, estos autores sitúan el número de hongos liquenizados en 484 especies. En general, los géneros de hongos liquenizados mejor representados serían *Buellia* (*Physciaceae*), *Caloplaca* s.l. (*Teloschistaceae*), *Cladonia* (*Cladoniaceae*), *Lecanora* (*Lecanoraceae*), y *Verrucaria* (*Verrucariaceae*), a la espera de una confirmación basada en datos moleculares (Figura 6).

Con el inicio del siglo XXI, el desarrollo de las herramientas de análisis molecular ha permitido mejorar el conocimiento de la diversidad de la biota fúngica liquenizada de la Antártida y, en especial, resolver dudas taxonómicas (p. ej. Dyer y Murtagh 2001; Poulsen et al. 2001; Lee et al. 2008; Lindblom y Søchting 2008; Ruprecht et al. 2010, 2012b; Søchting y Castello 2012; Søchting et al. 2014a; Pérez-Ortega et al. 2015; Garrido-Benavent et al. 2016; Ertz et al. 2017). Estos estudios han incrementado el número de especies conocidas de hongos liquenizados hasta cifras cercanas a las 500 especies (incluyendo las Islas Georgias del Sur), lo que supone alrededor del 3.3% de las especies conocidas a nivel mundial. El uso de secuencias *barcoding* de ADN ha sido fundamental a la hora de identificar el hongo presente en talos muy deteriorados recolectados en ambientes extremos como los Valles Secos de McMurdo (Pérez-Ortega et al. 2012a). Con diferentes algoritmos de delimitación de especies, estos autores demostraron la presencia de entre 26 y 27 taxones, de los cuales alrededor de un 55% podrían representar con alta probabilidad nuevas especies para la ciencia. De hecho, algunas de éstas han sido recientemente descritas (Søchting et al. 2014a; Garrido-Benavent et al. 2016).

2.5. Diversidad de fotobiontes

Al igual que ocurre en otras regiones de clima menos adverso del planeta, la diversidad de algas liquenizadas antárticas está poco estudiada. Aoki et al. (1998) aislaron de líquenes antárticos y cultivaron con éxito *Elliptochloris bilobata*, *Trebouxia incrustata* y *T.* cf. *impressa*. Sin embargo, el procedimiento de aislamiento, cultivo y estudio ultraestructural de las células en el que se basa la taxonomía de estos organismos fotosintéticos (p. ej. Friedl 1989) resulta complicado y no permite una

rápida identificación de los fotobiontes. En particular, el cultivo de fotobiontes generalmente requiere del uso de material recolectado recientemente ("talos frescos") y

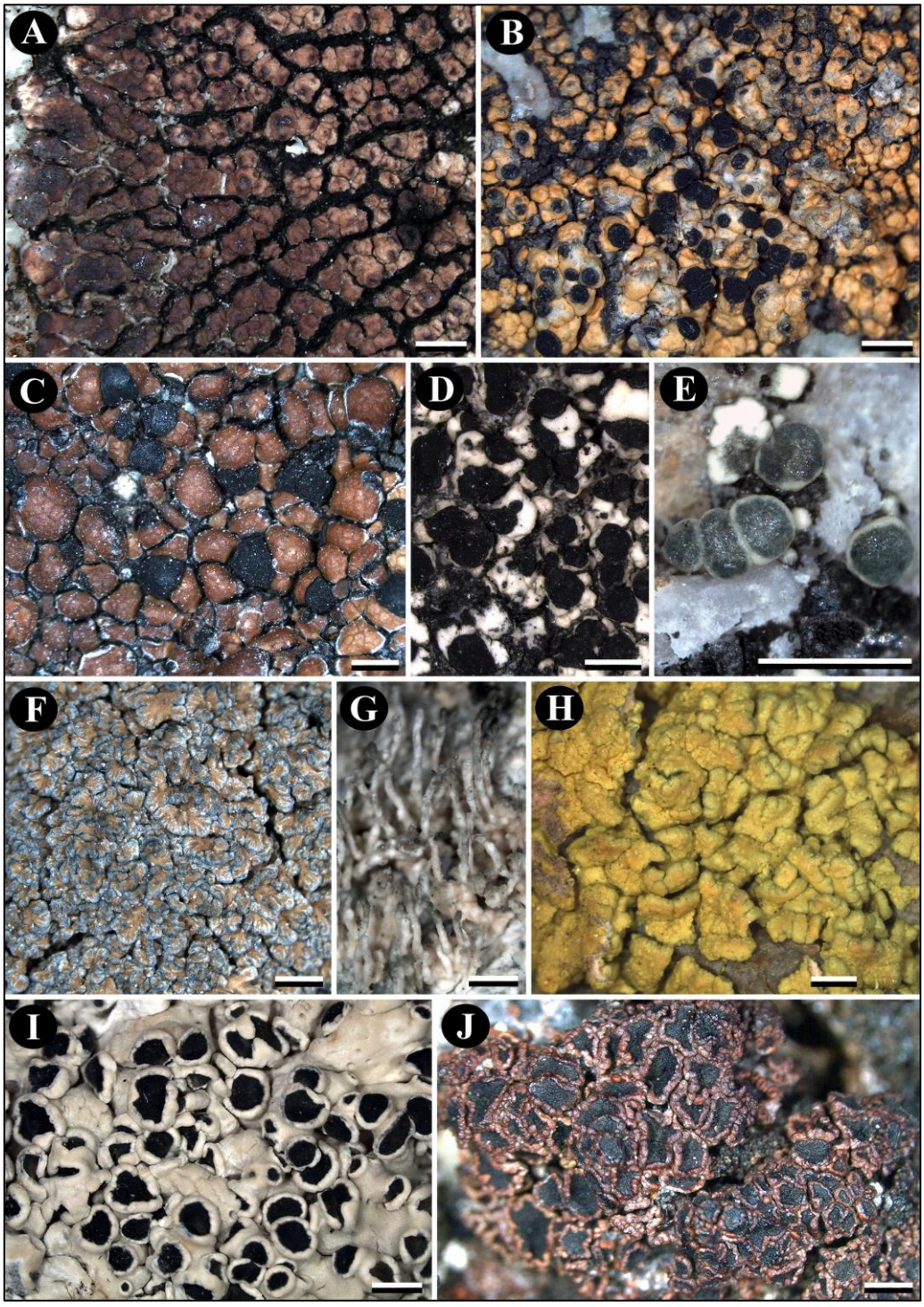

Figura 6. Hongos liquenizados de la Antártida. (A) *Acarospora macrocyclos*. (B) *Buellia anisomera*. (C) *Lecidea atrobrunnea*. (D) *Lecanora physciella*. (E) *L. polytropa*. (F) *Pannaria hookeri*. (G) *Pertusaria corallophora*. (H) *Pleopsidium chlorophanum*. (I) *Tephromela atra*. (J) *Rinodina olivaceobrunnea*. Escalas: 1 mm (Fotografías macroscópicas: IGB; ejemplares recolectados en la Isla Adelaida, Antártida Marítima, por U. Søchting).

debido a la logística propia de la Antártida, en la mayoría de los casos las muestras tardan varios meses en llegar a su destino, lo que disminuye la tasa de éxito de los cultivos. En cambio, el uso de marcadores moleculares específicos del genoma algal ha contribuido recientemente a la mejora del conocimiento de la diversidad de fotobiontes a partir de muestras ambientales de líquenes. Uno de los primeros estudios en este sentido fue realizado por Romeike et al. (2002), quienes muestrearon la diversidad de algas liquenizadas en varias especies del hongo *Umbilicaria* a lo largo de un transecto de aprox. 5.000 km en la Península Antártica, encontrando hasta 5 linajes diferentes, todos ellos pertenecientes al género *Trebouxia*. Ejemplos de asociaciones poco estrictas entre hongos y algas liquenizadas han sido descritos por Wirtz et al. (2003) y Engelen et al. (2010). Los primeros autores obtuvieron secuencias de los cianobiontes de cinco líquenes recolectados en la Isla Livingston (Antártida Marítima) y observaron que todos ellos compartían la misma cianobacteria, y sólo dos albergaban una segunda cianobacteria. Engelen et al. (2010) identificaron hasta tres especies diferentes de ficobiontes, pertenecientes a dos géneros distintos (*Trebouxia* y *Asterochloris*), involucrados simbióticamente con el hongo liquenizado *Lepraria borealis*. La interpretación de estos patrones asociativos se hizo en términos de la fuerte presión selectiva a la que los micobiontes están sometidos en estas regiones de clima adverso, que favorecen asociaciones simbióticas menos selectivas del hongo respecto al fotobionte. Asimismo, de los Ríos et al. (2005) propusieron la hipótesis de que la baja disponibilidad de algas en algunos microhábitats líticos antárticos tiene como consecuencia que los micobiontes se asocien con un *pool* relativamente reducido de algas compatibles. Estudios recientes que contemplaban una diversa gama de líquenes detectaron niveles variables de selectividad en la interacción hongo-alga (Pérez-Ortega et al. 2012a; Ruprecht et al. 2012a; Engelen et al. 2016). Recientemente, Zúñiga et al. (2017) han demostrado la existencia de una gran diversidad genética en *Nostoc* de vida libre y asociados a hongos liquenizados pertenecientes al género *Peltigera* en la Antártida Marítima. Finalmente, el uso de datos genéticos y técnicas de microscopía electrónica también ha permitido la descripción de una nueva especie de ficobionte en líquenes antárticos, *Asterochloris sejongensis*, bajo la perspectiva de la taxonomía integradora (Kim et al. 2017).

2.6. Patrones biogeográficos en los hongos liquenizados

El conocimiento de la distribución geográfica global de un número considerable de hongos liquenizados antárticos, al igual que ocurre con otras criptógamas, es limitado. Ello tiene dos explicaciones. Por una parte, y como se ha señalado anteriormente, la escasez de colecciones, muchas de ellas incluso con características morfológicas inadecuadas para su estudio; por otra, la escasa bibliografía no sólo referente a la Antártida, sino también a todo el hemisferio austral, que permita establecer rangos de distribución más exactos para los distintos elementos de la biota liquénica. Hertel (1984, 1987, 1988), en sus referencias a los líquenes lecidoides, señaló que pese a que la Antártida Continental presentaba taxones endémicos (p. ej. género *Austrolecia*), el mayor número de endemismos estaba presente en la Antártida Marítima

y zona subantártica. En el continente, sin embargo, abundaban las especies de amplia distribución. Un patrón similar mostrarían las especies de *Caloplaca* s.l. (Søchting y Olech 1995). Estas observaciones fueron recalcadas unos años después por Kappen (2000) para asociar el elevado grado de endemismo a condiciones climáticas menos adversas. Por otra parte, en la revisión florística de Castello y Nimis (1997), el porcentaje de especies endémicas se estableció en el 38%, mientras que el de taxones bipolares y cosmopolitas, en conjunto, llegaba al 41.5%. De hecho, la importancia del elemento bipolar en la biota liquénica antártica ya había sido subrayada décadas antes por Lamb (1948). Más tarde, Øvstedal y Lewis Smith (2001) aunaron toda la información disponible hasta el momento y establecieron 5 patrones de distribución geográfica para los líquenes antárticos: 1) cosmopolita, 2) sur del Hemisferio Sur, 3) región magallánica (sur de Suramérica), 4) bipolar y 5) antártico-endémica. De los más de 350 hongos liquenizados que estos autores documentaron, el patrón que recibió un mayor número de especies fue también el patrón bipolar, con 148 (un 39.1% del total de especies), seguido del antártico-endémico (128 spp., 33.5%) y las cosmopolitas (26 spp., 6.9%). Además de estas cifras, los autores destacaron el gran número de especies bipolares en localidades situadas a menores latitudes (p. ej. 41% en las Islas Orcadas del Sur), y la rareza de especies cosmopolitas en localidades con condiciones climáticas más adversas (p. ej. 7% en la Antártida Continental). A diferencia de Hertel (1984, 1987, 1988), estos autores señalaron que el grado de endemismo era mayor en la Antártida Continental que en la Antártida Marítima, con más del 50% de las especies endémicas (Øvstedal y Lewis Smith 2001). Estudios posteriores a nivel local y regional, o bien refutarían (Søchting et al. 2004), o bien apoyarían (Singh et al. 2015b) esas observaciones iniciales.

Por otro lado, al considerar en conjunto la biota liquénica de diferentes territorios del hemisferio austral (p. ej. Antártida, Nueva Zelanda, Tierra del Fuego y Tasmania), varios autores habrían reconocido, en general, un marcado carácter circumpolar y cosmopolita, y por otra parte, que dicha biota era más similar entre regiones geográficamente más cercanas (Lindsay 1977; Walker 1985; Hertel 1987; Galloway 1991). De hecho, Feuerer y Hawksworth (2007) determinaron analíticamente el agrupamiento en términos florísticos de la región subantártica con las restantes regiones australes. Respecto a los mecanismos responsables de las similitudes florísticas entre dichas regiones, los trabajos de Hertel (1984), Engelsksjøn y Jørgensen (1986), Stenroos (1993) y Søchting y Olech (1995) ya habían augurado un papel clave de la dispersión a larga distancia. Más aún, tanto Engelsksjøn y Jørgensen (1986) primero, como Galloway (1991) y Søchting y Olech (1995) después, sostuvieron que los fuertes vientos del oeste, o las corrientes marinas que circulan en el mismo sentido, pudieron facilitar el intercambio de propágulos entre regiones y, en último lugar, ocasionar los patrones biogeográficos observados hoy en día. Seppelt (1995) expuso un ejemplo de la elevada capacidad de recolonización de los líquenes, al constatar que las Islas Windmill poseían una biota liquénica abundante y diversa a pesar de que estas islas perdieron la capa de hielo hace solo 5.500 años, durante el Holoceno. Finalmente, Muñoz et al. (2004) demostraron mediante análisis estadísticos que la conectividad por viento, y no

la proximidad geográfica, era la responsable mayoritaria de las similitudes florísticas en el Hemisferio Sur, y por tanto de los patrones de distribución de plantas (incluyendo líquenes) observados en la actualidad.

Aunque de un modo más comedido, explicaciones basadas en la vicarianza ya fueron expuestas por Galloway (1987) para explicar, aunque sin referirse explícitamente a la Antártida, los patrones de distribución disyuntos de los líquenes australes. En particular, este autor subrayó la importancia que pudo tener la fragmentación de las masas continentales. Seppelt (1995), incluso, trató de explicar las disyunciones de ciertos líquenes marítimos, como algunas especies del género *Verrucaria*, dentro de la Antártida. Según él, las poblaciones disyuntas se habrían originado por el efecto obliterante de las masas de hielo en las áreas costeras, que impedirían la expansión de estas especies por toda la costa, relegándolas a áreas disyuntas. Sin embargo, como se ha visto más recientemente, la evolución en los patrones de distribución de las plantas australes parece estar dominada mayormente por dispersión, y no por vicarianza (p. ej. Sanmartín y Ronquist 2004; Winkworth et al. 2015).

3. Origen de la biota liquénica antártica

3.1. Etapa "pre-molecular"

A lo largo del siglo XX, numerosos estudiosos de la biota liquénica antártica manifestaron su opinión sobre el origen de la misma (p. ej. Lamb 1948, 1970; Dodge 1973; Lindsay 1977; Hertel 1987; Seppelt 1995). En general, las hipótesis planteadas estaban enfocadas a dos grupos de líquenes antárticos con diferente distribución geográfica: los de amplia distribución (p. ej. bipolares) y los endémicos. Los datos en los que estaban basadas dichas hipótesis eran eminentemente florísticos, provenientes de catalogaciones de la biota liquénica antártica, tanto a nivel local, como a nivel global.

Uno de los primeros autores en plantear una explicación acerca del origen de la biota liquénica antártica fue Lamb (1948, 1949, 1954, 1970). En primera instancia, éste se mostró dubitativo a la hora de asignar un origen austral o boreal para los líquenes bipolares antárticos. Quizás influenciado por las ideas expuestas previamente por Du Rietz (1940), de que el origen más probable de una especie era aquél en donde el género al que pertenece presentaba más especies, Lamb (1948) sugirió un origen predominantemente austral para especies de los géneros de hongos *Sphaerophorus*, *Placopsis* y *Neuropogon*. Para apoyar su planteamiento, Lamb afirmó que la mayoría de líquenes bipolares se encontraban en los territorios más cercanos a Tierra del Fuego, como la Tierra de Graham (Península Antártida), por lo que habría sido posible el intercambio de propágulos entre ambas zonas y la eventual colonización del Hemisferio Norte a través de la Cordillera de los Andes y las Montañas Rocosas norteamericanas. Unas décadas después, Lamb (1970) subrayaría el papel que pudieron haber jugado el viento o las aves en la colonización antártica de líquenes existentes en la zona subantártica después del último periodo glacial.

Respecto al origen de las especies que en aquel momento se consideraban endémicas de la Antártida y regiones adyacentes, Lamb (1948) planteó una hipótesis basada en la vicarianza. Según él, algunas especies de hongos liquenizados del género *Verrucaria* y *Staurothele* australes presentarían su respectiva especie vicariante en el Hemisferio Norte. Desgraciadamente, no estableció de manera explícita ni un marco temporal, ni las causas responsables de dicha vicarianza. Un año después, nuevas evidencias glaciológicas llevaron a Lamb (1949) a reconsiderar su perspectiva sobre el origen de los líquenes endémicos antárticos. Así, puesto que los hábitats de este continente susceptibles de haber sido colonizados por vegetación habrían quedado expuestos en los últimos 10.000 años, Lamb lanzó la hipótesis de que los líquenes endémicos persistieron en la Antártida durante las últimas glaciaciones refugiados en *nunataks* continentales. Según este autor, la supuesta baja tasa evolutiva de los líquenes no podría explicar el elevado grado de endemismo observado en la Antártida. De acuerdo con esta hipótesis, Lamb (1970) atribuiría a las especies endémicas un origen pre-pleistocénico, apoyándose en las consideraciones de Dahl (1946) sobre geomorfología y glaciología, que proponían que las montañas costeras antárticas habrían impedido la formación de placas de hielo continuas, dejando espacios expuestos

en la costa. Así, este autor sugirió que no sólo los *nunataks* pudieron ser refugio de los líquenes en el interior del continente, sino que también pudieron existir refugios u oasis costeros. Otra evidencia que Lamb usó para defender su concepción de origen antiguo para las especies endémicas fue la presencia de caracteres morfológicos singulares en algunas especies endémicas antárticas. Por ejemplo, destacó que algunas especies de los géneros *Caloplaca* s.l., *Lecania* y *Bacidia* presentaban un biotipo fruticuloso muy característico (Figura 7), mientras que en otras regiones del planeta, todas las especies de dichos géneros eran únicamente crustáceas (Lamb 1954, 1970). La singularidad morfológica de estas especies antárticas fue razón suficiente para para considerarlas como "antiguas y muy evolucionadas". Finalmente, este autor concluyó su trabajo muy cauteloso, enfatizando la necesidad de conocer mejor la biota liquénica no sólo antártica, si no también austral, para tener una idea más certera del nivel de endemismo en los líquenes antárticos.

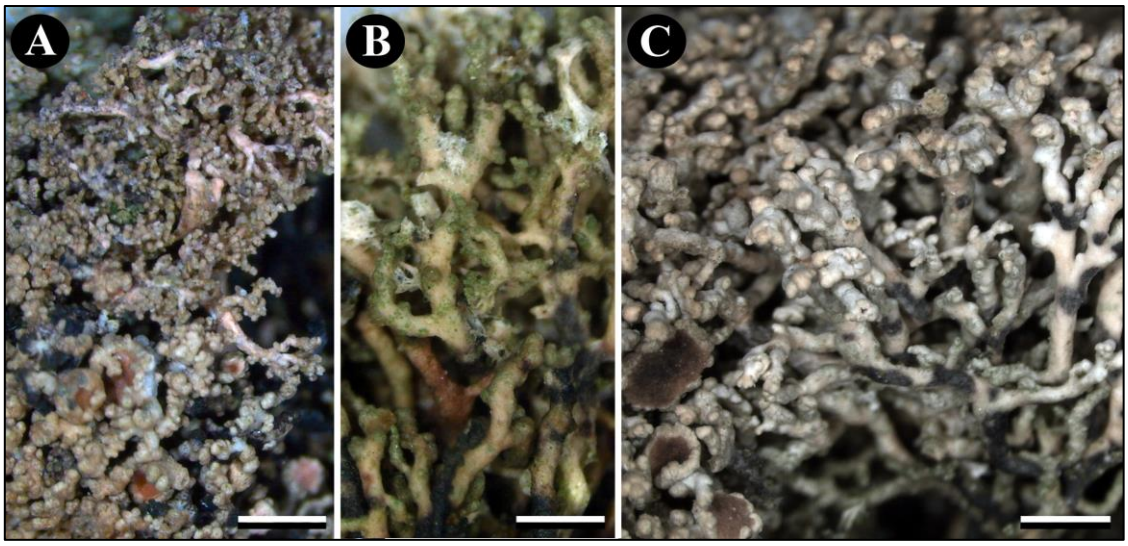

Figura 7. Especies de talo fruticuloso pertenecientes a géneros que habitualmente forman talos de biotipo crustáceo. (A) *Catillaria corymbosa*. (B) *C. corymbosa*, detalle en donde se pueden observar células de algas. (C) *Lecania brialmontii*. Escalas: 1 mm. (Fotografías macroscópicas: IGB; ejemplares recolectados en la Isla Adelaida, Antártida Marítima, por U. Søchting).

Otro autor que investigó el origen de la biota liquénica en la Antártida fue Dodge. Quizás movido por un concepto equívoco de endemismo (ver Castello y Nimis 1995) y por el desarrollo en la década de los sesenta de la tectónica de placas, Dodge consideró al continente antártico como un refugio antiguo para especies de hongos liquenizados (Dodge 1948, 1964, 1973). Así, por ejemplo, los taxones presentes en la Antártida continental derivarían de especies gondwánicas que habrían sobrevivido al último periodo glacial en *nunataks* y, con el cambio climático, habrían ampliado su rango de distribución a lo largo del continente, a la vez que especiaban localmente. Esta última sería la razón por la cual, según este autor, existirían un gran número de especies continentales endémicas. En cambio, para los líquenes de la Península Antártica sugirió la mayor conexión con Tierra del Fuego como determinante para su origen. De hecho,

propuso que los líquenes bipolares habrían colonizado la Antártida mediante migración desde las cadenas montañosas del norte, centro y sur del continente americano (Dodge 1964).

Tanto Lamb como Dodge, por tanto, habrían considerado el origen temporal de la biota liquénica antártica como mixto, incluyendo especies endémicas relictas, y otras de amplia distribución como recientes colonizadoras. Esta postura fue en realidad la más aceptada por autores sucesivos, como Ahmadjian (1970), Lindsay (1977), Filson (1982) y Jørgensen (1983). Walker (1985) también concibió un origen dual para explicar los patrones de distribución de miembros del grupo *Neuropogon*, dentro del género de hongos liquenizados *Usnea*. Asimismo, Hertel (1987) consideró el gran número de taxones lecideoides saxícolas de las islas subantárticas como prueba de un origen más antiguo, en contraposición a las especies del continente, generalmente de distribución más amplia y, por tanto, de origen reciente.

Otro liquenólogo que impulsó la liquenología austral en la segunda mitad del siglo XX fue D. J. Galloway. En su trabajo de revisión de 1991, que versaba sobre los líquenes endémicos de la región austral en general, interpretó que los endemismos podrían haber resultado de la evolución de ancestros debido a largos periodos de aislamiento, o bien podrían constituir taxones con distribuciones relictas, que habían sobrevivido a extinciones causadas por cambios climáticos o geográficos. Aplicado al continente antártico, Galloway (1991) opinó que la flora de la Antártida Continental era principalmente post-pleistocénica, y ello difería del origen de la flora de la Antártida insular, más relicta y pre-pleistocénica.

Ya bien entrada la década de los 90, Søchting y Olech (1995) interpretaron el origen de las especies del género *Caloplaca* s.l. bipolares de la Antártida, especialmente las muscícolas y terrícolas (un tercio del total), como resultado de migraciones entre hemisferios a través de las cadenas montañosas americanas (Cordillera Andina y Montañas Rocosas) o de una conexión Malasio-Papuana. En cambio, afirmaron que la dispersión a larga distancia desde el Ártico a la Antártida era poco probable, contradiciendo hasta cierto punto la opinión mostrada por Stenroos (1993) para el origen de las algunas especies de *Cladonia* australes. Por otra parte, Søchting y Olech (1995) destacaron el alto grado de endemismo mostrado por las *Caloplaca* s.l. de hábitats costeros de la Antártida Marítima. Para estas especies, estos autores dedujeron un origen antiguo e independiente del de las especies árticas que crecían en estos mismos ambientes. En concreto, justificaron el aislamiento entre ambas regiones polares por la incapacidad de las diásporas de dispersarse a larga distancia a través de los trópicos y subtrópicos. Dicho aislamiento histórico ya había sido señalado años antes por Kärnefelt (1990) para muchas especies de hongos liquenizados del Hemisferio Sur. Además, Søchting y Olech (1995) sugirieron que las zonas de la Antártida Marítima, así como las de Tierra del Fuego y la Patagonia, que habían estado más tiempo libres de hielo eran las áreas desde donde especies endémicas de *Caloplaca* s.l. habrían evolucionado y persistido y finalmente desde allí recolonizado otras regiones antárticas situadas más al este después del último periodo glacial.

Seppelt (1995) evaluó las diferentes hipótesis presentadas por otros autores para admitir, una vez más, el origen mixto de la biota liquénica antártica. Según este autor, el origen de los hongos liquenizados presentes en la Península Antártica era antiguo para algunas especies que se habrían refugiado allí durante las glaciaciones mientras habrían desaparecido del resto del continente. A nivel de la Antártida Continental, Seppelt (1995) sugirió que algunas especies habrían podido sobrevivir a las glaciaciones en *nunataks*, con posterior expansión de su rango de distribución, mientras que otras habrían colonizado el continente mediante migración desde la Península Antártica, o incluso desde el sur de Suramérica, en épocas recientes, entre el Pleistoceno y Holoceno. Al igual que Lamb (1970), Stenroos (1993) y Søchting y Olech (1995), Seppelt (1995) señaló el papel del viento como posible mecanismo para la recolonización de islas y regiones recientemente expuestas. Para apoyar la hipótesis de especies refugiadas en *nunataks*, Seppelt y después también Øvstedal y Smith (2001), adujeron la presencia actual de líquenes en picos montañosos remotos (Siple 1938; Engelskjøn 1986; Ryan et al. 1989) y la existencia de líquenes endolíticos (casmo- o criptoendolíticos) en regiones de clima extremo como los Valles Secos de McMurdo (p. ej. Kappen et al. 1981; Friedmann 1982).

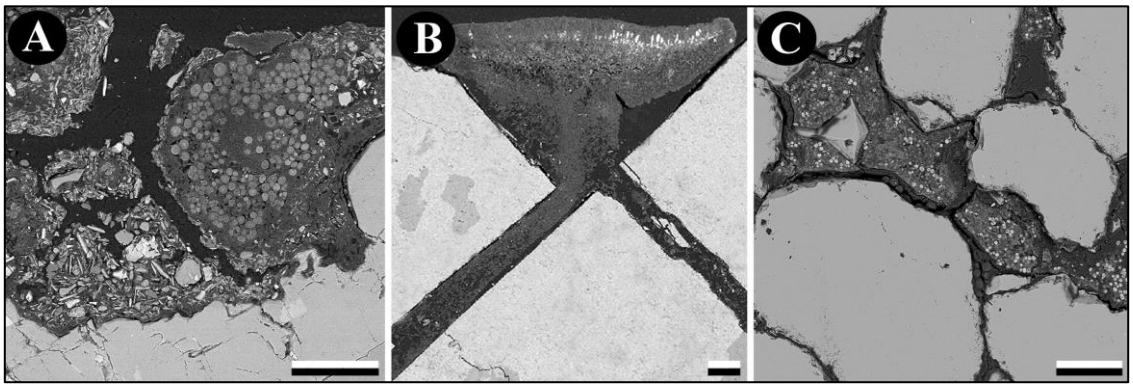

Figura 8. Crecimiento epilítico (A), casmoendolítico (B) y criptoendolítico (C) de talos liquénicos. Escalas: 100 μm. (Fotografías de microscopía electrónica: AdR).

Finalmente, los últimos trabajos de esta etapa "pre-molecular" a considerar son los de Castello y Nimis (1997), Kappen (2000), Øvstedal y Lewis Smith (2001) y Peat et al. (2007). En general, todos estos autores reinterpretaron las cifras de endemismos y especies con distribución más amplia (p. ej. bipolar) y recogieron evidencias de otros estudios para señalar, una vez más, el origen temporal mixto de la biota liquénica antártica. Castello y Nimis (1997) propusieron un origen reciente para las especies del continente antártico –Cuaternario– mediado por eventos de dispersión a larga distancia, y un origen antiguo, para especies de la región subantártica. Kappen (2000), al igual que había hecho Lamb en 1970, manifestó la opinión que las especies endémicas del continente antártico no habrían tenido suficiente tiempo, en los 10.000 años de deshielo, para evolucionar y que por tanto corresponderían más bien a una biota relicta, que habría persistido refugiada en *nunataks* (p. ej. Valles Secos de McMurdo). La existencia de poblaciones relictas a elevadas latitudes, entre 72º y 84º Sur, ha sido también propuesta en recientes estudios florísticos (Green et al. 2011b; Green et al. 2015).

Øvstedal y Lewis Smith (2001), además, enfatizaron el papel de la dispersión a larga distancia como mecanismo responsable de la similitud entre la biota liquénica de la Península Antártica y la de Tierra del Fuego. Para justificar el posible intercambio de propágulos entre ambos territorios, estos autores se basaron en los resultados de captura de diásporas exóticas y polen en localidades antárticas de Kappen y Straka (1988), Lewis Smith (1991), Linskens et al. (1993) y Marshall (1996a) así como otros que evidenciaban dispersión local de propágulos liquénicos (Rudolph 1970; Marshall 1996b). Por último, al analizar la diversidad y los patrones de distribución de la biota Antártica de manera sistemática, Peat et al. (2007) propusieron que es probable que parte de los líquenes tuviera "un origen antiguo y vicariante".

3.2. Etapa "molecular"

Dyer y Murtagh (2001) y Murtagh et al. (2002) establecieron posiblemente el inicio de la etapa molecular en el estudio biogeográfico de los líquenes antárticos. Mediante filogenias del marcador molecular nuclear *Internal Transcribed Spacer* (*nrITS*) y amplificación aleatoria de ADN-polimórfico (*RAPDS*), destacaron la marcada divergencia genética de los especímenes antárticos de *Xanthoria elegans* respecto a los recolectados en otras regiones del planeta, sin llegar a proponer una explicación histórica de tal observación. Dentro de la Antártida, destacaron la similitud genética (1 único nucleótido diferente) entre especímenes de *Buellia frigida* recolectados en localidades separadas más de 600 km en la Antártida continental oriental. Por otra parte, observaron que dos especímenes de *X. elegans*, recolectados uno en la Antártida Marítima y el otro en la Base Mawson localizada en la Antártida Continental oriental (localidades separadas unos 4.960 km), presentaban secuencias del *nrITS* idénticas, de lo que dedujeron la existencia de un número relativamente bajo de genotipos en toda la Antártida.

Usando dos marcadores moleculares (*nrITS*, *β-tubulin*), Crespo et al. (2002) reconocieron un grupo monofilético que incluía muestras de *Parmelia saxatilis* provenientes de la Antártida, Patagonia, Ártico, Europa boreal, Norteamérica y algunas montañas elevadas mediterráneas. En vista de la poca divergencia genética observada, incluso entre especímenes de la Península de Kola (Rusia) y la Antártida, estos autores interpretaron que la dispersión de isidios facilitada por aves en tiempos relativamente recientes, podría ser el mecanismo responsable del patrón de distribución actual de este liquen. Sin embargo, el origen austral o boreal de esta especie no estaba incluido explícitamente en esta hipótesis.

Simultáneamente, Romeike et al. (2002) emplearon datos filogenéticos para contestar explícitamente a la pregunta del origen de la biota liquénica antártica. Para ello, usaron como caso de estudio el género de hongos liquenizados *Umbilicaria*. Así pues, estos autores sugirieron que las poblaciones actuales de *Umbilicaria* presentes en la Antártida derivarían tanto de múltiples eventos independientes de colonización desde regiones templadas, como de raros eventos de dispersión a larga distancia de ecotipos preadaptados a las condiciones climáticas adversas del continente. Asimismo, en este

trabajo los autores pusieron de relieve la posibilidad de que algas y hongos hubieran colonizado el continente independientemente, y que el proceso de "reliquenización" se pudo producir gracias a la baja selectividad del hongo respecto al alga.

Unos años después, Reeb et al. (2007) observaron similitudes genéticas entre especímenes de *Pleopsidium chlorophanum* de la Antártida y otros de Sudáfrica y Norte de Europa (p. ej. Noruega) usando diferentes marcadores, aunque dichos autores no lo interpretaron en términos biogeográficos. El mismo año, Seymour et al. (2007) llevaron a cabo una revisión molecular de especies antárticas neuropogonoides del género *Usnea*. En este estudio se detectaron niveles variables de diversidad genética intraespecífica en las especies consideradas, pero no se observó una correlación clara entre el origen geográfico y el grado de similitud genética de las muestras. En los sucesivos trabajos de Wirtz et al. (2008, 2012), la similitud genética entre poblaciones antárticas y norteamericanas de las especies *U. sphacelata* y *U. lambii* se interpretó como resultado de dispersión a larga distancia directa o gradual a través de los Andes o, alternativamente, a la existencia de poblaciones relictas en el Hemisferio Norte.

Por otra parte, Lindblom y Søchting (2008) demostraron con evidencias filogenéticas el patrón de distribución bipolar de *Xanthomendoza borealis*. Para su origen, sin embargo, propusieron dos hipótesis a la espera de ser probadas por análisis más complejos. Por una parte, y puesto que el género *Xanthomendoza* tiene más especies en el Hemisferio Norte, estos autores alegaron un origen reciente para *X. borealis*, que habría colonizado la Antártida Continental mediante dispersión a larga distancia directa entre ambos polos por aves o viento, sin descartar una migración a lo largo de las cadenas montañosas americanas. En segundo lugar, recurrieron a la existencia de poblaciones relictas en el continente antártico que se habrían originado tras la fragmentación de las masas continentales y que habrían resistido los periodos glaciales. Desafortunadamente, estos autores no aportaron en su trabajo datos cuantitativos de diversidad y diferenciación genética entre poblaciones boreales y australes de *X. borealis*. En el trabajo filogenético de Søchting y Castello (2012) se demostró el patrón de distribución y posible origen antártico de *Austroplaca darbishirei*, cuyas poblaciones continentales y marítimas diferían sutilmente a nivel genético. Igualmente, estos autores evidenciaron el patrón de distribución bipolar de la especie hermana *A. soropelta*, cuyo origen fue explicado de la manera reversa al de *X. borealis*. Es decir, propusieron que lo más probable era que *A. soropelta* fuera un taxón austral, porque así lo eran la mayoría de especies próximas. La colonización del Hemisferio Norte habría sido *a posteriori*, en tiempos recientes, dada la escasa diferenciación morfológica y genética entre especímenes de localidades australes y boreales. En este punto hay que resaltar que el uso de la información contenida en los marcadores genéticos desde inicios del siglo XXI no sólo ha permitido reevaluar los patrones biogeográficos establecidos en estudios previos, sino que también ha tenido una fuerte repercusión a nivel de la sistemática y taxonomía liquénica. Por ejemplo, la familia de hongos ascomicetes liquenizados *Teloschistaceae*, en la cual se incluye *Caloplaca* s.l., ha sufrido en los últimos años un fuerte reordenamiento de las especies a

nivel genérico (Arup et al. 2013). Algunos géneros, incluso su propio nombre científico, han sido propuestos para resaltar el origen geográfico de las especies que agrupa, como por ejemplo *Austroplaca*, *Dufourea*, *Gondwania*, *Shackletonia* y *Xanthopeltis*, todos ellos con especies restringidas mayormente al hemisferio austral. Por último, Roca-Valiente (2013) realizó un estudio exhaustivo de la diversidad genética y morfológica del liquen *Rhizocarpon geographicum* con un muestreo a nivel mundial que permitió detectar similitudes genéticas entre muestras de Alaska, Tierra del Fuego y la Antártida Marítima. En este estudio se detectaron, además, dos linajes bipolares con representantes antárticos.

Sin embargo, ha sido el estudio filogeográfico del liquen bipolar *Cetraria aculeata* el que ha marcado el mayor hito en la investigación del origen de la biota liquénica antártica (Fernández-Mendoza et al. 2011; Domaschke et al. 2012; Fernández-Mendoza y Printzen 2013; ver Printzen et al. 2013). Aparte de abordar el origen de su patrón de distribución bipolar (ver más abajo), estos estudios emplearon análisis de genética de poblaciones, filogenéticos y reconstrucciones genealógicas para demostrar que la máxima diversidad genética del micobionte estaba en el Ártico, y que ésta declinaba en dirección a la región antártica. Esta observación hizo que se planteara un origen boreal para dicha especie, con posterior colonización del hemisferio austral. Con el fin de testar dicha hipótesis, Fernández-Mendoza y Printzen (2013) compararon diferentes modelos migratorios baja un marco de coalescencia. Los resultados apoyaron la hipótesis de un origen boreal para el este liquen antártico. Además, por primera vez se incorporó un marco temporal al análisis de reconstrucción de cambios de carácter con el fin de estudiar la expansión geográfica de *C. aculeata* a lo largo del tiempo. En conjunto, todos estos análisis confirmaron que las poblaciones antárticas de *C. aculeata* se originaron en el Pleistoceno, probablemente tras una colonización desde Patagonia. Estos autores interpretaron la reducida diversidad genética de las poblaciones antárticas de mico- y fotobiontes como ejemplo de efecto fundador y sugirieron, aunque de manera algo especulativa, el posible papel que pudieron tener unas aves llamadas "págalos" (familia *Stercorariidae*; en inglés "Skuas") en la dispersión de propágulos vegetativos de *C. aculeata* entre Patagonia y la Península Antártida.

Los últimos estudios publicados hasta la fecha que han abordado aspectos filogeográficos de la biota liquénica antártica han sido los llevados a cabo por Jones et al. (2013, 2015) sobre el liquen endémico *Buellia frigida*. En 2013, estos autores analizaron la diversidad de fotobiontes y la selectividad que mostraba el micobionte. En varias localidades situadas en la región del Mar de Ross, mostraron como el micobionte se asociaba con el mismo haplotipo de fotobionte, del género *Trebouxia*. Sin embargo, en los Valles Secos, *B. frigida* estaba asociada a multitud de genotipos algales, al igual que habían mostrado previamente Pérez-Ortega et al. (2012a). Dado que este patrón había sido también observado para *Umbilicaria aprina* por los otros autores, Jones et al. (2013) plantearon la posibilidad de que los Valles Secos de McMurdo habrían actuado como refugio para los fotobiontes en sucesivos periodos glaciales, permitiendo el mantenimiento de una diversidad genética comparativamente elevada en los fotobiontes.

De hecho, un estudio anterior de De Wever et al. (2009) sobre algas clorófitas antárticas habría sostenido ya la existencia de refugios glaciales para estos organismos tanto en la Antártida Marítima como en la Continental. Alternativamente, Jones et al. (2013) sugirieron que la elevada longevidad de los líquenes en estas localidades tan áridas continentales habría facilitado la acumulación de mutaciones en el genoma algal, dando lugar a un *pool* genéticamente diverso de fotobiontes. Jones et al. (2015) analizaron la diversidad genética de los micobiontes de *B. frigida* con microsatélites. De dichos análisis concluyeron que tanto los Valles Secos de McMurdo como las Montañas Reina Maud pudieron haber actuado como refugios glaciales continentales para *B. frigida*, puesto que la mayoría de alelos privados (únicos) los encontraron allí. Asimismo, estos autores documentaron niveles moderados de diferenciación genética entre las distintas localidades donde *B. frigida* fue recolectada. En vista de estos resultados, adujeron que tanto el patrón de vientos dominante como las barreras físicas (p. ej. glaciares) existentes en la región de estudio impedirían la dispersión y posterior asentamiento de propágulos, principalmente esporas, entre localidades.

4. El patrón de distribución geográfica bipolar

4.1. Definición e incidencia

El eminente ictiólogo soviético L. S. Berg (1933) aplicó el término bipolar para referirse a la distribución geográfica de una especie o de especies emparentadas que abarca las regiones polares, templadas o subtropicales de ambos hemisferios, pero no a las tropicales. Más adelante, Moore y Chater (1971) añadirían un criterio latitudinal a dicha definición. Así pues, las especies bipolares serían aquellas presentes, al menos, en latitudes superiores a los 55º N en el Hemisferio Norte (p. ej. Alaska, norte de Europa) y al mismo tiempo en latitudes no inferiores a los 52º S en el Hemisferio Sur (aproximadamente a nivel del Estrecho de Magallanes), independientemente de su presencia en otras regiones del planeta. Muchos autores sucesivos han considerado los términos "anfitropical" y "antitropical" como sinónimos de bipolar cuando se referían a este tipo de distribución disyunta.

La irrupción de las tecnologías de secuenciación de ácidos nucleicos y, en especial aquellas de alto rendimiento (del inglés, "*high-throughput sequencing*") ha permitido confirmar la existencia de taxones bipolares en organismos pertenecientes a todos los niveles de organización, tanto en procariotas como, especialmente, en eucariotas. Sul et al. (2013) determinaron la existencia de especies de bacteria marinas compartidas entre ambos polos, mientras que de Cárcer et al. (2015) demostraron que parte de los linajes de virus del Ártico y la Antártida eran idénticos. En eucariotas microscópicos, la existencia de taxones bipolares, concretamente en ambientes acuáticos del Ártico y la Antártida, se ha confirmado para foraminíferos plantónicos y bentónicos (Darling et al. 2000; Pawlowski et al. 2007), dinoflagelados (Montresor et al. 2003), ciliados (Di Giuseppe et al. 2013) y diatomeas (van de Vijver et al. 2005). Asimismo, análisis basados en secuenciación masiva de suelos han revelado similitudes a diferentes niveles taxonómicos entre las comunidades fúngicas edáficas de ambos polos (Tedersoo et al. 2014; Cox et al. 2016).

En general, los amplios rangos de distribución de estos microorganismos han sido explicados desde la hipótesis de "*Everything is everywhere, but, the environment selects*", propuesta por Baas Becking (1934). Según ésta, las especies de diferentes tipos de organismos podrían estar presentes en cualquier localidad del planeta siempre y cuando las condiciones ambientales les fueran adecuadas para sobrevivir. Dicha ubicuidad vendría dada por la supuesta gran capacidad colonizadora de los organismos microscópicos que forman estructuras minúsculas para la dispersión como esporas y quistes. Sin embargo, diferentes estudios sobre biogeografía microbiana han refutado esta hipótesis a la vez que han aportado nuevas evidencias de patrones biogeográficos en microorganismos, como puede ser la existencia de niveles variables de endemismo y cosmopolitismo incluso en bacterias (ver Martiny et al. 2006; van der Gast 2015).

Sin embargo, han sido los estudios sobre briófitos y plantas vasculares bipolares los que han enriquecido en mayor grado la literatura sobre este tipo tan particular de distribución geográfica. Así, Raven (1963), Moore y Chatter (1971) y Wen y Ickert-

Bond (2009) revisaron la distribución anfitropical o bipolar actual de alrededor de 30 especies de plantas y vaticinaron que las disyunciones se habrían establecido a partir del Mioceno, probablemente debido a eventos de dispersión a larga distancia entre continentes. Nathan (2006) apuntó que eventos climáticos extremos e incluso ciertos vectores como los animales podían transformar este tipo de dispersión de ser muy rara, a ser más habitual de lo esperado. Por otra parte, las evidencias existentes hasta el momento hicieron suponer a Raven (1963) y Wen y Ickert-Bond (2009) que la direccionalidad de la migración intercontinental habría sido mayormente norte-sur, en particular entre Norteamérica y Suramérica. Gracias, una vez más, a la información escondida en el ADN y al uso de métodos de reconstrucción biogeográfica y de datación basada en el reloj molecular, en los últimos años ha crecido el número de estudios cuyo objetivo ha sido estimar un marco temporal para el origen de los patrones de distribución bipolar en vegetales.

En plantas vasculares, destacan los estudios efectuados sobre el género *Carex* (*Cyperaceae*), que es uno de los que contiene un mayor número de especies bipolares (Moore y Chater 1971). Trabajos sucesivos testaron tres mecanismos que podrían explicar este tipo de distribución en *Carex*: evolución convergente, vicariancia y dispersión a larga distancia (Escudero et al. 2010; Villaverde et al. 2012). En general, los resultados obtenidos apoyaron a la dispersión a larga distancia entre Norteamérica y Suramérica como el mecanismo más plausible para la adquisición de un rango austral en la distribución de varias especies de *Carex*, aunque no se pudo confirmar si esta dispersión habría sido directa o mediante migración progresiva a través de las cadenas montañosas del continente americano (Escudero et al. 2010; Villaverde et al. 2015a,b). Tanto en estos estudios como en un estudio simultáneo que marcó un hito en la historia de la biogeografía de plantas bipolares, el realizado por Popp et al. (2011) sobre *Empetrum*, se mencionó el posible papel de las aves migratorias como vectores de dispersión de frutos o semillas entre regiones separadas por miles de kilómetros de distancia. Finalmente, Spalik et al. (2010) y Amarilla et al. (2015) sugirieron que especies bipolares de los géneros *Munroa* y *Lilaeopsis* habrían seguido la ruta de migración alternativa, es decir, de sur a norte para explicar su distribución geográfica actual.

En briófitos se repite en cierto modo el escenario planteado para las plantas vasculares. Hedenäs (2009), Piñeiro et al. (2012) y Lewis et al. (2014a) han estudiado los patrones de distribución bipolar de especies pertenecientes a los géneros *Sarmentypnum*, *Cinclidium* y *Tetraplodon*, respectivamente. Mediante diferentes análisis de los datos genéticos y estimación de tiempos de divergencia concluyeron que el origen de esas especies era eminentemente boreal y que entre el Mioceno y Pleistoceno se habrían establecido poblaciones en el hemisferio austral gracias a eventos directos de dispersión a larga distancia. Lewis et al. (2014a) señalaron que en dicha dispersión habrían mediado aves migratorias, posiblemente del orden *Charadriiformes*. En otro trabajo del mismo año, estos autores demostraron que aves migratorias que se

desplazan frecuentemente entre regiones a elevadas latitudes de ambos hemisferios presentaban diásporas de briófitos enganchadas a su plumaje (Lewis et al. 2014b).

4.2. Los líquenes bipolares

Los hongos liquenizados son el grupo de organismos con una mayor abundancia de especies con distribución bipolar o anfitropical. Como ya se ha comentado, aproximadamente el 40% de las especies presentes en la Antártida y en la islas subantárticas son bipolares (Øvstedal y Lewis Smith 2001). Asimismo, las regiones alpina y esteparia de la Patagonia y Nueva Zelanda también son ricas en taxones bipolares, como bien apuntan los estudios de Galloway y Bartlett (1986), Bjerke y Elvebakk (2004) y Galloway (2003). Según Galloway y Aptroot (1995), la primera mención de líquenes bipolares fue realizada por T. Taylor en la primera mitad del siglo XIX. Posteriormente, el eminente geógrafo G. E. Du Rietz elaboraría uno de los primeros tratados detallados de plantas con distribución bipolar en los territorios australes, en donde incluiría también a los líquenes (Du Rietz 1940). Aparte de los trabajos de Galloway centrados en Nueva Zelanda, la mayoría de las interpretaciones sobre el origen del patrón de distribución bipolar en los líquenes se han realizado en el contexto de la liquenología antártica (ver arriba). Gracias a los trabajos basados en datos genéticos, poco a poco se van conociendo los mecanismos responsables de la distribución en el espacio y en el tiempo de los líquenes bipolares. En general, estos son los mismos que los postulados en los estudios de plantas y briófitos, es decir, la vicarianza y dispersión a larga distancia. Los datos genéticos y de estimación de tiempos de divergencia parecen favorecer la segunda opción (p. ej. Fernández-Mendoza y Printzen 2013). Sin embargo, todavía se requieren más evidencias empíricas antes de poder ofrecer una respuesta global a la pregunta de cuándo y cómo se originó este rango de distribución en estos organismos simbióticos funcionalmente tan complejos. Por el momento, varias hipótesis se han propuesto para explicar el origen de especies bipolares pertenecientes a los géneros de hongos liquenizados *Sphaerophorus* (Högnabba y Wedin 2003), *Cladonia* (Myllys et al. 2003), *Usnea* (Wirtz et al. 2008) y *Lichenomphalia* (Geml et al. 2012) y quedan a la espera de ser testadas con potentes herramientas estadísticas. Estos y otros aspectos de la bipolaridad en líquenes serán tratados en profundidad en varios capítulos de esta tesis.

OBJETIVOS Y ESTRUCTURA DE LA TESIS

"*From my earliest childhood I nourished and cherished the desire to make a creditable journey in a new country, and write such a respectable account of its natural history as should give me a niche amongst the scientific explorers of the globe I inhabit, and hand my name down as a useful contributor of original matter*". – Sir Joseph Dalton Hooker

Esta tesis se enmarca en el contexto de la liquenología antártica. A pesar de ser ésta una disciplina que cuenta con casi dos siglos de historia, en las últimas décadas se ha visto especialmente impulsada por la irrupción de las técnicas de la biología molecular, que han permitido abordar el estudio de la diversidad de líquenes antárticos desde una nueva óptica más integradora, incorporando el marco evolutivo a diversas cuestiones que habían suscitado largos debates históricos.

El objetivo general de la presente tesis doctoral es contribuir al conocimiento de la diversidad y del origen de la biota liquénica antártica desde distintas perspectivas, destacando la taxonómica y la biogeográfica, usando herramientas propias de la filogenética y la genética de poblaciones que, en conjunto, permiten explorar la filogeografía de los líquenes antárticos. Para lograr este objetivo general se proponen los siguientes objetivos específicos:

- Estudio taxonómico de grupos problemáticos de hongos liquenizados y liquenícolas antárticos a través de una aproximación holística que aúne la metodología tradicional (morfología, anatomía, ecología y química) y técnicas de la biología molecular, en particular, el uso de secuencias de ADN, para la descripción y asignación filogenética de nuevos géneros y especies.
- Estudio del origen temporal de líquenes antárticos mediante análisis filogeográficos de los micobiontes y fotobiontes que los componen:

  a) Estudio de *Mastodia tessellata* (*Verrucariaceae*, Ascomycota) y su fotobionte, *Prasiola* (*Trebouxiophyceae*, Chlorophyta), a partir de muestras recolectadas en Antártida, Tierra del Fuego (Suramérica) y Norteamérica. Este liquen representa un ejemplo paradigmático de talo liquénico configurado por un hongo asociado a un único fotobionte, que pertenece al género de algas verdes foliáceas y macroscópicas *Prasiola*.

  b) Estudio de los hongos liquenizados *Pseudephebe pubescens* y *P. minuscula* (*Parmeliaceae*, Ascomycota), a partir de un muestreo llevado a cabo a nivel mundial, con poblaciones en todos los continentes.
- Evaluación filogeográfica del rango de distribución bipolar en *M. tessellata*, *P. pubescens* y *P. minuscula* y revisión bibliográfica sobre hongos y algas liquenizados bipolares, para caracterizar este patrón de distribución en líquenes.

Esta tesis doctoral se compone de cinco apartados:

1. **Introducción general**, en donde se abordan aspectos básicos de la biología de líquenes, la liquenología en la Antártida, incluido el origen de la biota liquénica antártica, así como una primera consideración sobre el patrón de distribución bipolar en organismos con diferentes niveles de complejidad, desde bacterias hasta líquenes y plantas vasculares.
2. **Metodología**, sección enfocada en la descripción de aspectos básicos de la zona de muestreo, de las especies objeto de estudio y de los métodos y técnicas analíticos empleados.

3. **Resultados**, que integra siete capítulos que a su vez representan siete trabajos de investigación, los cuales pueden ser agrupados en dos bloques: **Bloque 1**, que incorpora les tres primeros capítulos que tratan aspectos taxonómicos y sistemáticos de grupos poco conocidos de hongos liquenizados y liquenícolas antárticos, y **Bloque 2**, configurado por cuatro capítulos enfocados a profundizar en la filogeografía de especies con distribución bipolar o anfitropical frecuentes en la región antártica. Cuatro de estos trabajos han sido ya publicados en revistas indexadas, mientras que otros están en proceso de revisión:

   Capítulo 1: *Charcotiana* y *Amundsenia*, dos nuevos géneros en la familia de hongos liquenizados *Teloschistaceae* (subfamilia *Xanthorioideae*), incluyendo dos nuevas especies de la Antártida Continental; y *Austroplaca frigida*, un nombre nuevo para una especie antártica continental.
   Título del artículo científico publicado: "*Charcotiana* and *Amundsenia*, two new genera in *Teloschistaceae* (lichenized Ascomycota, subfamily *Xanthorioideae*) hosting two new species from continental Antarctica, and *Austroplaca frigida*, a new name for a continental Antarctic species"
   Autores del artículo científico publicado: Ulrik Søchting, Isaac Garrido-Benavent, Rod Seppelt, Miris Castello, Sergio Pérez-Ortega, Asunción de los Ríos, Leopoldo García Sancho, Patrik Frödén y Ulf Arup.
   Datos de Publicación: Lichenologist 46(6): 763–782 (2014).
   doi:10.1017/S0024282914000395
   Objetivo del trabajo. Identificar especies de hongos liquenizados antárticos pertenecientes a la familia *Teloschistaceae* (Ascomycota) cuya adscripción taxonómica era problemática de acuerdo a la literatura disponible. Con esta finalidad se plantea un estudio taxonómico integrador que combine caracteres de la sistemática liquenológica tradicional (morfología, anatomía y química de los talos liquénicos), con datos genéticos provenientes de tres marcadores moleculares, dos nucleares (*nrITS*, *nrLSU*) y uno mitocondrial (*mrSSU*). A través de reconstrucciones filogenéticas se infiere la posición filogenética de los nuevos linajes dentro de la familia *Teloschistaceae* (Arup et al. 2013). Además, se evalúa la posición de la especies *Caloplaca frigida*, que se combina en el género *Austraplaca*, y la especie ártica *C. approximata*, que se combina en el nuevo género *Amundsenia*, de acuerdo a dicho nuevo marco clasificatorio.

   Capítulo 2: *Austrostigmidium*, un género nuevo de hongos liquenícolas austral de la familia *Teratosphaeriaceae* emparentado con hongos meristemáticos colonizadores de rocas.
   Título del artículo científico publicado: "*Austrostigmidium*, a new austral genus of lichenicolous fungi close to rock-inhabiting meristematic fungi in *Teratosphaeriaceae*"

Autores del artículo científico publicado: Sergio Pérez-Ortega, Isaac Garrido-Benavent y Asunción de los Ríos
Datos de Publicación: Lichenologist 47(3): 143–156 (2015).
doi:10.1017/S0024282915000031
Objetivo del trabajo. Estudio de la taxonomía y biología de un hongo liquenícola presente habitualmente en colecciones del liquen *Mastodia tessellata* en Antártida y Tierra del Fuego. Se utiliza con este fin un marco que abarca el estudio de caracteres morfológicos y anatómicos para caracterizar a la especie, el uso de marcadores filogenéticos (*nrLSU* y *nrSSU*) para ubicar su posición filogenética, y, por último, el uso de microscopía de fluorescencia y electrónica de trasmisión (TEM) con el fin de profundizar en el tipo de relación entre los simbiontes formadores del huésped (mico- y fotobionte) y su simbionte liquenícola, caracterizando las interacciones celulares a nivel ultraestructural.

Capítulo 3: *Shackletonia cryodesertorum* (*Teloschistaceae*, Ascomycota), una nueva especie de los Valles Secos de McMurdo de la Antártida, con breves apuntes sobre la biogeografía del género *Shackletonia*.
Título del artículo científico publicado: "*Shackletonia cryodesertorum* (*Teloschistaceae*, Ascomycota), a new species from the McMurdo Dry Valleys (Antarctica) with notes on the biogeography of the genus *Shackletonia*"
Autores del artículo científico publicado: Isaac Garrido-Benavent, Ulrik Søchting, Asunción de los Ríos y Sergio Pérez-Ortega
Datos de Publicación: Mycological Progress (2016). doi:10.1007/s11557-016-1204-x
Objetivo del trabajo. Estudio taxonómico de especímenes de los Valles Secos de McMurdo (Antártida Continental) pertenecientes a la familia *Teloschistaceae* que no habían podido ser atribuidos a ninguna especie conocida en estudios anteriores ni morfológica ni molecularmente (Pérez-Ortega et al. 2012). Una vez asignados al género *Shackletonia*, se establece un marco temporal para estudiar la evolución de dicho género en el hemisferio austral así como para datar el origen de *S. cryodesertorum*, un endemismo Antártico descrito en el trabajo.

Capítulo 4: De Alaska a la Antártida: delimitación de especies y diversidad genética en *Prasiola* (*Trebouxiophyceae*), un alga clorófita foliácea asociada con el hongo liquenizado bipolar *Mastodia tessellata*.
Título del artículo científico publicado: "From Alaska to Antarctica: Species boundaries and genetic diversity of *Prasiola* (*Trebouxiophyceae*), a foliose chlorophyte associated with the bipolar lichen-forming fungus *Mastodia tessellata*"
Autores del artículo científico publicado: Isaac Garrido-Benavent, Sergio Pérez-Ortega y Asunción de los Ríos

Datos de Publicación: Molecular Phylogenetics and Evolution 107: 117–131 (2017).
http://dx.doi.org/10.1016/j.ympev.2016.10.013
Objetivo del trabajo. Estudiar la diversidad genética del fotobionte del hongo liquenizado bipolar *Mastodia tessellata*, que pertenece al género de algas verdes foliáceas *Prasiola*. Con este fin se utilizan tres marcadores moleculares, dos nucleares (*nrITS*, *RPL10A*) y uno del cloroplasto (*tufA*) obtenidos de especímenes recolectados a lo largo de un gradiente latitudinal en Norteamérica, Tierra del Fuego y Antártida. El número creciente de estudios que ha descubierto linajes crípticos en algas verdes y, en particular, fotobiontes liquénicos, es elevado (p. ej. Malavasi et al. 2016; Škaloud et al. 2016), por lo que, en primer lugar, se realiza un estudio de delimitación de especies con el objetivo de revelar el número de linajes asimilables a especies a lo largo de la distribución de la especie, como paso preliminar a estudios filogeográficos posteriores. En segundo lugar, se propone estudiar la estructura filogeográfica de las poblaciones de *Prasiola* liquenizada mediante la inferencia de haplotipos y las relaciones genealógicas entre ellos, y el uso de algoritmos que permitan la inferencia de grupos genéticos. A partir de los resultados obtenidos se pretende caracterizar de forma más precisa esta simbiosis tan particular y en especial construir hipótesis sobre el origen de la distribución bipolar y presencia en el continente antártico del liquen *M. tessellata*.

Capítulo 5: La dispersión directa y conjunta del hongo liquenizado *Mastodia tessellata* (Ascomycota) y su fotobionte explica su distribución bipolar.
Título del artículo científico enviado: “No need for stepping stones: Direct, joint dispersal of the lichen-forming fungus *Mastodia tessellata* (Ascomycota) and its photobiont explains their bipolar distribution.”
Autores del artículo científico enviado: Isaac Garrido-Benavent, Asunción de los Ríos, Fernando Fernández-Mendoza y Sergio Pérez-Ortega.
Revista: Journal of Biogeography (enviado).
Objetivo del trabajo. Dilucidar las factores históricos responsables de la presencia en la Antártida y la distribución bipolar de los simbiontes del liquen *Mastodia tessellata*. Al igual que en el capítulo anterior, en primer lugar se plantea un análisis de delimitación de especies como paso preliminar al estudio de la filogeografía de *M. tessellata*. Se utilizan secuencias de ADN provenientes de tres marcadores nucleares (*nrITS*, *Mcm7* y *EF-1α*). Además, a partir de la secuenciación de un nuevo marcador del cloroplasto (*rbcL*) y el análisis de especímenes adicionales se propone corroborar las hipótesis de límites de especies propuestas en el Capítulo 4 para el fotobionte, *Prasiola*. En segundo lugar, se plantea un estudio filogeográfico robusto de mico- y fotobiontes compuesto por un análisis de la diversidad genética y relaciones genealógicas entre haplotipos, la elaboración de cronogramas usando diferentes estrategias de calibración según se trate de mico- o fotobionte, y la comparación de diferentes

hipótesis de flujo génico entre las regiones de estudio bajo un marco Bayesiano y de coalescencia, para determinar el origen geográfico de los simbiontes y la direccionalidad histórica de la migración.

Capítulo 6: Estudio filogeográfico global de las especies del género de hongos liquenizados *Pseudephebe* (*Parmeliaceae*, Ascomycota), con especial atención al origen de las poblaciones de la Antártida.
Título del artículo científico: "A world-wide phylogeographic overview of the lichen-forming fungi genus *Pseudephebe* (*Parmeliaceae*, Ascomycota) offers new insights into the origin of the Antarctic lichen biota"
Autores del artículo científico enviado: Isaac Garrido-Benavent, Sergio Pérez-Ortega, Asunción de los Ríos, Helmut Mayrhofer y Fernando Fernández-Mendoza.
Revista: Molecular Ecology (en preparación).
Objetivo del trabajo. Investigar los límites de especies y la filogeografía de dos especies de micobionte del género *Pseudephebe* con distribución anfitropical y poblaciones en la Antártida: *P. pubescens* y *P. minuscula*, en base a datos de seis marcadores genéticos (*nrITS*, *Mcm7*, *GAPDH*, *EF-1α*, *L1* y *PGK*) y un muestreo extensivo de especímenes llevado a cabo a nivel mundial, con poblaciones en todos los continentes, incluyendo localidades en la Antártida Marítima y Continental. A partir de estos datos genéticos se pretende obtener una visión global de la estructura filogeográfica de los micobiontes y determinar el marco temporal en el que las dos se originaron, haciendo especial hincapié en el origen de sus poblaciones antárticas y la adquisición de la distribución anfitropical actual.

Capítulo 7: Pasado, presente y futuro en la investigación de hongos y algas liquenizados bipolares.
Título del artículo científico enviado: "Past, present and future of research in bipolar lichen-forming fungi and their photobionts"
Autores del artículo científico enviado: Isaac Garrido-Benavent, Asunción de los Ríos y Sergio Pérez-Ortega.
Revista: American Journal of Botany (trabajo de revisión invitado para número especial dedicado a la distribución bipolar en organismos vegetales)
Objetivo del trabajo. Revisar de manera crítica el conocimiento sobre la distribución bipolar en hongos liquenizados y sus respectivos fotobiontes. Comparar los hallazgos derivados del uso de marcadores moleculares en las últimas dos décadas en el contexto de las hipótesis propuestas hasta la fecha sobre el origen de este rango de distribución disyunto. Las primeras alusiones al patrón de distribución bipolar datan de mediados del siglo XIX, y aunque es un patrón presente en otros organismos como plantas vasculares y briófitos, el mayor número de ejemplos se encuentra entre los hongos liquenizados, con más

de 160 especies con dicha distribución en Antártida e islas adyacentes. En esta revisión también se examina el papel jugado por la dispersión a larga distancia, evaluando los diferentes vectores de dispersión y la importancia del nicho ecológico en el origen de la distribución bipolar. Finalmente, se propone una revisión de los conceptos "bipolar" y "anfitropical" y se ofrece una visión general de las grandes cuestiones aún vigentes sobre la distribución bipolar de hongos liquenizados y sus fotobiontes y las posibles líneas futuras de trabajo.

4. **Discusión general**, sección en la que se ofrece una visión integrada de los resultados obtenidos en esta tesis en el contexto de la liquenología en general y, en particular, de la liquenología antártica.
5. **Conclusiones**, apartado final en el que se enumerarán las contribuciones principales de esta tesis al conocimiento de la biota liquénica antártica.
6. **Bibliografía**, que recoge las referencias bibliográficas expuestas desde la Introducción hasta la Discusión general.
7. **Anexos**, en los que se recogen los autores de los nombres científicos presentados en esta tesis (Anexo I), así como un breve glosario de términos importantes que se repiten en diferentes apartados del manuscrito (Anexo II).

METODOLOGÍA

1. Zonas de muestreo

El material biológico usado en la presente tesis doctoral ha sido recolectado en diferentes áreas geográficas, con muestreos específicos para los distintos bloques de estudio:

a) En el Bloque 1 (Capítulos 1, 2, 3), el material proviene de diferentes colecciones de líquenes efectuadas en los Valles Secos de McMurdo de la Antártida (Capítulo 1 y 3), en otras localidades antárticas al norte de la Tierra de Victoria, las islas Windmill, Coulman y Ross, y la Costa de Ingrid Christensen (Capítulo 1), y en la Península Antártica y Tierra del Fuego (Suramérica) (Capítulo 2). El material se encuentra depositado en diferentes herbarios de universidades e instituciones de investigación públicas: MAF (Universidad Complutense de Madrid), MA (Real Jardín Botánico, Madrid), C (University of Copenhagen, Dinamarca), HO (Tasmanian Herbarium, Australia), LD (Lund University Botanical Museum, Suecia), UPS (The Museum of Evolution Herbarium, Uppsala University, Suecia) y O (Natural History Museum, University of Oslo, Noruega).

b) En el Bloque 2, para los estudios filogeográficos del mico- y fotobionte de *Mastodia tessellata* (Capítulos 4 y 5), se han utilizado especímenes recolectados a lo largo de un gradiente latitudinal que incluye la Antártida Marítima, Tierra del Fuego y Norteamérica. En la Antártida se recolectaron individuos en la localidad peninsular Caleta Cierva así como en las islas adyacentes Avian, Yalour, Rongé, Livingston, Greenwich y Rey Jorge; en Tierra del Fuego, se recolectó en la Península Brunswick y en las islas Basket, Chair, Picton y Navarino; y en Norteamérica se recogió material del Parque Nacional Glacier Bay y Petersburg (Alaska, Estados Unidos) y de Port Edward (Columbia Británica, Canadá). Por otra parte, el Capítulo 6 de este mismo Bloque 2 corresponde a un estudio filogeográfico de las especies del género de hongos liquenizados *Pseudephebe*, a partir de un muestreo a nivel mundial con localidades en: Alaska y Montana (Norteamérica); Bolivia y Chile, incluyendo Tierra del Fuego; Antártida peninsular y continental; Groenlandia, Islandia, Noruega, Escocia, Austria, Suiza, Francia, Kosovo, Montenegro, España y Portugal (Europa); China; y Nueva Zelanda. El material se encuentra disponible en el herbario MA (Real Jardín Botánico, Madrid), MAF (Universidad Complutense de Madrid), GZU (Graz University, Austria), OTA (Otago University Herbarium, Nueva Zelanda), LPB (Herbario Nacional de Bolivia), KUN-L (Kunming Institute of Botany, China) y C (University of Copenhagen, Dinamarca)

En los distintos capítulos de esta tesis se proporciona información más específica para cada localidad de muestreo: situación geográfica, coordenadas (latitud y longitud), altitud, autor y fecha de la recolección, y ambiente en donde crecía la muestra.

2. Material biológico

Este apartado está centrado en las especies que han sido objeto de estudio filogeográfico: *Mastodia tessellata* y su fotobionte *Prasiola borealis*, y *Pseudephebe pubescens* y *P. minuscula* (Bloque 2). La descripción de los géneros y especies del Bloque 1 están incluidas en los respectivos capítulos.

Para los cuatro taxones anteriores se incluye: a) una breve diagnosis en donde quedan reflejados los caracteres macro- y microscópicos más relevantes para su identificación, acompañados de una lámina fotográfica, así como el hábitat y su distribución mundial; b) una selección de publicaciones en donde se han tratado aspectos taxonómicos y/o biogeográficos de utilidad para contextualizar los estudios llevados a cabo en la presente tesis doctoral; y c) un mapa con las citas disponibles para cada taxón georeferenciadas obtenidas a través de la Infraestructura Mundial de Información en Biodiversidad (GBIF, del inglés *Global Biodiversity Information Facility*). Otros aspectos relativos al número de especímenes estudiados y localidades concretas de muestro para cada taxón se pueden encontrar en los Capítulos 4 y 5 (*Mastodia tessellata* y su fotobionte) y 6 (*Pseudephebe pubescens* y *P. minuscula*).

Los autores de los nombres científicos que aparecen en los diferentes apartados de esta tesis se especifican en el Anexo I.

2.1. *Mastodia tessellata* (Hook. f. y Harv.) Hook. f. y Harv., Bot. Antarc. Voy.: 499 (1847) (*Verrucariaceae*, Ascomycota)

(Figura 9)

Diagnosis del micobionte: hongo liquenizado que forma líquenes de biotipo foliáceo, con talo irregularmente lobulado, coriáceo, de tamaño variable, hasta aproximadamente 2 cm de envergadura. Ascomas de tipo peritecioide y conidiomas distribuidos de manera irregular, generalmente en el haz de las láminas y hacia las áreas distales, donde la lámina aparece generalmente con mayores niveles de melanización. En el talo, las hifas fúngicas forman una matriz más o menos regular que envuelve y aísla grupos de células del alga (Figura 1, Introducción). Peritecios subglobosos, entre 200–300 µm de diámetro, inmersos, con una zona periostiolar prominente, de color marrón oscuro hasta negros en los ejemplares más maduros. Cavidad del peritecio, o lóculo, gelatinosa, con perífisis presentes alrededor del ostiolo. Himenio embebido en una matriz gelatinosa, con paráfisis evanescentes; ascas bitunicadas, que rápidamente pierden una pared (delicuescente), octospóricas, de hasta 50 × 15 µm, claviformes o subcilíndricas. Ascosporas hasta 18 × 5 µm, de subelípticas a fusiformes, con los extremos redondeados, ni septadas ni ornamentadas, hialinas. Conidiomas subglobosos, de alrededor de 250 µm de diámetro, inmersos en el talo, con una zona periostiolar prominente y de marrón oscuro a negros. Conidios de subglobosos a elipsoidales, alrededor de 2 × 1 µm e hialinos. Sustancias extraíbles en acetona ausentes.

Diagnosis del fotobionte, *Prasiola borealis* M. Reed (*Trebouxiophyceae*, Chlorophyta): especímenes adultos no liquenizados de entre 0.5–1.2 cm de alto, formados por 3–4 láminas de entre 20–40 µm de grosor (en estado liquenizado pueden alcanzar un grosor 0.2 mm) y de color verde claro en individuos jóvenes y verde oscuro en los más adultos, irregularmente redondeadas o en forma de cuña, lobuladas y a veces arrugadas y agrietadas, con los extremos curvados hacia dentro, y que crecen a partir de un mismo punto basal, ocasionalmente estipitado, formado por sustancias extracelulares adhesivas. Inicialmente, cada lámina es monostromática, *i.e*. formada por una única capa de células, mientras que las láminas viejas son polistromáticas, incluyendo entre 6 y 8 capas. Las células se agrupan en tétradas (grupos de 4 células) y éstas se disponen en áreas cuadradas o poligonales, dejando un espacio relativamente ancho entre ellas. En vista superficial, las células son cuadrangulares o rectangulares, de entre 4–9 µm de diámetro; en vista transversal, las células presentan una morfología oblonga, de 11–14 µm de altitud y se disponen a modo de empalizada. La reproducción parece llevarse a cabo mediante la producción de acinetos, un tipo especial de células de reposo y resistencia, de pared gruesa, que pueden finalmente transformase en aplanosporangios.

Hábitat y distribución: liquen que crece en roquedos costeros (zona supralitoral alta) del Océano Pacífico norte (Columbia Británica, Alaska), Tierra del Fuego (Suramérica) e Islas Malvinas, Islas Kerguelen, Tasmania, o en rocas a altitudes más elevadas en la Antártida Peninsular y Continental (Figura 10). También existe alguna cita antigua de las costas orientales de Siberia (Rusia), así como de la presencia del alga no liquenizada en las Islas Kuriles (Japón-Rusia) y en el norte de Europa. Tanto el liquen como el alga en estado de vida libre pueden ser considerados ornitocoprófilos, pues suelen vivir asociados a posaderos y nidos de ave con abundantes deposiciones fecales.

Referencias bibliográficas seleccionadas: Nylander (1884), Reed (1902), Nagai (1940), Brodo (1976), Murray (1963), Aptroot y van der Knaap (1993), Kohlmeyer et al. (2004), Kovačik y Pereira (2001), Lud et al. (2001), Øvstedal y Lewis Smith (2001), Rindi et al. (2007), Pérez-Ortega et al. (2010), Moniz et al. (2014), Guiry y Guiry (2017).

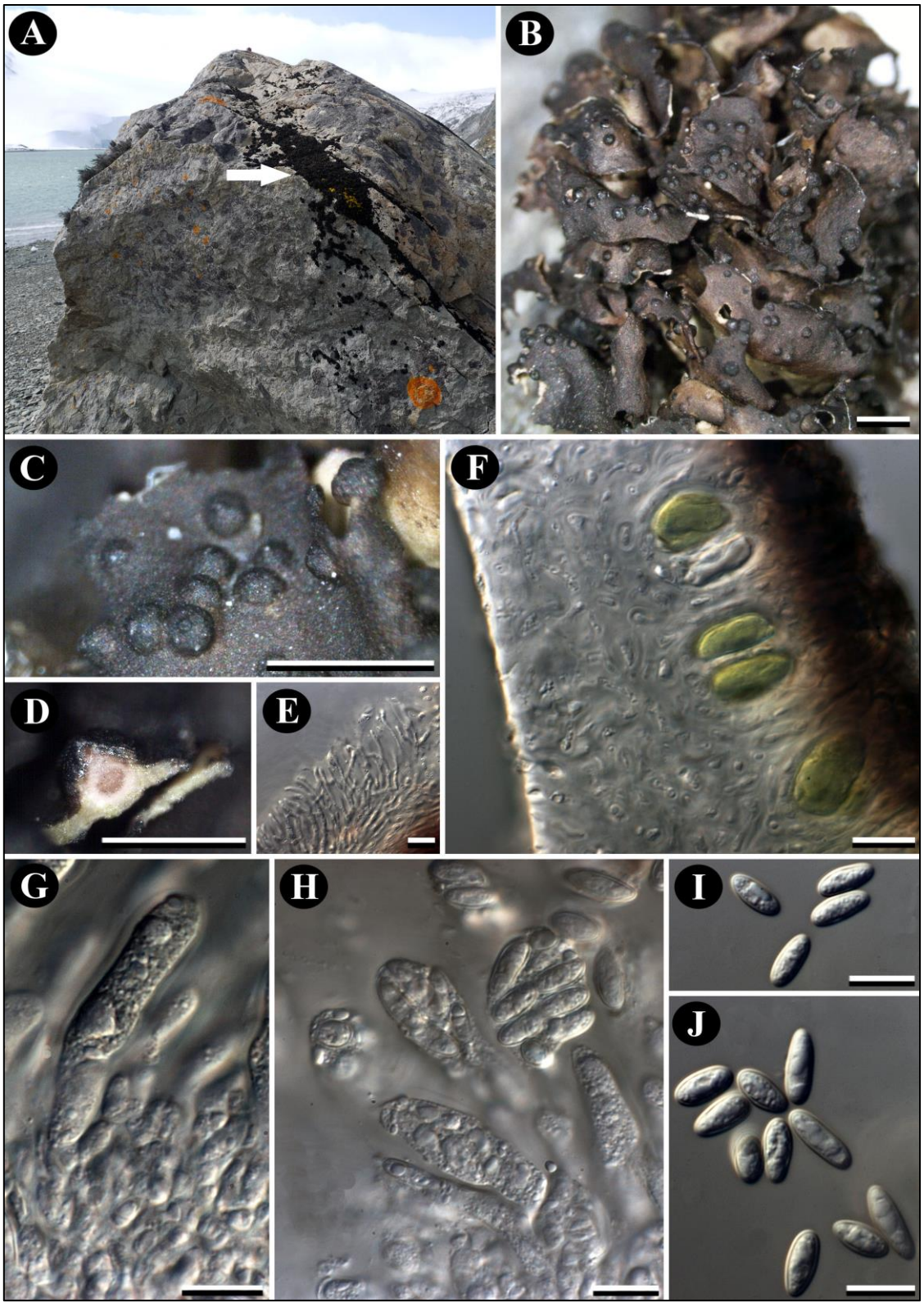

Figura 9. *Mastodia tessellata*. (A) Hábitat de *M. tessellata* en rocas cercanas al mar en la Isla Livingston (Antártida Marítima), con la flecha blanca indicando un grupo denso de talos del liquen. (B) Aspecto externo del talo liquénico. (C) Peritecios. (D) Sección transversal de un peritecio. (E) Perífisis. (F) Sección transversal del talo en donde se aprecian células algales e hifas. (G) Asca inmadura. (H) Ascas maduras. (I–J)

Esporas. Escalas: (B–C) = 1 mm, (D) = 0.5 mm, (E–J) = 10 µm. (Fotografía paisaje: AdR; Fotografías macro- y microscópicas: IGB; ejemplar estudiado recolectado en la Isla Livingston, Antártida Marítima, por A. de los Ríos).

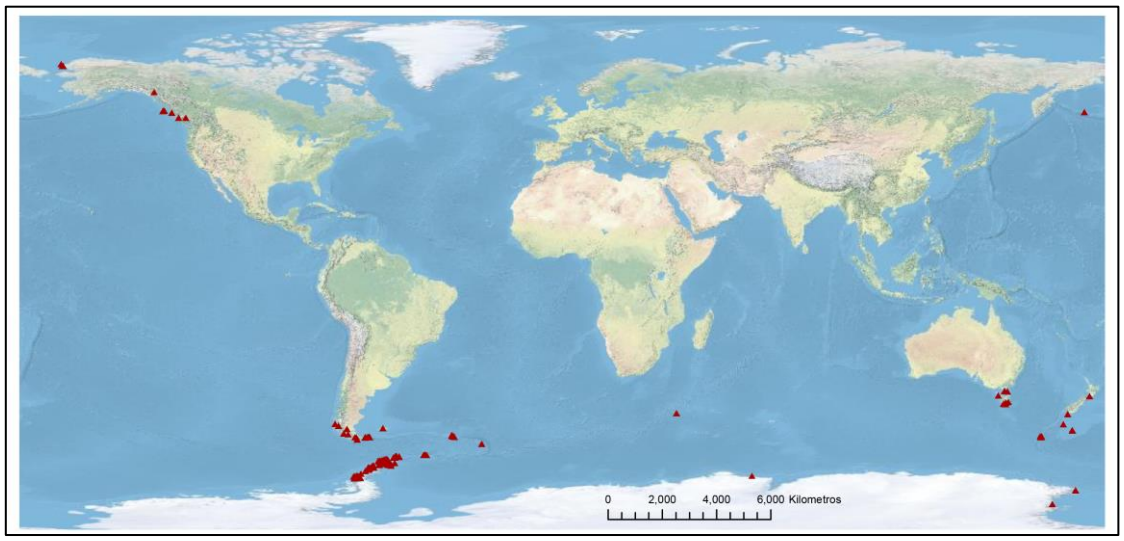

Figura 10. Distribución conocida de *Mastodia tessellata* de acuerdo a la base de datos del GBIF (último acceso: 1 Marzo 2017). Los triángulos rojos indican las localidades donde se ha localizado este liquen.

2.2. *Pseudephebe pubescens* (L.) M. Choisy, Icon. Lich. Univ.: sine pag. (1930) (*Parmeliaceae*, Ascomycota)

(Figura 11)

Diagnosis: hongo liquenizado que forma líquenes de biotipo fruticuloso, con talos decumbentes o raramente con aspecto arbustivo, de hasta 10 cm de longitud y aproximadamente 1 cm de altura, generalmente alargados, de ramificación irregularmente densa, isótoma o dicotómica, con distancia intermodal entre 1–3 mm, con ramas finas de sección más o menos circular, hasta 0.2 mm de diámetro, de marrón oscuro a negras, con los extremos más estrechos y redondeados. Superficie mate o ligeramente brillante, con pseudocifelas más o menos conspicuas. Apotecios muy raros, cuando están presentes, lecanorinos, de color marrón oscuro, de hasta 5.5 mm de diámetro. Ascas claviformes, de pared gruesa, K/I+ azul, de tipo *Lecanora*, octosporadas. Ascosporas elipsoidales, no septadas, hialinas, de hasta 12 × 8 µm. Conidiomas, cuando están presentes, inmersos en el talo, formando ligeros abultamientos oscuros de hasta 0.4 mm principalmente cerca de las axilas. Conidios simples, baciliformes, no pigmentados, de tamaño alrededor de 5–7 × 1 µm. Sustancias extraíbles en acetona presentes en algunos talos, principalmente ácido norestíctico y raramente un ácido similar al girofórico. En la simbiosis participan algas unicelulares del género *Trebouxia* (*Trebouxiophyceae*, Chlorophyta).

Hábitat y distribución: liquen que crece sobre rocas silíceas expuestas en las regiones polares, y en el piso alpino y oromediterráneo de zonas templadas, con localidades en las Montañas Rocosas (en Estados Unidos y Canadá), Groenlandia, Andes, Antártida Marítima, norte de Europa y principales cordilleras del sur de Europa, en Siberia (Rusia), Japón, en varias cordilleras asiáticas, Australia y Nueva Zelanda (Figura 12).

Referencias bibliográficas seleccionadas: Brodo y Hawksworth (1977), Brodo et al. (2001), Øvstedal y Lewis Smith (2001), Smith et al. (2009), Stenroos et al. (2016), Boluda et al. (2016).

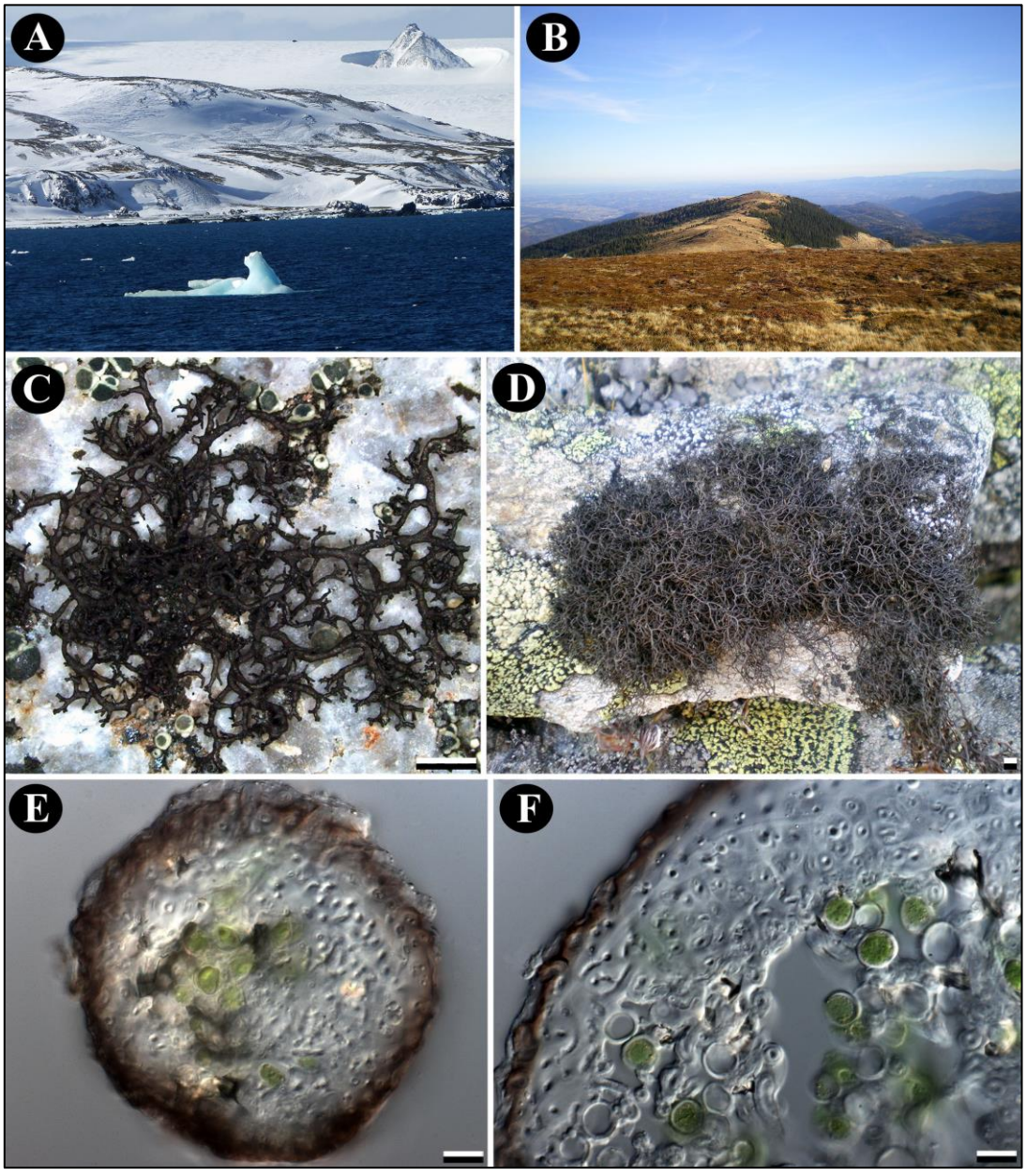

Figura 11. Las morfoespecies *Pseudephebe minuscula* y *P. pubescens*. (A) Paisaje de la Antártida Marítima. (B) Koralpe (Alpes al sureste de Austria). (C) *Pseudephebe minuscula*, talo recolectado en la Antártida. (D) *Pseudephebe pubescens*, talo

recolectado en Koralpe. (E) Sección transversal de una rama de *P. minuscula*. (F) Sección transversal de una rama de *P. pubescens*. Escalas: (C–D) = 1 mm, (E–F) = 10 µm. (Fotografía paisaje: AdR y IGB; Fotografías macro- y microscópicas: IGB; ejemplar de *P. minuscula* estudiado recolectado en la Isla Adelaida, Antártida Marítima, por U. Søchting; ejemplar de *P. pubescens* estudiado recolectado en Koralpe, sureste de Austria, por I. Garrido-Benavent).

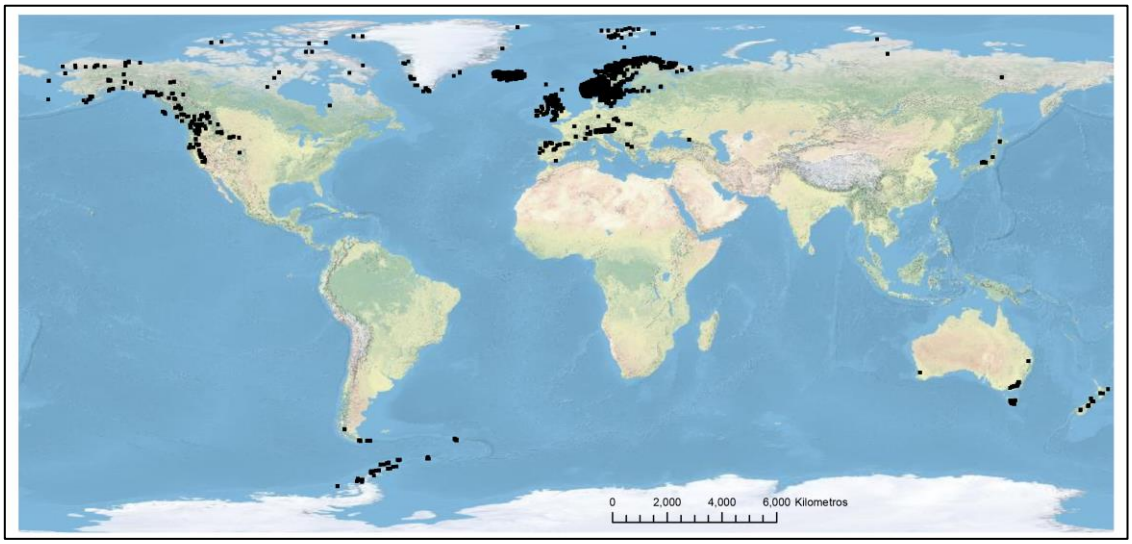

Figura 12. Distribución conocida de la morfoespecie *Pseudephebe pubescens* de acuerdo a la base de datos del GBIF (último acceso: 1 Marzo 2017). Los cuadrados negros indican las localidades donde se ha localizado este liquen.

2.3. *Pseudephebe minuscula* (Arnold) Brodo y D. Hawksw., Opera Botanica 42: 140 (1977) (*Parmeliaceae*, Ascomycota)

(Figura 11)

Diagnosis: hongo liquenizado que forma líquenes de biotipo fruticuloso, con talo generalmente postrado y decumbente, más o menos circular, profusamente ramificado de forma isótoma o dicótoma, con distancia intermodal entre 0.2–1 mm, aunque en algunos talos maduros de ambientes climáticamente severos con aspecto crustáceo en el centro, hasta 10 cm de diámetro y 1 cm de altura, con ramas de sección desde circular a aplanada, menor de 0.1 mm de diámetro, con los extremos más estrechos y redondeados, y de color marrón oscuro o casi negro. Superficie más o menos brillante, y en donde se observan ocasionalmente pseudocifelas, algunas veces perforadas. Apotecios raros, de 1–3 mm, lecanorinos, con el excípulo ligeramente verrugoso, marrón oscuro. Ascas claviformes, de pared gruesa, K/I+ azul, de tipo *Lecanora*, octosporados. Ascosporas elipsoidales de hasta 10 × 7 µm, constituidas por un única célula hialina. Conidiomas raramente presentes, y cuando lo están, inmersos en el talo,

con ostiolo dilatado y formando abultamientos talinos. Conidios simples, baciliformes, no pigmentados, hasta 8 × 1.1 µm. Sustancias extraíbles en acetona presentes, principalmente el ácido norestíctico. En la simbiosis participan algas unicelulares del género *Trebouxia* (*Trebouxiophyceae*, Chlorophyta).

Hábitat y distribución: liquen rupícola, con preferencia por rocas ácidas expuestas, que está presente en regiones alpinas de zonas templadas (Montañas Rocosas en Estados Unidos, y diversas cordilleras en Europa), además de distintas regiones árticas (Alaska, Canadá, Groenlandia, norte de Europa y Siberia) y Antártida (Marítima y Continental), donde es relativamente común (Figura 13).

Referencias bibliográficas seleccionadas: Brodo y Hawksworth (1977), Brodo et al. (2001), Øvstedal y Lewis Smith (2001), Smith et al. (2009), Stenroos et al. (2016), Boluda et al. (2016).

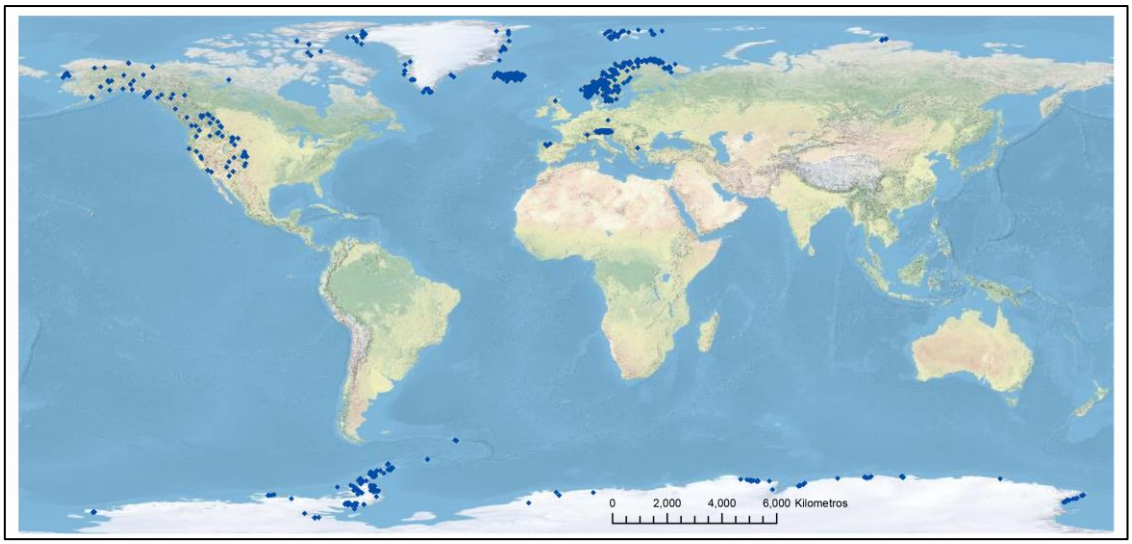

Figura 13. Distribución conocida de la morfoespecie *Pseudephebe minuscula* de acuerdo a la base de datos del GBIF (último acceso: 1 Marzo 2017). Los diamantes azules indican las localidades donde se ha localizado este liquen.

Observaciones: la existencia de talos de *Pseudephebe* con morfología intermedia entre *P. pubescens* y *P. minuscula* es bien conocida (p. ej. Brodo y Hawksworth 1977). Este es uno de los motivos que llevaron a Boluda et al. (2016) a presentar el primer trabajo de delimitación de especies en un contexto filogenético, usando tres loci (*nrITS*, *Mcm7* y *RPB1*), y aportando, además, información sobre la química de los especímenes. Estos autores sugirieron que los caracteres que se han utilizado tradicionalmente para separar ambas especies son demasiado variables, especialmente en *P. minuscula*, pero que los datos genéticos sí apoyarían la existencia de dos taxones, que han sido atribuidos a *P. pubescens* y *P. minuscula*. Además, demostraron la presencia de pseudocifelas y ácido norestítico en ambas especies. Finalmente, Boluda et al. (2016)

proponen denominar como *P. pubescens* aggr. a aquellos individuos no analizados molecularmente.

3. Métodos de análisis

Al igual que ocurre para la zona de estudio y material biológico, los métodos analíticos empleados en la presente tesis doctoral son específicos para cada bloque de estudio (Figura 14). En el Bloque 1 se estudian caracteres relevantes en la sistemática y taxonomía tradicional de líquenes, como los morfológicos, anatómicos y químicos (Figura 14A). En los Bloques 1 y 2 se emplean diferentes tipos de análisis filogenéticos para delimitar especies usando varios marcadores moleculares específicos para micobiontes y fotobiontes (Figura 14B). Adicionalmente, en el Bloque 2 se implementa una metodología enfocada al estudio filogeográfico de las especies de interés detalladas anteriormente (Figura 14B). Aunque en cada capítulo de la presente tesis doctoral se especificarán los métodos analíticos empleados, a continuación se exponen en breve y/o de manera esquemática los mismos.

3.1. Estudios morfológicos, anatómicos y químicos

- Para el estudio morfológico y realización de fotografías a escala macroscópica en los diferentes capítulos y secciones de esta tesis se usó un microscopio de disección Leica S8APO equipado con un sistema de captura de imágenes tipo Leica EC3. Algunas láminas fotográficas contienen imágenes de paisaje y de líquenes en su ambiente cuya autoría quedará expuesta en los respectivos pies de figura (IGB: Isaac Garrido Benavent; AdR: Asunción de los Ríos; SPO: Sergio Pérez Ortega).

- Para el estudio microscópico y la toma de microfotografías se usaron preparaciones en portaobjetos que fueron visualizadas en un microscopio Zeiss Axioplan 2 equipado con contraste de interferencia diferencial (DIC, "Nomarski") y provisto de una cámara digital Zeiss AxioCam. Este mismo microscopio fue utilizado junto con un equipo para microscopía de fluorescencia que incluía un Filtro Zeiss Set 49 (luz emitida, 463 nm) para visualizar interacciones celulares entre simbiontes, y diferentes componentes celulares y extracelulares en los Capítulos 2 y 3.

- El estudio ultraestructural incluido en el Capítulo 2 se realizó con un microscopio electrónico de transmisión Zeiss EM910. La metodología empleada en la preparación de muestras y obtención de cortes ultrafinos se realizó siguiendo de los Ríos y Ascaso (2001), que se puede resumir brevemente en los siguientes pasos:

1) Fijación de las muestras con glutaraldehído en tampón fosfato sódico 100 mM (pH 7.1) durante 24 horas a 4º C.

2) Lavados con tampón fosfato sódico 100 mM (pH 7.1).

3) Fijación en tetróxido de osmio (OsO_4) al 1% con tampón fosfato sódico 100 mM (pH 7.1) durante 3 horas a temperatura ambiente y en oscuridad.

4) Lavados con tampón fosfato sódico 100 mM (pH 7.1).

5) Deshidratación con etanol a concentraciones crecientes (30, 50, 70, 90 y 100%) y con óxido de propileno a temperatura ambiente.

7) Infiltración de las muestras en resina "Spurr" y polimerización en estufa a 70º C durante 24 horas.

8) Obtención de cortes ultrafinos (70–90 nm) con micrótomo Ultracut-E (Reichert).

9) Tinción de los cortes con citrato de plomo (Reynolds 1963).

- El estudio del patrón de compuestos metabólicos secundarios existente en diversas especies de la familia *Teloschistaceae* correspondiente a los Capítulos 1 y 3 se realizó mediante cromatografía líquida de alta eficacia (HPLC, del inglés *High Performance Liquid Chromatography*). La composición relativa de metabolitos secundarios fue calculada usando una absorbancia a 270 nm de acuerdo con Søchting (1997). Este estudio, que corresponde al Capítulo 1 de la presente tesis, se llevó a cabo en la Universidad de Copenhague (Dinamarca).

Parte del trabajo experimental del Capítulo 1 se llevó a cabo en el laboratorio de la Universidad de Copenhague (Dinamarca) gracias a una beca del proyecto europeo SYNTHESYS (*Synthesys of Systematic Resources*) concedida al doctorando en 2013 y por tanto se usaron equipos y/o metodologías ligeramente distintas a las expuestas en esta sección de la tesis, quedándose debidamente explicadas en el respectivo apartado de Material y Métodos de dicho capítulo.

3.2. Extracción de ADN, PCRs, tratamiento de las secuencias y obtención de *datasets*

En general, el ADN genómico se extrajo a partir de pequeños fragmentos del talo liquénico, como ascomas (Capítulo 2), pequeñas areolas de talos crustáceos (Capítulo 3), porciones distales de unos pocos mm^2 en talos foliáceos (Capítulos 4–5), o ramas individuales en talos fruticulosos (Capítulo 6). Asimismo, previamente a la extracción del ADN; el material fue inspeccionado bajo el microscopio de disección para cerciorarse de la ausencia de otros organismos potencialmente contaminantes y, posteriormente, congelado en nitrógeno líquido (o en el congelador a -80º C) y pulverizado mediante el uso de un molino (Retsch MM 200). Cabe destacar que en el Capítulo 1 la amplificación de los *loci* utilizados en el estudio se realizó mediante PCR directa, sin previa extracción del ADN (ver Arup 2006).

Los estudios filogenéticos y filogeográficos llevados a cabo en los Capítulos 1–6 se han basado en secuencias de ADN (Figura 14). Aunque la metodología puede ser ligeramente distinta en el Capítulo 1 (ver motivos arriba), en general, la obtención y tratamiento inicial de las secuencias, así como la generación última de alineamientos de secuencias (*datasets*) consta de los siguientes pasos estándar:

1) Extracción del ADN genómico, que se llevó a cabo a través de uno de estos dos protocolos que usan en alguno de sus pasos iniciales el surfactante catiónico bromuro de hexadeciltrimetilamonio, o CTAB (Cubero et al. 1999; Werth et al. 2016). El método de Cubero et al. (1999), que se emplea en los Capítulos 2–5 de esta tesis, fue diseñado para la extracción eficiente de ADN de muestras de hongos liquenizados y no liquenizados, tanto frescas como herborizadas, y consta brevemente de los siguientes pasos:

i) Precipitación del ADN en tampón de CTAB que contiene, adicionalmente, Tris y el agente quelante ácido etilendiaminotetraacético (EDTA). También se puede añadir PVPP (polivinil polipirrolidona) para facilitar la eliminación de la mayoría de inhibidores polifenólicos.

ii) Suspensión del pellet en una solución de NaCl 1.2 M, y precipitación en un volumen de cloroformo:isoamilalcohol (24:1).

iii) Lavado final con etanol al 70%.

iv) Elución del ADN con agua filtrada estéril (Sigma®)

Por su parte, el método de Werth et al. (2016) es un método nuevo diseñado para el aislamiento rápido de ADN genómico para estudios enfocados a la preparación de librerías genómicas en líquenes, y queda resumido como sigue:

a) Lisado celular en tampón de CTAB, y centrifugación para eliminar restos celulares.

b) Unión del ADN a una membrana de fibra de vidrio bajo concentraciones elevadas de un agente caotrópico, en particular, el cloruro de guanidinio (CH_6ClN_3).

c) Dos lavados con etanol al 70%.

d) Elución del ADN con tampones elaborados a base de Tris-HCl y EDTA a un pH básico de entre 8–9.

2) Selección de marcadores moleculares y su amplificación por PCR (del inglés *Polymerase Chain Reaction*). Los *loci* seleccionados para los distintos capítulos de esta tesis varían en función del objetivo del estudio y del tipo de simbionte analizado (Tabla 1). Para el micobionte se ha usado el *locus nrITS* del ADN ribosómico nuclear, ampliamente empleado en estudios filogenéticos, de delimitación de especies (código de barras fúngico), y filogeográficos (Fernández-Mendoza et al. 2011; Schoch et al. 2012; Leavitt et al. 2013). Los fragmentos *LSU* y *SSU* nucleares así como el *SSU* mitocondrial han sido usados en trabajos enfocados a dilucidar relaciones filogenéticas a niveles taxonómicos más elevados (p. ej. Lumbsch et al. 2001; Schoch et al. 2009; Pérez-Ortega et al. 2010; Arup et al. 2013). Los *loci EF-1α*, *Mcm7* y *GAPDH* han sido usados tanto en aproximaciones filogenéticas como filogeográficas (Fernández-Mendoza y Printzen 2013; Sork y Werth 2014; Boluda et al. 2016). Sin embargo, los *loci L1* y *PGK* (Stielow

et al. 2015) (Capítulo 6), no habían sido utilizados previamente para la delimitación de especies y genética de poblaciones en hongos liquenizados. Para los fotobiontes, se usan los *loci nrITS*, *tufA* y *rbcL*, los cuales han sido propuestos como marcadores adecuados para inferir relaciones filogenéticas y explorar los niveles de variabilidad intraespecífica en distintos grupos de algas (Rindi et al. 2007; Saunders y Kucera 2010; del Campo et al. 2013; Moniz et al. 2014). Los cebadores ("*primers*", en inglés) empleados para la PCR con el fin de amplificar los distintos *loci* se obtuvieron de la literatura (ver capítulos correspondientes) pero en muchos casos también se diseñaron *de novo* a partir de secuencias, o bien disponibles en la base de datos GENBANK, o bien obtenidas inicialmente con los cebadores originales, mediante el *software* PRIMER-BLAST (Ye et al. 2012). Las condiciones de PCR se detallan igualmente en cada capítulo de tesis.

Tabla 1. *Loci* empleados en cada capítulo de tesis para cada simbionte.

Capítulo	*Loci* (simbionte)
1	*nrITS*, *nuLSU*, *mtSSU* (micobionte)
2	*nuLSU*, *nuSSU* (micobionte)
3	*nrITS*, *nuLSU*, *mtSSU* (micobionte)
4	*nrITS*, *tufA*, *RPL10A* (fotobionte)
5	*nrITS*, *EF-1α*, *Mcm7* (micobionte) *nrITS*, *tufA*, *RPL10A*, *rbcL* (fotobionte)
6	*nrITS*, *Mcm7*, *GAPDH*, *EF-1α*, *L1*, *PGK* (micobionte)

3) Purificación y secuenciación de los productos de la PCR, la primera mediante el *kit* comercial UltraClean PCR Clean-Up Kit (MOBIO Laboratories, Inc.) y, la segunda, llevada a cabo por el método de Sanger en diferentes laboratorios externos (Macrogen Europe, Holanda; Microsynth, Austria).

4) Revisión de la calidad de los electroferogramas y ensamblaje de los mismos para generar secuencias únicas, para lo cual se usaron los programas BIOEDIT v.7.0.9 (Hall 1999) y SEQMANII v.5.07© (Dnastar Inc.).

5) Testeado de las secuencias mediante la herramienta BLAST (del inglés *Basic Local Alignment Search Tool*; Altschul et al. 1990) en la base de datos de GENBANK (accesible por https://www.ncbi.nlm.nih.gov/genbank/) para comprobar que dichas secuencias no se correspondían a las de hongos/algas contaminantes.

6) Alineamiento de las secuencias y preparación de los diferentes conjuntos de datos ("*datasets*"), usando los programas BIOEDIT v.7.0.9 (Hall 1999), GBLOCKS v.0.91b (Castresana 2000), MAFFT v.7.222 (Katoh et al. 2002) y MUSCLE v.3.6 (Edgar 2004), mientras que los algoritmos de alineamiento y los parámetros empleados se detallan en cada uno de los capítulos.

7) Estimación de los modelos evolutivos de sustitución nucleotídica para cada conjunto de datos, empleando los programas informáticos JMODELTEST v.2.1.6 (Darriba et al. 2012) y PARTITIONFINDER v.1.1.1 (Lanfear et al. 2012).

3.3. Estudios filogenéticos y filogeográficos

Los árboles filogenéticos reconstruidos en los tres capítulos del Bloque 1 y Capítulo 4 (Bloque 2) tienen como objetivo situar en un contexto filogenético las especies objeto de estudio para la posterior discusión taxonómica y, en su caso, descripción de nuevos taxones (Figura 14A). En general, las filogenias se han inferido a partir de dos aproximaciones: la máxima verosimilitud, empleando los programas RAxML (Stamatakis 2006; Stamatakis et al. 2008) y PHYML v.3.0 (Guindon et al. 2010), y la inferencia Bayesiana, usando diferentes estrategias implementadas en BEAST v.1.7 (Suchard y Rambaut 2009; Drummond et al. 2012) y MRBAYES v.3.2.3 (Ronquist et al. 2012). Brevemente, la primera intenta estimar la filogenia más probable que pueda generarse a partir de los datos disponibles y un modelo de sustitución nucleotídica, mientras que en la segunda se calcula una probabilidad posterior para cada árbol posible dado un modelo de sustitución nucleotídica y unos datos. Las filogenias se infirieron usando, bien un único locus, bien *loci* concatenados, y usaron secuencias disponibles en la base de datos GENBANK, incluyendo en todos los casos un grupo externo, o *outgroup*.

En el Bloque 2, que está centrado en el estudio genético de los simbiontes del liquen *Mastodia tessellata* y de los micobiontes de las dos especies de *Pseudephebe*, además de inferir filogenias (Capítulo 4), se lleva a cabo un estudio de delimitación de especies que sigue una aproximación de descubrimiento y validación de hipótesis de especies (p. ej. Rannala 2015; Hotaling et al. 2016) (Figura 14B). Brevemente, los métodos de descubrimiento de especies usan datos genéticos y algoritmos determinados con el fin de identificar evidencias de subestructura genética en las poblaciones estudiadas que puedan ser atribuibles a más de un taxón. Cada uno de estos algoritmos utiliza una aproximación distinta para encontrar posibles especies. El algoritmo GMYC (Pons et al. 2006) se basa en las distribuciones de la longitud de las ramas derivadas de relaciones entre individuos de una misma especie (modelizadas acorde a la teoría de la coalescencia) y relaciones entre especies (que siguen un modelo de tipo Yule o *Pure Birth*). El algoritmo ABGD (Puillandre et al. 2012) trata de encontrar el llamado *barcoding gap* en la distribución de distancias genéticas entre las secuencias de una región genómica informativa utilizada para diferenciar especies. Este algoritmo se basa en la hipótesis de que existe un hueco o *gap* en la distribución de secuencias que permite separar las distancias intraespecíficas de las interespecíficas (Puillandre et al. 2012). Adicionalmente, las redes multi-*locus* construidas mediante el algoritmo NEIGHBORNET (Bryant y Moulton 2004) a partir de matrices estandarizadas de distancias genéticas pueden dar también una idea sobre la existencia de más de un taxón comparando el grado de reticulación entre los diferentes individuos muestreados. En conjunto, todos estos análisis permiten elaborar hipótesis iniciales sobre límites de especies que son comparadas en una segunda fase (validación) usando conjuntos de datos de varios *loci* y una metodología Bayesiana, por ejemplo, mediante el test de

Bayes Factors, o BFD (del inglés *Bayes Factor Delimitation*, Grummer et al. 2014), o comparando la existencia de flujo génico entre especies putativas (p. ej. MIGRATE-N, Beerli 2006; Beerli y Palczewski 2010).

En el Bloque 2 también se lleva a cabo un estudio profundo de la estructura filogeográfica y diversidad genética de los distintos componentes de la simbiosis liquénica (Figura 14B). El análisis de la estructura filogeográfica es abordado mediante la inferencia de poblaciones intraspecíficas no filogenéticas con distintos algoritmos de agrupamiento genético (p. ej. BAPS, Corander y Marttinen 2006, Corander et al. 2008; STRUCTURE, Pritchard et al. 2000; Falush et al. 2003; DAPC, Jombart et al. 2010). Los niveles de divergencia y diferenciación entre las poblaciones geográficas (*i.e*. conjunto de individuos provenientes de una única localidad o región mayor de estudio) son evaluados mediante el cálculo de diferentes índices (Dxy, Nei 1987; Fst, Weir y Cockerham 1984). Asimismo, se infieren las relaciones genealógicas desde un punto de vista estadísticamente parsimonioso entre haplotipos para cada marcador usando el método TCS (Clement et al. 2002) y los resultados se expresan en forma de redes de haplotipos. Por último, también se evalúan los niveles de polimorfismo del ADN para los distintos *datasets* genéticos por medio de distintos estadísticos calculados con el *software* DNASP (Librado y Rozas 2009).

Los diferentes estudios filogeográficos de esta tesis se complementan con análisis de estimación de tiempos de divergencia (Capítulo 5; Capítulo 6; véase también Capítulo 3) y comparación de hipótesis de flujo génico (Capítulo 5). Los primeros se llevan a cabo utilizando distintas estrategias de calibración (primaria y/o secundaria) sobre conjuntos de datos de uno o varios *loci* en BEAST y *BEAST (Heled y Drummond 2010; Drummond et al. 2012). Las hipótesis de flujo génico entre regiones (migración) se comparan mediante el programa MIGRATE-N (Beerli 2006; Beerli y Palczewski 2010). La presencia de alelos compartidos entre dos especies (o poblaciones) puede ser considerada como indicación de flujo génico o polimorfismo ancestral. MIGRATE-N asume que todo el polimorfismo compartido deriva de flujo génico, mientras que otras aproximaciones, como la llevada a cabo por el software IMA2 (Hey 2010), aceptan la existencia de polimorfismo ancestral y flujo génico después de la divergencia entre linajes. En general, los resultados de las estimas de tiempos de divergencia y la inferencia del mejor modelo de flujo génico son usados para plantear hipótesis biogeográficas para las especies objeto de estudio. En cualquier caso, los apartados correspondientes de cada capítulo ofrecen información más detallada de los métodos filogenéticos y filogeográficos empleados en la presente tesis.

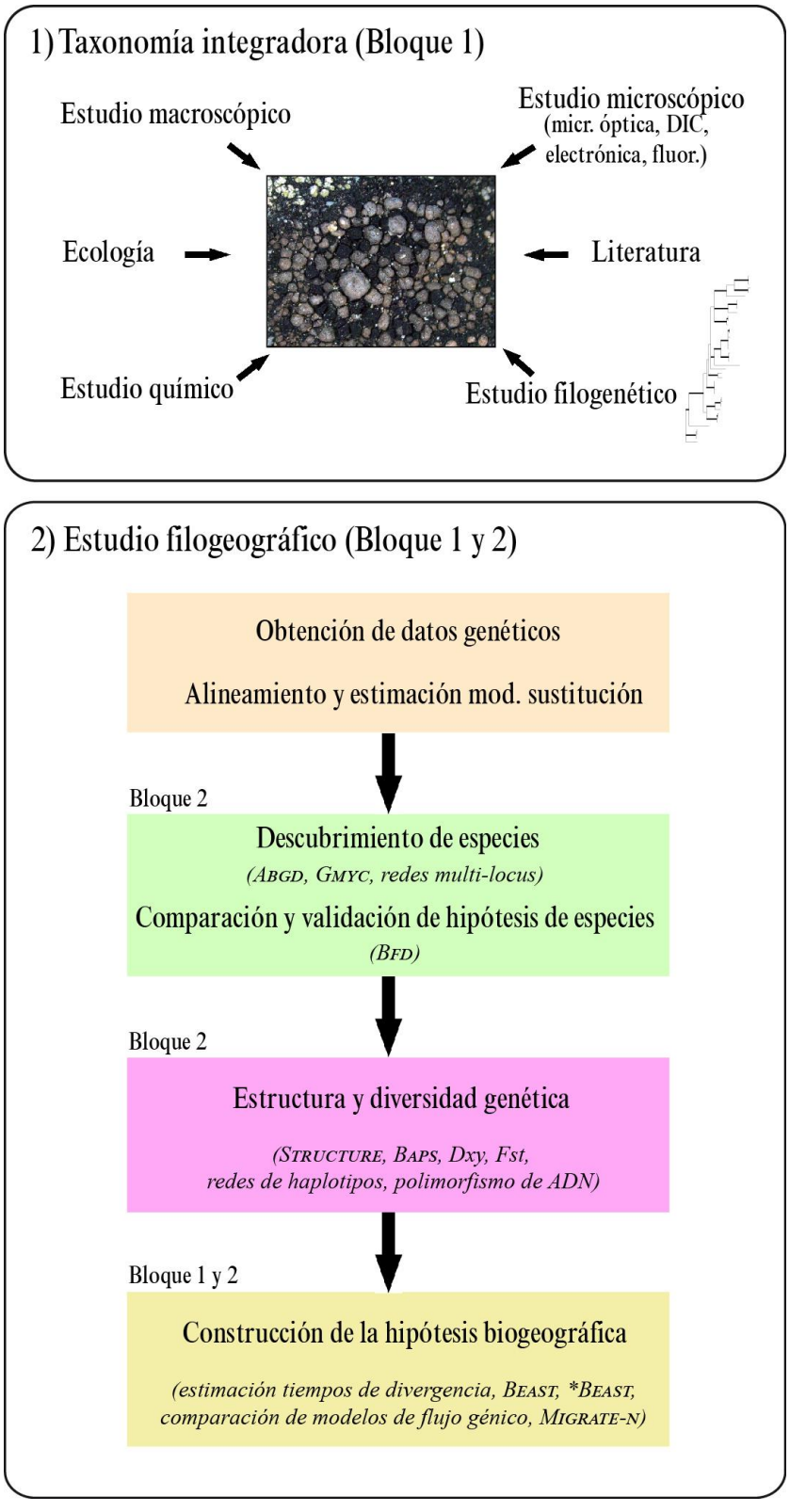

Figura 14. Metodología implementada en la presente tesis doctoral. (A) Taxonomía integradora (Bloque 1). (B) Estudio filogeográfico (Bloques 1 y 2).

RESULTADOS

"*Every species has come into existence coincident both in space and time with a pre-existing closely allied species. Description or law, it challenged the theory of special creation and bruited the idea of evolution in a tone of thunderous innuendo*." – David Quammen

CAPÍTULO 1 (*CHAPTER 1*)

Charcotiana y *Amundsenia*, dos nuevos géneros en la familia de hongos liquenizados *Teloschistaceae* (subfamilia *Xanthorioideae*), incluyendo dos nuevas especies de la Antártida Continental; y *Austroplaca frigida*, un nombre nuevo para una especie antártica continental.

Referencia del artículo científico publicado:

Søchting U, **Garrido-Benavent I**, Seppelt R, Castello M, Pérez-Ortega S, de los Ríos A, Sancho LG, Patrik Frödén y Arup A (2014) *Charcotiana* and *Amundsenia*, two new genera in *Teloschistaceae* (lichenized Ascomycota, subfamily *Xanthorioideae*) hosting two new species from continental Antarctica, and *Austroplaca frigida*, a new name for a continental Antarctic species. Lichenologist 46(6): 763–782 doi:10.1017/S0024282914000395

Abstract

Based on a combined three-locus analysis two new genera, *Charcotiana* and *Amundsenia*, are proposed in the lichen family *Teloschistaceae* (Ascomycota), subfamily *Xanthorioideae*. *Charcotiana* includes the new species *C. antarctica*, which is known only from Continental Antarctica. The bipolar genus *Amundsenia* includes the new species *A. austrocontinentalis*, which is also known only from Continental Antarctica, and the Arctic species *Caloplaca approximata* which is here combined into the new genus. The two new genera are phylogenetically distinct, but poor in morphological characters; the new species consist mainly of minute apothecia in cracks of rocks located in the climatically harshest regions of the Antarctic. They are somewhat similar to another continental Antarctic species, *Austroplaca frigida*, which is described as a new name based on the illegitimate name *Caloplaca frigida*. The distribution of the four species is mapped.

1. Introduction

The knowledge of Antarctic *Teloschistaceae* (Ascomycota) has expanded significantly in recent years (Søchting & Øvstedal 1992, 1998; Olech & Søchting 1993; Søchting & Olech 1995, 2000; Olech 2004; Søchting et al. 2004, 2014b; Lindblom & Søchting 2008; Søchting & Castello 2012), and numerous new species have been described, all in the genus *Caloplaca*. The highest diversity has been recorded in the Maritime Antarctic, and particularly towards the lower latitudes as is the general trend for lichens (Peat et al. 2007). However, recent expeditions to Continental Antarctica have brought back lichen collections disclosing species that are unknown in the more mesic parts of Antarctica, in spite of those parts having been most intensively explored (Olech 2004; Søchting et al. 2004). Two such species, which appear to have so far passed unnoticed also by the Antarctic lichen flora authors (Dodge 1973; Øvstedal & Smith 2001), are described here as new to science. The phylogenetic analysis of three loci has made it possible to establish their taxonomic affiliation in relation to the recently published taxonomy of the *Teloschistaceae* (Arup et al. 2013). Based on their position in the molecular phylogenetic tree of *Teloschistaceae*, we have found it necessary to place them in two new genera, also including the Arctic species known as *Caloplaca approximata*.

2. Material and Methods

The study includes material collected during Antarctic expeditions to Continental Antarctica by the Italian Antarctic Research Programme (PNRA) (1988–1996), Australian Antarctic Division (1971–2010) and the New Zealand Antarctic Program (2007, 2009). The collections are kept in designated herbaria. Collections formerly in ADT are now lodged in the Tasmanian Herbarium (HO). Distribution data for *Amundsenia* (= *Caloplaca*) *approximata* are based on specimens from C, LD, O and UPS.

2.1. Morphology and anatomy

Macroscopic descriptions are based on observations made with a Wild Heerbrugg M5-53204 dissecting microscope. Measurements were made using a mounted Nikon DS-Fi1 camera combined with the software NIS-Elements. For the apothecia, only the thickness of the whole margin and the proper exciple was measured because the distinction of thalline and proper exciple was frequently unclear. Sections were cut by hand or using a Reichert-Jung Cryostat 2800 Frigocut E microtome. Measurements were taken using an Olympus BX60 microscope. All measurements were made on material mounted in water. Ascospores were measured outside the asci, and ascospore size is given as an average with standard deviation; extremes are given in parentheses. The thickness of spore septa is measured at the outer wall in accordance with Vondrák et al. (2013). The number of measurements is indicated in parentheses.

2.2. PCR-amplification and alignment

Thirteen new nuclear rDNA sequences of the internal transcribed spacer region (*nrITS*) and three of the large subunit (*nuLSU*), together with a further three new sequences of the small subunit of the mitochondrial ribosomal RNA gene (*mtSSU*), were produced. The PCR amplifications were carried out using direct PCR following Arup (2006). The primers used were ITS1F (Gardes & Bruns 1993) and ITS4 (White et al. 1990) for *nrITS*, AL1R (Döring et al. 2000), LR5 or LR6 (Vilgalys & Hester 1990) for *nuLSU*, and mrSSU1 (Zoller et al. 1999) and mrSSU7 (Zhou & Stanosz 2001) for *mtSSU*. The PCR settings followed Ekman (2001) or Arup et al. (2013). PCR products were electrophoresed in a 1% agarose gel and visualized using ethidium bromide or GelRed™ (Biotium). Products were cleaned using a Cycle Pure Kit (Qiagen or Five Prime). The primers used for the PCR were also used in the sequencing reaction in combination with LR3 and LR3R (Vilgalys & Hester 1990) for *nuLSU*; sequencing was carried out by MACROGEN Inc., Korea. Sequences were assembled using CLC MAIN WORKBENCH v.4.1.2. Additional sequences were downloaded from GENBANK. Voucher information and GENBANK accession numbers are provided in Appendix 1 for both the new and the downloaded sequences.

Two alignments were produced: one combined alignment with 86 species including three loci, *nrITS*, *nuLSU* and *mtSSU*, representing the three subfamilies in *Teloschistaceae*, and another with 39 *nrITS* sequences representing relevant clades of the subfamily *Xanthorioideae* (Arup et al. 2013). For the combined analysis, *Physcia aipolia* and *Amandinea punctata* were used as outgroups. For the *nrITS* analysis, *Parvoplaca tiroliensis* was used as outgroup. Ambiguously aligned regions were removed from all alignments before analyses.

2.3. Phylogenetic analyses

The alignments of the three different genes were first analysed separately to check for incongruence between genes, but no incongruences were found. A conflict was assumed to be significant if two different relationships (one monophyletic and one non-monophyletic) were both supported with posterior probabilities 0.95 or higher (Buckley et al. 2002). A suitable model of molecular evolution for each of the loci was selected using the Bayesian Information Criterion (BIC, Schwarz 1978) as implemented in JMODELTEST v.2.1.4 (Guindon & Gascuel 2003; Darriba et al. 2012), evaluating only the 24 models available in MRBAYES v.3.2 (Ronquist et al. 2012). The GTR+I+Γ model was found to be optimal for both the *nrITS* and *nuLSU* datasets for the combined analysis, but HKY+I+Γ for the *mtSSU* data set. The *nrITS* alignment was also analysed separately using the evolutionary model GTR+I+Γ. Bayesian tree inference was carried out using Markov chain Monte Carlo (MCMC) as implemented in MRBAYES v.3.2. In the combined analysis, the three genes included were treated as separate partitions. Parameters used in the analyses followed those of Arup et al. (2013), except for the branch length prior that was set to an exponential with mean 1/10. Three parallel runs of Markov chain Monte Carlo were performed, each with 7 chains, 6 of which were

incrementally heated with a temperature of 0.10. Analyses were diagnosed every 100.000 generations and automatically halted when convergence was reached.

Convergence was defined as a standard deviation of splits (with frequency ≥ 0.1) between runs below 0.01. Every 1.000th tree was sampled and the first 50% of the runs were removed as burn-in. PAUP* v.4.0b10 (Swofford 2002) was used to construct 50% majority rule consensus trees from the post-burn-in tree samples, and FIGTREE v.1.4 (http://tree.bio.ed.ac.uk/software/figtree/) and APPLE WORKS v.6.2.9 (Apple Computers Inc.) to illustrate them.

2.4. Secondary chemistry

The secondary metabolite pattern was identified using HPLC and analysed separately for thallus and apothecia. The relative composition of the secondary compounds was calculated based on absorbance at 270 nm, according to Søchting (1997).

3. Results and Discussion

3.1. Molecular analyses

The combined analysis of the *nrITS*, *nuLSU* and *mtSSU* dataset included 41 terminal species and a total of 2.030 positions. A 50% majority-rule consensus tree is presented in Figure 1. The tree splits into three main clades corresponding to the three subfamilies proposed by Arup et al. (2013). *Xanthorioideae* and *Teloschistoideae* are well supported here, in concordance with Arup et al. (2013), but *Caloplacoideae* has lower support (PP = 0.84) in this rather limited analysis. All the new sequences are clearly nested within *Xanthorioideae*, with the new genus *Charcotiana* on a separate branch in the middle of the subfamily. For practical reasons, the analyses presented here include fewer taxa than those presented in Arup et al. (2013) and the support for the backbone structure of the tree is therefore lower for many nodes. However, even in analyses with three genes and a more extensive species sampling (data not shown), the placement of *Charcotiana* is the same and we have been unable to accommodate it within any of the already defined genera in the subfamily. The other new genus, *Amundsenia*, appears as the sister clade of *Squamulea* with high support (Figure 1).

The analysis of only *nrITS* data included 39 sequences and a total of 544 positions. A 50% majority-rule consensus tree is presented in Figure 2. In this analysis, the genus *Amundsenia* is weakly supported, whereas the support was strong in the combined three gene analyses (PP = 1; Figure 1). The two species of the genus show some intraspecific variation, one variable position in *A. austrocontinentalis* and six variable positions in *A. approximata* with up to 5 differences between specimens, but they clearly appear as monophyletic with full support. The variation is slightly greater in *Charcotiana antarctica*, with eight variable positions with up to five differences

between specimens. *Caloplaca frigida* is well nested within the genus *Austroplaca*, with the two sorediate species *A. darbishirei* and *A. soropelta* as its closest relatives.

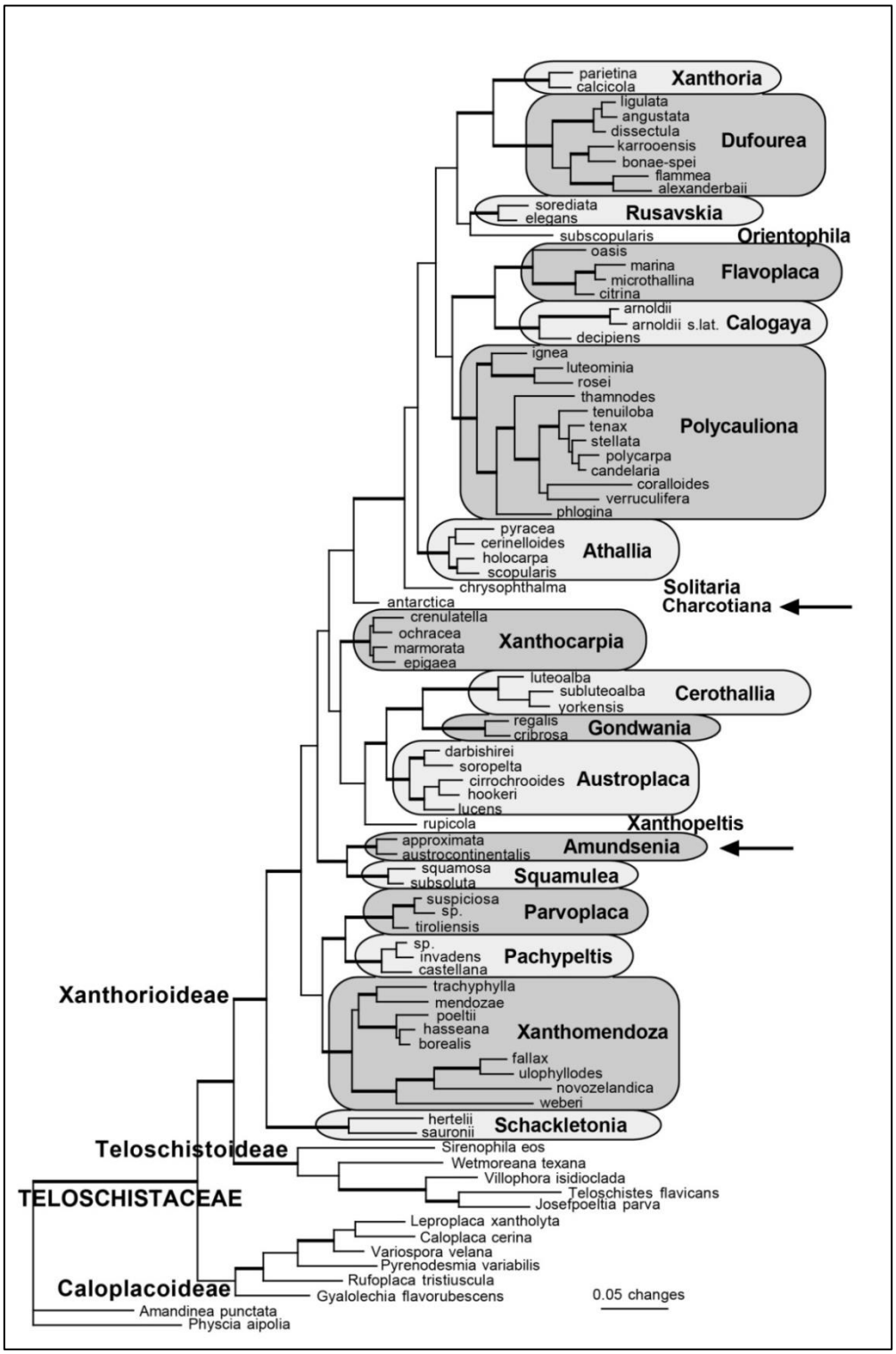

Figure 1. 50% majority-rule consensus tree of *nrITS*, *nuLSU* and *mtSSU* data using Bayesian MCMC. Nodes with posterior probabilities (PP) ≥ 0.95 are shown in bold.

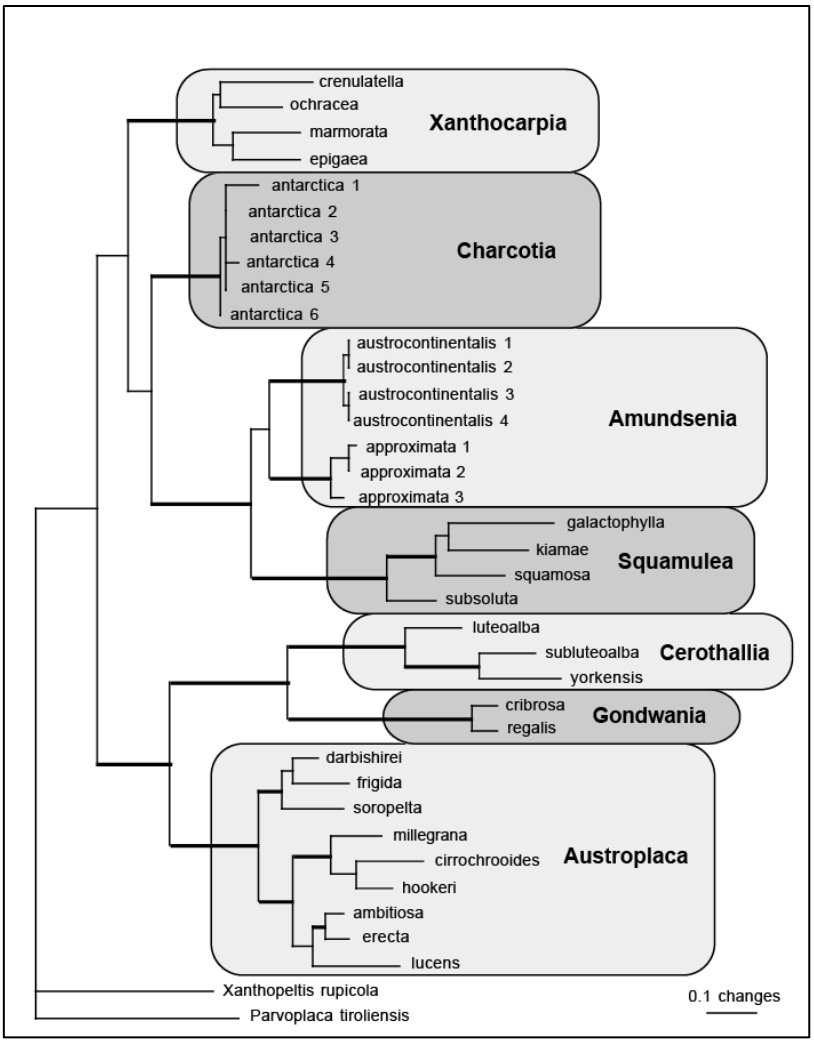

Figure 2. 50% majority-rule consensus tree of *nrITS* data using Bayesian MCMC. Nodes with posterior probabilities (PP) ≥ 0.95 are shown in bold.

3.2. Secondary chemistry

Only chemosyndrome A of Søchting (1997) was shown to occur in the two new species. This chemosyndrome is dominated by parietin, but in addition has small proportions of emodin, teloschistin, parietinic acid and fallacinal. It is the most frequent chemosyndrome in the subfamily *Xanthorioideae*.

3.3. Taxonomy

Charcotiana Søchting, Garrido- Benavent & Arup gen. nov.

MYCOBANK NO.: MB 808600

Type: *Charcotiana antarctica* Søchting, Garrido-Benavent, Pérez-Ortega, Seppelt & Castello

Diagnosis: Thallus saxicolous, crustose, areolate, orange. Apothecia sparse or abundant, zeorine with orange disc. Spores polardiblastic.

Secondary chemistry: Apothecia and thalli contain parietin (dominant) and small proportions of teloschistin, fallacinal, parietinic acid and emodin. Chemosyndrome A of Søchting (1997).

Etymology: The genus is named after the significant French polar explorer and scientist Jean-Baptiste Charcot (1867–1936).

Distribution: *Charcotiana* is known only from Continental Antarctica.

Notes: So far, *C. antarctica* is the only species included in the genus. *Charcotiana* is defined primarily on molecular phylogenetic characters and is similar to several other crustose genera in the subfamily with regard to main morphology, anatomy and secondary chemistry. However, it has a strong tendency to develop stipitate apothecia, a feature that is rare in most genera. Such apothecia occur, for example, in *Austroplaca*, *Calogaya* and *Gondwania*, but the species in those genera normally produce distinct lobes or are subfruticose. Stipitate apothecia also occur in *Gyalolechia stipitata* in subfamily *Caloplacoideae*, but this genus is characterized by a fragilin dominated secondary chemistry (Arup et al. 2013).

Charcotiana antarctica Søchting, Garrido-Benavent, Pérez-Ortega, Seppelt & Castello sp. nov. (Figure 3)

MYCOBANK NO.: MB 808602

Diagnosis: Thallus crustose, orange, bullate to areolate with minutely lobate margins, most often distinctly stipitate, particularly when fertile. Apothecia crowded, often stipitate and irregular, with excluded margin. Spores polardiblastic, 12 × 6.5 mm; septum *c*. 3.5 mm.

Type: Antarctica, Northern Victoria Land, Daniell Peninsula, Cape Phillips, 73º 050’ S, 169º 35’ E, on volcanic rock, 7 January 1996, *F. Bersan* (TSB A833 –holotype; MA-Lich 18175, C–isotypes).

Thallus crustose, saxicolous, up to 3 cm wide, consisting of scattered areoles. Prothallus absent. Areoles small, initially isolated and bullate, eventually coalescing, forming larger irregular-shaped areoles that are minutely lobate at margins, pale to deep orange, 0.1–3.0 mm wide (n = 40) and 0.1–0.6 mm (n = 34) thick. A large proportion of the specimens studied have a ramified structure with finger-like protrusions that continue branching, thus giving an overall coralloid appearance. Yellowish white dead tissue abundant in some samples, especially in old or abraded areoles. Thallus cortex paraplectenchymatous with cell lumina 2.5–4.5 mm wide (n = 12). Photobiont trebouxioid.

Apothecia lecanorine to mostly zeorine, mainly one per areole, numerous, rather crowded, regular to deformed by compression, sessile, often stipitate on top of finger-

like protrusions of the thallus, in which case they are slightly constricted at the base, 0.2–1.2 mm diam. (n = 26). Disc flat to somewhat convex in mature apothecia, deep orange to dark orange-brown when old, sometimes bright, epruinose. Apothecial margin particularly in very young apothecia rather thick, (60–) 95 ± 16 (–120) mm (n = 24). Thalline exciple rarely persistent, more often excluded early but still visible below the proper exciple of older apothecia, mainly pale orange. Proper exciple distinct, thin, often difficult to observe in deformed mature apothecia, (20–) 43 ± 11 (–70) mm thick (n = 45), concolorous with the disc. Proper exciple tissue prosoplectenchymatous, fan-shaped, consisting of non-isodiametric cells with lumina 4.5–6.0 mm long (n = 7) and *c*. 2 mm wide (n = 4). Hypothecium hyaline, consisting of densely interwoven hyphae. Hymenium hyaline, (51–) 58 ± 6 (–66) mm high (n = 8). Epithecium with dark orange, medium coarse epipsamma. Paraphyses (1.6–) 2.3 ± 0.4 (–3.9) mm thick (n = 64), simple to apically sparingly branched, septate, cylindrical with attenuate apex to moniliform and apically gradually slightly inflated, with (2.9–) 5.2 ± 0.9 (–7) mm thick (n = 49) apical cells. Asci clavate, with 8 spores, (39.5–) 48 ± 6 (–61) mm (n = 18) long and (13.5–) 16 ± 2.5 (–21) mm (n = 16) wide. Ascospores polardiblastic, ellipsoid, rarely subcylindrical with rounded ends, (8.5–) 12 ± 1.5 (–16) × (5–) 6.5 ± 0.7 (–8) mm (n = 90); length/breadth ratio (1.3–) 1.9 ± 0.3 (–2.9); ascospore septa (2.4–) 3.6 ± 0.7 (–5.7) mm thick; ratio of ascospore length/septum width (2–) 3.4 ± 0.5 (–4.6).

Conidiomata not seen.

Secondary chemistry: Thallus and apothecia K+ purple. Chemosyndrome A of Søchting (1997).

Etymology: The name reflects the distribution of this species, so far known only from Continental Antarctica and nearby islands.

Ecology and distribution: Based on the known localities, the species can grow on acid rocks, sand and dead mosses. *Charcotiana antarctica* grows in a wide spectrum of microhabitats including large stones, scoria debris, pebbles, rubble or gravel, silt, vulcanites, charnockite and coarse-grained granite. It is commonly found growing in small crevices of rocks where it may be able to retain a more humid environment. It is known from coastal sites at 25 meters above sea level (m a.s.l.). to high mountain ranges at 1.457 m a.s.l, but most of the samples were collected at 215–652 m a.s.l. Accompanying species are, for example, *Buellia frigida*, *Lecanora mons-nivis*, *L. physciella*, *Lecidea cancriformis*, *Pleopsidium chlorophanum*, *Umbilicaria decussata* and *Rusavskia elegans*. The moss *Syntrichia sarconeurum* was also seen accompanying them.

Charcotiana antarctica is so far known from Continental Antarctica, including several islands close to the continent margin (Coulman, Ross and Windmill islands) (Figure 4). According to the number of extant collections, *C. antarctica* is expected to be a common but often neglected species in Continental Antarctica. However, it has never been recorded from Maritime Antarctica or the Subantarctic Islands.

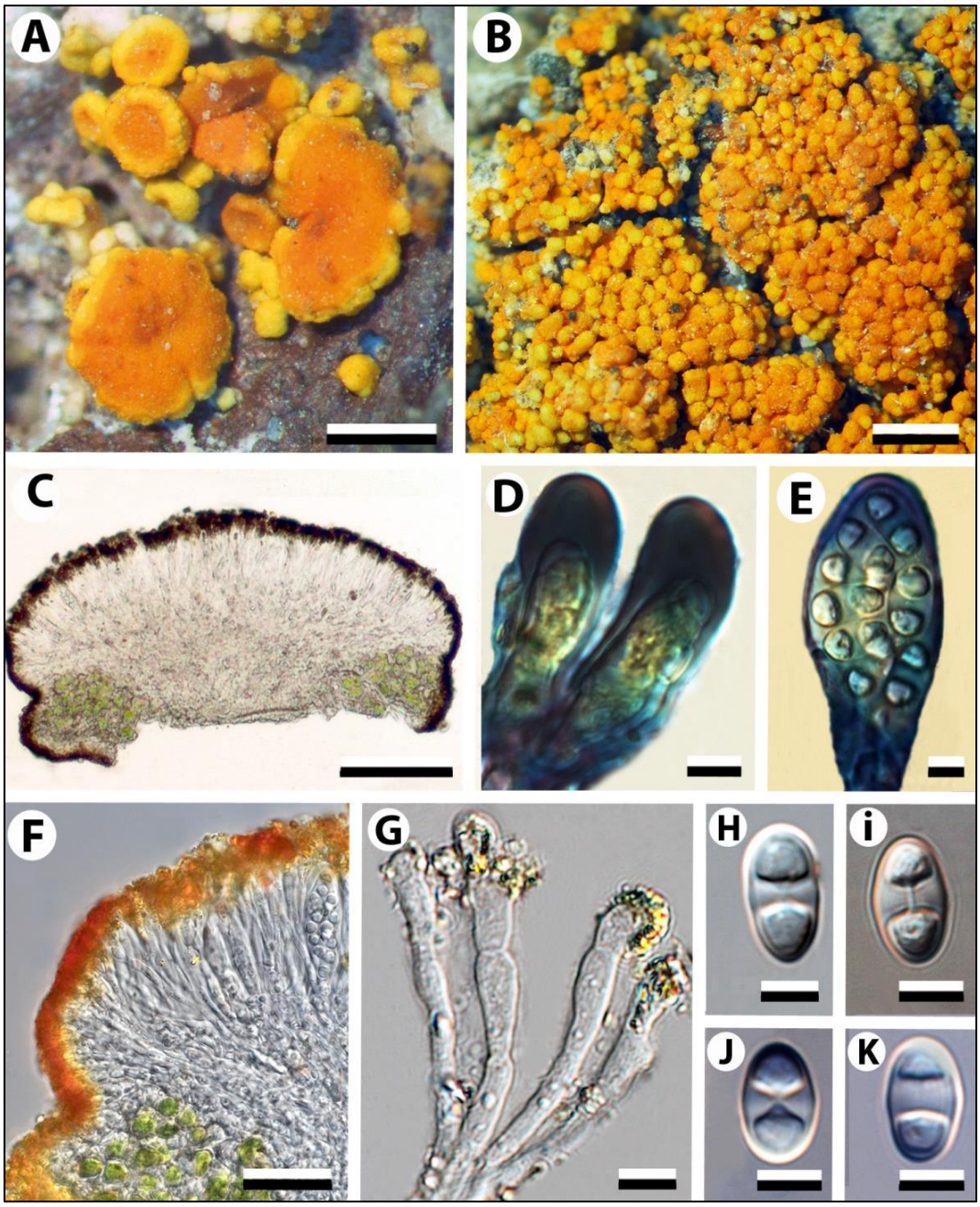

Figure 3. *Charcotiana antarctica*, habitus (A–B) and anatomical characters (C–K). (A) holotype (*F. Bersan*, TSB A833). (B) Sterile, granular thallus on sandy soil (*R. Bargagli*, TSB A580). (C) Cross section of an apothecium. (D) Young asci. (E) Mature ascus. (F) Cross section of a proper exciple. (G) Paraphyses. (H–K) Ascospores. Scales: A–B = 0.5 mm, C = 100 µm, D–E & G–K = 5 µm, F = 10 µm. (Photographs: IGB).

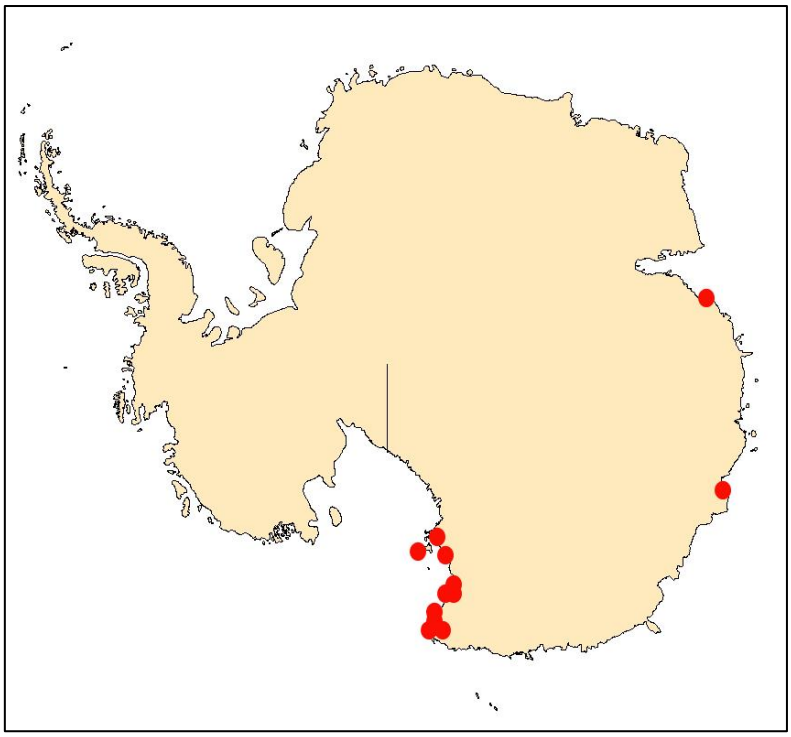

Figure 4. *Charcotiana antarctica*, distribution.

Notes: Specimens growing on sandy soil and mosses (ADT 25057, ADT 25393, ADT 25233, ADT 25051) develop a continuous, granular thallus, up to 10 mm wide, consisting of strongly aggregated, sometimes slightly fused, bullate (granule-like) areoles, (80–) 157 ± 49.5 (–260) mm wide (n = 20). They can be somewhat more greenish yellow when growing in the shade. Old areoles may become black. Moreover, these thalli are strongly coralloid (Figure 3B) and usually sterile. Apothecia from epigaeic specimens were seen only in ADT 25051.

Additional material studied: Antarctica: Northern Victoria Land: Cape Hallett region, Football Saddle, 652 m a.s.l., 72º 30’ 20.1” S, 169º 42’ 42.7” E, 2004, *R. D. Seppelt* (ADT 25067, ADT 25040, ADT 25051, ADT 25038, ADT 25057, ADT 25454); 72º 31’ S, 169º 45’ E, 1996, *F. Bersan* (TSB A829); NW end of Cape Hallett summit, 373.6 m a.s.l., 72º 19’ 20.9” S, 170º 15’ 20.8” E, 2004, *R. D. Seppelt* (ADT 25292, ADT 25286); Cape Christie, 523.8 m a.s.l., 72º 17’ 41.2” S, 169º 55’ 39.9” E, 2004, *R. D. Seppelt* (ADT 25388); 448.8 m a.s.l., 72º 18’ 10.4” S, 169º 58’ 53.9” E, 2004, *R. D. Seppelt* (ADT 25393); Red Castle Ridge: 323 m a.s.l., 72º 26’ 50.9” S, 169º 56’ 44.7” E, 2004, *R. D. Seppelt* (ADT 25233); 342 m a.s.l., 72º 26’ 53.5” S, 169º 56’ 51” E, 2004, *R. D. Seppelt* (ADT 25223); Daniell Peninsula, Cape Phillips, 73º 5’ S, 169º 35’ E, 1994, *R. Bargagli* (TSB A922, TSB A580); Wood Bay, Mt. Melbourne, Edmonson Point, 74º 21’ S, 165º 6’ E, 1995, *F. Bersan* (TSB A815); Deep Freeze Range, Boomerang Glacier, 74º 33’ S, 163º 54’ E, 1991, *S. Sedmak* (TSB A885); Coulman Island, 73º 19’ S, 169º 45’ E, 1989, *P. Modenesi* (TSB A353). Southern Victoria Land: Ross Island, Cape Crozier, 182 m a.s.l., 77º 31.801’ S, 169º 17.458’ E, 2007, *L. G. Sancho* (MAF-Lich 18885, MAF-Lich 18885-2, MAF-Lich 18886, MAF-

Lich 18886-2, MAF-Lich 18888, MAF-Lich 18889, MAF-Lich 18891, MAF-Lich 18891-2, MAF-Lich 18894, MAF-Lich 18895, MAF-Lich 18898, MAF-Lich 18903, MAF-Lich 18891, MAF-Lich 18903-2, MAF-Lich 18905); 158 m a.s.l., 77º 31.877' S, 169º 16.652' E, 2007, *L. G. Sancho* (MAF-Lich 18900); 212 m a.s.l., 77º 31.682' S, 169º 17.345' E, 2007, *L. G. Sancho* (MAF-Lich 18882, MAF-Lich 18883, MAF-Lich 18884, MAF-Lich 18887, MAF-Lich 18887-2, MAF-Lich 18892, MAF-Lich 18893, MAF-Lich 18896, MAF-Lich 18897, MAF-Lich 18882 MAF-Lich 18897-2, MAF-Lich 18897-3, MAF-Lich 18897-4, MAF-Lich 18899); Cape Crozier, 77º 27' S, 169º 14' E, 2010, *J. Smykla* (KRAM-L-63612 as *Caloplaca erecta*); Tripp Bay, Cape Ross, 76º 45' S, 163º 0' E, 1994, *R. Bargagli* (TSB A684); Dry Valleys, Miers Valley, 480 m a.s.l., 78º 5' 47.1" S, 163º 41' 33.6" E, 2000, *R. D. Seppelt* (ADT 21960). Windmill Islands: Ford Island, central, 66º 24' S, 110º 32' E, 1983, *R. D. Seppelt* (ADT 14247); Holl Island, central part of the island, 66º 25' S, 110º 25' E, 1989, *R. D. Seppelt* (ADT 19258). Ingrid Christensen Coast: Vestfold Hills, gully on south side of Trajer Valley, 68º 36' 0" S, 78º 27' 30" E, 1979, *R. D. Seppelt* (ADT 8755); east end of Lake Druzhby, 25 m a.s.l., 68º 34' 25" S, 78º 24' 0" E, 1979, *R. D. Seppelt* (ADT 8278).

Amundsenia Søchting, Garrido- Benavent, Arup & Frödén gen. nov.

MYCOBANK NO.: MB 808601

Type: *Amundsenia austrocontinentalis* Garrido-Benavent, Søchting, Pérez-Ortega & Seppelt

Diagnosis: Thallus saxicolous, crustose, orange. Apothecia sparse, dispersed, orange. Spores polardiblastic, small, with short spore septum.

Secondary chemistry: Apothecia and thalli contain parietin (dominant) and small proportions of teloschistin, fallacinal, parietinic acid and emodin. Chemosyndrome A of Søchting (1997).

Etymology: The genus is named after the successful Norwegian polar explorer Roald Amundsen (1872–1928), who was the first man to reach the South Pole.

Distribution: *Amundsenia* is so far known only from the Arctic and Subarctic, and from Continental Antarctica.

Notes: As seen from Figure 1, the genus *Amundsenia* is a monophyletic clade that belongs in the subfamily *Xanthorioideae*. Its sister group, the genus *Squamulea*, has a different proper exciple consisting of paraplectenchymatous tissue, usually a squamulose to lobate thallus and it occurs in subtropical to temperate regions. Therefore we have chosen not to merge the two sister groups. Currently two species are accepted in *Amundsenia*.

Amundsenia approximata (Lynge) Søchting, Arup & Frödén comb. nov. (Figure 5)

MYCOBANK NO.: MB 808603

Caloplaca vitellinula f. *approximata* Lynge, Lich. N. Zemlya: 222 (1928). – *Caloplaca approximata* (Lynge) H. Magn., Ark. Bot. 33A (1): 130 (1946); type: Russia, Novaya Zemlya, Mashigin Fjord, Langs en bæk på N-siden af Blaafjell Basin, 1 August 1921, *Lynge* (O-L-1206 –lectotype, selected here).

For a description of *A. approximata* see Hansen et al. (1987).

Distribution: *Amundsenia approximata* is widely distributed in the Arctic region, as shown in Figure 6. It was previously recorded from Antarctica based on a collection from McMurdo, Ross Island, in Continental Antarctica (Søchting & Øvstedal 1992), where the other species of the genus, *A. austrocontinentalis*, is fairly common. With the present knowledge, we assume that the specimen was actually *A. austrocontinentalis*. A further record from Signy Island, South Orkney Islands (RILS 1056, BAS) cited by Øvstedal & Smith (2001) proved to be an erroneous identification. Accordingly, *A. approximata* is not considered to occur in Antarctica.

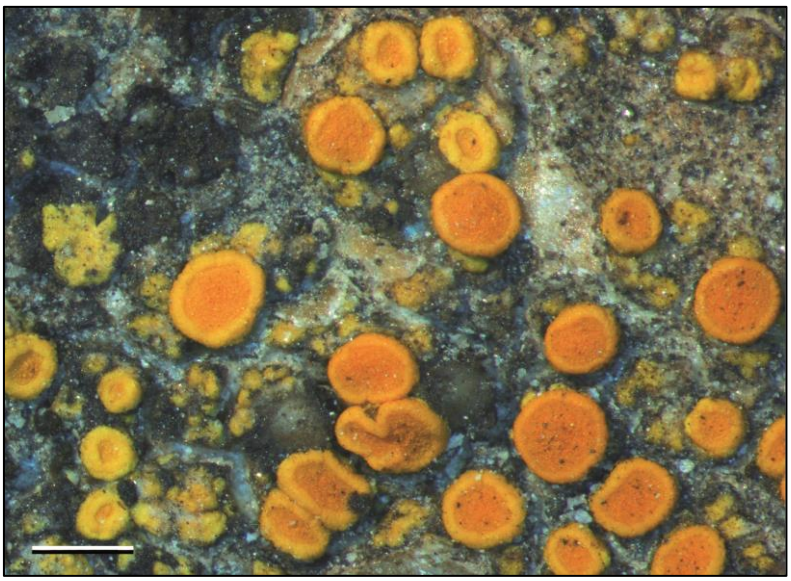

Figure 5. *Amundsenia approximata*, habitus (*Søchting* 4471). Scale: 0.5 mm. (Photograph: IGB).

Notes: The distinction of *Caloplaca cacuminum* from *A. approximata* is not clear. *Caloplaca cacuminum* was described from the Alps in 1953, and was later reported from Greenland (Hansen et al. 1987). Molecular studies are needed to establish if the two species can be merged.

Selected material studied: Greenland: Disko Island, Qeqertarsuaq/Godhavn, 69.271º N, 53.503º W, 1982, *Poelt & Ullrich* (GZU); S-Greenland, Narsaq Community, Narsarssuaq, Sutuluaqqap Quappaa Kua, 61º 9.3’ N, 45º 24’ W, 2005, *U. Søchting* 10490 (C); Umanak, Marmorilik, 71.322º N, 51.374º W, 1983, *Poelt & Ullrich* (GZU).

—Iceland: N-Múlasysla, NW of Mödrudalur, Vegaskard, 65º 26' 30" N, 15º 58' W, 1997, *U. Søchting* 7529 (C). —Norway: Finnmark: Alta county, Vassbotndalen, UTM: EC 6964, 1983, *U. Søchting* 4471 (C). Hordaland: Ulvik kommune, Finse, Mt. St. Finsenuten, UTM: 32W 041606 672088, 2002, *U. Arup* L02346 (UPS). Nordland: Vega Island, Valla, 65.666º N, 11.929º E, 1972, *G. Degelius* (UPS). Oppland: Dovre, Grimsdal at Verkensætri, UTM: NP 2881, 1985, *U.* Søchting 5321 (C); Dovre, Tverråi, N of Grimsdalshytta, UTM: NP 3385, 1985, *U. Søchting* 5443 (C). Sor-Trondelag: Oppdal, Alpine Station, UTM: NQ1457, 1983, *Sivertsen* (C). Troms: S of Skibotndalen, between Luhcajávri and Stuoraoaivi, 69º 15' N, 20º 24' E, 2003, *U. Søchting* 10080 (C). —Svalbard: Albert I Land, Mitrahalvøya, Erlingvatnet, UTM: VJ 26 01, 1989, *U. Søchting* 6039 (C); Nordenskjöld Land, Reindalen N of Sørhytta, UTM: WG 2058, 1989, *U. Søchting* 5530 (C); Oscar II Land, Brøggerhalvøya, Kiærstranda, UTM: VH2464, 1989, *U. Søchting* 6117 (C); Sabine Land, Sassendalen at Fredheim, 78º 21' 23" N, 16º 57' 42" E, 1986, *U. Søchting* 5855 (C). —Russia: Central Siberia: Taimyr Peninsula, Byrranga Mts, in the vicinity of northern extremity of Levinson-Lessing Lake, 74º 33' N, 98º 34' E, 1994, *M. Zhurbenko* 94474 (C); Jamalo-Nenetskij, Raiis Massive, Alpine meadow W of 134 km railway post, 67º N, 65º 35' E, 1993, *U. Søchting* 6693 (C). —Sweden: Härjedalen: Ulvberget, *U. Arup* L02239 (LD); Tännäs, 6km SE of Mt. Skarsen, 1988, *R. Santesson* 32467 (UPS). Jämtland: Undersåker par., Mt. Välliste, 8 km WSW of Undersåker, UTM: RT90: 702049 136637, 2002, *U. Arup* L02084 (LD); Åre, Stalltjärnstugan, 63.475º N, 12.559º E, 1952, *Sundell* (UPS). Norrbotten: Lule Lappmark, Jokkmokk par., Padjelanta National Park, foot of Allak *c*. 3.5 km SSW of the peak Allaktjåhkkå, UTM: RT90: 7479814 1535934, *U. Arup* L04213 (LD); Torne Lappmark, Abisko, Abiskojåkk, 68.308º N, 18.661º E, 1919, *Magnusson* 2683b (UPS). Västerbotten: Åsele Lappmark, Vilhelmina parish, *c*. 20 km ESE of Saxnäs, UTM: WN 356021, 1991, *U. Søchting* 6294 (C). —USA: Alaska: Denali Park at access road, 65º 33' N, 148º 53' W, 1996, *U. Søchting* 7454 (C).

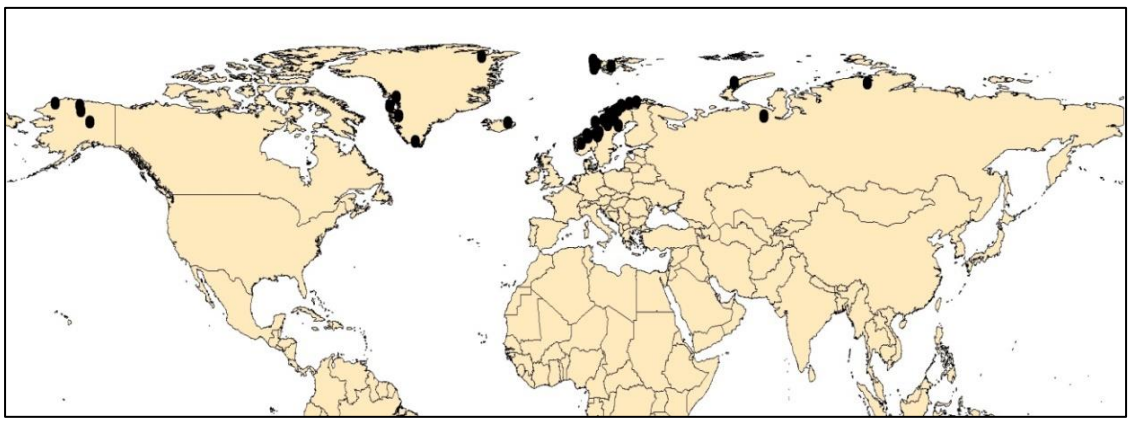

Figure 6. *Amundsenia approximata*, distribution.

Amundsenia austrocontinentalis Garrido-Benavent, Søchting, Pérez- Ortega & Seppelt sp. nov. (Figure 7)

MYCOBANK NO.: MB 808604

Diagnosis: Thallus crustose, composed of flat areoles that are irregular to minutely lobate at the margins, deep yellow to pale orange. Apothecia sessile, with flat, matt discs, usually with orange pruina. Apothecium margin very thick in young apothecia. Spores polardiblastic, 11 × 5.5 mm; septum *c*. 3 mm.

Type: Antarctica, Ingrid Christensen Coast, Vestfold Hills, Mule Peninsula, west of Clear Lake, 8 m a.s.l., 68º 39' S, 77º 57' 20" E, on small stones in a glacial till, 2 February 1979, *R. D. Seppelt* (ADT 8895 –holotype; C–isotype).

Thallus crustose, saxicolous, areolate, up to 3 cm wide. Prothallus absent. Areoles 0.2–0.8 mm wide (n = 26) and 0.1–0.3 mm high (n = 25), flat, with irregular to sometimes minutely lobate margins, deep yellow to pale orange, becoming whitish when abraded or dead. Thallus cortex paraplectenchymatous with cell lumina 2.2–3.5 mm wide (n = 20). Photobiont trebouxioid.

Apothecia lecanorine to zeorine when mature, usually one per areole, scarce to numerous, rather dispersed but occasionally aggregated, regular to deformed by compression, sessile, 0.2–1.5 mm wide (n = 61). Disc mainly flat, rarely slightly concave when well developed, and sometimes somewhat convex when mature, mostly pale orange, matt, usually with orange pruina. Apothecial margin initially very thick, but eventually often excluded and hidden below the disc, (50–) 117 ± 35 (–220) mm thick (n = 38). Thalline exciple often persistent, but may also be excluded early, deep greenish yellow to pale orange. Proper exciple distinct, thick even in mature apothecia, (30–) 61 ± 14 (–90) mm (n = 56), concolorous with the disc or slightly paler. Proper exciple tissue prosoplectenchymatous consisting of non-isodiametric cells with lumina 3.8–7.5 mm long and 1–2 mm wide (n = 15). Hypothecium hyaline, consisting of densely interwoven hyphae. Hymenium hyaline, (43–) 58 ± 7.5 (–76) mm high (n = 43). Epithecium with dark orange medium coarse epipsamma. Paraphyses (1.7–) 2.4 ± 0.4 (–3.1) mm thick (n = 63), septate, simple to sparingly branched at the top, mostly moniliform, apically gradually slightly inflated or rarely with an attenuated cap, (3.1–) 4.7 ± 0.7 (–6.2) mm thick (n = 120) apical cells. Asci clavate, with 8 spores, (41.5–) 46.5 ± 4 (–54) mm long and (12–) 12.5 ± 1 (–14.5) mm wide (n = 10). Ascospores polardiblastic, ellipsoid, rarely subcylindrical with rounded ends, (8–) 11 ± 1 (–13.5) × (4–) 5.5 ± 0.5 (–6.5) mm (n = 86); length/width ratio (1–) 2 ± 0.2 (–2.6); ascospore septa (2–) 2.9 ± 0.3 (–3.5) mm thick; ratio of ascospore length/septum width (3–) 3.8 ± 0.4 (–5).

Conidiomata not seen.

Secondary chemistry: Thallus and apothecia K+ purple. Chemosyndrome A of Søchting (1997).

Etymology: The name *austrocontinentalis* is based on the currently known distribution of the new species, which has been found in Continental Antarctica.

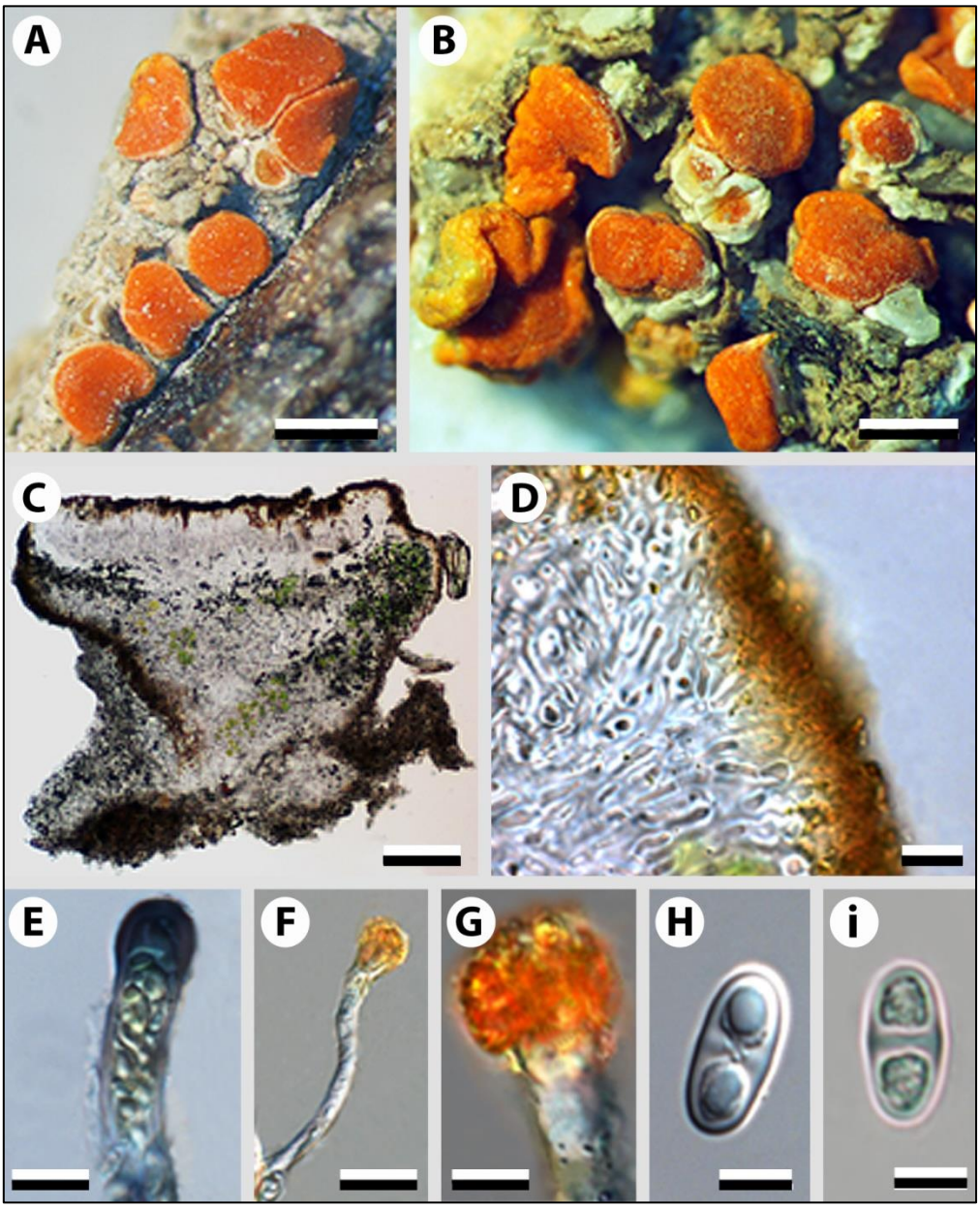

Figure 7. *Amundsenia austrocontinentalis*, habitus (A–B) and anatomical characters (C–I). (A) Holotype (*R. D. Seppelt*, ADT 8895). (B) Apothecia (*J. Raggio*, MAF-Lich 18901). (C) Cross section of an apothecium. (D) Cross section of a proper exciple. (E) Mature ascus. (F) Paraphyse. (G) Paraphyse apical cell. (H–I) Ascospores. Scales A–B = 0.5 mm, C = 100 µm, D–F = 10 µm, G–I = 5 µm. (Photographs: IGB).

Ecology and distribution: *Amundsenia austrocontinentalis* is frequently found growing on granite rocks but some specimens have been found on stone flakes in moraine debris, rock fragments amongst dolerite blocks in felsenmeer or on scoria rubble in scree. This species commonly grows in small crevices of large granitic rocks

in more or less exposed areas. It is known from the supralitoral level in coastal sites (8 m a.s.l.) to mountains, 320–750 m a.s.l. Accompanying species: *Austroplaca darbishirei*, *Lecanora* spp., *Lecidea cancriformis*, *Muellerella pygmaea* and *Rhizoplaca melanophthalma*. The species is so far known only from Continental Antarctica, in the Vestfold Hills (Ingrid Christensen Coast) and Southern Victoria Land (Figure 8). It may be locally abundant, for example in the McMurdo Dry Valleys.

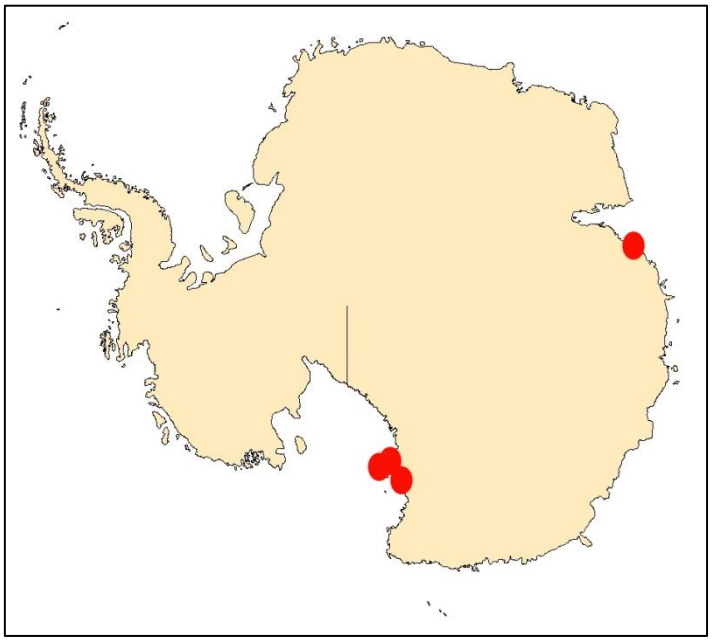

Figure 8. *Amundsenia austrocontinentalis*, distribution.

Notes: There are three samples (ADT 21115, ADT 20302, ADT 19147) whose spore morphology and septum differ from the other specimens analysed, and that better resemble those of *Amundsenia approximata*, especially in the shorter septa, (2.1–) 2.5 ± 0.2 (–2.9) mm, ratio of ascospore length/septum width (4.3–) 5.5 ± 0.8 (–8.3) (n = 26). However, the spore size of these peculiar specimens is far greater compared with the latter species: (11–) 13.5 ± 1.5 (–17.5) × (5.5–) 6.5 ± 0.5 (–8) mm, length/width ratio (1.5–) 2.1 ± 0.3 (–2.8) (n = 26), whereas *A. approximata* has mean values of 11 ± 1.5 × 4 ± 0.5 mm (n = 10). Accordingly, we have decided not to use any quantitative data of the three samples mentioned above when computing the different measurements for *A. austrocontinentalis*. Moreover, the apothecia of the sample ADT 21115 are clearly stipitate as in *Charcotiana antarctica*, with a protrusion (stipe) 0.10–0.25 mm tall and overall height between 0.3–0.7 mm (n = 7). Morphology, colour, secondary chemistry and other microscopic features are the same as in the other *A. austrocontinentalis* samples. At present, *nrITS* sequences are not available for these three specimens; therefore, we cannot corroborate the novelty of a putative new species either.

Even though *C. antarctica* and *A. austrocontinentalis* are molecularly well delimited and normally also macroscopically distinct, they may occasionally be difficult to separate (Supplementary Table 1). *Charcotiana antarctica* can be distinguished by its deeper orange thallus, with scattered, bullate areoles that usually form protrusions, which can develop into somewhat branched-coralloid structures, deep orange, epruinose discs, and stipitate apothecia with thin apothecial margins. The latter feature should be used with caution because both species are quite variable, even within the same sample, and show overlapping value ranges. Additionally, the thallus of *A. austrocontinentalis* is commonly paler, with flat areoles, with flat, matt discs covered by orange pruina, and with thicker apothecial and proper margins. Microscopically, it can be difficult to separate the two species due to the overlapping ranges, but *C. antarctica* tends to have longer spores with thicker septa compared to those of *A. austrocontinentalis*.

Both *C. antarctica* and *A. austrocontinentalis* tend to reduce their interface with the rock substratum by the formation of microstipitate areoles and apothecia. This is a characteristic of many other Antarctic lichens, including *Austroplaca frigida* (see below), and is even more pronounced where the thallus becomes microfruticose with all photosynthetically active parts elevated from the rock, as seen in *Caloplaca scolecomarginata* and *Huea coralligera* (Ott & Sancho 1993; Søchting & Olech 2000); this separation from the rock may improve temperature conditions in the photosynthetic and reproductive parts of the lichen and was previously noted, particularly in eutrophicated sites, by Lamb (1968), Jacobsen & Kappen (1988) and Olech (1990).

Additional material studied: Antarctica: Ingrid Christensen Coast: Vestfold Hills, 500 m South of Pauk Lake, 25 m a.s.l., 68º 34’ 40” S, 78º 28’ 30” E, 1979, *R. D. Seppelt* (ADT 9015). Southern Victoria Land: Ross Island, Scott Base Area, 150 m NW seismic station, 77º 51’ S, 166º 45’ E, 1997, *R. D. Seppelt* (ADT 20302); Kar Plateau, south eastern end, 76º 56’ S, 162º 20’ E, 1992, *R. D. Seppelt* (ADT 19147); McMurdo Dry Valleys, Garwood Valley, 78º 2.046’ S, 163º 56.237’ E, 1999, *R. D. Seppelt* (ADT 21115); 360 m a.s.l., 78º 1’ 36.4” S, 163º 51’ 36.4” E, 2009, *J. Raggio* (MAF-Lich 18901); Upper Garwood, 688 m a.s.l., 78º 2.173’ S, 163º 50.191’ E, 2009, *A. de los Ríos* (MAF-Lich 18171); 671 m a.s.l., 78º 3.454’ S, 163º 48.531’ E, 2009, *A. de los Ríos* (MAF-Lich 18173); Upper Garwood/Upper Miers Valleys area, *c*. 1 km ESE of Shangri-La Camp, 750 m a.s.l., 78º 3’ 28.4” S, 163º 46’ 10” E, 2009, *R. D. Seppelt* (ADT 27534); *c*. 1.5 km ENE of Shangri-La Camp, 750 m a.s.l., 78º 3’ 29.6” S, 163º 49’ 17.8” E , 2009, *R. D. Seppelt* (ADT 27537); Miers Valley, 320 m a.s.l., 78º 5’ 50.6” S, 163º 43’ 7.3” E, 2000, *R. D. Seppelt* (ADT 21966); between both glaciers, close to a stream, 171 m a.s.l., 78º 6.012’ S, 163º 48.603’ E, 2009, *A. de los Ríos* (MAF-Lich 18174); plateau, 521 m a.s.l., 78º 6.825’ S, 163º 51.225’ E, 2009, *A. de los Ríos* (MAF-Lich 18172).

Austroplaca frigida Søchting & Garrido-Benavent nom. nov. (Figure 9)

MYCOBANK NO.: MB 808605

Caloplaca frigida Søchting in Søchting & Olech. Bibl. Lichenol. 75: 24 (2000), nom. illeg., non *Caloplaca frigida* (Paulson) Zahlbr. (1930)

Type: Antarctic Continent, Dronning Maud Land, Vestfjella, the nunatak Basen, January 1992, *G. Thor* 10559 (S –holotype; C, CRA–isotypes).

Austroplaca frigida may be an overlooked species in Continental Antarctica (Figure 10). It has not been collected outside Continental Antarctica so far. It was described in Søchting & Olech (2000) as *Caloplaca frigida* by Søchting, who overlooked that the combination *Caloplaca frigida* (Paulson) Zahlbruckner had been made in 1930 in Cat. Lich. Univers. 7: 139 based on the basionym *Placodium frigidum* Paulson 1925.

The molecular analysis based on *nrITS* sequences has shown *Caloplaca frigida* Søchting to belong into *Austroplaca* (Figure 2), and to be closely related to two Antarctic species, *A. soropelta* and *A. darbishirei*, which have well-developed orange-yellow thalli producing soredia (Søchting & Castello 2012). *Austroplaca frigida* is often reduced to scattered apothecia; it may be confused with the above species, but has a narrower spore septum (1.5–2 mm).

Selected material studied: Antarctica: Southern Victoria Land: Kar Plateau south east end, 76º 56’ S, 162º 20’ E, 1992, *R. D. Seppelt* (ADT 19175); Garwood Valley, 78º 2.046’ S, 163º 56.237’ E, 1999, *R. D. Seppelt* (ADT 21118); 78º 2.103’ S, 163º 56.38’ E, 1999, *R. D. Seppelt* (ADT 21126); 78º 2.046’ S, 163º 56.237’ E, 1999, *R. D. Seppelt* (ADT 21117); 78º 2.103’ S, 163º 56.38’ E, 1999, *R. D. Seppelt* (ADT 21125); 78º 2.103’ S, 163º 56.38’ E, 1999, *R. D. Seppelt* (ADT 21123); 78º 2.89’ S, 165º 42.29’ E, 2009, *Sancho & Seppelt* (MAF); McMurdo Dry Valleys, Upper Garwood Valley area, *c*. 1 km W of Shangri-La camp, 78º 2’ 53.5” S, 163º 42’ 17.5” E, 2009, *R. D. Seppelt* (ADT 27513); 340 m a.s.l., 78º 1’ 38.4” S, 163º 50’ 20” E, 2009, *J. Raggio* (MAF-Lich 18890, MAF-Lich 18890-2, MAF-Lich 18904); plateau, 78º 1’ 38.4” S, 163º 30’ 20” E, 2009, *J. Raggio* (MAF-Lich 18902, MAF-Lich 18902-2). Windmill Islands: Ford Island, central, 66º 24’ 25” S, 110º 30’ 50” E, 1983, *R. D. Seppelt* (ADT 14232).

Figure 9. *Austroplaca frigida*, habitus (*J. Raggio*, MAF-Lich 18902-2). Scale: 0.5 mm. (Photograph: IGB).

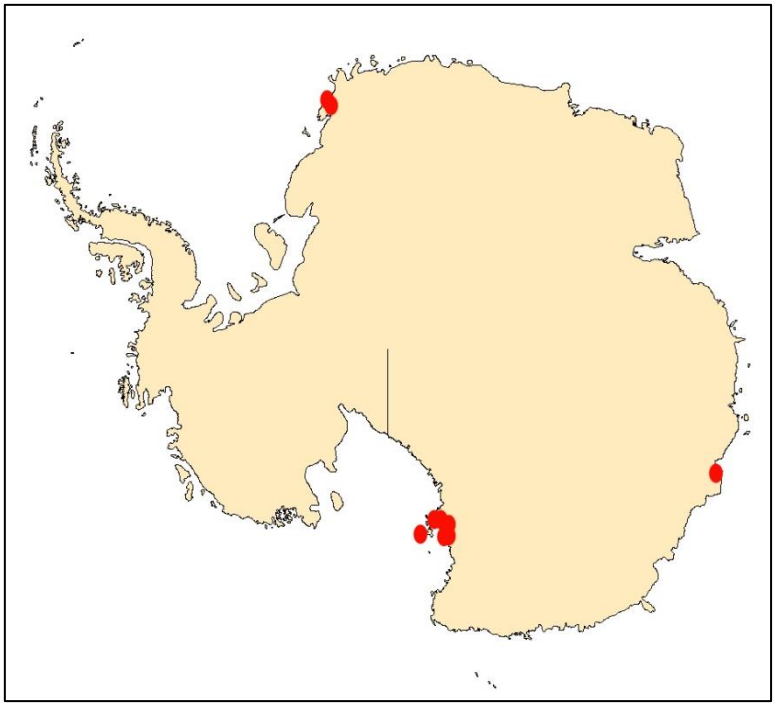

Figure 10. *Austroplaca frigida*, distribution.

Supplementary Table 1. Morphological and anatomical comparison between *Charcotiana antarctica* and *Amundsenia austrocontinentalis*.

	Areole width (mm)	Areole height (mm)	Thallus with ± coralloid protrusions	Thallus colour	Apothecium diam. (mm)	Apothecial margin (µm)	Proper margin (µm)	Disc colour	Disc pruinose
Charcotiana antarctica	0.1–3 (n = 40)	0.1–0.6 (n = 34)	Often	Pale to mostly deep orange	0.2–1.2 (n = 26)	(60–) 95 ± 16 (–120) (n = 24)	(20–) 43 ± 11 (–70) (n = 45)	Deep orange to dark orange brown when old	Never
Amundsenia austrocontinentalis	0.2–0.8 (n = 26)	0.1–0.3 (n = 25)	Never	Deep yellow to pale orange	0.2–1.5 (n = 61)	(50–) 117 ± 35 (–220) (n = 38)	(30–) 61 ± 14 (–90) (n = 56)	Mostly pale orange	Usually

	Paraphyse apical cell width (µm)	Spore length × width (µm)	Spore length/width ratio	Spore septum width (µm)	Ratio of ascospore length/septum width
Charcotiana antarctica	(2.9–) 5.2 ± 0.9 (–7) (n = 49)	(8.5–) 12 ± 1.5 (–16) × (5–) 6.5 ± 0.5 (–8) (n = 90)	(1.3–) 1.9 ± 0.3 (–2.9)	(2.4–) 3.6 ± 0.7 (–5.7)	(2–) 3.4 ± 0.5 (–4.6)
Amundsenia austrocontinentalis	(3.1–) 4.7 ± 0.7 (–6.2) (n = 120)	(8–) 11 ± 1 (–13.5) × (4–) 5.5 ± 0.5 (–6.5) (n = 86)	(1–) 2 ± 0.2 (–2.6)	(2–) 2.9 ± 0.3 (–3.5)	(3–) 3.8 ± 0.4 (–5)

Appendix 1. Sequences used in any of the two phylogenetic analyses: newly produced in bold and others downloaded from GENBANK.

Species	Country, collector, collector nr, herbarium	*nrITS*	*nuLSU*	*mtSSU*
Amandinea punctata	Unknown	AF250780	AY340536	AY143399
Amundsenia austrocontinentalis 1	Antarctica, Upper Garwood, *A. de los Ríos*, MAF-Lich 18173	JX036068		**KJ789975**
A. austrocontinentalis 2	Antarctica, Miers Valley, *A. de los Ríos*, MAF-Lich 18174	JX036036		
A. austrocontinentalis 3	Antarctica, McMurdo Dry Valleys, *Seppelt* 27537, HO	**KJ789961**		
A. austrocontinentalis 4	Antarctica, Miers Valley, *Seppelt* 21966, HO	**KJ789962**		
A. approximata 1	Greenland, *Søchting* 10490, C	**KJ789963**		
A. approximata 2	Sweden, *Arup* L02084, LD	**KJ789964**		
A. approximata 3	Norway, *Arup* L08179, LD	**KJ789965**	**KJ789972**	**KJ789974**
Athallia cerinelloides	Sweden, *Arup* L06208, LD (*nrITS*); Swe., *Arup* L07202, LD (*nuLSU*, *mtSSU*)	KC179339	KC179147	KC179477
A. holocarpa	Sweden, *Arup* L04019, LD	J346540	KC179148	KC179478
A. pyracea	Sweden, *Arup* L04039, LD	J346553	KC179149	KC179479
A. scopularis	Iceland, *Søchting* 7521, C	KC179340	KC179150	KC179480
Austroplaca ambitiosa	U.K., Falkland Isl., *Lewis Smith* 11027, AAS (*nrITS*, *nuLSU*)	KC179081	KC179151	
	Chile, *Søchting* 11271, C (*mtSSU*)			KC179481
A. cirrochrooides	Chile, *Søchting* 11300, C	KC179082	KC179152	KC179482

A. darbishirei	Antarctica, Antarctic Peninsula, *Søchting* 11401, C	KC179083	KC179153	KC179483
A. erecta	New Zealand, 26-3-2000, *Eagle*, C	KC179084		
A. frigida 1	Antarctica, Dry Valleys, Garwood Valley, *J. Raggio*, MAF-Lich 18904	JX036061		
A. frigida 2	Antarctica, Dry Valleys, Garwood Valley, *J. Raggio*, MAF-Lich 18890	JX036062		
A. frigida 3	Antarctica, Dry Valleys, Garwood Valley plateau, *J. Raggio*, MAF-Lich 18902-2	JX036127		
A. hookeri	Antarctica, South Shetland Isl., *Søchting* 7611, C	KC179085	KC179154	KC179484
A. lucens	France, Kerguelen Isl., *Søchting* 9417, C	KC179087	KC179155	KC179485
A. millegrana	Chile, Søchting 11330, C (ITS); *Søchting* 10176, C (*nuLSU*)	KC179088	KC179156	
	Chile, *Søchting* 10350, C			KC179486
A. soropelta	Iceland, Frödén 650, LD (*nrITS*); Iceland, *Søchting* 7536, C (*nuLSU*, *mtSSU*)	KC179089	KC179157	KC179487
Calogaya arnoldii	Sweden, Arup L06205, LD (*nrITS*); Sweden, *Søchting* 10610, C (*nuLSU*)	KC179342	KC179165	
C. arnoldii s.lat	Denmark, *Søchting* 7472, C	KC179343	KC179166	KC179497
C. decipiens	Denmark, 1995, *Søchting*, C	KC179344	KC179167	
	Sweden, *Arup* L06187, LD			KC179498
Caloplaca cerina	Norway, Svalbard, *Elvebakk* 03:084, TROM	KC179425	KC179168	KC179499
Cerothallia luteoalba	Sweden, *Frödén* 1869, LD	KC179099	KC179177	KC179511
C. subluteoalba	Australia, VIC, *Kondratyuk* 20433, LD isotype	KC179100		KC179512
C. yorkensis	Australia, VIC, *Kärnefelt* 996101, LD	KC179101	KC179178	KC179513
Charcotiana antarctica 1	Antarctica, Victoria Land, *Bersan* A815, TSB	**KJ789966**		**KJ789976**
C. antarctica 2	Antarctica, Victoria Land, *Bersan* A833, TSB	**KJ789967**		

C. antarctica 3	Antarctica, Northern Victoria Land, *Seppelt* 25454, HO	**KJ789968**		
C. antarctica 4	Antarctica, Northern Victoria Land, *Seppelt* 25292, HO	**KJ789969**		
C. antarctica 5	Antarctica, Southern Victoria Land, *Smykla*, KRAM-L-63612	**KJ789970**	**KJ789973**	
C. antarctica 6	Antarctica, Northern Victoria Land, *Seppelt* 25038, HO	**KJ789971**		
Dufourea alexanderbaii	South Africa, *Feuerer & Thell* 60487b, LD holotype	KC179350	KC179179	KC179514
D. angustata	Australia, NSW, *Kondratyuk* 20483, CANB holotype	KC179351	KC179180	
	Australia, NSW, *Kärnefelt* 20045001 & *Kondratyuk*, LD			KC179515
D. bonae-spei	South Africa, *Feuerer & Thell* 60485ab, LD	KC179353		
	South Africa, *Feuerer & Thell* 60493a, LD		KC179181	KC179516
D. dissectula	South Africa, *Feuerer & Thell* 604796, LD holotype	KC179355	KC179182	KC179517
D. flammea	South Africa, *Feuerer & Thell* 60488a, HBG	KC179357	KC179183	KC179518
D. karrooensis	South Africa, *Wetschnig W. & U.*, GZU 133-8p	KC179358		
	South Africa, 10-9-2010, *Fröberg* s.n., LD		KC179184	KC179519
D. ligulata	Australia, TAS, *Frödén* 1234, LD	KC179359	KC179185	KC179520
Flavoplaca citrina	Sweden, *Arup* L03013, LD	DQ173224	KC179186	KC179521
F. marina	U.K., England, *Arup* L92106, LD (*nrITS*); Swe., *Arup* L04057, LD (*nuLSU,mtSSU*)	AF353946	KC179187	KC179522
F. microthallina	Sweden, *Søchting* 7480, C	KC179368	KC179188	KC179523
F. oasis	Sweden, *Arup* L03017, LD	FJ346546	KC179189	KC179524
Gondwania cribrosa	Australia, TAS, *Søchting* 11581, C	KC179102	KC179192	KC179526
G. regalis	Antarctica, Antarctic Peninsula, *Søchting* 11416, C	KC179103		

	Antarctica, Antarctic Peninsula, *Søchting* 11427, C		KC179193	KC179527
Gyalolechia flavorubescens	Estonia, *Søchting* 10127, C	KC179439	KC179197	KC179531
Josefpoeltia parva	Argentina, *Frödén* 1671, LD	KC179296	KC179204	KC179539
Leproplaca xantholyta	Austria, *Arup* L97278, LD (*nrITS*), Spain, *Søchting* 9675, C (*nuLSU*, *mtSSU*)	KC179451	KC179208	KC179542
Orientophila subscopularis	Japan, *Frisch* Jp99, LD holotype	KC179375		KC179546
Pachypeltis castellana	Denmark, Greenland, *Søchting* 10500, C (*nrITS*)	KC179105		
	Greenland, *Søchting* 10470, C (*mtSSU*)			KC179547
P. invadens	Norway, Svalbard, *Elvebakk* 03:109, TROM	KC179108	KC179212	KC179548
Pachypeltis sp.	China, *Abbas & Mahamat* 500113, XJUG	KC179110	KC179214	KC179550
Parvoplaca sp.	Sweden, *Arup* L10208, LD	KC179113	KC179215	KC179551
P. suspiciosa	Russia, *Hermansson* 16839, priv. herb.	KC179115		
	Sweden, *Hermansson* 18005, priv. herb.			**KJ810561**
P. tiroliensis	Sweden, *Arup* L02364, LD (*nrITS*); Sweden, *Frödén* 1945, LD (*nuLSU*, *mtSSU*)	KC179116	KC179216	KC179552
Physcia aipolia	Unknown (*nrITS*, *mtSSU*); Wedin 6145, BM (*nuLSU*)	AF250803	AY300857	AY143406
Polycauliona candelaria	Iceland, *Søchting* 7488, C	KC179379	KC179217	KC179553
P. coralloides	Mexico, *Søchting* 9887, C	KC179380	KC179218	KC179554
P. ignea	Mexico, *Moberg* 10402, UPS (*nrITS*); Mexico, *Søchting* 9879, C (*nuLSU*, *mtSSU*)	KC179382	KC179219	KC179555
P. luteominia	U.S.A., California, *Wetmore* 73797, LD	KC179387		
	U.S.A., California, *Søchting* 11219, C		KC179220	KC179556
P. phlogina	Sweden, *Göransson* L02055, LD	DQ173235	KC179221	KC179557

P. polycarpa	U.S.A., Minnestota, *Wetmore* 80511, LD	KC179389		
	Denmark, 3.V.1995 *Fredtoft*, C (*nuLSU*); Denmark, *Søchting* 10507, C (*mtSSU*)		KC179222	KC179558
P. rosei	U.S.A., California, *Arup* L89165, LD (*nrITS*)	KC179390		
	U.S.A., California, *Søchting* 11225, C (*nuLSU*, *mtSSU*)		KC179223	KC179559
P. stellata	U.S.A., California, *Arup* L09154, LD	KC179400	KC179229	KC179566
P. tenax	U.S.A., California, *Westberg* 949, LD	KC179401	KC179230	KC179567
P. tenuiloba	Mexico, *Nash* 40170, LD	KC179402	KC179231	KC179568
P. thamnodes	Mexico, *Søchting* 9878, C	KC179403	KC179232	KC179569
P. verruculifera	Sweden, *Arup* L06209, LD (*nrITS*); Iceland, *Søchting* 7522, C (*nuLSU*, *mtSSU*)	KC179404	KC179233	KC179570
Pyrenodesmia variabilis	Austria, *Arup* s.n., LD (*nrITS*); Sweden, *Arup* L03134, LD (*nuLSU*, *mtSSU*)	AF353963	KC179234	KC179572
Rufoplaca tristiuscula	Norway, *Arup* L08171, LD	KC179460	KC179237	KC179575
Rusavskia elegans	Iceland, *Søchting* 7530, C	KC179406		
	Russia, *Zhurbenko* 96376, C		KC179238	KC179576
R. sorediata	Norway, *Lindblom* 1229, BG (*nrITS*); Iceland, *Søchting* 7538, C (*nuLSU*, *mtSSU*)	AY453647	KC179239	KC179577
Shackletonia hertelii	Chile, *Søchting* 10349, C	KC179118		KC179579
	Antarctica, South Shetland Isl., *Søchting* 7932, C		KC179240	
S. sauronii	Antarctica, South Shetland Isl., *Søchting* 7654, C	KC179120	KC179241	KC179580
Sirenophila eos	Australia, NSW, *Kärnefelt* 20044702, LD	KC179300	KC179246	KC179585
Solitaria chrysophthalma	Sweden, *Arup* L03101, LD	KC179408	KC179251	KC179590
Squamulea galactophylla	U.S.A., Kansas, *Morse* 10997, LD	KC179122		

S. kiamae	Australia, NSW, *Kondratyuk* 20480, LD isotype	KC179123		
S. squamosa	U.S.A., Arizona, *Kärnefelt* AM960105, LD	KC179125	KC179252	KC179591
S. subsoluta	Austria, *Arup* L97072, LD	AF353954	KC179253	KC179592
Teloschistes flavicans	Chile, *Frödén* 1624, LD	KC179317	KC179255	KC179594
Variospora velana	Italy, *Arup* L07194, LD (*nrITS*); Italy, *Arup* L07123, LD (*nuLSU*, *mtSSU*)	KC179476	KC179265	KC179605
Villophora isidioclada	Chile, *Søchting* 10185, C	KC179325	KC179266	KC179606
Wetmoreana texana	Mexico, *Søchting* 9925, C	KC179337	KC179273	KC179612
Xanthocarpia crenulatella	Austria, *Søchting* 9359, C	KC179126	KC179274	KC179613
X. epigaea	Spain, *Etayo* 21453, C (*nrITS*, *nuLSU*); Germany, 2006, *Huneck*, C (*mtSSU*)	KC179127	KC179275	KC179614
X. marmorata	Italy, *Arup* L07030, LD	KC179131	KC179276	KC179615
X. ochracea	France, 1998, *Roux*, C (*nrITS*); Italy, *Arup* L07009, LD (*nuLSU*);	KC179132	KC179277	
	Italy, *Arup* L07124, LD (*mtSSU*)			KC179616
Xanthopeltis rupicola	Chile, *Frödén* 1654, LD	KC179146	KC179286	KC179626
Xanthoria calcicola	Sweden, *Arup* L97372, LD	AF353944		
	Spain, *Søchting* 9627, C		KC179287	KC179627
X. parietina	Denmark, 2002, *Søchting* s. n., C	KC179411		KC179629
	Denmark, *Søchting* 7157, C		KC179289	
Xanthomendoza borealis	Greenland, *Søchting* 10499, C	KC179133		
	Russia, *Zhurbenko* 94411, UPS		KC179278	KC179617

X. fallax	Austria, *Arup* L97529, LD (*nrITS*); U.S.A., Wisconsin *Søchting* 9566, C (*nuLSU*)AF353955		KC179279	
	U.S.A., Michigan, *Søchting* 9566, C (*mtSSU*)			KC179618
X. hasseana	U.S.A.,Arizona, *Søchting* 7014, C	KC179136	KC179280	KC179619
X. mendozae	Chile, *Søchting* 10209, C	KC179138	KC179281	KC179620
X. novozelandica	New Zealand, *Kärnefelt* 999003, LD	KC179140	–	KC179621
X. poeltii	Sweden, *Kondratyuk* 2, LD holotype	KC179142		KC179622
	Denmark, *Søchting* 7473, C		KC179282	
X. trachyphylla	U.S.A., North Dakota, *Wetmore* 80270, LD	KC179143	KC179283	KC179623
X. ulophyllodes	Russia, 2006 *Kuznetsova*, H (*nrITS*), U.S.A., Wisconsin, *Søchting* 9571(*nuLSU*, *mtSSU*)	KC179144	KC179284	KC179624
X. weberi	U.S.A., North Carolina, *Søchting* 7241, C	KC179145	KC179285	KC179625

CAPÍTULO 2 (*CHAPTER 2*)

Austrostigmidium, un género nuevo de hongos liquenícolas austral de la familia *Teratosphaeriaceae* (*Capnodiales*, Ascomycota) emparentado con hongos meristemáticos colonizadores de rocas.

Referencia del artículo científico publicado:

Pérez-Ortega S, **Garrido-Benavent I** y de los Ríos A (2015) *Austrostigmidium*, a new austral genus of lichenicolous fungi close to rock-inhabiting meristematic fungi in *Teratosphaeriaceae*. Lichenologist 47(3): 143–156 doi:10.1017/S0024282915000031

Abstract

The new genus of lichenicolous fungi *Austrostigmidium* is described from Antarctica and Tierra del Fuego (Chile). It is characterized by the presence of black pseudothecia, pseudoparaphyses, fissitunicate, I-, KI- asci and 3-septate hyaline ascospores. So far, the only known species grows on *Mastodia tessellata* (*Verrucariales*, *Eurotiomycetes*). The new genus is compared with anatomically close genera. Based on *nuLSU* and *nuSSU* markers we inferred its phylogenetic relationships and found that it belongs to the family *Teratosphaeriaceae* (*Capnodiales*, *Dothideomycetes*) and is closely related to rock-inhabiting fungal species, as well as to the hyphomycetous lichenicolous fungus *Xanthoriicola*. Finally, the host-parasite interface has been analysed by means of transmission electron microscopy and fluorescence microscopy in order to describe the interactions among the new fungus and the symbionts forming the host lichen.

1. Introduction

Lichenicolous fungi represent a highly specialized group of fungi with life strategies ranging from saprotrophs to aggressive parasites (Lawrey & Diederich 2003). This wide range of nutritional modes further reflects the high phylogenetic diversity found in this group of fungi, recently revealed by several molecular studies (Crespo et al. 2010b; Millanes et al. 2011; Diederich et al. 2013; Ertz et al. 2013; Frisch et al. 2014; Pérez-Ortega et al. 2014; Suija et al. 2014). While research on lichenicolous fungi has received increased interest during the past decades, it is clearly geographically biased, with a greater focus concentrated in certain areas. Thus, if we compare polar and subpolar regions of both hemispheres, arctic and subarctic areas have received much more attention (e.g. Zhurbenko & Laursen 2003; Zhurbenko 2009a,b; Zhurbenko 2010) than their equivalents in the Southern Hemisphere (Lawrey & Diederich 2003; Hawksworth & Iturriaga 2006; Etayo & Sancho 2008). One aspect of lichenicolous infections that has received little attention is the characterization of the host-parasite interfaces (de los Ríos & Grube 2000; Grube & de los Ríos 2001; Lawrey & Diederich 2003). This is probably due to the need for more sophisticated techniques than light microscopy to identify and ultrastructurally characterize the interactions between lichenicolous fungi and components of the lichen host. During our study on the phylogeography of the lichen-forming fungus *Mastodia tessellata*, a lichenicolous fungus was discovered that grew abundantly on the surface of this species in samples collected in Antarctica and Tierra del Fuego. Morphological and anatomical characters, such as the perithecioid ascomata, the presence of periphyses and bitunicate 8-spored asci with 3-septate hyaline ascospores led us to consider its affinities with the genus *Pseudostigmidium*, recently described from southern South America (Etayo & Sancho 2008) and with *Stigmidium*. However, the presence of some characters deviating from these two genera led us to describe a new genus.

Here we describe the new genus *Austrostigmidium*, with the new species *A. mastodiae*, and discuss its possible affinities with apparently closely related genera. Furthermore, we shed light on its phylogenetic relationships by means of *nuLSU* and *nuSSU* markers data, demonstrating its adscription to the *Teratosphaeriaceae* (*Capnodiales*, *Dothideomycetes*). Finally, using transmission electron and fluorescence microscopies, we show that the new taxon interacts preferentially with the photobiont of *Mastodia tessellata* and discuss possible implications of these interactions for the lichen symbiosis.

2. Material and methods

2.1. Morphological studies

Specimens were examined under a Leica S8APO dissecting microscope, and macroscopic photographs were taken with a Leica EC3 image capture system. Hand-

made sections of ascomata were observed using a Zeiss Axioplan 2 microscope fitted with "Nomarski" differential interference contrast (DIC) and photographs were taken with a Zeiss AxioCam digital camera. Microscopic observations and measurements were made using material mounted in H_2O by means of the Zeiss Axiovision 4.8 image analyser system. 10% KOH, Lugol's iodine, without (I) or with (K/I) pre-treatment with KOH, lactophenol cotton blue and Blue Cresyl (BCr) were used both for tissue dissociation and examination, and for testing possible colour reactions of ascomatal elements and vegetative hyphae. Regarding measurements, the average, followed by its standard deviation and the maximum and minimum values (in parentheses) are given in each case. The length/width ratio gives minimum and maximum values, average and its standard deviation.

The voucher and type specimens are deposited in MA. Author citations follow MYCOBANK (http://www.mycobank.org/).

2.2. Taxon sampling, DNA extraction, PCR amplification, and DNA sequencing

DNA sequences were generated from five specimens from populations of Tierra del Fuego (Chile) and Antarctica (Appendix 1). Due to the tiny size of the fruiting bodies, about 10–15 pseudothecia were sampled from the same host thallus portion. A sterilized razor blade and an acupuncture needle were used for removing the pseudothecia from thalli and for cleaning their surface. The remnants were then further inspected under both the dissecting and light microscopes in order to avoid contamination by other fungi or algae. Genomic DNA isolation was performed by means of a modified version of the CTAB method (Cubero et al. 1999). In order to establish the phylogenetic position of the selected taxa we amplified, partially, the *nuLSU* and *nuSSU* rDNA regions, using the primer pairs LR0R (Rehner & Samuels 1994) and LR5 (Vilgalys & Hester 1990) for *nuLSU*, and nssu131–nssu1088 (Kauff & Lutzoni 2002) for *nuSSU*. PCR reactions were performed in a total volume of twenty microlitres, containing 5 µl of template DNA, 2 µl of each primer (10 µM), 10 µl of DNA AmpliTools Fast Master Mix (2x) (Biotools®); final volume was reached by adding distilled water. The PCR cycle for *nuLSU* was: an initial 5 min heating phase at 95°C, followed by 25 cycles of 28 s at 95°C, 28 s at 52°C and 30 s at 72°C, followed by identical 10 cycles but using 50°C for the annealing step; for *nuSSU*: initial denaturation for 5 min at 95°C, followed by 10 cycles of 30 s at 95°C, 30 s at 56°C and 30 s at 72°C, followed by identical 25 cycles but using 52°C for the annealing step; the final elongation for both *nuLSU* and *nuSSU* was 15 s at 72°C. The PCR reactions were visualized on 1% agarose gel stained with PRONASAFE nucleic acid stain solution (CONDA Laboratories). PCR products were purified and cleaned using the UltraClean® PCR Clean-Up Kit (MOBIO Laboratories, Inc.). Both complementary DNA strands were sequenced at MACROGEN EUROPE (The Netherlands). Electropherograms were checked and assembled using SEQMANII v.5.07© (Dnastar Inc.).

2.3. Sequence alignment and phylogenetic analysis

We retrieved 48 *nuLSU* and 23 *nuSSU* sequences from the GENBANK corresponding to species in the *Teratosphaeriaceae* (and 3 outgroup species) based on BLAST searches of the new generated sequences and previous studies on the family (Ruibal et al. 2009; Egidi et al. 2014). We aligned them together with the new sequences generated in this study (5 *nuLSU*, 2 *nuSSU*) (Appendix 1) using MUSCLE v.3.6 (Edgar 2004) and the resulting alignments were manually examined in BIOEDIT v.7.0.9 (Hall 1999). GBLOCKS v.0.91b (Castresana 2000) was used to remove ambiguously aligned regions, using the least restrictive options for removing gaps and allowing for gap in less than 50% of the sequences. The combined *nuLSU* + *nuSSU* dataset consisted of 1.677 bp (722 bp for *nuLSU* and 955 bp for *nuSSU*). JMODELTEST v.2.1.4 (Darriba et al. 2012) was used to select the best nucleotide substitution model for subsequent analyses using the Bayesian Information Criterion (BIC, Schwarz 1978). The GTR+I+Γ model was selected for *nuLSU* and the K80+I for *nuSSU*. Partitions were used for the combined *nuLSU* + *nuSSU* dataset in both analyses. The taxa *Capnodium coffeae*, *Leptoxyphium fumago* and *Polychaeton citri* were selected as outgroup. Maximum likelihood (ML) analyses were carried out using the online version of RAxML-HPC2 implemented in CIPRES Science Gateway (Stamatakis 2006; Stamatakis et al. 2008; Miller et al. 2010). Nodal support was evaluated using 1.000 bootstrap pseudoreplicates. Bayesian analyses were those implemented in MRBAYES v.3.2.2 on the CIPRES Science Gateway (Miller et al. 2010; Ronquist et al. 2012). Two parallel, simultaneous runs with four-chain runs were performed over 10 M generations starting with a random tree. Sampling was performed after every 100th step; the first 25% of saved data was discarded as "burn-in" and the 50% majority-rule consensus tree and posterior probabilities (PP) were calculated from the rest of trees. Convergence of chains and ESS values were checked in TRACER v.1.6 (http://tree.bio.ed.ac.uk/software/tracer/). Phylogenetic trees were visualized in FIGTREE v.1.3.1 and ADOBE ILLUSTRATOR CS5® was used for artwork. Bootstrap support values equal or higher than 70 and Bayesian posterior probabilities equal or higher than 0.95 were regarded as significantly supported. The combined, *nuLSU* + *nuSSU* ML tree was chosen as the working phylogenetic hypothesis.

2.4. Transmission electron microscopy

Small fragments of *Mastodia tessellata* thalli dwelling *Austrostigmidium* pseudothecia were fixed in 3% glutaraldehyde and 1% osmium tetroxide, dehydrated in a graded ethanol series, and embedded in Spurr's resin following the protocol described in de los Ríos & Ascaso (2001). Ultrathin sections were post-stained with lead citrate (Reynolds 1963) and observed in a Zeiss EM910 transmission electron microscope (TEM).

3. Results

3.1. Taxonomy

Austrostigmidium Pérez-Ortega & Garrido-Benavent, gen. nov. (Figure 1–2)

MYCOBANK NO.: MB 811127

Type: *Austrostigmidium mastodiae* Pérez-Ortega & Garrido-Benavent

Diagnosis: Vegetative hyphae present, hyaline to dark brown; pseudothecia sessile to semi-immersed, globose to subglobose; pseudothecial wall brown, paraplectenchymatous, ostiolate; periphyses abundant; short pendant filaments (pseudoparaphyses) present; asci clavate to subcylindrical, fissitunicate, ocular chamber present, I-, KI-; ascospores hyaline, not ornamented, 3-septate. Pycnidia sessile or with one third immersed in the host thallus, conical to subglobose; conidiogenous cells more or less ampulliform; conidiospores hyaline, simple, bacilliform, straight to curved.

Etymology: The generic name refers to its geographic origin (*australis*, southern) and *Stigmidium*, a genus to which the new taxon resembles anatomically.

Distribution: *Austrostigmidium* is known only from Maritime Antarctica and Tierra del Fuego (Chile).

Austrostigmidium mastodiae Pérez-Ortega & Garrido-Benavent sp. nov. (Figure 1–2)

MYCOBANK NO.: MB 811128

Type: Antarctica. South Shetlands. Livingston Island. Glaciar Rocoso, 3 m a.s.l.; 62º 42.824’ S, 60º 24.548’ W, 31 Jan 2014, *A. de los Ríos* (MA-Lich 18215).

Diagnosis: Vegetative hyphae hyaline to dark brown, torulose; pseudothecia globose to subglobose, (58−) 95.5 ± 18.9 (−130); pseudothecial wall brown, paraplectenchymatous, composed of 4−9 layers of polygonal cells; periphyses abundant; short pendant filaments (pseudoparaphyses) composed of two cells; hymenial gel I-, KI-; asci clavate to subcylindrical, fissitunicate, ocular chamber present (30.5−) 39.6 ± 4.8 (−48) × (8−) 11.1 ± 1.6 (−14.4) µm, 8-spored, I-, KI-; ascospores hyaline, not ornamented, 3-septate, halonate when young, (14.5−) 16.7 ± 1.3 (−20) × (3.5−) 4.1 ± 0.5 (−5) µm. Pycnidia present, conical to subglobose, (34−) 48 ± 10.1 (−65) × (32−) 36.7 ± 3.9 (−43) µm; conidiogenous cells more or less ampulliform, simple, hyaline, (3.5−) 5.1 ± 0.8 (−7) × (2.5−) 2.8 ± 0.25 (−3) µm; conidiospores hyaline, simple, bacilliform, straight to curved, (2.5−) 3. 4 ± 0.6 (−5) × (1−) 1.8 ± 0.2 (−1.5) µm.

Etymology: The epithet *mastodiae* refers to the host genus.

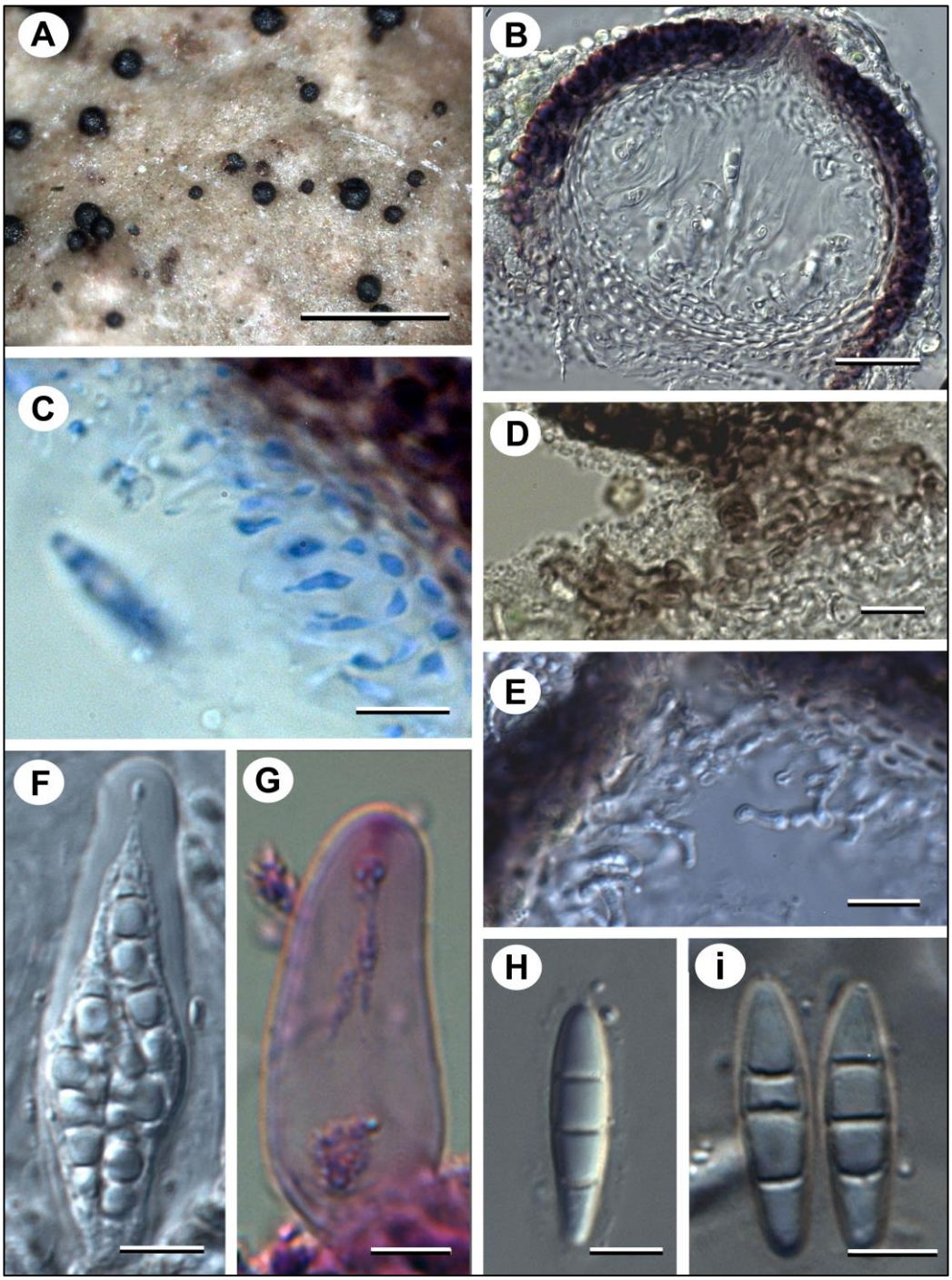

Figure 1. *Austrostigmidium mastodiae*, habitus (A) and anatomical characters (B–I). (A) Pseudothecia on the surface of *Mastodia tessellata*. (B) Longitudinal section of a pseudothecium (DIC). (C) Pendant filaments (pseudoparaphyses) in lactophenol cotton blue. (D) Detail of brown vegetative hyphae below the pseudothecium. (E) Periphyses (DIC). (F) Mature ascus showing ascospores (DIC). (G) Ascus tip in BCr showing ocular chamber and the stained apical apparatus. (H) Young ascospore with an apparent halo (DIC). (I) Mature ascospores (DIC). Scales: A = 500 µm, B = 25 µm, C–E= 10 µm, F–I = 5 µm. (Photographs: SPO & IGB).

Vegetative hyphae usually hyaline to light brown, torulose, usually immersed in the host thallus, rarely observed on the thallus surface, then dark brown, 2−3 µm width, I-, KI-, BCr+ violet. Pseudothecia globose to subglobose, black, usually with glossy appearance, (58−) 95.5 ± 18.9 (−130) µm (n = 36) in diam., sessile on the host thallus, or with the base slightly immersed; ostiolate, with a central ostiolum (12−) 15.5 ± 2.2 (−18) µm in size (n = 12). Pseudothecial wall brown, K- (turning dark brown to blackish), (10−) 14 ± 3.8 (−23) µm, usually paler in the lower third, even hyaline in the basal part in contact with the host thallus, paraplectenchymatous, composed of several layers of polygonal cells (4−9), these being (2−) 3.8 ± 1.4 (−8) × (1−) 2.3 ± 0.5 (−3.4) µm in size (n = 28), with a thin cell wall; inner wall layers hyaline. Periphyses abundant around the ostiolum, hyaline, simple or slightly branched towards the apex, septate with a rounded apex, (10.5−) 14.3 ± 3 (−21.5) × (1.5−) 1.7 ± 0.28 (−2.5) µm (n = 16). Short pendant filaments (pseudoparaphyses) composed of two cells found in all specimens (9−) 12.3 ± 2.7 (−15.5) × (1.5−) 1.6 ± 0.21 (−2.5) µm (n = 13), but some specimens show longer filaments up to 20 µm. Other interascal filaments not observed. Hymenial gel I-, KI-. Asci clavate to subcylindrical, fissitunicate, ocular chamber present at least in young asci, no external gelatin observed, (30.5−) 39.6 ± 4.76 (−48) × (8−) 11.1 ± 1.65 (−14.4) µm (n = 23), 8-spored, I-, KI-, wall BCr-, epiplasm BCr+ violet, apical apparatus revealed with BCr in form of a ± light purple multilayered area stained above the ocular chamber. Ascospores hyaline, not ornamented, 3-septate (with a fourth septum in some mature ascospores), sometimes slightly constricted at the septum, apex blunted, halonate when young (1−4 µm thick), (14.5−) 16.7 ± 1.3 (−20) × (3.5−) 4.1 ± 0.5 (−5) µm in size [length/width ratio = (3.2−) 4.2 ± 0.6 (−5.8) (n = 86)].

Pycnidia present, sessile or with one third immersed in the host thallus, black, usually with glossy appearance, conical to subglobose, dispersed or aggregated in groups, (34−) 48 ± 10.09 (−65) × (32−) 36.75 ± 3.88 (−43) µm (n = 24); conidiomatal wall brown, K- (turning dark brown to blackish), (6−) 8 ± 4.6 (−13) µm, paler in the basal part, paraplectenchymatous, composed of several layers of cells (2−5), these being rectangular and similar in size to those in ascomata wall. Conidiogenous cells more or less ampulliform (upper third narrower), simple, hyaline, (3.5−) 5.06 ± 0.8 (−7) × (2.5−) 2.76 ± 0.25 (−3) µm (n = 30). Conidiospores hyaline, simple, bacilliform, straight to curved, (2.5−) 3.34 ± 0.64 (−5) × (1−) 1.37 ± 0.21 (−1.5) µm.

Other material studied: *Austrostigmidium mastodiae*: Antarctica. South Shetlands, Livingston Island, Punta Hanna, seashore, 0−5 meters above sea level (m. a.s.l.), 62˚ 39’ S, 60˚ 37’ W, 12 Feb 2012, *C. Laguna Fiol* s/n (MA-Lich 18202); South Shetlands, King George Island (Isla 25 de Mayo), Potter Peninsula, Peñon VI, 0−5 m a.s.l., 62.261203° S; 58.618951° W, 22 Dic 2009, *F. Fernández-Mendoza* & *S. Domaschke* (MA-Lich 18203); South Shetland Islands, King George Island (Isla 25 de Mayo), Potter Peninsula, Stranger Point, 0−5 m a.s.l., 62.261502° S; 58.617572° W, 22 Dec 2009, *F. Fernández-Mendoza* & *S. Domaschke* (MA-Lich 18206); Avian Island (Adelaide Island), seashore, 0−5 m a.s.l., 67° 46’ S, 68° 53’ W, 27 Jan 2007, *J.C. García Galindo* & *J. Romagni* (MA-Lich 18210); Rongé Island, seashore, 0−5 m a.s.l.,

64° 43’ S, 60° 54’ W, 25 Jan 2007, *J.C. García Galindo* & *J. Romagni* (MA-Lich 18211); Antarctic Peninsula, Cierva Cove, seashore, 0−5 m a.s.l., 64° 09’ S, 60° 57’ W, 26 Jan 2007, *J.C. García Galindo* & *J. Romagni* (MA-Lich 18212); Yalour Island, seashore, 0−5 m a.s.l., 65° 15’ S, 64° 11’ W, 26 Jan 2007, *J.C. García Galindo* & *J. Romagni* (MA-Lich 18209); —Chile. XII Región, Tierra del Fuego, Isla Basket, seashore, 0−2 m a.s.l., 54º 42' 13" S; 71º 34' 53" W, 17 Dec 2009, *S. Pérez-Ortega 3179bis* (MA-Lich 18204); *Ibidem, S. Pérez-Ortega 3242bis* (MA-Lich 18213); Beagle Channel, Isla Chair, Bahía Darwin, seashore, 0−5 m a.s.l., 54º 53' 59" S; 70º 00' 48" W, 16 Dec 2009, *S. Pérez-Ortega 3227* (MA-Lich 18207); Peninsula Brunswick, near to Cape Froward, San Nicolás Bay, 0−5 m a.s.l., 53º 47' 7.4" S, 70º 58' 38" W, 18 Dec. 2009, *U. Søchting* (MA-Lich 18208).

Stigmidium acetabuli: Spain. Aragón, Teruel, Tramacastilla, road from Tramacastilla to Villar del Cobo, *Quercus faginea* forest, 30TXK163732, 1460 m a.s.l., on *Pleurosticta acetabulum*, 5 Sept 2010, *S. Pérez-Ortega* 1539 (MA-Lich 18216).

Pseudostigmidium nephromiarium: Chile. Región de Magallanes and Chilean Antarctica, Navarino Island, Cerro Bandera, 250 m a.s.l., 54º 57’ 10”S, 67º 38’ 33” W, 19 Jan 2008, *S. Pérez-Ortega* (MA-Lich 18217).

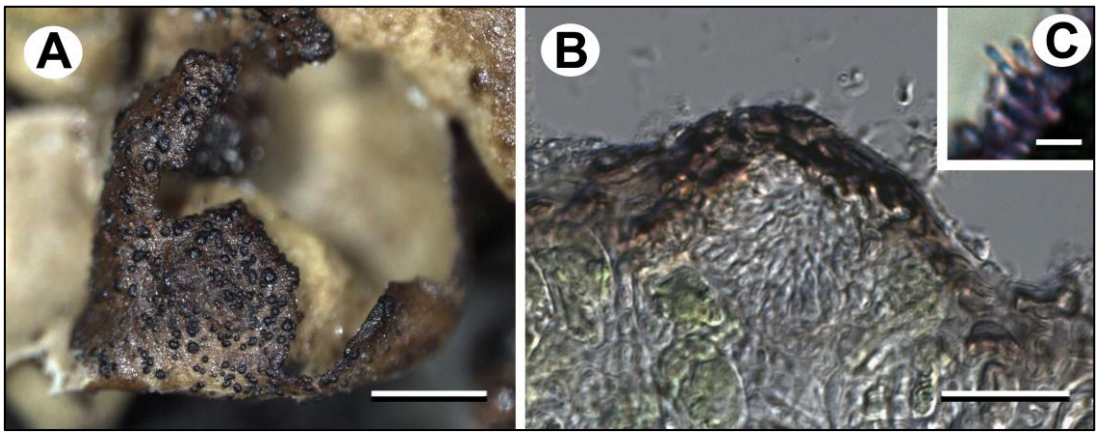

Figure 2. *Austrostigmidium mastodiae*, pycnidia and conidiospores. (A) Pycnidia on *Mastodia tessellata*. (B) Longitudinal section of a pycnidium. (C) Conidiogenous cells and conidium in BCr. Scales: A = 500 µm, B = 25 µm, C = 5 µm. (Photographs: SPO & IGB).

3.2. Phylogenetic relationships

We generated a total of 7 rDNA sequences (5 *nuLSU* and 2 *nuSSU*, Appendix 1). The final alignment consisted in 53 sequences and 1.677 characters (722 corresponding to *nuLSU*, and 955 to *nuSSU*). Bayesian and ML analyses resulted in similar and congruent topologies, so that only the best tree obtained in the ML search is shown in Figure 3 with posterior probabilities added to supported branches. The five specimens of *Austrostigmidium mastodiae* formed a single, well-supported clade both by posterior

probability (PP = 1) and bootstrap (B = 100%). Within this clade, three specimens (I346, I347, s1479) appear together within a well-supported group (PP = 1, B = 100%), whereas the relationships of this group with the two remaining specimens (I344 and I345) stay unclear. The former three specimens were collected in Tierra del Fuego whereas the latter two were from Antarctica. *Austrostigmidium mastodiae* formed a supported clade together with specimens of *Xanthoriicola physciae* and species of the genus *Friedmanniomyces* (*F. endolithicus* and *F. simplex*) (PP = 1, B = 88%). However, phylogenetic relationships among these three groups remain unresolved. This clade composed by *Austrostigmidium*, *Xanthoriicola* and *Friedmanniomyces* constitutes the sister clade of a group composed by *Elasticomyces elasticus* and *Monticola elongata* (PP = 0.99, B = 97%).

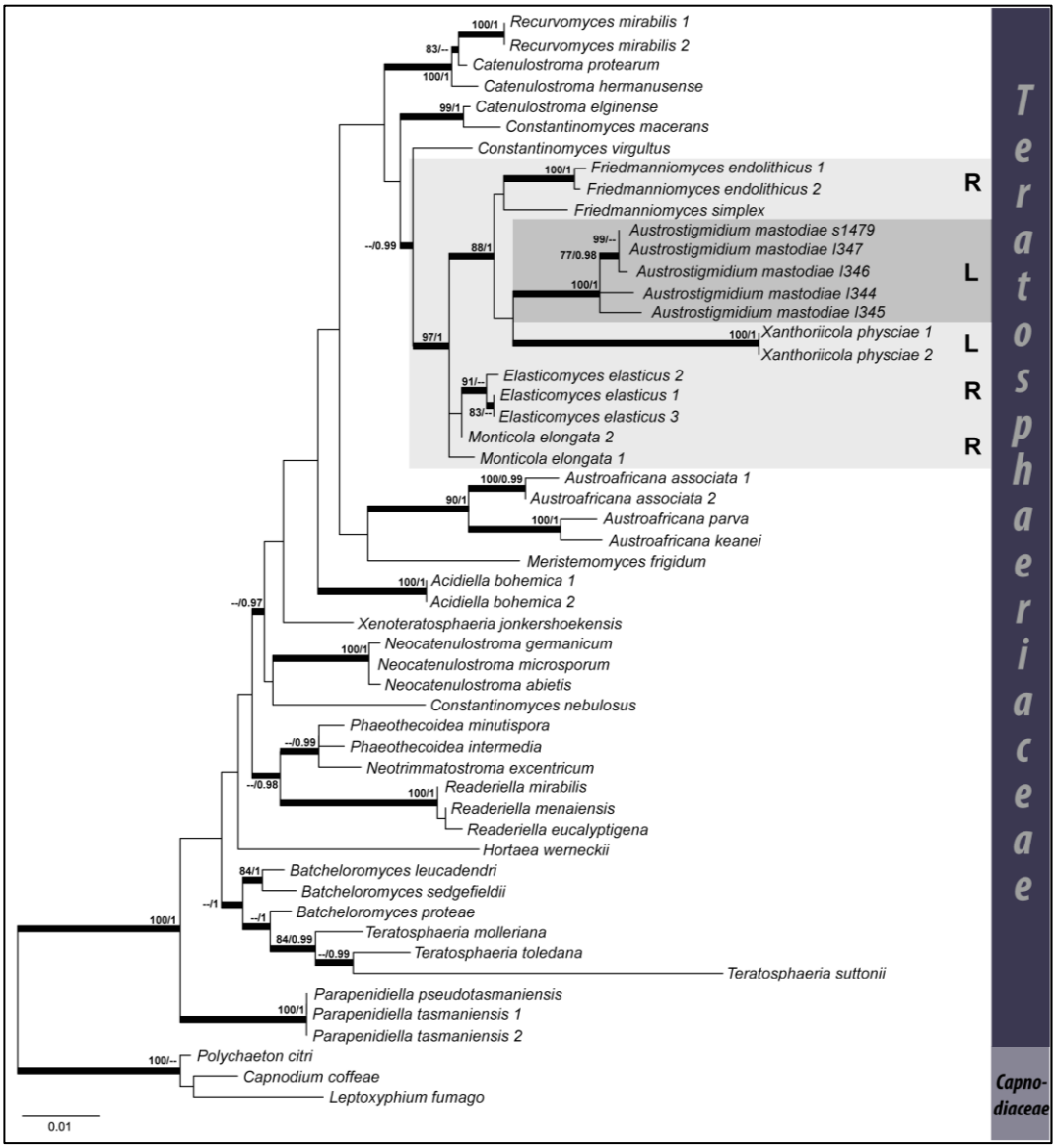

Figure 3. Maximum likelihood phylogenetic tree obtained in the RAxML analysis (Bayesian analysis recovered a similar topology). Bold branches depict either bootstrap (B) or/and posterior probabilities (PP) support, figures are given above the branches

(B/PP). *Austrostigmidium mastodiae* is highlighted in dark grey and the group to which it belongs in light grey. R = rock-inhabiting fungi, L = lichenicolous fungi.

3.3. Host-parasite interface

Austrostigmidium mastodiae shows close interactions with the thallus of *Mastodia tessellata*, especially with the photobiont partner. Vegetative hyphae of *A. mastodiae* arise from the base of the pseudothecium and penetrate into the host thallus (Figure 1D). We often observed the decrease of living photobiont cells beneath the pseudothecia, this being particularly visible under the fluorescence microscope. Figure 4A–B show the same thallus section with the surface of a pseudothecium using transmitted light (Figure 4A) and fluorescence (Figure 4B) microscopy. In Figure 4A, it is possible to observe photobiont cells with a healthy appearance only in the lower part of the host thallus. These cells showed a chlorophyll autofluorescence signal (red color) by fluorescence microscopy (Figure 4B). The autofluorescence signal was much lower, when observable, in damaged algal cells situated beneath the pseudothecium (arrows in Figure 4A–B), highlighting the lack of viability of these photobiont cells. The host-parasite interface of this lichenicolous infection has been characterized by means of transmission electron microscopy (TEM). Host fungal and lichenicolous hyphae were clearly distinctive using TEM (Figure 4C). *Mastodia* hyphae ("M") usually show longer and much larger cells than *Austrostigmidium* ("A"), which usually has more torulose hyphae (Figure 4C). Cell walls are also thicker in *M. tessellata* hyphae (0.7–0.8 µm *vs* 0.3–0.4 µm). On the other hand, *Austrostigmidium* hyphae showed a large number of electron-dense osmophylic globules in the cytoplasm.

Our TEM study reveals frequent interactions of *Austrostigmidium* hyphae with the photobiont cells of *M. tessellata*, but not with the mycobiont hyphae. In Figure 4D–F it is possible to observe the sequence of interactions between the photobiont cells and *Austrostigmidium* hyphae. In Figure 4D it is shown how *Mastodia* hyphae interact with a *Prasiola borealis* cell forming the typical complex haustorial system with multiple lobes, as described in Pérez-Ortega et al. (2010). It is also possible to observe *Austrostigmidium* hyphae near the photobiont cell but still without any visible interaction. In a second stage (Figure 4E), *Austrostigmidium* hyphae clearly interact with the *P. borealis* cell and push the cell wall producing an invagination. Finally, in Figure 4F it is possible to observe a completely degraded photobiont cell with both *Mastodia* and *Austrostigmidium* hyphae attacking it and inducing the collapse of photobiont cells. *Mastodia* and *Austrostigmidium* hyphae penetrated the host cell wall but it is even possible to observe intracellular haustoria by an *Austrostigmidium* hypha (arrow).

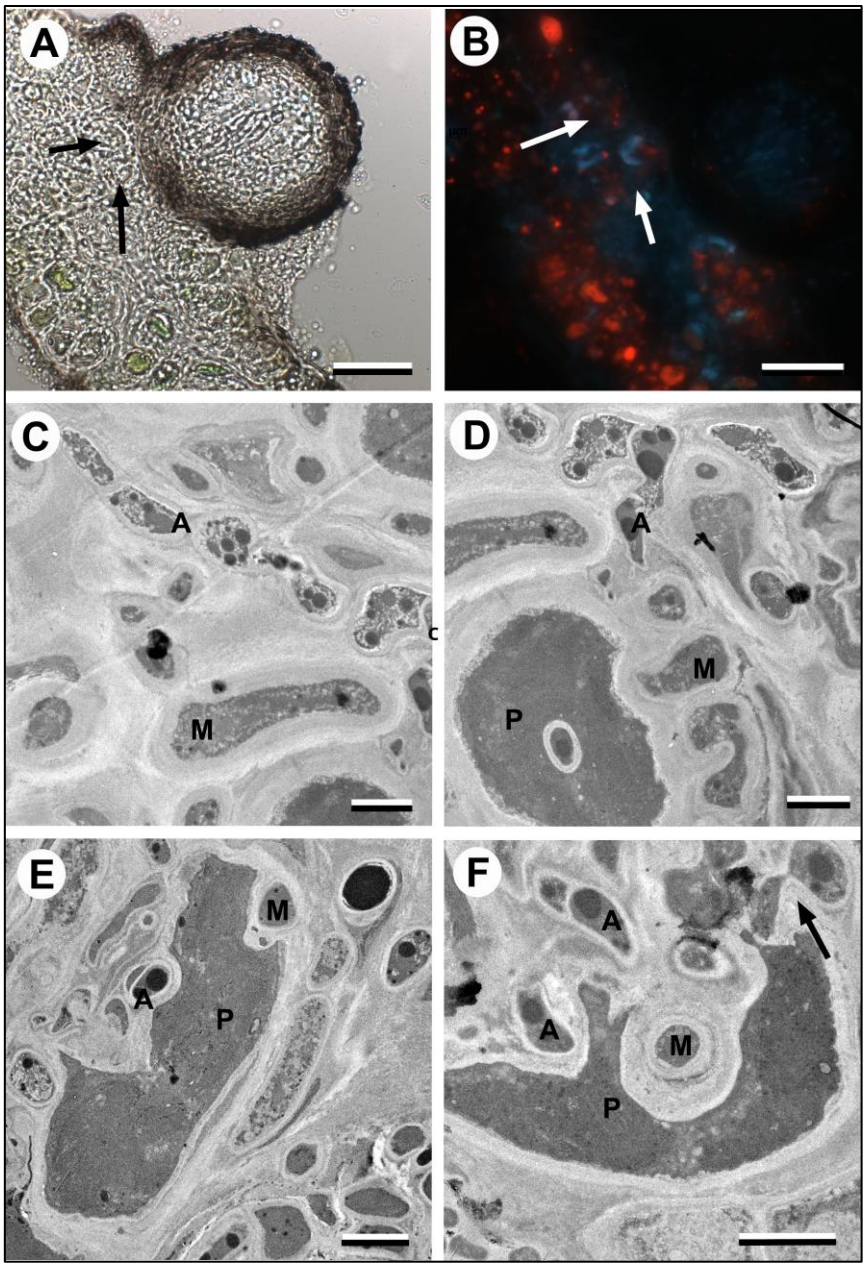

Figure 4. *Austrostigmidium mastodiae*, anatomical and ultrastructural interactions. (A) Light microscopy image of a section of *Mastodia* thallus with an *Austrostigmidium* pseudothecium, arrows point to collapsed photobiont cells. (B) Same section in fluorescence microscopy, arrows point the same collapsed photobiont cells showing faint fluorescence signal (red). (C) TEM image showing an *A. mastodiae* hypha ("A") with numerous osmophylic globules and *M. tessellata* hyphae ("M"). (D) TEM image showing *M. tessellata* hyphae ("M") interacting with a *Prasiola borealis* cell ("P"), *Austrostigmidium* hyphae ("A") are situated near the photobiont cell but do not interact. (E) TEM image showing fungal hyphae ("M" and "A") interacting with a photobiont cell ("P") and producing the invagination of the cell. (F) TEM image showing penetrations of the cell wall produced by *Autrostigmidium* ("A") and *M. tessellata* ("M") and the *Austrostigmidium* intracellular haustorium into the collapsed photobiont cell (arrow). Scales: A–B = 25 µm, C–F= 2 µm. (Photographs: AdR & IGB & SPO).

4. Discussion

The new genus *Austrostigmidium* is described for material of a pseudothecioid species with 3-septate ascospores growing on *Mastodia tessellata*. A new genus is proposed as the new species does not fit any available genus. *Austrostigmidium* shows affinities with the recently described *Pseudostigmidium* (Etayo & Sancho 2008). This genus, described from southern South America, occurs on epiphytic macrolichens from the *Peltigerales* and is characterized by its conical to subconical ascomata, the lack of hamathecial filaments, presence of periphyses and 3-septate ascospores. These characters are shared with *Austrostigmidium*. The main difference between both genera relies on the structure of the ascomatal wall. In *Pseudostigmidium*, the wall is composed of a network or more or less radial torulose hyphae (Etayo & Sancho 2008), whereas *Austrostigmidium* has a paraplectenchymatous wall composed of polygonal cells. Only *P. biseptatum* shows a different paraplectenchymatous wall structure. This species is also deviant regarding ascospore septation, showing 2-septate ascospores, and shape of the ascomata, subglobose in *P. biseptatum* and conical in other species of the genus. Therefore we consider that *A. mastodiae* does not belong to *Pseudostimidium* s. str., but its relationships to *P. biseptatum* need to be studied further.

Austrostigmidium also shows close affinities with *Stigmidium*. This genus is divided into several groups and may be polyphyletic (Calatayud & Triebel 2003, Roux & Triebel 1994). *Stigmidium* and *Austrostigmidium* share the presence of hyaline to dark brown vegetative hyphae, paraplectenchymatous wall of the pseudothecia, bitunicate asci with an ocular chamber and an apical apparatus revealed by BCr. *Stigmidium* shows a range of suprahymenial elements, from short to long pseudoparaphyses (Roux & Triebel 1994; Calatayud & Triebel 2003). In *Austrostigmidium* most of the specimens studied showed short pseudoparaphyses of the type-a (composed of two cells of unequal length) (Roux & Triebel 1994). This type of pseudoparaphyses appears in *Stigmidium* s. str. (Roux & Triebel 1994). Long suprahymenial filaments were found in one specimen which are more similar to those of the type-b *sensu* Roux & Triebel (1994) and present in the *Stigmidium placynthii* group (Roux & Triebel 1994). The presence of both types of suprahymenial filaments in the same species is intriguing and deserves further research in order to find out whether this anomaly is due to the abnormal expansion of the periphyses towards lower areas of the pseudothecium cavity. Other ascomatal characters in these specimens do not differ from the rest.

Thus, the main differences between *Stigmidium* and *Pseudostigmidium* rely on ascospore characters. *Stigmidium* always has 1-septate ascospores, although species of the *Stigmidium psorae* group (Calatayud & Triebel 2003) may have 1-3-5-septate ascospores, but only when ascospores are old, and then they become brown. In *Austrostigmidium*, ascospores are always 3-septate, with a fourth septum appearing in very mature ascospores, but never turning brown. Furthermore, *Austrostigmidium* has ascospores with thicker cell walls than *Stigmidium*.

Other genera showing similarities with *Austrostigmidium* are *Epibryon*, *Sphaerellothecium* and *Clauzadella*. *Epibryon* is a genus of predominantly bryophilous species with I+, KI+ blue hymenial gel, lacking periphyses and an ocular chamber in the asci, and most of the species show setae in the ascomata (Döbbeler 1978, 1985). It has been recently ascribed within the *Chaetothyriales* in the family *Epibryaceae* (Gueidan et al. 2014). *Sphaerellothecium* differs by a typical superficial network of brown vegetative hyphae and the presence of interascal paraphysoids (Roux & Triebel 1994). As in *Austrostigmidium*, *Sphaerellothecium* species may show 3-septate ascospores in some species, but they tend to turn brown when mature. Finally, *Clauzadella* also shows 3-septate ascospores; it is characterized by the presence of large pseudothecia (0.2–0.3 mm) with walls tinged by a characteristic violet pigment (Navarro-Rosinés & Roux 1996).

Molecular analyses revealed the phylogenetic adscription of the new genus *Austrostigmidium* to the family *Teratosphaeriaceae* (*Capnodiales*), more precisely to the clade *Teratosphaeriaceae* I (according to Egidi et al. 2014), as the family *Teratosphaeriaceae* has been shown to be polyphyletic by Ruibal et al. (2009). Several anatomical characters in *Austrostigmidium* support its inclusion within *Teratosphaeriaceae*, such as the presence of ostiolate pseudothecia with periphysate canal, pseudoparaphyses, 8-spored bitunicate asci with multilayered endotunica and the presence of a mucoid sheath in the ascospores (Crous et al. 2007). Other characters common within the family, such as the presence of stroma or the 2-septate ascospores turning brown when mature, are absent in *Austrostigmidium*. The clade containing the new genus also comprises the lichenicolous genus *Xanthoriicola*, a hyphomycetous lichenicolous fungus with broad cupulate enteroblastic conidiogenous cells generating dark brown, simple and warted conidia which grow on the apothecia of *Xanthoria parietina* (Ruibal et al. 2011) and *Friedmanniomyces*, a hyphomycetous rock-inhabiting endemic genus from Antarctica with pale to dark brown hyphae, having simple to multicellular conidia (Selbmann et al. 2005). The sister clade to the group *Austrostigmidium-Friedmanniomyces-Xanthoriicola* consists of two rock-inhabiting genera, *Elasticomyces* described from Antarctica and *Monticola* described from Italy. Basal to these two clades is *Constantinomyces*, another recently described genus of rock-inhabiting fungi including species from the Iberian Peninsula and Mallorca (Egidi et al. 2014).

Rock-inhabiting fungi are slow-growing microorganisms associated with natural rocky substrata (Egidi et al. 2014). These organisms show physiological and physical characters related to stress tolerance, such as the presence of melanin-like compounds in their cell walls, lack of morphologically differentiated sexual phases and production of few metabolites and morphological structures for survival (Egidi et al. 2014; Sterflinger 2006). It has been pointed out that rock-inhabiting fungi may be the probable ancestors of the lichenized order *Verrucariales* (Gueidan et al. 2008). Now with the presence of two lichenicolous fungi, *Austrostigmidium* and *Xanthoriicola*, in a clade of predominantly rock-inhabiting fungi, it is clear that this group of fungi can also be the

ancestor of some groups of lichenicolous fungi. This switch of lifestyle is not surprising; on the one hand it has been shown that some rock-inhabiting fungi are able to form associations with lichen photobionts, at least in culture (Gorbushina et al. 2005), and on the other hand, Selbmann et al. (2013) have recently shown that lichens constitute a very valuable niche for black meristematic fungi in Antarctica, where epilithic conditions are very often prohibitive for life. In this study, the species *Friedmanniomyces endolithicus* was isolated from *Lecidea cancriformis*, and *Elasticomyces elasticus* was isolated from *Lecanora fuscobrunnea*, *Lecanora* sp. and *Usnea antarctica*. Furthermore, a similar switch of lifestyle has already been reported within the recently described order *Lichenostigmatales* (Ertz et al. 2013).

It has been shown how *A. mastodiae* interacts with its host *Mastodia tessellata*. These interactions are not morphogenetic, as they do not produce deformations or galls in the host thallus. *Austrostigmidium mastodiae* does not produce any apparent damage in the host thallus, at least not any observable under the dissecting microscope. Based on this observation, *A. mastodiae* is a commensalistic species, according to Hawksworth (1982). However, this study using transmission electron microscopy has revealed close interactions between *A. mastodiae* hyphae and the photobiont cells of *M. tessellata*, those of the alga *Prasiola borealis* (Pérez-Ortega et al. 2010; Moniz et al. 2012a,b). These interactions result in the total collapse of photobiont cells, once the lichenicolous fungus interacts with them. Whereas *M. tessellata* produces peg-like haustoria and biotrophic intraparietal penetrations (Pérez-Ortega et al. 2010), *A. mastodiae* seems to first push against the cell wall producing invaginations and later it penetrates into the cell wall and plasma membrane. Pérez-Ortega et al. (2010) highlighted that the symbiosis between *M. tessellata* and *Prasiola borealis* was not similar to other known lichen symbioses. Instead, this case seems to be more a dynamic equilibrium dependent on biotic and abiotic factors. The presence of a further fungus interacting with the photobiont cells appears to collapse the system and lead to the common loss of photobiont cells beneath the pseudothecia of *Austrostigmidium*. It is likely that the collapse of photobionts cells is dependent on several factors as the fitness of the lichen symbiosis at the time the infection occurs, and other abiotic factor such as the level of nitrogen and phosphorous available in the habitat (Pérez-Ortega et al. 2010). A higher incidence of *Austrostigmidium* pseudothecia has been observed in those localities close to penguin colonies.

Interactions between lichenicolous fungi and the photobiont cells of their hosts are common (Rambold & Triebel 1992; de los Ríos & Grube 2000; de los Ríos et al. 2002). One of the best illustrated examples is how the lichenicolous fungus *Zwackhiomyces coepulonus* attacks and kills the photobiont cells of its host *Xanthoria parietina* by means of intracellular haustoria (Grube & Hafellner 1990; de los Ríos et al. 2002). Infection by *Austrostigmidium mastodiae* does not seem as harmful for the host as cases where the lichenicolous fungus directly interacts with the mycobiont cells (de los Ríos & Grube 2000; Grube & de los Ríos 2001; de los Ríos et al. 2002). Lawrey & Diederich (2003) raised the hypothesis that “highly stable and specialized biotrophic interactions

will exhibit modes of nutrient acquisition involving only one lichen biont and little host damage". Thus, considering the observations made in this study, *A. mastodiae* can be considered a highly stable and specialized biotrophic association.

Appendix 1. Specimens in this study and their accession numbers.

Species	*nuLSU*	*mtSSU*
Acidiella bohemica 1	KF901985	-
A. bohemica 2	KF901984	-
Austroafricana associata 1	KF901827	
A. associata 2	KF901824	-
A. keanei	KF901830	-
A. parva	KF901831	-
Batcheloromyces leucadendri	KF937221	-GU214515
B. proteae	KF901833	AY251102
B. sedgefieldii	KF937222	-
Capnodium coffeae	DQ247800	DQ247808
Catenulostroma elginense	EU019252.2	GU214517
C. hermanusense	KF902089	-
C. protearum	KF902090	-
Constantinomyces macerans	KF310005	AY843266
C. nebulosus	KF310014	-
C. virgultus	GU323964	-
Elasticomyces elasticus 1	GU250375	GU250332
E. elasticus 2	KF309992	GU250353
E. elasticus 3	GU250376	GU250333
Friedmanniomyces endolithicus 1	GU250366	GU250322
F. endolithicus 2	GU250367	GU250326
F. simplex	GU250368	NG016527
Hortaea werneckii	EU019270	Y18693
Leptoxyphium fumago	GU214430	GU214535
Meristemomyces frigidum	KF310013	-
Monticola elongata 1	GU250398	
M. elongata 2	KF309994	-
Neocatenulostroma abietis	KF937226	DQ678040
N. germanicum	KF901989	GU214518
N. microsporum	KF901814	GU214520
N. excentricum	KF901840	-
Parapenidiella pseudotasmaniensis	KF901844	-
P. tasmaniensis 1	KF902132	-
P. tasmaniensis 2	KF901843	
Phaothecoidea intermedia	KF902106	-
P. minutispora	KF442565	-
Polychaeton citri	GU214469	-
Austrostigmidium mastodiae I344	KP282858	-
A. mastodiae I345	KP282859	-
A. mastodiae I346	KP282860	-
A. mastodiae I347	KP282861	KP282863
A. mastodiae s1479	KP282862	KP282864
Readeriella eucalyptigena	KF442566	-
R. menaiensis	KF442569	-
R. mirabilis	EU754209	EU754110
Recurvomyces mirabilis 1	GU250372	GU250329
R. mirabilis 2	KC315876	KC315865
Teratosphaeria molleriana	GU214508	GU214607
T. suttonii	KF902162	GU214616
T. toledana	KF901924	GU214618
Xanthoriicola physciae 1	JN040489	-
X. physciae 2	KF176965	-
Xenoteratosphaeria jonkershoekensis	KF937250	GU296200

CAPÍTULO 3 (*CHAPTER 3*)

Shackletonia cryodesertorum (*Teloschistaceae*, Ascomycota), una nueva especie de los Valles Secos de McMurdo de la Antártida, con breves apuntes sobre la biogeografía del género *Shackletonia*.

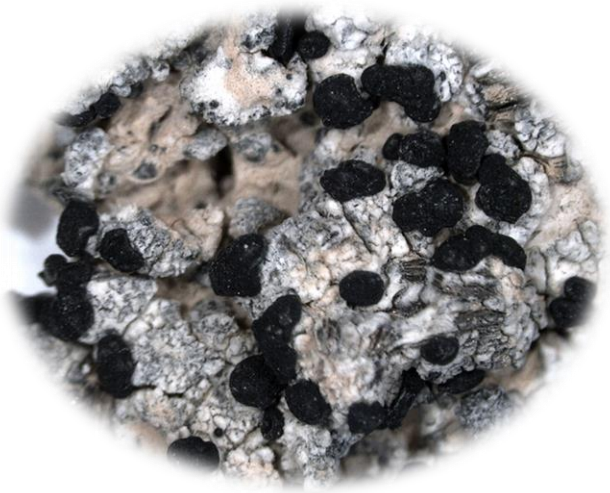

Referencia del artículo científico publicado:

Garrido-Benavent I, Søchting U, de los Ríos A y Pérez-Ortega S (2016) *Shackletonia cryodesertorum* (*Teloschistaceae*, Ascomycota), a new species from the McMurdo Dry Valleys (Antarctica) with notes on the biogeography of the genus *Shackletonia*. Mycological Progress doi:10.1007/s11557-016-1204-x

Abstract

A new species of *Shackletonia* (*Teloschistaceae*, Ascomycota) is described from the McMurdo Dry Valleys in Antarctica, one of the regions with the harshest conditions on Earth. Distinctive traits of the new taxon are the grey thallus, its black lecideine apothecia with a dark greenish blue exterior side of the exciple, *Lecidea* green pigment present at the cortex and exciple, emodin-dominated anthraquinones only in the epithecium, and spores on average 11.2 × 6.0 µm with 3.6 µm wide septum. New chemical data from HPLC analyses further supports the uniqueness of the genus *Shackletonia* regarding secondary metabolite production within subfamily *Xanthorioideae*. Based on data from three molecular markers (*nrITS*, *nuLSU* and *mtSSU*) we found the new species sister to *S. sauronii*, a species so far known only from Livingston Island (Antarctica). Using secondary calibrations we inferred a long-time evolution of *Shackletonia* in the Southern Hemisphere, which separated from the remaining lineages of *Xanthorioideae* between the late Cretaceous and the early Paleogene, and diversified during the late Paleocene and early Oligocene.

1. Introduction

Knowledge on the lichen family *Teloschistaceae* (Ascomycota) has expanded considerably in the last decade. Several long-standing questions on evolutionary history and ecology are being solved thanks to novel technological and conceptual advances. For instance, Gaya et al. (2015) have recently assessed the synergistic effect of intrinsic and extrinsic factors on the diversification burst this family of fungi has undergone. Such radiation is one of the key reasons explaining its fascinating high species richness, with *c*. 1.000 estimated taxa (Arup et al. 2013). The use of molecular tools has also made possible to suggest new taxonomical rearrangements within this complicated group of lichenized fungi (e.g. Arup et al. 2013). Thus, new genera have been proposed to accommodate lineages sharing traits such as habitus, secondary compounds and/or geographic distribution (Arup et al. 2013; Søchting et al. 2014a,b). However, more data are needed to confirm with higher statistical support the phylogenetic relationships among some taxa, especially at the backbone of the *Teloschistaceae* phylogeny.

In addition, it is necessary to expand sampling to remote regions where isolated lineages can occur and help to improve the accuracy of molecular phylogenies. The Antarctic continent is almost covered by ice and only 0.5% of the territory corresponds to ice-free areas (Peat et al. 2007). More than thirty species of *Teloschistaceae* occur in the continent (Søchting & Olech 1995; Øvstedal & Lewis Smith 2001; Søchting et al. 2004; Søchting et al. 2014a and references therein). During the study of the relationships among myco- and photobionts in the McMurdo Dry Valleys (Pérez-Ortega et al. 2012a) an unknown species of *Teloschistaceae* with dark apothecia was discovered, which was initially presumed to be a member of the genus *Huea*.

A molecular analysis based on three markers has been conducted in order to determine its phylogenetic adscription within the *Teloschistaceae* using the recent classification by Arup et al. (2013). Here, we prove that such species belongs to the genus *Shackletonia* and represents a new species. This taxon is further characterized by means of standard morphological, anatomical and chemical studies. Finally, dating analyses based on two alternative methods are performed in order to shed light on the evolution and biogeography of the genus *Shackletonia* as well as the proposed new species.

2. Material and Methods

2.1. Sampling area

A detailed description of the climatic and geological properties of the sampling area that could influence lichen growth and dispersal can be found in Pérez-Ortega et al. (2012a).

2.2. Morphological and anatomical studies

Macroscopic descriptions are based on observations made with a Leica S8APO dissecting microscope equipped with a Leica EC3 image capture system. Handmade sections of ascomata were observed in a Zeiss Axioplan 2 microscope fitted with "Nomarski" differential interference contrast (DIC) and photographs were taken with a Zeiss AxioCam digital camera. Microscopic measurements were made on material mounted in water by means of the Zeiss Axiovision 4.8 imaging system. Chemicals used either for tissue dissociation and examination, or for testing possible colour reactions of ascomatal elements and vegetative hyphae were: 10% KOH (K), Lugol's iodine, without (I) or with (K/I) pre-treatment with K, sodium hypochlorite (C), concentrated nitric acid (cN) and 10% nitric acid (10% N). Fluorescence microscopy using the filter set for DAPI (Zeiss Filter Set 49; Ex⁄Em: 365⁄420–470) was employed to visualize individual hyphae as well as to detect anthraquinone granules on ascocarp sections. Ascospores were measured outside the asci. The average is followed by its standard deviation, and the maximum and minimum values are given in parentheses. The thickness of spore septum was measured at the outer wall. The number of measurements is indicated in parentheses. All specimens are deposited in MA-Lich. Author citations follow MYCOBANK (http://www.mycobank.org/). Macro- and microscopic details of the new species are shown in Figures 1–2.

2.3. Taxon sampling, DNA extraction, PCR amplification, and DNA sequencing

Total DNA was isolated from four specimens by means of a modified version of the CTAB method (Cubero et al. 1999). To extract DNA, we aimed at isolating fragments of thallus over sections of apothecia, thus avoiding taking dikaryotic or diploid tissue. Three markers were selected for this study following Arup et al. (2013). The nuclear ribosomal large subunit (*nrLSU*) and the small subunit of the mitochondrial ribosomal RNA gene (*mtSSU*) were amplified from two out of four specimens, whereas the internal transcribed spacer region (*nrITS*) was sequenced for all specimens in a previous work (Pérez-Ortega et al. 2012a). The primers used were LR3 and LR7 (Vilgalys & Hester 1990) for *nrLSU*, and mrSSU1 (Zoller et al. 1999) and mrSSU7 (Zhou & Stanosz 2001) for *mtSSU*. The following PCR temperature profiles were employed: 5 min at 94° C, then 35 cycles of 1 min at 94° C, 1 min at 54 or 56° C (*nrLSU* and *mtSSU*, respectively), 3 min at 72° C, with a final extension of 10 min at 72° C. The PCR reactions were visualized with a 1% agarose gel stained with PRONASAFE nucleic acid stain solution (CONDA Laboratories). PCR products were purified and cleaned using the UltraClean® PCR Clean-Up Kit (MOBIO Laboratories, Inc.). Both complementary DNA strands were sequenced at MACROGEN EUROPE (The Netherlands) using the same primer set as for the initial amplifications. Electropherograms were checked and assembled using SEQMANII v.5.07© (DNASTAR Inc.). Accession numbers for the new sequences are provided in Appendix 1.

2.4. Sequence alignment and phylogenetic analyses

We produced two datasets: 1) Dataset A included an extensive sampling of *nrITS* sequences from species from most genera of subfamily *Xanthorioideae* (Arup et al. 2013; Søchting et al. 2014b) and, 2) Dataset B corresponded to a reduced three-marker alignment (*nrITS*, *nuLSU* and *mtSSU*) including only those members of *Xanthorioideae* with at least two available markers. *Leproplaca xantholyta* was selected as outgroup following Arup et al. (2013). A total of 132 sequences (66 *nrITS*, 31 *nuLSU* and 35 *mtSSU*) were downloaded from GENBANK (Appendix 1). Unaligned sequence files were submitted to the CIPRES Science Gateway web server (Miller et al. 2010) and the MAFFT algorithm (Katoh et al. 2002; Katoh & Toh 2008) was selected to construct the base alignment using default parameters. Resulting alignments were edited in BIOEDIT v.7.0.9 (Hall 1999) by delimiting and removing obvious ambiguously aligned regions. Species-specific introns were also identified and transformed into single nucleotide positions (single event) when possible. We further divided the *nrITS* into three regions, namely *ITS1*, *5.8S* and *ITS2*. Best fitting nucleotide substitution models were obtained with JMODELTEST v.2.1.4 (Darriba et al. 2012) and using the Akaike Information Criterion (AIC, Akaike 1974). Thus, considering Dataset A, the GTR+Γ was selected for the *ITS1* and *ITS2*, and the K80+Γ for the *5.8S*, whereas the best-fitting models for Dataset B were GTR+I+Γ (*ITS1*, *nuLSU*), K80+I (*5.8S*), K80+Γ (*ITS2*) and HKY+I+Γ (*mtSSU*). Maximum likelihood (ML) and two Bayesian approaches were used for inferring phylogenetic relationships in both datasets. The online beta version of PHYML v.3.0 (Guindon et al. 2010), which includes an automatic model selection by Smart Model Selection (SMS), was used for ML analyses. Both NNI and SPR were selected for tree rearrangement, and bootstrapping was performed using 1.000 pseudoreplicates. Prior to concatenation (Dataset B), we also inferred ML trees for each locus with PHYML v.3.0, using 1.000 bootstrap pseudoreplicates, to test for topological incongruence among them, assuming bootstrap values ≥ 70% as significant for conflicting relationships among the same set of taxa (Mason-Gamer & Kellogg 1996). Subsequently, a Bayesian analysis was implemented in MRBAYES v.3.2.3 (Ronquist et al. 2012) on the CIPRES Science Gateway. Two parallel, simultaneous runs with four-chain runs were performed over 1×10^7 generations starting with a random tree. Sampling was performed after every 100th step. An ultrametric tree was also inferred in a Bayesian framework using BEAST v.1.7 (Suchard & Rambaut 2009; Drummond et al. 2012) as implemented in CIPRES Science Gateway. Adequacy of a strict clock model was firstly assessed for each locus using MEGA v.5.0 (Tamura et al. 2011) on ML and Bayesian topologies (Supplementary Table 1). BEAST analyses were then performed using an uncorrelated relaxed lognormal molecular clock (Drummond et al. 2006) for the whole *nrITS* (*ITS1 + 5.8S + ITS2*) and *mtSSU* regions, a strict clock for *nuLSU*, and a Yule tree prior assuming a constant lineage birth rate for each branch in the tree. Two runs of 2.5×10^7 generations each, sampling every 2.500 step, were combined. For both Bayesian analyses, the first 25% of saved data was discarded as burn-in. The 50% majority-rule consensus tree (MRBAYES) and the maximum clade credibility tree (BEAST) with the corresponding posterior probabilities (PP) were calculated from the

rest of trees. TRACER v.1.6 (http://tree.bio.ed.ac.uk/software/tracer/) was used to check for convergence of chains. Effective sample size (ESS) greater than 200, average standard deviation of split frequencies (ASDSF) values below 0.01 and potential scale reduction factors (PSRF) values approaching 1.00 were established as indicators of convergence.

Phylogenetic trees were visualized in FIGTREE v.1.4.2 (http://tree.bio.ed.ac.uk/software/figtree/) and ADOBE ILLUSTRATOR CS5 and PHOTOSHOP CS5 were used for artwork. Nodes displaying bootstrap support values equal or higher than 70% and Bayesian posterior probabilities equal or higher than 0.95 were regarded as significantly supported. Phylogenetic relationships deriving from Dataset A analyses are depicted in Figure 3.

2.5. Molecular dating

We performed a dating analysis for the main lineages within *Xanthorioideae* through a secondary calibration approach implemented in BEAST on the concatenated three-marker dataset. A time estimate of 62.61 MA (74.03–51.85 MA, 95% highest posterior density, HPD) was used for calibrating the *Caloplaca-Xanthoria* and *Xanthomendoza* split based on results of Gaya et al. (2015). This calibration was set as a prior using a normal distribution (mean = 62.61, stdev = 5.5). We also estimated divergence dates using substitution rates. Since these have never been inferred from *Teloschistaceae*, we used two alternative substitution rates for *nrITS*: 3.41×10^{-3} s/s/MA (*Melanohalea*, Leavitt et al. 2012b) and 2.43×10^{-3} s/s/MA (*Montanelia*, Leavitt et al. 2015b). Substitution rates for other loci were co-estimated under a uniform prior between 10^{-5} and 10. The topological prior and clock settings were selected as above. Two independent MCMC runs of 2×10^{7} generations were combined and a 10% burn-in was used. Data-free analyses were also run and showed no strong influence of the priors on posterior estimates.

2.6. Intrageneric variation in *Shackletonia*

We aimed at assessing the genetic variability within *Shackletonia*, where the new species is phylogenetically positioned. An additional alignment including all species was then constructed with MAFFT v.7 (Katoh & Standley 2013) using the G-INS-I strategy, *Unalignlevel* to 0.4 and the "Leave gappy regions" option activated. Alignment ends were trimmed to the shortest sequence using the FABOX v.1.41 online toolbox (Villesen 2007) and edited *a posteriori* by eye in BIOEDIT v.7.0.9 in order to correct obvious ambiguously aligned regions. For the highly variable *nrITS* region, GBLOCKS v.0.91b (Castresana 2000) was further used as an automatic procedure to deal with gappy regions, allowing for smaller final blocks and half gap positions. Ambiguous nucleotides were converted into N ("any base"). DNA polymorphism levels were evaluated after excluding gaps by calculating segregating sites (*s*), nucleotide diversity (π), average number of nucleotide differences (*k*), number of haplotypes (*h*) and haplotype diversity (*Hd*) with DNASP v.5.10 (Librado & Rozas 2009). Two high-diverse genera of *Xanthorioideae* with a considerable amount of molecular data,

Xanthomendoza and *Austroplaca*, were also analysed for comparison. Results are displayed in Supplementary Table 2.

2.7. Secondary chemistry

The secondary metabolite pattern was identified using HPLC and analysed separately for thallus and apothecia. The relative composition of the secondary compounds was calculated based on absorbance at 270 nm according to Søchting (1997).

3. Results

3.1. Taxonomy

Shackletonia cryodesertorum Garrido-Benavent, Søchting & Pérez-Ortega sp. nov. (Figure 1–2)

MYCOBANK NO.: MB 815626

Diagnosis: Thallus crustose, with a minute to deeply cracked greyish surface. Apothecia lecideine, mostly aggregate, completely black, epruinose, with a dark greenish blue outer exciple. Epithecium dark greenish blue with scattered anthraquinone granules. *Lecidea* green pigment present at the cortex and exciple. Exciple I/KI+ violet. Medulla I+ violet. Spores 11.2 × 6.0 µm; septum 3.6 µm.

Type: Antarctica, Victoria Land, McMurdo Dry Valleys, Upper Garwood, 78° 03.673’ S, 163° 47.455’ E, 541 m a.s.l., on granite rock, *A. de los Ríos*, 12 Dec 2009, holotype MA-Lich 18381.

Etymology: The epithet refers to the Antarctic region where this species was found, the McMurdo Dry Valleys, typically considered a cold (from the greek κρύο “*cryo-”*) desert (from the latin desertus, “*desertorum*”) due to its harsh climatic conditions.

Thallus crustose, epilithic, rather continuous, up to 20 mm wide and 3–7 mm thick. Surface completely rugose, minute to deeply cracked or rimose, grey to dirty greyish, often blackish within the cracks, in some areas pale brownish tinged, epruinose. Cortex 30–60 µm thick, with a thin layer of a dark greenish blue pigment at the top (reaching 20 µm thick) which turns pale towards the bottom, paraplectenchymatous with cells ± isodiametric and lumina ranging 1.6–4.5 µm wide, K-, C-, KC-, I/KI+ violet to deep blue, 10% N-, cN+ strongly pinkish (*Lecidea* green, Wetmore 1996). Epicortex hyaline or sometimes brownish, composed of necrotic fungal tissue up to 90 µm high, I+ violet. Medulla I+ violet.

Ascomata lecideine, numerous to usually aggregate, rounded to deformed by compression, sessile, not or slightly constricted at the base, 0.4–1.1 mm wide and 0.1–

0.3 mm high (n = 15). Disc flat to convex when mature, usually deformed and minutely cracked when compressed, totally black, epruinose. Proper margin distinct, mostly prominent but indistinguishable in mature and flexuous apothecia, (50–) 80 ± 20.4 (–100) µm thick (n = 15), concolorous to the disc. Outer part of the exciple dark greenish blue up to 20 µm, prosoplectenchymatous, consisting of non-isodiametric cells with lumina 3.5–10 µm long and 1–2 µm wide (n = 15), I/KI+ violet, cN+ strongly pinkish (*Lecidea* green). Hypothecium hyaline to brownish, consisting of densely interwoven hyphae. Subhymenium present, up to 20 µm high. Hymenium hyaline to faintly blue, (52–) 60.4 ± 7.5 (–75.2) µm high (n = 8). Epithecium dark greenish blue to blackish with dispersed deep-orange anthraquinone granules, K+ faintly violet, C-, cN+ strongly pinkish (*Lecidea* green). Paraphyses (1.7–) 2.2 ± 0.3 (–2.9) µm thick (n = 25), septate, simple to sparingly branched at the top, widening towards the apices, with blue-tinged cell walls, apical cells (3–) 4.3 ± 0.6 (–5.3) µm thick (n = 20). Asci clavate, *Teloschistes*-type, with 8 spores, (39.6–) 42 ± 2 (–45) µm long and (11.8–) 14 ± 2.6 (–18) wide (n = 5), usually arranged at different heights. Ascospores polardiblastic, ellipsoid, (10.1–) 11.2 ± 0.7 (–12.7) × (5–) 6 ± 0.6 (–7.3) µm (n = 24); length/width ratio (1.6–) 1.9 ± 0.2 (–2.3); ascospore septa (3.1–) 3.6 ± 0.3 (–4.2) µm thick; ratio of ascospore length/septum width (1.2–) 1.7 ± 0.2 (–2).

Conidiomata not seen.

Secondary chemistry: The extractable anthraquinones from apothecia consist mainly of emodin (89%) with smaller amounts of emodinal (7%), emodic acid (3%) and parietin (1%) based on absorption at 270 nm. No anthraquinones were detected from the thallus.

Photobiont: Algal cells deeply embedded in the medulla, chlorococcoid, including two haplotypes in the *Trebouxia* sp. URa2 clade (Pérez-Ortega et al. 2012a; Ruprecht et al. 2012a). This is an undescribed species phylogenetically related to *T. arboricola* and *T. decolorans*, and associated mostly with Antarctic lecideoid taxa, but also with species of *Lecanora*, *Rhizoplaca*, *Caloplaca* s.l. and *Umbilicaria* (Pérez-Ortega et al. 2012a; Ruprecht et al. 2012a).

Habitat and distribution: All specimens were growing on large granite rocks, especially in cracks and small crevices. No other microhabitats are so far known, and no other lichen species were seen growing together with it. Nevertheless, *Buellia frigida* and *Lecidea* spp. are common in the area. *Shackletonia cryodesertorum* is known from two out of three McMurdo Dry Valleys (Garwood and Miers), although it is expected to occur in other areas in continental Antarctica.

Additional examined material: Antarctica, McMurdo Dry Valleys, Upper Garwood, 78° 02.010’ S, 163° 50.686’ E, 710 m a.s.l., *A. de los Ríos* 16 Dec 2009, MA-Lich 18378; Miers Valley, The Altiplano, 78° 06.787' S, 163° 46.936' E, 541 m a.s.l., *A. de los Ríos*, 27 Nov 2009, MA-Lich 18379; *ibidem*, *A. de los Ríos*, 27 Nov 2009, MA-Lich 18380.

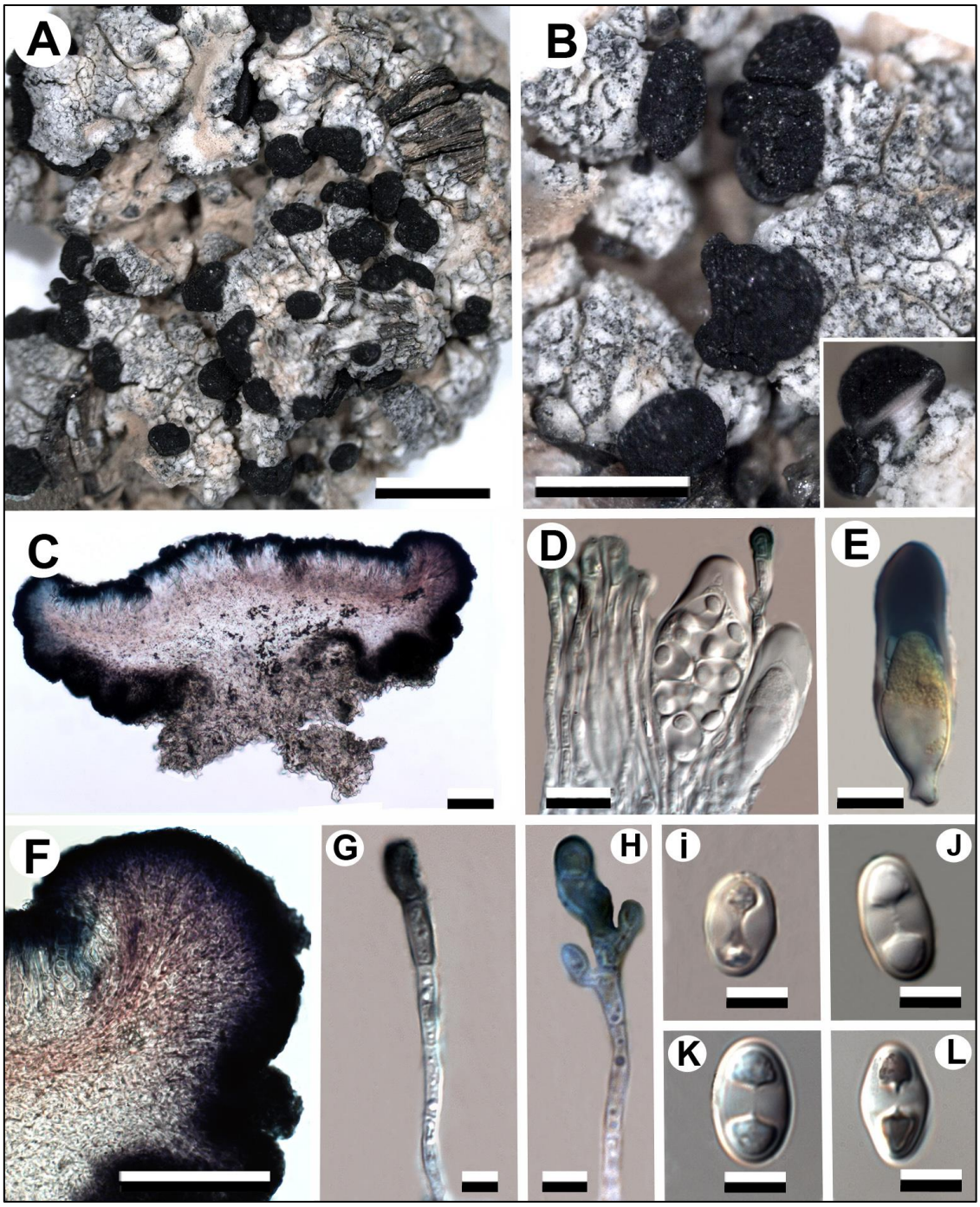

Figure 1. *Shackletonia cryodesertorum*, type (*A. de los Ríos*, MA-Lich 18381), macroscopic (A–B) and microscopic (C–L) characters. (A) Habitus. (B) Apothecia; detail of apothecial section in small box. (C) Apothecial section. (D) Young and mature asci and paraphyses. (E) I/K+ reaction showing a typical *Teloschistes*-type ascus. (F) Detail of exciple. (G–H) Paraphyses. (I–L) Ascospores. Scales: (A–B) = 1 mm, (C,F) = 50 μm, (D–E) = 10 μm, (G–L) = 5 μm. (Photographs: IGB).

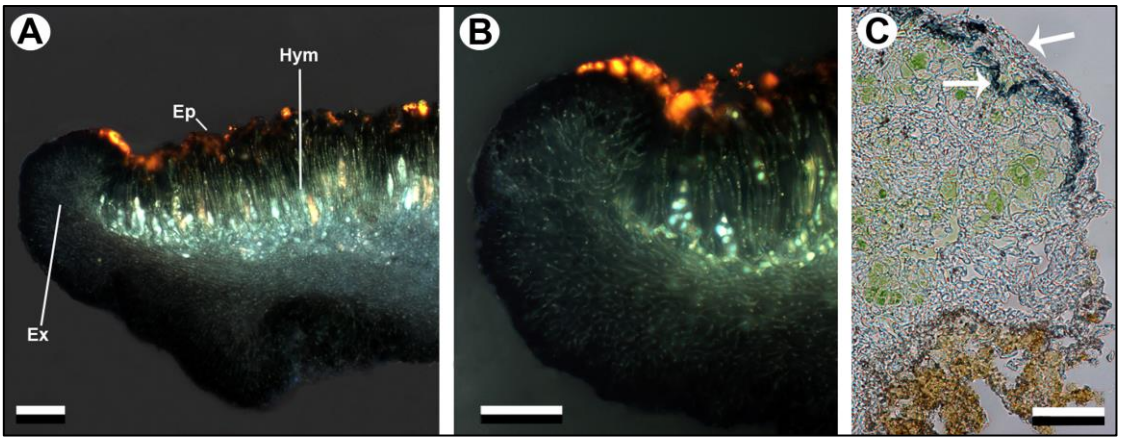

Figure 2. *Shackletonia cryodesertorum*, type (*A. de los Ríos*, MA-Lich 18381). (A–B) Apothecial section in fluorescence microscopy using filter set for DAPI (Zeiss Filter Set 49) (Ep = epithecium, Ex = exciple, Hym = hymenium). (C) Thallus section (from top to bottom, arrows indicate the necral layer or epicortex and the dark-greenish-blue-pigmented upper cortex, respectively). Scales: (A–C) = 50 μm. (Photographs: IGB & SPO).

3.2. Molecular analyses

Four *nrITS* and two new *mtSSU* and one *nuLSU* sequences were generated for this study from four Antarctic collections (Appendix 1). Dataset A (*nrITS*) alignment comprised 70 taxa and 527 characters, of which 292 were variable and 254 parsimony-informative. The combined three-marker analysis (Dataset B) comprises 37 taxa and 2.094 characters, 565 of them being variable and 406 parsimony-informative. Analyses made in BEAST produced ESS higher than 200 for all parameters in both cases. The MRBAYES analysis reached an average standard deviation of split frequencies of 0.01 after 8.15×10^5 (Dataset A) and 2.315×10^6 (Dataset B) generations. The ML analysis resulted in a single best ML tree of Ln = –6965.8152 (Dataset A) and Ln = –11366.3557 (Dataset B). No statistically-supported conflict was observed among the topologies obtained with these three methods or among the three markers included in Dataset B, and the BEAST-resulting topology from Dataset A is presented in Figure 3.

In general, the phylogenetic relationships within *Xanthorioideae* recovered in all analyses agree with previous findings from Arup et al. (2013) and Søchting et al. (2014a). Minor differences in among-genera relationships regarding Arup et al. (2013), such as the supported sister relationship of *Xanthocarpia* and *Austroplaca* in the *nrITS* BEAST analyses, could be derived from the use of a slightly different taxa sampling or treatment of gappy regions. BEAST analyses using a proper clock model for each locus recovered higher inner-clade support values than the ML and MRBAYES ones (Figure 4). However, uncertain sister relationships of some taxa within *Xanthorioideae*, such as *Charcotiana*, have not yet been solved (Søchting et al. 2014a). On the other hand, the monophyly of the genus *Shackletonia* and the among-species relationships were unequivocally supported by both *nrITS* (Figure 3) and three-marker datasets (Figure 4). Otherwise, only BEAST analyses supported its basal phylogenetic position to the

remaining *Xanthorioideae* groups. Molecular data obtained from four samples of *Shackletonia cryodesertorum* were identical and placed it sister to the parasitic species *S. sauronii* (PP > 0.95, B > 70), and both, in turn, are sister to a monophyletic group containing the remaining *Shackletonia* species (Figure 3).

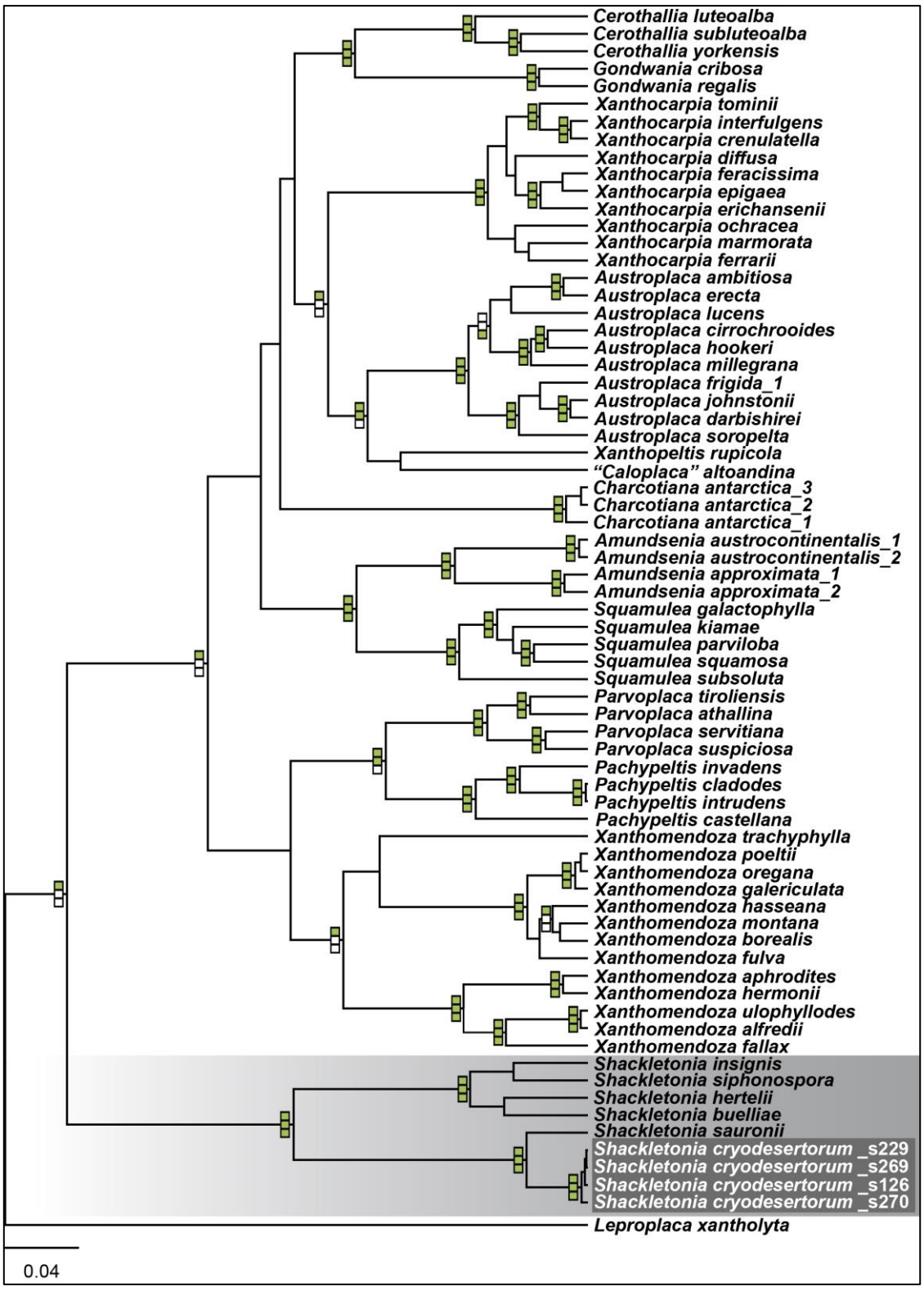

◀Figure 3. Maximum clade credibility (MCC) phylogenetic tree calculated using BEAST and based on *nrITS* sequences of the 70 specimens shown in Appendix 1. From top to bottom, squares filled with green colour represent significant statistical support obtained with BEAST (PP ≥ 0.95), MRBAYES (PP ≥ 0.95), and PHYML (B ≥ 70) analyses, respectively.

A chronogram based on the analysis of the combined matrix of three loci and using a secondary calibration on the node representing the split of *Caloplaca-Xanthoria* and *Xanthomendoza* (Gaya et al. 2015) is depicted in Figure 4. It includes 95% HPD intervals only for those nodes supported by at least one phylogenetic reconstruction method (ML, and two Bayesian). According to this analysis, *Shackletonia* began to diversify between the late Paleocene and the early Oligocene, with a mean estimate of 42.8 MA (95% HPD 56.7–30.3), while the new species *S. cryodesertorum* originated between the early Oligocene and the middle Miocene (mean = 20.4, 95% HPD 30.2–11.5). The estimated average substitution rates for each locus were 3.24×10^{-3} s/s/MA (*nrITS*), 4.5×10^{-4} s/s/MA (*nuLSU*) and 4.71×10^{-4} s/s/MA (*mtSSU*). Divergence time estimates using the mean *nrITS* substitution rate from *Melanohalea* were largely congruent with the previous approach, in concordance with previous results (e.g. Amo de Paz et al. 2011; Leavitt et al. 2012b, in *Parmeliaceae*). Thus, diversification of *Shackletonia* was dated back to 38.7 MA (95% HPD 50.1–28.1) whereas the origin of the new species was estimated around 18.5 MA (95% HPD 27.4–10.7). The co-estimated mean substitution rates for the *nuLSU* and *mtSSU* loci were 4.96×10^{-4} s/s/MA and 5.16×10^{-4} s/s/MA, respectively. Both analyses agree in estimating the separation of *Shackletonia* from the remaining lineages of subfamily *Xanthorioideae* between the late Cretaceous and the early Paleogene (mean estimates ranging from 70.5 to 64 MA). In addition, congruency of results from these two analyses to those from Gaya et al. (2015) is revealed by considering highly similar age estimates for the diversification of *Xanthocarpia* and *Xanthomendoza*. On the other hand, calibrating through a mean *nrITS* substitution rate from *Montanelia* produced discordant and higher age estimates for all nodes than the previous ones. For comparison, Supplementary Table 3 shows selected node ages and their respective 95% HPD from each analysis, including also results from Gaya et al. (2015).

Shackletonia has been shown as a highly variable genus at the three molecular markers used when compared to other *Xanthorioideae* genera (e.g. *Xanthomendoza* and *Austroplaca*) richer both in known species diversity and molecular data availability (Supplementary Table 2). A large amount of singleton sites and indels account for much of *Shackletonia* intrageneric genetic diversity. On the other hand, divergence between *S. cryodesertorum-sauronii* clade to the remaining *Shackletonia* species is mostly explained by singleton variable sites and one-position-long indels.

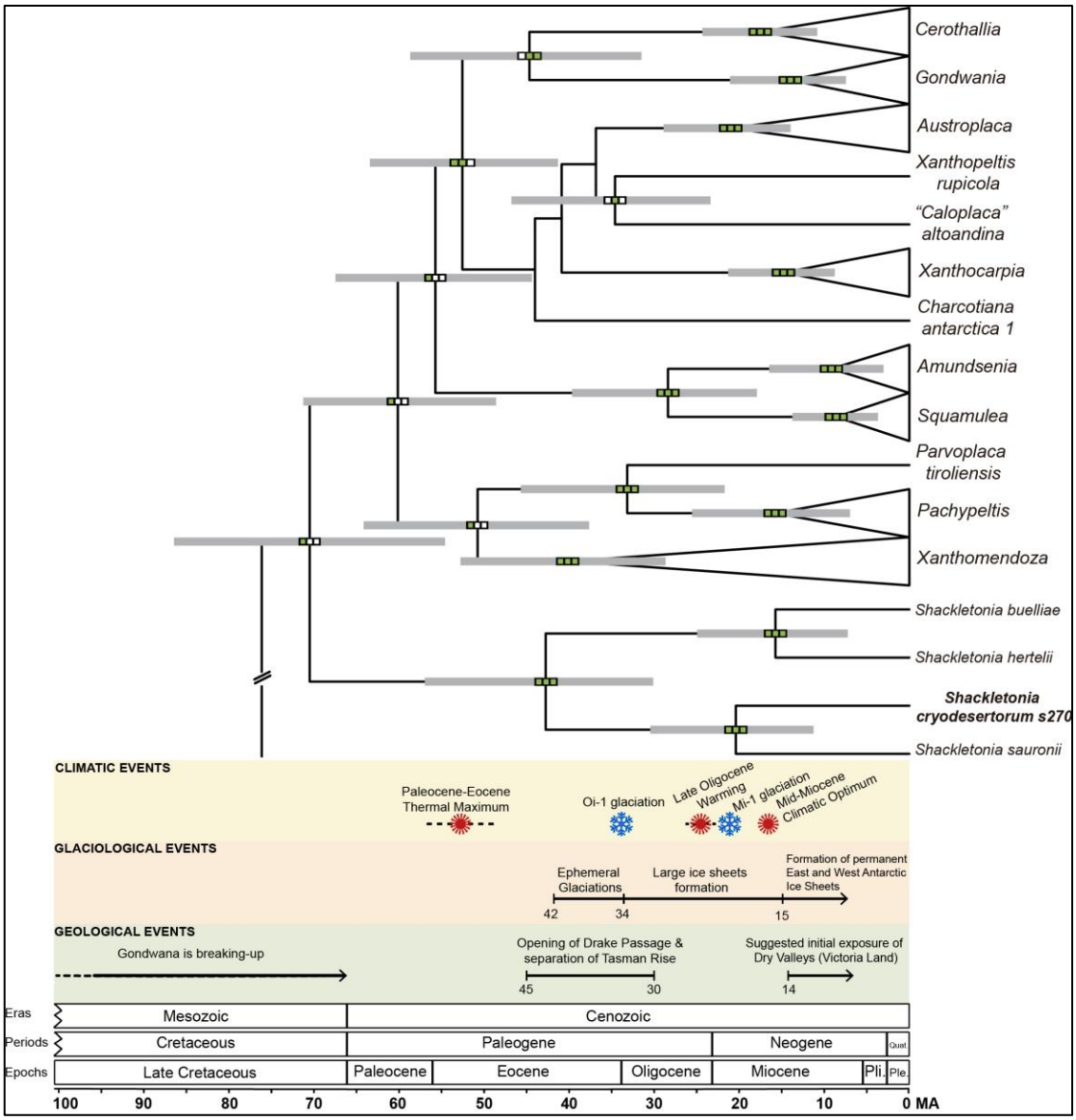

Figure 4. Time-calibrated MCC tree estimated from a concatenated dataset of ribosomal (*nrITS* and *nrLSU*) and mitochondrial (*mtSSU*) markers from lineages of subfamily *Xanthorioideae* using BEAST. Bars show the 95% highest posterior density intervals (HPD) only for those nodes supported by at least one phylogenetic reconstruction method. From left to right, squares filled with green colour represent significant statistical support obtained with BEAST (PP ≥ 0.95), MRBAYES (PP ≥ 0.95) and PHYML (B ≥70) analyses, respectively. Climatic, glaciological, and geological events occurring mostly in the Southern Hemisphere, and particularly in Antarctica, follow Zachos et al. (2001) and Convey et al. (2008). MA: million years ago.

4. Discussion

The new species is unequivocally placed within *Shackletonia*, a genus comprising lichenized, lichenicolous and muscicolous species, so far known from Antarctica and southern Patagonia (Arup et al. 2013). *Shackletonia*, phylogenetically located at the base of subfamily *Xanthorioideae* (Arup et al. 2013; Søchting et al. 2014a), is distinguished from other *Xanthorioideae* groups by its unique chemistry, producing 5- and 7-chloroemodin and their derivatives (Søchting et al. 2004). The new species *S. cryodesertorum* is well distinguished from the other species in the genus by its ecology and morpho-anatomical features. Thus, it grows on naked granitic rocks differing from the lichenicolous and muscicolous lifestyle shown by other species in the genus like *S. buelliae*, *S. sauronii* and *S. siphonospora* (Olech & Søchting 1993; Søchting et al. 2004). *Shackletonia insignis* also occurs saxicolous preferring sheltered crevices on rocks and developing microfruticose to pulvinate thalli composed of vertical lobes and attached to the substrate by means of rhizomorph-like hyphal strands with pedicellate ends (Søchting et al. 2004). Parts of some *S. cryodesertorum* thalli sometimes develop microfruticose morphs, with rhizomorph-like structures on the bottom as well. This seems to be a common feature displayed by lichens growing on Antarctic rocks and could be related with higher water retention capacity and light harvesting efficiency (Sojo et al. 1997; Valladares et al. 1998). *Shackletonia hertelii* differs by its areolate thalli, the initial dark orange colour of the apothecial disc and the apically non-inflated paraphyses (Søchting et al. 2004). *Shackletonia sauronii* is the sister species of *S. cryodesertorum*, and differs from the new taxon by the presence of dark reddish orange discs in young apothecia, barely visible to short septate, slightly longer spores, hardly thickened apical cells of paraphyses and I- medulla. (Søchting et al. 2004). The black ascomata of the new species also separates it from species of the *Caloplaca sideritis* group, which are characterized by their grey or whitish thallus lacking anthraquinones, and apothecia always reacting K+ purple (Wetmore 1996). Members of *Huea* and *Pyrenodesmia* (*sensu* Arup et al. 2013) also show blackish or black apothecia. *Huea* species differ from *S. cryodesertorum* by showing different chemical reactions and epithecium lacking anthraquinones whereas *Pyrenodesmia* species have a different thallus morphology, pigmentation, chemosyndrome type and microhabitat preferences. Finally, *S. cryodesertorum* resembles *Caloplaca exsecuta*, a taxon only known from the Northern Hemisphere, which also contains the pigment *Lecidea* green (Bachmann 1890). However, *C. exsecuta* shows a different habitus, disc and epithecium pigmentation and spore dimensions (Søchting et al. 2008).

Shackletonia buelliae, *S. siphonospora* and *S. cryodesertorum* share the presence of dark greenish blue pigment in the exciple. The formation of *Lecidea* green instead of anthraquinones is commonly observed in strongly light-exposed *Teloschistaceae* in polar regions (Hansen et al. 1987; Søchting 1989; Søchting & Seppelt 2003). As the chemical nature of *Lecidea* green is unknown, it is so far not established whether it is a result of a chemical transformation of anthraquinones or not. *Shackletonia buelliae* and the new species also share the I+ violet reaction of the exciple, cortex and medulla, with

or without prior addition of K (Olech & Søchting 1993). This reaction is very rare in *Teloschistaceae* and was formerly reported from *Caloplaca cladodes* (Poelt & Pelleter 1984). *Caloplaca magni-filii* is another species with amyloid medulla (Hansen et al. 1987).

A particular trait of *S. cryodesertorum* thalli is the existence of a necral layer or epicortex. Such a structure is considered a useful taxonomic character for several species of *Teloschistaceae* (Wetmore 1996), including *Caloplaca agrata*, *C. hueana*, *C. pellodella* and *C. sonorae*, all occurring in tropical areas and non-calcareous rocks (Wetmore 1996). On the other hand, a thicker cortex could improve thallus water capacity (Pérez-Ortega et al. 2012b), thus facilitating the survival in cold deserts such as the McMurdo Dry Valleys (Kappen 1982, 2000), but it has also been postulated to be the result of exposure to higher light intensities (Grube 2010).

The two alternative dating methods used to investigate the evolution in time of our target lineage yielded similar results. The genus *Shackletonia*, so far known mainly from Antarctica, diverged from the remaining groups in *Xanthorioideae* between the late Cretaceous and the early Paleogene (Supplementary Table 3). Furthermore, *Shackletonia* radiation is dated back at some point during the late Paleocene and early Oligocene (56.7–28.1 MA). This period corresponds with the opening of the Drake Passage and a progressive temperature decline, firstly generating ephemeral glaciers during the mid-Eocene (*c*. 42 MA) (Birkenmajer et al. 2005; Miller et al. 2005), and later ending up in the initiation of large Antarctic ice sheets at the Eocene-Oligocene boundary (*c*. 34 MA). These changes boosted important changes in the Antarctic biota like the replacement of native Antarctic plants with cold-tolerating species such as *Nothofagus* trees (Francis et al. 2008). Other genera in our phylogeny, including the more or less geographically restricted *Gondwania*, *Pachypeltis* and *Xanthocarpia*, the widely disjunct *Amundsenia*, *Austroplaca*, *Cerothallia* and *Xanthomendoza* and the cosmopolitan *Squamulea*, largely diversified throughout the late Paleogene and Neogene (< 34 MA), when the global paleoclimate was characterized by changing conditions (Zachos et al. 2001). These times further concur with inferred ages for the radiation of many parmelioid genera (Amo de Paz et al. 2011; Divakar et al. 2015). Finally, *S. cryodesertorum-sauronii* split is dated back at some point during the Oligocene and Miocene, and this timing partially overlaps with age estimates for the initial exposure of the Dry Valleys (Sugden et al. 2006).

From a biogeographic point of view, phylogenetic and dating results suggest a long-time evolution of *Shackletonia* in the Southern Hemisphere, particularly Antarctica. Only *S. hertelii* occurs also in Patagonia. A similar pattern was proposed for the neuropogonoid species of *Usnea*, which could have originated and dispersed from Antarctica to southern South America (Wirtz et al. 2008).

Key to *Shackletonia* species

1 On detritus, soil or mosses; ascospores simple, *c*. 16 × 5 µm ***S. siphonospora***

1* On rock or lichenicolous on saxicolous lichens; ascospores polardiblastic 2

2 Lichenicolous 3

2* On rock 5

3 Lichenicolous on *Psoroma* sp., or more rarely on *Pannaria* sp.; ascospores on average ≤ 12 µm long **"Caloplaca"** ***psoromatis***

3* Lichenicolous on *Buellia* sp.; ascospores on average ≥ 12 µm long 4

4. Thallus not visible, changes in host thalli not evident; ascospore septum 4–6 µm wide on average; with 5-chloroemodin ***S. buelliae***

4* Thallus visible, producing colour and size changes in host thalli; ascospore septum poorly differentiated, 2.5–3 µm wide; with 7-chloroemodin ***S. sauronii***

5 Thallus with 5-chloroemodin; apical cells of paraphyses not or slightly inflated 6

5* Thallus without 5-chloroemodin; apical cells of paraphyses inflated up to 5 µm thick ***S. cryodesertorum***

6 Thallus crustose, dark greyish; apical cells of paraphyses not inflated; saxicolous on maritime rocks or sometimes lichenicolous ***S. hertelii***

6* Thallus microfruticose, bluish grey to very pale grey; apical cells of paraphyses gradually inflated, up to 2.5 µm thick; in rock crevices ***S. insignis***

Supplementary Table 1. Test for strict molecular clock for each locus in Dataset A and B conducted in MEGA v.5. Tested under two different topologies (ML and Bayesian). *denotes rejection of the null hypothesis (i.e. equal rates)

	ML estimate				MrBayes consensus			
nrITS GTR+I+Γ (Dataset A)	ln*L*	Param	(+Γ)	(+I)	ln*L*	Param	(+Γ)	(+I)
With Clock	-7095.856	79	1.115	0.36	-7099.121	79	1.191	0.35
Without Clock	-6960.321	147	1.15	0.32	-6960.203	147	1.2	0.33
P (Ho: = rates)		$5.2e^{-11}$*				$8.96e^{-12}$*		
nrITS TN93+I+Γ (Dataset B)	ln*L*	Param	(+Γ)	(+I)	ln*L*	Param	(+Γ)	(+I)
With Clock	-5444.788	40	0.977	0.28	-5452.139	40	0.913	0.32
Without Clock	-5388.285	75	0.96	0.32	-5363.874	75	0.89	0.30
P (Ho: = rates)		$8.65e^{-4}$*				$3.63e^{-11}$*		
nuLSU GTR+I+Γ (Dataset B)	ln*L*	Param	(+Γ)	(+I)	ln*L*	Param	(+Γ)	(+I)
With Clock	-2753.380	42	0.778	0.63	-2746.279	42	0.793	0.64
Without Clock	-2722.074	73	0.76	0.64	-2718.789	73	0.78	0.64
P (Ho: = rates)		0.45				0.72		
mtSSU HKY+I+Γ (Dataset B)	ln*L*	Param	(+Γ)	(+I)	ln*L*	Param	(+Γ)	(+I)
With Clock	-3006.041	42	0.706	0.59	-3025.628	42	0.789	0.63
Without Clock	-2948.207	77	0.81	0.64	-2946.274	77	0.82	0.64
P (Ho: = rates)		$4.9e^{-4}$*				$7.73e^{-9}$*		

Supplementary Table 2. Polymorphism statistics for each marker (*nrITS*, *nuLSU*, *mtSSU*) from datasets corresponding to the *Xanthorioideae* genera *Shackletonia*, *Xanthomendoza* and *Austroplaca*. *s* (number of polymorphic sites), *k* (average number of nucleotide differences) and π (nucleotide diversity). *n* refers to species included in Appendix 1.

	Shackletonia			*Xanthomendoza*			*Austroplaca*		
Datasets	*nrITS*	*nuLSU*	*mtSSU*	*nrITS*	*nuLSU*	*mtSSU*	*nrITS*	*nuLSU*	*mtSSU*
s	102	27	33	99	34	37	63	28	25
Singleton variable sites	36	27	15	33	20	11	35	19	13
Parsimony informative sites	66	0	18	66	14	26	28	9	12
Eta (total number of mutations)	117	27	33	113	34	38	68	29	25
k	51.13	18	19.5	35.705	14.133	17.8	21.444	10.048	9.619
π	0.11164	0.02466	0.02624	0.07934	0.01860	0.02561	0.04797	0.01317	0.01196
Sites with alignment gaps or missing data	40	10	37	18	3	8	8	0	2
Number of sites (bp)	498	740	780	468	763	703	455	763	806
Species included (n)	6/6	3/6	4/6	13/13	6/13	6/13	9/9	7/9	7/9

Supplementary Table 3. Divergence time estimates (MA) of selected nodes obtained using different secondary calibration approaches with BEAST. Proposed geological periods take into account estimated ages within 95% HPD obtained from the first two analyses. Results of Gaya et al. (2015) are provided for comparison

	Calibrated node approach	*Melanohalea nrITS* substitution rate[a]	*Montanelia nrITS* substitution rate[b]	Gaya et al. (2015)	Geological period
Shackletonia and remaining *Xanthorioideae* lineages split	70.5 (54.8–86.2)	64 (51.4–77.9)	89.3 (70.9–107.7)	--	Late Cretaceous-Paleogene
Shackletonia crown group	42.8 (30.3–56.7)	38.7 (28.1–50.1)	54.2 (39.4–71)	--	Late Paleocene-Early Oligocene
Shackletonia cryodesertorum origin	20.4 (11.5–30.2)	18.5 (10.7–27.4)	25.9 (14.7–37.6)	--	Late Oligocene-Early Miocene
Xanthocarpia crown group	14.79 (9–21.1)	13.5 (8.7–18.9)	18.8 (12.1–25.9)	*c*. 14 (5.5–25.5)	Early/Middle Miocene
Xanthomendoza crown group	40.12 (28.9–52.5)	36.4 (26.9–46.9)	50.9 (37–64.8)	*c*. 43 (31–56)	Eocene-Early Oligocene
Caloplaca-Xanthoria and *Xanthomendoza* split	60.15 (48.8–71)	54.2 (43–65.8)	76 (60–91.8)	62.61 (74.03–51.85)	Late Cretaceous-Paleogene

[a] 3.41×10^{-3} s/s/MA (Leavitt et al. 2012b); [b] 2.43×10^{-3} s/s/MA (Leavitt et al. 2015b).

Appendix 1. List of taxa used in this study, with collection data and GENBANK accession numbers; newly produced sequences are in bold.

Taxa	Country, collector, collector no., herbarium	*nrITS*	*nuLSU*	*mtSSU*
Amundsenia austrocontinentalis 1	Antarctica, Upper Garwood, *A. de los Ríos*, MAF-Lich 18173	JX036068	-	KJ789975
A. austrocontinentalis 2	Antarctica,McMurdo Dry Valleys, *Seppelt* 27537, HO	KJ789961	-	-
A. approximata 1	Greenland, *Søchting* 10490, C	KJ789963	-	-
A. approximata 2	Norway, *Arup* L08179, LD	KJ789965	KJ789972	KJ789974
Austroplaca ambitiosa	UK, Falkland Isl., *Lewis Smith* 11027, AAS (*nrITS*, *nuLSU*); Chile, *Søchting* 11271, C (*mtSSU*)	KC179081	KC179151	KC179481
A. cirrochrooides	Chile, *Søchting* 11300, C	KC179082	KC179152	KC179482
A. darbishirei	Antarctica, Antarctic Peninsula, *Søchting* 11401, C	KC179083	KC179153	KC179483
A. erecta	New Zealand, *Eagle*, C	KC179084	-	-
A. frigida	Antarctica, Dry Valleys, Garwood Valley, *J. Raggio*, MAF-Lich 18904	JX036061	-	-
A. hookeri	Antarctica, South Shetland Isl., *Søchting* 7611, C	KC179085	KC179154	KC179484
A. johnstonii	Antarctica, South Shetland Isl., *Søchting* 7927, C	KC179086	-	-
A. lucens	France, Kerguelen Isl., *Søchting* 9417, C	KC179087	KC179155	KC179485
A. millegrana	Chile, *Søchting* 11330, C (*nrITS*); *Søchting* 10176, C (*nuLSU*); Chile, *Søchting* 10350, C (*mtSSU*)	KC179088	KC179156	KC179486
A. soropelta	Iceland, *Frödén* 650, LD (*nrITS*); Iceland, *Søchting* 7536, C (*nuLSU*, *mtSSU*)	KC179089	KC179157	KC179487
"Caloplaca" altoaldina	Argentina, *Frödén* 1700, LD	KC179094	KC179170	KC179503
Cerothallia luteoalba	Sweden, *Frödén* 1869, LD	KC179099	KC179177	KC179511
C. subluteoalba	Australia, VIC, *Kondratyuk* 20433, LD isotype	KC179100	-	KC179512
C. yorkensis	Australia, VIC, *Kärnefelt* 996101, LD	KC179101	KC179178	KC179513
Charcotiana antarctica 1	Antarctica, Victoria Land, *Bersan* A815, TSB	KJ789966	-	KJ789976
C. antarctica 2	Antarctica, Northern Victoria Land, *Seppelt* 25454, HO	KJ789968	-	-
C. antarctica 3	Antarctica, Southern Victoria Land, *Smykla*, KRAM-L-63612	KJ789970	KJ789973	-
Gondwania cribrosa	Australia, Tasmania, *Søchting* 11581, C	KC179102	KC179192	KC179526
G. regalis	Antarctica, Antarctic Peninsula, *Søchting* 11416, C	KC179103	-	-
	Antarctica, Antarctic Peninsula, *Søchting* 11427, C	-	KC179193	KC179527
Leproplaca xantholyta	Austria, *Arup* L97278, LD (*nrITS*); Spain, *Søchting* 9675, C (*nuLSU*, *mtSSU*)	KC179451	KC179208	KC179542
Pachypeltis castellana	Denmark, Greenland, *Søchting* 10500, C (*nrITS*)	KC179105	-	-
	Greenland, *Søchting* 10470, C (*mtSSU*)	-	-	KC179547

P. cladodes	USA, Wyoming, *Wetmore* 81439, LD	KC179106	-	-
P. intrudens	Afghanistan, *Soelberg* s.n., C	KC179107	-	-
P. invadens	Norway, Svalbard, *Elvebakk* 03:109, TROM	KC179108	KC179212	KC179548
Parvoplaca athallina	Antarctica, Antarctic Peninsula, *Søchting* 11393, C	KC179111	-	-
P. servitiana	Greece, *Spribille* 16225, CBFS JV6974	JN641778	-	-
P. suspiciosa	Russia, *Hermansson* 16839, McCune priv. herb.	KC179115	-	-
P. tiroliensis	Sweden, *Arup* L02364, LD (*nrITS*); Sweden, *Frödén* 1945, LD (*nuLSU*, *mtSSU*)	KC179116	KC179216	KC179552
Shackletonia buelliae	Antarctica, South Shetland Isl., *Søchting* 7583, C	KC179117	-	KC179578
***S. cryodesertorum* s126**	Antarctica, McMurdo Dry Valleys, Upper Garwood, *A. de los Ríos*, MA-Lich 18381, holotype	JX036057	-	**KU599932**
S. cryodesertorum s229	Antarctica, McMurdo Dry Valleys, Upper Garwood, *A. de los Ríos*, MA-Lich 18378	JX036132	-	-
S. cryodesertorum s269	Antarctica, McMurdo Dry Valleys, Miers Valley, The Altiplano, *A. de los Ríos*, MA-Lich 18379	JX036143	-	-
S. cryodesertorum s270	Antarctica, McMurdo Dry Valleys, Miers Valley, The Altiplano, *A. de los Ríos*, MA-Lich 18380	JX036144	**KU599931**	**KU599933**
S. hertelii	Chile, *Søchting* 10349, C (*nrITS*, *mtSSU*); Antarctica, South Shetland Isl., *Søchting* 7932, C (*nuLSU*)	KC179118	KC179240	KC179579
S. insignis	Antarctica, South Shetland Isl., *Søchting* 7933, C	KC179119	-	-
S. sauronii	Antarctica, South Shetland Isl., *Søchting* 7654, C	KC179120	KC179241	KC179580
S. siphonospora	Antarctica, South Shetland Isl., *Søchting* 7883, C	KC179121	-	-
Squamulea galactophylla	USA, Kansas, *Morse* 10997, LD	KC179122	-	-
S. kiamae	Australia, NSW, *Kondratyuk* 20480, LD isotype	KC179123	-	-
S. parviloba	USA, Texas, *Wetmore* 87830, LD	KC179124	-	-
S. squamosa	USA, Arizona, *Kärnefelt* AM960105, LD	KC179125	KC179252	KC179591
S. subsoluta	Austria, *Arup* L97072, LD	AF353954	KC179253	KC179592
Xanthocarpia crenulatella	Austria, *Søchting* 9359, C	KC179126	KC179274	KC179613
X. diffusa	Spain, 2007, *Llimona*, BCN	HQ699659	-	-
X. epigaea	Spain, *Etayo* 21453, C (*nrITS*, *nuLSU*); Germany, 2006, *Huneck*, C (*mtSSU*)	KC179127	KC179275	KC179614
X. erichansenii	Greenland, *Hansen* 734, LD	KC179128	-	-
X. feracissima	USA, Minnesota, *Morse* 14178, LD	KC179129	-	-
X. ferrari	Russia, *Vondrák* JV6531, CBFS	HQ699662	-	-
X. interfulgens	Iran, *Vondrák* JV5777, CBFS	HQ699639	-	-
X. marmorata	Italy, *Arup* L07030, LD	KC179131	KC179276	KC179615

X. ochracea	France, 1998, *Roux*, C (*nrITS*); Italy, *Arup* L07009, LD (*nuLSU*); Italy, *Arup* L07124, LD (*mtSSU*)	KC179132	KC179277	KC179616
X. tominii	Kazakhstan, *Vondrák* JV7273, CBFS	HQ699626	-	-
Xanthomendoza alfredii	Russia, *Obermayer* 50-P3, GZU holotype	AM263332	-	-
X. aphrodites	Cyprus, *Kalb* 1807/15808, Kalb priv. herb. holotype	AM408411	-	-
X. borealis	Greenland, *Søchting* 10499, C	KC179133	-	-
	Russia, *Zhurbenko* 94411, UPS	-	KC179278	KC179617
X. fallax	Austria, *Arup* L97529, LD (*nrITS*); USA, Wisconsin *Søchting* 9566, C (*nuLSU*); USA, Michigan, *Søchting* 9566, C (*mtSSU*)	AF353955	KC179279	KC179618
X. fulva	Chile, *Frödén* 1544, LD	KC179134	-	-
X. galericulata	Mexico, *Søchting* 9898, C	KC179135	-	-
X. hasseana	USA, Arizona, *Søchting* 7014, C	KC179136	KC179280	KC179619
X. hermonii	Syria, *Kondratyuk* 20128, LD isotype	KC179137	-	-
X. montana	USA, Montana, *Wetmore* 80956, M (*nrITS*); USA, California, *Knudsen* 3384, H (*nuLSU*); USA, *Nash* 34659, LD (*mtSSU*)	AY081157	JQ301582	EU680944
X. oregana	USA, Oregon, *McCune* 31146, LD	KC179141	-	-
X. poeltii	Sweden, *Kondratyuk* 2, LD holotype (*nrITS*, *mtSSU*); Denmark, *Søchting* 7473, C (*nuLSU*)	KC179142	KC179282	KC179622
X. trachyphylla	USA, North Dakota, *Wetmore* 80270, LD	KC179143	-	-
X. ulophyllodes	Russia, 2006 *Kuznetsova*, H (*nrITS*), USA, Wisconsin, *Søchting* 9571 (*nuLSU*, *mtSSU*)	KC179144	KC179284	KC179624
Xanthopeltis rupicola	Chile, *Frödén* 1654, LD	KC179146	KC179286	KC179626

CAPÍTULO 4 (*CHAPTER 4*)

De Alaska a la Antártida: delimitación de especies y diversidad genética en *Prasiola* (*Trebouxiophyceae*), un alga clorófita foliácea asociada con el hongo liquenizado bipolar *Mastodia tessellata*.

Referencia del artículo científico publicado:

Garrido-Benavent I, Pérez-Ortega S y de los Ríos A (2017) From Alaska to Antarctica: Species boundaries and genetic diversity of *Prasiola* (*Trebouxiophyceae*), a foliose chlorophyte associated with the bipolar lichen-forming fungus *Mastodia tessellata*. Molecular Phylogenetics and Evolution 107: 117–131 dx.doi.org/10.1016/j.ympev.2016.10.013

Abstract

Symbiotic associations between green algae (Chlorophyta) and fungi give rise to morphologically and eco-physiologically distinct entities, or so-called, lichens. In one of the most peculiar of these associations, the partners are species of the macroscopic genus *Prasiola* (*Trebouxiophyceae*) and the ascomycete *Mastodia tessellata* (*Verrucariaceae*). This is the only known case of a lichen symbiosis involving a foliose green alga. Despite intense research targeted at understanding the biology of this particular association, little is known about the genetic variability of its symbionts. This study focuses on the photobiont partner of this lichen and was designed to explore and compare its genetic diversity along a latitudinal axis from Alaska to Antarctica. Molecular sequence data were generated for three loci: two nuclear markers (*nrITS*, *RPL10A*) and one plastid-encoded marker (*tufA*). The usefulness of the *Prasiola nrITS* and *RPL10A* data was examined at the species and intraspecific levels. We used the population assignment tests implemented in BAPS and STRUCTURE and two algorithmic species delimitation procedures (ABGD, GMYC) to generate species boundary discovery hypotheses, which were subsequently tested using Bayes Factors. Population genetic differentiation and structure were also assessed through fixation indices, polymorphism statistics and haplotype networks. Based on the results of the species validation method, we propose that at least two species of *Prasiola* associate with the lichen-forming fungus *Mastodia tessellata*. Of these, *P. borealis* is broadly distributed in Alaska, Tierra del Fuego and the Antarctic Peninsula, whereas the second, undescribed, species is restricted to the Antarctic Peninsula. We detected significant phylogeographic substructure in *P. borealis*, including greater haplotype diversity in the Tierra del Fuego populations. Our findings provide new data that will be useful to unravel the cryptic diversity and phylogeographic patterns of the green alga partners of lichens.

1. Introduction

With *c*. 4.500 described species, the green algae are an extraordinarily diverse group of eukaryotic macro- and microorganisms that date back to 700–1.500 MA (Herron et al. 2009; Guiry 2012). Difficulties in the systematics of these organisms are two-fold. First, morphological homoplasy and stasis along with phenotypic plasticity are common at different phylogenetic depths (e.g. Fraser et al. 2009a; Škaloud & Rindi 2013; Verbruggen 2014). And second, the multiple species concepts that phycologists have applied to accommodate the singularities of their respective groups of interest often prevent establishing broadly accepted species delimitation criteria across the whole lineage (Leliaert et al. 2014).

The systematics of green algae associated with lichen-forming fungi is no exception. While fungal species delimitation based on traditional morpho-anatomical and chemical characters is relatively straightforward, the circumscription of symbiont algae is particularly challenging. For over a decade, studies have been unravelling the diversity of lichen-associated photobionts within a phylogenetic framework. The consequence of this research effort has been the revision of traditional species concepts and even the description of new taxa (Kroken & Taylor 2000; Škaloud & Peksa 2010; Nelsen et al. 2011; Vančurová et al. 2015). So far, the use of numerous coalescent-based methods to document and describe species based on DNA sequences (see Fujita et al. 2012) has been limited, most studies having focused on selectivity and specificity (Sadowska-Dés et al. 2014; Leavitt et al. 2015c). However, in many groups of chlorophytes involved in lichen symbioses, further evidence based on multi-locus data is required.

Contrasting patterns of lichen photobiont phylodiversity have been observed at high phylogenetic levels. For instance, the lichen-forming fungus family *Parmeliaceae*, with more than 2.500 species showing a wide variety of ecological and geographic ranges, is strictly associated with green micro-algae of the genus *Trebouxia* (e.g. Fernández-Mendoza et al. 2011; Leavitt et al. 2015c). Likewise, nearly all *Peltigerales* associate with *Nostoc* cyanobacterium either as a primary or secondary photobiont (Rikkinen 2013), while orders including many tropical species such as *Arthoniales* and *Ostropales* have symbiotic relationships preferentially with the *Trentepohliales* (Nelsen et al. 2011). In contrast, members of the widespread family *Verrucariaceae* associate with at least seven photobiont genera from three different phyla (reviewed in Thüs et al. 2011). The relationship between the lichen-forming fungus *Mastodia tessellata* and a macroscopic green alga of the genus *Prasiola* (*Prasiolales*, *Trebouxiophyceae*) has long drawn the attention of biologists as the only known lichen with a foliose photobiont (Kohlmeyer et al. 2004; Pérez-Ortega et al. 2010). Descriptions of this symbiosis have ranged from a mycophycobiosis or putative "fungal infestation" (Reed 1902; Parader & Ahmadjian 2000; Rindi et al. 2007) to a primitive or borderline lichen (Kováčik & Pereira 2001; Lud et al. 2001; Kohlmeyer et al. 2004). Based on electron microscopy observations, Pérez-Ortega et al. (2010) claimed that the fungal partner of this lichen provokes the altered arrangement of algal cells, and that the cells of both bionts undergo

intimate interactions albeit with negligible impacts on macromorphology. These authors also highlighted the complexity of this symbiotic relationship, which rather than being strictly attributed to parasitism, mutualism or saprophytism, may be described as a dynamic equilibrium in which the photobiont under certain conditions is able to "escape" from the mycobiont.

Despite the long-standing debate about the nature and ecological implications of this uncommon association, little is known about the genetic variability of these symbionts. In early work, it was acknowledged that two species of *Prasiola* associated with Ascomycetes. In the Northern Hemisphere, Reed (1902) designated as *Prasiola borealis*, green algae colonised by a fungus he described as *Guignardia alaskana*. Lichenised *Prasiola* specimens from the Antarctic and Subantarctic regions were initially ascribed to *Prasiola crispa* ssp. *antarctica* (Kováčik & Pereira 2001; Lud et al. 2001; Kohlmeyer et al. 2004). However, more recent studies have shown that both *P. delicata* and *P. borealis* associate with *Mastodia tessellata* in the Northern and both hemispheres respectively (Pérez-Ortega et al. 2010; Moniz et al. 2012a, 2014). Further, Moniz et al. (2012b) used molecular data to resurrect *Prasiola antarctica* (= *P. crispa* ssp. *antarctica)* to accommodate a distinct Antarctic lineage, yet the specimens of this species examined so far show no distinct signs of fungal presence meaning that the species of Antarctic *Prasiola* associated with *M. tessellata* remain unknown.

In this study, we compiled a comprehensive molecular dataset extracted from specimens of *Prasiola* collected in Alaska, Tierra del Fuego and the Antarctic Peninsula. Three molecular markers were selected for the alga, including the plastid-encoded elongation factor Tu (*tufA*) gene, the nuclear ribosomal Internal Transcribed Spacer (*nrITS*), and the nuclear *RPL10A* gene. The latter encodes the protein RPL10, required to join together 40S and 60S subunits into a functional 80S ribosome (Eisinger et al. 1997). The markers *tufA* and *nrITS* have been often used in barcode and phylogenetic studies of several groups of green algae (e.g. Leliaert et al. 2009; Saunders & Kucera 2010; Rindi et al. 2011; Sadowska-Dés et al. 2014; Moya et al. 2015). In contrast, the *RPL10A* gene has been seldom used for evolutionary analyses in Chlorophyta (del Campo et al. 2013). Moreover, there are no literature data available on *nrITS* and *RPL10A* markers for *Prasiola*.

The aims of our study were: (1) to test the use of *nrITS* and *RPL10A* markers for evolutionary analyses at intermediate and low taxonomic levels in *Prasiola*, (2) to explore the population structure of the *Mastodia tessellata* photobiont, (3) to propose and validate species boundaries for lichenized *Prasiola* using a multi-locus approach, and (4), to shed light on the genetic structure and differentiation within each delimited species across its distribution range.

2. Material and Methods

2.1. Taxon sampling

We collected 140 individual samples of *Prasiola*, each one consisting of 3–4 blades arising from a common holdfast (Figure 1). The majority of them showed evident signs of fungal colonisation, i.e. brownish subglobose fungal perithecia on the blade surface (Figure 1B–C). Free-living *Prasiola* specimens, particularly those growing along with the lichenized ones, were also obtained to check whether they were unlichenized forms of the same algal taxa. Additionally, we obtained DNA sequences from pure cultures of *Prasiola crispa* and *Prasiolopsis ramosa* from the SAG Culture Collection (SAG strain numbers 43.96 and 26.83, respectively).

Sampling was done at 15 coastal localities along a latitudinal transect that includes Alaska (2 loc.), Tierra del Fuego (6 loc.) and the Antarctic Peninsula (7 loc.). Further details of the localities are given in Appendix 1. Up to 18 samples per locality were collected, then air dried and, finally, stored at the herbarium of the Real Jardín Botánico de Madrid (MA).

2.2. DNA extraction, PCR, and sequencing

Blade surfaces of hydrated thalli were thoroughly scraped under a dissecting microscope to remove contaminating epiphytic micro-algae. After several rinse cycles in distilled water, small blade fragments (*c*. 2 × 2 mm) first inspected under the light microscope were collected for DNA extraction. Fragments were then dried, frozen in liquid nitrogen (-196° C) and pulverized using a Retsch MM 200 mixer mill and metallic beads. A modified version of the CTAB method (Cubero et al. 1999) was used to isolate genomic DNA. The plastid-encoded *tufA* gene, and the *nrITS* and protein-coding *RPL10A* nuclear markers were amplified. To improve amplification efficacy, we designed new internal primers with PRIMER-BLAST (Ye et al. 2012) and followed a nested PCR protocol. Details of the primers and PCR settings used in this study are found in Supplementary Tables 4–5, respectively. The initial and nested PCR reactions were run in a total volume of 25 microlitres, containing 3–5 µl of template DNA or 1 µl of the first reaction (nested), 1.25 µl of each primer (10 µM), 2.5 µl of reaction buffer (Biotools®), 5 µl of dNTPs (1 mM), 1 µl of $MgCl_2$ (50 mM) and 0.5 U of DNA polymerase (Biotools®); distilled water was used to make up the final volume. AmpliTools Fast Master Mix (2x) (Biotools®) or PCR-PuRe-Taq Ready-to-Go Beads© (GE Healthcare) were also used in some reactions following the manufacturers' instructions. The identity of novel *nrITS* sequences was checked in BLAST, and only hits displaying 80–90% similarity to any other GENBANK-available members of *Prasiolaceae* (e.g. *Stichococcus*, *Desmococcus* and *Diplosphaera*, Guiry & Guiry 2016) were selected as candidate *nrITS* for *Prasiola*. PCR products were electrophorized in 1.5% agarose gels stained with PRONASAFE nucleic acid stain solution (CONDA Laboratories). After purification using the UltraClean® PCR Clean-Up Kit (MOBIO Laboratories, Inc.), DNA strands were finally sequenced at MACROGEN EUROPE (The Netherlands).

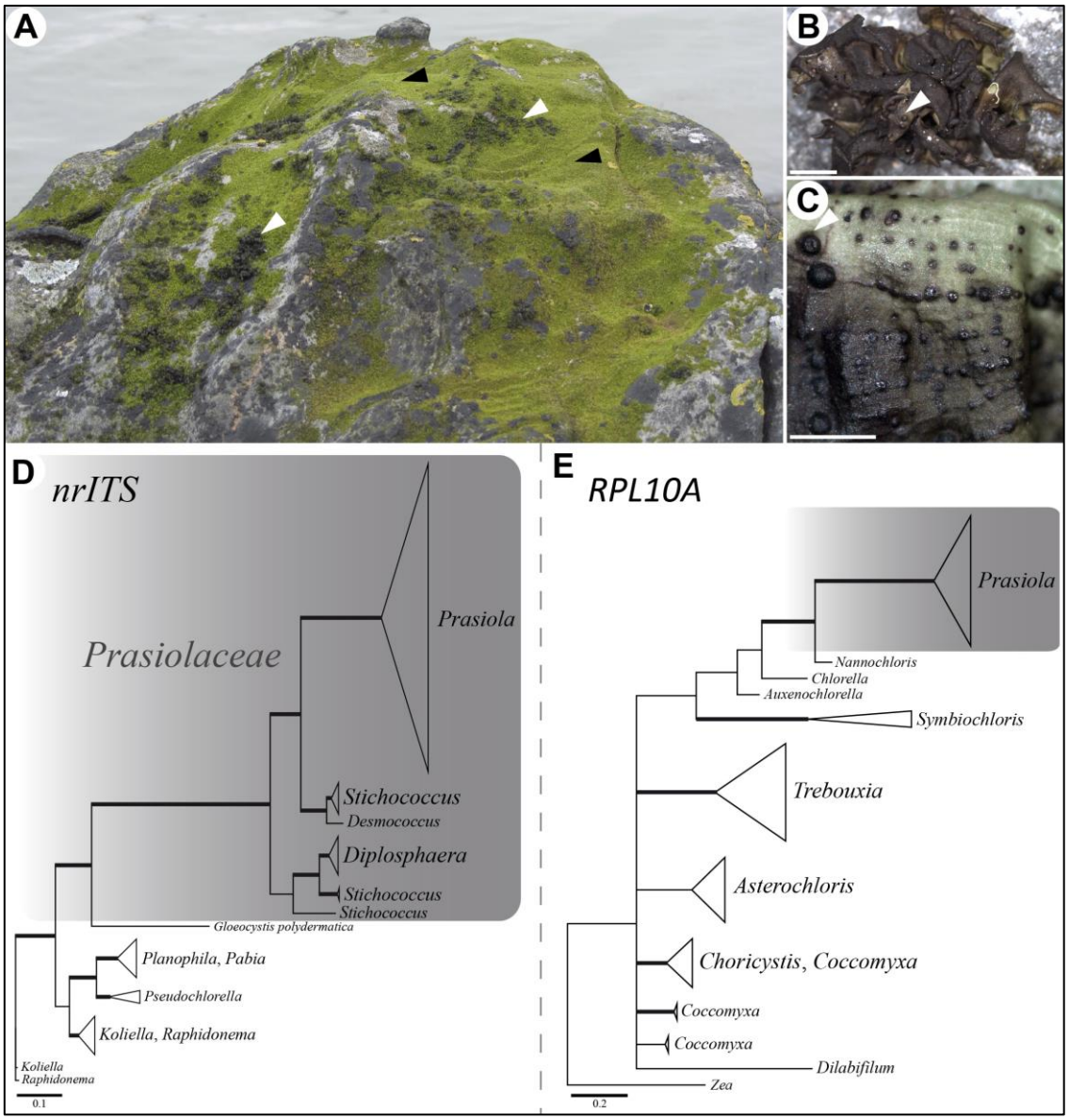

Figure 1. (A) Lichenized (white arrow tips) and free-living (black arrow tips) *Prasiola* specimens growing on a boulder near the seashore in Petersburg, Alaska. (B) and (C) lichenized *Prasiola* blades showing fungal perithecia at different development stages (white arrow tips). (D) and (E) MrBayes 50% majority-rule consensus trees depicting phylogenetic relationships of *Prasiola* with other members of Chlorophyta based on *nrITS* and *RPL10A* data. Thickened branches indicate Bayesian posterior probability (PP) ≥ 95%. Scales: (B–C) = 1 mm. (Photographs and phylogenetic trees: SPO & IGB).

2.3. DNA sequence analysis

Electropherograms were checked, trimmed and assembled using SEQMANII v.5.07© (Dnastar Inc.). GENBANK accessions are given in Appendix 1. We followed Steeves et al. (2005) and Bergemann et al. (2009) when dealing with sequences showing a few ambiguous sites. These were collapsed into existing haplotypes to avoid artificial inflation of genetic diversity through the addition of new haplotypes. Alignments were

carried out in GENEIOUS® v.9.0.2 using MAFFT v.7.222 (Katoh et al. 2002). Each single-locus dataset was tested for recombination using five alternative methods: the PHI test (Bruen et al. 2006), as implemented in the software SPLITSTREE4 v.4.13.1 (Huson & Bryant 2006); the four-gamete test conducted in DNASP v.5.10 (Librado & Rozas 2009), and the RDP, GENECONV, MAXCHI methods, which are available in the software RDP4 version Beta 39 (Martin et al. 2010). The latter three analyses were carried out using default parameters as suggested in Martin et al. (2010). Substitution models for each alignment used in this study were estimated in JMODELTEST v.2.1.6 (Darriba et al. 2012) based on the Akaike Information Criterion (AIC, Akaike 1974).

2.4. Single-gene phylogenies

We compiled three datasets consisting of newly generated *nrITS*, *tufA* and *RPL10A* sequences, which were subsequently reduced to haplotypes using FABOX v.1.41 online toolbox (Villesen 2007) (Appendix 1). An arbitrary haplotype of each locus was used to conduct *blastn* searches to select and download data for other Chlorophyta taxa from GENBANK. We prioritized sequences obtained from pure cultured (SAG, UTEX, CCAP) over environmental samples (Appendix 2–4). Twenty-four *nrITS* accessions belonging to members of Chlorophyta were chosen, and aligned with 23 haplotypes obtained from lichenized or free-living *Prasiola* samples (dataset *nrITS*-A). GBLOCKS v.0.91b (Castresana 2000) was used to remove ambiguously aligned regions and large gaps by using varying levels of stringency. GBLOCKS settings and initial and final features of each alignment are shown in Supplementary Table 6. For the *tufA* locus, twenty-seven accessions including all available *Prasiola* taxa were selected and aligned with four haplotypes obtained from lichenized or free-living *Prasiola* specimens (dataset *tufA*-A). Two species of *Rosenvingiella* were used as outgroup. Finally, 8 *RPL10A* haplotypes obtained from lichenized, free-living and cultured *Prasiola* were aligned with twenty-six sequences of other Chlorophyta, and the green plant *Zea mays* was used as the outgroup (dataset *RPL10A*-A). The alignment was reduced to the first 111 bp, which partially corresponds to an exonic region conserved across lineages. Phylogenetic relationships were inferred using two approaches. Maximum Likelihood (ML) reconstructions were carried out in the online version of RAxML-HPC2 implemented in CIPRES Science Gateway web server (Stamatakis 2006, 2008; Miller et al. 2010). Nodal support was computed from 1.000 bootstrap pseudoreplicates. Subsequently, a Bayesian inference method was implemented in MRBAYES v.3.2.3 (Ronquist et al. 2012). Protein-coding data were divided into three partitions corresponding to codon positions, enabling substitution model parameters to vary independently across partitions. Two parallel, simultaneous four-chain runs were executed over 1×10^7 generations starting with a random tree, and sampling after every 100th step. We discarded the first 20% of data as burn-in. The 50% majority-rule consensus tree and corresponding posterior probabilities (PP) were calculated from the remaining trees. Average standard deviation of split frequencies (ASDSF) values below 0.01 and potential scale reduction factors (PSRF) values approaching 1.00 were set as indicators of chain convergence.

2.5. Population assignment tests

A Bayesian framework was used to assess the level of genetic stratification in single and multi-locus genotype data. We used BAPS v.6 (Corander & Marttinen 2006; Corander et al. 2008) to identify clusters with different allele frequencies independently from each molecular dataset. Sequence data were previously converted into single nucleotide polymorphism (SNP) files in MESQUITE v.3.01 (Maddison & Maddison 2014). BAPS analyses used a model that accounted for dependences present between the marker loci or sites within aligned sequences (Corander & Tang 2007), codon linkage models, and were run with *K* values ranging from 2 to 10, with 10 replicates for each value. Multi-locus analyses were based only on individuals with at least two markers including *nrITS*, as this marker displays four times the variability than others. The result with the highest log likelihood was selected as optimal and used to infer admixed individuals. Settings included a minimum size of two individuals per cluster, using 100 iterations, 200 reference individuals and 100 iterations per reference individuals (Corander & Marttinen 2006). To further investigate population ascription of individuals, we also employed STRUCTURE v.2.3.4 (Pritchard et al. 2000; Falush et al. 2003). It has been suggested that both Bayesian approaches should be used, at least when low levels of differentiation among groups are expected (Latch et al. 2006). PGDSPIDER v.2.0.7.2 (Lischer & Excoffier 2012) was used to transform haplotypes into alleles to avoid bias due to genetic relatedness in multi-locus analyses. Four different datasets were analysed: A: *tufA-RPL10A*, B: *tufA-nrITS*, C: *RPL10A-nrITS*, and D: three-locus dataset. In datasets B, C and D, individuals without *nrITS* data were excluded. Ten replicate runs consisting of 50.000 burn-in generations, followed by 500.000 iterations, with *K* ranging from 1 to 10 were performed in each dataset. Each analysis used a model allowing admixture, no prior population information, a uniform alpha prior, whereas allele frequencies were kept independent among gene pools in order to avoid overestimating the number of gene pools (Falush et al. 2003). We used the online platform CLUMPAK (Kopelman et al. 2015) to delimit the optimum number of clusters (best *K*) according to Evanno et al. (2005). We also considered ln(Pr(X|K)) values to identify the *k* for which Pr(K = k) is highest (STRUCTURE manual, section 5.1). The *POPHELPER* R package (Francis 2016) was employed to graph admixture results.

2.6. Species discovery methods

When combined with genetic clustering analyses, species discovery strategies based on single-locus datasets provide valuable background information to build hypotheses of species limits. We first employed the Automatic Barcode Gap Discovery method (ABGD, Puillandre et al. 2012), a distance-based approach which automatically finds breaks in the distribution of genetic pairwise distances, allowing intra- and interspecific distances to overlap. It was remotely run at http://wwwabi.snv.jussieu.fr/public/abgd/abgdweb.html, using the Kimura two parameters (K2P) model to calculate genetic distances between individuals, and TS/TV values obtained from MEGA v.5.2 (Tamura et al. 2011). As the exact threshold values indicating the presence of more than one species in the dataset are unknown for the

markers used and our target group, we set the remaining parameters to default values. ABGD analyses were run with the following datasets: newly generated *nrITS*, *tufA*, and *RPL10A* sequence data obtained from lichenized specimens (datasets *nrITS*-B, *tufA*-B, *RPL10A*-B, respectively), and the extended *tufA*-A dataset. Later, we utilized the Generalized Mixed Yule Coalescent model (GMYC, Pons et al. 2006; Fujisawa & Barraclough 2013). GMYC uses a prior on the gene tree that assumes a mixture of a Yule branching process for the species tree and a coalescent model within populations. Both single and multiple threshold models were implemented in the GMYC web server (http://species.h-its.org/gmyc/; Zhang 2015). To test the effect of incorporating sequences from outgroup taxa on the GMYC delimitation results, we constructed alignments without (datasets *nrITS*-B, *RPL10A*-B) or including several outgroup sequences (datasets *nrITS*-A, *nrITS*-C with only the *Stichococcus* and *Desmococcus* outgroup sequences, and *RPL10A*-C). For the *tufA* gene, we used dataset *tufA*-C, which is the same as *tufA*-A but without duplicate sequences. Ultrametric trees used in the GMYC analyses were computed in BEAST v.1.8.1 (Drummond et al. 2012) using a strict clock, a coalescent constant population size prior (Monaghan et al. 2009), and substitution models as presented in Supplementary Table 6. Prior parameters and operators were set to default for the *nrITS* analysis, whereas three partitions were specified in the *tufA* and *RPL10A* analyses, unlinking substitution rate parameters and base frequencies across codon positions and setting a uniform prior (initial value = 1, upper value = 5, lower value = 0) for each codon relative rate parameter. Two runs of 2×10^7 generations each, sampling every 2.000 step, were performed in CIPRES Science Gateway and then combined with LOGCOMBINER v.1.8.1. The first 20% of data was discarded as burn-in, and the maximum clade credibility tree with the corresponding posterior probabilities (PP) calculated from the remaining trees.

2.7. Species validation method

We evaluated the different species hypotheses recovered by genetic structure analyses (BAPS, STRUCTURE) and single-gene-based discovery methods (ABGD, s/mGMYC) using the Bayes Factor Delimitation (BFD) method of Grummer et al. (2014). This approach allows for topological uncertainty in gene trees and incongruences among gene trees which is desirable in scenarios of recent divergences or in phylogeographic studies dealing with large sample numbers (e.g. Chen et al. 2014; Hedin et al. 2015). Competing species delimitation hypotheses were generated with *BEAST (Heled & Drummond 2010; Drummond et al. 2012). Analyses were performed under a strict clock for each locus, with mean clock rate fixed to 1.0 for *nrITS* whereas rates were co-estimated for the other loci. A Yule tree prior, which assumes a constant lineage birth rate for each branch in the tree, and the piecewise linear and constant root model for population size were used following Grummer et al. (2014). Hyperpriors for the species population mean and Yule speciation process parameters were given an inverse gamma distribution with an initial value of 0.015 or 1, shape parameter of 3 or 1 and scale of 0.3 or 1, respectively. Clock rates for *RPL10A* and *tufA* were co-estimated under a uniform prior (0, 5). Informative priors were also given for the remaining

parameters across all analyses. To avoid overparameterization, less complex substitution models, such as HKY, were used (Supplementary Table 6). No outgroup species was included as *BEAST works with two or more species (Heled & Drummond 2010). Two replicate runs of 50 M generations, saving every 5.000th tree, were performed using the CIPRES Science Gateway. Convergence across separate runs was assumed if effective sample sizes (ESS) were >200, which was checked in TRACER v.1.6 (http://tree.bio.ed.ac.uk/software/tracer/). Calculation of marginal likelihoods estimates (MLE) for each replicate run was done using Path Sampling (PS, Lartillot & Philippe 2006) and Stepping-Stone (SS, Xie et al. 2011). PS and SS runs were conducted with default settings. We averaged MLE across runs and calculated Bayes Factors following Hedin et al. (2015). Results were interpreted according to Kass & Raftery (1995), who consider 2lnBF > 10 as "decisive" support for a hypothesis.

2.8. Polymorphism statistics, haplotype networks, and neutrality tests

We first calculated genetic diversity estimators for each marker to discuss their suitability for inter- and intraspecific studies. DNASP v.5.10 (Librado & Rozas 2009) was used to compute the number of segregating sites (*s*), number of haplotypes (*h*), haplotype diversity (*Hd*), average number of nucleotide differences (*k*), nucleotide diversity (π) either using the Jukes & Cantor (1969) correction or not, and parsimony informative sites. Next, DNA polymorphism was evaluated for each marker according to: a) potential evolutionary units delineated by the species discovery-validation analyses, and b) the geographic origin of samples. Sequences corresponding to the Antarctic individuals with extraction codes I107 and I443 (hap16_*its*, hap3_*rpl*, hap3_*tuf*) were not included in the second analysis as they were genetically identical. For the *RPL10A* marker, we used a partial alignment containing the initial exonic region to compute total DNA polymorphism, but the whole sequence length was used in the case of geographic analyses. Gaps were not considered in calculations. Statistical parsimony using the method TCS (Clement et al. 2002) as implemented in POPART v.1.7 (Leigh & Bryant 2015) was used to infer relationships among haplotypes. Finally, deviations from neutrality, which are useful for inferring past population size changes, were tested with Tajima's *D* and Fu's *Fs* statistics in DNASP v.5.10 using the number of segregating sites. The significance of these tests was assessed based on 10^4 coalescent simulations.

2.9. Quantifying genetic divergence and differentiation

We used the average number of nucleotide substitutions per site between sampling localities of each species (Dxy, Nei 1987) as a proxy to measure the extent of genetic divergence. It is especially important to treat each putative species separately because equivocal concepts of species limits could confound an extrinsic barrier to dispersal with intrinsic reproductive barriers (Pante et al. 2015). Further, levels of genetic differentiation were determined by calculating the estimator Θ for Wright's fixation index Fst (Weir & Cockerham 1984) based on allele frequencies. Dxy and Fst values between sampling localities were estimated in ARLEQUIN v.3.5 (Excoffier &

Lischer 2010) and results were graphically represented with a collection of R functions (R Development Core Team 2013) implemented in *r-lequin* (http://heidi.chnebu.ch/doku.php?id=r-lequin). Prior to computations, haplotype input files were constructed with DNASP v.5.10, including gaps and invariable sites. Individuals from the three sampling localities of Navarino Island were pooled together to balance sampling sizes. The *tufA* dataset was not used for this purpose due to low levels of polymorphism.

3. Results

3.1. Sequence data and polymorphism

We generated 362 new DNA sequences from three molecular markers: 119 *nrITS*, 109 *RPL10A* and 134 *tufA* (Appendix 1). 353 sequences were acquired from fungus-colonised blades, while the remaining sequences were derived from free-living or cultured *Prasiola*. Alignment lengths were 791 and 574 base pairs for *nrITS* and *tufA*, respectively. Only the first 111 bp of the whole *RPL10A* dataset could be unambiguously aligned and were informative enough for subsequent analyses. The remaining sequence data were those of a hypervariable region that could be aligned exclusively when samples were grouped according to separate geographic regions. Likewise, del Campo et al. (2013) noticed that most exons of the *RPL10A* gene showed approximately similar sizes of 100–200 bp and were conserved across distantly related lineages. No statistically significant recombination events were detected in any of the tests (p-value > 0.5) and the weak signal found only in MAXCHI analysis of the *nrITS* dataset was assumed to be more the result of homoplasy due to the high polymorphism observed than due to true recombination. The *nrITS* dataset showed the highest values of nucleotide diversity and segregating sites, whereas the *tufA* marker showed the lowest level of polymorphism. Values for these and other genetic diversity statistics are summarized in Supplementary Table 7.

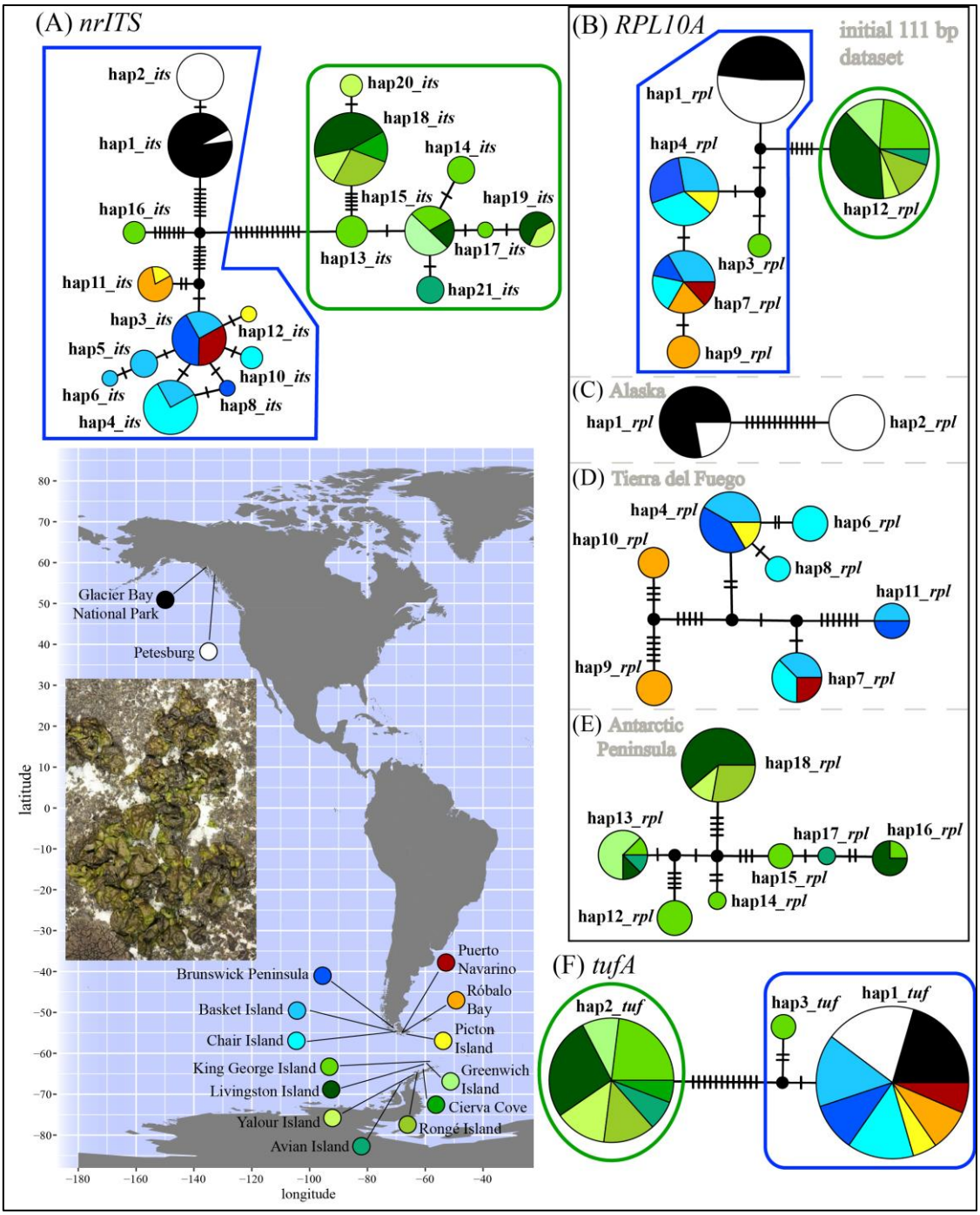

Figure 2. Statistical parsimony networks for haplotypes of the nuclear *nrITS* (A) and *RPL10A* (B–E) loci, and plastid-encoded *tufA* (F) in lichenized *Prasiola borealis* (dark blue lines) and *Prasiola* sp. (green lines). Colors indicate the localities where individuals were collected (these also appear in the map). The sizes of the circles in the networks are proportional to the numbers of individuals bearing the haplotype; black-filled circles indicate missing haplotypes. Mutations are shown as hatch marks. Haplotype codes follow Appendix 1. Note that haplotypes in network B are based on the 111 bp-long *RPL10A* dataset.

3.2. Phylogenetic relationships in single-locus analyses

A total of 23 *nrITS*, 4 *tufA* and 8 *RPL10A* haplotypes were used to infer the phylogenetic tree for each loci. Of these, 21 *nrITS*, 3 *tufA* and 6 *RPL10A* haplotypes corresponded to lichenized *Prasiola* individuals collected in different localities (Figure 2). ASDSF and PSRF values indicated convergence of chains in all Bayesian runs. The *nrITS* sequences produced in this study formed a monophyletic group sister to members of *Prasiolaceae* (*Stichococcus*, *Desmococcus* and *Diplosphaera*) (Figure 1D). *Diplosphaera* formed a monophyletic group, and *Stichococcus* was recovered as polyphyletic, as observed in previous works based on *rbcL* and *nuSSU* markers (Thüs et al. 2011). Relationships among haplotypes were congruent across different alignments and phylogenetic methods used (Supplementary Figure 1). The ML tree revealed three supported monophyletic clades, each including individuals from a single geographical region (Alaska, Tierra del Fuego or the Antarctic Peninsula). Within the Tierra del Fuego clade, a haplotype from Navarino Island (hap11_*its*) appeared basal to the remaining haplotypes (hap3–10,12_*its*) with bootstrap support over 70%. The relative position of hap16_*its* recovered from two individuals from King George Island was uncertain. Figure 3 shows the phylogenetic relationships of the *tufA* haplotypes. Thus, haplotypes hap1_*tuf* (Alaska and Tierra del Fuego) and hap3_*tuf* (King George Island) fell within a monophyletic clade containing samples of *Prasiola furfuracea* and *P. borealis*. The relative position of a haplotype recovered from the majority of the Antarctic lichenized specimens (hap2_*tuf*) remained unclear. Further, the unlichenized *Prasiola* sample collected in Alaska (I438, hap4_*tuf*) was phylogenetically assigned to a monophyletic clade with *P. delicata*. Finally, in the *RPL10A* tree, *Prasiola* haplotypes formed a supported monophyletic group sister to a sample of *Nannochloris normandinae* (*Chlorellaceae*) (Figure 1E, Supplementary Figure 2). No structure was recovered within the ingroup, only for a small clade including lichenized and free-living specimens from Alaska (hap1–2_*rpl*). An Antarctic haplotype (hap12_*rpl*) and a cultured *Prasiola crispa* sequence appeared basal to the remaining *Prasiola* but with low support. Relationships among other taxa included in our analyses are not further discussed as they were not the focus of this study.

►Figure 3. MRBAYES 50% majority-rule consensus tree showing phylogenetic relationships of lichenized and free-living (hap1–3_*tuf*) and free-living (hap4_*tuf*) *Prasiola* based on *tufA* data. Branches in bold indicate statistical support from Bayesian posterior probabilities (PP ≥ 0.95, above) and/or ML bootstrap values (B ≥ 70%, below). The geographic origin of specimens are signaled by colored dots: north-western North America (black), Tierra del Fuego (blue), northern Europe (red), Tasmania (yellow), and Antarctic Peninsula (green). GENBANK accession numbers are indicated for each tip node.

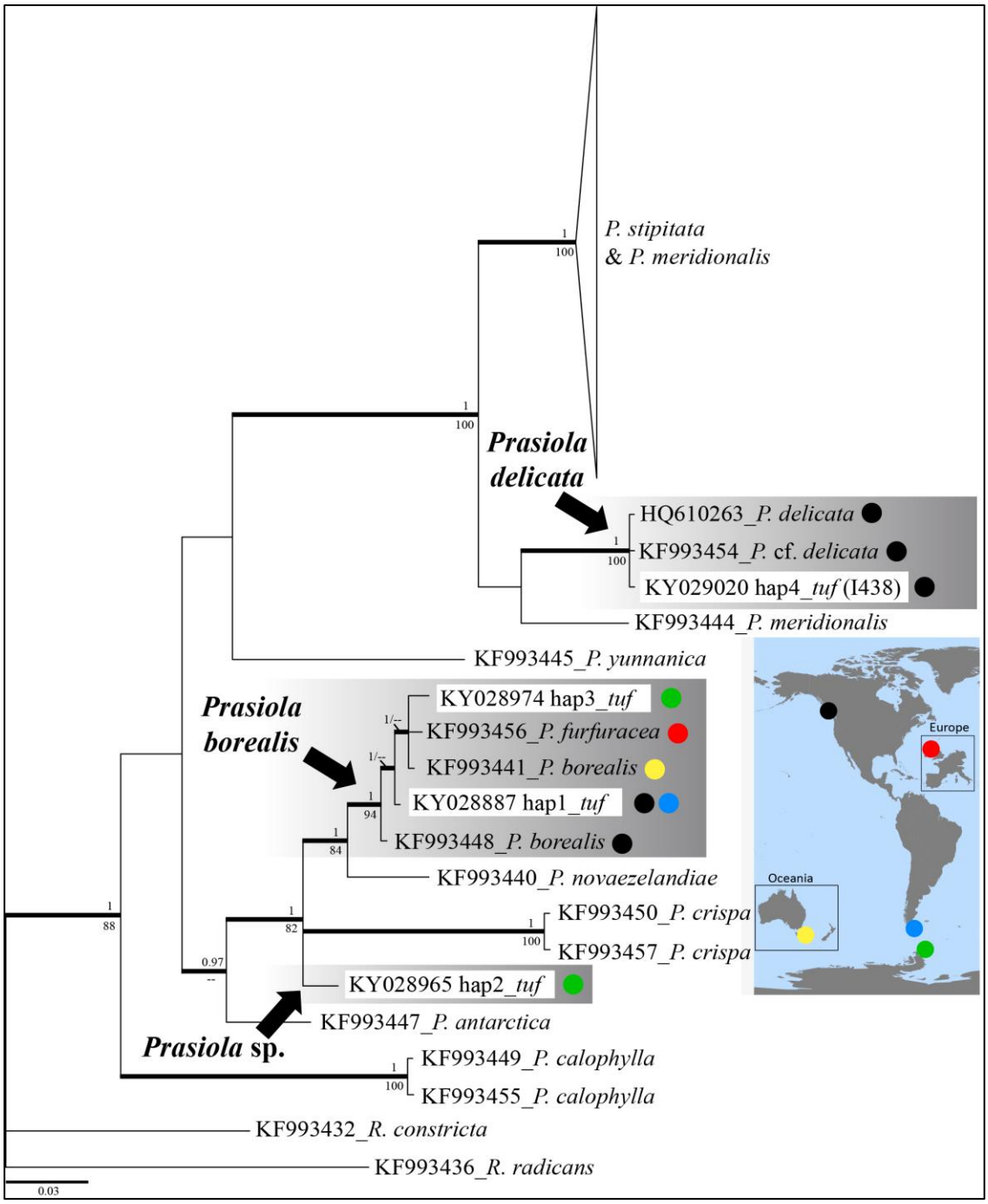

3.3. Inference of population structure

The number of SNP extracted from the *nrITS*, *RPL10A* and *tufA* datasets were 53, 12 and 15, respectively. Single-locus clusters (SLCs) or populations inferred with BAPS ranged from 3 for *tufA* to 5 for *nrITS* and *RPL10A* (Figure 4). Individuals from Alaska and Tierra del Fuego were grouped together in the *tufA* analysis, although they were shown as different in *nrITS* and *RPL10A* analyses. Further, *nrITS* and *RPL10A* population assignments of individuals from Tierra del Fuego and the Antarctic Peninsula did not match. Thus, the *nrITS* SLC output assembled all Tierra del Fuego samples into one cluster and the Antarctic individuals into two distinct clusters, while the best solution for *RPL10A* consisted of two groups for Tierra del Fuego and one

group for the Antarctic Peninsula. The three SLC analyses were consistent in assigning a distinct genetic cluster for two Antarctic individuals collected from King George Island (I107 and I443). In addition, the optimum number of mixture clusters identified in the combined three-marker dataset was five (Figure 4) and these corresponded to the same populations inferred from the *nrITS* dataset alone. Admixture analysis revealed significant signs of admixture only in 3 individuals with missing data (data not shown).

The Bayesian clustering analyses implemented in STRUCTURE based on haplotype instead of SNP data revealed clear population substructuring in the dataset. The optimal *K* by Evanno ranged from 2 (*tufA-RPL10A*, *tufA-nrITS*, three-marker datasets) to 3 (*RPL10A-nrITS* dataset). The best *K* inferred with the alternative calculation method returned identical results except for the three-marker dataset (*K* = 3). Admixed ancestry was inferred for two Antarctic individuals from King George Island (I107 and I443) in all analyses. Individuals from Tierra del Fuego showed variable percentages of admixture when considering *K* = 3 (three-marker and *nrITS-RPL10A* datasets). The STRUCTURE results averaged over 10 runs are presented in Figure 5.

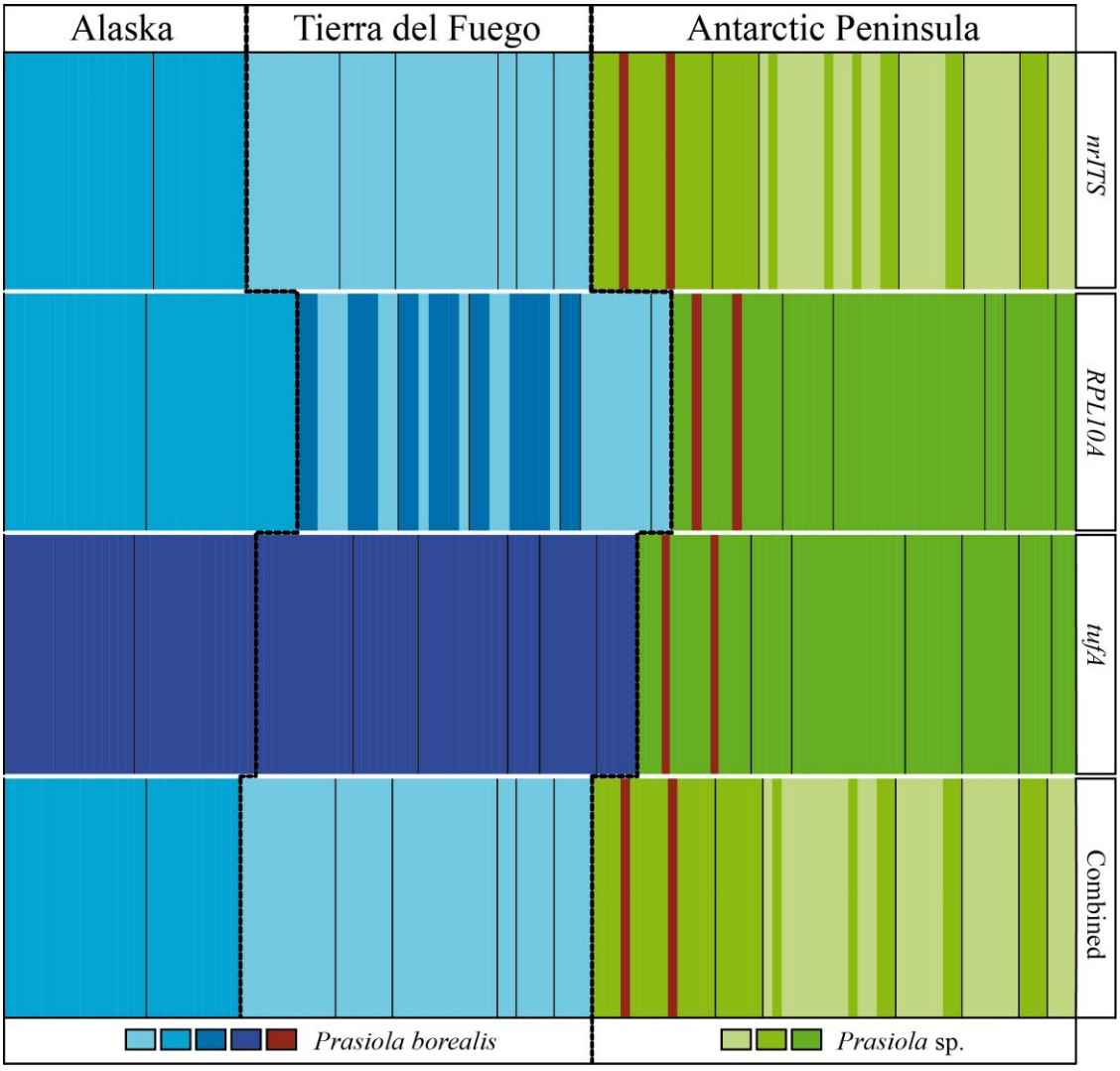

◀Figure 4. Mixture results from Bayesian clustering analyses conducted with BAPS using SNP data from lichenized *Prasiola* specimens collected in Alaska, Tierra del Fuego and Antarctica. The three top panels show individual population assignments based on single locus data (SLCs) while the fourth panel shows results based on a combined matrix of SNP from the three loci (*nrITS*, *RPL10A* and *tufA*). Different genetic clusters are indicated with different colors. According to the species discovery-validation approach, individuals in purple, deep red and different shades of blue are assigned to *P. borealis* while different shades of green indicate Antarctic individuals of a second, as yet undescribed, *Prasiola* species.

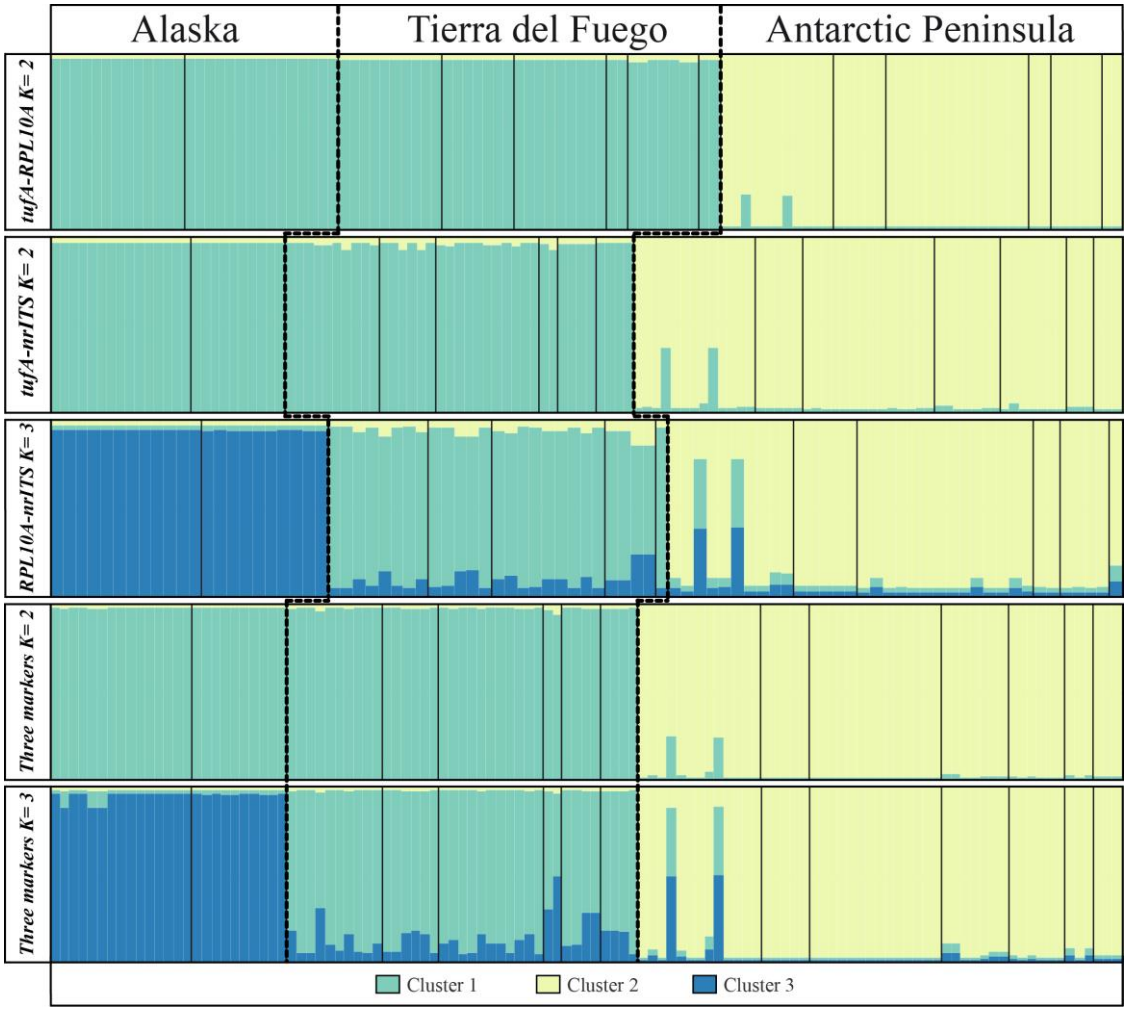

Figure 5. Admixture results of Bayesian clustering analyses with STRUCTURE using haplotype data from lichenized *Prasiola* specimens collected in Alaska, Tierra del Fuego and Antarctica. The three top panels show individual population assignments inferred under the best *K* model based on different combinations of two loci, while the two bottom panels show individual population assignments inferred under $K = 2$ and $K = 3$ for a combined multi-locus dataset (*nrITS*, *RPL10A* and *tufA*). Vertical bars represent individual assignment probabilities to different genetic clusters indicated with colors. The examined number of specimens varies across tests whereas the order of individuals is equivalent across panels.

3.4. Species delimitation

Transition/transversion rates calculated for the *nrITS*-B, *RPL10A*-B, *tufA*-B and *tufA*-A datasets were 1.924, 3.1, 1.18 and 1.85, respectively. ABGD analysis of the *nrITS*-B dataset rendered biologically unrealistic results when considering extreme prior thresholds (i.e. all specimens included in only one species or in as many as 20 different species). Intermediate values of *P* led to a more consistent result with 5 partitions or species detected (*P* = 0.0017 to 0.0077). Initial and recursive partitions in the *RPL10A*-B analyses converged on 3 partitions (*P* = 0.0129 to 0.0215). When considering the *tufA*-B dataset, the ABGD result supported two partitions (*P* = 0.0077 to 0.0215), one corresponding to specimens from Alaska, Tierra del Fuego and two individuals from King George Island (I107 and I443), and a second including all remaining Antarctic samples. Finally, twelve partitions (*P* = 0.0010 to 0.0215) were found for *tufA*-A; our target group was split into two and haplotype ascriptions matched those of the previous analysis. Results of GMYC delineation and corresponding likelihood ratio tests (LRT) are summarized in Supplementary Table 1. When outgroup taxa were excluded, the inferred number of species was unrealistically high using both the simple-threshold (7 entities, LRT ns) or multiple-threshold (12 entities) in the *nrITS*-B dataset analysis. Single-threshold analysis of *RPL10A*-B gave rise to two entities (LRT ns). The inclusion of outgroup sequences to increase the Yule proportion of the tree either over-lumped (*nrITS*-C sGMYC) or over-split (*nrITS*-C mGMYC) the putative number of lichenized *Prasiola* species. Only sGMYC analysis of the extended *nrITS*-A dataset supported the two-species hypothesis. Single- and multiple-threshold results for the *tufA*-C dataset, considering all available *Prasiola* sequences, resulted in 12 putative species (LRT ns), two of which corresponded to our lichenized specimens. Phylogenetic relationships inferred for these taxa are consistent with the results of Moniz et al. (2014) and Heesch et al. (2016) and are depicted in Figure 3.

Finally, we compared two alternative species delimitation models according to the scenarios supported by more than one discovery analysis. Model 1 consisted of five species supported either by the BAPS multi-locus clustering result or by the *nrITS*-B ABGD delimitation output. Model 2 defined two entities corresponding to the two main clusters estimated using STRUCTURE, and were also in agreement with the ABGD and sGMYC delimitation results obtained for the *tufA* and *RPL10A* datasets, respectively. Marginal likelihood values for the considered models averaged over two runs and calculated through PS and SS are shown in Supplementary Table 2. Bayes Factor comparisons positively, but not strongly, favoured the two species model over the five species model.

3.5. Genetic polymorphism, population differentiation, phylogeographic structure and neutrality tests

According to the species delimitation results and phylogenetic analyses based on *tufA* molecular data (Figure 3), we divided our data into two sets. The first set was ascribed to the species *Prasiola borealis* and included samples collected in Alaska,

Tierra del Fuego, and two specimens from King George Island (I107 and I443). The second group was provisionally named *Prasiola* sp., and consisted of individuals from the Antarctic Peninsula. Genetic diversity indices and neutrality test results for each putative species are reported in Supplementary Table 3. Nucleotide and haplotype diversities were greater for *Prasiola borealis* than *Prasiola* sp. across all markers. No haplotypes were shared among species, while individuals from Alaska and Tierra del Fuego shared a *tufA* haplotype. In *Prasiola borealis*, the patterns of population differentiation (Fst) and distance-based genetic (Dxy) divergence for the *nrITS* and *RPL10A* markers showed two well-differentiated groups of regional populations (Alaska and Tierra del Fuego) (Figure 6). Alaska displayed the lowest values of both nucleotide and haplotype diversities. Also within this region, the two sampling localities differed genetically in that each one has its particular *nrITS* haplotype. The Tierra del Fuego sampling localities were genetically more homogeneous despite particularly high Dxy values in some pairwise comparisons of the *nrITS* marker (Figure 6). For the Antarctic *Prasiola* sp., *nrITS* and *RPL10A* haplotype diversities were similar when the full length of the second marker was considered. King George Island showed intermediate levels of differentiation with respect to all other sampling localities, whereas the Greenwich and Avian islands showed the highest Fst values in several pairwise comparisons. Conversely, higher values of Dxy were observed for the King George, Greenwich and Avian islands when compared with other sampling localities (Figure 6). Given the limited sampling effort in some Antarctic localities (i.e. Cierva Cove, Avian Island), any further interpretation of genetic differentiation and divergence patterns would be tentative.

We found a strong geographical signal in *nrITS* and *RPL10A* haplotype networks (Figure 2). The *nrITS* network revealed 19 haplotypes (Figure 2A). For *Prasiola borealis*, haplotypes from Alaska, Tierra del Fuego and King George Island were separated by more than 10 nucleotide substitutions. Within Tierra del Fuego, a star-like pattern was observed with two haplotypes being the most widespread and two haplotypes being restricted to Navarino Island. For *Prasiola* sp., King George and Livingston islands were richer in terms of haplotype diversity. Restricted haplotypes emerged for the King George, Avian and Yalour islands. When considering the initial exonic region of the *RPL10A* marker, the 6 haplotypes detected were also geographically structured (Figure 2B). Restricted haplotypes were detected in Navarino and King George islands. When the full-length *RPL10A* marker was considered, we were able to detect additional genetic diversity within each geographic region (Figure 2C–E). Thus, the two Alaskan sampling localities shared one of the two haplotypes (Figure 2C), as occurred for the *nrITS* marker. In Tierra del Fuego, the haplotype network depicted 7 haplotypes, some restricted to Navarino Island or Darwin Bay (Chair Island) (Figure 2D). For *Prasiola* sp., the TCS method unveiled 7 haplotypes (Figure 2E). As for *nrITS*, the King George and Livingston islands harboured greater numbers of distinct haplotypes. Restricted haplotypes were also found for the King George and Avian islands. Finally, the *tufA* haplotype network (Figure 2F) provided no

further insight into the genetic diversity of both *Prasiola* species, due to the low amount of polymorphism.

Neither Tajima's *D* nor Fu's *Fs* neutrality tests were significant for either of our two putative species, which could point to evolution according to mutation-drift equilibrium (Supplementary Table 3). On the contrary, when analysing the full-length *RPL10A* sequence, positive and significant values of *D* (3.04407) and *Fs* (14.672) were observed for the extant Alaskan localities of *Prasiola borealis*. This finding could be congruent with a recent founder event or substantial population contraction scenario (Schneider & Excoffier 1999).

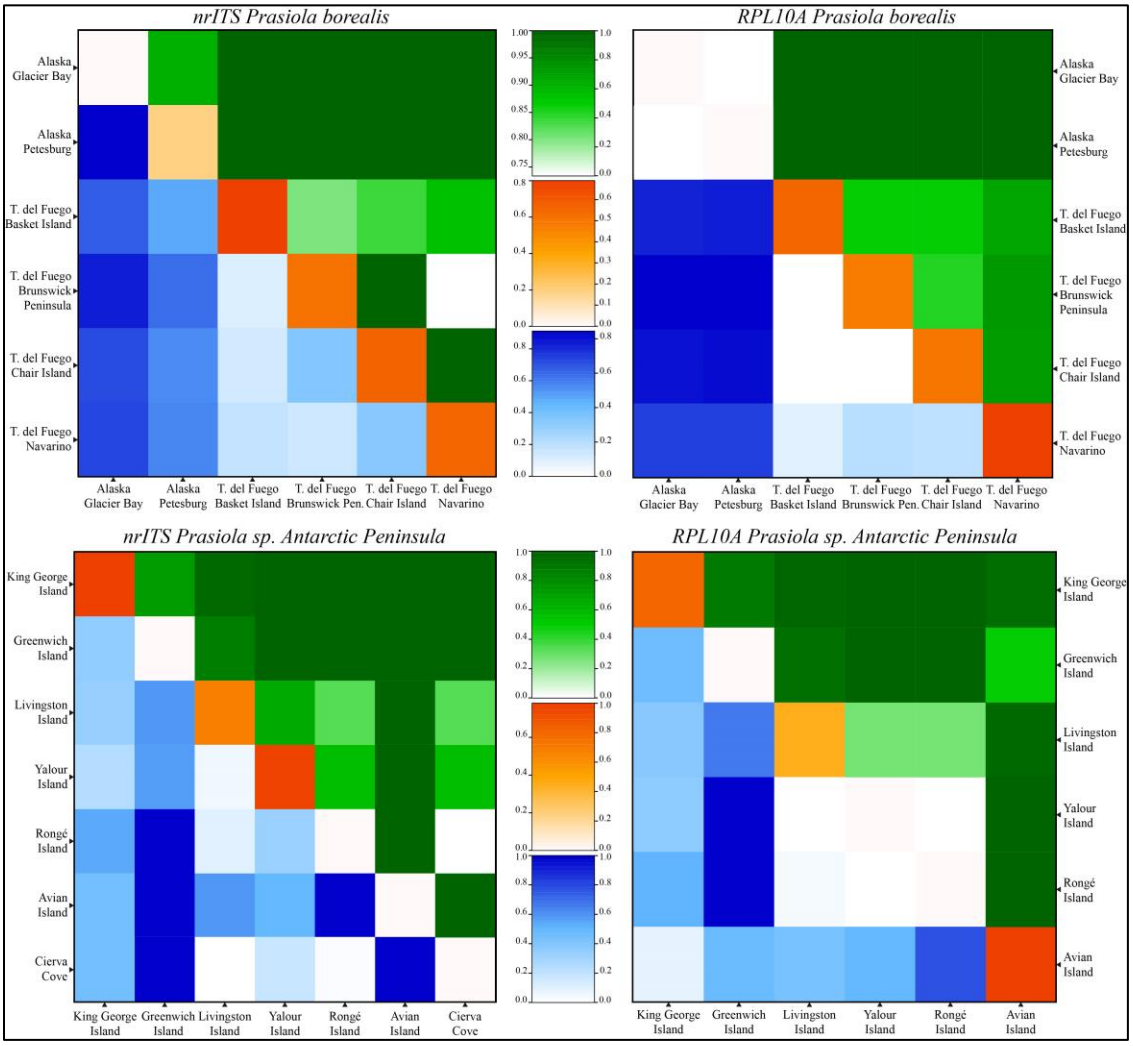

Figure 6. Genetic divergence (Dxy, above diagonal, green shades), genetic differentiation (Fst, below diagonal, blue shades), and within group genetic diversity (π, diagonal, orange shades) between sampling localities in each putative species based on *nrITS* and *RPL10A* data. Scales on left- and right-hand sides of central bars correspond to graphs on left and right, respectively.

4. Discussion

This spatially-comprehensive study of prasiolacean species provides information on diversity within the genus *Prasiola* and on the evolutionary history and biogeography of its lichenized species. Recent investigations in the family *Prasiolaceae* have moved on from morphology-based circumscription of taxa to delimitation approaches employing DNA data (Rindi et al. 2004; Heesch et al. 2012, 2016; Moniz et al. 2012a; Kim et al. 2015). So far, phylogenetic appraisals of this family have been based on nuclear (*nuSSU*) and plastid (*rbcL*, *psaB*, and *tufA*) markers showing low levels of variability (e.g. Rindi et al. 2007; Moniz et al. 2014). However, while these markers are useful to resolve relationships among genera and species, their performance has not proved as satisfactory when trying to disentangle more complex evolutionary relationships such as those shown by the closely related *P. meridionalis*, *P. stipitata* and *P. linearis* (Moniz et al. 2012b, 2014). In the present study, we generated for the first time sequences of *nrITS* and *RPL10A* markers for members of *Prasiola*. Both of these loci are shown to be hypervariable and perform well at intermediate taxonomic levels (inter- and intraspecific relationships).

Phylogenetic reconstructions based on *nrITS* data allocated our *Prasiola* sequences to a monophyletic group sister to *Diplosphaera*, *Stichococcus* and *Desmococcus* (Figure 1D). These results confirm the relationships previously inferred in several phylogenetic studies (De Wever et al. 2009; Thüs et al. 2011). At the species level, *nrITS* discriminated well between candidate species of *Prasiola*. Particularly, the Alaskan (I438) and Antarctic (I60, I83) free-living and lichenized *Prasiola* were revealed as clearly distinct lineages in Bayesian and ML topologies (Supplementary Figure 1). In addition, sequences recovered from lichenized thalli specimens clustered in three supported clades, each corresponding to a different geographic area. Phylogenetic relationships inferred for *tufA* were largely congruent with the results of Moniz et al. (2014) and Heesch et al. (2016) and are illustrated in Figure 3. Two haplotypes (hap1,3_*tuf*) formed a monophyletic clade together with *P. furfuracea* and *P. borealis*, while hap2_*tuf* appeared basal to a clade containing the latter two species and *P. novaezelandiae*. Supraspecific units could be delimited in our study using a partially exonic region of the *RPL10A* gene. The intronic region was not possible to align further than at the regional level. The usefulness of both exons and introns of the *RPL10A* gene for phylogenetic reconstructions at different taxonomic depths was described by del Campo et al. (2013). Specifically, these authors found that exonic nucleotide sequences were sufficiently decisive to recover unambiguous relationships among either distantly related taxa (e.g. animals, plants, fungi) or within particular lineages, such as genera of *Trebouxiophyceae*. According to the genetic variability found here among *Prasiola* species in both nuclear *nrITS* and *RPL10A*, we propose these markers as good molecular tools for resolving phylogenetic uncertainties in *Prasiolaceae*. Remarkably, intronic *RPL10A* regions also showed enough resolution for fine scale population analyses.

To date, only a few studies have addressed species delimitation in Chlorophyta using a discovery-validation approach (Sadowska-Dés et al. 2014; Malavasi et al. 2016; Škaloud et al. 2016). Here we combined population assignment tests (BAPS, STRUCTURE) with delimitation strategies based either on distances between sequences (ABGD) or the coalescent theory (GMYC) to address the discovery of species. Population assignment analyses are valuable tools for species discovery, as they work at the interface between population genetic and phylogenetic analyses (e.g. Hedin et al. 2015; Hotaling et al. 2016). Further, estimation of admixture can help unveil intermediate individuals that have retained ancestral polymorphisms or suffered introgressive hybridization (Engel et al. 2005). The two cluster approaches identified contrasting genetic clusters (Figure 4–5). STRUCTURE analyses were more conservative than BAPS and suggested either two or three subpopulations whereas BAPS, which tends to overestimate numbers of clusters (Latch et al. 2006), recovered three to five clusters. We observed a clear dominance of the *nrITS* data over the mixture results of the multi-locus BAPS analyses. A likely explanation is that the *nrITS* marker might have as many as four times more SNPs than the other two markers. Corander & Marttinen (2006) argued that BAPS is a more powerful tool to identify hidden structure within populations, so it could be that our BAPS results mirrored a mixed pattern which includes inter- and intraspecific groups.

Species delimitation algorithms based on genetic distances and coalescent theory also provided discrepant results in terms of the suggested number of species. Thus, while ABGD outputs were generally conservative for all markers, s/mGMYC tests based on the *nrITS* marker rendered a high number of entities. Some studies have documented spurious inflations of inferred species diversity that do not correspond to species-level lineages when using GMYC (Miralles & Vences 2013; Hamilton et al. 2014). In our study, GMYC output seemed mostly affected by taxon sampling coverage (Miralles & Vences 2013; Talavera et al. 2013; Dellicour & Flot 2015). Thus, when lichenized *Prasiola* datasets were analysed without outgroups, inferred species were overestimated (7 sGMYC and 12 mGMYC) due to the deep genetic structuring observed in our *nrITS* data. This is thought to affect estimation of the coalescence point (Hamilton et al. 2011). Conversely, the inclusion of other members of *Prasiolaceae* constrained delimitations to a reduced number of entities for the lichenized *Prasiola*, which seems more realistic. GMYC analyses using *RPL10A* produced inconsistent results depending also on the taxon sampling, although they always recovered a smaller number of entities compared with the *nrITS* tests. Finally, we observed that the *tufA* marker is particularly consistent in delimiting species in *Prasiola*, which is in agreement with previous works (Saunders & Kucera 2010; Moniz et al. 2014; Heesch et al. 2016).

Using the BFD approach (Grummer et al. 2014) to validate the most plausible species hypothesis, the two-species model of lichenized *Prasiola* was favoured over the least inclusive hypothesis of five species. The BFD method, just as other validation methods like SPEDESTEM (Ence & Carstens 2011) or Bayesian Phylogenetic and Phylogeography (BP&P, Yang & Rannala 2010), accounts for gene-tree discordance,

incomplete lineage sorting, recently-diverged species with gene flow and ancestral polymorphism retention (Fujita et al. 2012). The first of the two putative species was found to correspond to *P. borealis*, as *tufA* haplotypes hap1_*tuf* and hap3_*tuf* fell within a monophyletic clade including this species (Figure 3). The second species, *Prasiola* sp., likely represents an unknown lineage within this genus.

The recognition of two species associated with *Mastodia tessellata* has major implications for the taxonomy and biogeography of *Prasiola*. Recent works using *rbcL* and *tufA* data have established three distinct clades of *Prasiola* in Antarctica corresponding to the species *Prasiola crispa*, *P. antarctica* and *P. glacialis* (Moniz et al. 2012b, 2014). The former two species share an identical gross morphology and habitat (nitrogen-rich soil and rocks in penguin rookeries), yet their *rbcL* sequences differ by 25 bp (Moniz et al. 2012b). Lichenized *Prasiola* from Antarctica are also commonly found living in these habitats but, genetically, they form a distinct lineage (Figure 3). Unfortunately, no *tufA* sequences of *P. glacialis* were available for comparison but this species shows a clearly distinct ecology, occurring in non-permanent freshwater habitats distant from the possibility of fertilization by birds (Moniz et al. 2012b). Thus, it seems unlikely that the lichenized Antarctic *Prasiola* found in our study could be regarded as conspecific to any of the known three species. The description of a new taxonomic entity, however, requires a polyphasic taxonomic study with multiple lines of evidence (i.e. morphology, culture growth, genetics, ecology, mode of reproduction) (Dayrat 2005; Carstens et al. 2013; Malavasi et al. 2016). Special mention should be made of Antarctic samples I107 and I443. The species discovery-validation approach supports their inclusion within *P. borealis* but the STRUCTURE multi-locus results suggested their admixed origin (Figure 5). Varying levels of admixture in natural populations have been attributed to retention of ancestral polymorphism and introgressive hybridisation (Engel et al. 2005). For two species to hybridise, populations of parental species should at least grow sympatrically and reproduce sexually. At present, we have no evidence of *P. borealis* growing in the Antarctic Peninsula with the exception of these two specimens. Further, mechanisms of sexual reproduction are poorly understood in this genus (Rindi 2010). We cannot, however, rule out the more parsimonious alternative explanation to consider these genotypes part of the total genetic diversity found in *P. borealis*, likely originated by genetic differentiation in a geographically disjunct population. More comprehensive sampling in other geographic areas of the Southern Hemisphere could reveal new genetic clusters within *P. borealis* and help us understand the origin of these specimens.

We confirmed the strict relationship of *Mastodia tessellata* with members of the genus *Prasiola* across most of its distribution range. However the distribution pattern of the two *Prasiola* species found in symbiosis are rather distinct. *Prasiola borealis* occurs in Alaska and Tierra del Fuego. This amphitropical disjunct distribution is supported by the null genetic divergence found between specimens from these regions based on *tufA* marker data. Molecular studies have shown that this species was present in the northern Pacific coast of North America (Rindi et al. 2007) and Tierra del Fuego (Pérez-Ortega

et al. 2010), but also in Tasmania (Moniz et al. 2012a) and New Zealand (Heesch et al. 2012). Interestingly, Moniz et al. (2014) found free-living specimens of *P. furfuracea* collected in Galway (Ireland) to be nearly genetically identical to *P. borealis* samples from British Columbia and Tasmania. Assuming the conspecificity of both taxa will have two major consequences. In the first place, *P. borealis* should be considered a synonym of *P. furfuracea* according to nomenclatural priority (Moniz et al. 2014). Secondly, the extended geographic range for this algal species would raise new questions about the constraints in space and time of the distribution of this lichen symbiosis. In contrast, the second species found in our study, *Prasiola* sp., seems to be restricted to the Antarctic Peninsula. *Mastodia tessellata* has been reported in numerous coastal localities across Antarctica and in numerous sub-Antarctic islands. Further studies are needed to confirm the endemic character of this taxon in the Antarctic Peninsula.

The bipolar distribution of *Prasiola borealis* along the Alaska-Tierra del Fuego axis prompts the question of how did this distribution arise. Widely disjunct distributions were early interpreted in terms of vicariance (break-up of an ancestral range) or long-distance dispersal (colonisation of a new area) (Du Rietz 1940; Raven 1963). The low admixture estimated in all multi-locus STRUCTURE analyses (Figure 5), the high estimates of genetic differentiation (Fst, Figure 6) between both regional sampling localities, and the highly structured haplotype networks (Figure 2) argue against recurrent genetic exchange, and rather suggest a single historical dispersal event. Transequatorial dispersal events have been postulated to explain amphitropical distributions in plants (Villaverde et al. 2015a,b), mosses (Lewis et al. 2014a) and lichen-forming fungi (Fernández-Mendoza & Printzen 2013).

Lichen symbionts may show different patterns of selectivity and specificity (e.g. Thüs et al. 2011; Pérez-Ortega et al. 2012a; Leavitt et al. 2015c). The lichen involving *Mastodia tessellata* has been proposed as an example of highly reciprocal specificity (Pérez-Ortega et al. 2010). Here, we show that two *Prasiola* species contribute to this symbiosis across its distribution range. Further, Moniz et al. (2014) recently found *Prasiola delicata* blades with signs of lichenization in British Columbia. We found no lichenized *Prasiola delicata* specimens. However, a *tufA* sequence from a free-living individual collected in Alaska (I438) was shown here to be identical to two samples labelled as *P.* cf. *delicata* and *P. delicata* in Moniz et al. (2014). The occurrence of several photobionts across the distribution of *M. tessellata* questions the current hypothesis of highly reciprocal specificity and points to interchangeable photobionts depending on the area as reported in other species (Fernández-Mendoza et al. 2011).

5. Conclusions

Because of a lack and plasticity of characters, species delimitation in algae had been until recently an arduous task. This task has been made appreciably easier by the introduction of several new DNA taxonomy tools, but these tools also have their flaws and different methods can give rise to contrasting results. Based on comprehensive geographic sampling and three molecular markers, our study indicates the usefulness of a species discovery-validation approach to test multiple hypotheses delimiting the *Prasiola* species associated with *Mastodia tessellata*. Two putative *Prasiola* species were identified: *P. borealis*, showing a striking bipolar distribution that could be explained by a historical dispersal event; and a likely new species restricted to the Antarctic Peninsula. Our finding of several *Prasiola* species associated with *Mastodia tessellata* across its distribution range, the relatively common presence of *P. furfuracea* (= *P. borealis*) in Europe without reports of the mycobiont, and the bipolar disjunction found in *P. borealis* build a promising scenario for future research that seeks to understand the processes that have shaped –in space and time– this remarkable lichen symbiosis.

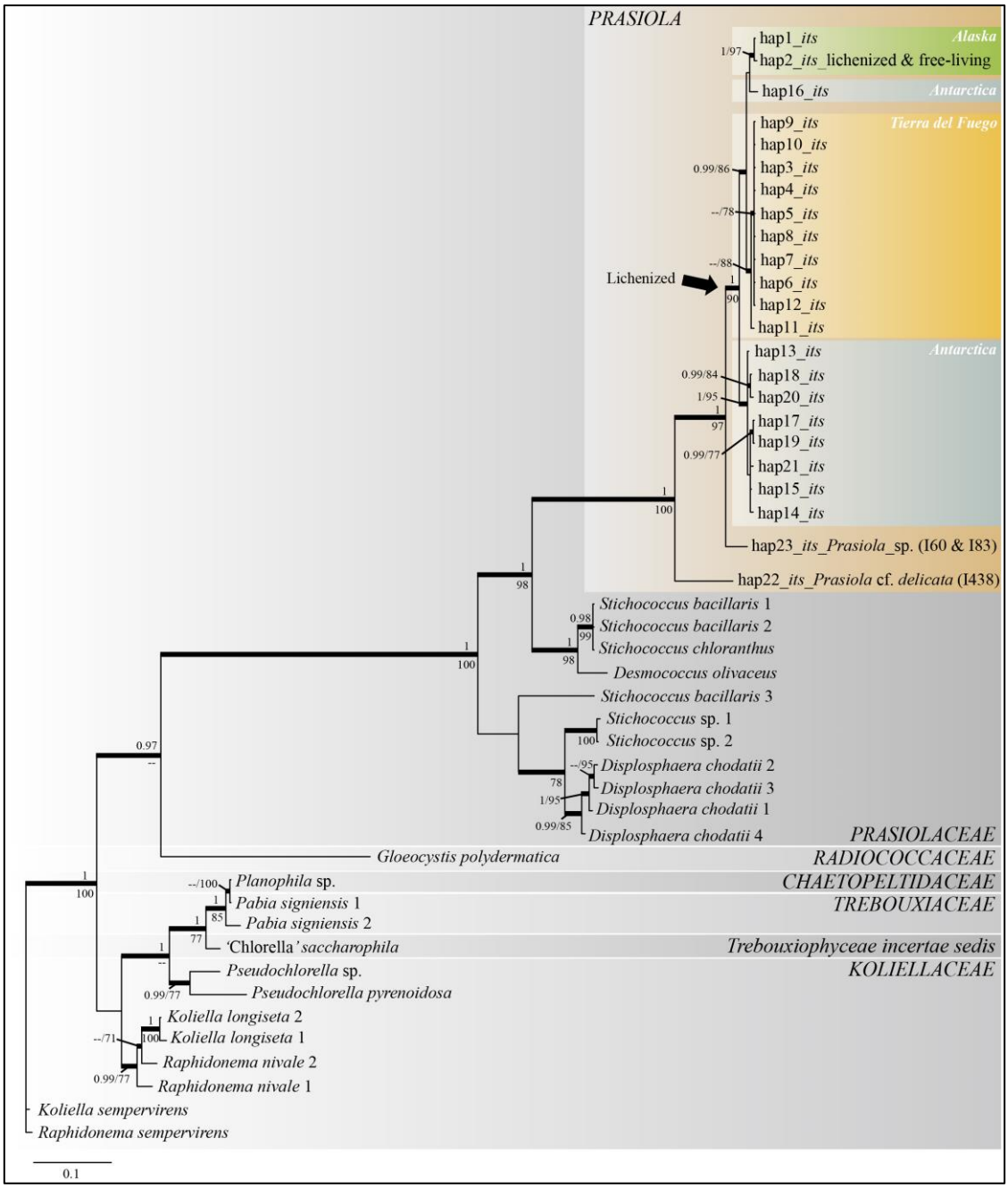

Supplementary Figure 1. MRBAYES 50% majority-rule consensus tree showing phylogenetic relationships of lichenized and free-living *Prasiola* with other members of Chlorophyta based on *nrITS* data. The geographic origin of the main clades is also shown. Sequence data and accession numbers are available in Appendix 1. Family adscription of taxa follows ALGAEBASE (http://www.algaebase.org/; last accession 05/05/2016). Thickened branches indicate Bayesian posterior probabilities (PP ≥ 0.95, above) from the MRBAYES analysis and/or ML bootstrap values (B ≥ 70%, below) from the RAxML analysis.

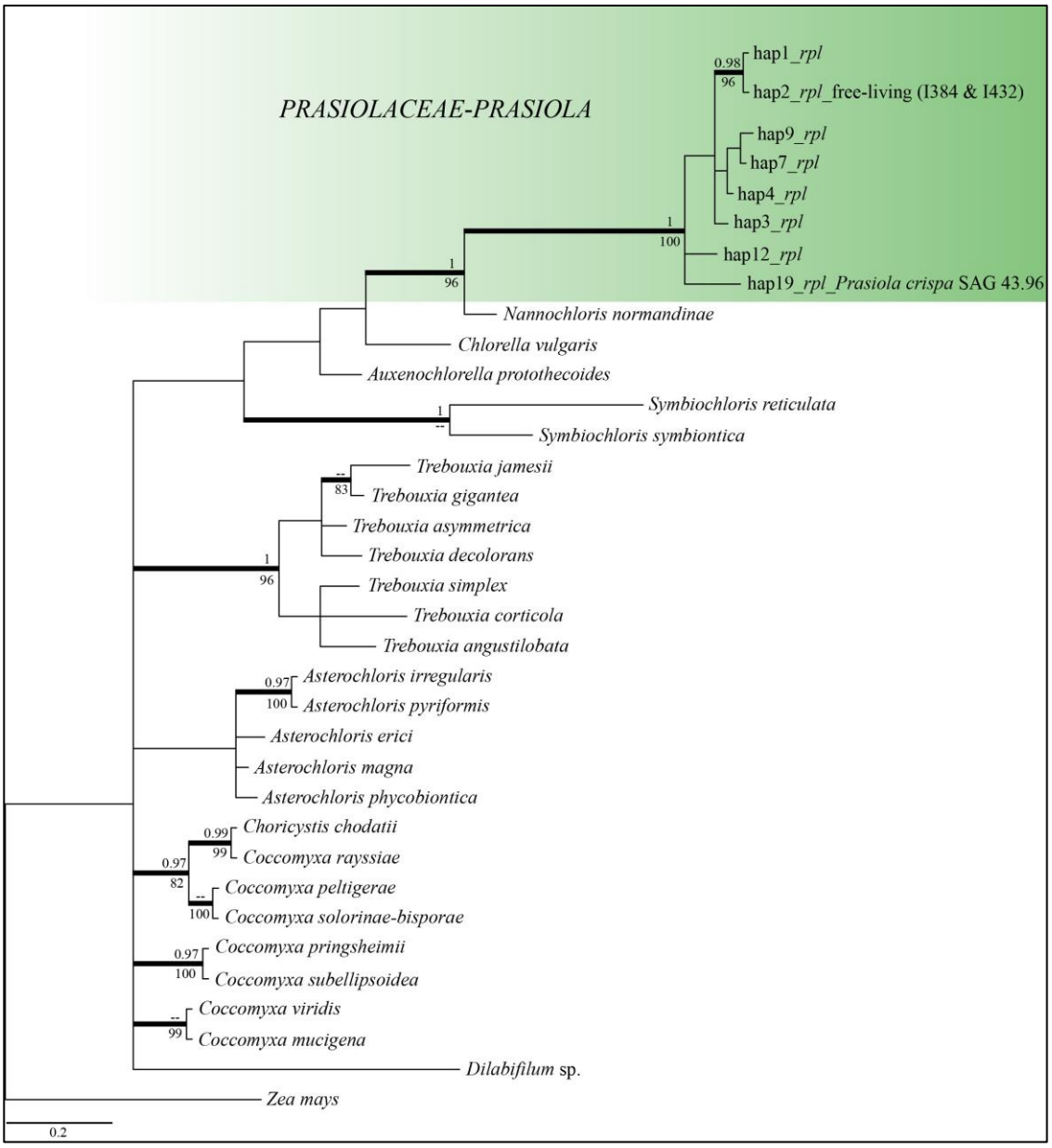

Supplementary Figure 2. MRBAYES 50% majority-rule consensus tree showing phylogenetic relationships of lichenized, free-living, and cultured *Prasiola* (highlighted in green) with other members of Chlorophyta based on *RPL10A* data. Sequence data and accession numbers are available in Appendix 1. Branches in bold indicate Bayesian posterior probabilities (PP ≥ 0.95, above) from the MRBAYES analysis and/or ML bootstrap values (B ≥ 70%, below) from the RAxML analysis.

Supplementary Table 1. Summary results of the delimitation analyses using simple and multiple threshold GMYC models and datasets either excluding (*nrITS*-B, *RPL10A*-B) or including (*nrITS*-A, *nrITS*-C, *RPL10A*-C, *tufA*-C) outgroup sequences.

sGMYC	Likelihood null model	Likelihood GMYC model	LR test p-value	Number of ML entities (confidence interval)	Number of *Prasiola* entities
nrITS-A	292.8752	298.2313	0.0047 (**)	18 (3–29)	2
nrITS-B	140.4253	141.6294	0.299 (ns)	7 (1–8)	7
nrITS-C	169.2985	172.9305	0.0264 (*)	3 (3–20)	1
RPL10A-B	20.34751	20.35993	0.987 (ns)	2 (1–5)	2
RPL10A-C	29.68955	31.92859	0.106 (ns)	6 (2–9)	1
tufA-C	69.74654	72.58169	0.0587 (ns)	12 (4–14)	2
mGMYC					
nrITS-A	292.8752	299.2547	0.0016 (**)	22 (10–22)	5
nrITS-B	140.4253	143.5391	0.044 (*)	12 (5–12)	12
nrITS-C	169.2985	173.0388	0.023 (*)	17 (3–17)	13
RPL10A-C	29.68955	31.92859	0.106 (ns)	6 (2–7)	1
tufA-C	69.74654	72.58169	0.0587 (ns)	12 (4–13)	2

*P < 0.05, ** P < 0.01

Supplementary Table 2. Marginal likelihood and Bayes Factor values for two alternative species delimitation hypotheses and their motivation. Best model highlighted in bold.

	Distinct species	Motivation	Path Sampling		Stepping-Stone	
			Ln (Marginal Likelihood)	2ln (Bayes Factor)	Ln (Marginal Likelihood)	2ln (Bayes Factor)
Model 1 (5 spp.)	sp1: Alaska[a] sp2: T. Fuego[a] sp3: Antarctica 1[b] sp4: Antarctica 2[c] sp5: Antarctica 3[d]	BAPS multi-locus clustering, ABGD *nrITS*-B	-2652.437	4.652	-2652.516	4.716
Model 2 (2 spp.)	sp1: Alaska[a], T. Fuego[a], Antarctica 1[b] sp2: Antarctica 2[c], Antarctica 3[d]	STRUCTURE multi-locus clustering, ABGD *tufA*-A and tufA-B, s/mGMYC *tufA*-C, sGMYC *RPL10A*-B, sGMYC *nrITS*-A	**-2650.111**	**n/a**	**-2650.158**	**n/a**

[a] All individuals

[b] Individuals with hap16_*its*

[c] Individuals with hap13–15,17,19,21_*its*

[d] Individuals with hap18,20_*its*

Supplementary Table 3. Polymorphism statistics and neutrality tests results for each marker (*nrITS*, *RPL10A*, *tufA*), species and geographic origin. (ns: not significant).

Dataset	n	bp	gaps	*s*	*h*	*Hd*	*k*	π	π(JC)	Tajima's *D*	Fu's *Fs*
nrITS P. borealis Alaska	26	783	9	1	2	0.471	0.471	0.00061	0.00061	1.30276 (ns)	1.437 (ns)
nrITS P. borealis Tierra del Fuego	37	783	8	9	9	0.797	1.673	0.00216	0.00216	-0.66558 (ns)	-2.432 (ns)
nrITS P. borealis All localities	65	783	12	29	11	0.847	8.434	0.01094	0.01107	1.21395 (ns)	5.509 (ns)
nrITS Prasiola sp. Antarctica	50	779	5	13	8	0.756	4.774	0.00617	0.00621	1.93347 (ns)	3.278 (ns)
RPL10A P. borealis Alaska	29	868	12	13	2	0.488	6.34	0.00741	0.00748	3.04407 (**)	14.672 (***)
RPL10A P. borealis Tierra del Fuego	37	879	23	27	7	0.826	6.742	0.00788	0.00794	0.14634 (ns)	5.547 (ns)
RPL10A P. borealis All localities	68	111	0	7	5	0.705	2.572	0.02317	0.0238	1.8985 (ns)	3.761 (ns)
RPL10A Prasiola sp. Antarctica	38	842	12	17	7	0.724	4.908	0.00591	0.00595	0.69664 (ns)	3.600 (ns)
tufA P. borealis Alaska	31	574	0	0	1	0	0	0	0	n/a	n/a
tufA P. borealis Tierra del Fuego	47	574	0	0	1	0	0	0	0	n/a	n/a
tufA P. borealis All localities	80	574	0	3	2	0.049	0.148	0.00026	0.00026	-1.41353 (ns)	0.047 (ns)
tufA Prasiola sp. Antarctica	52	574	0	0	1	0	0	0	0	n/a	n/a

** sig. P < 0.01, *** sig. P < 0.001

Supplementary Table 4. Loci and primers used in the present study. Primers designed for the present work are highlighted in bold.

Locus	Genome	Primer name	Orientation (F/R)	Primer sequence (5'–3')	Reference
nrITS	Nuclear	nr-SSU-1780-5' Algal	F	CTGCGGAAGGATCATTGATTC	Piercey-Normore & DePriest (2001)
		ITSpras1F	**F**	**TCTATCAACAACCCCACAGC**	**This study**
		ITS4T	R	GGTTCGCTCGCCGCTACTA	Kroken & Taylor (2000)
		ITSprasR1	**R**	**GGTTAGTTTCTTTTCCTCCGC**	**This study**
RPL10A	Nuclear	L10a-F	F	GCTNAACAAGAACAAGAAGC	del Campo et al. (2013)
		rpl10aF-1pras	**F**	**CAGCTAAGAAATATGCGGCT**	**This study**
		L10aR	R	SACGTTCTGCCAGTTCTTCTT	del Campo et al. (2013)
		rpl10aR-1pras	**R**	**ATAGACGCCTTGATGTCATT**	**This study**
tufA	Chloroplast	tufAF	F	TGAAACAGAAMAWCGTCATTATGC	Famà et al. (2002)
		tufAF-pras	**F**	**GGTTCGCCGGAAATACAAT**	**This study**
		tufAR	R	CCTTCNCGAATMGCRAAWCGC	Famà et al. (2002)
		tufAR-pras	**R**	**CAGTAACATCAGTTGTTCG**	**This study**

Supplementary Table 5. PCR settings.

PCR product	PCR round	Primer pair (F/R)	PCR protocol
nrITS	1st	nr-SSU-1780-5' Algal/ITS4T	95°C (5 min), 35 cycles of 95°C (20 sec) + 55°C (25 sec) + 72°C (25 sec), 72°C (15 sec), 4°C (∞)
	2nd (nested)	ITSpras1F/ITSprasR1	95°C (5 min), 35 cycles of 95°C (30 sec) + 57°C (1 min) + 72°C (1 min 30 sec), 72°C (10 min), 4°C (∞)
RPL10A	1st	L10a-F/L10a-R	95°C (5 min), 40 cycles of 95°C (25 sec) + 55°C (30 sec) + 72°C (32 sec), 72°C (15 sec), 4°C (∞)
	2nd (nested)	rpl10aF-1pras/rpl10aR-1pras	94°C (2 min), 35 cycles of 94°C (30 sec) + 55°C (30 sec) + 72°C (1 min), 72°C (7 min), 4°C (∞)
tufA	1st	tufAF/tufAR	94°C (4 min), 34 cycles of 94°C (30 sec) + 52°C (1 min) + 72°C (1 min 30 sec), 72°C (5 min), 4°C (∞)
	2nd (nested)	tufAF-pras/tufAR-pras	

Supplementary Table 6. GBLOCKS settings and inferred optimum substitution models for all datasets in Material and Methods sections 2.4 and 2.6.

Analyses made in Section 2.4.						
	nrITS-A GBlocks-a	*nrITS*-A GBlocks-b	*nrITS*-A GBlocks-c	*nrITS*-A GBlocks-d	*RPL10A*-A	*tufA*-A
Minimum number of sequences for a conserved position	25	25	25	25	n/a	n/a
Minimum number of sequences for a flanking position	42	42	42	42	n/a	n/a
Maximum number of contiguous non-conserved positions	4	4	4	4	n/a	n/a
Minimum length of a block	10	10	5	5	n/a	n/a
Allowed gap positions	None	With Half	With Half	All	n/a	n/a
Final alignment length (bp) after processing (% original length)	258 (27%)	529 (56%)	577 (62%)	627 (67%)	n/a	n/a
Final number of blocks	7	21	28	8	n/a	n/a
Substitution Model (AIC, best)	GTR+Γ	GTR+I+Γ	GTR+I+Γ	GTR+I+Γ	HKY+I+Γ	GTR+Γ
Substitution Model (AIC, first less complex that can be used in BEAST)	HKY+Γ	HKY+Γ	HKY+I+Γ	HKY+I+Γ	HKY+Γ	HKY+I+Γ

Analyses made in Section 2.6.		
Dataset	Substitution Model (AIC, best)	Substitution Model (AIC, first less complex that can be used in BEAST)
nrITS-A	GTR+I+Γ	HKY+I+Γ
nrITS-B	GTR+Γ	HKY+Γ
nrITS-C	GTR+Γ	HKY+Γ
RPL10A-B	K80	HKY
RPL10A-C	HKY+Γ	/
tufA-C	GTR+Γ	HKY+I+Γ

Supplementary Table 7. Summary of genetic diversity statistics of *nrITS*, *RPL10A* (only the first unambiguously aligned 111 bp), and *tufA* sequences of lichenized *Prasiola*.

	nrITS	*RPL10A (partial)*	*tufA*
Number of sequences	115	106	132
Alignment length (bp)	791	111	574
Sites with alignment gaps or missing data	24	0	0
Number of polymorphic (segregating) sites, *s*	50	12	15
Parsimony informative sites	48	12	15
Number of haplotypes, *h*	19	6	3
Haplotype diversity, *Hd*	0.906	0.753	0.499
Average number of nucleotide differences, *k*	15.023	4.46	6.321
Nucleotide diversity, π	0.01959	0.04018	0.01101
Nucleotide diversity (Jukes and Cantor), π(JC)	0.01996	0.04189	0.01118

Appendix 1. Samples used in this study, with details on collection data (region, sampling locality, date, collector, longitude, latitude), as well as *nrITS*, *RPL10A* and *tufA* haplotype codes for each sample, and GENBANK accession numbers.

Extraction Code	Collection details (region, sampling locality, date, collector)	Longitude	Latitude	*nrITS*	*nrITS* GENBANK Accession number	*RPL10A*	*RPL10A* GENBANK accession number	*tufA*	*tufA* GENBANK accession number
I44 (I388)	Alaska (USA), Glacier Bay National Park, Gustavus, Barlett Cove. Seashore, 0-5 m a.s.l. 12/7/2012. Leg. *S. Pérez-Ortega*. Loc. 589b	58° 26' 58" N	135° 53' 56" W	hap1	KX987871	hap1	KY028779	hap1	KY028887
I45	Alaska (USA), Glacier Bay National Park, Gustavus, Barlett Cove. Seashore, 0-5 m a.s.l. 12/7/2012. Leg. *S. Pérez-Ortega*. Loc. 589b	58° 26' 58" N	135° 53' 56" W	/	/	hap1	KY028780	hap1	KY028888
I46 (I386)	Alaska (USA), Glacier Bay National Park, Gustavus, Barlett Cove. Seashore, 0-5 m a.s.l. 12/7/2012. Leg. *S. Pérez-Ortega*. Loc. 589b	58° 26' 58" N	135° 53' 56" W	hap1	KX987872	/	/	hap1	KY028889
I48	Alaska (USA), Glacier Bay National Park, Gustavus, Barlett Cove. Seashore, 0-5 m a.s.l. 12/7/2012. Leg. *S. Pérez-Ortega*. Loc. 589b	58° 26' 58" N	135° 53' 56" W	hap1	KX987873	hap1	KY028781	hap1	KY028890
I50	Alaska (USA), Glacier Bay National Park, Gustavus, Barlett Cove. Seashore, 0-5 m a.s.l. 12/7/2012. Leg. *S. Pérez-Ortega*. Loc. 589b	58° 26' 58" N	135° 53' 56" W	hap1	KX987874	hap1	KY028782	hap1	KY028891
I51	Alaska (USA), Glacier Bay National Park, Gustavus, Barlett Cove. Seashore, 0-5 m a.s.l. 12/7/2012. Leg. *S. Pérez-Ortega*. Loc. 589b	58° 26' 58" N	135° 53' 56" W	hap1	KX987875	/	/	hap1	KY028892
I52	Alaska (USA), Glacier Bay National Park, Gustavus, Barlett Cove. Seashore, 0-5 m a.s.l. 12/7/2012. Leg. *S. Pérez-Ortega*. Loc. 589b	58° 26' 58" N	135° 53' 56" W	hap1	KX987876	/	/	hap1	KY028893
I53	Alaska (USA), Glacier Bay National	58° 26' 58" N	135° 53' 56" W	hap1	KX987877	hap1	KY028783	hap1	KY028894

	Park, Gustavus, Barlett Cove. Seashore, 0-5 m a.s.l. 12/7/2012. Leg. *S. Pérez-Ortega*. Loc. 589b								
I54b	Alaska (USA), Glacier Bay National Park, Gustavus, Barlett Cove. Seashore, 0-5 m a.s.l. 12/7/2012. Leg. *S. Pérez-Ortega*. Loc. 589b	58° 26' 58" N	135° 53' 56" W	hap1	KX987878	hap1	KY028784	hap1	KY028895
I55	Alaska (USA), Glacier Bay National Park, Gustavus, Barlett Cove. Seashore, 0-5 m a.s.l. 12/7/2012. Leg. *S. Pérez-Ortega*. Loc. 589b	58° 26' 58" N	135° 53' 56" W	hap1	KX987879	hap1	KY028785	hap1	KY028896
I369	Alaska (USA), Glacier Bay National Park, Gustavus, Barlett Cove. Seashore, 0-5 m a.s.l. 12/7/2012. Leg. S. Pérez-Ortega. Loc. 589b	58° 26' 58" N	135° 53' 56" W	hap1	KX987880	/	/	/	/
I375	Alaska (USA), Glacier Bay National Park, Gustavus, Barlett Cove. Seashore, 0-5 m a.s.l. 12/7/2012. Leg. *S. Pérez-Ortega*. Loc. 589b	58° 26' 58" N	135° 53' 56" W	/	/	hap1	KY028786	/	/
I376	Alaska (USA), Glacier Bay National Park, Gustavus, Barlett Cove. Seashore, 0-5 m a.s.l. 12/7/2012. Leg. *S. Pérez-Ortega*. Loc. 589b	58° 26' 58" N	135° 53' 56" W	hap1	KX987881	hap1	KY028787	hap1	KY028897
I427	Alaska (USA), Glacier Bay National Park, Gustavus, Barlett Cove. Seashore, 0-5 m a.s.l. 12/7/2012. Leg. *S. Pérez-Ortega*. Loc. 589b	58° 26' 58" N	135° 53' 56" W	hap1	KX987882	hap1	KY028788	hap1	KY028898
I428	Alaska (USA), Glacier Bay National Park, Gustavus, Barlett Cove. Seashore, 0-5 m a.s.l. 12/7/2012. Leg. *S. Pérez-Ortega*. Loc. 589b	58° 26' 58" N	135° 53' 56" W	hap1	KX987883	hap1	KY028789	hap1	KY028899
I429	Alaska (USA), Glacier Bay National Park, Gustavus, Barlett Cove. Seashore, 0-5 m a.s.l. 12/7/2012. Leg. *S. Pérez-Ortega*. Loc. 589b	58° 26' 58" N	135° 53' 56" W	hap1	KX987884	hap1	KY028790	hap1	KY028900

I430	Alaska (USA), Glacier Bay National Park, Gustavus, Barlett Cove. Seashore, 0-5 m a.s.l. 12/7/2012. Leg. *S. Pérez-Ortega*. Loc. 589b	58° 26' 58" N	135° 53' 56" W	hap1	KX987885	hap1	KY028791	hap1	KY028901
I431	Alaska (USA), Glacier Bay National Park, Gustavus, Barlett Cove. Seashore, 0-5 m a.s.l. 12/7/2012. Leg. *S. Pérez-Ortega*. Loc. 589b	58° 26' 58" N	135° 53' 56" W	hap1	KX987886	hap1	KY028792	hap1	KY028902
I266	Alaska (USA), Petersburg, South Mitkof Island, Summer Strait. Seashore, on sedimentary rocks, 0-5 m a.s.l. 25/06/2012. *Leg. S. Pérez-Ortega, T. Spribille & K. Dillman*. Loc. 558	56° 33' 10" N	132° 38' 41" W	hap2	KX987887	hap2	KY028793	hap1	KY028903
I267	Alaska (USA), Petersburg, South Mitkof Island, Summer Strait. Seashore, on sedimentary rocks, 0-5 m a.s.l. 25/06/2012. Leg. *S. Pérez-Ortega, T. Spribille & K. Dillman*. Loc. 558	56° 33' 10" N	132° 38' 41" W	hap2	KX987888	hap2	KY028794	hap1	KY028904
I268	Alaska (USA), Petersburg, South Mitkof Island, Summer Strait. Seashore, on sedimentary rocks, 0-5 m a.s.l. 25/06/2012. Leg. *S. Pérez-Ortega, T. Spribille & K. Dillman*. Loc. 558	56° 33' 10" N	132° 38' 41" W	hap2	KX987889	hap2	KY028795	hap1	KY028905
I270	Alaska (USA), Petersburg, South Mitkof Island, Summer Strait. Seashore, on sedimentary rocks, 0-5 m a.s.l. 25/06/2012. Leg. *S. Pérez-Ortega, T. Spribille & K. Dillman*. Loc. 558	56° 33' 10" N	132° 38' 41" W	hap2	KX987890	hap2	KY028796	hap1	KY028906
I271	Alaska (USA), Petersburg, South Mitkof Island, Summer Strait. Seashore, on sedimentary rocks, 0-5 m a.s.l. 25/06/2012. Leg. *S. Pérez-*	56° 33' 10" N	132° 38' 41" W	hap2	KX987891	hap2	KY028797	hap1	KY028907

	Ortega, T. Spribille & K. Dillman. Loc. 558								
I273	Alaska (USA), Petersburg, South Mitkof Island, Summer Strait. Seashore, on sedimentary rocks, 0-5 m a.s.l. 25/06/2012. Leg. *S. Pérez-Ortega, T. Spribille & K. Dillman.* Loc. 558	56° 33' 10" N	132° 38' 41" W	hap2	KX987892	hap2	KY028798	hap1	KY028908
I274	Alaska (USA), Petersburg, South Mitkof Island, Summer Strait. Seashore, on sedimentary rocks, 0-5 m a.s.l. 25/06/2012. Leg. *S. Pérez-Ortega, T. Spribille & K. Dillman.* Loc. 558	56° 33' 10" N	132° 38' 41" W	hap1	KX987893	hap1	KY028799	hap1	KY028909
I275	Alaska (USA), Petersburg, South Mitkof Island, Summer Strait. Seashore, on sedimentary rocks, 0-5 m a.s.l. 25/06/2012. Leg. *S. Pérez-Ortega, T. Spribille & K. Dillman.* Loc. 558	56° 33' 10" N	132° 38' 41" W	hap2	KX987894	hap2	KY028800	hap1	KY028910
I276	Alaska (USA), Petersburg, South Mitkof Island, Summer Strait. Seashore, on sedimentary rocks, 0-5 m a.s.l. 25/06/2012. Leg. *S. Pérez-Ortega, T. Spribille & K. Dillman.* Loc. 558	56° 33' 10" N	132° 38' 41" W	/	/	hap1	KY028801	hap1	KY028911
I277	Alaska (USA), Petersburg, South Mitkof Island, Summer Strait. Seashore, on sedimentary rocks, 0-5 m a.s.l. 25/06/2012. Leg. *S. Pérez-Ortega, T. Spribille & K. Dillman.* Loc. 558	56° 33' 10" N	132° 38' 41" W	/	/	hap2	KY028802	hap1	KY028912
I433	Alaska (USA), Petersburg, South Mitkof Island, Summer Strait. Seashore, on sedimentary rocks, 0-5 m a.s.l. 25/06/2012. Leg. *S. Pérez-*	56° 33' 10" N	132° 38' 41" W	hap2	KX987895	hap2	KY028803	hap1	KY028913

	Ortega, T. Spribille & K. Dillman. Loc. 558								
I434	Alaska (USA), Petersburg, South Mitkof Island, Summer Strait. Seashore, on sedimentary rocks, 0-5 m a.s.l. 25/06/2012. Leg. *S. Pérez-Ortega, T. Spribille & K. Dillman*. Loc. 558	56° 33' 10" N	132° 38' 41" W	hap2	KX987896	hap2	KY028804	hap1	KY028914
I435	Alaska (USA), Petersburg, South Mitkof Island, Summer Strait. Seashore, on sedimentary rocks, 0-5 m a.s.l. 25/06/2012. Leg. *S. Pérez-Ortega, T. Spribille & K. Dillman*. Loc. 558	56° 33' 10" N	132° 38' 41" W	/	/	hap2	KY028805	hap1	KY028915
I436	Alaska (USA), Petersburg, South Mitkof Island, Summer Strait. Seashore, on sedimentary rocks, 0-5 m a.s.l. 25/06/2012. Leg. *S. Pérez-Ortega, T. Spribille & K. Dillman*. Loc. 558	56° 33' 10" N	132° 38' 41" W	/	/	hap1	KY028806	hap1	KY028916
I437	Alaska (USA), Petersburg, South Mitkof Island, Summer Strait. Seashore, on sedimentary rocks, 0-5 m a.s.l. 25/06/2012. Leg. *S. Pérez-Ortega, T. Spribille & K. Dillman*. Loc. 558	56° 33' 10" N	132° 38' 41" W	/	/	hap1	KY028807	hap1	KY028917
I130-1	Tierra del Fuego (Chile), Brunswick Peninsula, San Nicolás Bay, near Cabo Froward, XII Región. Seashore, 0-5 m a.s.l. 18/12/2009. Leg. *S. Pérez-Ortega*. Loc. 434-435	53° 50' 46" S	71° 7' 4" W	/	/	hap4	KY028808	hap1	KY028918
I242	Tierra del Fuego (Chile), Brunswick Peninsula, San Nicolás Bay, near Cabo Froward, XII Región. Seashore, 0-5 m a.s.l. 18/12/2009. Leg. *S. Pérez-Ortega*. Loc. 434-435	53° 50' 46" S	71° 7' 4" W	hap3	KX987897	hap4	KY028809	hap1	KY028919

I249-3	Tierra del Fuego (Chile), Brunswick Peninsula, San Nicolás Bay, near Cabo Froward, XII Región. Seashore, 0-5 m a.s.l. 18/12/2009. Leg. *S. Pérez-Ortega*. Loc. 434-435	53° 50' 46" S	71° 7' 4" W	/	/	hap11	KY028810	hap1	KY028920
I483	Tierra del Fuego (Chile), Brunswick Peninsula, San Nicolás Bay, near Cabo Froward, XII Región. Seashore, 0-5 m a.s.l. 18/12/2009. Leg. *S. Pérez-Ortega*. Loc. 434-435	53° 50' 46" S	71° 7' 4" W	hap3	KX987898	hap4	KY028811	hap1	KY028921
I484	Tierra del Fuego (Chile), Brunswick Peninsula, San Nicolás Bay, near Cabo Froward, XII Región. Seashore, 0-5 m a.s.l. 18/12/2009. Leg. *S. Pérez-Ortega*. Loc. 434-435	53° 50' 46" S	71° 7' 4" W	hap7	KX987899	hap4	KY028812	hap1	KY028922
I485	Tierra del Fuego (Chile), Brunswick Peninsula, San Nicolás Bay, near Cabo Froward, XII Región. Seashore, 0-5 m a.s.l. 18/12/2009. Leg. *S. Pérez-Ortega*. Loc. 434-435	53° 50' 46" S	71° 7' 4" W	hap3	KX987900	/	/	hap1	KY028923
I486	Tierra del Fuego (Chile), Brunswick Peninsula, San Nicolás Bay, near Cabo Froward, XII Región. Seashore, 0-5 m a.s.l. 18/12/2009. Leg. *S. Pérez-Ortega*. Loc. 434-435	53° 50' 46" S	71° 7' 4" W	hap8	KX987901	hap4	KY028813	hap1	KY028924
I487	Tierra del Fuego (Chile), Brunswick Peninsula, San Nicolás Bay, near Cabo Froward, XII Región. Seashore, 0-5 m a.s.l. 18/12/2009. Leg. *S. Pérez-Ortega*. Loc. 434-435	53° 50' 46" S	71° 7' 4" W	hap3	KX987902	hap11	KY028814	hap1	KY028925
I127	Tierra del Fuego (Chile), Beagle Channel, Basket Island, XII Región. Seashore, 0-5 m a.s.l. 17/12/2009. Leg. *S. Pérez-Ortega*. Loc. 432-433	54° 42' 13" S	71° 34' 53" W	/	/	hap4	KY028815	hap1	KY028926
I128	Tierra del Fuego (Chile), Beagle	54° 42' 13" S	71° 34' 53" W	/	/	hap4	KY028816	hap1	KY028927

	Channel, Basket Island, XII Región. Seashore, 0-5 m a.s.l. 17/12/2009. Leg. *S. Pérez-Ortega*. Loc. 432-433								
I232	Tierra del Fuego (Chile), Beagle Channel, Basket Island, XII Región. Seashore, 0-5 m a.s.l. 17/12/2009. Leg. *S. Pérez-Ortega*. Loc. 432-433	54° 42' 13" S	71° 34' 53" W	hap3	KX987903	/	/	hap1	KY028928
I233	Tierra del Fuego (Chile), Beagle Channel, Basket Island, XII Región. Seashore, 0-5 m a.s.l. 17/12/2009. Leg. *S. Pérez-Ortega*. Loc. 432-433	54° 42' 13" S	71° 34' 53" W	hap4	KX987904	hap7	KY028817	hap1	KY028929
I234-2	Tierra del Fuego (Chile), Beagle Channel, Basket Island, XII Región. Seashore, 0-5 m a.s.l. 17/12/2009. Leg. *S. Pérez-Ortega*. Loc. 432-433	54° 42' 13" S	71° 34' 53" W	hap4	KX987905	hap7	KY028818	hap1	KY028930
I237b	Tierra del Fuego (Chile), Beagle Channel, Basket Island, XII Región. Seashore, 0-5 m a.s.l. 17/12/2009. Leg. *S. Pérez-Ortega*. Loc. 432-433	54° 42' 13" S	71° 34' 53" W	hap5	KX987906	/	/	hap1	KY028931
I240	Tierra del Fuego (Chile), Beagle Channel, Basket Island, XII Región. Seashore, 0-5 m a.s.l. 17/12/2009. Leg. *S. Pérez-Ortega*. Loc. 432-433	54° 42' 13" S	71° 34' 53" W	hap5	KX987907	hap11	KY028819	hap1	KY028932
I478	Tierra del Fuego (Chile), Beagle Channel, Basket Island, XII Región. Seashore, 0-5 m a.s.l. 17/12/2009. Leg. *S. Pérez-Ortega*. Loc. 432-433	54° 42' 13" S	71° 34' 53" W	hap3	KX987908	hap4	KY028820	hap1	KY028933
I479	Tierra del Fuego (Chile), Beagle Channel, Basket Island, XII Región. Seashore, 0-5 m a.s.l. 17/12/2009. Leg. *S. Pérez-Ortega*. Loc. 432-433	54° 42' 13" S	71° 34' 53" W	hap6	KX987909	hap4	KY028821	hap1	KY028934
I480	Tierra del Fuego (Chile), Beagle Channel, Basket Island, XII Región. Seashore, 0-5 m a.s.l. 17/12/2009. Leg. *S. Pérez-Ortega*. Loc. 432-433	54° 42' 13" S	71° 34' 53" W	hap3	KX987910	hap4	KY028822	hap1	KY028935

I481	Tierra del Fuego (Chile), Beagle Channel, Basket Island, XII Región. Seashore, 0-5 m a.s.l. 17/12/2009. Leg. *S. Pérez-Ortega*. Loc. 432-433	54° 42' 13" S	71° 34' 53" W	hap4	KX987911	hap7	KY028823	hap1	KY028936
I482	Tierra del Fuego (Chile), Beagle Channel, Basket Island, XII Región. Seashore, 0-5 m a.s.l. 17/12/2009. Leg. *S. Pérez-Ortega*. Loc. 432-433	54° 42' 13" S	71° 34' 53" W	hap5	KX987912	hap11	KY028824	hap1	KY028937
I137	Tierra del Fuego (Chile), Beagle Channel, Darwin Bay, Chair Island, XII Región. Seashore, 0-5 m a.s.l. 16/12/2009. Leg. *S. Pérez-Ortega*. Loc. 429-431	54° 54' 2" S	70° 00' 30" W	hap9	KX987913	hap6	KY028825	hap1	KY028938
I138	Tierra del Fuego (Chile), Beagle Channel, Darwin Bay, Chair Island, XII Región. Seashore, 0-5 m a.s.l. 16/12/2009. Leg. *S. Pérez-Ortega*. Loc. 429-431	54° 54' 2" S	70° 00' 30" W	hap10	KX987914	hap8	KY028826	hap1	KY028939
I221	Tierra del Fuego (Chile), Beagle Channel, Darwin Bay, Chair Island, XII Región. Seashore, 0-5 m a.s.l. 16/12/2009. Leg. *S. Pérez-Ortega*. Loc. 429-431	54° 54' 2" S	70° 00' 30" W	hap4	KX987915	hap7	KY028827	hap1	KY028940
I222	Tierra del Fuego (Chile), Beagle Channel, Darwin Bay, Chair Island, XII Región. Seashore, 0-5 m a.s.l. 16/12/2009. Leg. *S. Pérez-Ortega*. Loc. 429-431	54° 54' 2" S	70° 00' 30" W	hap4	KX987916	hap7	KY028828	hap1	KY028941
I223	Tierra del Fuego (Chile), Beagle Channel, Darwin Bay, Chair Island, XII Región. Seashore, 0-5 m a.s.l. 16/12/2009. Leg. *S. Pérez-Ortega*. Loc. 429-431	54° 54' 2" S	70° 00' 30" W	hap4	KX987917	/	/	hap1	KY028942
I488	Tierra del Fuego (Chile), Beagle Channel, Darwin Bay, Chair Island,	54° 54' 2" S	70° 00' 30" W	hap9	KX987918	hap6	KY028829	hap1	KY028943

	XII Región. Seashore, 0-5 m a.s.l. 16/12/2009. Leg. *S. Pérez-Ortega*. Loc. 429-431								
I489	Tierra del Fuego (Chile), Beagle Channel, Darwin Bay, Chair Island, XII Región. Seashore, 0-5 m a.s.l. 16/12/2009. Leg. *S. Pérez-Ortega*. Loc. 429-431	54° 54' 2" S	70° 00' 30" W	hap9	KX987919	hap6	KY028830	hap1	KY028944
I490	Tierra del Fuego (Chile), Beagle Channel, Darwin Bay, Chair Island, XII Región. Seashore, 0-5 m a.s.l. 16/12/2009. Leg. S. Pérez-Ortega. Loc. 429-431	54° 54' 2" S	70° 00' 30" W	hap4	KX987920	hap6	KY028831	hap1	KY028945
I491	Tierra del Fuego (Chile), Beagle Channel, Darwin Bay, Chair Island, XII Región. Seashore, 0-5 m a.s.l. 16/12/2009. Leg. *S. Pérez-Ortega*. Loc. 429-431	54° 54' 2" S	70° 00' 30" W	hap10	KX987921	hap8	KY028832	hap1	KY028946
I492	Tierra del Fuego (Chile), Beagle Channel, Darwin Bay, Chair Island, XII Región. Seashore, 0-5 m a.s.l. 16/12/2009. Leg. *S. Pérez-Ortega*. Loc. 429-431	54° 54' 2" S	70° 00' 30" W	hap4	KX987922	/	/	hap1	KY028947
I493	Tierra del Fuego (Chile), Beagle Channel, Darwin Bay, Chair Island, XII Región. Seashore, 0-5 m a.s.l. 16/12/2009. Leg. *S. Pérez-Ortega*. Loc. 429-431	54° 54' 2" S	70° 00' 30" W	hap4	KX987923	hap7	KY028833	hap1	KY028948
I139	Tierra del Fuego (Chile), Beagle Channel, Picton Island, XII Región. Seashore, 0-5 m a.s.l. 23/1/2008. Leg. *S. Pérez-Ortega*. Loc. 222	55° 1' 10" S	66° 55' 39" W	/	/	hap5	KY028834	hap1	KY028949
I145	Tierra del Fuego (Chile), Beagle Channel, Picton Island, XII Región. Seashore, 0-5 m a.s.l. 23/1/2008.	55° 1' 10" S	66° 55' 39" W	hap11	KX987924	/	/	hap1	KY028950

	Leg. *S. Pérez-Ortega*. Loc. 222								
I210	Tierra del Fuego (Chile), Beagle Channel, Picton Island, XII Región. Seashore, 0-5 m a.s.l. 23/1/2008. Leg. *S. Pérez-Ortega*. Loc. 222	55° 1' 10" S	66° 55' 39" W	hap12	KX987925	/	/	hap1	KY028951
I497	Tierra del Fuego (Chile), Beagle Channel, Picton Island, XII Región. Seashore, 0-5 m a.s.l. 23/1/2008. Leg. *S. Pérez-Ortega*. Loc. 222	55° 1' 10" S	66° 55' 39" W	/	/	hap5	KY028835	hap1	KY028952
I216	Tierra del Fuego (Chile), Beagle Channel, Róbalo Bay, Navarino Island, XII Región. Seashore, 0-5 m a.s.l. 25/1/2008. Leg. *S. Pérez-Ortega.* Loc. 223	54° 56' 4" S	67° 40' 34" W	/	/	hap9	KY028836	hap1	KY028953
I153b	Tierra del Fuego (Chile), Beagle Channel, Róbalo Bay, Navarino Island, XII Región. Seashore, 0-5 m a.s.l. 25/1/2008. Leg. *S. Pérez-Ortega.* Loc. 223	54° 56' 4" S	67° 40' 34" W	/	/	hap9	KY028837	hap1	KY028954
I499	Tierra del Fuego (Chile), Beagle Channel, Róbalo Bay, Navarino Island, XII Región. Seashore, 0-5 m a.s.l. 25/1/2008. Leg. *S. Pérez-Ortega.* Loc. 223	54° 56' 4" S	67° 40' 34" W	hap11	KX987926	hap10	KY028838	hap1	KY028955
I500	Tierra del Fuego (Chile), Beagle Channel, Róbalo Bay, Navarino Island, XII Región. Seashore, 0-5 m a.s.l. 25/1/2008. Leg. *S. Pérez-Ortega*. Loc. 223	54° 56' 4" S	67° 40' 34" W	/	/	hap10	KY028839	hap1	KY028956
I501	Tierra del Fuego (Chile), Beagle Channel, Róbalo Bay, Navarino Island, XII Región. Seashore, 0-5 m a.s.l. 25/1/2008. Leg. S. Pérez-Ortega. Loc. 223	54° 56' 4" S	67° 40' 34" W	hap11	KX987927	hap10	KY028840	hap1	KY028957
I502	Tierra del Fuego (Chile), Beagle	54° 56' 4" S	67° 40' 34" W	hap11	KX987928	hap9	KY028841	hap1	KY028958

	Channel, Róbalo Bay, Navarino Island, XII Región. Seashore, 0-5 m a.s.l. 25/1/2008. Leg. *S. Pérez-Ortega*. Loc. 223								
I503	Tierra del Fuego (Chile), Beagle Channel, Róbalo Bay, Navarino Island, XII Región. Seashore, 0-5 m a.s.l. 25/1/2008. Leg. *S. Pérez-Ortega*. Loc. 223	54° 56' 4" S	67° 40' 34" W	hap11	KX987929	hap9	KY028842	hap1	KY028959
I156	Tierra del Fuego (Chile), Beagle Channel, Puerto Navarino, Navarino Island, XII Región. Seashore, 0-5 m a.s.l. 27/1/2008. Leg. S. Pérez-Ortega. Loc. 227	54° 55' 48" S	68° 20' 45" W	/	/	hap7	KY028843	hap1	KY028960
I504	Tierra del Fuego (Chile), Beagle Channel, Puerto Navarino, Navarino Island, XII Región. Seashore, 0-5 m a.s.l. 27/1/2008. Leg. *S. Pérez-Ortega*. Loc. 227	54° 55' 48" S	68° 20' 45" W	hap3	KX987930	/	/	hap1	KY028961
I505	Tierra del Fuego (Chile), Beagle Channel, Puerto Navarino, Navarino Island, XII Región. Seashore, 0-5 m a.s.l. 27/1/2008. Leg. *S. Pérez-Ortega*. Loc. 227	54° 55' 48" S	68° 20' 45" W	hap3	KX987931	/	/	hap1	KY028962
I506	Tierra del Fuego (Chile), Beagle Channel, Puerto Navarino, Navarino Island, XII Región. Seashore, 0-5 m a.s.l. 27/1/2008. Leg. *S. Pérez-Ortega*. Loc. 227	54° 55' 48" S	68° 20' 45" W	hap3	KX987932	/	/	hap1	KY028963
I507	Tierra del Fuego (Chile), Beagle Channel, Puerto Navarino, Navarino Island, XII Región. Seashore, 0-5 m a.s.l. 27/1/2008. Leg. *S. Pérez-Ortega*. Loc. 227	54° 55' 48" S	68° 20' 45" W	hap3	KX987933	hap7	KY028844	hap1	KY028964
I95	Antarctica, South Shetlands, King	62.261502° S	58.617572° W	hap13	KX987934	hap12	KY028845	hap2	KY028965

	George Island, Potter Peninsula, Stranger Point. Seashore, 0-5 m a.s.l. 22/12/2009. Leg. *F. Fernández-Mendoza & S. Domaschke.*								
I104b	Antarctica, South Shetlands, King George Island, Potter Peninsula, Stranger Point. Seashore, 0-5 m a.s.l. 22/12/2009. Leg. *F. Fernández-Mendoza & S. Domaschke.*	62.261502° S	58.617572° W	hap14	KX987935	/	/	hap2	KY028966
I105	Antarctica, South Shetlands, King George Island, Potter Peninsula, Stranger Point. Seashore, 0-5 m a.s.l. 22/12/2009. Leg. *F. Fernández-Mendoza & S. Domaschke.*	62.261502° S	58.617572° W	hap15	KX987936	hap14	KY028846	hap2	KY028967
I107	Antarctica, South Shetlands, King George Island, Potter Peninsula, Stranger Point. Seashore, 0-5 m a.s.l. 22/12/2009. Leg. *F. Fernández-Mendoza & S. Domaschke.*	62.261502° S	58.617572° W	hap16	KX987937	hap3	KY028847	hap3	KY028968
I112	Antarctica, South Shetlands, King George Island, Potter Peninsula, Stranger Point. Seashore, 0-5 m a.s.l. 22/12/2009. Leg. *F. Fernández-Mendoza & S. Domaschke.*	62.261502° S	58.617572° W	hap13	KX987938	/	/	hap2	KY028969
I203	Antarctica, South Shetlands, King George Island, Potter Peninsula, Stranger Point. Seashore, 0-5 m a.s.l. 22/12/2009. Leg. *F. Fernández-Mendoza & S. Domaschke.*	62.261502° S	58.617572° W	/	/	hap16	KY028848	hap2	KY028970

I440	Antarctica, South Shetlands, King George Island, Potter Peninsula, Stranger Point. Seashore, 0-5 m a.s.l. 22/12/2009. Leg. *F. Fernández-Mendoza & S. Domaschke.*	62.261502° S	58.617572° W	hap13	KX987939	hap12	KY028849	hap2	KY028971
I441	Antarctica, South Shetlands, King George Island, Potter Peninsula, Stranger Point. Seashore, 0-5 m a.s.l. 22/12/2009. Leg. *F. Fernández-Mendoza & S. Domaschke.*	62.261502° S	58.617572° W	hap13	KX987940	hap12	KY028850	hap2	KY028972
I442	Antarctica, South Shetlands, King George Island, Potter Peninsula, Stranger Point. Seashore, 0-5 m a.s.l. 22/12/2009. Leg. *F. Fernández-Mendoza & S. Domaschke.*	62.261502° S	58.617572° W	hap17	KX987941	/	/	hap2	KY028973
I443	Antarctica, South Shetlands, King George Island, Potter Peninsula, Stranger Point. Seashore, 0-5 m a.s.l. 22/12/2009. Leg. *F. Fernández-Mendoza & S. Domaschke.*	62.261502° S	58.617572° W	hap16	KX987942	hap3	KY028851	hap3	KY028974
I444	Antarctica, South Shetlands, King George Island, Potter Peninsula, Stranger Point. Seashore, 0-5 m a.s.l. 22/12/2009. Leg. *F. Fernández-Mendoza & S. Domaschke.*	62.261502° S	58.617572° W	hap15	KX987943	hap12	KY028852	hap2	KY028975
I454	Antarctica, South Shetlands, King George Island, Potter Peninsula, Stranger Point. Seashore, 0-5 m a.s.l. 22/12/2009. Leg. *F. Fernández-Mendoza & S. Domaschke.*	62.261502° S	58.617572° W	hap15	KX987944	hap13	KY028853	hap2	KY028976

I455	Antarctica, South Shetlands, King George Island, Potter Peninsula, Stranger Point. Seashore, 0-5 m a.s.l. 22/12/2009. Leg. *F. Fernández-Mendoza & S. Domaschke.*	62.261502° S	58.617572° W	hap14	KX987945	hap15	KY028854	hap2	KY028977
I456	Antarctica, South Shetlands, King George Island, Potter Peninsula, Stranger Point. Seashore, 0-5 m a.s.l. 22/12/2009. Leg. *F. Fernández-Mendoza & S. Domaschke.*	62.261502° S	58.617572° W	hap14	KX987946	hap15	KY028855	hap2	KY028978
I508	Antarctica, South Shetlands, Greenwich Island. Seashore, 0-5 m a.s.l. 28/1/2013. Leg. *J. E. González Pastor.*	62° 26' 53.55" S	59° 55' 45.81" W	hap15	KX987947	hap13	KY028856	hap2	KY028979
I509	Antarctica, South Shetlands, Greenwich Island. Seashore, 0-5 m a.s.l. 28/1/2013. Leg. *J. E. González Pastor.*	62° 26' 53.55" S	59° 55' 45.81" W	hap15	KX987948	hap13	KY028857	hap2	KY028980
I510	Antarctica, South Shetlands, Greenwich Island. Seashore, 0-5 m a.s.l. 28/1/2013. Leg. *J. E. González Pastor.*	62° 26' 53.55" S	59° 55' 45.81" W	hap15	KX987949	hap13	KY028858	hap2	KY028981
I511	Antarctica, South Shetlands, Greenwich Island. Seashore, 0-5 m a.s.l. 28/1/2013. Leg. *J. E. González Pastor.*	62° 26' 53.55" S	59° 55' 45.81" W	hap15	KX987950	hap13	KY028859	hap2	KY028982
I512	Antarctica, South Shetlands, Greenwich Island. Seashore, 0-5 m a.s.l. 28/1/2013. Leg. *J. E. González Pastor.*	62° 26' 53.55" S	59° 55' 45.81" W	hap15	KX987951	hap13	KY028860	hap2	KY028983
I165	Antarctica, South Shetlands, Livingston Island, Española Cove. Seashore, 0-5 m a.s.l. 27/1/2014.	62° 39' 07.35" S	60° 22' 11.58" W	hap18	KX987952	hap18	KY028861	hap2	KY028984

	Leg. *A. de los Ríos.*								
I166	Antarctica, South Shetlands, Livingston Island, Española Cove. Seashore, 0-5 m a.s.l. 27/1/2014. Leg. *A. de los Ríos.*	62° 39' 07.35" S	60° 22' 11.58" W	hap19	KX987953	hap16	KY028862	hap2	KY028985
I167	Antarctica, South Shetlands, Livingston Island, Española Cove. Seashore, 0-5 m a.s.l. 27/1/2014. Leg. *A. de los Ríos.*	62° 39' 07.35" S	60° 22' 11.58" W	hap18	KX987954	hap18	KY028863	hap2	KY028986
I168	Antarctica, South Shetlands, Livingston Island, Española Cove. Seashore, 0-5 m a.s.l. 27/1/2014. Leg. *A. de los Ríos.*	62° 39' 07.35" S	60° 22' 11.58" W	hap18	KX987955	hap18	KY028864	hap2	KY028987
I169	Antarctica, South Shetlands, Livingston Island, Española Cove. Seashore, 0-5 m a.s.l. 27/1/2014. Leg. *A. de los Ríos.*	62° 39' 07.35" S	60° 22' 11.58" W	hap18	KX987956	hap18	KY028865	hap2	KY028988
I170	Antarctica, South Shetlands, Livingston Island, Española Cove. Seashore, 0-5 m a.s.l. 27/1/2014. Leg. *A. de los Ríos.*	62° 39' 07.35" S	60° 22' 11.58" W	hap18	KX987957	hap18	KY028866	hap2	KY028989
I171	Antarctica, South Shetlands, Livingston Island, Española Cove. Seashore, 0-5 m a.s.l. 27/1/2014. Leg. *A. de los Ríos.*	62° 39' 07.35" S	60° 22' 11.58" W	/	/	hap18	KY028867	/	/
I176	Antarctica, South Shetlands, Livingston Island, Española Cove. Seashore, 0-5 m a.s.l. 27/1/2014. Leg. *A. de los Ríos.*	62° 39' 07.35" S	60° 22' 11.58" W	hap18	KX987958	hap18	KY028868	hap2	KY028990
I187	Antarctica, South Shetlands, Livingston Island, Española Cove. Seashore, 0-5 m a.s.l. 27/1/2014. Leg. *A. de los Ríos.*	62° 39' 07.35" S	60° 22' 11.58" W	hap15	KX987959	/	/	/	/
I381	Antarctica, South Shetlands, Livingston Island, Española Cove.	62° 39' 07.35" S	60° 22' 11.58" W	hap18	KX987960	hap18	KY028869	hap2	KY028991

	Seashore, 0-5 m a.s.l. 27/1/2014. Leg. *A. de los Ríos.*								
I447	Antarctica, South Shetlands, Livingston Island, Española Cove. Seashore, 0-5 m a.s.l. 27/1/2014. Leg. A. de los Ríos.	62° 39' 07.35" S	60° 22' 11.58" W	hap18	KX987961	hap18	KY028870	hap2	KY028992
I448	Antarctica, South Shetlands, Livingston Island, Española Cove. Seashore, 0-5 m a.s.l. 27/1/2014. Leg. *A. de los Ríos.*	62° 39' 07.35" S	60° 22' 11.58" W	hap19	KX987962	hap16	KY028871	hap2	KY028993
I449	Antarctica, South Shetlands, Livingston Island, Española Cove. Seashore, 0-5 m a.s.l. 27/1/2014. Leg. *A. de los Ríos.*	62° 39' 07.35" S	60° 22' 11.58" W	hap18	KX987963	hap18	KY028872	hap2	KY028994
I450	Antarctica, South Shetlands, Livingston Island, Española Cove. Seashore, 0-5 m a.s.l. 27/1/2014. Leg. *A. de los Ríos.*	62° 39' 07.35" S	60° 22' 11.58" W	hap18	KX987964	hap18	KY028873	hap2	KY028995
I451	Antarctica, South Shetlands, Livingston Island, Española Cove. Seashore, 0-5 m a.s.l. 27/1/2014. Leg. *A. de los Ríos.*	62° 39' 07.35" S	60° 22' 11.58" W	hap19	KX987965	hap16	KY028874	hap2	KY028996
I453	Antarctica, South Shetlands, Livingston Island, Española Cove. Seashore, 0-5 m a.s.l. 27/1/2014. Leg. *A. de los Ríos.*	62° 39' 07.35" S	60° 22' 11.58" W	hap15	KX987966	hap13	KY028875	hap2	KY028997
I286	Antarctica, Yalour Island. Seashore, 0-5 m a.s.l. 26/1/2007. Leg. J. C. García Galindo & J. Romagni.	65° 15' S	64° 01' W	hap20	KX987967	/	/	hap2	KY028998
I288	Antarctica, Yalour Island. Seashore, 0-5 m a.s.l. 26/1/2007. Leg. *J. C. García Galindo & J. Romagni.*	65° 15' S	64° 01' W	hap20	KX987968	/	/	hap2	KY028999
I291	Antarctica, Yalour Island. Seashore, 0-5 m a.s.l. 26/1/2007. Leg. *J. C. García Galindo & J. Romagni.*	65° 15' S	64° 01' W	hap18	KX987969	hap18	KY028876	hap2	KY029000

I292	Antarctica, Yalour Island. Seashore, 0-5 m a.s.l. 26/1/2007. Leg. *J. C. García Galindo & J. Romagni.*	65° 15' S	64° 01' W	hap18	KX987970	hap18	KY028877	hap2	KY029001
I459	Antarctica, Yalour Island. Seashore, 0-5 m a.s.l. 26/1/2007. Leg. *J. C. García Galindo & J. Romagni.*	65° 15' S	64° 01' W	hap18	KX987971	/	/	hap2	KY029002
I460	Antarctica, Yalour Island. Seashore, 0-5 m a.s.l. 26/1/2007. Leg. *J. C. García Galindo & J. Romagni.*	65° 15' S	64° 01' W	hap19	KX987972	/	/	hap2	KY029003
I462	Antarctica, Yalour Island. Seashore, 0-5 m a.s.l. 26/1/2007. Leg. *J. C. García Galindo & J. Romagni.*	65° 15' S	64° 01' W	hap19	KX987973	/	/	hap2	KY029004
I300	Antarctica, Rongé Island. Seashore, 0-5 m a.s.l. 25/1/2007. Leg. *J. C. García Galindo & J. Romagni.*	64° 43' S	62° 34' W	hap18	KX987974	/	/	hap2	KY029005
I302	Antarctica, Rongé Island. Seashore, 0-5 m a.s.l. 25/1/2007. Leg. *J. C. García Galindo & J. Romagni.*	64° 43' S	62° 34' W	/	/	hap18	KY028878	hap2	KY029006
I463	Antarctica, Rongé Island. Seashore, 0-5 m a.s.l. 25/1/2007. Leg. *J. C. García Galindo & J. Romagni.*	64° 43' S	62° 34' W	hap18	KX987975	hap18	KY028879	hap2	KY029007
I464	Antarctica, Rongé Island. Seashore, 0-5 m a.s.l. 25/1/2007. Leg. *J. C. García Galindo & J. Romagni.*	64° 43' S	62° 34' W	hap18	KX987976	/	/	hap2	KY029008
I465	Antarctica, Rongé Island. Seashore, 0-5 m a.s.l. 25/1/2007. Leg. *J. C. García Galindo & J. Romagni.*	64° 43' S	62° 34' W	hap18	KX987977	hap18	KY028880	hap2	KY029009
I466	Antarctica, Rongé Island. Seashore, 0-5 m a.s.l. 25/1/2007. Leg. *J. C. García Galindo & J. Romagni.*	64° 43' S	62° 34' W	hap18	KX987978	hap18	KY028881	hap2	KY029010
I467	Antarctica, Rongé Island. Seashore, 0-5 m a.s.l. 25/1/2007. Leg. *J. C. García Galindo & J. Romagni.*	64° 43' S	62° 34' W	hap18	KX987979	hap18	KY028882	hap2	KY029011
I309	Antarctica, Avian Island (Adelaide Island). Seashore, 0-5 m a.s.l.	67° 46' S	68° 53' W	hap21	KX987980	/	/	hap2	KY029012

	27/1/2007. Leg. *J. C. García Galindo & J. Romagni.*								
I311	Antarctica, Avian Island (Adelaide Island). Seashore, 0-5 m a.s.l. 27/1/2007. Leg. *J. C. García Galindo & J. Romagni.*	67° 46' S	68° 53' W	/	/	hap13	KY028883	hap2	KY029013
I318	Antarctica, Avian Island (Adelaide Island). Seashore, 0-5 m a.s.l. 27/1/2007. Leg. *J. C. García Galindo & J. Romagni.*	67° 46' S	68° 53' W	hap21	KX987981	hap17	KY028884	hap2	KY029014
I470	Antarctica, Avian Island (Adelaide Island). Seashore, 0-5 m a.s.l. 27/1/2007. Leg. *J. C. García Galindo & J. Romagni.*	67° 46' S	68° 53' W	hap21	KX987982	/	/	hap2	KY029015
I473	Antarctica, Antarctic Peninsula, Cierva Cove. Seashore, 0-5 m a.s.l. 26/1/2007. Leg. *J. C. García Galindo & J. Romagni.*	64° 09' S	60° 57' W	hap18	KX987983	/	/	hap2	KY029016
I475	Antarctica, Antarctic Peninsula, Cierva Cove. Seashore, 0-5 m a.s.l. 26/1/2007. Leg. *J. C. García Galindo & J. Romagni.*	64° 09' S	60° 57' W	hap18	KX987984	/	/	hap2	KY029017
I476	Antarctica, Antarctic Peninsula, Cierva Cove. Seashore, 0-5 m a.s.l. 26/1/2007. Leg. *J. C. García Galindo & J. Romagni.*	64° 09' S	60° 57' W	hap18	KX987985	/	/	hap2	KY029018
I384	Alaska (USA), Petersburg, South Mitkof Island, Summer Strait. Seashore, on sedimentary rocks, 0-5 m a.s.l. 25/06/2012. Leg. *S. Pérez-Ortega, T. Spribille & K. Dillman.* Loc. 558	56° 33' 10" N	132° 38' 41" W	/	/	hap2	KY028885	/	/
I432	Alaska (USA), Petersburg, South Mitkof Island, Summer Strait. Seashore, on sedimentary rocks, 0-5	56° 33' 10" N	132° 38' 41" W	hap2	KX987986	hap2	KY028886	hap1	KY029019

	m a.s.l. 25/06/2012. Leg. *S. Pérez-Ortega, T. Spribille & K. Dillman*. Loc. 558								
I408	SAG 43.96	/	/	/	/	hap19	KY012794	/	/
I438	Alaska (USA), Petersburg, Mitkof Island, Summer Strait. Seashore, on sedimentary rocks, 0-1 m a.s.l. 24/06/2012. Leg. *S. Pérez-Ortega, T. Spribille & K. Dillman*. Loc. 558	56° 44' 29" N	132° 56' 23" W	hap22	KX987987	/	/	hap4	KY029020
I60	Antarctica, South Shetlands, Livingston Island, Hannah Point. Seashore, 0-5 m a.s.l. 12/2/2012. Leg. *C. Laguna Fiol*	62° 39' S	60° 37' W	hap23	KX987988	/	/	/	/
I83	Antarctica, South Shetlands, King George Island, Potter Peninsula, Stranger Point. Seashore, 0-5 m a.s.l. 22/12/2009. Leg. *F. Fernández-Mendoza & S. Domaschke.*	62.261502° S	58.617572° W	hap23	KX987989	/	/	/	/

Appendix 2. GENBANK samples used for constructing the *nrITS*-A dataset used in the single-locus analysis.

Taxon	Strain or Isolate	Family (*sensu* ALGAEBASE-accessed April 2016)	GENBANK accession number
'Chlorella' saccharophila	CCAP 211/57	*Trebouxiophyceae incertae sedis*	FR865676
Desmococcus olivaceus	SAG 1.92	*Prasiolaceae*	KM020049
Diplosphaera chodatii 1	FontaineM22-1	*Prasiolaceae*	KF317621
Diplosphaera chodatii 2	FontaineDV2-2	*Prasiolaceae*	KF317625
Diplosphaera chodatii 3	FontaineDV4-3	*Prasiolaceae*	KF317627
Diplosphaera chodatii 4	FontaineDV5-2	*Prasiolaceae*	KF317629
Gloeocystis polydermatica	CCAP 31/5	*Radiococcaceae*	FR865740
Koliella longiseta 1	SAG 470-1	*Koliellaceae*	HE610126
Koliella longiseta 2	SAG 470-1	*Koliellaceae*	AJ431677
Koliella sempervirens	CCALA 363	*Koliellaceae*	AJ431673
Pabia signiensis 1	SAG 7.90	*Trebouxiaceae*	KM116464
Pabia signiensis 2	SAG 2110	*Trebouxiaceae*	KM116465
Planophila sp.	CCAP 462/1	*Chaetopeltidaceae*	FR865753
Pseudochlorella sp.	CCAP 211/1A	*Koliellaceae*	FM958479
Pseudochlorella pyrenoidosa	SAG 18.95	*Koliellaceae*	AM422986
Raphidonema nivale 1	CCCryo<DEU>:274-06	*Koliellaceae*	HQ404891
Raphidonema nivale 2	CCAP 470/4	*Koliellaceae*	AJ431676
Raphidonema sempervirens	CCAP 470/6	*Koliellaceae*	AJ431674
Stichococcus bacillaris 1	SAG 379-1b	*Prasiolaceae*	AJ431678
Stichococcus bacillaris 2	SAG 379-2	*Prasiolaceae*	HE610125
Stichococcus bacillaris 3	FG2/4.2	*Prasiolaceae*	KM020048
Stichococcus chloranthus	UTEX 315	*Prasiolaceae*	AM412751
Stichococcus sp. 1	IOAC542S	*Prasiolaceae*	KC817132
Stichococcus sp. 2	IOAC805S	*Prasiolaceae*	KC817137

Appendix 3. GENBANK samples used for constructing the *tufA*-A dataset used in the single-locus analysis.

Taxon	Strain or Isolate	Family (*sensu* ALGAEBASE-accessed April 2016)	GENBANK accession number
Prasiola antarctica	P31	*Prasiolaceae*	KF993447
Prasiola borealis	P4	*Prasiolaceae*	KF993441
Prasiola borealis	P33	*Prasiolaceae*	KF993448
Prasiola calophylla	P41	*Prasiolaceae*	KF993449
Prasiola calophylla	P61	*Prasiolaceae*	KF993455
Prasiola crispa	P43	*Prasiolaceae*	KF993450
Prasiola crispa	P65	*Prasiolaceae*	KF993457
Prasiola furfuracea	P62	*Prasiolaceae*	KF993456
Prasiola delicata	GWS005076	*Prasiolaceae*	HQ610263
Prasiola cf. *delicata*	GALW015795	*Prasiolaceae*	KF993454
Prasiola meridionalis	F12	*Prasiolaceae*	KF993433
Prasiola meridionalis	F21	*Prasiolaceae*	KF993434
Prasiola meridionalis	F30	*Prasiolaceae*	KF993438
Prasiola meridionalis	F31	*Prasiolaceae*	KF993439
Prasiola meridionalis	P7	*Prasiolaceae*	KF993442
Prasiola meridionalis	P8	*Prasiolaceae*	KF993443
Prasiola meridionalis	P10	*Prasiolaceae*	KF993444
Prasiola novaezelandiae	P2	*Prasiolaceae*	KF993440
Prasiola stipitata	GWS003898	*Prasiolaceae*	HQ610265
Prasiola stipitata	GWS004462	*Prasiolaceae*	HQ610267
Prasiola stipitata	F26	*Prasiolaceae*	KF993437
Prasiola stipitata	P26	*Prasiolaceae*	KF993446
Prasiola stipitata	P40	*Prasiolaceae*	KF993451
Prasiola stipitata	P54	*Prasiolaceae*	KF993452
Prasiola stipitata	P55	*Prasiolaceae*	KF993453
Prasiola stipitata	P39	*Prasiolaceae*	KF993458
Prasiola yunnanica	P16	*Prasiolaceae*	KF993445
Rosenvingiella constricta	F01	*Prasiolaceae*	KF993432
Rosenvingiella radicans	F25	*Prasiolaceae*	KF993436

Appendix 4. GENBANK samples used for constructing the *RPL10A*-A dataset used in the single-locus analysis.

Taxon	Strain or Isolate	Family (*sensu* ALGAEBASE-accessed April 2016)	GENBANK accession number
Asterochloris erici	SAG 32.85	*Trebouxiaceae*	JX179048
Asterochloris irregularis	SAG 33.85	*Trebouxiaceae*	JX179050
Asterochloris magna	UTEX 902	*Trebouxiaceae*	JX179051
Asterochloris phycobiontica	SAG 26.81	*Trebouxiaceae*	JX179052
Asterochloris pyriformis	UTEX 1713	*Trebouxiaceae*	JX179053
Auxenochlorella protothecoides	710	*Chlorellaceae*	JX857642
Chlorella vulgaris	UTEX 259	*Chlorellaceae*	EF411214
Choricystis chodatii	SAG 216-2	*Coccomyxaceae*	JX196849
Coccomyxa mucigena	SAG 216-4	*Coccomyxaceae*	JX196850
Coccomyxa peltigerae	SAG 216-5	*Coccomyxaceae*	JX179054
Coccomyxa pringsheimii	SAG 216-7	*Coccomyxaceae*	JX179056
Coccomyxa rayssiae	SAG 216-8	*Coccomyxaceae*	JX179057
Coccomyxa solorinae-bisporae	SAG 216-10	*Coccomyxaceae*	JX179058
Coccomyxa subellipsoidea	SAG 216-13	*Coccomyxaceae*	JX179062
Coccomyxa viridis	SAG 216-14	*Coccomyxaceae*	JX179064
Dilabifilum sp.	SAG 2038	*Ulvales incertae sedis*	JX179066
Nannochloris normandinae	SAG 9.82	*Chlorellaceae*	JX179070
Symbiochloris reticulata	DretLp	*Trebouxiaceae*	JX179067
Symbiochloris symbiontica	SAG 27.81	*Trebouxiaceae*	JX179069
Trebouxia angustilobata	SAG 2204	*Trebouxiaceae*	JF414661
Trebouxia asymmetrica	SAG 48.88	*Trebouxiaceae*	JX179071
Trebouxia corticola	UTEX 909	*Trebouxiaceae*	JX179072
Trebouxia decolorans	UTEX B781	*Trebouxiaceae*	JX179073
Trebouxia gigantea	UTEX 2231	*Trebouxiaceae*	JX179074
Trebouxia jamesii	UTEX 2233	*Trebouxiaceae*	JF414663
Trebouxia simplex	SAG 2207	*Trebouxiaceae*	JF414662
Zea mays	clone 881852	*Poaceae*	EU976371

CAPÍTULO 5 (*CHAPTER 5*)

La dispersión directa y conjunta del hongo liquenizado *Mastodia tessellata* (Ascomycota) y su fotobionte explica su distribución bipolar.

Referencia del artículo científico en revisión:

Garrido-Benavent I, de los Ríos A, Fernández-Mendoza F y Pérez-Ortega S (2017) No need for stepping stones: Direct, joint dispersal of the lichen-forming fungus *Mastodia tessellata* (Ascomycota) and its photobiont explains their bipolar distribution. Journal of Biogeography (in rev.)

Abstract

Although a high percentage of Antarctic lichens are known to occur also at high latitudes or alpine habitats in the Northern Hemisphere, few studies have formally investigated the historical processes at the origin of such bipolar distribution pattern. A species delimitation approach together with the use of dated phylogenies and joint migration analyses were conducted to examine phylogeographic patterns in the bipolar lichen-forming fungus *Mastodia tessellata* (*Verrucariaceae,* Ascomycota) and its photobionts (*Prasiola, Trebouxiophyceae,* Chlorophyta) along a North America-Antarctica latitudinal axis. We show that *M. tessellata* comprises two fungal species which in turn associate with three different photobiont lineages along the studied distribution range. Independent estimation of divergence ages for myco- and photobionts agreed in a mid-Miocene to Pliocene species split in the Southern Hemisphere, and a late Miocene to Pleistocene acquisition of the bipolar distribution. Comparison of migration models and genetic diversity patterns suggested an austral origin for the bipolar species. The complex evolutionary history of *Mastodia tessellata* s.l. can be explained by a combination of vicariant and direct long-distance dispersal mechanisms, the latter probably bird-mediated. We provide novel evidence for a pre-Pleistocene long-term evolution of lichens in Antarctica, as well as the importance of Southern to Northern Hemisphere migratory routes in shaping bipolar distributions.

1. Introduction

In the 19th century, Humboldt (1817), Darwin (1872), and Wallace (1880) converged on a common point, their fascination for disjunct amphitropical plant distributions. Since then, a number of vascular plants, mosses, liverworts and lichens have been shown to be present in polar regions and temperate mountain areas of both hemispheres, and largely absent from the tropics. In earlier times, this pattern was interpreted in terms of either vicariance (Du Rietz 1940; Briggs 1987) or long-distance dispersal (Darwin 1872; Raven 1963). More recently, the use of molecular markers and reliable time-calibrated phylogenetic methods (Yang & Donoghue 2016) has allowed setting up a temporal context for the origin of such distributions, across different organism groups. Until now, Miocene to Pleistocene long-distance dispersal has been proposed to have shaped the amphitropical distributions of species in some vascular plant genera (e.g. *Empetrum* Popp et al. 2011; *Munroa*, Amarilla et al. 2015; *Carex*, Villaverde et al. 2015a,b) and bryophytes (*Cinclidium*, Piñeiro et al. 2012; *Tetraplodon*, Lewis et al. 2014a).

Lichen-forming fungi stand out as the organism group showing most amphitropically disjunct species (Du Rietz 1940; Galloway & Aptroot 1995), although this may in some cases be due to an underestimation of diversity using overly broad species concepts. The Antarctic continent represents the most extreme example with up to 40% of the occurring species (*c.* 148 spp.) showing bipolar distribution patterns (Øvstedal & Lewis Smith 2001). The origin of lichenized and non-lichenized fungi in Antarctica has been debated since long, with most authors acknowledging endemic taxa as ancient relicts, and bipolar taxa as recent, post-Pleistocene colonisers (e.g. Lamb 1970; Hertel 1987; Galloway 1991; Bridge & Spooner 2012). The molecular era has yielded relatively few studies dealing with the origin of bipolar Antarctic lichen-forming fungi. Patterns shown by *Xanthomendoza borealis* and *Usnea lambii* were interpreted based on genetic affinities (i.e. tree topology), and long-distance dispersal was suggested as one possible mechanism shaping their distributions (Lindblom & Søchting 2008; Wirtz et al. 2008). Only Fernández-Mendoza & Printzen (2013) provided a model-based, robust statistical evidence for a boreal origin and subsequent southward migration of *Cetraria aculeata* during the Pleistocene. In general, this Northern to Southern Hemisphere migration route in relatively recent times, which is coherent with that of most vascular plants (Wen & Ickert-Bond 2009) has been often hypothesized for other bipolar lichens occurring in South America and New Zealand (Myllys et al. 2003; Geml et al. 2012).

In this study we focus on *Mastodia tessellata* (*Verrucariaceae*, Ascomycota), a saxicolous, foliose lichen which occurs in nutrient-rich spots of the supralittoral zone in cold, oceanic to hyper-oceanic climates (Kohlmeyer et al. 2004). Its distribution range goes from the Southern Hemisphere, mainly Antarctica and neighbouring islands, Tierra del Fuego (Chile), Tasmania and New Zealand, and extends to the Pacific coast of Alaska and Canada (Øvstedal & Lewis Smith 2001; Kohlmeyer et al. 2004). *Mastodia tessellata* represents a paradigmatic case since it is one of the very few species of

lichen-forming fungi associated with a macroscopic, foliose alga. In a previous work, we showed that at least two photobiont species of the trebouxiophycean genus *Prasiola* are involved in this symbiosis (Garrido-Benavent et al. 2017). Furthermore, we confirmed a bipolar distribution for the primarily recognised photobiont, *P. borealis*, whereas a second, undescribed *Prasiola* species was restricted to Antarctica. Patterns of genetic diversity and genealogical relationships among haplotypes of the former species suggested a Southern to Northern Hemisphere migration (Garrido-Benavent et al. 2017).

The exceptional biology of our target species allows for jointly unravelling the evolutionary history of the fungal and algal partner, as in other coevolving systems (e.g. host-pathogen interactions). For this reason, we extend here our previous study in order to discern the macro- and microevolutionary causes that underlie their disjunct distribution pattern. First, we will evaluate the occurrence of cryptic speciation in the mycobiont after several photobiont species were recognized to take part in lichenization (Moniz et al. 2014; Garrido-Benavent et al. 2017). Precise delineation of independently evolving lineages will therefore avoid confusion when interpreting the role of extrinsic and intrinsic barriers to gene flow (Pante et al. 2015). Second, we will build temporal frameworks for the evolution of myco- and photobiont lineages to test their fit to classical hypotheses of bipolar distributions. Thus, models accounting for vicariance will be supported if age estimates date back to the major tectonic events leading to the breakup of Pangaea and Gondwana (mid-Jurassic to Late Cretaceous, roughly 174–66 million years ago, MA, Scotese 2001; Mao et al. 2012). Conversely, disjunction ages dating from the Miocene to Pleistocene will strongly favour trans-tropical long-distance dispersal (Wen & Ickert-Bond 2009; Fernández-Mendoza & Printzen 2013; Lewis et al. 2014a). Finally, different migration models will be statistically compared and demographic parameters estimated to accurately reflect the evolutionary history of the delimited lineages.

2. Material and Methods

2.1. Study area and sampling design

Sampling aimed at covering most of the disjunct distributional range of *Mastodia tessellata*, including 16 localities from both hemispheres: two from Alaska (USA), one from British Columbia (Canada), six from Tierra del Fuego (Chile) and seven from the Antarctic Peninsula and neighbouring islands (Supplementary Figure 1). A total of 315 lichenized specimens were molecularly analysed: 69 from North America, 135 from Tierra del Fuego and 111 from the Antarctic region (Appendix 1). *Verrucaria tessellatula* was selected as the fungal outgroup. The photobiont dataset also included nine free-living *Prasiola* specimens collected in the same studied region and a cultured sample of *P. crispa* (SAG code 43.96).

2.2. Amplification and DNA sequence analyses

Three unlinked, nuclear fungal markers were amplified: the internal transcribed spacer of the nuclear ribosomal DNA (*nrITS*), the protein-coding elongation factor 1-α (*EF-1α*) and the DNA replication licensing factor of the mini-chromosome maintenance complex 7 (*Mcm7*). For the algae, we used the three loci (*nrITS*, *RPL10A* and *tufA*) dataset published in Garrido-Benavent et al. (2017), which we expanded with new samples and a fourth locus, the plastidial RuBisco large subunit (*rbcL*). To improve amplification, we designed new primers with PRIMER-BLAST (Ye et al. 2012) to use in nested PCRs (Supplementary Table 1–2). PCR reactions were performed according to information in Supplementary Table 3. Algal *tufA*, *nrITS* and *RPL10A* amplifications conditions, as well as further procedures for obtaining and assembling electropherograms, checking and aligning sequences, and recombination testing can be found in Garrido-Benavent et al. (2017). Details on localities and specimens are given in Appendix 1. Optimal substitution models and partition schemes for each dataset were estimated in PARTITIONFINDER v.1.1.1 (Lanfear et al. 2012), using the greedy scheme-search algorithm. Less complex models were usually allowed when poor estimations of overall likelihood were yielded due to overparameterization.

2.3. Species discovery

To evaluate the presence of cryptic species in the mycobiont dataset, we used the Automatic Barcode Gap Discovery (ABGD) method (Puillandre et al. 2012), which automatically finds breaks in the distribution of genetic pairwise distances in single-locus datasets. We restricted ABGD runs to the marker proposed as fungal barcode, *nrITS* (Schoch et al. 2012). Then, multi-locus allelic data were used to estimate evolutionary populations under an admixture model as implemented in STRUCTURE v.2.3.4 (Pritchard et al. 2000; Falush et al. 2003). We chose the three criteria proposed in Mayer et al. (2015) to determine the optimum number of clusters (*K*): a high ΔK, no single individual-based group and a stable assignment of individuals over replications. Setting of run parameters and results summarization in ABGD and STRUCTURE analyses followed Garrido-Benavent et al. (2017). For the photobiont, analyses were restricted to the newly generated *rbcL* and *tufA* data, and focused on corroborating lineage adscription found in our previous work. For each locus, maximum clade credibility trees were constructed including most GENBANK-available members of *Prasiolaceae* using BEAST v.1.8.1 as implemented in the CIPRES Science Gateway (Suchard & Rambaut 2009; Miller et al. 2010; see below for details on BEAST analysis settings). Finally, multi-locus networks were generated for both symbionts using the NEIGHBORNET algorithm (Bryant & Moulton 2004) as implemented in SPLITSTREE v.4.13.1 from non-standardized distance matrices between individuals calculated in POFAD v.1.07 (Joly & Bruneau 2006).

2.4. Species validation

First, we compared alternative mycobiont species delimitation models inferred from ABGD and STRUCTURE groupings, and multi-locus networks using the Bayes

Factor Delimitation (BFD) method (Grummer et al. 2014). Because this method departs from a multispecies coalescent method, it can accommodate discordance between gene phylogenies. The outgroup was included in all analyses to allow testing a single-species model (Chen et al. 2014). Analyses were run using *BEAST (Heled & Drummond 2010; Drummond et al. 2012). Settings, priors, running conditions and marginal likelihood (ML) calculations followed Garrido-Benavent et al. (2017).

To provide further evidence on population/species boundaries and their permeability in both symbionts data, we used the Bayesian software MIGRATE-N v.3.6.11 (Beerli 2006; Beerli & Palczewski 2010), which interprets all shared polymorphism resulted from gene flow. Four alternative delimitation models were ranked using BF (Supplementary Figure 2A). Five Antarctic specimens were inferred to be genetically distinct and to belong to a different population/species than the core of the Antarctic specimens, and were thus treated as a separate population. As MIGRATE-N does not allow imposing unconnected populations, in our case candidate species, we consistently retained bidirectional gene-flow between them while imposing low prior expectations on migration rates (*M*) as a model compromise (see Allen et al. 2016). Analyses used multi-locus sequence data, variable rates among loci, starting values for Θ and *M* calculated from Wright's Fst, random starting trees, empirical base frequencies and locus-specific transition:transversion ratios for the myco- (*nrITS*: 2.17, *EF-1α*: 1.57, *Mcm7*: 1.38) and photobiont (*nrITS*: 1.17, *rbcL*: 2.76, *RPL10A*: 3.13, *tufA*: 2.02) as calculated in MEGA v.5.2 (Tamura et al. 2011). We chose uniform priors for Θ (Min. = 0, Max. = 0.15, Delta = 0.015) and *M* (Min. = 0, Max. = 8.000, Delta = 1.000) and conducted four replicates for each model with a static heating scheme using four chains (1, 1.5, 3, 10^5). We discarded 40.000 trees as burn-in and recorded 65.000 steps with an increment of 100. ESS values > 1.000 and posterior distributions of the parameters, recorded as single peaks with smooth curves, were considered for convergence assessment.

For model comparisons, 2 ln Bayes Factors were calculated from averaged ML (BFD) and ML approximated by thermodynamic integration ("Bézier") in MIGRATE-N (Beerli & Palczewski 2010). 2 ln BF values above 10 indicate very strong evidence against a model as compared with the best (Kass & Raftery 1995).

2.5. Evaluation of species genetic diversity and phylogeographic structure

Polymorphism statistics, genetic divergence and differentiation, neutrality tests and genealogical relationships among haplotypes in each validated mycobiont species were calculated following Garrido-Benavent et al. (2017). We additionally inspected the level of genetic stratification with Bayesian population assignment tests conducted in BAPS v.6 (Corander et al. 2006, 2008) and STRUCTURE v.2.3.4. BAPS multi-locus analyses used single nucleotide polymorphism (SNP) data, a codon linkage model, a linked clustering model, and were run with individual values of *K* ranging from two to 10 and 10 replicates for each value of *K*. STRUCTURE was run with the *locprior* option turned on for sampling location information to assist clustering (Hubisz et al. 2009). For

photobionts, we used only the *rbcL* and *tufA* datasets to calculate DNA polymorphism and haplotype networks.

2.6. Molecular dating analysis

We reconstructed a temporal framework for the divergence of the validated myco- and photobiont species as well as the main phylogeographically differentiated clusters within them. Due to the lack of a suitable fossil record within *Verrucariaceae*, two different fungal *nrITS* average mutation rates were imposed on the multi-locus mycobiont dataset: 2.52×10^{-3} s/s/MA (*Erysiphales*, Takamatsu & Matsuda 2004) and 3.41×10^{-3} s/s/MA (*Melanohalea*, Leavitt et al. 2012b). Analyses were implemented in *BEAST, unlinking clock and tree models among datasets, and imposing a strict clock on each dataset (Supplementary Table 4), and using a Yule process and a piecewise linear and constant root as the species tree prior and population size model, respectively. Priors replicated the species validation settings. *EF-1α* and *Mcm7* substitution rates were co-estimated using a uniform prior (initial value = 1, upper = 5, lower = 0). Single-locus haplotype chronograms were then calculated using inferred average substitution rates for *EF-1α* and *Mcm7* (Supplementary Table 5) and a coalescent constant size tree prior in BEAST v.1.8.1.

Because *Prasiola* lacks a suitable fossil record, we used a two-step approach to set photobiont diversification in a time frame. First, we compiled a dataset consisting of 73 representatives of Streptophyta and Chlorophyta, from which members of classes *Chlorophyceae* and *Trebouxiophyceae* (including the target genus *Prasiola* and its closest relative *Rosenvingiella*) exhibited a more intensive sampling (Appendix 2). Molecular data included the nuclear small ribosomal subunit (*18S*), and four chloroplast protein-coding genes extracted from complete plastid genomes: the beta subunit of ATP synthase (*atpB*), P700 chlorophyll a-apoprotein A2 (*psaB*), the *tufA*, and the *rbcL*. First, obvious ambiguously aligned regions in *18S* dataset were removed using the less stringent settings and half gap positions allowed in GBLOCKS v.0.91b (Castresana 2000). After confirming topological congruence among datasets, we generated a concatenated alignment which included 308 sequences and a total of 7.867 bp. Sequence data from the glaucophyte *Cyanophora paradoxa* was used to root the tree (Herron et al. 2009). Several fossils and secondary molecular-based calibrations across Viridiplantae, and several nodes constrained as monophyletic were imposed when setting the analysis (Supplementary Table 6). As starting tree, we used a ML topology obtained in RAxML-HPC2 as implemented in the CIPRES Science Gateway web server (Stamatakis 2006, 2008; Miller et al. 2010) which was transformed into an ultrametric tree using the *chronos* function in the *ape* R package (Paradis et al. 2004). The analysis was run in BEAST v.1.8.1 using a lognormal relaxed molecular clock for all markers (Supplementary Table 7), and a Birth-Death process tree prior. Average substitution rates for each marker were co-estimated under a uniform prior (initial value = 1, upper = 5, lower = 0). Remaining parameters were set to default.

We subsequently draw the *tufA* mean substitution rate from the posterior distribution of the first analysis, particularly for the clade including all *Prasiolaceae* members (Supplementary Table 8). This rate was imposed on a) a rooted, two-marker dataset including all lichenised *Prasiola* for which *tufA* and *rbcL* sequences were available (85 specimens included), and b) an unrooted, four-marker dataset (*tufA*, *rbcL*, *nrITS* and *RPL10A*) for which at least two markers were available (67 specimens included). Preliminary runs using a relaxed molecular clock showed that the marginal distribution of the standard deviation of the rate variation included 0 and therefore a strict clock was imposed on all markers. Additionally, we constructed chronograms for *tufA* and *rbcL* using an extended sampling of lichenized and non-lichenized *Prasiolaceae* (GENBANK data).

Overall running instructions included variable chain lengths ranging from 2.5×10^7 (single-locus analyses) to 2×10^8 steps (multi-locus analyses), saving always 10.000 trees. After selecting an adequate burn-in, and checking for convergence in TRACER v.1.5 (http://tree.bio.ed.ac.uk/software/tracer/), the mean heights of the post-burnin tree samples were annotated in TREEANNOTATOR v.1.8.1 (Drummond et al. 2012). 50% majority rule consensus trees were constructed using FIGTREE v.1.4 (http://tree.bio.ed.ac.uk/software/figtree/). ADOBE ILLUSTRATOR CS5 was used for artwork.

2.7. Joint migration analysis

Gene flow directionality, population connectivity and demographic parameters in bipolar myco- and photobiont species were further evaluated with MIGRATE-N v.3.6.11. Under a Bayesian-coalescent framework, this software allows for estimating historical effective population sizes ($\Theta = x\mathrm{N}e\mu$; x is a multiplier that depends on the ploidy and inheritance of data, Beerli 2010) and migration rates ($M = m/\mu$) for multiple populations. Six competing models for each biont were constructed according to two opposite migratory routes: from Northern to Southern Hemisphere, or *vice versa* (Supplementary Figure 2B). For reference, two null models were also compared: one in which all populations were grouped into one panmictic deme, and a second in which all possible connections among these populations were allowed. Analyses settings and model comparisons were done as above. Subsequently, we manually calculated the number of immigrants per generation (xNm) from the mean estimates of the mutation-scaled migration parameter M.

3.1 Results

3.1. Molecular datasets

Nine-hundred and twelve of the 1.277 used sequences were generated for this study. The mycobiont dataset comprised 753 sequences (251 *nrITS*, 251 *EF-1α*, and 251 *Mcm7*), whereas the algal dataset included 524 sequences (133 *nrITS*, 96 *rbcL*, 119

RPL10A and 176 *tufA*). Data on alignments and estimated substitution models used in different analyses are in Supplementary Table 9–11. The MAXCHI recombination detection method only found a weak, non-statistically significant signal in the *EF-1α* matrix, which was assumed to be the result of homoplasy due to the high polymorphism shown by this marker. Specific information on the photobiont *nrITS* and *RPL10A* datasets was provided in Garrido-Benavent et al. (2017).

3.2. Delimitation of non-phylogenetic demes

We found 16 *nrITS*, 15 *EF-1α* and 11 *Mcm7* mycobiont haplotypes. *nrITS* ABGD, multi-locus STRUCTURE (best *K*) and multi-locus network analyses were coherent in splitting the dataset into two clusters that we further treated as candidate species (Figure 1B–D, Supplementary Figure 3). The first included all specimens from North America, Tierra del Fuego and five from Antarctica; the second comprised all remaining Antarctic specimens. The BFD method also supported a two-species over a one-species model (Supplementary Table 12) and BF comparisons in MIGRATE-N further favoured the inclusion of five Antarctic individuals within the North American and Tierra del Fuego cluster, and supported the genetic isolation between candidate species even in Antarctica, where both are present (Supplementary Table 13). Three Tierra del Fuego specimens (1.2% of all samples) showed an admixed fraction over 10% (Figure 1D), a result derived not of sharing alleles but from the lack of support, as it can be observed in the BAPS result (Figure 1E) and in the haplotype networks (Figure 2).

For the photobiont, six *rbcL* and three *tufA* haplotypes were recovered. Inner nodes in *rbcL* and *tufA* topologies received low statistical support, despite both recovered a monophyletic clade including most Southern Hemisphere representatives of *Prasiola* (Supplementary Figure 4–5). *rbcL* topologies supported allocation of photobiont sequences in three distantly related lineages. Thus, North American (*hap1*, *hap2*, *hap3*), Tierra del Fuego (*hap4*) and the Antarctic (*hap5*) haplotypes clustered within a *P. borealis-furfuracea* clade; the Antarctic *Prasiola* sp. haplotype (*hap6*) was closely related to a *P.* cf. *crispa* sample (EF589146 accession); and a British Columbia haplotype (*hap7*) to *P. delicata* (Figure 2, Supplementary Figure 4, Appendix 3). Phylogenetic adscription of the *tufA* haplotypes was identical to that reported in Garrido-Benavent et al. (2017). Newly generated *nrITS* and *RPL10A* sequences for *P. delicata* showed almost no polymorphism and will not be considered further. MIGRATE-N supported a model with no gene flow between bipolar *P. borealis* and the undescribed Antarctic *Prasiola* sp. (Supplementary Table 13).

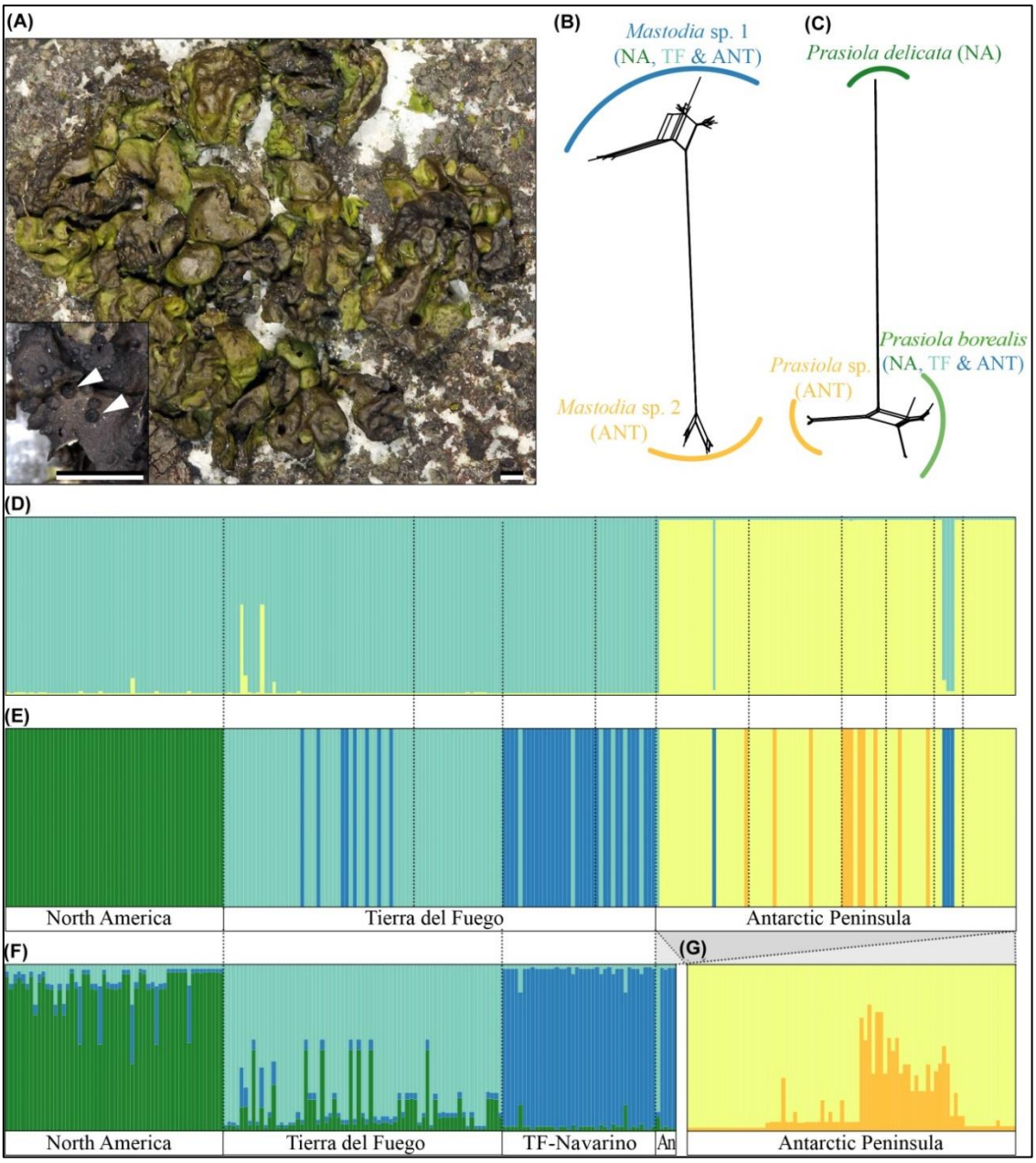

Figure 1. Species delimitation and genetic structure in *Mastodia tessellata* s.l. (A) *Mastodia* sp. 1 and *Prasiola borealis* association in Alaska, with a detail of perithecia (fungal structures producing sexual spores, white arrow tips). (B) and (C) SPLITSTREE NEIGHBORNET diagrams obtained from multi-locus myco- and photobiont datasets, respectively. Delimited species are highlighted: NA, North America; TF, Tierra del Fuego (Chile); ANT, Antarctica. (D) Mycobiont genetic admixture inferred with STRUCTURE under $K = 2$. (E) Mycobiont genetic mixture estimated with BAPS using SNP data. (F) *Mastodia* sp. 1 genetic admixture inferred under $K = 3$ in STRUCTURE. (G) *Mastodia* sp. 2 genetic admixture inferred under $K = 2$ in STRUCTURE. All analyses used multi-locus data. Colours in vertical bars represent assignment probabilities to different genetic clusters. Scale A = 2 mm (Photographs: SPO & IGB).

3.3. Genetic polymorphism, population differentiation, neutrality tests, and phylogeographic structure

According to the species delimitation results, we divided our mycobiont data into two sets, provisionally named *Mastodia* sp. 1 and *Mastodia* sp. 2, which shared no haplotypes (two-species model) in any studied loci. Genetic diversity indices, neutrality tests and genetic differentiation and divergence for each validated species are summarized in Supplementary Figure 6 and Supplementary Table 14. Nucleotide and haplotype diversities were greater for *Mastodia* sp. 1 than for the Antarctic *Mastodia* sp. 2 across all markers. In *Mastodia* sp. 1, the patterns of population differentiation (Fst) and distance-based (Dxy) divergence in *nrITS* revealed two-well differentiated groups of regional populations: North America and Tierra del Fuego. Within the latter, populations from Navarino and Picton islands showed further differentiation. Overall, Tierra del Fuego exhibited higher *Hd* and π values for *nrITS* and *Mcm7* than North America, whereas the reversed was true for *EF-1α Hd*. The Antarctic *Mastodia* sp. 1 population was more closely related to Navarino and Picton islands (*nrITS*, *EF-1α*) and its five individuals showed relatively high values of *Hd* and π. In *Mastodia* sp. 2, four haplotypes were found in each dataset, and no clear patterns of population differentiation and divergence were found. Regarding the photobiont, North American populations of *P. borealis* showed higher *Hd* and π than Tierra del Fuego and Antarctic ones for the *rbcL* data. Antarctic *Prasiola* sp. individuals shared the same haplotype. Extending the *tufA* molecular sampling in comparison to Garrido-Benavent et al. (2017) did not provided further insight into the genetic diversity of lichenized *Prasiola*. No significant deviations from neutrality were found in any case.

A strong geographic structure was found in the populations of *Mastodia* sp. 1. The *nrITS* data comprised 12 haplotypes split into three-separated and well-supported clades (Figure 2, Supplementary Figure 7). North American haplotypes were closely related to those found in Tierra del Fuego. Navarino and Picton islands haplotypes were included in a separate subnetwork. Specimens from King George Island (Antarctica) shared haplotypes with Tierra del Fuego populations, while haplotypes from Avian Island were particularly related to those found in Navarino and Picton islands. The *EF-1α* and *Mcm7* networks showed a star-like pattern in which an abundant, central haplotype was widespread in both hemispheres (Figure 2A). Some Navarino and Picton islands and Antarctic *EF-1α* haplotypes were resolved in a subnetwork separated by many mutational steps. *Mastodia* sp. 2 networks are in general formed by an abundant central haplotype and few minor ones that are geographically restricted (Figure 2B). For *Prasiola borealis*, the *rbcL* network revealed a predominant Tierra del Fuego haplotype to which Antarctic and a subnetwork of North American haplotypes were connected (Figure 2D). North America and Tierra del Fuego shared a *tufA* haplotype (Figure 2E).

The number of SNPs inferred from the mycobiont *nrITS*, *EF-1α* and *Mcm7* datasets were 50, 52 and 19, respectively. Multi-locus inference of mixture populations carried out in BAPS divided *Mastodia* sp. 1 into three clusters: one including all North American individuals, and two with Tierra del Fuego individuals. Remarkably, one of

these two included most Navarino and Picton islands samples and the five specimens from Antarctica ascribed to *Mastodia* sp. 1 (Figure 1E). This result agrees with the level of genetic stratification found in STRUCTURE (Figure 1F). Antarctic *Mastodia* sp. 2 was partitioned in two clusters (Figure 1E), coinciding with the higher amount of admixed individuals found in Livingston, Yalour and Rongé islands (Figure 1G).

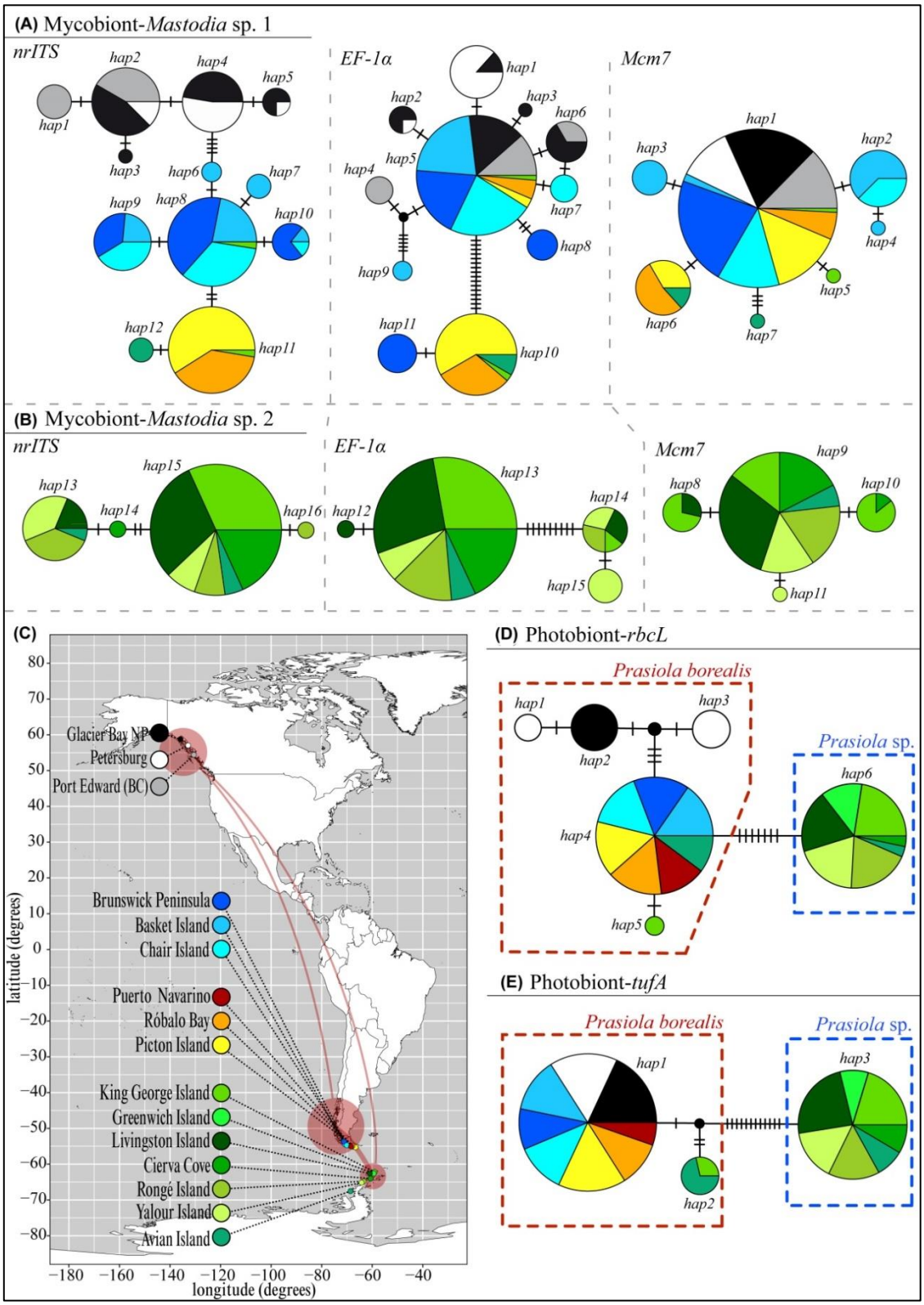

◀Figure 2. Statistical parsimony networks for haplotypes of *Mastodia tessellata* s.l. myco- and photobionts. (A) and (B) *nrITS*, *EF-1α* and *Mcm7* networks for *Mastodia* sp. 1 and *Mastodia* sp. 2, respectively. (C) Map showing sampling localities and a representation of interregional genetic connectivity in *Mastodia* sp. 1. The red circles are scaled to represent the proportion of haplotypes found in each of the three geographic regions (North America, Tierra del Fuego and Antarctica) averaged across loci; connectors represent the proportion of haplotypes shared between the regions averaged across the three loci. (D) and (E) *rbcL* and *tufA* networks for *Prasiola borealis* (dashed red line) and *Prasiola* sp. (dashed blue line), respectively. Colours indicate the localities where individuals were collected (these also appear in the map). The sizes of the circles in the networks are proportional to the numbers of individuals bearing the haplotype; small, black-filled circles indicate missing haplotypes. Mutations are shown as hatch marks. Haplotype codes follow Appendix 1.

3.4. Estimation of divergence times

The estimation of population divergence times is based on phylochronogram reconstructions carried out on multi- and single-locus reconstructions (Supplementary Figure 4–5,7–10,12–13). The main events for both symbionts are summarized in Figure 3. The highly concordant age estimates observed in myco- and photobiont phylogenies support the adequacy of the alternative secondary calibrations implemented in both symbionts. In the fungus, the use of a *Melanohalea nrITS* substitution rate produced younger estimates, but 95% HPD intervals largely overlapped to those obtained using the more slowly evolving *nrITS* rate of *Erysiphales* (Figure 3). For simplicity, results and discussion are based only on the latter. The topology of the multispecies coalescent tree obtained in *BEAST using the main fungal geographical lineages (Supplementary Figure 10) is well resolved. The tMRCA of the bipolar *Mastodia* sp. 1 and Antarctic *Mastodia* sp. 2 was estimated to be 8.04 MA (95% HPD 12.02–3.69). Extant widely disjunct distribution of *Mastodia* sp. 1 was achieved in the Pleistocene, *c.* 0.77 MA (95% HPD 1.39–0.27). Single-locus analyses inferred mean age estimates for *Mastodia* sp. 1 and sp. 2 divergence ranging from 4.74 (*Mcm7*) to 14.38 (*nrITS*) MA (Figure 3, Supplementary Figure 7–9), which fall in the mid-Miocene to mid-Pliocene. The *nrITS* chronogram estimated the divergence between North American and Tierra del Fuego haplotypes to be 3.02 MA (95% HPD, 4.64–1.59).

The maximum credibility tree of Viridiplantae showed high resolution (Supplementary Figure 11). The classes *Trebouxiophyceae*, *Chlorophyceae* and *Ulvophyceae* were resolved each as monophyletic, with *Trebouxiophyceae* as sister to the other two classes (Herron et al. 2009; De Wever et al. 2009; but see Cocquyt 2009). The monophyly of the family *Prasiolaceae* within *Trebouxiophyceae* was statistically supported, and its diversification was dated back to 416.35 MA (95% HPD 470.56–358.61), which falls in the Silurian-Devonian transition. The divergence of *Prasiola* from its closest relatives, *Rosenvingiella* and *Rosenvingiellopsis*, was estimated to have occurred in the Early Cretaceous, *c.* 123.88 MA (95% HPD 151.6–99.44). The *BEAST topology illustrating the main photobiont geographical lineages supported the

previously reported distinction of the bipolar *P. borealis* and the undescribed Antarctic *Prasiola* species (Garrido-Benavent et al. 2017). This split was dated back to 8.26 MA (95% HPD 12.09–4.78) in the two-marker analysis (Supplementary Figure 12), or 4.33 MA (95% HPD 7.1–1.68) in the four-marker analysis (Supplementary Figure 13). However, none of these analyses could resolve the phylogenetic placement of populations within *P. borealis* with certainty. The diversification and establishment of a widely disjunct distribution in this taxon could be estimated to have occurred in the Pleistocene (mean values 2.06–1.95 MA, Supplementary Figure 12–13). For further interpretation we consider only results of the two-marker analysis, as the dataset used in the four-marker analysis includes fewer individuals and has a higher number of missing alleles which might mislead the obtained results. Average substitution rates for *Prasiolaceae tufA* and *rbcL* drawn from the first-step analysis were 1.28×10^{-3} and 9.57×10^{-4} s/s/MA, respectively (Supplementary Table 8). Using these rates, we estimated the diversification of the monophyletic clade including most restricted Southern Hemisphere (*P. antarctica*, *P. novaezelandiae*, *Prasiola* sp.) and bipolar (*P. borealis*/*furfuracea*, *P. crispa*) species to be during the Oligocene-Miocene transition (mean values 33.23 and 21.49 MA for *rbcL* and *tufA* chronograms, respectively). Divergence between lichenized *P. borealis* and *Prasiola* sp. was dated back to 17.18 MA (95% HPD 25.9–9.6, for *rbcL*, Supplementary Figure 4), or 10.05 MA (95% HPD 15.5–4.94, for *tufA*, Supplementary Figure 5). The acquisition of a bipolar distribution in *P. borealis* dated back to the late Miocene to Pleistocene (6.42 and 2.17 MA average values for *rbcL* and *tufA*, respectively). Nevertheless, age estimates obtained in the *rbcL* analysis should be taken with caution because branch lengths could be affected by a high degree of missing data in many sequences.

3.5. Joint migration analyses

Results of the MIGRATE-N analyses for the bipolar fungus *Mastodia* sp. 1 and associated bipolar algae *Prasiola borealis* are shown in Supplementary Table 15–16. For both symbionts, the best gene flow models were coherent in supporting a Southern to Northern Hemisphere migration route. Specifically, mycobiont Model 6 assumed Tierra del Fuego as source population and North America and Antarctica as sink populations (Supplementary Figure 2B). Photobiont Model 7 additionally supported a bidirectional gene flow between Tierra del Fuego and Antarctica.

Estimates of mutation-scaled population sizes (Θ) showed low precision in previous models (Supplementary Table 16). The 95% posterior densities spanned from one to three orders of magnitude. Average estimates of Antarctic Θ for both *Mastodia* sp. 1 and *Prasiola borealis* were an order of magnitude larger than those of the rest, most likely a result of the smaller sampling size. Conversely, North American populations exhibited the smallest values of Θ. On the other hand, high *x*Nm estimates were calculated from Tierra del Fuego into Antarctica. Average *x*Nm values estimated from Tierra del Fuego into North America lie below the "one migrant per generation" (Spieth 1974) significance threshold (Mills & Allendorft 1996) clearly reflecting that trans-tropical migration was a historical event and is not an ongoing process.

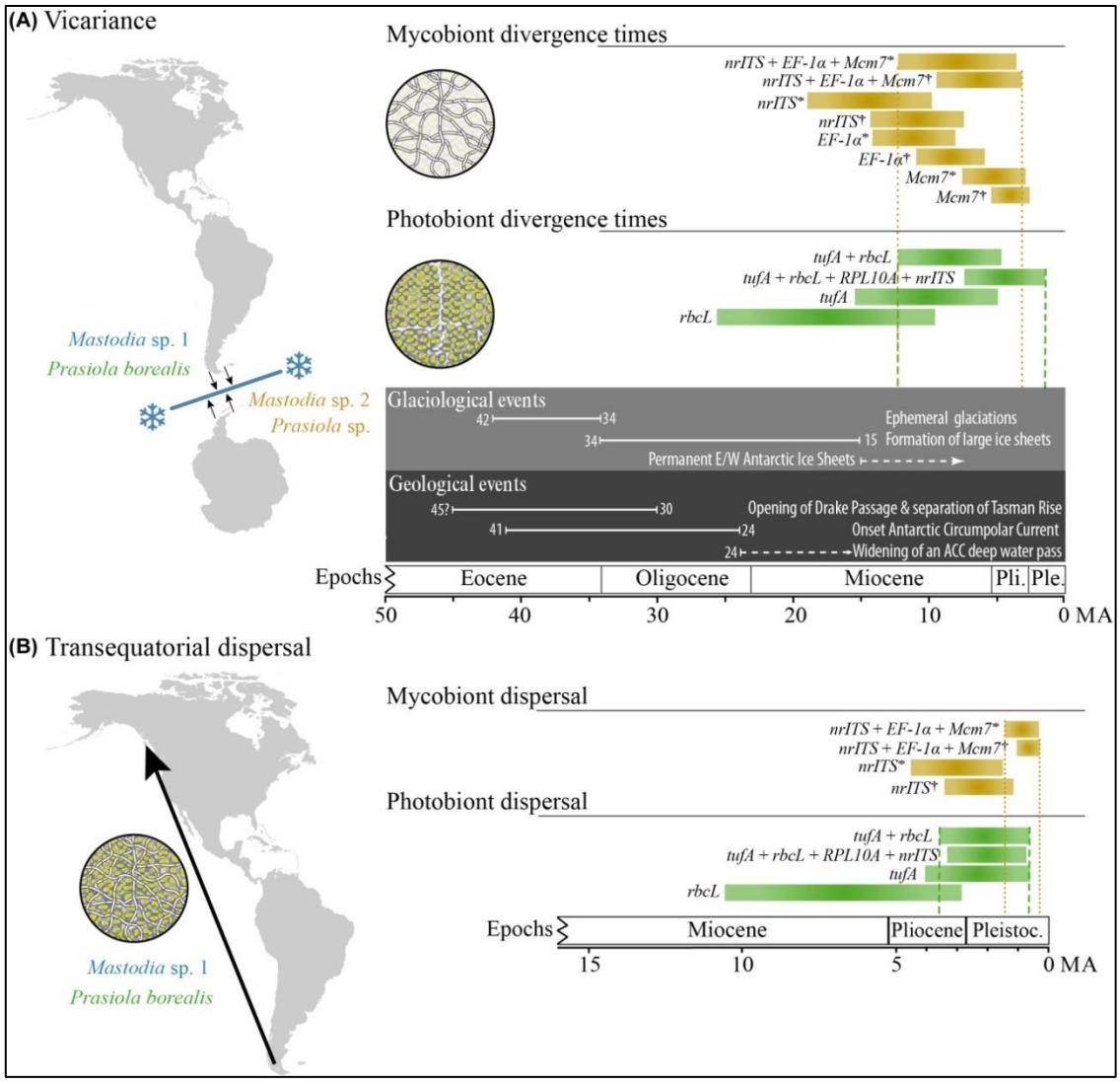

Figure 3. 95% High Posterior Density (HPD) age intervals obtained in BEAST and *BEAST to frame *Mastodia tessellata* s.l. symbionts evolution in time. (A) Temporal scenario for a vicariant speciation in Southern South America and Antarctica. Setting of glaciological, geologic and oceanographic events follow Convey et al. (2008), Feakins et al. (2012), Scher et al. (2015), and Lear & Lunt (2016). * and † denote age estimates obtained using an *Erysiphales* (Takamatsu & Matsuda 2004) or *Melanohalea* (Leavitt et al. 2012b) *nrITS*, or co-estimated *EF-1α* and *Mcm7*, mycobiont substitution rates, respectively. (B) Temporal framework for a long-distance dispersal event shaping the bipolar distribution of *Mastodia* sp. 1 and *Prasiola borealis*. The black arrow indicates the most plausible migration route as inferred with MIGRATE-N. In (A) and (B) yellowish brown and green colours of HPD bars are for myco- and photobionts, respectively. MA: million years ago.

4. Discussion

4.1. *Mastodia tessellata sensu lato*

The species discovery-validation approach based on sequence data allowed the identification of two myco- and three photobionts involved in *M. tessellata* symbiosis (Figure 1, Supplementary Table 12–13). This lichen was previously thought to conform a single association with poorly differentiated morphological features (Kohlmeyer et al. 2004; Pérez-Ortega et al. 2010). More specifically, bipolar *Mastodia* sp. 1 and *P. borealis* were found to occur and associate in North America, Tierra del Fuego and more rarely in the Antarctic Peninsula. Oppositely, *Mastodia* sp. 2 and *Prasiola* sp. were restricted to the Antarctic Peninsula. We assume both fungal species to constitute sister lineages, while the algae *P. novaezelandiae* is phylogenetically interspersed between *P. borealis* and *Prasiola* sp. (Supplementary Figure 4–5). Interestingly, we confirmed the association of *Mastodia* sp. 1 with a third algal species, *P. delicata*, in coastal British Columbia (Moniz et al. 2014). An overall assessment of the fungal and algal lineages involved in this particular symbiosis, as well as their taxonomic status, are pending for further sampling in other areas of the Southern Hemisphere (e.g. Kerguelen Islands, New Zealand and Tasmania).

4.2. Speciation in the Southern Hemisphere

The 95% HPD age intervals estimated for the divergence between Tierra del Fuego and Antarctic myco- and photobionts were highly concordant (Figure 3A), suggesting that the evolution of both symbionts has been driven by a common mechanism. The divergence between the Antarctic and bipolar *Mastodia* species identified in our study is estimated during the mid-Miocene to Pliocene (roughly 17–5.6 MA). A vicariant hypothesis for the origin of both species seems likely, but not in the context of the physical separation of South American and Antarctic landmasses (*c.* 45–23.9 MA, see Convey et al. 2008; Scher et al. 2015; Lear & Lunt 2016, and references therein). It seems reasonable that an ancestral species may have had a more or less continuous range in austral coasts up to the mid-Miocene warm period (Feakins et al. 2012). After the mid-Miocene optimum, the opening of the Shackleton Fracture Zone (22 MA) and the subsequent topographic restructuration of the North Scotia Ridge (16–11 MA) (Barker & Thomas 2004) resulted in a progressive intensification of the Antarctic Circumpolar Current (ACC). This element alone or summed to climate cooling and the re-establishment of Antarctic ice sheets might have limited gene flow among already disjunct lichen populations, thus reinforcing allopatric speciation in Antarctica and Tierra del Fuego. Likewise, González-Wevar et al. (2016) have also reported an ACC-driven, mid-Miocene to Pliocene origin for the divergence of some Antarctic and Subantarctic marine invertebrate taxa. In contrast, our dating results are incompatible with a relatively recent (Quaternary) origin of myco- and photobionts species mediated by dispersal between Antarctica and Southern South America (Figure 3A). In fact, dispersal in and out of Antarctica is presumed to be rare due to the surrounding Southern Ocean, therefore allowing the Antarctic biota to evolve in relative

isolation (Barnes et al. 2006). However, alternative geographic scenarios cannot be fully discarded. It is possible that the Antarctic *Mastodia* species may have originated away from the Antarctic Peninsula-Tierra del Fuego axis that we considered in our study, and has later dispersed into its current distribution.

The present study provides new insights into the long-debated issue of the origin of Antarctic lichen biota. The reciprocal monophyly in disjunct species of both *M. tessellata* s.l. symbionts (Figure 2, Supplementary Figure 7–10,12–13), and the clear-cut pattern shown in admixture analyses (Figure 1; for photobionts see Figure 5 in Garrido-Benavent et al. 2017) suggest an independent, long-term survival of lichenized *Mastodia* sp. 2 and *Prasiola* sp. in maritime Antarctica. These observations support the premise of an ancient, pre-Pleistocene origin of Antarctic lichens invoked by earlier lichenologists (Lamb 1970; Hertel 1987; Castello & Nimis 1997). In a previous work, we proved a Paleogene-Neogene diversification of the primarily Antarctic genus *Shackletonia* (*Teloschistaceae*, Ascomycota, Garrido-Benavent et al. 2016). Evidence for in situ persistence of Antarctic terrestrial biota over long timescales has been also reported in metazoans, such as springtails and mites (e.g. Convey et al. 2008; McGaughran et al. 2011). In cryptogams, different green algal lineages (De Wever et al. 2009) and the moss *Bryum argenteum* (Pisa et al. 2014) have been suggested to have survived through several glacial-interglacial cycles in local refugia. Similarly, our study lichen might have persisted in coastal ice-free refugia (see Lamb 1970) from at least the mid-Neogene. Moreover, geothermal areas in northern Antarctic Peninsula and Victoria Land, both hosting *M. tessellata* s.l. populations, have been postulated to act as glacial refugia for cryptogams (Fraser et al. 2014). Therefore, considering recolonisation from other "cryptic" oases in coastal continental Antarctica is also reasonable (Convey et al. 2008; Pugh & Convey 2008). In fact, the lower levels of DNA polymorphism estimated for most fungal and algal loci in the Antarctic species compared to the South American (Figure 2, Supplementary Table 14; Garrido-Benavent et al. 2017) might reflect the genetic consequences of bottlenecks derived from repeated Pleistocene glacial cycles and a later recolonisation (Hewitt 1996; Fraser et al. 2009b).

4.3. The acquisition of a bipolar distribution

We inferred a late Miocene to Pleistocene origin for the bipolar distribution of *Mastodia* sp. 1 and *P. borealis* (Figure 3B). Despite secondary calibrations are generally assumed to yield relatively inaccurate estimates, this time interval is incongruent with major tectonic events in the Mesozoic promoting vicariant intercontinental disjunctions (Galloway & Aptroot 1995). Thus, long-distance dispersal (LDD) is the most plausible mechanism for the acquisition of such amphitropical distribution. We advocate for a direct LDD between the two continents, because passive, coastal drift along the Pacific and through the tropics seems improbable given that the photobiont genus *Prasiola* is composed mainly of polar and cold-temperate species (Rindi et al. 2007), while the mycobiont relatives only occur in austral and cold-temperate areas (Galloway 2007; Pérez-Ortega et al. 2010) which do not withstand the warmer tropical coasts.

Model comparisons in MIGRATE-N were unequivocal in favouring a migration of both symbionts from Tierra del Fuego into North America (Supplementary Table 15–16). The larger mean estimates of Θ and the higher haplotype and nucleotide diversities in most loci for Tierra del Fuego populations compared to the North American add further credibility to an austral origin for the bipolar species (Figure 2, Supplementary Table 14,16). Oppositely, the low Θ values for North American populations are in agreement with a recovery after a founder effect, with more genetically homogeneous individuals (Supplementary Table 14,16). The extant genetic composition of *Mastodia* sp. 1 and lichenized *P. borealis* in our sampled North American populations still reflects a high degree of shared polymorphism (incomplete lineage sorting), especially in the low-copy, coding markers (Figure 2). Noteworthy, genetic differentiation for the mycobiont was found between Navarino and Picton islands and the remaining Tierra del Fuego populations (Figure 2, Supplementary Figure 6). A similar pattern was previously found in another mutualistic system, the *Nostoc* spp. associated with the *Gunnera magellanica* rhizome (Fernández-Martínez et al. 2013). In our study, as this pattern has been mainly found for the fungal partner, we hypothesize that dispersal of sexual or asexual spores within Tierra del Fuego is rather limited, likely by topographic (Cordillera Darwin) or oceanographic (currents flowing eastwards) factors. On the other hand, the strikingly large Θ values for Antarctic *Mastodia* sp. 1 and *P. borealis* mirror the high genetic diversity found in an otherwise relatively small sample size –five individuals (Figure 2, Supplementary Table 16). Also, migration estimates from Tierra del Fuego into Antarctica are substantially high (Supplementary Table 16) suggesting recent gene flow, likely in the Pleistocene (Supplementary Figures 7–10). In fact, some *nrITS*, *EF-1α*, and *Mcm7* (*Mastodia* sp. 1) and *rbcL* (*P. borealis*) haplotypes are shared between these regions (Figure 2). However, discerning whether such immigration into Antarctica occurred only once, or in multiple times, and involved migration of both bionts separately, or in combination, is challenging given the few available data.

Discussion on the agents (vectors, diaspores) involved in the establishment of bipolar distributions by LDD has long been subjected to speculation. In spite of the remarkable role of wind connectivity to shape the cryptogamic biota in the Southern Hemisphere (Muñoz et al. 2004), the probability of wind dispersion of small propagules such as ascospores (*c*. 9–20 μm) between hemispheres has been modelled as very unlikely (Wilkinson et al. 2012). It has also been suggested that water could have allowed the Southern Bull Kelp (*Durvillaea antarctica*) to recolonise the Southern Ocean after the Last Glacial Maximum (Fraser et al. 2009b). Wind and water connectivity between hemispheres is hampered by the Intertropical Convergent Zone (Wilkinson et al. 2012), hence transportation of *Mastodia* diaspores from the Southern into the Northern Hemisphere could be alternatively achieved via migratory birds. For example, the migration route and breeding colonies of the sooty shearwater (*Ardenna grisea*, *Procellariidae*) match to a great extent the current geographic distribution of bipolar *Mastodia* (BirdLife International 2015). In fact, this lichen is highly ornitocoprophilic (Kohlmeyer et al. 2004), which could facilitate that either sexual or asexual spores, both abundantly produced in most thalli, or even thallus fragments could

adhere to bird plumage or feet, and then carried along thousands of kilometres. Lewis et al. (2014b) found moss diaspores in feathers of trans-equatorial migrant shorebirds, and endozoochory has been also proven recently in other birds (Viana et al. 2016). The high similarity in genetic structure and age estimates of both symbionts (Figure 1,3; Garrido-Benavent et al. 2017) suggests that migration involved thallus fragments including fungal and algal cells.

4.4. A Northern Hemisphere photobiont switch

The assumption that lichen-forming fungi can associate with divergent photobionts across their geographic distribution is now well-accepted (Piercey-Normore & DePriest 2001; Yahr et al. 2006; Wornik & Grube 2010). Our phylogenetic results (Supplementary Figure 4–5) corroborate earlier reports of *M. tessellata* s.l. being associated with *P. delicata* in North American Pacific coasts (Moniz et al. 2014). In our case, horizontal acquisition of photobiont strains is likely to result from lichenization of germinated fungal meiospores. During this process, regional differences in photobiont availability (Fernandez-Mendoza 2013) and differences in the adaptation of algal lineages to local environmental conditions (e.g. Piercey-Normore & DePriest 2001; Yahr et al. 2006) may result in strongly contrasting regional patterns. The distributional ranges of lichenized *P. borealis* and *P. delicata*, as well as the non-lichenized *P. linearis* and *P. meridionalis* show a significant overlap in the Northern Pacific coast (Rindi et al. 2007, and references therein). Our calibrated *rbcL* and *tufA* phylogenies also suggest a long-term evolution of a clade containing *P. delicata* in the Northern Hemisphere (Supplementary Figure 4–5). These observations together with the fact that mycobiont haplotypes were shared between both lichenized *Prasiola*, points to *Mastodia* sp. 1 switching from *P. borealis* to *P. delicata* after the arrival of the former to North America in the Pleistocene (discussed above). In fact, switching to a locally adapted photobiont has been advocated to facilitate thriving in new environments, and drive mycobiont evolution (Fernández-Mendoza et al. 2011; Magain et al. 2016).

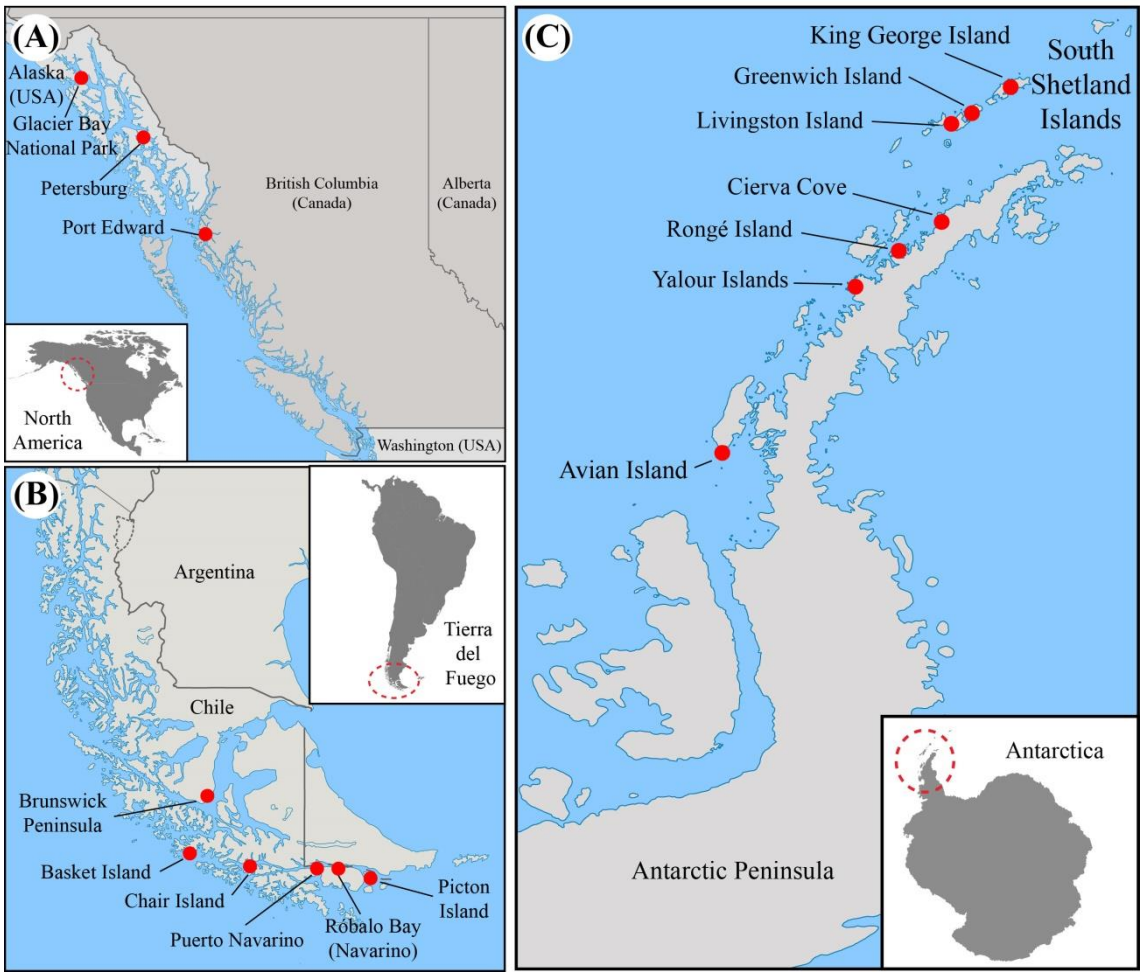

Supplementary Figure 1. Map of sampling localities for *Mastodia tessellata* s.l. (A) North America –3 localities. (B) Tierra del Fuego (Chile) –6 localities. (C) Antarctica –7 localities.

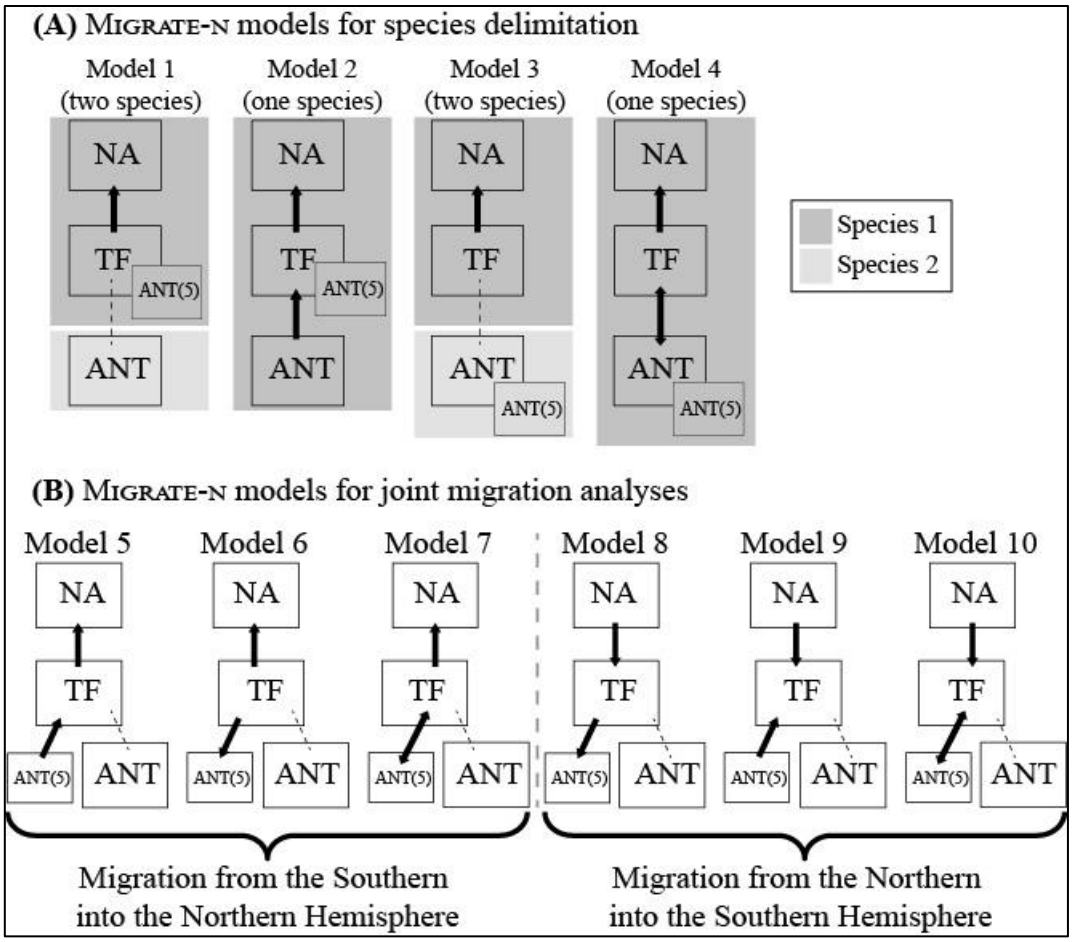

Supplementary Figure 2. Species delimitation and migration models tested in MIGRATE-N analyses. Migration models used for (A) species delimitation and (B) joint migration analyses of *Mastodia tessellata* s.l. myco- and photobionts in MIGRATE-N. (A) Separate species are highlighted in different shades of grey. The five genetically-distinct Antarctic individuals ("ANT(5)") were included within either Tierra del Fuego (Models 1,2) or the remaining Antarctic (Models 3,4) population. In (A) and (B) populations connected by a black arrow (representing gene flow) belong to a single species (namely Species 1, Species 2). Dashed lines represent absence of gene flow between populations and are used to highlight the existence of separate species. NA: North America; TF: Tierra del Fuego; ANT: Antarctica.

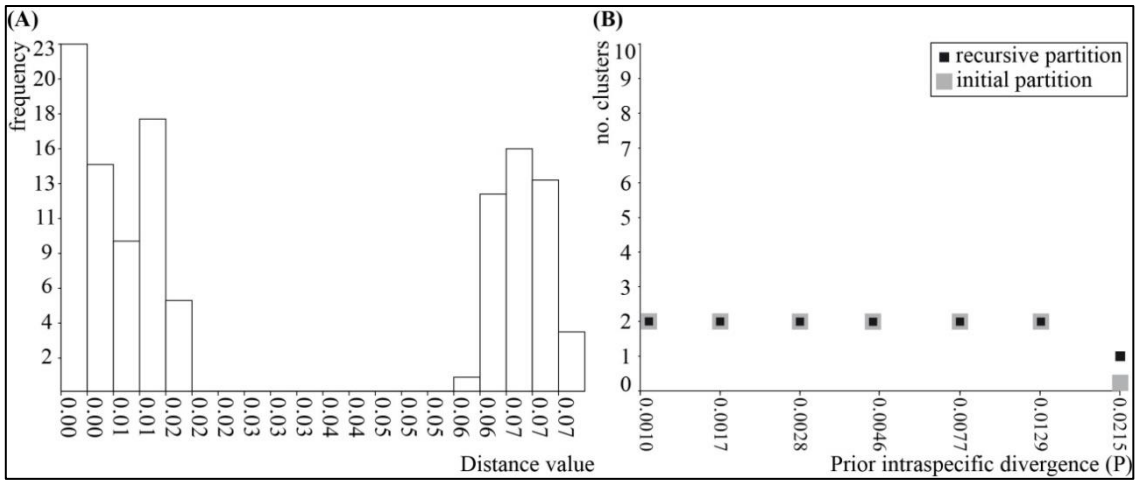

Supplementary Figure 3. ABGD analysis output. (A) Histogram showing the distribution of pairwise genetic distances (Kimura 2-parameter) among all sequences and the major barcode gap. (B) Plot showing how different values of "prior intraspecific genetic divergences" affect the number of clusters or hypothetical species recovered by the ABGD method. Note that recursive partitions are obtained by allowing the threshold to vary among species.

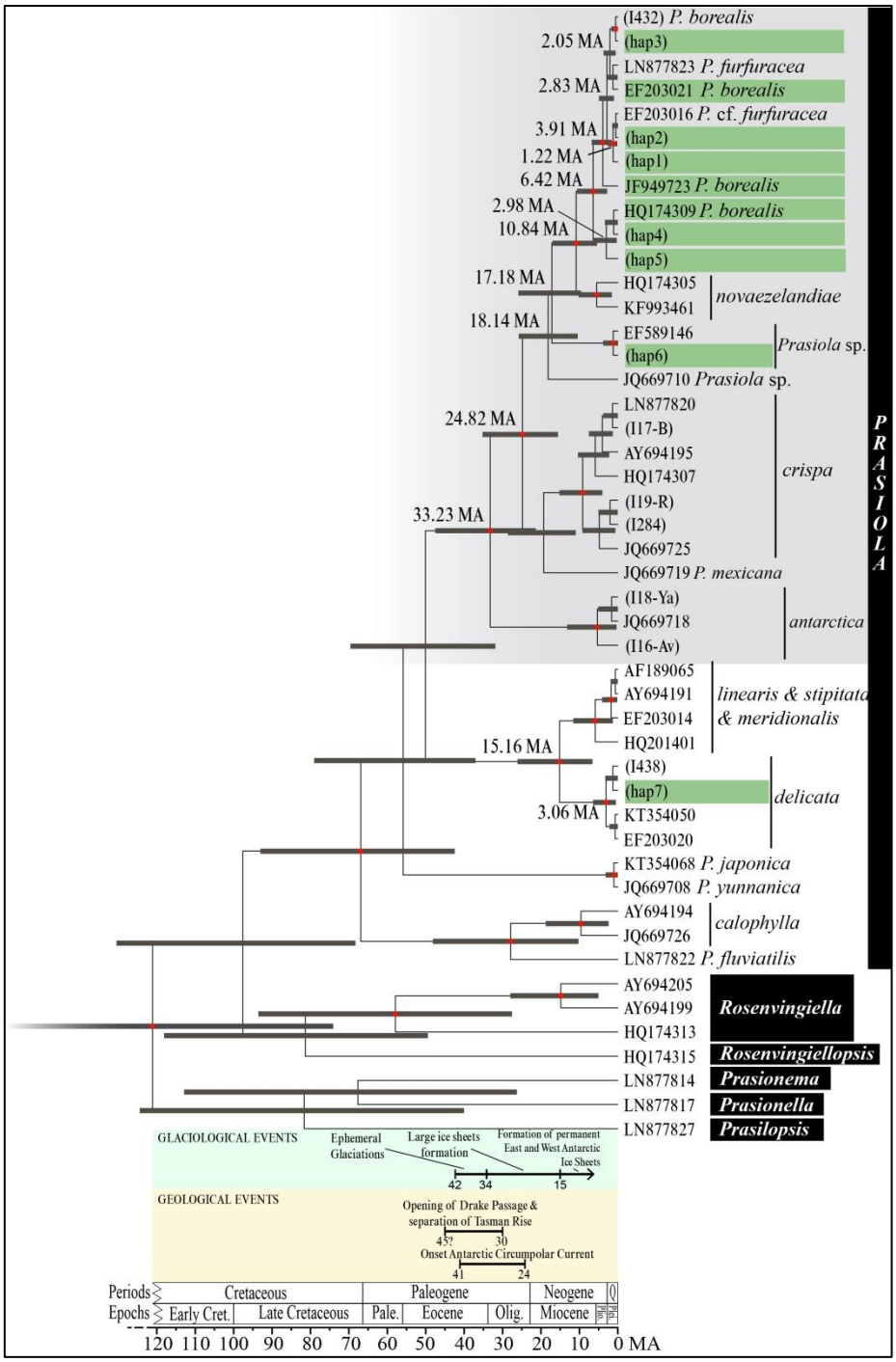

Supplementary Figure 4. Chronogram (maximum clade credibility tree) inferred in BEAST from *rbcL* data of selected *Prasiolaceae* members, including most *Prasiola* species. GENBANK accession numbers are indicated for each tip node. Lichenized accessions are highlighted in green. The shaded clade includes most Southern Hemisphere representatives of *Prasiola*. Bars show the 95% Highest Posterior Density (HPD) intervals for age estimates. Red dots on nodes represent significant statistical support obtained with BEAST (PP ≥ 0.95). Setting of glaciological, geological and oceanographic events follow Convey et al. (2008), Lear & Lunt (2016) and Scher et al. (2015). MA: million years ago.

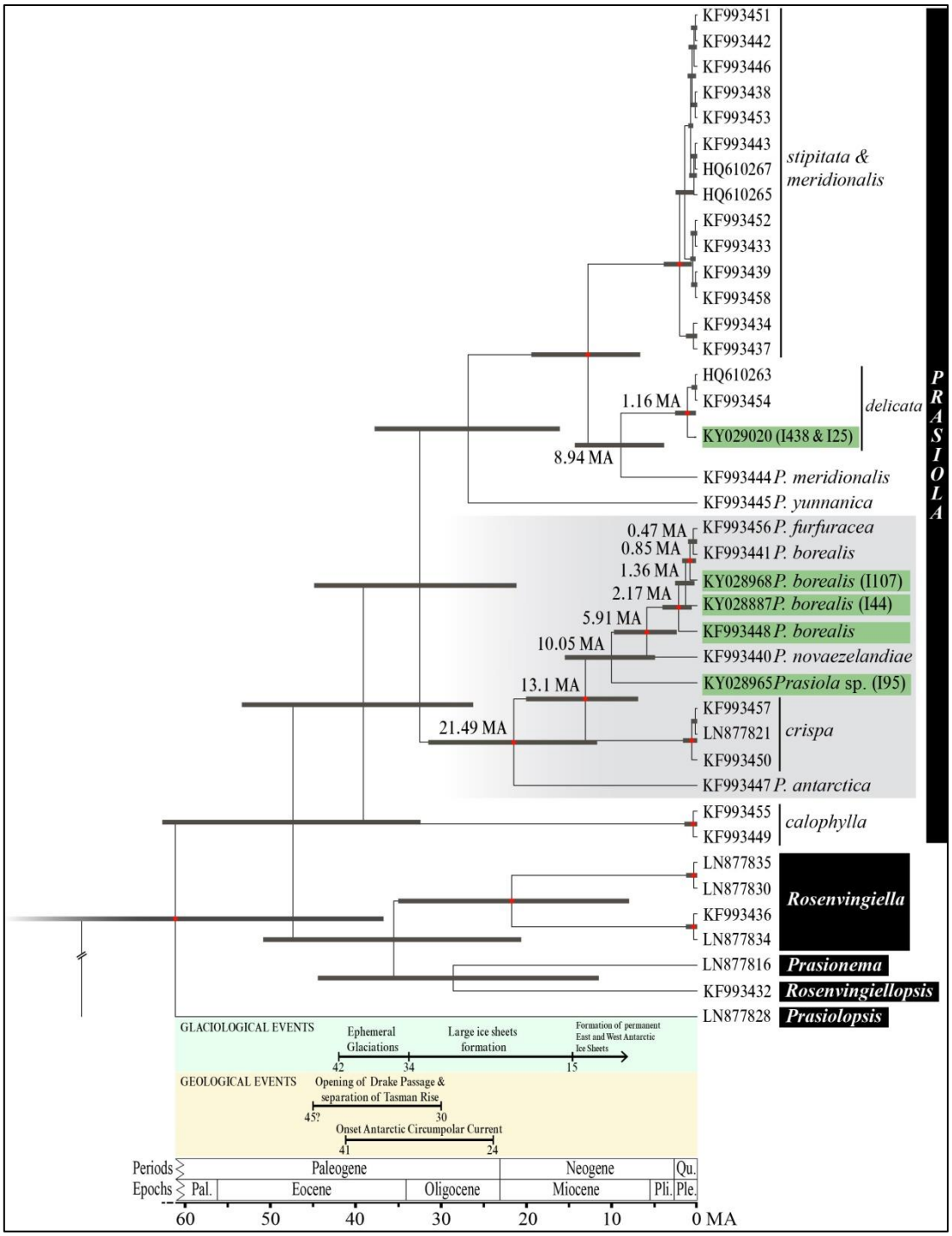

Supplementary Figure 5. Chronogram (maximum clade credibility tree) inferred in BEAST from *tufA* data of selected *Prasiolaceae* members, including most *Prasiola* species. GENBANK accession numbers are indicated for each tip node. Lichenized accessions are highlighted in green. The shaded clade includes most Southern Hemisphere representatives of *Prasiola*. Bars show the 95% Highest Posterior Density (HPD) intervals for age estimates. Red dots on nodes represent significant statistical support obtained with BEAST (PP ≥ 0.95). Setting of glaciological, geological and oceanographic events follow Convey et al. (2008), Lear & Lunt (2016) and Scher et al. (2015). MA: million years ago.

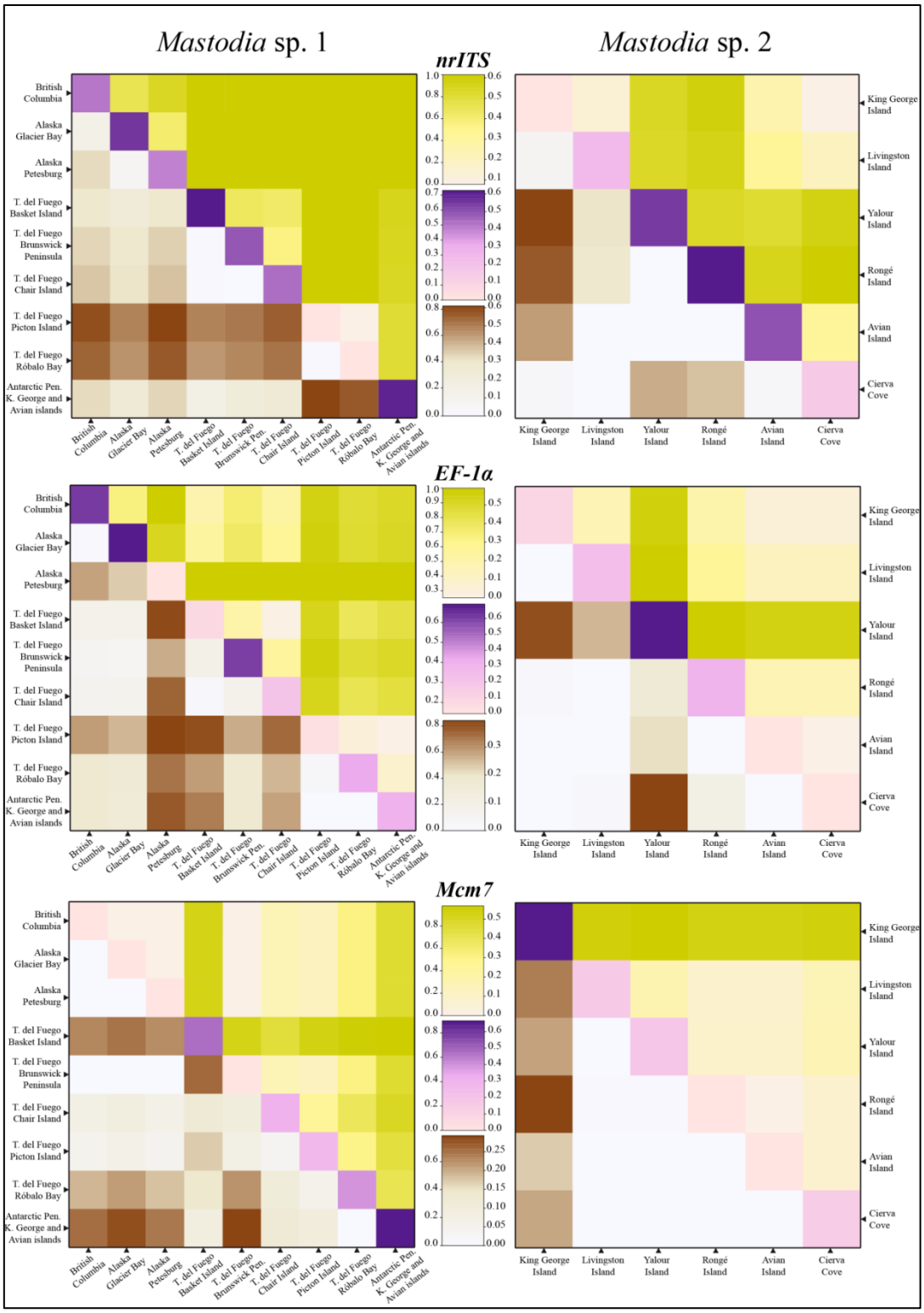

Supplementary Figure 6. Genetic divergence and differentiation in *Mastodia tessellata* s.l. mycobionts. Genetic divergence (Dxy, above diagonal, golden shades), genetic differentiation (Fst, below diagonal, brown shades), and within group genetic diversity (π, diagonal, purple shades) between sampling localities in each mycobiont species based on *nrITS*, *EF-1α* and *Mcm7* data. Scales on left- and right-hand sides of central bars correspond to graphs on left and right, respectively.

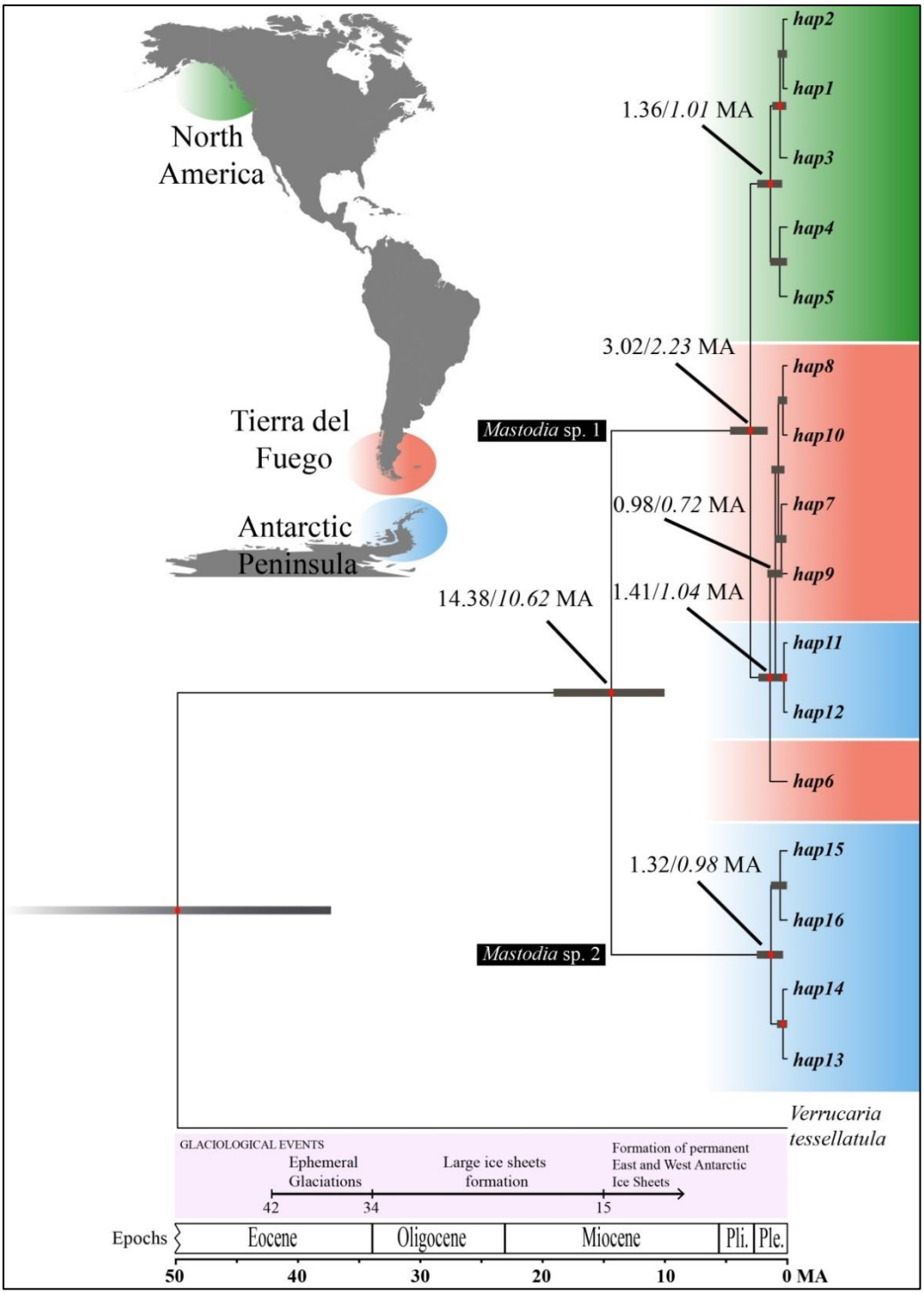

Supplementary Figure 7. Time-calibrated maximum clade credibility (MCC) tree estimated from the *nrITS* haplotype dataset of *Mastodia tessellata* s.l. mycobionts. The geographical origin of haplotypes is highlighted with different colours (see map). Age estimates for selected nodes were obtained using an *Erysiphales* (Takamatsu & Matsuda 2004) (on the left) or a *Melanohalea* (Leavitt et al. 2012b) (on the right, in italics) *nrITS* substitution rate. Bars show the 95% Highest Posterior Density (HPD) intervals for age estimates. Red dots on nodes represent significant statistical support obtained with BEAST (PP ≥ 0.95). Setting of glaciological events follows Convey et al. (2008). MA: million years ago.

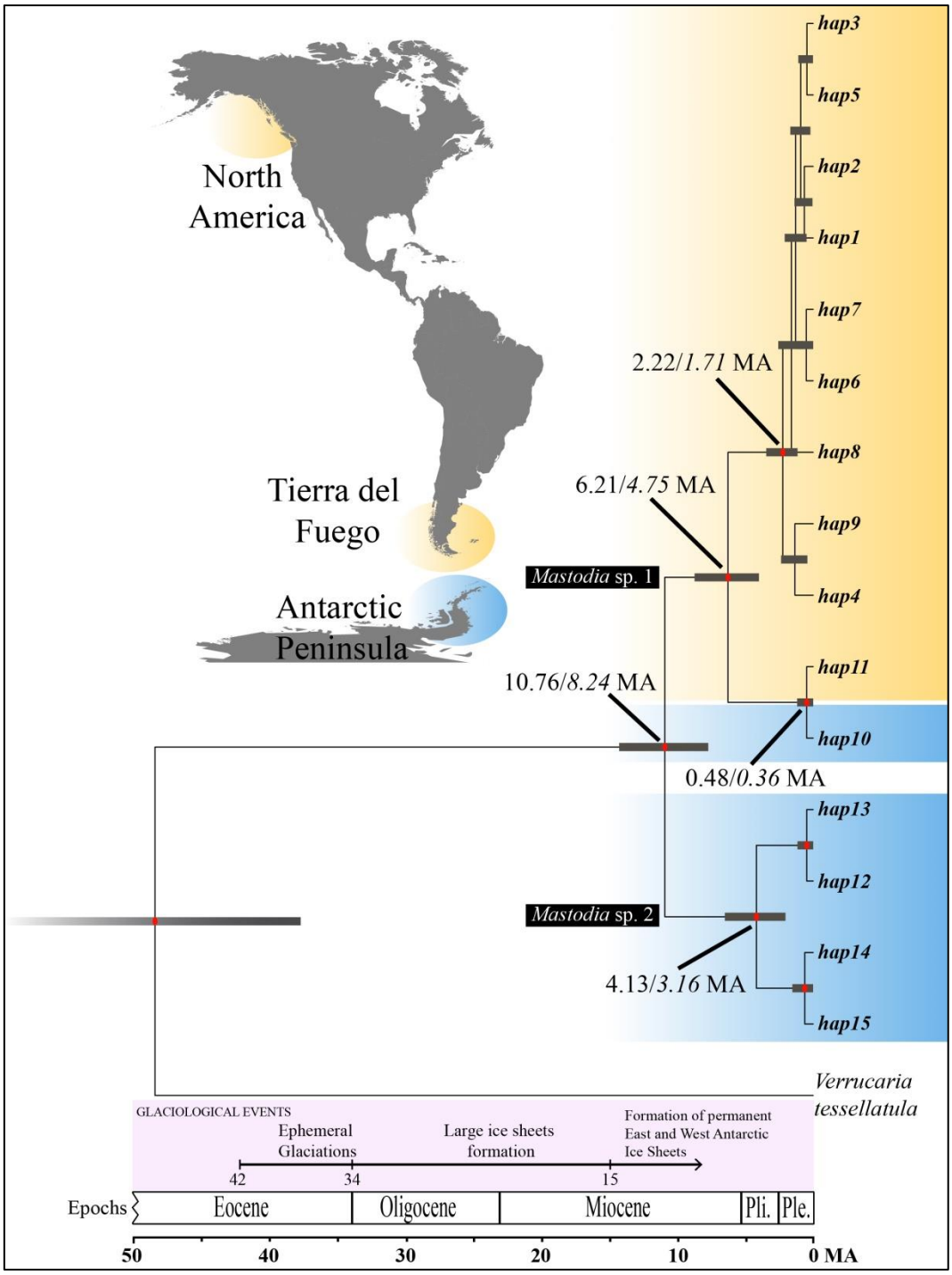

Supplementary Figure 8. Time-calibrated maximum clade credibility (MCC) tree estimated from the *EF-1α* haplotype dataset of *Mastodia tessellata* s.l. mycobionts. The geographical origin of haplotypes is highlighted with different colours (see map). Age estimates for selected nodes were obtained using co-estimated *EF-1α* substitution rates from analysis using an *Erysiphales* (Takamatsu & Matsuda 2004) (on the left), or a *Melanohalea* (Leavitt et al. 2012b) *nrITS* substitution rate (on the right, in italics). Bars show the 95% Highest Posterior Density (HPD) intervals for age estimates. Red dots on nodes represent significant statistical support obtained with BEAST (PP ≥ 0.95). Setting of glaciological events follows Convey et al. (2008). MA: million years ago.

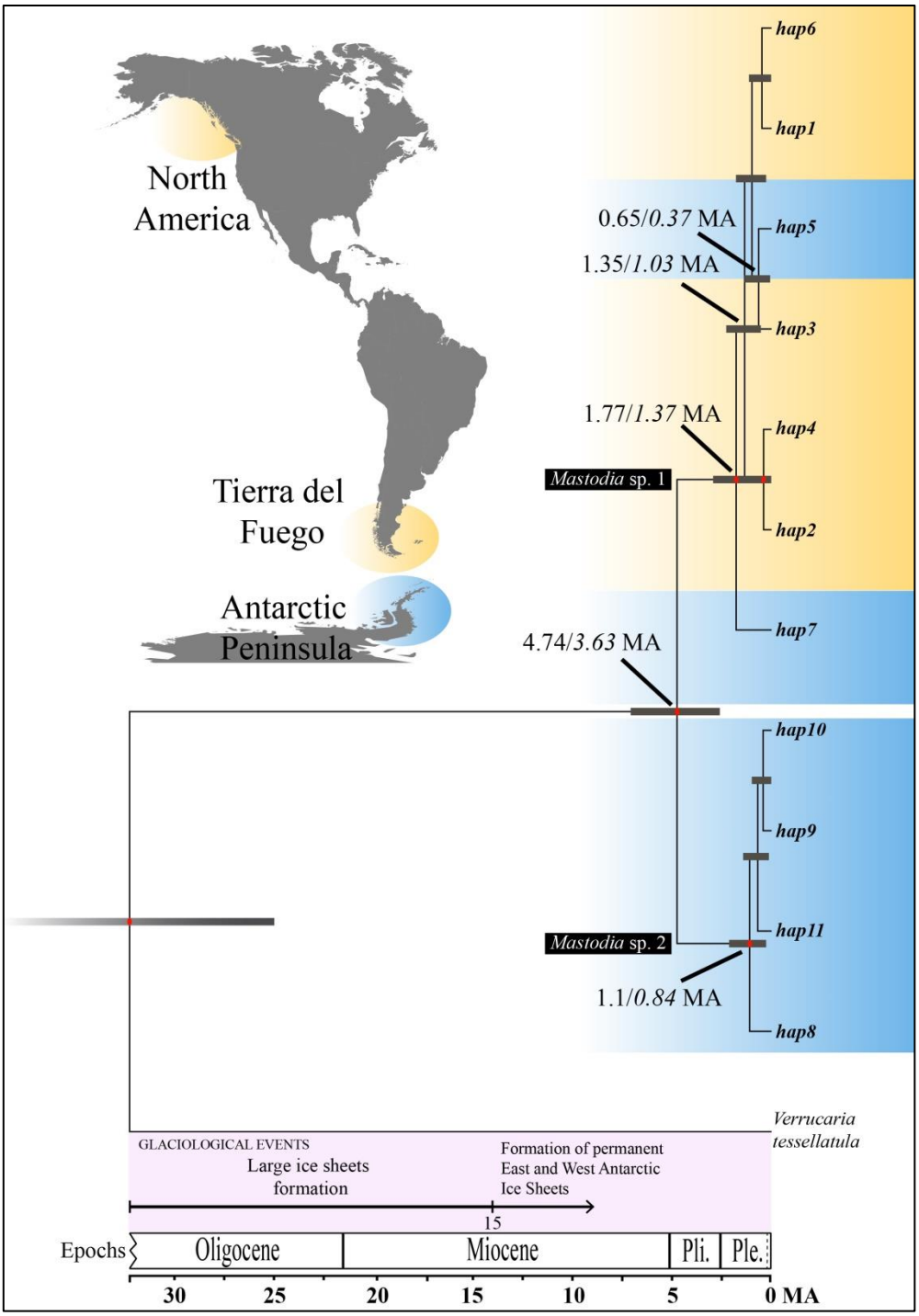

Supplementary Figure 9. Time-calibrated maximum clade credibility (MCC) tree estimated from the *Mcm7* haplotype dataset of *Mastodia tessellata* s.l. mycobionts. The geographical origin of haplotypes is highlighted with different colours (see map). Age estimates for selected nodes were obtained using co-estimated *Mcm7* substitution rates from analysis using an *Erysiphales* (Takamatsu & Matsuda 2004) (on the left), or a *Melanohalea* (Leavitt et al. 2012b) *nrITS* substitution rate (on the right, in italics). Bars show the 95% Highest Posterior Density (HPD) intervals for age estimates. Red dots on nodes represent significant statistical support obtained with BEAST (PP ≥ 0.95). Setting of glaciological events follows Convey et al. (2008). MA: million years ago.

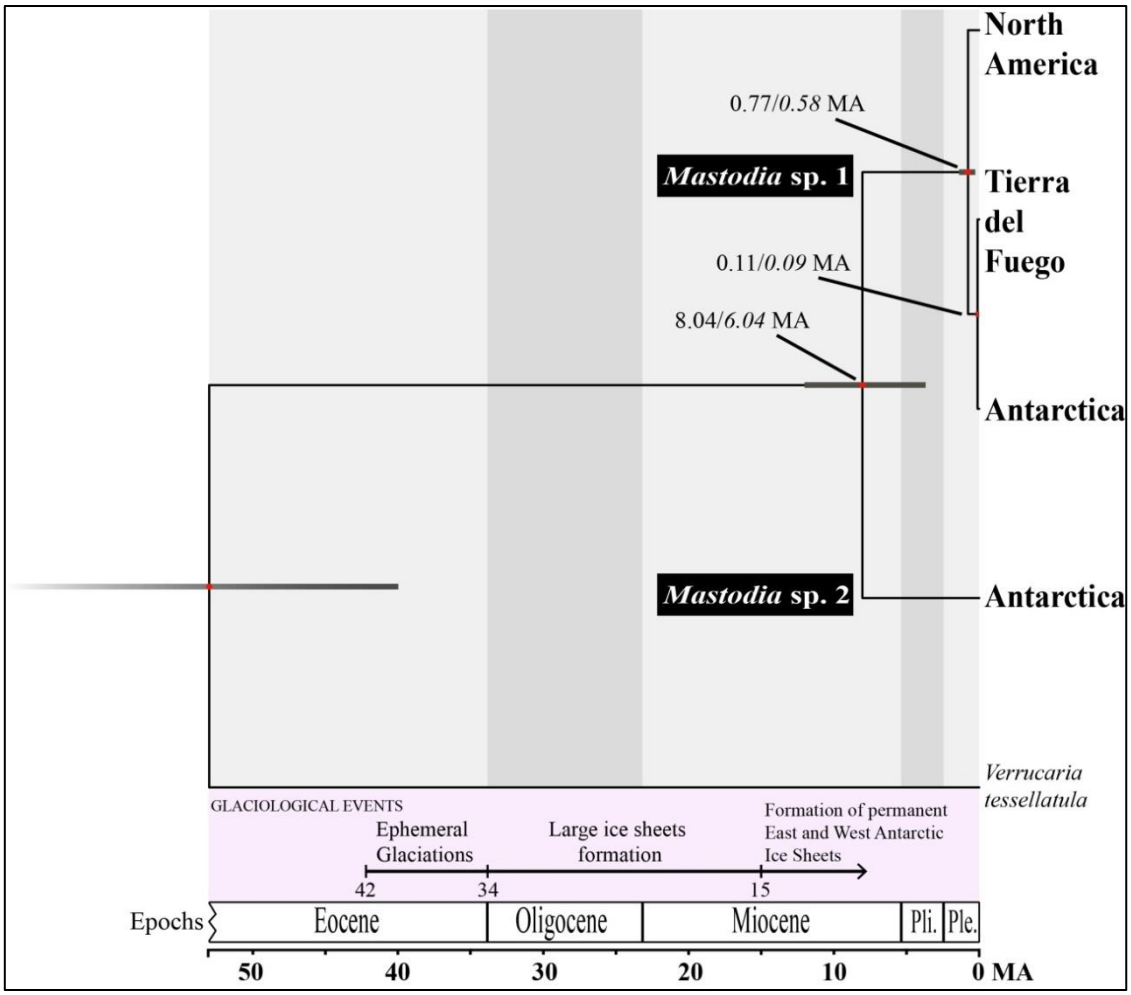

Supplementary Figure 10. Chronogram of *Mastodia tessellata* s.l. mycobionts using multi-locus data and the *BEAST population/species tree reconstruction method. Time-calibrated maximum clade credibility (MCC) tree and 95% Highest Posterior Density (HPD) age intervals (grey bars) inferred from *nrITS*, *EF-1α* and *Mcm7* using *BEAST population/species tree reconstruction method for *Mastodia tessellata* s.l. mycobionts. Age estimates for selected nodes were obtained using an *Erysiphales* (Takamatsu & Matsuda 2004) (on the left) or a *Melanohalea* (Leavitt et al. 2012b) (on the right, in italics) *nrITS* substitution rate. Red dots on nodes represent significant statistical support obtained with *BEAST (PP ≥ 0.95). Setting of glaciological events follows Convey et al. (2008). MA: million years ago.

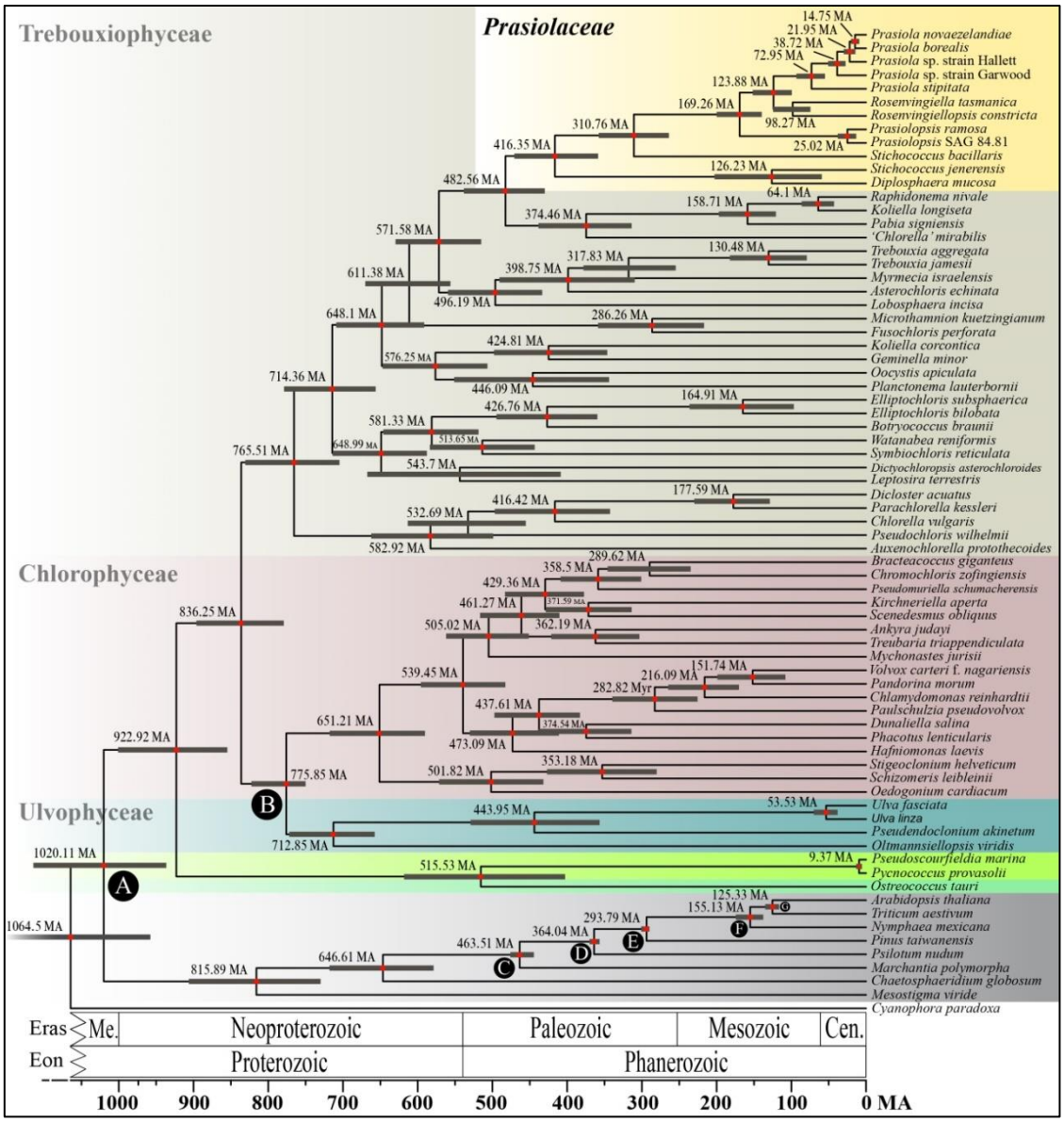

Supplementary Figure 11. Divergence times estimates in Viridiplantae including species of *Prasiola*. Five-locus maximum clade credibility (MCC) inferred in BEAST depicting phylogenetic relationships and divergence times estimates in Viridiplantae, including species of *Prasiola*. Classes *Ulvophyceae*, *Chlorophyceae* and *Trebouxiophyceae*, and family *Prasiolaceae* are indicated and highlighted in different colours. Class adscription of taxa follow AlgaeBase (Guiry & Guiry 2016). Bars show the 95% Highest Posterior Density (HPD) intervals for age estimates. Red dots on nodes represent significant statistical support obtained with BEAST (PP ≥ 0.95). Letters in circles indicate the nodes used for calibration (see Supplementary Table 6 for further information). MA: million years ago.

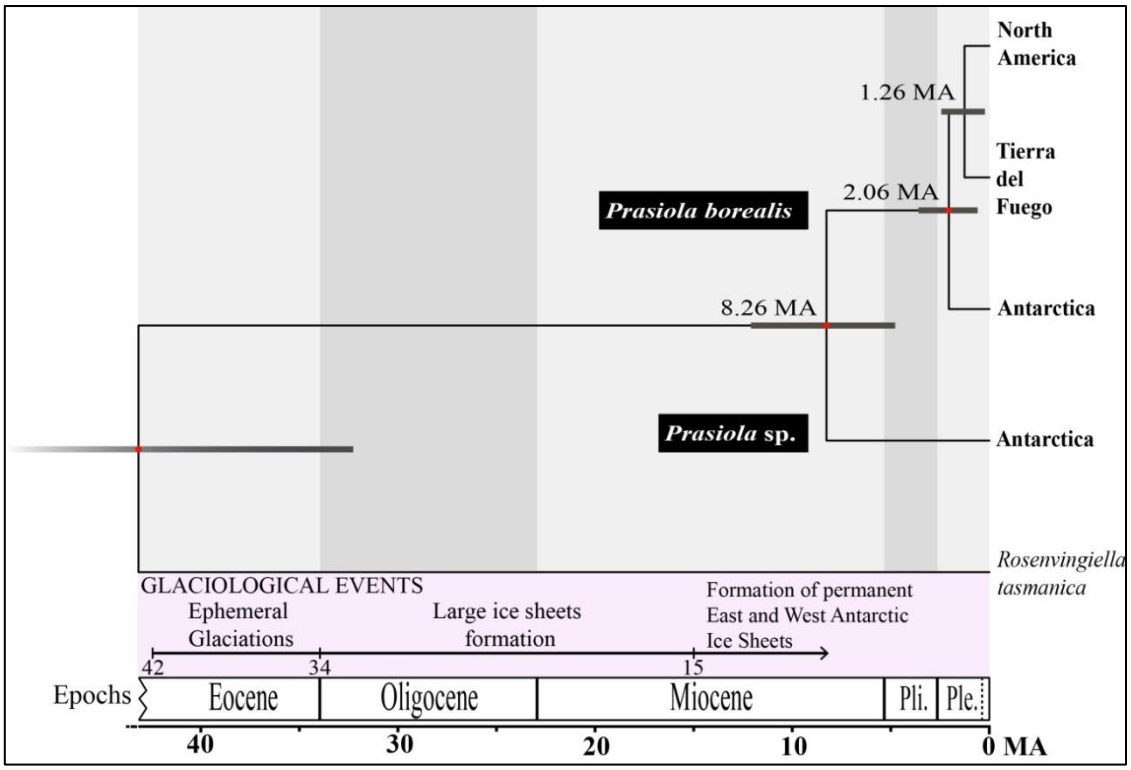

Supplementary Figure 12. Divergence times estimates for *Mastodia tessellata* s.l. photobionts inferred from a two-locus (*tufA*, *rbcL*) dataset. Time-calibrated maximum clade credibility (MCC) tree and 95% Highest Posterior Density (HPD) age intervals (grey bars) inferred from a two-locus (*tufA*, *rbcL*) dataset using *BEAST population/species tree reconstruction method for *Mastodia tessellata* s.l. photobionts. Red dots on nodes represent significant statistical support obtained with *BEAST (PP ≥ 0.95). Setting of glaciological events follows Convey et al. (2008). MA: million years ago.

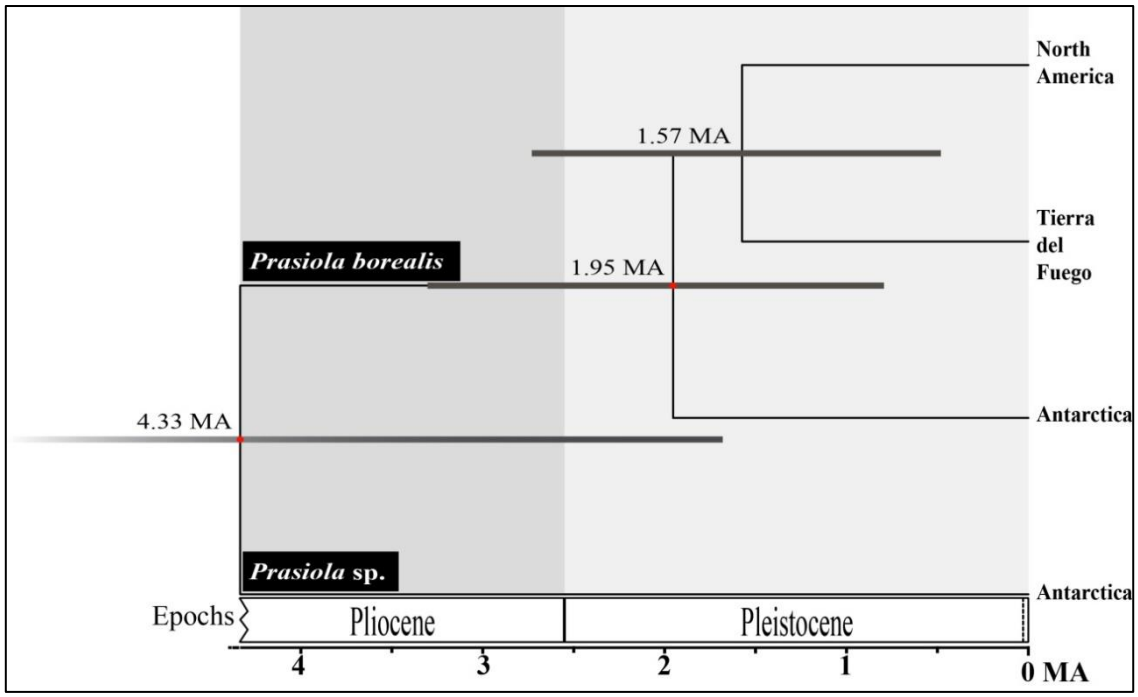

Supplementary Figure 13. Divergence times estimates for *Mastodia tessellata* s.l. photobionts inferred from a four-locus (*tufA*, *rbcL*, *nrITS*, *RPL10A*) dataset. Time-calibrated maximum clade credibility (MCC) tree and 95% Highest Posterior Density (HPD) age intervals (grey bars) inferred from a four-locus (*tufA*, *rbcL*, *nrITS*, *RPL10A*) dataset using *BEAST population/species tree reconstruction method for *Mastodia tessellata* s.l. photobionts. Red dots on nodes represent significant statistical support obtained with *BEAST (PP ≥ 0.95). MA: million years ago.

Supplementary Table 1. Loci and primers used in the current study for each biont. Primers designed for the present work are highlighted in bold.

	Locus	Primer name	Orientation (F/R)	Primer sequence (5'–3')	Reference
Mycobiont	*nrITS*	ITS1-LM	F	GAACCTGCGGAAGGATCATT	Myllys et al. (1999)
		ITS-Mast-F	**F**	**TAACAAGGTTTCCGTAGGTG**	**This study**
		ITS4	R	TCCTCCGCTTATTGATATGC	White et al. (1990)
	EF-1α	EFA-F	F	RGACAAGRCTCACATCAACGTSGT	Johannesson et al. (2000)
		EFA1-Mast	**F**	**CGACTCCGGCAAATCTACCA**	**This study**
		EFA-R	R	CCAGTRATCATGTTCTTGATGAART	Johannesson et al. (2000)
		EFA2-Mast	**R**	**TGAAGTCACGATGTCCTGGG**	**This study**
	Mcm7	Mcm7-709for	F	ACIMGIGTITCVGAYGTHAARCC	Schmitt et al. (2009)
		Mcm7-MastF	**F**	**GTGTTGGAGATCAACGCATTC**	**This study**
		Mcm7-1348rev	R	GAYTTDGCIACICCIGGRTCWCCCAT	Schmitt et al. (2009)
		Mcm7-MastR	**R**	**AGGTTGATATCGCCTCTGATT**	**This study**
Photobiont	*nrITS*	nr-SSU-1780-5' Algal	F	CTGCGGAAGGATCATTGATTC	Piercey-Normore & DePriest (2001)
		ITSpras1F	F	TCTATCAACAACCCCACAGC	Garrido-Benavent et al. (2017)
		ITS4T	R	GGTTCGCTCGCCGCTACTA	Kroken & Taylor (2000)
		ITSprasR1	R	GGTTAGTTTCTTTTCCTCCGC	Garrido-Benavent et al. (2017)
	rbcL	**rbcL-pras-F**	**F**	**GATATTGAACCAGTTGCAGG**	**This study**
		rbcL-pras-R	**R**	**GTCACGCATTAAATCAACGA**	**This study**
	RPL10A	L10a-F	F	GCTNAACAAGAACAAGAAGC	del Campo et al. (2013)
		rpl10aF-1pras	F	CAGCTAAGAAATATGCGGCT	Garrido-Benavent et al. (2017)
		L10aR	R	SACGTTCTGCCAGTTCTTCTT	del Campo et al. (2013)
		rpl10aR-1pras	R	ATAGACGCCTTGATGTCATT	Garrido-Benavent et al. (2017)
	tufA	tufAF	F	TGAAACAGAAMAWCGTCATTATGC	Famà et al. (2002)
		tufAF-pras	F	GGTTCGCCGGAAATACAAT	Garrido-Benavent et al. (2017)
		tufAR	R	CCTTCNCGAATMGCRAAWCGC	Famà et al. (2002)
		tufAR-pras	R	CAGTAACATCAGTTGTTCG	Garrido-Benavent et al. (2017)

Supplementary Table 2. PCR settings.

	Marker	PCR round	Primer pair (F/R)	PCR protocol
Mycobiont	*nrITS*	n/a	ITS1LM or ITS-MastF/ITS4	95 °C (5 min), 35 cycles of 95 °C (30 s) + 56 °C (1 min) + 72 °C (1 min 30 s), 72 °C (10 min), 4 °C (∞)
	EF-1α	1st	EFA1/EFA2	94 °C (8 min), 6 cycles of 94 °C (50 s) + 60 °C (50 s, touchdown -1 °C per cycle) + 72 °C (1 min 30 s), 32 cycles of 94 °C (50 s) + 54 °C (50 s) + 72 °C (1 min 30 s), 72 °C (10 min), 4 °C (∞)
		2nd (nested)	EFA1-Mast/EFA2-Mast	
	Mcm7	1st	Mcm7-709for/Mcm7-1384rev	95 °C (10 min), 6 cycles of 95 °C (45 s) + 58 °C (50 s, touchdown -1 °C per cycle) + 72 °C (1 min), 32 cycles of 95 °C (45 s) + 52 °C (50 s) + 72 °C (1 min), 72 °C (5 min), 4 °C (∞)
		2nd (nested)	MCM7-MastF/MCM7-MastR	
Photobiont	*nrITS*	1st	nr-SSU-1780-5' Algal/ITS4T	95 °C (5 min), 35 cycles of 95 °C (20 s) + 55 °C (25 s) + 72 °C (25 s), 72 °C (15 s), 4 °C (∞)
		2nd (nested)	ITSpras1F/ITSprasR1	95 °C (5 min), 35 cycles of 95 °C (30 s) + 57 °C (1 min) + 72 °C (1 min 30 s), 72 °C (10 min), 4 °C (∞)
	rbcL	n/a	rbcL-pras-F/rbcL-pras-R	95 °C (5 min), 35 cycles of 95 °C (25 s) + 53 °C (26 s) + 72 °C (30 s), 72 °C (15 s), 4 °C (∞)
	RPL10A	1st	L10a-F/L10a-R	95 °C (5 min), 40 cycles of 95 °C (25 s) + 55 °C (30 s) + 72 °C (32 s), 72 °C (15 s), 4 °C (∞)
		2nd (nested)	rpl10aF-1pras/rpl10aR-1pras	94 °C (2 min), 35 cycles of 94 °C (30 s) + 55 °C (30 s) + 72 °C (1 min), 72 °C (7 min), 4 °C (∞)
	tufA	1st	tufAF/tufAR	94 °C (4 min), 34 cycles of 94 °C (30 s) + 52 °C (1 min) + 72 °C (1 min 30 s), 72 °C (5 min), 4 °C (∞)
		2nd (nested)	tufAF-pras/tufAR-pras	

Supplementary Table 3. PCR reactions.

	Mycobiont (*nrITS*, *EF-1α*, *Mcm7)*	Photobiont (*rbcL*)
Template	3–5 µl DNA, or 1 µl first reaction (nested protocol)	4 µl DNA
Primer (10 µM)	1.25 µl (*nrITS*) 2.5 µl (*EF-1α*, *Mcm7*)	1.25 µl
Reaction buffer (Biotools®)	2.5 µl	n/a
dNTPs (1 mM)	5 µl	n/a
$MgCl_2$ (50 mM)	1 µl	n/a
DNA polymerase	0.5 U (Biotools®)	10 µl DNA AmpliTools Fast Master Mix (2x) (Biotools®)
Sterile, filtered water (Sigma®)	Variable	3.5 µl
Total reaction Volume	25 µl	20 µl

Supplementary Table 4.Test for strict molecular clock for each mycobiont locus conducted in MEGA v.5.2. Tested under two different topologies (ML and Bayesian). *denotes rejection of the null hypothesis (i.e. equal rates).

	ML estimate				MrBayes consensus			
nrITS [GTR+Γ]	ln*L*	Param	(+Γ)	(+I)	ln*L*	Param	(+Γ)	(+I)
With Clock	-1479.830	25	0.512	n/a	-1475.876	25	0.55	n/a
Without Clock	-1460.783	40	0.54	n/a	-1460.553	40	0.59	n/a
P (Ho: = rates)		0.147				0.433		
EF-1α [SYM]	ln*L*	Param	(+Γ)	(+I)	ln*L*	Param	(+Γ)	(+I)
With Clock	-1367.705	23	n/a	n/a	-1369.046	23	n/a	n/a
Without Clock	-1357.737	37	n/a	n/a	-1357.74	37	n/a	n/a
P (Ho: = rates)		0.867				0.752		
Mcm7 [GTR+I]	ln*L*	Param	(+Γ)	(+I)	ln*L*	Param	(+Γ)	(+I)
With Clock	-1230.675	20	n/a	0.13	-1228.976	20	n/a	0.17
Without Clock	-1226.185	30	n/a	0.13	-1226.004	30	n/a	0.17
P (Ho: = rates)		0.983				0.999		

Supplementary Table 5. Co-estimated *EF-1α* and *Mcm7* substitution rates from two analyses using different *nrITS* substitution rates. MA: million years ago.

	Erysiphales[a]	*Melanohalea*[b]
EF-1α	2.69×10^{-3} s/s/MA	3.515×10^{-3} s/s/MA
Mcm7	2.149×10^{-3} s/s/MA	2.803×10^{-3} s/s/MA

[a] 2.52×10^{-3} s/s/MA (Takamatsu & Matsuda 2004); [b] 3.41×10^{-3} s/s/MA (Leavitt et al. 2012b).

Supplementary Table 6. Calibrations used in the first-step photobiont BEAST dating analysis (Viridiplantae dataset). MA: million years ago.

Calibration		Evidence	Age (MA)	Geological Time	Prior distribution and settings	References
A	Split Streptophyta and Chlorophyta	Secondary calibration-Age estimates from previous studies	700–1500	Proterozoic	Uniform (initial = 1100, upper = 1500, lower = 700)	Hedges et al. (2004); Zimmer et al. (2007); De Wever et al. (2009)
B	Split *Ulvophyceae* and *Chlorophyceae*	*Proterocladus* fossil	750	Proterozoic	Exponential (initial = 750, mean = 30, offset = 750)	Butterfield et al. (1994); Herron et al. (2009)
C	Rise of land plants	First appearance of spore tetrads	432–476	Silurian-Ordovician	Uniform (initial = 454, upper = 476, lower = 432)	Kenrick & Crane (1997)
D	Emergence of Spermatophyta	Oldest known seeds	355–370	Devonian	Uniform (initial = 362, upper = 370, lower = 355)	Gillespie et al. (1981)
E	Split Angiosperms-Gymnosperms	Secondary calibration based on fossils used in previous studies	290–320	Carboniferous	Uniform (initial = 305, upper = 320, lower = 290)	Soltis et al. (2002)
F	*Nymphaeales* divergence	Earliest known fossil of *Nymphaeales*	115	Cretaceous	Exponential (initial = 115, mean = 30, offset = 115)	Friis et al. (2001)
G	Split Eudicots-Monocots	Appearance of tricolpate pollen	90–130	Cretaceous	Normal (initial = 125, mean = 125, stdev = 5)	Crane et al. (1995)

Supplementary Table 7. Test for strict molecular clock for each locus used in the photobiont first-step dating and conducted in MEGA v.5.2. Tested under two different topologies (ML and Bayesian). *denotes rejection of the null hypothesis (i.e. equal rates).

	ML estimate				MrBayes consensus			
18S GTR+I+Γ	ln*L*	Param	(+Γ)	(+I)	ln*L*	Param	(+Γ)	(+I)
With Clock	-13478.613	63	0.582	0.45	-13475.629	63	0.623	0.59
Without Clock	-13250.114	115	0.54	0.47	-13143.606	115	0.56	0.47
P (Ho: = rates)	9.7e-46*				1.8e-82*			
atpB GTR+I+Γ	ln*L*	Param	(+Γ)	(+I)	ln*L*	Param	(+Γ)	(+I)
With Clock	-36483.532	70	1.080	0.40	-36390.457	70	0.976	0.40
Without Clock	-36094.537	129	1.09	0.38	-35849.127	129	0.98	0.37
P (Ho: = rates)	9.5e-98*				1.3e-155*			
psaB GTR+I+Γ	ln*L*	Param	(+Γ)	(+I)	ln*L*	Param	(+Γ)	(+I)
With Clock	-54092.377	74	1.013	0.43	-53755.644	74	0.865	0.40
Without Clock	-53557.039	137	1.00	0.40	-53300.876	137	0.87	0.39
P (Ho: = rates)	1.7e-149*				7.01e-119*			
rbcL GTR+I+Γ	ln*L*	Param	(+Γ)	(+I)	ln*L*	Param	(+Γ)	(+I)
With Clock	-32007.229	82	1.201	0.47	-32007.229	82	1.201	0.47
Without Clock	-31802.035	153	1.26	0.44	-31802.035	153	1.26	0.44
P (Ho: = rates)	6.9e-28*				6.89e-28*			
tufA GTR+I+Γ	ln*L*	Param	(+Γ)	(+I)	ln*L*	Param	(+Γ)	(+I)
With Clock	-27905.824	63	1.066	0.36	-28000.889	63	1.006	0.34
Without Clock	-27739.503	115	1.03	0.35	-278000.47	115	1.00	0.35
P (Ho: = rates)	1.0e-25*				1.98e-36*			

Supplementary Table 8. Inferred substitution rates for selected markers from first- and second-step photobiont dating analyses. First column are overall mean values obtained in the first-step analysis, while values in the second column correspond with mean substitution rates drawn specifically from *Prasiolaceae* (first-step analysis). Rates used in *tufA* and *rbcL* single-locus dating analyses are in bold. MA: million years ago.

Marker (location)	Overall mean rate	*Prasiolaceae* mean rate
18S (nuclear)	9.416×10^{-5} s/s/MA	5.05×10^{-5} s/s/MA
tufA (plastidial)	1.109×10^{-3} s/s/MA	**1.28×10^{-3} s/s/MA**
rbcL (plastidial)	6.078×10^{-4} s/s/MA	**9.57×10^{-4} s/s/MA**
atpB (plastidial)	1.208×10^{-3} s/s/MA	1.54×10^{-3} s/s/MA
psaB (plastidial)	1.1×10^{-3} s/s/MA	1.33×10^{-3} s/s/MA

Supplementary Table 9. Substitution models used in myco- and photobiont species delimitation analyses. Superscript numbers within parentheses indicate the best partition scheme found in PARTITIONFINDER and implemented in BEAST or *BEAST analyses.

	Dataset (un-/rooted)	Alignment length (bp)	Partition	Inferred model
Mycobiont	*nrITS* (unrooted)	580	n/a	GTR
	nrITS (rooted)	589	n/a	GTR+Γ
	EF-1α (unrooted)	525	intron	TrNef$^{(1)}$
			exon (1st cod. pos.)	K80$^{(2)}$
			exon (2nd cod. pos.)	K80$^{(2)}$
			exon (3rd cod. pos.)	K80$^{(2)}$
	EF-1α (rooted)	535	intron	TrNef$^{(1)}$
			exon (1st cod. pos.)	K80$^{(2)}$
			exon (2nd cod. pos.)	K80$^{(2)}$
			exon (3rd cod. pos.)	K80$^{(2)}$
	Mcm7 (unrooted)	585	exon (1st cod. pos.)	HKY$^{(1)}$
			exon (2nd cod. pos.)	K80$^{(2)}$
			exon (3rd cod. pos.)	HKY$^{(1)}$
	Mcm7 (rooted)	585	exon (1st cod. pos.)	K80$^{(1)}$
			exon (2nd cod. pos.)	K80$^{(1)}$
			exon (3rd cod. pos.)	HKY$^{(2)}$
Photobiont	*rbcL* (unrooted)	780	exon (1st cod. pos.)	K80$^{(1)}$
			exon (2nd cod. pos.)	K80$^{(1)}$
			exon (3rd cod. pos.)	HKY$^{(2)}$
	rbcL (rooted)	780	exon (1st cod. pos.)	TrNef+I$^{(1)}$
			exon (2nd cod. pos.)	TrNef+I$^{(1)}$
			exon (3rd cod. pos.)	GTR+Γ$^{(2)}$
	tufA (unrooted)	574	exon (1st cod. pos.)	TrN+I$^{(1)}$
			exon (2nd cod. pos.)	K80$^{(2)}$
			exon (3rd cod. pos.)	HKY$^{(3)}$
	tufA (rooted)	574	exon (1st cod. pos.)	GTR+Γ$^{(1)}$
			exon (2nd cod. pos.)	K80+I$^{(2)}$
			exon (3rd cod. pos.)	GTR+I$^{(3)}$

Supplementary Table 10.Substitution models imposed in the first-step photobiont BEAST dating analysis.

Marker (location)	Alignment length (bp)	Partition	Inferred model	Less complex model used in BEAST
18S (nuclear)	1594	n/a	GTR+I+Γ	HKY+I+Γ
atpB (plastidial)	1410	exon (1st cod. pos.)	GTR+I+Γ	HKY+I+Γ
		exon (2nd cod. pos.)	GTR+I+Γ	HKY+I+Γ
		exon (3rd cod. pos.)	GTR+I+Γ	HKY+I+Γ
psaB (plastidial)	2205	exon (1st cod. pos.)	SYM+I+Γ	HKY+I+Γ
		exon (2nd cod. pos.)	GTR+I+Γ	HKY+I+Γ
		exon (3rd cod. pos.)	GTR+I+Γ	HKY+I+Γ
rbcL (plastidial)	1428	exon (1st cod. pos.)	GTR+I+Γ	HKY+I+Γ
		exon (2nd cod. pos.)	SYM+I+Γ	HKY+I+Γ
		exon (3rd cod. pos.)	GTR+I+Γ	HKY+I+Γ
tufA (plastidial)	1230	exon (1st cod. pos.)	GTR+I+Γ	HKY+I+Γ
		exon (2nd cod. pos.)	GTR+I+Γ	HKY+I+Γ
		exon (3rd cod. pos.)	GTR+I+Γ	HKY+I+Γ

Supplementary Table 11. Substitution models used in the second-step photobiont dating analysis. Superscript numbers within parentheses indicate the best partition scheme found in PARTITIONFINDER and implemented in *BEAST analyses.

Analysis	Marker (location)	Alignment length (bp)	Partition	Inferred model	Less complex model used in *BEAST
Two-marker (85 specimens included)	*tufA* (plastid)	574	exon (1st cod. pos.)	TrN$^{(1)}$	n/a
			exon (2nd cod. pos.)	K80$^{(2)}$	n/a
			exon (3rd cod. pos.)	GTR$^{(3)}$	KKY
	rbcL (plastid)	780	exon (1st cod. pos.)	TrN$^{(1)}$	n/a
			exon (2nd cod. pos.)	K80$^{(2)}$	n/a
			exon (3rd cod. pos.)	GTR$^{(3)}$	HKY
Four-marker (67 specimens)	*nrITS* (nuclear)	791	n/a	TrN+I+Γ$^{(1)}$	n/a
	RPL10A (nuclear)	111	exon (1st cod. pos.)	TrN+I+Γ$^{(1)}$	n/a
			exon (2nd cod. pos.)	HKY$^{(2)}$	n/a
			exon (3rd cod. pos.)	TrN+I+Γ$^{(1)}$	n/a
	tufA (plastid)	574	exon (1st cod. pos.)	HKY$^{(2)}$	n/a
			exon (2nd cod. pos.)	HKY$^{(3)}$	n/a
			exon (3rd cod. pos.)	HKY$^{(4)}$	n/a
	rbcL (plastid)	780	exon (1st cod. pos.)	HKY$^{(4)}$	n/a
			exon (2nd cod. pos.)	HKY$^{(2)}$	n/a
			exon (3rd cod. pos.)	HKY$^{(3)}$	n/a

Supplementary Table 12. Marginal likelihood and Bayes Factor values for two alternative species delimitation hypotheses in the fungal partner of *Mastodia tessellata* and their motivation. Best model in bold.

Model	Distinct species	Motivation	Path Sampling		Stepping-Stone	
			Ln (Marginal likelihood)	2ln (Bayes Factor)	Ln (Marginal likelihood)	2ln (Bayes Factor)
Model 1 (1 spp.)	n/a	Fungus with a wide distribution	-4455.7	23.6	-4455.7	23.4
Model 2 (2 spp.)	sp1: N. America[a],T. Fuego[b], Antarctica[c] sp2: Antarctica[d]	STRUCTURE multi-locus clustering, ABGD of *nrITS*, multi-locus network	**-4443.9**	**n/a**	**-4444**	**n/a**

[a] Individuals with *nrITS* haplotypes: *hap1*, *hap2*, *hap3*, *hap4*, *hap5*

[b] Individuals with *nrITS* haplotypes: *hap6*, *hap7*, *hap8*, *hap9*, *hap10*, *hap11*

[c] Individuals with *nrITS* haplotypes: *hap11*, *hap12*

[d] Individuals with *nrITS* haplotypes: *hap13*, *hap14*, *hap15*, *hap16*

Supplementary Table 13. Best gene flow models for candidate species of *Mastodia tessellata* s.l. myco- and photobionts assessed with MIGRATE-N. Comparisons were based on the Bézier Lml estimator and Bayes Factors (2 ln BF). Best models are highlighted in bold text. BF values above 10 indicate a very strong evidence against a model as compared with the best. Square brackets are used to indicate groups of populations, '↔' indicates population connectivity/gene flow, and ';' denotes no connectivity. See Supplementary Figure 2A for further description of models. NA: North America; TF: Tierra del Fuego; ANT: Antarctica.

Biont	Model	Description	Bézier Lml	2 ln BF Bézier
Mycobiont	**1**	**[NA↔[TF+ANT(5)]]; ANT**	**-3812.29**	**0**
	2	[NA↔ [TF+ANT(5)] ↔ANT]	-4459.48	1294.38
	3	[NA↔TF]; [ANT(5)+ANT]	-3945.32	266.06
	4	[NA↔TF] ↔ [ANT(5)+ANT]	-4603.9	1583.22
Photobiont	**1**	**[NA↔[TF+ANT(5)]]; ANT**	**-4031.74**	**0**
	2	[NA↔ [TF+ANT(5)] ↔ANT]	-4233.59	403.7
	3	[NA↔TF]; [ANT(5)+ANT]	-4064.89	66.3
	4	[NA↔TF] ↔ [ANT(5)+ANT]	-4253.02	442.56

Supplementary Table 14. Polymorphism statistics and neutrality test results for each myco- (*nrITS*, *EF-1α*, *Mcm7*) and photobiont (*rbcL*, *tufA*) marker, species and geographic origin. (ns: not significant).

Dataset	n	sites	gaps	*s*	*h*	*Hd*	*k*	π	π(JC)	Tajima's *D*
nrITS Mastodia sp.1 N. America	54	577	0	4	5	0.673	0.876	0.00152	0.00152	-0.00376 (ns; P > 0.1)
nrITS Mastodia sp.1 T. Fuego	107	577	0	6	6	0.71	1.41	0.00244	0.00245	0.51714 (ns; P > 0.1)
nrITS Mastodia sp.1 T. Antarctica	5	577	0	3	3	0.7	1.4	0.00243	0.00243	-0.17475 (ns; P > 0.1)
nrITS Mastodia sp.1 All localities	166	577	0	15	12	0.84	3.75	0.0065	0.00654	1.09545 (ns; P > 0.1)
nrITS Mastodia sp.2 Antarctica	84	580	0	4	4	0.35	0.989	0.00171	0.00171	0.48526 (ns; P > 0.1)
EF-1α Mastodia sp.1 N. America	54	509	2	6	6	0.746	1.148	0.00226	0.00227	-0.3209 (ns; P > 0.1)
EF-1α Mastodia sp.1 T. Fuego	107	509	2	26	6	0.633	8.176	0.01613	0.01648	1.92934 (ns; 0.1>P>0.05)
EF-1α Mastodia sp.1 Antarctica	5	509	2	16	2	0.4	6.4	0.01262	0.0129	-1.22187 (ns; P > 0.1)
EF-1α Mastodia sp.1 All localities	166	509	2	30	11	0.72	7.091	0.01399	0.01428	0.99133 (ns; P > 0.1)
EF-1α Mastodia sp.2 Antarctica	84	525	1	11	4	0.259	2.189	0.00418	0.00423	-0.01258 (ns; P > 0.1)
Mcm7 Mastodia sp.1 N. America	54	585	0	0	1	0	0	0	0	n/a
Mcm7 Mastodia sp.1 T. Fuego	107	585	0	4	5	0.524	0.611	0.00104	0.00105	-0.39005 (ns)
Mcm7 Mastodia sp.1 Antarctica	5	585	0	5	4	0.9	2.2	0.00376	0.00377	-0.56199 (ns)
Mcm7 Mastodia sp.1 All localities	166	585	0	8	7	0.407	0.481	0.00082	0.00082	-1.48661 (ns)
Mcm7 Mastodia sp.2 Antarctica	84	585	0	3	4	0.315	0.333	0.00057	0.00057	-0.82424 (ns)
rbcL P. borealis N. America	12	780	0	3	3	0.667	1.273	0.00163	0.00163	0.9223 (ns)
rbcL P. borealis T. Fuego	35	780	0	0	1	0	0	0	0	n/a
rbcL P. borealis Antarctica	5	780	0	1	2	0.4	0.4	0.00051	0.00051	-0.8165 (ns)
rbcL P. borealis All localities	52	780	0	7	5	0.425	1.61	0.00206	0.00207	0.10344 (ns)
rbcL Prasiola sp. Antarctica	32	780	0	0	1	0	0	0	0	n/a
tufA P. borealis N. America	32	574	0	0	1	0	0	0	0	n/a
tufA P. borealis T. Fuego	62	574	0	0	1	0	0	0	0	n/a
tufA P. borealis Antarctica	7	574	0	0	1	0	0	0	0	n/a
tufA P. borealis All localities	101	574	0	3	2	0.13	0.391	0.00068	0.00068	-0.58051 (ns)
tufA Prasiola sp. Antarctica	59	574	0	0	1	0	0	0	0	n/a

Supplementary Table 15. Best migration models for bipolar *Mastodia tessellata* s.l. symbionts assessed with MIGRATE-N. Comparisons were based on the Bézier Lml estimator and Bayes Factors (2 ln BF). Best models are highlighted in bold text. BF values above 10 indicate a very strong evidence against a model as compared with the best. Model description (see also Supplementary Figure 2B), number of estimated parameters and resulting probability are also provided for each model. S: Southern Hemisphere; N: Northern Hemisphere; TF: Tierra del Fuego; NA: North America; ANT: Antarctica.

Biont	Directionality	Model	Description and number of estimated parameters (Θ + M)	Bézier Lml	Model Probability	2 ln BF Bézier
Mycobionts (*Mastodia* sp. 1 & sp. 2)	n/a	Null	No connections (single population) (1 + 0)	-5076.57	~ 0	2541.08
		Null	All possible connections among the 4 populations (4 + 12)	-4656.34	~ 0	1700.62
Bipolar mycobiont (*Mastodia* sp. 1)	S -> N	5	TF migration into NA. ANT migration into TF. (4 + 2)	-3829.29	7.897×10^{-11}	46.52
		6	**TF migration into NA and ANT. (4 + 2)**	**-3806.03**	**0.998**	**0**
		7	TF migration into NA and ANT. ANT migration into TF. (4 + 3)	-3817.84	7.416×10^{-6}	23.62
	N -> S	8	NA migration into TF. TF migration into ANT. (4 + 2)	-3821.82	1.386×10^{-7}	31.58
		9	NA migration into TF. ANT migration into TF. (4 + 2)	-3960.56	7.72×10^{-68}	309.06
		10	NA migration into TF. TF migration into ANT and *vice versa* (4 + 3)	-3832.12	4.66×10^{-12}	52.18
Photobionts (*Prasiola*	n/a	Null	No connections (single population) (1 + 0)	-4424.57	~ 0	845.62

borealis & *Prasiola* sp.)		Null	All possible connections among the 4 populations (4 + 12)	-4287.1	~ 0	570.68
Bipolar photobiont (*Prasiola borealis*)	S -> N	5	TF migration into NA. ANT migration into TF. (4 + 2)	-4021.24	3.467×10^{-9}	38.96
		6	TF migration into NA and ANT. (4 + 2)	-4014.01	4.785×10^{-6}	24.5
		7	**TF migration into NA and ANT. ANT migration into TF. (4 + 3)**	**-4001.76**	**9.999×10^{-1}**	**0**
	N -> S	8	NA migration into TF. TF migration into ANT. (4 + 2)	-4012.32	2.593×10^{-5}	21.12
		9	NA migration into TF. ANT migration into TF. (4 + 2)	-4103.53	6.336×10^{-45}	203.54
		10	NA migration into TF. TF migration into ANT and *vice versa* (4 + 3)	-4017.45	1.534×10^{-7}	31.38

Supplementary Table 16. Mutation-scaled population size (Θ) and migration rates (*M*) of the best migration model for the bipolar *Mastodia tessellata* s.l. symbionts calculated with MIGRATE-N. Mean parameter values were used to calculate the average number of migrants per generation (*x*Nm). See also Supplementary Table 15 and Supplementary Figure 2 for further details. Msp1: *Mastodia* sp. 1; Msp2: *Mastodia* sp. 2; Pbo: *Prasiola borealis*; Psp: *Prasiola* sp.; NA: North America; TF: Tierra del Fuego; ANT: Antarctica.

	2.5%	25%	Mode	75%	97.5%	Median	Mean	*x*Nm
Mycobiont Model 6: Southern to Northern Hemisphere. **TF migration into NA and ANT.**								
Θ_{Msp1NA}	0.00000	0.00000	0.00075	0.00180	0.00450	0.00185	0.00163	–
Θ_{Msp1TF}	0.00280	0.00530	0.00695	0.00840	0.01120	0.00705	0.00704	–
$\Theta_{Msp1ANT}$	0.00000	0.00000	0.00335	0.01070	0.11600	0.01075	0.02888	–
Θ_{Msp2}	0.00050	0.00270	0.00415	0.00550	0.00780	0.00425	0.00417	–
$M_{Msp1TF->Msp1NA}$	0.0	160.0	274.7	405.3	784.0	333.3	386.3	0.630
$M_{Msp1TF->Msp1ANT}$	1418.7	2069.3	2882.7	4853.3	7840.0	4130.7	4273.1	123.407
Photobiont Model 7: Southern to Northern Hemisphere. **TF migration into NA and ANT. ANT migration into TF.**								
Θ_{PboNA}	0.00000	0.00000	0.00005	0.00090	0.00270	0.00095	0.00053	–
Θ_{PboTF}	0.00000	0.00000	0.00005	0.00120	0.00340	0.00125	0.00094	–
Θ_{PboANT}	0.00000	0.00000	0.00155	0.00330	0.01690	0.00335	0.00539	–
Θ_{Psp}	0.00000	0.00050	0.00145	0.00250	0.00440	0.00205	0.00173	–
$M_{PboTF->PboNA}$	0.0	80.0	157.3	234.7	394.7	184.0	179.9	0.095
$M_{PboANT->PboTF}$	0.0	0.0	50.7	90.7	202.7	88.0	53.3	0.050
$M_{PboTF->PboANT}$	0.0	69.3	210.7	565.3	2032.0	520.0	1140.9	6.149

Appendix 1. Samples used in this study, with details on collection data (region, sampling locality, date, collector, longitude, latitude), as well as haplotype codes for each myco- and photobiont sample.

					Mycobiont			Photobiont			
Species (mycobiont/photobiont)	Extraction	Collection	Longitude	Latitude	*nrITS*	*EF1-α*	*Mcm7*	*tufA*	*rbcL*	*RPL10A*	*nrITS*
Mastodia sp.1/*Prasiola borealis*	I38-1	Alaska (USA), Glacier Bay National Park, Gustavus, Barlett Cove. Seashore, 0-5 m a.s.l. 12/7/2012. Leg. *S. Pérez-Ortega.* Loc. 589b	58° 26' 58" N	135° 53' 56" W	hap4	hap1	hap1	-	-	-	-
Mastodia sp.1/*Prasiola borealis*	I39	Alaska (USA), Glacier Bay National Park, Gustavus, Barlett Cove. Seashore, 0-5 m a.s.l. 12/7/2012. Leg. *S. Pérez-Ortega.* Loc. 589b	58° 26' 58" N	135° 53' 56" W	hap4	hap5	hap1	-	-	-	-
Mastodia sp.1/*Prasiola borealis*	I40	Alaska (USA), Glacier Bay National Park, Gustavus, Barlett Cove. Seashore, 0-5 m a.s.l. 12/7/2012. Leg. *S. Pérez-Ortega.* Loc. 589b	58° 26' 58" N	135° 53' 56" W	hap5	hap2	hap1	hap1	-	-	-
Mastodia sp.1/*Prasiola borealis*	I41	Alaska (USA), Glacier Bay National Park, Gustavus, Barlett Cove. Seashore, 0-5 m a.s.l. 12/7/2012. Leg. *S. Pérez-Ortega.* Loc. 589b	58° 26' 58" N	135° 53' 56" W	hap2	hap6	hap1	-	-	-	-
Mastodia sp.1/*Prasiola borealis*	I42dupl1	Alaska (USA), Glacier Bay National Park, Gustavus, Barlett Cove. Seashore, 0-5 m a.s.l. 12/7/2012. Leg. *S. Pérez-Ortega.* Loc. 589b	58° 26' 58" N	135° 53' 56" W	hap2	hap6	hap1	-	-	-	-
Mastodia sp.1/*Prasiola borealis*	I42dupl2	Alaska (USA), Glacier Bay National Park, Gustavus, Barlett Cove. Seashore, 0-5 m a.s.l. 12/7/2012. Leg. *S. Pérez-Ortega.* Loc. 589b	58° 26' 58" N	135° 53' 56" W	hap2	hap5	hap1	-	-	-	-
Mastodia sp.1/*Prasiola borealis*	I43	Alaska (USA), Glacier Bay National Park, Gustavus, Barlett Cove. Seashore, 0-5 m a.s.l. 12/7/2012. Leg. *S. Pérez-Ortega.* Loc. 589b	58° 26' 58" N	135° 53' 56" W	hap2	hap5	hap1	-	-	-	-
Mastodia sp.1/*Prasiola borealis*	I44	Alaska (USA), Glacier Bay National Park, Gustavus, Barlett Cove. Seashore, 0-5 m a.s.l. 12/7/2012. Leg. *S. Pérez-Ortega.* Loc. 589b	58° 26' 58" N	135° 53' 56" W	hap5	hap2	hap1	hap1	-	hap1	hap1
Mastodia sp.1/*Prasiola borealis*	I45	Alaska (USA), Glacier Bay National Park, Gustavus, Barlett Cove. Seashore, 0-5 m a.s.l. 12/7/2012. Leg. *S. Pérez-Ortega.* Loc. 589b	58° 26' 58" N	135° 53' 56" W	hap2	hap6	hap1	hap1	-	hap1	-
Mastodia sp.1/*Prasiola borealis*	I46dupl1	Alaska (USA), Glacier Bay National Park, Gustavus, Barlett Cove. Seashore, 0-5 m a.s.l. 12/7/2012. Leg. *S. Pérez-Ortega.* Loc. 589b	58° 26' 58" N	135° 53' 56" W	hap4	hap5	hap1	hap1	hap2	-	hap1
Mastodia sp.1/*Prasiola borealis*	I46dupl2	Alaska (USA), Glacier Bay National Park, Gustavus, Barlett Cove. Seashore, 0-5 m a.s.l. 12/7/2012. Leg. *S. Pérez-Ortega.* Loc. 589b	58° 26' 58" N	135° 53' 56" W	hap2	hap5	hap1	-	-	-	-
Mastodia sp.1/*Prasiola borealis*	I47dupl1	Alaska (USA), Glacier Bay National Park, Gustavus, Barlett Cove. Seashore, 0-5 m a.s.l. 12/7/2012. Leg. *S. Pérez-Ortega.* Loc. 589b	58° 26' 58" N	135° 53' 56" W	hap2	hap5	hap1	-	-	-	-

Mastodia sp.1/*Prasiola borealis*	I47dupl2	Alaska (USA), Glacier Bay National Park, Gustavus, Barlett Cove. Seashore, 0-5 m a.s.l. 12/7/2012. Leg. *S. Pérez-Ortega.* Loc. 589b	58° 26' 58" N	135° 53' 56" W	hap4	hap5	hap1	-	-	-	-
Mastodia sp.1/*Prasiola borealis*	I48dupl1	Alaska (USA), Glacier Bay National Park, Gustavus, Barlett Cove. Seashore, 0-5 m a.s.l. 12/7/2012. Leg. *S. Pérez-Ortega.* Loc. 589b	58° 26' 58" N	135° 53' 56" W	hap2	hap6	hap1	hap1	-	hap1	hap1
Mastodia sp.1/*Prasiola borealis*	I48dupl2	Alaska (USA), Glacier Bay National Park, Gustavus, Barlett Cove. Seashore, 0-5 m a.s.l. 12/7/2012. Leg. *S. Pérez-Ortega.* Loc. 589b	58° 26' 58" N	135° 53' 56" W	hap4	hap6	hap1	-	-	-	-
Mastodia sp.1/*Prasiola borealis*	I49	Alaska (USA), Glacier Bay National Park, Gustavus, Barlett Cove. Seashore, 0-5 m a.s.l. 12/7/2012. Leg. *S. Pérez-Ortega.* Loc. 589b	58° 26' 58" N	135° 53' 56" W	hap3	hap3	hap1	-	-	-	-
Mastodia sp.1/*Prasiola borealis*	I50	Alaska (USA), Glacier Bay National Park, Gustavus, Barlett Cove. Seashore, 0-5 m a.s.l. 12/7/2012. Leg. *S. Pérez-Ortega.* Loc. 589b	58° 26' 58" N	135° 53' 56" W	hap4	hap5	hap1	hap1	-	hap1	hap1
Mastodia sp.1/*Prasiola borealis*	I51dupl1	Alaska (USA), Glacier Bay National Park, Gustavus, Barlett Cove. Seashore, 0-5 m a.s.l. 12/7/2012. Leg. *S. Pérez-Ortega.* Loc. 589b	58° 26' 58" N	135° 53' 56" W	hap4	hap1	hap1	hap1	-	-	hap1
Mastodia sp.1/*Prasiola borealis*	I51dupl2	Alaska (USA), Glacier Bay National Park, Gustavus, Barlett Cove. Seashore, 0-5 m a.s.l. 12/7/2012. Leg. *S. Pérez-Ortega.* Loc. 589b	58° 26' 58" N	135° 53' 56" W	hap2	hap6	hap1	-	-	-	-
Mastodia sp.1/*Prasiola borealis*	I52	Alaska (USA), Glacier Bay National Park, Gustavus, Barlett Cove. Seashore, 0-5 m a.s.l. 12/7/2012. Leg. *S. Pérez-Ortega.* Loc. 589b	58° 26' 58" N	135° 53' 56" W	hap2	hap5	hap1	hap1	-	-	hap1
Mastodia sp.1/*Prasiola borealis*	I53dupl1	Alaska (USA), Glacier Bay National Park, Gustavus, Barlett Cove. Seashore, 0-5 m a.s.l. 12/7/2012. Leg. *S. Pérez-Ortega.* Loc. 589b	58° 26' 58" N	135° 53' 56" W	hap4	hap5	hap1	hap1	-	hap1	hap1
Mastodia sp.1/*Prasiola borealis*	I53dupl2	Alaska (USA), Glacier Bay National Park, Gustavus, Barlett Cove. Seashore, 0-5 m a.s.l. 12/7/2012. Leg. *S. Pérez-Ortega.* Loc. 589b	58° 26' 58" N	135° 53' 56" W	hap5	hap2	hap1	-	-	-	-
Mastodia sp.1/*Prasiola borealis*	I54	Alaska (USA), Glacier Bay National Park, Gustavus, Barlett Cove. Seashore, 0-5 m a.s.l. 12/7/2012. Leg. *S. Pérez-Ortega.* Loc. 589b	58° 26' 58" N	135° 53' 56" W	hap2	hap5	hap1	hap1	-	hap1	hap1
Mastodia sp.1/*Prasiola borealis*	I55	Alaska (USA), Glacier Bay National Park, Gustavus, Barlett Cove. Seashore, 0-5 m a.s.l. 12/7/2012. Leg. *S. Pérez-Ortega.* Loc. 589b	58° 26' 58" N	135° 53' 56" W	hap4	hap5	hap1	hap1	-	hap1	hap1
Mastodia sp.1/*Prasiola borealis*	I369	Alaska (USA), Glacier Bay National Park, Gustavus, Barlett Cove. Seashore, 0-5 m a.s.l. 12/7/2012. Leg. *S. Pérez-Ortega.* Loc. 589b	58° 26' 58" N	135° 53' 56" W	-	-	-	-	-	-	hap1
Mastodia sp.1/*Prasiola borealis*	I375	Alaska (USA), Glacier Bay National Park, Gustavus, Barlett Cove. Seashore, 0-5 m a.s.l. 12/7/2012. Leg. *S. Pérez-Ortega.* Loc. 589b	58° 26' 58" N	135° 53' 56" W	-	-	-	-	-	hap1	-
Mastodia sp.1/*Prasiola borealis*	I376	Alaska (USA), Glacier Bay National Park, Gustavus, Barlett Cove. Seashore, 0-5 m a.s.l. 12/7/2012. Leg.	58° 26' 58" N	135° 53' 56" W	-	-	-	hap1	-	hap1	hap1

		S. Pérez-Ortega. Loc. 589b									
Mastodia sp.1/*Prasiola borealis*	I427	Alaska (USA), Glacier Bay National Park, Gustavus, Barlett Cove. Seashore, 0-5 m a.s.l. 12/7/2012. Leg. *S. Pérez-Ortega.* Loc. 589b	58° 26' 58" N	135° 53' 56" W	-	-	-	hap1	hap2	hap1	hap1
Mastodia sp.1/*Prasiola borealis*	I428	Alaska (USA), Glacier Bay National Park, Gustavus, Barlett Cove. Seashore, 0-5 m a.s.l. 12/7/2012. Leg. *S. Pérez-Ortega.* Loc. 589b	58° 26' 58" N	135° 53' 56" W	-	-	-	hap1	hap2	hap1	hap1
Mastodia sp.1/*Prasiola borealis*	I429	Alaska (USA), Glacier Bay National Park, Gustavus, Barlett Cove. Seashore, 0-5 m a.s.l. 12/7/2012. Leg. *S. Pérez-Ortega.* Loc. 589b	58° 26' 58" N	135° 53' 56" W	-	-	-	hap1	hap2	hap1	hap1
Mastodia sp.1/*Prasiola borealis*	I430	Alaska (USA), Glacier Bay National Park, Gustavus, Barlett Cove. Seashore, 0-5 m a.s.l. 12/7/2012. Leg. *S. Pérez-Ortega.* Loc. 589b	58° 26' 58" N	135° 53' 56" W	-	-	-	hap1	hap2	hap1	hap1
Mastodia sp.1/*Prasiola borealis*	I431	Alaska (USA), Glacier Bay National Park, Gustavus, Barlett Cove. Seashore, 0-5 m a.s.l. 12/7/2012. Leg. *S. Pérez-Ortega.* Loc. 589b	58° 26' 58" N	135° 53' 56" W	-	-	-	hap1	hap2	hap1	hap1
Mastodia sp.1/*Prasiola borealis*	I265	Alaska (USA), Petersburg, South Mitkof Island, Summer Strait. Seashore, on sedimentary rocks, 0-5 m a.s.l. 25/06/2012. Leg. *S. Pérez-Ortega, T. Spribille & K. Dillman.* Loc. 558	56° 33' 10" N	132° 38' 41" W	hap4	hap1	hap1	-	-	-	-
Mastodia sp.1/*Prasiola borealis*	I266	Alaska (USA), Petersburg, South Mitkof Island, Summer Strait. Seashore, on sedimentary rocks, 0-5 m a.s.l. 25/06/2012. Leg. *S. Pérez-Ortega, T. Spribille & K. Dillman.* Loc. 558	56° 33' 10" N	132° 38' 41" W	hap4	hap1	hap1	hap1	-	hap2	hap2
Mastodia sp.1/*Prasiola borealis*	I267	Alaska (USA), Petersburg, South Mitkof Island, Summer Strait. Seashore, on sedimentary rocks, 0-5 m a.s.l. 25/06/2012. Leg. *S. Pérez-Ortega, T. Spribille & K. Dillman.* Loc. 558	56° 33' 10" N	132° 38' 41" W	hap4	hap1	hap1	hap1	-	hap2	hap2
Mastodia sp.1/*Prasiola borealis*	I268	Alaska (USA), Petersburg, South Mitkof Island, Summer Strait. Seashore, on sedimentary rocks, 0-5 m a.s.l. 25/06/2012. Leg. *S. Pérez-Ortega, T. Spribille & K. Dillman.* Loc. 558	56° 33' 10" N	132° 38' 41" W	hap4	hap1	hap1	hap1	-	hap2	hap2
Mastodia sp.1/*Prasiola borealis*	I269	Alaska (USA), Petersburg, South Mitkof Island, Summer Strait. Seashore, on sedimentary rocks, 0-5 m a.s.l. 25/06/2012. Leg. *S. Pérez-Ortega, T. Spribille & K. Dillman.* Loc. 558	56° 33' 10" N	132° 38' 41" W	hap4	hap1	hap1	-	-	-	-
Mastodia sp.1/*Prasiola borealis*	I270dupl1	Alaska (USA), Petersburg, South Mitkof Island, Summer Strait. Seashore, on sedimentary rocks, 0-5 m a.s.l. 25/06/2012. Leg. *S. Pérez-Ortega, T. Spribille & K. Dillman.* Loc. 558	56° 33' 10" N	132° 38' 41" W	hap5	hap2	hap1	hap1	-	hap2	hap2
Mastodia sp.1/*Prasiola borealis*	I270dupl2	Alaska (USA), Petersburg, South Mitkof Island, Summer Strait. Seashore, on sedimentary rocks, 0-5 m a.s.l. 25/06/2012. Leg. *S. Pérez-Ortega, T.*	56° 33' 10" N	132° 38' 41" W	hap4	hap1	hap1	-	-	-	-

		Spribille & K. Dillman. Loc. 558									
Mastodia sp.1/*Prasiola borealis*	I271	Alaska (USA), Petersburg, South Mitkof Island, Summer Strait. Seashore, on sedimentary rocks, 0-5 m a.s.l. 25/06/2012. Leg. *S. Pérez-Ortega, T. Spribille & K. Dillman.* Loc. 558	56° 33' 10" N	132° 38' 41" W	hap4	hap1	hap1	hap1	-	hap2	hap2
Mastodia sp.1/*Prasiola borealis*	I273	Alaska (USA), Petersburg, South Mitkof Island, Summer Strait. Seashore, on sedimentary rocks, 0-5 m a.s.l. 25/06/2012. Leg. *S. Pérez-Ortega, T. Spribille & K. Dillman.* Loc. 558	56° 33' 10" N	132° 38' 41" W	hap4	hap1	hap1	hap1	-	hap2	hap2
Mastodia sp.1/*Prasiola borealis*	I274dupl1	Alaska (USA), Petersburg, South Mitkof Island, Summer Strait. Seashore, on sedimentary rocks, 0-5 m a.s.l. 25/06/2012. Leg. *S. Pérez-Ortega, T. Spribille & K. Dillman.* Loc. 558	56° 33' 10" N	132° 38' 41" W	hap2	hap1	hap1	hap1	-	hap1	hap1
Mastodia sp.1/*Prasiola borealis*	I274dupl2	Alaska (USA), Petersburg, South Mitkof Island, Summer Strait. Seashore, on sedimentary rocks, 0-5 m a.s.l. 25/06/2012. Leg. *S. Pérez-Ortega, T. Spribille & K. Dillman.* Loc. 558	56° 33' 10" N	132° 38' 41" W	hap4	hap1	hap1	-	-	-	-
Mastodia sp.1/*Prasiola borealis*	I275	Alaska (USA), Petersburg, South Mitkof Island, Summer Strait. Seashore, on sedimentary rocks, 0-5 m a.s.l. 25/06/2012. Leg. *S. Pérez-Ortega, T. Spribille & K. Dillman.* Loc. 558	56° 33' 10" N	132° 38' 41" W	hap2	hap1	hap1	hap1	hap3	hap2	hap2
Mastodia sp.1/*Prasiola borealis*	I276	Alaska (USA), Petersburg, South Mitkof Island, Summer Strait. Seashore, on sedimentary rocks, 0-5 m a.s.l. 25/06/2012. Leg. *S. Pérez-Ortega, T. Spribille & K. Dillman.* Loc. 558	56° 33' 10" N	132° 38' 41" W	hap2	hap1	hap1	hap1	-	hap1	-
Mastodia sp.1/*Prasiola borealis*	I277	Alaska (USA), Petersburg, South Mitkof Island, Summer Strait. Seashore, on sedimentary rocks, 0-5 m a.s.l. 25/06/2012. Leg. *S. Pérez-Ortega, T. Spribille & K. Dillman.* Loc. 558	56° 33' 10" N	132° 38' 41" W	hap4	hap1	hap1	hap1	-	hap2	-
Mastodia sp.1/*Prasiola borealis*	I433	Alaska (USA), Petersburg, South Mitkof Island, Summer Strait. Seashore, on sedimentary rocks, 0-5 m a.s.l. 25/06/2012. Leg. *S. Pérez-Ortega, T. Spribille & K. Dillman.* Loc. 558	56° 33' 10" N	132° 38' 41" W	-	-	-	hap1	hap3	hap2	hap2
Mastodia sp.1/*Prasiola borealis*	I434	Alaska (USA), Petersburg, South Mitkof Island, Summer Strait. Seashore, on sedimentary rocks, 0-5 m a.s.l. 25/06/2012. Leg. *S. Pérez-Ortega, T. Spribille & K. Dillman.* Loc. 558	56° 33' 10" N	132° 38' 41" W	-	-	-	hap1	hap3	hap2	hap2
Mastodia sp.1/*Prasiola borealis*	I435	Alaska (USA), Petersburg, South Mitkof Island, Summer Strait. Seashore, on sedimentary rocks, 0-5 m a.s.l. 25/06/2012. Leg. *S. Pérez-Ortega, T. Spribille & K. Dillman.* Loc. 558	56° 33' 10" N	132° 38' 41" W	-	-	-	hap1	hap3	hap2	-
Mastodia sp.1/*Prasiola borealis*	I436	Alaska (USA), Petersburg, South Mitkof Island, Summer Strait. Seashore, on sedimentary rocks, 0-5 m a.s.l. 25/06/2012. Leg. *S. Pérez-Ortega, T.*	56° 33' 10" N	132° 38' 41" W	-	-	-	hap1	hap1	hap1	-

		Spribille & K. Dillman. Loc. 558									
Mastodia sp.1/*Prasiola borealis*	I437	Alaska (USA), Petersburg, South Mitkof Island, Summer Strait. Seashore, on sedimentary rocks, 0-5 m a.s.l. 25/06/2012. Leg. *S. Pérez-Ortega, T. Spribille & K. Dillman.* Loc. 558	56° 33' 10" N	132° 38' 41" W	-	-	-	hap1	hap1	hap1	-
Mastodia sp.1/*Prasiola delicata*	I23-1	British Columbia (Canada), Port Edward. Seashore, 0-5 m a.s.l. 22/6/2012. Leg. *S. Pérez-Ortega & T. Spribille.* Loc. 554	54° 15' 12" N	130° 15' 26" W	hap2	hap4	hap1	-	-	-	-
Mastodia sp.1/*Prasiola delicata*	I24-1	British Columbia (Canada), Port Edward. Seashore, 0-5 m a.s.l. 22/6/2012. Leg. *S. Pérez-Ortega & T. Spribille.* Loc. 554	54° 15' 12" N	130° 15' 26" W	hap2	hap5	hap1	hap4	-	-	hap22
Mastodia sp.1/*Prasiola delicata*	I25	British Columbia (Canada), Port Edward. Seashore, 0-5 m a.s.l. 22/6/2012. Leg. *S. Pérez-Ortega & T. Spribille.* Loc. 554	54° 15' 12" N	130° 15' 26" W	hap1	hap6	hap1	hap4	-	hap20	-
Mastodia sp.1/*Prasiola delicata*	I26	British Columbia (Canada), Port Edward. Seashore, 0-5 m a.s.l. 22/6/2012. Leg. *S. Pérez-Ortega & T. Spribille.* Loc. 554	54° 15' 12" N	130° 15' 26" W	hap2	hap4	hap1	-	-	-	-
Mastodia sp.1/*Prasiola delicata*	I27dupl1	British Columbia (Canada), Port Edward. Seashore, 0-5 m a.s.l. 22/6/2012. Leg. *S. Pérez-Ortega & T. Spribille.* Loc. 554	54° 15' 12" N	130° 15' 26" W	hap1	hap6	hap1	hap4	-	-	hap22
Mastodia sp.1/*Prasiola delicata*	I27dupl2	British Columbia (Canada), Port Edward. Seashore, 0-5 m a.s.l. 22/6/2012. Leg. *S. Pérez-Ortega & T. Spribille.* Loc. 554	54° 15' 12" N	130° 15' 26" W	hap2	hap5	hap1	-	-	-	-
Mastodia sp.1/*Prasiola delicata*	I28	British Columbia (Canada), Port Edward. Seashore, 0-5 m a.s.l. 22/6/2012. Leg. *S. Pérez-Ortega & T. Spribille.* Loc. 554	54° 15' 12" N	130° 15' 26" W	hap2	hap4	hap1	hap4	-	-	hap22
Mastodia sp.1/*Prasiola delicata*	I29	British Columbia (Canada), Port Edward. Seashore, 0-5 m a.s.l. 22/6/2012. Leg. *S. Pérez-Ortega & T. Spribille.* Loc. 554	54° 15' 12" N	130° 15' 26" W	hap1	hap5	hap1	hap4	hap7	hap20	hap22
Mastodia sp.1/*Prasiola delicata*	I30	British Columbia (Canada), Port Edward. Seashore, 0-5 m a.s.l. 22/6/2012. Leg. *S. Pérez-Ortega & T. Spribille.* Loc. 554	54° 15' 12" N	130° 15' 26" W	hap1	hap6	hap1	hap4	-	-	-
Mastodia sp.1/*Prasiola delicata*	I31	British Columbia (Canada), Port Edward. Seashore, 0-5 m a.s.l. 22/6/2012. Leg. *S. Pérez-Ortega & T. Spribille.* Loc. 554	54° 15' 12" N	130° 15' 26" W	hap2	hap4	hap1	-	-	-	-
Mastodia sp.1/*Prasiola delicata*	I32	British Columbia (Canada), Port Edward. Seashore, 0-5 m a.s.l. 22/6/2012. Leg. *S. Pérez-Ortega & T. Spribille.* Loc. 554	54° 15' 12" N	130° 15' 26" W	hap2	hap5	hap1	hap4	-	hap20	hap22
Mastodia sp.1/*Prasiola delicata*	I33	British Columbia (Canada), Port Edward. Seashore, 0-5 m a.s.l. 22/6/2012. Leg. *S. Pérez-Ortega & T. Spribille.* Loc. 554	54° 15' 12" N	130° 15' 26" W	hap2	hap5	hap1	hap4	-	hap20	hap22
Mastodia sp.1/*Prasiola delicata*	I34	British Columbia (Canada), Port Edward. Seashore, 0-5 m a.s.l. 22/6/2012. Leg. *S. Pérez-Ortega & T.*	54° 15' 12" N	130° 15' 26" W	hap1	hap5	hap1	hap4	-	-	hap24

		Spribille. Loc. 554									
Mastodia sp.1/*Prasiola delicata*	I35	British Columbia (Canada), Port Edward. Seashore, 0-5 m a.s.l. 22/6/2012. Leg. *S. Pérez-Ortega & T. Spribille.* Loc. 554	54° 15' 12" N	130° 15' 26" W	hap2	hap5	hap1	hap4	-	hap20	hap22
Mastodia sp.1/*Prasiola delicata*	I36	British Columbia (Canada), Port Edward. Seashore, 0-5 m a.s.l. 22/6/2012. Leg. *S. Pérez-Ortega & T. Spribille.* Loc. 554	54° 15' 12" N	130° 15' 26" W	hap1	hap5	hap1	hap4	-	hap20	hap22
Mastodia sp.1/*Prasiola delicata*	I37	British Columbia (Canada), Port Edward. Seashore, 0-5 m a.s.l. 22/6/2012. Leg. *S. Pérez-Ortega & T. Spribille.* Loc. 554	54° 15' 12" N	130° 15' 26" W	hap2	hap5	hap1	-	-	-	-
Mastodia sp.1/*Prasiola delicata*	I422	British Columbia (Canada), Port Edward. Seashore, 0-5 m a.s.l. 22/6/2012. Leg. *S. Pérez-Ortega & T. Spribille.* Loc. 554	54° 15' 12" N	130° 15' 26" W	-	-	-	hap4	hap7	hap20	hap22
Mastodia sp.1/*Prasiola delicata*	I423	British Columbia (Canada), Port Edward. Seashore, 0-5 m a.s.l. 22/6/2012. Leg. *S. Pérez-Ortega & T. Spribille.* Loc. 554	54° 15' 12" N	130° 15' 26" W	-	-	-	hap4	hap7	hap20	hap22
Mastodia sp.1/*Prasiola delicata*	I424	British Columbia (Canada), Port Edward. Seashore, 0-5 m a.s.l. 22/6/2012. Leg. *S. Pérez-Ortega & T. Spribille.* Loc. 554	54° 15' 12" N	130° 15' 26" W	-	-	-	hap4	hap7	hap20	hap22
Mastodia sp.1/*Prasiola delicata*	I425	British Columbia (Canada), Port Edward. Seashore, 0-5 m a.s.l. 22/6/2012. Leg. *S. Pérez-Ortega & T. Spribille.* Loc. 554	54° 15' 12" N	130° 15' 26" W	-	-	-	hap4	hap7	hap20	hap22
Mastodia sp.1/*Prasiola delicata*	I426	British Columbia (Canada), Port Edward. Seashore, 0-5 m a.s.l. 22/6/2012. Leg. *S. Pérez-Ortega & T. Spribille.* Loc. 554	54° 15' 12" N	130° 15' 26" W	-	-	-	hap4	hap7	hap20	hap22
Mastodia sp.1/*Prasiola borealis*	I130-1_dupl1	Tierra del Fuego (Chile), Brunswick Peninsula, San Nicolás Bay, near Cabo Froward, XII Región. Seashore, 0-5 m a.s.l. 18/12/2009. Leg. *S. Pérez-Ortega.* Loc. 434-435	53° 50' 46" S	71° 7' 4" W	hap8	hap11	hap1	hap1	-	hap4	-
Mastodia sp.1/*Prasiola borealis*	I130-1_dupl2	Tierra del Fuego (Chile), Brunswick Peninsula, San Nicolás Bay, near Cabo Froward, XII Región. Seashore, 0-5 m a.s.l. 18/12/2009. Leg. *S. Pérez-Ortega.* Loc. 434-435	53° 50' 46" S	71° 7' 4" W	hap10	hap5	hap1	-	-	-	-
Mastodia sp.1/*Prasiola borealis*	I241	Tierra del Fuego (Chile), Brunswick Peninsula, San Nicolás Bay, near Cabo Froward, XII Región. Seashore, 0-5 m a.s.l. 18/12/2009. Leg. *S. Pérez-Ortega.* Loc. 434-435	53° 50' 46" S	71° 7' 4" W	hap8	hap5	hap1	-	-	-	-
Mastodia sp.1/*Prasiola borealis*	I242	Tierra del Fuego (Chile), Brunswick Peninsula, San Nicolás Bay, near Cabo Froward, XII Región. Seashore, 0-5 m a.s.l. 18/12/2009. Leg. *S. Pérez-Ortega.* Loc. 434-435	53° 50' 46" S	71° 7' 4" W	hap8	hap11	hap1	hap1	-	hap4	hap3
Mastodia sp.1/*Prasiola borealis*	I243dupl1	Tierra del Fuego (Chile), Brunswick Peninsula, San Nicolás Bay, near Cabo Froward, XII Región.	53° 50' 46" S	71° 7' 4" W	hap8	hap11	hap1	-	-	-	-

		Seashore, 0-5 m a.s.l. 18/12/2009. Leg. *S. Pérez-Ortega*. Loc. 434-435									
Mastodia sp.1/*Prasiola borealis*	I243dupl2	Tierra del Fuego (Chile), Brunswick Peninsula, San Nicolás Bay, near Cabo Froward, XII Región. Seashore, 0-5 m a.s.l. 18/12/2009. Leg. *S. Pérez-Ortega*. Loc. 434-435	53° 50' 46" S	71° 7' 4" W	hap10	hap5	hap1	-	-	-	-
Mastodia sp.1/*Prasiola borealis*	I243b_dupl1	Tierra del Fuego (Chile), Brunswick Peninsula, San Nicolás Bay, near Cabo Froward, XII Región. Seashore, 0-5 m a.s.l. 18/12/2009. Leg. *S. Pérez-Ortega*. Loc. 434-435	53° 50' 46" S	71° 7' 4" W	hap8	hap11	hap1	-	-	-	-
Mastodia sp.1/*Prasiola borealis*	I243b_dupl2	Tierra del Fuego (Chile), Brunswick Peninsula, San Nicolás Bay, near Cabo Froward, XII Región. Seashore, 0-5 m a.s.l. 18/12/2009. Leg. *S. Pérez-Ortega*. Loc. 434-435	53° 50' 46" S	71° 7' 4" W	hap10	hap5	hap1	-	-	-	-
Mastodia sp.1/*Prasiola borealis*	I244b	Tierra del Fuego (Chile), Brunswick Peninsula, San Nicolás Bay, near Cabo Froward, XII Región. Seashore, 0-5 m a.s.l. 18/12/2009. Leg. *S. Pérez-Ortega*. Loc. 434-435	53° 50' 46" S	71° 7' 4" W	hap8	hap5	hap1	-	-	-	-
Mastodia sp.1/*Prasiola borealis*	I245dupl1	Tierra del Fuego (Chile), Brunswick Peninsula, San Nicolás Bay, near Cabo Froward, XII Región. Seashore, 0-5 m a.s.l. 18/12/2009. Leg. *S. Pérez-Ortega*. Loc. 434-435	53° 50' 46" S	71° 7' 4" W	hap8	hap11	hap1	-	-	-	-
Mastodia sp.1/*Prasiola borealis*	I245dupl2	Tierra del Fuego (Chile), Brunswick Peninsula, San Nicolás Bay, near Cabo Froward, XII Región. Seashore, 0-5 m a.s.l. 18/12/2009. Leg. *S. Pérez-Ortega*. Loc. 434-435	53° 50' 46" S	71° 7' 4" W	hap10	hap5	hap1	-	-	-	-
Mastodia sp.1/*Prasiola borealis*	I131	Tierra del Fuego (Chile), Brunswick Peninsula, San Nicolás Bay, near Cabo Froward, XII Región. Seashore, 0-5 m a.s.l. 18/12/2009. Leg. *S. Pérez-Ortega*. Loc. 434-435	53° 50' 46" S	71° 7' 4" W	hap9	hap5	hap1	-	-	-	-
Mastodia sp.1/*Prasiola borealis*	I132	Tierra del Fuego (Chile), Brunswick Peninsula, San Nicolás Bay, near Cabo Froward, XII Región. Seashore, 0-5 m a.s.l. 18/12/2009. Leg. *S. Pérez-Ortega*. Loc. 434-435	53° 50' 46" S	71° 7' 4" W	hap9	hap5	hap1	-	-	-	-
Mastodia sp.1/*Prasiola borealis*	I133dupl1	Tierra del Fuego (Chile), Brunswick Peninsula, San Nicolás Bay, near Cabo Froward, XII Región. Seashore, 0-5 m a.s.l. 18/12/2009. Leg. *S. Pérez-Ortega*. Loc. 434-435	53° 50' 46" S	71° 7' 4" W	hap8	hap11	hap1	-	-	-	-
Mastodia sp.1/*Prasiola borealis*	I133dupl2	Tierra del Fuego (Chile), Brunswick Peninsula, San Nicolás Bay, near Cabo Froward, XII Región. Seashore, 0-5 m a.s.l. 18/12/2009. Leg. *S. Pérez-Ortega*. Loc. 434-435	53° 50' 46" S	71° 7' 4" W	hap10	hap5	hap1	-	-	-	-
Mastodia sp.1/*Prasiola borealis*	I134	Tierra del Fuego (Chile), Brunswick Peninsula, San Nicolás Bay, near Cabo Froward, XII Región.	53° 50' 46" S	71° 7' 4" W	hap8	hap8	hap1	-	-	-	-

		Seashore, 0-5 m a.s.l. 18/12/2009. Leg. *S. Pérez-Ortega*. Loc. 434-435									
Mastodia sp.1/*Prasiola borealis*	I135	Tierra del Fuego (Chile), Brunswick Peninsula, San Nicolás Bay, near Cabo Froward, XII Región. Seashore, 0-5 m a.s.l. 18/12/2009. Leg. *S. Pérez-Ortega*. Loc. 434-435	53° 50' 46" S	71° 7' 4" W	hap8	hap5	hap1	-	-	-	-
Mastodia sp.1/*Prasiola borealis*	I136	Tierra del Fuego (Chile), Brunswick Peninsula, San Nicolás Bay, near Cabo Froward, XII Región. Seashore, 0-5 m a.s.l. 18/12/2009. Leg. *S. Pérez-Ortega*. Loc. 434-435	53° 50' 46" S	71° 7' 4" W	hap9	hap5	hap1	-	-	-	-
Mastodia sp.1/*Prasiola borealis*	I246dupl1	Tierra del Fuego (Chile), Brunswick Peninsula, San Nicolás Bay, near Cabo Froward, XII Región. Seashore, 0-5 m a.s.l. 18/12/2009. Leg. *S. Pérez-Ortega*. Loc. 434-435	53° 50' 46" S	71° 7' 4" W	hap8	hap11	hap1	-	-	-	-
Mastodia sp.1/*Prasiola borealis*	I246dupl2	Tierra del Fuego (Chile), Brunswick Peninsula, San Nicolás Bay, near Cabo Froward, XII Región. Seashore, 0-5 m a.s.l. 18/12/2009. Leg. *S. Pérez-Ortega*. Loc. 434-435	53° 50' 46" S	71° 7' 4" W	hap8	hap8	hap1	-	-	-	-
Mastodia sp.1/*Prasiola borealis*	I246b	Tierra del Fuego (Chile), Brunswick Peninsula, San Nicolás Bay, near Cabo Froward, XII Región. Seashore, 0-5 m a.s.l. 18/12/2009. Leg. *S. Pérez-Ortega*. Loc. 434-435	53° 50' 46" S	71° 7' 4" W	hap8	hap8	hap1	hap1	-	-	-
Mastodia sp.1/*Prasiola borealis*	I247dupl1	Tierra del Fuego (Chile), Brunswick Peninsula, San Nicolás Bay, near Cabo Froward, XII Región. Seashore, 0-5 m a.s.l. 18/12/2009. Leg. *S. Pérez-Ortega*. Loc. 434-435	53° 50' 46" S	71° 7' 4" W	hap8	hap11	hap1	-	-	-	-
Mastodia sp.1/*Prasiola borealis*	I247dupl2	Tierra del Fuego (Chile), Brunswick Peninsula, San Nicolás Bay, near Cabo Froward, XII Región. Seashore, 0-5 m a.s.l. 18/12/2009. Leg. *S. Pérez-Ortega*. Loc. 434-435	53° 50' 46" S	71° 7' 4" W	hap8	hap8	hap1	-	-	-	-
Mastodia sp.1/*Prasiola borealis*	I247-2	Tierra del Fuego (Chile), Brunswick Peninsula, San Nicolás Bay, near Cabo Froward, XII Región. Seashore, 0-5 m a.s.l. 18/12/2009. Leg. *S. Pérez-Ortega*. Loc. 434-435	53° 50' 46" S	71° 7' 4" W	hap8	hap8	hap1	-	-	-	-
Mastodia sp.1/*Prasiola borealis*	I248	Tierra del Fuego (Chile), Brunswick Peninsula, San Nicolás Bay, near Cabo Froward, XII Región. Seashore, 0-5 m a.s.l. 18/12/2009. Leg. *S. Pérez-Ortega*. Loc. 434-435	53° 50' 46" S	71° 7' 4" W	hap9	hap5	hap1	-	-	-	-
Mastodia sp.1/*Prasiola borealis*	I249	Tierra del Fuego (Chile), Brunswick Peninsula, San Nicolás Bay, near Cabo Froward, XII Región. Seashore, 0-5 m a.s.l. 18/12/2009. Leg. *S. Pérez-Ortega*. Loc. 434-435	53° 50' 46" S	71° 7' 4" W	hap9	hap5	hap1	-	-	-	-
Mastodia sp.1/*Prasiola borealis*	I249-2	Tierra del Fuego (Chile), Brunswick Peninsula, San Nicolás Bay, near Cabo Froward, XII Región.	53° 50' 46" S	71° 7' 4" W	hap8	hap5	hap1	-	-	-	-

		Seashore, 0-5 m a.s.l. 18/12/2009. Leg. *S. Pérez-Ortega.* Loc. 434-435									
Mastodia sp.1/*Prasiola borealis*	I249-3	Tierra del Fuego (Chile), Brunswick Peninsula, San Nicolás Bay, near Cabo Froward, XII Región. Seashore, 0-5 m a.s.l. 18/12/2009. Leg. *S. Pérez-Ortega.* Loc. 434-435	53° 50' 46" S	71° 7' 4" W	hap9	hap5	hap1	hap1	hap4	hap11	-
Mastodia sp.1/*Prasiola borealis*	I483	Tierra del Fuego (Chile), Brunswick Peninsula, San Nicolás Bay, near Cabo Froward, XII Región. Seashore, 0-5 m a.s.l. 18/12/2009. Leg. *S. Pérez-Ortega.* Loc. 434-435	53° 50' 46" S	71° 7' 4" W	-	-	-	hap1	hap4	hap4	hap3
Mastodia sp.1/*Prasiola borealis*	I484	Tierra del Fuego (Chile), Brunswick Peninsula, San Nicolás Bay, near Cabo Froward, XII Región. Seashore, 0-5 m a.s.l. 18/12/2009. Leg. *S. Pérez-Ortega.* Loc. 434-435	53° 50' 46" S	71° 7' 4" W	-	-	-	hap1	hap4	hap4	hap7
Mastodia sp.1/*Prasiola borealis*	I485	Tierra del Fuego (Chile), Brunswick Peninsula, San Nicolás Bay, near Cabo Froward, XII Región. Seashore, 0-5 m a.s.l. 18/12/2009. Leg. *S. Pérez-Ortega.* Loc. 434-435	53° 50' 46" S	71° 7' 4" W	-	-	-	hap1	hap4	-	hap3
Mastodia sp.1/*Prasiola borealis*	I486	Tierra del Fuego (Chile), Brunswick Peninsula, San Nicolás Bay, near Cabo Froward, XII Región. Seashore, 0-5 m a.s.l. 18/12/2009. Leg. *S. Pérez-Ortega.* Loc. 434-435	53° 50' 46" S	71° 7' 4" W	-	-	-	hap1	hap4	hap4	hap8
Mastodia sp.1/*Prasiola borealis*	I487	Tierra del Fuego (Chile), Brunswick Peninsula, San Nicolás Bay, near Cabo Froward, XII Región. Seashore, 0-5 m a.s.l. 18/12/2009. Leg. *S. Pérez-Ortega.* Loc. 434-435	53° 50' 46" S	71° 7' 4" W	-	-	-	hap1	hap4	hap11	hap3
Mastodia sp.1/*Prasiola borealis*	I127	Tierra del Fuego (Chile), Beagle Channel, Basket Island, XII Región. Seashore, 0-5 m a.s.l. 17/12/2009. Leg. *S. Pérez-Ortega.* Loc. 432-433	54° 42' 13" S	71° 34' 53" W	hap8	hap5	hap2	hap1	hap4	hap4	-
Mastodia sp.1/*Prasiola borealis*	I128	Tierra del Fuego (Chile), Beagle Channel, Basket Island, XII Región. Seashore, 0-5 m a.s.l. 17/12/2009. Leg. *S. Pérez-Ortega.* Loc. 432-433	54° 42' 13" S	71° 34' 53" W	hap8	hap5	hap3	hap1	-	hap4	-
Mastodia sp.1/*Prasiola borealis*	I129dupl1	Tierra del Fuego (Chile), Beagle Channel, Basket Island, XII Región. Seashore, 0-5 m a.s.l. 17/12/2009. Leg. *S. Pérez-Ortega.* Loc. 432-433	54° 42' 13" S	71° 34' 53" W	hap9	hap5	hap2	-	-	-	-
Mastodia sp.1/*Prasiola borealis*	I129dupl2	Tierra del Fuego (Chile), Beagle Channel, Basket Island, XII Región. Seashore, 0-5 m a.s.l. 17/12/2009. Leg. *S. Pérez-Ortega.* Loc. 432-433	54° 42' 13" S	71° 34' 53" W	hap8	hap5	hap2	-	-	-	-
Mastodia sp.1/*Prasiola borealis*	I232	Tierra del Fuego (Chile), Beagle Channel, Basket Island, XII Región. Seashore, 0-5 m a.s.l. 17/12/2009. Leg. *S. Pérez-Ortega.* Loc. 432-433	54° 42' 13" S	71° 34' 53" W	hap7	hap9	hap3	hap1	-	-	hap3
Mastodia sp.1/*Prasiola borealis*	I233	Tierra del Fuego (Chile), Beagle Channel, Basket Island, XII Región. Seashore, 0-5 m a.s.l. 17/12/2009. Leg. *S. Pérez-Ortega.* Loc. 432-433	54° 42' 13" S	71° 34' 53" W	hap7	hap5	hap3	hap1	-	hap7	hap4

Mastodia sp.1/*Prasiola borealis*	I234	Tierra del Fuego (Chile), Beagle Channel, Basket Island, XII Región. Seashore, 0-5 m a.s.l. 17/12/2009. Leg. *S. Pérez-Ortega.* Loc. 432-433	54° 42' 13" S	71° 34' 53" W	hap8	hap5	hap3	-	-	-	-
Mastodia sp.1/*Prasiola borealis*	I234-2_dupl1	Tierra del Fuego (Chile), Beagle Channel, Basket Island, XII Región. Seashore, 0-5 m a.s.l. 17/12/2009. Leg. *S. Pérez-Ortega.* Loc. 432-433	54° 42' 13" S	71° 34' 53" W	hap8	hap5	hap3	hap1	-	hap7	hap4
Mastodia sp.1/*Prasiola borealis*	I234-2_dupl2	Tierra del Fuego (Chile), Beagle Channel, Basket Island, XII Región. Seashore, 0-5 m a.s.l. 17/12/2009. Leg. *S. Pérez-Ortega.* Loc. 432-433	54° 42' 13" S	71° 34' 53" W	hap10	hap5	hap1	-	-	-	-
Mastodia sp.1/*Prasiola borealis*	I235	Tierra del Fuego (Chile), Beagle Channel, Basket Island, XII Región. Seashore, 0-5 m a.s.l. 17/12/2009. Leg. *S. Pérez-Ortega.* Loc. 432-433	54° 42' 13" S	71° 34' 53" W	hap7	hap9	hap3	-	-	-	-
Mastodia sp.1/*Prasiola borealis*	I236dupl1	Tierra del Fuego (Chile), Beagle Channel, Basket Island, XII Región. Seashore, 0-5 m a.s.l. 17/12/2009. Leg. *S. Pérez-Ortega.* Loc. 432-433	54° 42' 13" S	71° 34' 53" W	hap8	hap5	hap2	-	-	-	-
Mastodia sp.1/*Prasiola borealis*	I236dupl2	Tierra del Fuego (Chile), Beagle Channel, Basket Island, XII Región. Seashore, 0-5 m a.s.l. 17/12/2009. Leg. *S. Pérez-Ortega.* Loc. 432-433	54° 42' 13" S	71° 34' 53" W	hap8	hap5	hap1	-	-	-	-
Mastodia sp.1/*Prasiola borealis*	I237dupl1	Tierra del Fuego (Chile), Beagle Channel, Basket Island, XII Región. Seashore, 0-5 m a.s.l. 17/12/2009. Leg. *S. Pérez-Ortega.* Loc. 432-433	54° 42' 13" S	71° 34' 53" W	hap8	hap5	hap2	-	-	-	-
Mastodia sp.1/*Prasiola borealis*	I237dupl2	Tierra del Fuego (Chile), Beagle Channel, Basket Island, XII Región. Seashore, 0-5 m a.s.l. 17/12/2009. Leg. *S. Pérez-Ortega.* Loc. 432-433	54° 42' 13" S	71° 34' 53" W	hap9	hap5	hap2	-	-	-	-
Mastodia sp.1/*Prasiola borealis*	I237b	Tierra del Fuego (Chile), Beagle Channel, Basket Island, XII Región. Seashore, 0-5 m a.s.l. 17/12/2009. Leg. *S. Pérez-Ortega.* Loc. 432-433	54° 42' 13" S	71° 34' 53" W	hap6	hap5	hap4	hap1	-	-	hap5
Mastodia sp.1/*Prasiola borealis*	I238	Tierra del Fuego (Chile), Beagle Channel, Basket Island, XII Región. Seashore, 0-5 m a.s.l. 17/12/2009. Leg. *S. Pérez-Ortega.* Loc. 432-433	54° 42' 13" S	71° 34' 53" W	hap9	hap5	hap2	-	-	-	-
Mastodia sp.1/*Prasiola borealis*	I238b	Tierra del Fuego (Chile), Beagle Channel, Basket Island, XII Región. Seashore, 0-5 m a.s.l. 17/12/2009. Leg. *S. Pérez-Ortega.* Loc. 432-433	54° 42' 13" S	71° 34' 53" W	hap8	hap5	hap2	-	-	-	-
Mastodia sp.1/*Prasiola borealis*	I239	Tierra del Fuego (Chile), Beagle Channel, Basket Island, XII Región. Seashore, 0-5 m a.s.l. 17/12/2009. Leg. *S. Pérez-Ortega.* Loc. 432-433	54° 42' 13" S	71° 34' 53" W	hap9	hap5	hap2	-	-	-	-
Mastodia sp.1/*Prasiola borealis*	I240	Tierra del Fuego (Chile), Beagle Channel, Basket Island, XII Región. Seashore, 0-5 m a.s.l. 17/12/2009. Leg. *S. Pérez-Ortega.* Loc. 432-433	54° 42' 13" S	71° 34' 53" W	hap6	hap5	hap2	hap1	-	hap11	hap5
Mastodia sp.1/*Prasiola borealis*	I478	Tierra del Fuego (Chile), Beagle Channel, Basket Island, XII Región. Seashore, 0-5 m a.s.l. 17/12/2009. Leg. *S. Pérez-Ortega.* Loc. 432-433	54° 42' 13" S	71° 34' 53" W	-	-	-	hap1	hap4	hap4	hap3
Mastodia sp.1/*Prasiola borealis*	I479	Tierra del Fuego (Chile), Beagle Channel, Basket Island, XII Región. Seashore, 0-5 m a.s.l.	54° 42' 13" S	71° 34' 53" W	-	-	-	hap1	hap4	hap4	hap6

		17/12/2009. Leg. *S. Pérez-Ortega*. Loc. 432-433									
Mastodia sp.1/*Prasiola borealis*	I480	Tierra del Fuego (Chile), Beagle Channel, Basket Island, XII Región. Seashore, 0-5 m a.s.l. 17/12/2009. Leg. *S. Pérez-Ortega*. Loc. 432-433	54° 42' 13" S	71° 34' 53" W	-	-	-	hap1	hap4	hap4	hap3
Mastodia sp.1/*Prasiola borealis*	I481	Tierra del Fuego (Chile), Beagle Channel, Basket Island, XII Región. Seashore, 0-5 m a.s.l. 17/12/2009. Leg. *S. Pérez-Ortega*. Loc. 432-433	54° 42' 13" S	71° 34' 53" W	-	-	-	hap1	hap4	hap7	hap4
Mastodia sp.1/*Prasiola borealis*	I482	Tierra del Fuego (Chile), Beagle Channel, Basket Island, XII Región. Seashore, 0-5 m a.s.l. 17/12/2009. Leg. *S. Pérez-Ortega*. Loc. 432-433	54° 42' 13" S	71° 34' 53" W	-	-	-	hap1	hap4	hap11	hap5
Mastodia sp.1/*Prasiola borealis*	I137	Tierra del Fuego (Chile), Beagle Channel, Darwin Bay, Chair Island, XII Región. Seashore, 0-5 m a.s.l. 16/12/2009. Leg. *S. Pérez-Ortega*. Loc. 429-431	54° 54' 2" S	70° 00' 30" W	hap9	hap5	hap1	hap1	-	hap6	hap9
Mastodia sp.1/*Prasiola borealis*	I138	Tierra del Fuego (Chile), Beagle Channel, Darwin Bay, Chair Island, XII Región. Seashore, 0-5 m a.s.l. 16/12/2009. Leg. *S. Pérez-Ortega*. Loc. 429-431	54° 54' 2" S	70° 00' 30" W	hap9	hap5	hap2	hap1	-	hap8	hap10
Mastodia sp.1/*Prasiola borealis*	I224	Tierra del Fuego (Chile), Beagle Channel, Darwin Bay, Chair Island, XII Región. Seashore, 0-5 m a.s.l. 16/12/2009. Leg. *S. Pérez-Ortega*. Loc. 429-431	54° 54' 2" S	70° 00' 30" W	hap8	hap5	hap1	-	-	-	-
Mastodia sp.1/*Prasiola borealis*	I224b	Tierra del Fuego (Chile), Beagle Channel, Darwin Bay, Chair Island, XII Región. Seashore, 0-5 m a.s.l. 16/12/2009. Leg. *S. Pérez-Ortega*. Loc. 429-431	54° 54' 2" S	70° 00' 30" W	hap9	hap5	hap1	-	-	-	-
Mastodia sp.1/*Prasiola borealis*	I225	Tierra del Fuego (Chile), Beagle Channel, Darwin Bay, Chair Island, XII Región. Seashore, 0-5 m a.s.l. 16/12/2009. Leg. *S. Pérez-Ortega*. Loc. 429-431	54° 54' 2" S	70° 00' 30" W	hap8	hap7	hap2	-	-	-	-
Mastodia sp.1/*Prasiola borealis*	I226dupl2	Tierra del Fuego (Chile), Beagle Channel, Darwin Bay, Chair Island, XII Región. Seashore, 0-5 m a.s.l. 16/12/2009. Leg. *S. Pérez-Ortega*. Loc. 429-431	54° 54' 2" S	70° 00' 30" W	hap8	hap5	hap1	-	-	-	-
Mastodia sp.1/*Prasiola borealis*	I227	Tierra del Fuego (Chile), Beagle Channel, Darwin Bay, Chair Island, XII Región. Seashore, 0-5 m a.s.l. 16/12/2009. Leg. *S. Pérez-Ortega*. Loc. 429-431	54° 54' 2" S	70° 00' 30" W	hap8	hap7	hap2	-	-	-	-
Mastodia sp.1/*Prasiola borealis*	I228	Tierra del Fuego (Chile), Beagle Channel, Darwin Bay, Chair Island, XII Región. Seashore, 0-5 m a.s.l. 16/12/2009. Leg. *S. Pérez-Ortega*. Loc. 429-431	54° 54' 2" S	70° 00' 30" W	hap8	hap7	hap2	-	-	-	-
Mastodia sp.1/*Prasiola borealis*	I228b	Tierra del Fuego (Chile), Beagle Channel, Darwin Bay, Chair Island, XII Región. Seashore, 0-5 m a.s.l. 16/12/2009. Leg. *S. Pérez-Ortega*. Loc. 429-431	54° 54' 2" S	70° 00' 30" W	hap8	hap7	hap2	-	-	-	-
Mastodia sp.1/*Prasiola borealis*	I229	Tierra del Fuego (Chile), Beagle Channel, Darwin Bay, Chair Island, XII Región. Seashore, 0-5 m a.s.l. 16/12/2009. Leg. *S. Pérez-Ortega*. Loc. 429-431	54° 54' 2" S	70° 00' 30" W	hap9	hap5	hap1	-	-	-	-
Mastodia sp.1/*Prasiola borealis*	I230	Tierra del Fuego (Chile), Beagle Channel, Darwin Bay, Chair Island, XII Región. Seashore, 0-5 m a.s.l. 16/12/2009. Leg. *S. Pérez-Ortega*. Loc. 429-431	54° 54' 2" S	70° 00' 30" W	hap9	hap5	hap1	-	-	-	-

Mastodia sp.1/*Prasiola borealis*	I231	Tierra del Fuego (Chile), Beagle Channel, Darwin Bay, Chair Island, XII Región. Seashore, 0-5 m a.s.l. 16/12/2009. Leg. *S. Pérez-Ortega.* Loc. 429-431	54° 54' 2" S	70° 00' 30" W	hap9	hap5	hap1	-	-	-	-
Mastodia sp.1/*Prasiola borealis*	I219	Tierra del Fuego (Chile), Beagle Channel, Darwin Bay, Chair Island, XII Región. Seashore, 0-5 m a.s.l. 16/12/2009. Leg. *S. Pérez-Ortega.* Loc. 429-431	54° 54' 2" S	70° 00' 30" W	hap8	hap5	hap1	-	-	-	-
Mastodia sp.1/*Prasiola borealis*	I220	Tierra del Fuego (Chile), Beagle Channel, Darwin Bay, Chair Island, XII Región. Seashore, 0-5 m a.s.l. 16/12/2009. Leg. *S. Pérez-Ortega.* Loc. 429-431	54° 54' 2" S	70° 00' 30" W	hap10	hap5	hap1	-	-	-	-
Mastodia sp.1/*Prasiola borealis*	I221	Tierra del Fuego (Chile), Beagle Channel, Darwin Bay, Chair Island, XII Región. Seashore, 0-5 m a.s.l. 16/12/2009. Leg. *S. Pérez-Ortega.* Loc. 429-431	54° 54' 2" S	70° 00' 30" W	hap9	hap5	hap1	hap1	-	hap7	hap4
Mastodia sp.1/*Prasiola borealis*	I221-2	Tierra del Fuego (Chile), Beagle Channel, Darwin Bay, Chair Island, XII Región. Seashore, 0-5 m a.s.l. 16/12/2009. Leg. *S. Pérez-Ortega.* Loc. 429-431	54° 54' 2" S	70° 00' 30" W	hap8	hap5	hap2	-	-	-	-
Mastodia sp.1/*Prasiola borealis*	I222	Tierra del Fuego (Chile), Beagle Channel, Darwin Bay, Chair Island, XII Región. Seashore, 0-5 m a.s.l. 16/12/2009. Leg. *S. Pérez-Ortega.* Loc. 429-431	54° 54' 2" S	70° 00' 30" W	hap8	hap5	hap1	hap1	hap4	hap7	hap4
Mastodia sp.1/*Prasiola borealis*	I222-2	Tierra del Fuego (Chile), Beagle Channel, Darwin Bay, Chair Island, XII Región. Seashore, 0-5 m a.s.l. 16/12/2009. Leg. *S. Pérez-Ortega.* Loc. 429-431	54° 54' 2" S	70° 00' 30" W	hap8	hap5	hap1	-	-	-	-
Mastodia sp.1/*Prasiola borealis*	I222-3	Tierra del Fuego (Chile), Beagle Channel, Darwin Bay, Chair Island, XII Región. Seashore, 0-5 m a.s.l. 16/12/2009. Leg. *S. Pérez-Ortega.* Loc. 429-431	54° 54' 2" S	70° 00' 30" W	hap8	hap5	hap1	-	-	-	-
Mastodia sp.1/*Prasiola borealis*	I223	Tierra del Fuego (Chile), Beagle Channel, Darwin Bay, Chair Island, XII Región. Seashore, 0-5 m a.s.l. 16/12/2009. Leg. *S. Pérez-Ortega.* Loc. 429-431	54° 54' 2" S	70° 00' 30" W	hap8	hap5	hap1	hap1	-	-	hap4
Mastodia sp.1/*Prasiola borealis*	I223-2	Tierra del Fuego (Chile), Beagle Channel, Darwin Bay, Chair Island, XII Región. Seashore, 0-5 m a.s.l. 16/12/2009. Leg. *S. Pérez-Ortega.* Loc. 429-431	54° 54' 2" S	70° 00' 30" W	hap8	hap5	hap1	-	-	-	-
Mastodia sp.1/*Prasiola borealis*	I341	Tierra del Fuego (Chile), Beagle Channel, Darwin Bay, Chair Island, XII Región. Seashore, 0-5 m a.s.l. 16/12/2009. Leg. *S. Pérez-Ortega.* Loc. 429-431	54° 54' 2" S	70° 00' 30" W	hap8	hap5	hap1	-	-	-	-
Mastodia sp.1/*Prasiola borealis*	I488	Tierra del Fuego (Chile), Beagle Channel, Darwin Bay, Chair Island, XII Región. Seashore, 0-5 m a.s.l. 16/12/2009. Leg. *S. Pérez-Ortega.* Loc. 429-431	54° 54' 2" S	70° 00' 30" W	-	-	-	hap1	hap4	hap6	hap9
Mastodia sp.1/*Prasiola borealis*	I489	Tierra del Fuego (Chile), Beagle Channel, Darwin Bay, Chair Island, XII Región. Seashore, 0-5 m a.s.l. 16/12/2009. Leg. *S. Pérez-Ortega.* Loc. 429-431	54° 54' 2" S	70° 00' 30" W	-	-	-	hap1	hap4	hap6	hap9
Mastodia sp.1/*Prasiola borealis*	I490	Tierra del Fuego (Chile), Beagle Channel, Darwin Bay, Chair Island, XII Región. Seashore, 0-5 m a.s.l. 16/12/2009. Leg. *S. Pérez-Ortega.* Loc. 429-431	54° 54' 2" S	70° 00' 30" W	-	-	-	hap1	-	hap6	hap4
Mastodia sp.1/*Prasiola borealis*	I491	Tierra del Fuego (Chile), Beagle Channel, Darwin Bay, Chair Island, XII Región. Seashore, 0-5 m a.s.l.	54° 54' 2" S	70° 00' 30" W	-	-	-	hap1	hap4	hap8	hap10

		16/12/2009. Leg. *S. Pérez-Ortega.* Loc. 429-431									
Mastodia sp.1/*Prasiola borealis*	I492	Tierra del Fuego (Chile), Beagle Channel, Darwin Bay, Chair Island, XII Región. Seashore, 0-5 m a.s.l. 16/12/2009. Leg. *S. Pérez-Ortega.* Loc. 429-431	54° 54' 2" S	70° 00' 30" W	-	-	-	hap1	hap4	-	hap4
Mastodia sp.1/*Prasiola borealis*	I493	Tierra del Fuego (Chile), Beagle Channel, Darwin Bay, Chair Island, XII Región. Seashore, 0-5 m a.s.l. 16/12/2009. Leg. *S. Pérez-Ortega.* Loc. 429-431	54° 54' 2" S	70° 00' 30" W	-	-	-	hap1	hap4	hap7	hap4
Mastodia sp.1/*Prasiola borealis*	I139	Tierra del Fuego (Chile), Beagle Channel, Picton Island, XII Región. Seashore, 0-5 m a.s.l. 23/1/2008. Leg. *S. Pérez-Ortega.* Loc. 222	55° 1' 10" S	66° 55' 39" W	hap11	hap10	hap1	hap1	-	hap5	-
Mastodia sp.1/*Prasiola borealis*	I140	Tierra del Fuego (Chile), Beagle Channel, Picton Island, XII Región. Seashore, 0-5 m a.s.l. 23/1/2008. Leg. *S. Pérez-Ortega.* Loc. 222	55° 1' 10" S	66° 55' 39" W	hap11	hap10	hap1	-	-	-	-
Mastodia sp.1/*Prasiola borealis*	I141	Tierra del Fuego (Chile), Beagle Channel, Picton Island, XII Región. Seashore, 0-5 m a.s.l. 23/1/2008. Leg. *S. Pérez-Ortega.* Loc. 222	55° 1' 10" S	66° 55' 39" W	hap11	hap10	hap1	-	-	-	-
Mastodia sp.1/*Prasiola borealis*	I142	Tierra del Fuego (Chile), Beagle Channel, Picton Island, XII Región. Seashore, 0-5 m a.s.l. 23/1/2008. Leg. *S. Pérez-Ortega.* Loc. 222	55° 1' 10" S	66° 55' 39" W	hap11	hap10	hap1	hap1	-	-	-
Mastodia sp.1/*Prasiola borealis*	I143dupl1	Tierra del Fuego (Chile), Beagle Channel, Picton Island, XII Región. Seashore, 0-5 m a.s.l. 23/1/2008. Leg. *S. Pérez-Ortega.* Loc. 222	55° 1' 10" S	66° 55' 39" W	hap11	hap5	hap1	hap1	-	-	-
Mastodia sp.1/*Prasiola borealis*	I143dupl2	Tierra del Fuego (Chile), Beagle Channel, Picton Island, XII Región. Seashore, 0-5 m a.s.l. 23/1/2008. Leg. *S. Pérez-Ortega.* Loc. 222	55° 1' 10" S	66° 55' 39" W	hap11	hap10	hap1	-	-	-	-
Mastodia sp.1/*Prasiola borealis*	I144	Tierra del Fuego (Chile), Beagle Channel, Picton Island, XII Región. Seashore, 0-5 m a.s.l. 23/1/2008. Leg. *S. Pérez-Ortega.* Loc. 222	55° 1' 10" S	66° 55' 39" W	hap11	hap10	hap1	-	-	-	-
Mastodia sp.1/*Prasiola borealis*	I145dupl1	Tierra del Fuego (Chile), Beagle Channel, Picton Island, XII Región. Seashore, 0-5 m a.s.l. 23/1/2008. Leg. *S. Pérez-Ortega.* Loc. 222	55° 1' 10" S	66° 55' 39" W	hap11	hap10	hap6	hap1	hap4	-	hap11
Mastodia sp.1/*Prasiola borealis*	I145dupl2	Tierra del Fuego (Chile), Beagle Channel, Picton Island, XII Región. Seashore, 0-5 m a.s.l. 23/1/2008. Leg. *S. Pérez-Ortega.* Loc. 222	55° 1' 10" S	66° 55' 39" W	hap11	hap10	hap1	-	-	-	-
Mastodia sp.1/*Prasiola borealis*	I146	Tierra del Fuego (Chile), Beagle Channel, Picton Island, XII Región. Seashore, 0-5 m a.s.l. 23/1/2008. Leg. *S. Pérez-Ortega.* Loc. 222	55° 1' 10" S	66° 55' 39" W	hap11	hap10	hap1	-	-	-	-
Mastodia sp.1/*Prasiola borealis*	I147	Tierra del Fuego (Chile), Beagle Channel, Picton Island, XII Región. Seashore, 0-5 m a.s.l. 23/1/2008. Leg. *S. Pérez-Ortega.* Loc. 222	55° 1' 10" S	66° 55' 39" W	hap11	hap10	hap1	hap1	-	-	-
Mastodia sp.1/*Prasiola borealis*	I148	Tierra del Fuego (Chile), Beagle Channel, Picton Island, XII Región. Seashore, 0-5 m a.s.l. 23/1/2008. Leg. *S. Pérez-Ortega.* Loc. 222	55° 1' 10" S	66° 55' 39" W	hap11	hap10	hap1	hap1	-	-	-

Mastodia sp.1/*Prasiola borealis*	I148-2	Tierra del Fuego (Chile), Beagle Channel, Picton Island, XII Región. Seashore, 0-5 m a.s.l. 23/1/2008. Leg. *S. Pérez-Ortega.* Loc. 222	55° 1' 10" S	66° 55' 39" W	hap11	hap10	hap1	-	-	-	-
Mastodia sp.1/*Prasiola borealis*	I208	Tierra del Fuego (Chile), Beagle Channel, Picton Island, XII Región. Seashore, 0-5 m a.s.l. 23/1/2008. Leg. *S. Pérez-Ortega.* Loc. 222	55° 1' 10" S	66° 55' 39" W	hap11	hap10	hap6	hap1	-	-	-
Mastodia sp.1/*Prasiola borealis*	I209	Tierra del Fuego (Chile), Beagle Channel, Picton Island, XII Región. Seashore, 0-5 m a.s.l. 23/1/2008. Leg. *S. Pérez-Ortega.* Loc. 222	55° 1' 10" S	66° 55' 39" W	hap11	hap10	hap1	hap1	-	-	-
Mastodia sp.1/*Prasiola borealis*	I210	Tierra del Fuego (Chile), Beagle Channel, Picton Island, XII Región. Seashore, 0-5 m a.s.l. 23/1/2008. Leg. *S. Pérez-Ortega.* Loc. 222	55° 1' 10" S	66° 55' 39" W	hap11	hap10	hap1	hap1	-	-	hap12
Mastodia sp.1/*Prasiola borealis*	I212dupl1	Tierra del Fuego (Chile), Beagle Channel, Picton Island, XII Región. Seashore, 0-5 m a.s.l. 23/1/2008. Leg. *S. Pérez-Ortega.* Loc. 222	55° 1' 10" S	66° 55' 39" W	hap11	hap10	hap6	-	-	-	-
Mastodia sp.1/*Prasiola borealis*	I212dupl2	Tierra del Fuego (Chile), Beagle Channel, Picton Island, XII Región. Seashore, 0-5 m a.s.l. 23/1/2008. Leg. *S. Pérez-Ortega.* Loc. 222	55° 1' 10" S	66° 55' 39" W	hap11	hap5	hap6	-	-	-	-
Mastodia sp.1/*Prasiola borealis*	I213	Tierra del Fuego (Chile), Beagle Channel, Picton Island, XII Región. Seashore, 0-5 m a.s.l. 23/1/2008. Leg. *S. Pérez-Ortega.* Loc. 222	55° 1' 10" S	66° 55' 39" W	hap11	hap10	hap6	hap1	hap4	-	-
Mastodia sp.1/*Prasiola borealis*	I214	Tierra del Fuego (Chile), Beagle Channel, Picton Island, XII Región. Seashore, 0-5 m a.s.l. 23/1/2008. Leg. *S. Pérez-Ortega.* Loc. 222	55° 1' 10" S	66° 55' 39" W	hap11	hap10	hap1	-	-	-	-
Mastodia sp.1/*Prasiola borealis*	I215	Tierra del Fuego (Chile), Beagle Channel, Picton Island, XII Región. Seashore, 0-5 m a.s.l. 23/1/2008. Leg. *S. Pérez-Ortega.* Loc. 222	55° 1' 10" S	66° 55' 39" W	hap11	hap10	hap1	-	-	-	-
Mastodia sp.1/*Prasiola borealis*	I215-2	Tierra del Fuego (Chile), Beagle Channel, Picton Island, XII Región. Seashore, 0-5 m a.s.l. 23/1/2008. Leg. *S. Pérez-Ortega.* Loc. 222	55° 1' 10" S	66° 55' 39" W	hap11	hap10	hap1	-	-	-	-
Mastodia sp.1/*Prasiola borealis*	I340	Tierra del Fuego (Chile), Beagle Channel, Picton Island, XII Región. Seashore, 0-5 m a.s.l. 23/1/2008. Leg. *S. Pérez-Ortega.* Loc. 222	55° 1' 10" S	66° 55' 39" W	hap11	hap10	hap1	-	-	-	-
Mastodia sp.1/*Prasiola borealis*	I494	Tierra del Fuego (Chile), Beagle Channel, Picton Island, XII Región. Seashore, 0-5 m a.s.l. 23/1/2008. Leg. *S. Pérez-Ortega.* Loc. 222	55° 1' 10" S	66° 55' 39" W	-	-	-	hap1	hap4	-	-
Mastodia sp.1/*Prasiola borealis*	I495	Tierra del Fuego (Chile), Beagle Channel, Picton Island, XII Región. Seashore, 0-5 m a.s.l. 23/1/2008. Leg. *S. Pérez-Ortega.* Loc. 222	55° 1' 10" S	66° 55' 39" W	-	-	-	hap1	hap4	-	-
Mastodia sp.1/*Prasiola borealis*	I496	Tierra del Fuego (Chile), Beagle Channel, Picton Island, XII Región. Seashore, 0-5 m a.s.l. 23/1/2008. Leg. *S. Pérez-Ortega.* Loc. 222	55° 1' 10" S	66° 55' 39" W	-	-	-	hap1	hap4	-	-
Mastodia sp.1/*Prasiola borealis*	I497	Tierra del Fuego (Chile), Beagle Channel, Picton Island, XII Región. Seashore, 0-5 m a.s.l. 23/1/2008.	55° 1' 10" S	66° 55' 39" W	-	-	-	hap1	hap4	hap5	-

		Leg. *S. Pérez-Ortega.* Loc. 222									
Mastodia sp.1/*Prasiola borealis*	I498	Tierra del Fuego (Chile), Beagle Channel, Picton Island, XII Región. Seashore, 0-5 m a.s.l. 23/1/2008. Leg. *S. Pérez-Ortega.* Loc. 222	55° 1' 10" S	66° 55' 39" W	-	-	-	hap1	-	-	-
Mastodia sp.1/*Prasiola borealis*	I216	Tierra del Fuego (Chile), Beagle Channel, Róbalo Bay, Navarino Island, XII Región. Seashore, 0-5 m a.s.l. 25/1/2008. Leg. *S. Pérez-Ortega.* Loc. 223	54° 56' 4" S	67° 40' 34" W	hap11	hap10	hap1	hap1	hap4	hap9	-
Mastodia sp.1/*Prasiola borealis*	I217	Tierra del Fuego (Chile), Beagle Channel, Róbalo Bay, Navarino Island, XII Región. Seashore, 0-5 m a.s.l. 25/1/2008. Leg. *S. Pérez-Ortega.* Loc. 223	54° 56' 4" S	67° 40' 34" W	hap11	hap10	hap6	hap1	-	-	-
Mastodia sp.1/*Prasiola borealis*	I217-2_dupl1	Tierra del Fuego (Chile), Beagle Channel, Róbalo Bay, Navarino Island, XII Región. Seashore, 0-5 m a.s.l. 25/1/2008. Leg. *S. Pérez-Ortega.* Loc. 223	54° 56' 4" S	67° 40' 34" W	hap11	hap5	hap6	-	-	-	-
Mastodia sp.1/*Prasiola borealis*	I217-2_dupl2	Tierra del Fuego (Chile), Beagle Channel, Róbalo Bay, Navarino Island, XII Región. Seashore, 0-5 m a.s.l. 25/1/2008. Leg. *S. Pérez-Ortega.* Loc. 223	54° 56' 4" S	67° 40' 34" W	hap11	hap10	hap6	-	-	-	-
Mastodia sp.1/*Prasiola borealis*	I218	Tierra del Fuego (Chile), Beagle Channel, Róbalo Bay, Navarino Island, XII Región. Seashore, 0-5 m a.s.l. 25/1/2008. Leg. *S. Pérez-Ortega.* Loc. 223	54° 56' 4" S	67° 40' 34" W	hap11	hap10	hap1	hap1	-	-	-
Mastodia sp.1/*Prasiola borealis*	I149	Tierra del Fuego (Chile), Beagle Channel, Róbalo Bay, Navarino Island, XII Región. Seashore, 0-5 m a.s.l. 25/1/2008. Leg. *S. Pérez-Ortega.* Loc. 223	54° 56' 4" S	67° 40' 34" W	hap11	hap10	hap6	-	-	-	-
Mastodia sp.1/*Prasiola borealis*	I150	Tierra del Fuego (Chile), Beagle Channel, Róbalo Bay, Navarino Island, XII Región. Seashore, 0-5 m a.s.l. 25/1/2008. Leg. *S. Pérez-Ortega.* Loc. 223	54° 56' 4" S	67° 40' 34" W	hap11	hap5	hap6	-	-	-	-
Mastodia sp.1/*Prasiola borealis*	I151	Tierra del Fuego (Chile), Beagle Channel, Róbalo Bay, Navarino Island, XII Región. Seashore, 0-5 m a.s.l. 25/1/2008. Leg. *S. Pérez-Ortega.* Loc. 223	54° 56' 4" S	67° 40' 34" W	hap11	hap10	hap1	-	-	-	-
Mastodia sp.1/*Prasiola borealis*	I152dupl1	Tierra del Fuego (Chile), Beagle Channel, Róbalo Bay, Navarino Island, XII Región. Seashore, 0-5 m a.s.l. 25/1/2008. Leg. *S. Pérez-Ortega.* Loc. 223	54° 56' 4" S	67° 40' 34" W	hap11	hap10	hap6	-	-	-	-
Mastodia sp.1/*Prasiola borealis*	I152dupl2	Tierra del Fuego (Chile), Beagle Channel, Róbalo Bay, Navarino Island, XII Región. Seashore, 0-5 m a.s.l. 25/1/2008. Leg. *S. Pérez-Ortega.* Loc. 223	54° 56' 4" S	67° 40' 34" W	hap11	hap5	hap6	-	-	-	-
Mastodia sp.1/*Prasiola borealis*	I153dupl1	Tierra del Fuego (Chile), Beagle Channel, Róbalo Bay, Navarino Island, XII Región. Seashore, 0-5 m a.s.l. 25/1/2008. Leg. *S. Pérez-Ortega.* Loc. 223	54° 56' 4" S	67° 40' 34" W	hap11	hap10	hap1	-	-	-	-
Mastodia sp.1/*Prasiola borealis*	I153dupl2	Tierra del Fuego (Chile), Beagle Channel, Róbalo Bay, Navarino Island, XII Región. Seashore, 0-5 m a.s.l. 25/1/2008. Leg. *S. Pérez-Ortega.* Loc. 223	54° 56' 4" S	67° 40' 34" W	hap11	hap5	hap1	-	-	-	-
Mastodia sp.1/*Prasiola borealis*	I153b	Tierra del Fuego (Chile), Beagle Channel, Róbalo Bay, Navarino Island, XII Región. Seashore, 0-5 m a.s.l. 25/1/2008. Leg. *S. Pérez-Ortega.* Loc. 223	54° 56' 4" S	67° 40' 34" W	hap11	hap10	hap1	hap1	hap4	hap9	-

Mastodia sp.1/*Prasiola borealis*	I154	Tierra del Fuego (Chile), Beagle Channel, Róbalo Bay, Navarino Island, XII Región. Seashore, 0-5 m a.s.l. 25/1/2008. Leg. *S. Pérez-Ortega.* Loc. 223	54° 56' 4" S	67° 40' 34" W	hap11	hap10	hap6	-	-	-	-
Mastodia sp.1/*Prasiola borealis*	I155	Tierra del Fuego (Chile), Beagle Channel, Róbalo Bay, Navarino Island, XII Región. Seashore, 0-5 m a.s.l. 25/1/2008. Leg. *S. Pérez-Ortega.* Loc. 223	54° 56' 4" S	67° 40' 34" W	hap11	hap10	hap1	hap1	-	-	-
Mastodia sp.1/*Prasiola borealis*	I499	Tierra del Fuego (Chile), Beagle Channel, Róbalo Bay, Navarino Island, XII Región. Seashore, 0-5 m a.s.l. 25/1/2008. Leg. *S. Pérez-Ortega.* Loc. 223	54° 56' 4" S	67° 40' 34" W	-	-	-	hap1	hap4	hap10	hap11
Mastodia sp.1/*Prasiola borealis*	I500	Tierra del Fuego (Chile), Beagle Channel, Róbalo Bay, Navarino Island, XII Región. Seashore, 0-5 m a.s.l. 25/1/2008. Leg. *S. Pérez-Ortega.* Loc. 223	54° 56' 4" S	67° 40' 34" W	-	-	-	hap1	hap4	hap10	-
Mastodia sp.1/*Prasiola borealis*	I501	Tierra del Fuego (Chile), Beagle Channel, Róbalo Bay, Navarino Island, XII Región. Seashore, 0-5 m a.s.l. 25/1/2008. Leg. *S. Pérez-Ortega.* Loc. 223	54° 56' 4" S	67° 40' 34" W	-	-	-	hap1	hap4	hap10	hap11
Mastodia sp.1/*Prasiola borealis*	I502	Tierra del Fuego (Chile), Beagle Channel, Róbalo Bay, Navarino Island, XII Región. Seashore, 0-5 m a.s.l. 25/1/2008. Leg. *S. Pérez-Ortega.* Loc. 223	54° 56' 4" S	67° 40' 34" W	-	-	-	hap1	-	hap9	hap11
Mastodia sp.1/*Prasiola borealis*	I503	Tierra del Fuego (Chile), Beagle Channel, Róbalo Bay, Navarino Island, XII Región. Seashore, 0-5 m a.s.l. 25/1/2008. Leg. *S. Pérez-Ortega.* Loc. 223	54° 56' 4" S	67° 40' 34" W	-	-	-	hap1	hap4	hap9	hap11
Mastodia sp.1/*Prasiola borealis*	I156	Tierra del Fuego (Chile), Beagle Channel, Puerto Navarino, Navarino Island, XII Región. Seashore, 0-5 m a.s.l. 27/1/2008. Leg. *S. Pérez-Ortega.* Loc. 227	54° 55' 48" S	68° 20' 45" W	-	-	-	hap1	hap4	hap7	-
Mastodia sp.1/*Prasiola borealis*	I504	Tierra del Fuego (Chile), Beagle Channel, Puerto Navarino, Navarino Island, XII Región. Seashore, 0-5 m a.s.l. 27/1/2008. Leg. *S. Pérez-Ortega.* Loc. 227	54° 55' 48" S	68° 20' 45" W	-	-	-	hap1	hap4	-	hap3
Mastodia sp.1/*Prasiola borealis*	I505	Tierra del Fuego (Chile), Beagle Channel, Puerto Navarino, Navarino Island, XII Región. Seashore, 0-5 m a.s.l. 27/1/2008. Leg. *S. Pérez-Ortega.* Loc. 227	54° 55' 48" S	68° 20' 45" W	-	-	-	hap1	hap4	-	hap3
Mastodia sp.1/*Prasiola borealis*	I506	Tierra del Fuego (Chile), Beagle Channel, Puerto Navarino, Navarino Island, XII Región. Seashore, 0-5 m a.s.l. 27/1/2008. Leg. *S. Pérez-Ortega.* Loc. 227	54° 55' 48" S	68° 20' 45" W	-	-	-	hap1	hap4	-	hap3
Mastodia sp.1/*Prasiola borealis*	I507	Tierra del Fuego (Chile), Beagle Channel, Puerto Navarino, Navarino Island, XII Región. Seashore, 0-5 m a.s.l. 27/1/2008. Leg. *S. Pérez-Ortega.* Loc. 227	54° 55' 48" S	68° 20' 45" W	-	-	-	hap1	hap4	hap7	hap3
Mastodia sp.1/*Prasiola borealis*	I93	Antarctica, South Shetlands, King George Island, Potter Peninsula, Stranger Point. Seashore, 0-5 m a.s.l. 22/12/2009. Leg. *F. Fernández-Mendoza & S. Domaschke.*	62.261502° S	58.617572° W	hap8	hap5	hap1	-	-	-	-
Mastodia sp.2/*Prasiola* sp.	I94	Antarctica, South Shetlands, King George Island, Potter Peninsula, Stranger Point. Seashore, 0-5 m a.s.l. 22/12/2009. Leg. *F. Fernández-Mendoza & S. Domaschke.*	62.261502° S	58.617572° W	hap15	hap13	hap10	-	-	-	-

Mastodia sp.2/ *Prasiola* sp.	I95	Antarctica, South Shetlands, King George Island, Potter Peninsula, Stranger Point. Seashore, 0-5 m a.s.l. 22/12/2009. Leg. *F. Fernández-Mendoza & S. Domaschke.*	62.261502° S	58.617572° W	hap15	hap13	hap10	hap3	hap6	hap12	hap13
Mastodia sp.2/ *Prasiola* sp.	I96	Antarctica, South Shetlands, King George Island, Potter Peninsula, Stranger Point. Seashore, 0-5 m a.s.l. 22/12/2009. Leg. *F. Fernández-Mendoza & S. Domaschke.*	62.261502° S	58.617572° W	hap15	hap13	hap9	-	-	-	-
Mastodia sp.2/ *Prasiola* sp.	I97	Antarctica, South Shetlands, King George Island, Potter Peninsula, Stranger Point. Seashore, 0-5 m a.s.l. 22/12/2009. Leg. *F. Fernández-Mendoza & S. Domaschke.*	62.261502° S	58.617572° W	hap15	hap13	hap9	-	-	-	-
Mastodia sp.2/ *Prasiola* sp.	I98-2	Antarctica, South Shetlands, King George Island, Potter Peninsula, Stranger Point. Seashore, 0-5 m a.s.l. 22/12/2009. Leg. *F. Fernández-Mendoza & S. Domaschke.*	62.261502° S	58.617572° W	hap15	hap13	hap10	-	-	-	-
Mastodia sp.2/ *Prasiola* sp.	I99	Antarctica, South Shetlands, King George Island, Potter Peninsula, Stranger Point. Seashore, 0-5 m a.s.l. 22/12/2009. Leg. *F. Fernández-Mendoza & S. Domaschke.*	62.261502° S	58.617572° W	hap15	hap13	hap8	-	-	-	-
Mastodia sp.2/ *Prasiola* sp.	I100	Antarctica, South Shetlands, King George Island, Potter Peninsula, Stranger Point. Seashore, 0-5 m a.s.l. 22/12/2009. Leg. *F. Fernández-Mendoza & S. Domaschke.*	62.261502° S	58.617572° W	hap15	hap13	hap10	-	-	-	-
Mastodia sp.2/ *Prasiola* sp.	I101dupl2	Antarctica, South Shetlands, King George Island, Potter Peninsula, Stranger Point. Seashore, 0-5 m a.s.l. 22/12/2009. Leg. *F. Fernández-Mendoza & S. Domaschke.*	62.261502° S	58.617572° W	hap15	hap13	hap9	-	-	-	-
Mastodia sp.2/ *Prasiola* sp.	I102dupl1	Antarctica, South Shetlands, King George Island, Potter Peninsula, Stranger Point. Seashore, 0-5 m a.s.l. 22/12/2009. Leg. *F. Fernández-Mendoza & S. Domaschke.*	62.261502° S	58.617572° W	hap15	hap13	hap9	-	-	-	-
Mastodia sp.2/ *Prasiola* sp.	I103-2	Antarctica, South Shetlands, King George Island, Potter Peninsula, Stranger Point. Seashore, 0-5 m a.s.l. 22/12/2009. Leg. *F. Fernández-Mendoza & S. Domaschke.*	62.261502° S	58.617572° W	hap15	hap13	hap8	-	-	-	-
Mastodia sp.2/ *Prasiola* sp.	I104b	Antarctica, South Shetlands, King George Island, Potter Peninsula, Stranger Point. Seashore, 0-5 m a.s.l. 22/12/2009. Leg. *F. Fernández-Mendoza & S. Domaschke.*	62.261502° S	58.617572° W	hap15	hap13	hap10	hap3	hap6	-	hap14
Mastodia sp.2/ *Prasiola* sp.	I105	Antarctica, South Shetlands, King George Island, Potter Peninsula, Stranger Point. Seashore, 0-5 m a.s.l. 22/12/2009. Leg. *F. Fernández-Mendoza & S. Domaschke.*	62.261502° S	58.617572° W	hap15	hap13	hap9	hap3	hap6	hap14	hap15

Mastodia sp.2/ *Prasiola* sp.	I106	Antarctica, South Shetlands, King George Island, Potter Peninsula, Stranger Point. Seashore, 0-5 m a.s.l. 22/12/2009. Leg. *F. Fernández-Mendoza & S. Domaschke.*	62.261502° S	58.617572° W	hap15	hap13	hap9	-	-	-	-
Mastodia sp.1/ *Prasiola borealis*	I107	Antarctica, South Shetlands, King George Island, Potter Peninsula, Stranger Point. Seashore, 0-5 m a.s.l. 22/12/2009. Leg. *F. Fernández-Mendoza & S. Domaschke.*	62.261502° S	58.617572° W	hap11	hap10	hap5	hap2	-	hap3	hap16
Mastodia sp.2/ *Prasiola* sp.	I109	Antarctica, South Shetlands, King George Island, Potter Peninsula, Stranger Point. Seashore, 0-5 m a.s.l. 22/12/2009. Leg. *F. Fernández-Mendoza & S. Domaschke.*	62.261502° S	58.617572° W	hap15	hap13	hap10	-	-	-	-
Mastodia sp.2/ *Prasiola* sp.	I110	Antarctica, South Shetlands, King George Island, Potter Peninsula, Stranger Point. Seashore, 0-5 m a.s.l. 22/12/2009. Leg. *F. Fernández-Mendoza & S. Domaschke.*	62.261502° S	58.617572° W	hap15	hap13	hap8	-	-	-	-
Mastodia sp.2/ *Prasiola* sp.	I112	Antarctica, South Shetlands, King George Island, Potter Peninsula, Stranger Point. Seashore, 0-5 m a.s.l. 22/12/2009. Leg. *F. Fernández-Mendoza & S. Domaschke.*	62.261502° S	58.617572° W	hap15	hap13	hap8	hap3	-	-	hap13
Mastodia sp.2/ *Prasiola* sp.	I113	Antarctica, South Shetlands, King George Island, Potter Peninsula, Stranger Point. Seashore, 0-5 m a.s.l. 22/12/2009. Leg. *F. Fernández-Mendoza & S. Domaschke.*	62.261502° S	58.617572° W	hap15	hap13	hap8	-	-	-	-
Mastodia sp.2/ *Prasiola* sp.	I114	Antarctica, South Shetlands, King George Island, Potter Peninsula, Stranger Point. Seashore, 0-5 m a.s.l. 22/12/2009. Leg. *F. Fernández-Mendoza & S. Domaschke.*	62.261502° S	58.617572° W	hap15	hap13	hap9	-	-	-	-
Mastodia sp.2/ *Prasiola* sp.	I116-2	Antarctica, South Shetlands, King George Island, Potter Peninsula, Stranger Point. Seashore, 0-5 m a.s.l. 22/12/2009. Leg. *F. Fernández-Mendoza & S. Domaschke.*	62.261502° S	58.617572° W	hap15	hap13	hap9	-	-	-	-
Mastodia sp.2/ *Prasiola* sp.	I117	Antarctica, South Shetlands, King George Island, Potter Peninsula, Stranger Point. Seashore, 0-5 m a.s.l. 22/12/2009. Leg. *F. Fernández-Mendoza & S. Domaschke.*	62.261502° S	58.617572° W	hap15	hap13	hap9	-	-	-	-
Mastodia sp.2/ *Prasiola* sp.	I203	Antarctica, South Shetlands, King George Island, Potter Peninsula, Stranger Point. Seashore, 0-5 m a.s.l. 22/12/2009. Leg. *F. Fernández-Mendoza & S. Domaschke.*	62.261502° S	58.617572° W	hap15	hap14	hap9	hap3	-	hap16	-
Mastodia sp.2/ *Prasiola* sp.	I440	Antarctica, South Shetlands, King George Island, Potter Peninsula, Stranger Point. Seashore, 0-5 m a.s.l. 22/12/2009. Leg. *F. Fernández-Mendoza & S. Domaschke.*	62.261502° S	58.617572° W	-	-	-	hap3	-	hap12	hap13

Mastodia sp.2/ *Prasiola* sp.	I441	Antarctica, South Shetlands, King George Island, Potter Peninsula, Stranger Point. Seashore, 0-5 m a.s.l. 22/12/2009. Leg. *F. Fernández-Mendoza & S. Domaschke.*	62.261502° S	58.617572° W	-	-	-	hap3	hap6	hap12	hap13
Mastodia sp.2/ *Prasiola* sp.	I442	Antarctica, South Shetlands, King George Island, Potter Peninsula, Stranger Point. Seashore, 0-5 m a.s.l. 22/12/2009. Leg. *F. Fernández-Mendoza & S. Domaschke.*	62.261502° S	58.617572° W	-	-	-	hap3	-	-	hap17
Mastodia sp.1/ *Prasiola borealis*	I443	Antarctica, South Shetlands, King George Island, Potter Peninsula, Stranger Point. Seashore, 0-5 m a.s.l. 22/12/2009. Leg. *F. Fernández-Mendoza & S. Domaschke.*	62.261502° S	58.617572° W	-	-	-	hap2	hap5	hap3	hap16
Mastodia sp.2/ *Prasiola* sp.	I444	Antarctica, South Shetlands, King George Island, Potter Peninsula, Stranger Point. Seashore, 0-5 m a.s.l. 22/12/2009. Leg. *F. Fernández-Mendoza & S. Domaschke.*	62.261502° S	58.617572° W	-	-	-	hap3	-	hap12	hap15
Mastodia sp.2/ *Prasiola* sp.	I454	Antarctica, South Shetlands, King George Island, Potter Peninsula, Stranger Point. Seashore, 0-5 m a.s.l. 22/12/2009. Leg. *F. Fernández-Mendoza & S. Domaschke.*	62.261502° S	58.617572° W	-	-	-	hap3	hap6	hap13	hap15
Mastodia sp.2/ *Prasiola* sp.	I455	Antarctica, South Shetlands, King George Island, Potter Peninsula, Stranger Point. Seashore, 0-5 m a.s.l. 22/12/2009. Leg. *F. Fernández-Mendoza & S. Domaschke.*	62.261502° S	58.617572° W	-	-	-	hap3	hap6	hap15	hap14
Mastodia sp.2/ *Prasiola* sp.	I456	Antarctica, South Shetlands, King George Island, Potter Peninsula, Stranger Point. Seashore, 0-5 m a.s.l. 22/12/2009. Leg. *F. Fernández-Mendoza & S. Domaschke.*	62.261502° S	58.617572° W	-	-	-	hap3	hap6	hap15	hap14
Mastodia sp.2/ *Prasiola* sp.	I508	Antarctica, South Shetlands, Greenwich Island. Seashore, 0-5 m a.s.l. 28/1/2013. Leg. *J. E. González Pastor.*	62° 26' 53.55" S	59° 55' 45.81" W	-	-	-	hap3	-	hap13	hap15
Mastodia sp.2/ *Prasiola* sp.	I509	Antarctica, South Shetlands, Greenwich Island. Seashore, 0-5 m a.s.l. 28/1/2013. Leg. *J. E. González Pastor.*	62° 26' 53.55" S	59° 55' 45.81" W	-	-	-	hap3	hap6	hap13	hap15
Mastodia sp.2/ *Prasiola* sp.	I510	Antarctica, South Shetlands, Greenwich Island. Seashore, 0-5 m a.s.l. 28/1/2013. Leg. *J. E. González Pastor.*	62° 26' 53.55" S	59° 55' 45.81" W	-	-	-	hap3	hap6	hap13	hap15
Mastodia sp.2/ *Prasiola* sp.	I511	Antarctica, South Shetlands, Greenwich Island. Seashore, 0-5 m a.s.l. 28/1/2013. Leg. *J. E. González Pastor.*	62° 26' 53.55" S	59° 55' 45.81" W	-	-	-	hap3	hap6	hap13	hap15
Mastodia sp.2/ *Prasiola* sp.	I512	Antarctica, South Shetlands, Greenwich Island. Seashore, 0-5 m a.s.l. 28/1/2013. Leg. *J. E. González Pastor.*	62° 26' 53.55" S	59° 55' 45.81" W	-	-	-	hap3	hap6	hap13	hap15

Mastodia sp.2/ *Prasiola* sp.	I56-2	Antarctica, South Shetlands, Livingston Island, near Base Juan Carlos I. Seashore, 0-5 m a.s.l. 2/2/2013. Leg. *J. E. González Pastor.*	62° 39' 07.35" S	60° 22' 11.58" W	hap15	hap13	hap9	-	-	-	-
Mastodia sp.2/ *Prasiola* sp.	I58	Antarctica, South Shetlands, Livingston Island, Hannah Point. Seashore, 0-5 m a.s.l. 12/2/2012. Leg. *C. Laguna Defior.*	62° 39' S	60° 37' W	hap15	hap13	hap9	-	-	-	-
Mastodia sp.2/ *Prasiola* sp.	I64b	Antarctica, South Shetlands, Livingston Island, Hannah Point. Seashore, 0-5 m a.s.l. 12/2/2012. Leg. *C. Laguna Defior.*	62° 39' S	60° 37' W	hap15	hap13	hap9	-	-	-	-
Mastodia sp.2/ *Prasiola* sp.	I73	Antarctica, South Shetlands, Livingston Island, Hannah Point. Seashore, 0-5 m a.s.l. 12/2/2012. Leg. *C. Laguna Defior.*	62° 39' S	60° 37' W	hap13	hap12	hap9	-	-	-	-
Mastodia sp.2/ *Prasiola* sp.	I74	Antarctica, South Shetlands, Livingston Island, Hannah Point. Seashore, 0-5 m a.s.l. 12/2/2012. Leg. *C. Laguna Defior.*	62° 39' S	60° 37' W	hap15	hap13	hap9	-	-	-	-
Mastodia sp.2/ *Prasiola* sp.	I75	Antarctica, South Shetlands, Livingston Island, Hannah Point. Seashore, 0-5 m a.s.l. 12/2/2012. Leg. *C. Laguna Defior.*	62° 39' S	60° 37' W	hap15	hap13	hap9	-	-	-	-
Mastodia sp.2/ *Prasiola* sp.	I76	Antarctica, South Shetlands, Livingston Island, Hannah Point. Seashore, 0-5 m a.s.l. 12/2/2012. Leg. *C. Laguna Defior.*	62° 39' S	60° 37' W	hap15	hap14	hap9	-	-	-	-
Mastodia sp.2/ *Prasiola* sp.	I77	Antarctica, South Shetlands, Livingston Island, Hannah Point. Seashore, 0-5 m a.s.l. 12/2/2012. Leg. *C. Laguna Defior.*	62° 39' S	60° 37' W	hap15	hap13	hap8	-	-	-	-
Mastodia sp.2/ *Prasiola* sp.	I165	Antarctica, South Shetlands, Livingston Island, Española Cove. Seashore, 0-5 m a.s.l. 27/1/2014. Leg. *A. de los Ríos.*	62° 39' 07.35" S	60° 22' 11.58" W	hap15	hap13	hap8	hap3	-	hap18	hap18
Mastodia sp.2/ *Prasiola* sp.	I166	Antarctica, South Shetlands, Livingston Island, Española Cove. Seashore, 0-5 m a.s.l. 27/1/2014. Leg. *A. de los Ríos.*	62° 39' 07.35" S	60° 22' 11.58" W	hap15	hap13	hap9	hap3	-	hap16	hap19
Mastodia sp.2/ *Prasiola* sp.	I167	Antarctica, South Shetlands, Livingston Island, Española Cove. Seashore, 0-5 m a.s.l. 27/1/2014. Leg. *A. de los Ríos.*	62° 39' 07.35" S	60° 22' 11.58" W	hap15	hap13	hap9	hap3	-	hap18	hap18
Mastodia sp.2/ *Prasiola* sp.	I168	Antarctica, South Shetlands, Livingston Island, Española Cove. Seashore, 0-5 m a.s.l. 27/1/2014. Leg. *A. de los Ríos.*	62° 39' 07.35" S	60° 22' 11.58" W	hap15	hap13	hap9	hap3	-	hap18	hap18
Mastodia sp.2/ *Prasiola* sp.	I169dupl1	Antarctica, South Shetlands, Livingston Island, Española Cove. Seashore, 0-5 m a.s.l. 27/1/2014. Leg. *A. de los Ríos.*	62° 39' 07.35" S	60° 22' 11.58" W	hap13	hap13	hap9	hap3	hap6	hap18	hap18
Mastodia sp.2/ *Prasiola* sp.	I169dupl2	Antarctica, South Shetlands, Livingston Island, Española Cove. Seashore, 0-5 m a.s.l. 27/1/2014. Leg. *A. de los Ríos.*	62° 39' 07.35" S	60° 22' 11.58" W	hap15	hap13	hap9	-	-	-	-
Mastodia sp.2/ *Prasiola* sp.	I169-2	Antarctica, South Shetlands, Livingston Island, Española Cove. Seashore, 0-5 m a.s.l. 27/1/2014.	62° 39' 07.35" S	60° 22' 11.58" W	hap15	hap13	hap9	-	-	-	-

		Leg. *A. de los Ríos.*									
Mastodia sp.2/ *Prasiola* sp.	I170	Antarctica, South Shetlands, Livingston Island, Española Cove. Seashore, 0-5 m a.s.l. 27/1/2014. Leg. *A. de los Ríos.*	62° 39' 07.35" S	60° 22' 11.58" W	hap15	hap14	hap9	hap3	-	hap18	hap18
Mastodia sp.2/ *Prasiola* sp.	I171	Antarctica, South Shetlands, Livingston Island, Española Cove. Seashore, 0-5 m a.s.l. 27/1/2014. Leg. *A. de los Ríos.*	62° 39' 07.35" S	60° 22' 11.58" W	hap15	hap13	hap9	-	-	hap18	-
Mastodia sp.2/ *Prasiola* sp.	I172dupl1	Antarctica, South Shetlands, Livingston Island, Española Cove. Seashore, 0-5 m a.s.l. 27/1/2014. Leg. *A. de los Ríos.*	62° 39' 07.35" S	60° 22' 11.58" W	hap15	hap13	hap9	-	-	-	-
Mastodia sp.2/ *Prasiola* sp.	I172dupl2	Antarctica, South Shetlands, Livingston Island, Española Cove. Seashore, 0-5 m a.s.l. 27/1/2014. Leg. *A. de los Ríos.*	62° 39' 07.35" S	60° 22' 11.58" W	hap13	hap13	hap9	-	-	-	-
Mastodia sp.2/ *Prasiola* sp.	I173	Antarctica, South Shetlands, Livingston Island, Española Cove. Seashore, 0-5 m a.s.l. 27/1/2014. Leg. *A. de los Ríos.*	62° 39' 07.35" S	60° 22' 11.58" W	hap15	hap13	hap9	-	-	-	-
Mastodia sp.2/ *Prasiola* sp.	I174	Antarctica, South Shetlands, Livingston Island, Española Cove. Seashore, 0-5 m a.s.l. 27/1/2014. Leg. *A. de los Ríos.*	62° 39' 07.35" S	60° 22' 11.58" W	hap15	hap13	hap9	-	-	-	-
Mastodia sp.2/ *Prasiola* sp.	I175	Antarctica, South Shetlands, Livingston Island, Española Cove. Seashore, 0-5 m a.s.l. 27/1/2014. Leg. *A. de los Ríos.*	62° 39' 07.35" S	60° 22' 11.58" W	hap15	hap13	hap9	-	-	-	-
Mastodia sp.2/ *Prasiola* sp.	I176	Antarctica, South Shetlands, Livingston Island, Española Cove. Seashore, 0-5 m a.s.l. 27/1/2014. Leg. *A. de los Ríos.*	62° 39' 07.35" S	60° 22' 11.58" W	hap15	hap13	hap9	hap3	-	hap18	hap18
Mastodia sp.2/ *Prasiola* sp.	I187	Antarctica, South Shetlands, Livingston Island, Española Cove. Seashore, 0-5 m a.s.l. 27/1/2014. Leg. *A. de los Ríos.*	62° 39' 07.35" S	60° 22' 11.58" W	-	-	-	-	-	-	hap15
Mastodia sp.2/ *Prasiola* sp.	I381	Antarctica, South Shetlands, Livingston Island, Española Cove. Seashore, 0-5 m a.s.l. 27/1/2014. Leg. *A. de los Ríos.*	62° 39' 07.35" S	60° 22' 11.58" W	-	-	-	hap3	hap6	hap18	hap18
Mastodia sp.2/ *Prasiola* sp.	I447	Antarctica, South Shetlands, Livingston Island, Española Cove. Seashore, 0-5 m a.s.l. 27/1/2014. Leg. *A. de los Ríos.*	62° 39' 07.35" S	60° 22' 11.58" W	-	-	-	hap3	-	hap18	hap18
Mastodia sp.2/ *Prasiola* sp.	I448	Antarctica, South Shetlands, Livingston Island, Española Cove. Seashore, 0-5 m a.s.l. 27/1/2014. Leg. *A. de los Ríos.*	62° 39' 07.35" S	60° 22' 11.58" W	-	-	-	hap3	-	hap16	hap19
Mastodia sp.2/ *Prasiola* sp.	I449	Antarctica, South Shetlands, Livingston Island, Española Cove. Seashore, 0-5 m a.s.l. 27/1/2014. Leg. *A. de los Ríos.*	62° 39' 07.35" S	60° 22' 11.58" W	-	-	-	hap3	hap6	hap18	hap18
Mastodia sp.2/ *Prasiola* sp.	I450	Antarctica, South Shetlands, Livingston Island, Española Cove. Seashore, 0-5 m a.s.l. 27/1/2014. Leg. *A. de los Ríos.*	62° 39' 07.35" S	60° 22' 11.58" W	-	-	-	hap3	hap6	hap18	hap18

Mastodia sp.2/ *Prasiola* sp.	I451	Antarctica, South Shetlands, Livingston Island, Española Cove. Seashore, 0-5 m a.s.l. 27/1/2014. Leg. *A. de los Ríos.*	62° 39' 07.35" S	60° 22' 11.58" W	-	-	-	hap3	hap6	hap16	hap19
Mastodia sp.2/ *Prasiola* sp.	I453	Antarctica, South Shetlands, Livingston Island, Española Cove. Seashore, 0-5 m a.s.l. 27/1/2014. Leg. *A. de los Ríos.*	62° 39' 07.35" S	60° 22' 11.58" W	-	-	-	hap3	hap6	hap13	hap15
Mastodia sp.2/ *Prasiola* sp.	I285	Antarctica, Yalour Island. Seashore, 0-5 m a.s.l. 26/1/2007. Leg. *J. C. García Galindo & J. Romagni.*	65° 15' S	64° 01' W	hap13	hap14	hap9	-	-	-	-
Mastodia sp.2/ *Prasiola* sp.	I286	Antarctica, Yalour Island. Seashore, 0-5 m a.s.l. 26/1/2007. Leg. *J. C. García Galindo & J. Romagni.*	65° 15' S	64° 01' W	hap15	hap15	hap9	hap3	-	-	hap20
Mastodia sp.2/ *Prasiola* sp.	I287	Antarctica, Yalour Island. Seashore, 0-5 m a.s.l. 26/1/2007. Leg. *J. C. García Galindo & J. Romagni.*	65° 15' S	64° 01' W	hap13	hap15	hap11	-	-	-	-
Mastodia sp.2/ *Prasiola* sp.	I288	Antarctica, Yalour Island. Seashore, 0-5 m a.s.l. 26/1/2007. Leg. *J. C. García Galindo & J. Romagni.*	65° 15' S	64° 01' W	hap15	hap13	hap9	hap3	hap6	-	hap20
Mastodia sp.2/ *Prasiola* sp.	I289	Antarctica, Yalour Island. Seashore, 0-5 m a.s.l. 26/1/2007. Leg. *J. C. García Galindo & J. Romagni.*	65° 15' S	64° 01' W	hap13	hap15	hap9	hap3	hap6	-	-
Mastodia sp.2/ *Prasiola* sp.	I291	Antarctica, Yalour Island. Seashore, 0-5 m a.s.l. 26/1/2007. Leg. *J. C. García Galindo & J. Romagni.*	65° 15' S	64° 01' W	hap13	hap15	hap9	hap3	hap6	hap18	hap18
Mastodia sp.2/ *Prasiola* sp.	I292	Antarctica, Yalour Island. Seashore, 0-5 m a.s.l. 26/1/2007. Leg. *J. C. García Galindo & J. Romagni.*	65° 15' S	64° 01' W	hap15	hap13	hap9	hap3	hap6	hap18	hap18
Mastodia sp.2/ *Prasiola* sp.	I293	Antarctica, Yalour Island. Seashore, 0-5 m a.s.l. 26/1/2007. Leg. *J. C. García Galindo & J. Romagni.*	65° 15' S	64° 01' W	hap13	hap13	hap9	-	-	-	-
Mastodia sp.2/ *Prasiola* sp.	I294	Antarctica, Yalour Island. Seashore, 0-5 m a.s.l. 26/1/2007. Leg. *J. C. García Galindo & J. Romagni.*	65° 15' S	64° 01' W	hap15	hap14	hap9	hap3	-	-	-
Mastodia sp.2/ *Prasiola* sp.	I295	Antarctica, Yalour Island. Seashore, 0-5 m a.s.l. 26/1/2007. Leg. *J. C. García Galindo & J. Romagni.*	65° 15' S	64° 01' W	hap13	hap13	hap9	-	-	-	-
Mastodia sp.2/ *Prasiola* sp.	I296	Antarctica, Yalour Island. Seashore, 0-5 m a.s.l. 26/1/2007. Leg. *J. C. García Galindo & J. Romagni.*	65° 15' S	64° 01' W	hap15	hap13	hap9	-	-	-	-
Mastodia sp.2/ *Prasiola* sp.	I459	Antarctica, Yalour Island. Seashore, 0-5 m a.s.l. 26/1/2007. Leg. *J. C. García Galindo & J. Romagni.*	65° 15' S	64° 01' W	-	-	-	hap3	-	-	hap18
Mastodia sp.2/ *Prasiola* sp.	I460	Antarctica, Yalour Island. Seashore, 0-5 m a.s.l. 26/1/2007. Leg. *J. C. García Galindo & J. Romagni.*	65° 15' S	64° 01' W	-	-	-	hap3	hap6	-	hap19
Mastodia sp.2/ *Prasiola* sp.	I462	Antarctica, Yalour Island. Seashore, 0-5 m a.s.l. 26/1/2007. Leg. *J. C. García Galindo & J. Romagni.*	65° 15' S	64° 01' W	-	-	-	hap3	hap6	-	hap19
Mastodia sp.2/ *Prasiola* sp.	I297	Antarctica, Rongé Island. Seashore, 0-5 m a.s.l. 25/1/2007. Leg. *J. C. García Galindo & J. Romagni.*	64° 43' S	62° 34' W	hap13	hap13	hap9	-	-	-	-
Mastodia sp.2/ *Prasiola* sp.	I298	Antarctica, Rongé Island. Seashore, 0-5 m a.s.l. 25/1/2007. Leg. *J. C. García Galindo & J. Romagni.*	64° 43' S	62° 34' W	hap13	hap13	hap9	hap3	-	-	-
Mastodia sp.2/ *Prasiola* sp.	I299	Antarctica, Rongé Island. Seashore, 0-5 m a.s.l. 25/1/2007. Leg. *J. C. García Galindo & J. Romagni.*	64° 43' S	62° 34' W	hap15	hap13	hap9	-	-	-	-
Mastodia sp.2/ *Prasiola* sp.	I300	Antarctica, Rongé Island. Seashore, 0-5 m a.s.l. 25/1/2007. Leg. *J. C. García Galindo & J. Romagni.*	64° 43' S	62° 34' W	hap15	hap14	hap9	hap3	-	-	hap18
Mastodia sp.2/ *Prasiola* sp.	I301	Antarctica, Rongé Island. Seashore, 0-5 m a.s.l. 25/1/2007. Leg. *J. C. García Galindo & J. Romagni.*	64° 43' S	62° 34' W	hap15	hap13	hap9	hap3	-	-	-

Mastodia sp.2/ *Prasiola* sp.	I302	Antarctica, Rongé Island. Seashore, 0-5 m a.s.l. 25/1/2007. Leg. *J. C. García Galindo & J. Romagni.*	64° 43' S	62° 34' W	hap15	hap13	hap9	hap3	hap6	hap18	-
Mastodia sp.2/ *Prasiola* sp.	I303	Antarctica, Rongé Island. Seashore, 0-5 m a.s.l. 25/1/2007. Leg. *J. C. García Galindo & J. Romagni.*	64° 43' S	62° 34' W	hap13	hap13	hap9	-	-	-	-
Mastodia sp.2/ *Prasiola* sp.	I304	Antarctica, Rongé Island. Seashore, 0-5 m a.s.l. 25/1/2007. Leg. *J. C. García Galindo & J. Romagni.*	64° 43' S	62° 34' W	hap15	hap13	hap9	-	-	-	-
Mastodia sp.2/ *Prasiola* sp.	I305	Antarctica, Rongé Island. Seashore, 0-5 m a.s.l. 25/1/2007. Leg. *J. C. García Galindo & J. Romagni.*	64° 43' S	62° 34' W	hap16	hap13	hap9	-	-	-	-
Mastodia sp.2/ *Prasiola* sp.	I306	Antarctica, Rongé Island. Seashore, 0-5 m a.s.l. 25/1/2007. Leg. *J. C. García Galindo & J. Romagni.*	64° 43' S	62° 34' W	hap13	hap13	hap9	-	-	-	-
Mastodia sp.2/ *Prasiola* sp.	I307	Antarctica, Rongé Island. Seashore, 0-5 m a.s.l. 25/1/2007. Leg. *J. C. García Galindo & J. Romagni.*	64° 43' S	62° 34' W	hap13	hap14	hap9	-	-	-	-
Mastodia sp.2/ *Prasiola* sp.	I308	Antarctica, Rongé Island. Seashore, 0-5 m a.s.l. 25/1/2007. Leg. *J. C. García Galindo & J. Romagni.*	64° 43' S	62° 34' W	hap13	hap13	hap9	-	-	-	-
Mastodia sp.2/ *Prasiola* sp.	I463	Antarctica, Rongé Island. Seashore, 0-5 m a.s.l. 25/1/2007. Leg. *J. C. García Galindo & J. Romagni.*	64° 43' S	62° 34' W	-	-	-	hap3	hap6	hap18	hap18
Mastodia sp.2/ *Prasiola* sp.	I464	Antarctica, Rongé Island. Seashore, 0-5 m a.s.l. 25/1/2007. Leg. *J. C. García Galindo & J. Romagni.*	64° 43' S	62° 34' W	-	-	-	hap3	hap6	-	hap18
Mastodia sp.2/ *Prasiola* sp.	I465	Antarctica, Rongé Island. Seashore, 0-5 m a.s.l. 25/1/2007. Leg. *J. C. García Galindo & J. Romagni.*	64° 43' S	62° 34' W	-	-	-	hap3	hap6	hap18	hap18
Mastodia sp.2/ *Prasiola* sp.	I466	Antarctica, Rongé Island. Seashore, 0-5 m a.s.l. 25/1/2007. Leg. *J. C. García Galindo & J. Romagni.*	64° 43' S	62° 34' W	-	-	-	hap3	hap6	hap18	hap18
Mastodia sp.2/ *Prasiola* sp.	I467	Antarctica, Rongé Island. Seashore, 0-5 m a.s.l. 25/1/2007. Leg. *J. C. García Galindo & J. Romagni.*	64° 43' S	62° 34' W	-	-	-	hap3	hap6	hap18	hap18
Mastodia sp.2/ *Prasiola* sp.	I309	Antarctica, Avian Island (Adelaide Island). Seashore, 0-5 m a.s.l. 27/1/2007. Leg. *J. C. García Galindo & J. Romagni.*	67° 46' S	68° 53' W	hap15	hap13	hap9	hap3	-	-	hap21
Mastodia sp.2/ *Prasiola* sp.	I311	Antarctica, Avian Island (Adelaide Island). Seashore, 0-5 m a.s.l. 27/1/2007. Leg. *J. C. García Galindo & J. Romagni.*	67° 46' S	68° 53' W	hap13	hap13	hap9	hap3	hap6	hap13	-
Mastodia sp.1/ *Prasiola borealis*	I312	Antarctica, Avian Island (Adelaide Island). Seashore, 0-5 m a.s.l. 27/1/2007. Leg. *J. C. García Galindo & J. Romagni.*	67° 46' S	68° 53' W	hap12	hap10	hap7	hap2	hap4	-	-
Mastodia sp.1/ *Prasiola borealis*	I313	Antarctica, Avian Island (Adelaide Island). Seashore, 0-5 m a.s.l. 27/1/2007. Leg. *J. C. García Galindo & J. Romagni.*	67° 46' S	68° 53' W	hap12	hap10	hap6	hap2	hap4	-	-
Mastodia sp.1/ *Prasiola borealis*	I315	Antarctica, Avian Island (Adelaide Island). Seashore, 0-5 m a.s.l. 27/1/2007. Leg. *J. C. García Galindo & J. Romagni.*	67° 46' S	68° 53' W	hap12	hap10	hap6	hap2	hap4	-	-
Mastodia sp.2/ *Prasiola* sp.	I318	Antarctica, Avian Island (Adelaide Island). Seashore, 0-5 m a.s.l. 27/1/2007. Leg. *J. C. García Galindo & J. Romagni.*	67° 46' S	68° 53' W	hap15	hap13	hap9	hap3	hap6	hap17	hap21
Mastodia sp.2/ *Prasiola* sp.	I319	Antarctica, Avian Island (Adelaide Island). Seashore, 0-5 m a.s.l. 27/1/2007. Leg. *J. C. García Galindo & J.*	67° 46' S	68° 53' W	hap15	hap13	hap9	hap3	-	-	-

		Romagni.									
Mastodia sp.2/ *Prasiola* sp.	I470	Antarctica, Avian Island (Adelaide Island). Seashore, 0-5 m a.s.l. 27/1/2007. Leg. *J. C. García Galindo & J. Romagni.*	67° 46' S	68° 53' W	-	-	-	hap3	-	-	hap21
Mastodia sp.2/ *Prasiola* sp.	I321	Antarctica, Antarctic Peninsula, Cierva Cove. Seashore, 0-5 m a.s.l. 26/1/2007. Leg. *J. C. García Galindo & J. Romagni.*	64° 09' S	60° 57' W	hap15	hap13	hap10	-	-	-	-
Mastodia sp.2/ *Prasiola* sp.	I322	Antarctica, Antarctic Peninsula, Cierva Cove. Seashore, 0-5 m a.s.l. 26/1/2007. Leg. *J. C. García Galindo & J. Romagni.*	64° 09' S	60° 57' W	hap15	hap13	hap9	-	-	-	-
Mastodia sp.2/ *Prasiola* sp.	I323	Antarctica, Antarctic Peninsula, Cierva Cove. Seashore, 0-5 m a.s.l. 26/1/2007. Leg. *J. C. García Galindo & J. Romagni.*	64° 09' S	60° 57' W	hap15	hap13	hap9	-	-	-	-
Mastodia sp.2/ *Prasiola* sp.	I324	Antarctica, Antarctic Peninsula, Cierva Cove. Seashore, 0-5 m a.s.l. 26/1/2007. Leg. *J. C. García Galindo & J. Romagni.*	64° 09' S	60° 57' W	hap15	hap13	hap9	-	-	-	-
Mastodia sp.2/ *Prasiola* sp.	I325	Antarctica, Antarctic Peninsula, Cierva Cove. Seashore, 0-5 m a.s.l. 26/1/2007. Leg. *J. C. García Galindo & J. Romagni.*	64° 09' S	60° 57' W	hap15	hap13	hap9	-	-	-	-
Mastodia sp.2/ *Prasiola* sp.	I326	Antarctica, Antarctic Peninsula, Cierva Cove. Seashore, 0-5 m a.s.l. 26/1/2007. Leg. *J. C. García Galindo & J. Romagni.*	64° 09' S	60° 57' W	hap15	hap13	hap9	-	-	-	-
Mastodia sp.2/ *Prasiola* sp.	I327	Antarctica, Antarctic Peninsula, Cierva Cove. Seashore, 0-5 m a.s.l. 26/1/2007. Leg. *J. C. García Galindo & J. Romagni.*	64° 09' S	60° 57' W	hap15	hap13	hap9	-	-	-	-
Mastodia sp.2/ *Prasiola* sp.	I328	Antarctica, Antarctic Peninsula, Cierva Cove. Seashore, 0-5 m a.s.l. 26/1/2007. Leg. *J. C. García Galindo & J. Romagni.*	64° 09' S	60° 57' W	hap15	hap13	hap9	-	-	-	-
Mastodia sp.2/ *Prasiola* sp.	I329	Antarctica, Antarctic Peninsula, Cierva Cove. Seashore, 0-5 m a.s.l. 26/1/2007. Leg. *J. C. García Galindo & J. Romagni.*	64° 09' S	60° 57' W	hap14	hap13	hap9	-	-	-	-
Mastodia sp.2/ *Prasiola* sp.	I330	Antarctica, Antarctic Peninsula, Cierva Cove. Seashore, 0-5 m a.s.l. 26/1/2007. Leg. *J. C. García Galindo & J. Romagni.*	64° 09' S	60° 57' W	hap15	hap13	hap9	-	-	-	-
Mastodia sp.2/ *Prasiola* sp.	I331	Antarctica, Antarctic Peninsula, Cierva Cove. Seashore, 0-5 m a.s.l. 26/1/2007. Leg. *J. C. García Galindo & J. Romagni.*	64° 09' S	60° 57' W	hap15	hap13	hap9	-	-	-	-
Mastodia sp.2/ *Prasiola* sp.	I332	Antarctica, Antarctic Peninsula, Cierva Cove. Seashore, 0-5 m a.s.l. 26/1/2007. Leg. *J. C. García Galindo & J. Romagni.*	64° 09' S	60° 57' W	hap15	hap13	hap9	hap3	-	-	-
Mastodia sp.2/ *Prasiola* sp.	I337	Antarctica, Antarctic Peninsula, Cierva Cove. Seashore, 0-5 m a.s.l. 26/1/2007. Leg. *J. C. García Galindo & J. Romagni.*	64° 09' S	60° 57' W	hap15	hap13	hap9	-	-	-	-

Mastodia sp.2/ *Prasiola* sp.	I473	Antarctica, Antarctic Peninsula, Cierva Cove. Seashore, 0-5 m a.s.l. 26/1/2007. Leg. *J. C. García Galindo & J. Romagni.*	64° 09' S	60° 57' W	-	-	-	hap3	-	-	hap18
Mastodia sp.2/ *Prasiola* sp.	I474	Antarctica, Antarctic Peninsula, Cierva Cove. Seashore, 0-5 m a.s.l. 26/1/2007. Leg. *J. C. García Galindo & J. Romagni.*	64° 09' S	60° 57' W	-	-	-	hap3	-	-	-
Mastodia sp.2/ *Prasiola* sp.	I475	Antarctica, Antarctic Peninsula, Cierva Cove. Seashore, 0-5 m a.s.l. 26/1/2007. Leg. *J. C. García Galindo & J. Romagni.*	64° 09' S	60° 57' W	-	-	-	hap3	hap6	-	hap18
Mastodia sp.2/ *Prasiola* sp.	I476	Antarctica, Antarctic Peninsula, Cierva Cove. Seashore, 0-5 m a.s.l. 26/1/2007. Leg. *J. C. García Galindo & J. Romagni.*	64° 09' S	60° 57' W	-	-	-	hap3	-	-	hap18
Prasiola crispa	I408	SAG 43.96	-	-	-	-	-	-	-	hap19	-
Prasiola sp. free-living	I60	Antarctica, South Shetlands, Livingston Island, Hannah Point. Seashore, 0-5 m a.s.l. 12/2/2012. Leg. *C. Laguna Defior.*	62° 39' S	60° 37' W	-	-	-	-	-	-	hap23
Prasiola sp. free-living	I83	Antarctica, South Shetlands, King George Island, Potter Peninsula, Stranger Point. Seashore, 0-5 m a.s.l. 22/12/2009. Leg. *F. Fernández-Mendoza & S. Domaschke.*	62.261502° S	58.617572° W	-	-	-	-	-	-	hap23
Prasiola borealis free-living	I432	Alaska (USA), Petersburg, South Mitkof Island, Summer Strait. Seashore, on sedimentary rocks, 0-5 m a.s.l. 25/06/2012. Leg. *S. Pérez-Ortega, T. Spribille & K. Dillman.* Loc. 558	56° 33' 10" N	132° 38' 41" W	-	-	-	hap1	hap8	hap2	hap2
Prasiola delicata free-living	I438	Alaska (USA), Petersburg, Mitkof Island, Summer Strait. Seashore, on sedimentary rocks, 0-1 m a.s.l. 24/06/2012. Leg. *S. Pérez-Ortega, T. Spribille & K. Dillman.* Loc. 558	56° 44' 29" N	132° 56' 23" W	-	-	-	hap4	hap9	-	hap22
Prasiola cf. *antarctica*	I16	Antarctica, Avian Island (Adelaide Island). Seashore, 0-5 m a.s.l. 27/1/2007. Leg. *J. C. García Galindo & J. Romagni.*	67° 46' S	68° 53' W	-	-	-	-	hap10	-	-
Prasiola crispa	I17	Antarctica, South Shetlands, Livingston Island, Byers Peninsula. Seashore, 0-5 m a.s.l. 5/2/2007. Leg. *J. C. García Galindo & J. Romagni.*	62° 38' S	61° 05' W	-	-	-	-	hap11	-	-
Prasiola cf. *antarctica*	I18	Antarctica, Yalour Island. Seashore, 0-5 m a.s.l. 26/1/2007. Leg. *J. C. García Galindo & J. Romagni.*	65° 15' S	64° 01' W	-	-	-	-	hap12	-	-
Prasiola crispa	I19	Antarctica, Rongé Island. Seashore, 0-5 m a.s.l. 25/1/2007. Leg. *J. C. García Galindo & J. Romagni.*	64° 43' S	62° 34' W	-	-	-	-	hap13	-	-
Prasiola crispa	I284	Antarctica, South Shetlands, King George Island, Potter Peninsula, Stranger Point. Seashore, 0-5 m a.s.l. 22/12/2009. Leg. *F. Fernández-Mendoza & S. Domaschke.*	62.261502° S	58.617572° W	-	-	-	-	hap14	-	-
Verrucaria tessellatula	I348	Tierra del Fuego, Leg. *S. Pérez-Ortega*			hap17	hap16	hap12	-	-	-	-

Appendix 2. GENBANK accession numbers of samples used for constructing the Viridiplantae dataset.

Species	Class	*rbcL*	*tufA*	*atpB*	*18S*	*psaB*
Ankyra judayi	*Chlorophyceae*	KT199255	KT199255	KT199255	U73469	KT199255
Arabidopsis thaliana	*Magnoliopsida*	NC000932	-	NC000932	X16077	NC000932
Asterochloris echinata	*Trebouxiophyceae*	KP318700	-	-	KP318687	-
Auxenochlorella protothecoides	*Trebouxiophyceae*	KC843975	KC843975	KC843975	KT158711	KC843975
Botryococcus braunii	*Trebouxiophyceae*	KM462884	KM462884	KM462884	KF673380	KM462884
Bracteacoccus giganteus	*Chlorophyceae*	KT625421	KT625421	KT625421	HQ246327	KT625421
Chaetosphaeridium globosum	*Coleochaetophyceae*	NC004115	-	NC004115	AF113506	NC004115
Chlamydomonas reinhardtii	*Chlorophyceae*	NC005353	NC005353	NC005353	AY665726	NC005353
Chlorella' *mirabilis*	*Trebouxiophyceae*	KM462865	KM462865	KM462865	-	KM462865
Chlorella vulgaris	*Trebouxiophyceae*	NC001865	NC001865	NC001865	AB162910	NC001865
Chromochloris zofingiensis	*Chlorophyceae*	KT199251	KT199251	KT199251	KR904902	KT199251
Cyanophora paradoxa	*Glaucophyceae*	NC001675	NC001675	NC001675	-	NC001675
Dicloster acuatus	*Trebouxiophyceae*	KM462885	KM462885	KM462885	AB037085	KM462885
Dictyochloropsis asterochloroides	*Trebouxiophyceae*	KC333606	-	-	KC333460	-
Diplosphaera mucosa	*Trebouxiophyceae*	AM260444	-	-	KF673370	-
Dunaliella salina	*Chlorophyceae*	GQ250046	GQ250046	GQ250046	-	GQ250046
Elliptochloris bilobata	*Trebouxiophyceae*	KM462887	KM462887	KM462887	FJ648517	KM462887
Elliptochloris subsphaerica	*Trebouxiophyceae*	FJ217382	-	-	KF144205	-
Fusochloris perforata	*Trebouxiophyceae*	KM462882	KM462882	KM462882	-	KM462882

Geminella minor	*Trebouxiophyceae*	KM462883	KM462883	KM462883	AF387151	KM462883
Hafniomonas laevis	*Chlorophyceae*	KT625415	KT625415	KT625415	-	KT625415
Kirchneriella aperta	*Chlorophyceae*	KT199250	KT199250	KT199250	AJ271859	KT199250
Koliella corcontica	*Trebouxiophyceae*	KM462874	KM462874	KM462874	AJ306536	KM462874
Koliella longiseta	*Trebouxiophyceae*	KM462868	KM462868	KM462868	AJ306535	KM462868
Leptosira terrestris	*Trebouxiophyceae*	EF506945	EF506945	EF506945	Z28973	EF506945
Lobosphaera incisa	*Trebouxiophyceae*	NC_025533	NC_025533	NC_025533	-	NC_025533
Marchantia polymorpha	*Marchantiopsida*	NC001319	-	NC001319	AB021684	NC001319
Mesostigma viride	*Mesostigmatophyceae*	NC002186	NC002186	NC002186	AJ250109	NC002186
Microthamnion kuetzingianum	*Trebouxiophyceae*	KM462876	KM462876	KM462876	KM676977	KM462876
Mychonastes jurisii	*Chlorophyceae*	KT625411	KT625411	KT625411	AF106074	KT625411
Myrmecia israelensis	*Trebouxiophyceae*	KM462861	KM462861	KM462861	-	KM462861
Nymphaea mexicana	*Magnoliopsida*	KF753633	-	KF753633	-	KF753633
Oedogonium cardiacum	*Chlorophyceae*	EU677193	EU677193	EU677193	EU123943	EU677193
Oltmannsiellopsis viridis	*Ulvophyceae*	DQ291132	DQ291132	DQ291132	D86495	DQ291132
Oocystis apiculata	*Trebouxiophyceae*	EF113459	-	EF113524	-	-
Ostreococcus tauri	*Mamiellophyceae*	NC008289	NC008289	NC008289	Y15814	NC008289
Pabia signiensis	*Trebouxiophyceae*	KM462866	KM462866	KM462866	AJ416108	KM462866
Pandorina morum	*Chlorophyceae*	AB044166	U09442	AB044179	LC066325	AB044455
Parachlorella kessleri	*Trebouxiophyceae*	FJ968741	FJ968741	FJ968741	KM020114	FJ968741
Paulschulzia pseudovolvox	*Chlorophyceae*	D86837	-	AB014040	U83120	AB044473
Phacotus lenticularis	*Chlorophyceae*	KT625422	KT625422	KT625422	AY009897	KT625422
Pinus taiwanensis	*Pinopsida*	KP771703	-	KP771703	EF673731	KP771703
Planctonema	*Trebouxiophyceae*	KM462880	KM462880	KM462880	-	KM462880

lauterbornii						
Prasiola "calophylla" strain Garwood	*Trebouxiophyceae*	EF589145	-	EU380546	-	EU380573
Prasiola "crispa" strain Hallet	*Trebouxiophyceae*	EF589146	-	GQ423923	-	GQ423928
Prasiola borealis	*Trebouxiophyceae*	JF949724	KF993441	-	-	JQ669689
Prasiola novaezelandiae	*Trebouxiophyceae*	KF993461	KF993440	-	-	KF993462
Prasiola stipitata	*Trebouxiophyceae*	JQ669729	KF993446	-	EF200526	JQ669692
Prasiolopsis ramosa	*Trebouxiophyceae*	LN877827	LN877828	-	AY762600	-
Prasiolopsis SAG84.81	*Trebouxiophyceae*	KM464713	KM464716	KM491794	-	KM464699
Pseudendoclonium akinetum	*Ulvophyceae*	AY835431	AY835431	AY835431	DQ011230	AY835431
Pseudochloris wilhelmii	*Trebouxiophyceae*	KM462886	KM462886	KM462886	KM020115	KM462886
Pseudomuriella schumacherensis	*Chlorophyceae*	KT199256	KT199256	KT199256	HQ292768	KT199256
Pseudoscourfieldia marina	*Pyramimonadophyceae*	U30279	AB561077	AB561015	AF122888	AB561037
Psilotum nudum	*Psilotopsida*	NC003386	-	NC003386	X81963	NC003386
Pycnococcus provasolii	*Pyramimonadophyceae*	FJ493498	FJ493498	FJ493498	KT878683	FJ493498
Raphidonema nivale	*Trebouxiophyceae*	EF589151	-	EU380547	AF448477	EU380574
Rosenvingiella constricta	*Trebouxiophyceae*	JF949725	LN877837	-	-	JQ669690
Rosenvingiella tasmanica	*Trebouxiophyceae*	JF949726	LN877835	-	-	JQ669700
Scenedesmus obliquus	*Chlorophyceae*	DQ396875	DQ396875	DQ396875	AJ249515	DQ396875
Schizomeris leibleinii	*Chlorophyceae*	HQ700713	HQ700713	HQ700713	KM020182	HQ700713
Stichococcus bacillaris	*Trebouxiophyceae*	KM462864	KM462864	KM462864	AJ311637	KM462864

Stichococcus jenerensis	*Trebouxiophyceae*	KM438447	KM438448	-	DQ275461	-
Stigeoclonium helveticum	*Chlorophyceae*	NC008372	NC008372	NC008372	JF680955	NC008372
Symbiochloris reticulata	*Trebouxiophyceae*	NC_025524	NC_025524	NC_025524	KC333463	NC_025524
Trebouxia aggregata	*Trebouxiophyceae*	EU123967	EU123976	EU123988	EU123942	EU123975
Trebouxia jamesii	*Trebouxiophyceae*	AJ969663	-	EF530542	-	-
Treubaria triappendiculata	*Chlorophyceae*	KT625410	KT625410	KT625410	-	KT625410
Triticum aestivum	*Liliopsida*	NC002762	-	NC002762	AY049040	NC002762
Ulva fasciata	*Ulvophyceae*	KT882614	KT882614	KT882614	DQ286547	KT882614
Ulva linza	*Ulvophyceae*	KX058323	KX058323	KX058323	JN093105	KX058323
Volvox carteri f. *nagariensis*	*Chlorophyceae*	AB076099	-	-	X53904	AB076148
Watanabea reniformis	*Trebouxiophyceae*	KM462863	KM462863	KM462863	X73991	KM462863

Appendix 3. GENBANK accession numbers of samples used for constructing the *rbcL* dataset for the single-locus dating analysis.

Taxon	Strain or Isolate	Collection origin	GENBANK accession number
Prasiola antarctica	GALW015710	Antarctica: King George Isl.	JQ669718
Prasiola borealis	GALW015301	Canada: British Columbia	EF203021
Prasiola borealis	P20	Tasmania	JF949723
Prasiola borealis	WELT A024286, isolate ASJ459	New Zealand	HQ174309
Prasiola calophylla	GALW014331	Ireland: Galway	AY694194
Prasiola calophylla	GALW015716	Ireland: Galway	JQ669726
Prasiola cf. *furfuracea*	GALW015416	USA: Alaska	EF203016
Prasiola crispa	SBDN 745_1	Norway: Svalbard	LN877820
Prasiola crispa	Gal	Ireland: Galway	AY694195
Prasiola crispa	UPN1037	Antarctica: Balleny Islands	HQ174307
Prasiola crispa (Holotype)	BMHolotype	United Kingdom: Isle of Skye	JQ669725
Prasiola delicata	JASM203	Japan: Hokkaido	KT354050
Prasiola delicata	GALW015302	Canada: British Columbia	EF203020
Prasiola fluviatilis	MP12.25A	Norway: Svalbard	LN877822
Prasiola furfuracea	SBDN 1042	France: Bretagne	LN877823
Prasiola japonica	MM22	Nepal: Kathmandu	KT354068
Prasiola linearis	/	USA: Washington	AF189065
Prasiola meridionalis	Oregon	USA: Oregon	AY694191
Prasiola mexicana	GALW015728	Mexico	JQ669719
Prasiola novaezelandiae	UPN1003	New Zealand	HQ174305
Prasiola novaezelandiae	P2	New Zealand	KF993461
Prasiola sp.	GALW015715	Antarctica: Garwood Val., McMurdo Dry Valleys	JQ669710
Prasiola stipitata	GALW015436	Iceland	EF203014
Prasiola stipitata	ASJ460	New Zealand	HQ201401
Prasiola yunnanica	GALW015731	China: Chanshan Mountains	JQ669708
*Prasiola*sp.	Hallett	Antarctica: Cape Hallett	EF589146
Prasiolopsis ramosa	CCALA 420	Switzerland	LN877827
Prasionella wendyae	SBDN_1141D	Norway: Svalbard	LN877817
Prasionema payeri	SH-2015a	Norway: Svalbard	LN877814
Rosenvingiella australis	UPN804	New Zealand	HQ174313
Rosenvingiella polyrhiza	Al	USA: Alaska	AY694205
Rosenvingiella radicans	Ovi	Spain: Oviedo	AY694199
Rosenvingiellopsis constricta	UPN1044	New Zealand	HQ174315

Appendix 4. GENBANK accession numbers of samples used for constructing the *tufA* dataset for the single-locus dating analysis.

Taxon	Strain or Isolate	Collection origin	GENBANK accession number
Prasiola antarctica	P31	Antarctica: Palmer Station	KF993447
Prasiola borealis	P4	Tasmania	KF993441
Prasiola borealis	P33	Canada: British Columbia	KF993448
Prasiola calophylla	P41	Ireland: Galway	KF993449
Prasiola calophylla	P61	Ireland: Galway	KF993455
Prasiola crispa	P43	Antarctica: King George Isl.	KF993450
Prasiola crispa	P65	Sweden: Gothenburg	KF993457
Prasiola crispa	SBDN 745_1	Norway: Svalbard	LN877821
Prasiola furfuracea	P62	Ireland: Galway	KF993456
Prasiola delicata	GWS005076	Canada: British Columbia	HQ610263
Prasiola cf. *delicata*	GALW015795	Canada: British Columbia	KF993454
Prasiola meridionalis	F12	USA: Alaska	KF993433
Prasiola meridionalis	F21	USA: Oregon	KF993434
Prasiola meridionalis	F30	USA: Washington	KF993438
Prasiola meridionalis	F31	Canada: British Columbia	KF993439
Prasiola meridionalis	P7	USA: Washington	KF993442
Prasiola meridionalis	P8	USA: California	KF993443
Prasiola meridionalis	P10	USA: California	KF993444
Prasiola novaezelandiae	P2	New Zealand	KF993440
Prasiola stipitata	GWS003898	Canada: New Brunswick	HQ610265
Prasiola stipitata	GWS004462	Canada: British Columbia	HQ610267
Prasiola stipitata	F26	Iceland	KF993437
Prasiola stipitata	P26	United Kingdom: Plymouth	KF993446
Prasiola stipitata	P40	Ireland: Galway	KF993451
Prasiola stipitata	P54	Norway: Finnoy	KF993452
Prasiola stipitata	P55	Ireland: Kilkee	KF993453
Prasiola stipitata	P39	Canada: Newfoundland	KF993458
Prasiola yunnanica	P16	China: Chanshan Mountains	KF993445
Rosenvingiellopsis constricta	F01	Canada: British Columbia	KF993432
Rosenvingiella radicans	F25	Iceland	KF993436

Rosenvingiella australis	SBDN 500	New Zealand	LN877830
Rosenvingiella tasmanica	SBDN 358	Tasmania	LN877835
Rosenvingiella radicans	SBDN 1183	Norway: Nordland	LN877834
Prasionema payeri	SBDN_745_6 A	Norway: Svalbard	LN877816
Prasiolopsis ramosa	CCALA 420	Switzerland	LN877828

CAPÍTULO 6 (*CHAPTER 6*)

Estudio filogeográfico global de las especies del género de hongos liquenizados *Pseudephebe* (*Parmeliaceae*, Ascomycota), con especial atención al origen de las poblaciones de la Antártida.

Título en inglés: "A world-wide phylogeographic overview of the amphitropical genus *Pseudephebe* (*Parmeliaceae*, Ascomycota) offers new insights into the origin of the Antarctic lichen biota"

Abstract

The origin of amphitropical distributions has been a matter of debate since naturalists recognized this pattern of distribution in the XIX century. The Antarctic lichen biota is characterized by a substantial number of amphitropical taxa, accounting for *c*. 40% of the total diversity. The time frame in which Antarctic populations of these taxa were originated remains largely unexplored. In this study, we focused on the lichen-forming fungal species *Pseudephebe minuscula* and *P. pubescens* (*Parmeliaceae*, Ascomycota) largely alleged to show amphitropical distributions. A six-locus dataset and an extensive sampling covering all of the Earth's continents is used to investigate species delimitation in these lichenized fungi, whereas population genetics, clustering and dating analyses, and genealogical reconstruction methods are employed to disentangle the origin of their contemporary disjunct distribution patterns as well as the origin of their Antarctic populations. Our results demonstrate the existence of three phylogenetic *Pseudephebe* species that diverged between the Miocene and Pliocene: *P. minuscula*, which is so far the only species showing an amphitropical distribution and growing in Antarctica; *P. pubescens*, which displays a distribution restricted to the European continent; and a third, undescribed *Pseudephebe* species from Alaska (USA). Overall, clustering, intraspecific variability and dating results suggest a boreal origin for *P. minuscula*, which dispersed into the Southern Hemisphere directly and/or through "mountain-hopping" during the Pleistocene. The Antarctic populations of this species are sorted into two genetically unrelated clusters, one including populations of Maritime Antarctica together with South American ones, and the second composed of populations from the Transantarctic Mountains (Continental Antarctica) and from the Arctic. Therefore, our data provide strong evidence that current Antarctic distribution of *P. minuscula* is the result of several relatively recent and independent dispersals.

1. Introduction

The systematic and phylogeographic study of lichenized fungi has gained momentum in the last two decades as a consequence of the introduction of phylogenetic and population genetic methods (Werth 2010, 2011; Leavitt et al. 2015a), resulting in a complete reassessment of biogeographic criteria in lichens. First, the use of time-calibrated phylogenies has shifted the geologic time frame used to interpret fungal evolution towards more recent geologic periods (Taylor & Berbee 2006). The divergence of fungal classes seems to date earlier than 300 MA (Prieto & Wedin 2013; Beimforde et al. 2014; Pérez-Ortega et al. 2016), while some of the most diverse families and genera of lichenized fungi may have diversified and spread multiple times across all continents in the last 60–10 MA (Divakar et al. 2012; Leavitt et al. 2012a,b,c; Prieto & Wedin 2013; Molina et al. 2017). Second, the use of population genetic datasets in species of lichenized fungi has revealed the presence of strong population differentiation between continents (Printzen et al. 2003) as well as long-range genetic connectivity in circumboreal (Buschbom 2007; Geml et al. 2010) and transequatorial (Geml et al. 2012; Fernández-Mendoza & Printzen 2013) pathways. While environmental filtering and the lichen's climatic niche are ultimately responsible for the observed distributional patterns (Leavitt & Lumbsch 2016), sometimes modulated through photobiont use (Fernández-Mendoza et al. 2011; Fernández-Mendoza 2013; Magain et al. 2016; Singh et al. 2016), the observed patterns of geographic connectivity seem to reflect events in the recent history of Earth more than a continuous panmictic metapopulation. Finally, although some species have been interpreted to be widely distributed (Crespo et al. 2002; Leavitt et al. 2013; Fernández-Mendoza & Printzen 2013), a growing tendency to interpret population structure solely as a result of speciation has resulted in the widespread opinion that most widely distributed morphospecies may in fact be composed of smaller, overlooked phylogenetic species. Some of these studies have unveiled cryptic species (Bickford et al. 2007; Crespo & Pérez-Ortega 2009) in either the fungal or the algal component of the symbiosis (e.g. Molina et al. 2004; Spribille et al. 2011; Garrido-Benavent et al. 2017). In fact, phylogeographic approaches have played a pivotal role in stressing the need for a broad revision of species concepts in many fungal lineages, a point also highlighted in studies of other microorganisms (Martiny et al. 2006; Bass et al. 2007; Fontaneto et al. 2008; Ryšánek et al. 2015).

Although concepts in lichen biogeography have recently improved, two major biogeographic hypotheses have rarely been tested. The first is the origin of amphitropically disjunct distributions, which puzzled botanists and lichenologists since Humboldt's times. Second, the origin of the Antarctic lichen biota, which lichenologists intensively debated along the twentieth century (e.g. Du Rietz 1940; Lamb 1948, 1970; Galloway 1991; Seppelt 1995). In reality, bipolarity in lichens was primarily discussed in the context of the origin of the Antarctic lichen biota, as *c*. 40% of the species of lichen-forming fungi in this continent display such distribution pattern (Øvstedal & Lewis Smith 2001). Before the use of DNA data and reliable time-calibrated phylogenetic methods (Yang & Donoghue 2016), most authors agreed on assigning a dual origin for Antarctic lichens, with some endemic species being old

and others displaying wider geographic distributions as recent colonisers (e.g. Lamb 1948, 1970; Galloway 1991; Seppelt 1995).

In the present study, we investigated the amphitropical distribution and origin of Antarctic populations of species in the lichen-forming genus *Pseudephebe* (*Parmeliaceae*, Ascomycota). Based on morphological characters, two species within this genus have been accepted since long: *P. minuscula* and *P. pubescens*. Both species are saxicolous on acidic rocks, their growth form is typically fruticose, and sexual reproductive structures are not common (Stenroos et al. 2016). It has been reported that *P. minuscula* and *P. pubescens* co-occur in polar regions (Arctic and Antarctica) but are also abundant in alpine habitats of temperate regions such as Central-Southern Europe, Australasia, and North and South America (Brodo & Hawksworth 1977; Galloway & Quilhot 1998; Øvstedal & Lewis Smith 2001; Galloway 2007; Herrera-Campos et al. 2016). However, recent assessments based on a combination of molecular, morphological and chemical data have contested traditional species circumscription in *Pseudephebe* (Boluda et al. 2016). These authors highlighted the presence of two monophyletic lineages which do not match the morphological species concepts in this genus.

The aim of our study is to analytically explore the geographic distribution of *Pseudephebe* species from both a macro- and a microevolutionary perspective, putting special attention to the spatial-temporal origin of their Antarctic populations. In the first place, we will investigate the existence of cryptic species using a denser individual and molecular sampling. Thus, numerous samples from all continents and a six-locus dataset will be subjected to a species discovery-validation approach. Then, we will analyse the phylogeographic structure of delimited species and set a temporal framework for the evolution of the recovered genetic lineages. The obtained results will be used to infer whether *Pseudephebe* diversification and acquisition of the current disjunct distribution was due to vicariance or long-distance dispersal. A vicariant scenario would be supported if disjunction age estimates date back to the major tectonic events leading to the breakup of Pangaea and Gondwana (mid-Jurassic to Late Cretaceous, roughly 174–66 MA, Scotese 2001; Mao et al. 2012), while long-distance dispersal will be favoured if these ages are close to recent time periods (i.e. Miocene-Pleistocene, Popp et al. 2011; Fernández-Mendoza & Printzen, 2013; Lewis et al. 2014a; Villaverde et al. 2015a,b). With this study we want to contribute to the general understanding of the origin of amphitropical distributions, but also to the origin of lichen populations in one of the most isolated and fascinating austral landscapes, Antarctica.

2. Material and Methods

2.1. Individual sampling

For the present study we assembled a comprehensive collection of *Pseudephebe* specimens intended to contain most of its distributional range. In total, we included 356 specimens collected in 26 localities covering all continental landmasses, including Antarctica. Sampling effort per locality was not even, depending on whether localities were assembled from herbarium collections or were newly collected with a population genetics scope. The specific number of samples per locality is specified in Appendix 1. An additional sample of *Bryoria bicolor* was included in the dataset as outgroup for the calibration of phylogenetic inferences (Appendix 1).

2.2. DNA extraction, PCR, and sequencing

A terminal branch for each specimen was placed in 1.5 ml Eppendorf tube, frozen at -80º C and ground in a Retsch cell grinder. The resulting powder was subjected to DNA extraction following the CTAB/guanidine hydrochloride method of Werth et al. (2016). Elution of nucleic acids was done in 40 µl of elution buffer. Six putatively unlinked, nuclear fungal markers were amplified: the Internal Transcribed Spacer of the nuclear ribosomal DNA (*nrITS*), and the protein-coding elongation factor 1-*α* (*EF-1α*), DNA replication licensing factor of the mini-chromosome maintenance complex 7 (*Mcm7*), glyceraldehyde-3-phosphate-dehydrogenase (*GAPDH*), phosphoglycerate kinase (*PGK*), and the small ribosomal protein 60S L10 (*L1*). The latter two are used for the first time in a phylogeographic context. *Pseudephebe*-specific primers were designed using PRIMER-BLAST (Ye et al. 2012) to improve amplification success (Supplementary Table 1). PCR reactions were carried out in a total volume of 15 µl, containing 2 µl of undiluted, template DNA, 0.45 µl of each primer (10 µM), 7.5 µl of reaction buffer (Kapa Biosystems), and 0.12 µl of DNA polymerase (Kapa Biosystems); final volume was reached by adding distilled water. Amplification conditions are summarized in Supplementary Table 2. PCR products were visualized in 1.5% agarose gels stained with Midori Green (NIPPON Genetics EUROPE). Automated Sanger sequencing of DNA strands was performed on an ABI 3730xl by Microsynth (Vienna).

2.3. DNA sequence analysis

Raw electropherograms were manually checked, trimmed and assembled using SEQMANII v.5.07© (Dnastar Inc.). The few sequences showing ambiguous sites were visually corrected and collapsed into locally co-occurring haplotypes to avoid artificial inflation of genetic diversity. Alignments were carried out in GENEIOUS® v.9.0.2 using MAFFT v.7.222 (Katoh et al. 2002) and introns and exons in protein-coding markers were adequately annotated. Each single-locus dataset was subsequently tested for recombination using four alternative methods: the PHI test (Bruen et al. 2006) implemented in the software SPLITSTREE4 v.4.13.1 (Huson & Bryant 2006), and the methods RDP, GENECONV, MAXCHI

available in the software RDP4 version Beta 39 (Martin et al. 2010). Default parameters were imposed in the latter three analyses (Martin et al. 2010). Optimal substitution models and partition schemes for each dataset were estimated using PARTITIONFINDER v.1.1.1 (Lanfear et al. 2012). The greedy scheme-search algorithm and the Bayesian Information Criterion (BIC, Schwarz 1978) were employed to infer the optimum substitution model and partition scheme using both linked and unlinked estimation of branch lengths.

2.4. Determination of species boundaries

We approximated the delimitation of phylogenetic species in *Pseudephebe* with a two-step approach. First, available *nrITS* and *Mcm7* sequences from GENBANK were downloaded and aligned with the newly generated data. The fungal barcode *nrITS* was selected for inferring species boundaries in the lichen-forming fungus with the distance-based, Automatic Barcode Gap Discovery method (ABGD, Puillandre et al. 2012) using its online implementation in http://www.abi.snv.jussieu.fr/public/abgd/abgdweb.html. This procedure automatically finds the barcode gap in the distribution of genetic pairwise distances among input sequences, allowing these to be sorted into hypothetical species. We used the Kimura two-parameters (K2P) model to estimate genetic distances, a transition/transversion value of 3.15 calculated with MEGA v.5.2 (Tamura et al. 2011) and different values for the relative gap width (*X*). Then, the genetic structure of the dataset was graphically explored using multi-locus networks generated using the NEIGHBORNET algorithm (Bryant & Moulton 2004) as implemented in SPLITSTREE v.4.13.1 on standardized distance matrices between individuals calculated in POFAD v.1.07 (Joly & Bruneau 2006). The *nrITS* and *Mcm7* datasets included individuals with sequences available for both markers, which were concatenated and subsequently reduced to multi-locus haplotypes. Then, sequence ends were trimmed to include the smaller number of missing nucleotides. The definitive analysis used the *genpofad* distance algorithm, a Jukes and Cantor correction for multiple hits, gaps coded as fifth state, while missing nucleotides and distances were both ignored.

The Bayes Factor Delimitation (BFD) method, which allows for topological uncertainty in gene trees and incongruences among gene trees (i.e. incomplete lineage sorting), was chosen to compare three different species boundary hypotheses compiled from previous analyses (Supplementary Table 3). Since its inception (Grummer et al. 2014), this approach has been widely applied when dealing with divergence of closely related species (Chen et al. 2014; Wei et al. 2016) or in phylogeographic studies using large sample numbers (Bagley et al. 2016; Garrido-Benavent et al. 2017). *BEAST (Heled & Drummond 2010; Drummond et al. 2012) was used to construct the different models, which included an outgroup to allow the one-species model to be tested (Chen et al. 2014). Simple data partitions and strict clocks were imposed on each marker after assessing convergence in preliminary, more parameter-rich *BEAST analyses. The mean clock rate was fixed to 1.0 for *nrITS* whereas rates were co-estimated for *Mcm7* under a uniform prior (0, 3). Analyses used a Yule tree prior, which assumes a constant lineage birth rate for each branch in the tree, and the piecewise linear and constant root model for population size (Grummer et al. 2014). These parameters were given

an uniform hyperprior (0.00015, 3), while remaining parameters used default priors. Two runs of 175 M generations, saving every 17.500th tree, were performed using the CIPRES Science Gateway (Miller et al. 2010) and then combined with LOGCOMBINER v.1.8.1. TRACER v.1.6 (http://tree.bio.ed.ac.uk/software/tracer/) was used to check for convergence, assumed if effective sample sizes (ESS) were > 200. Calculation of marginal likelihoods estimates (MLE) was done using Path Sampling (PS, Lartillot & Philippe 2006) and Stepping-Stone (SS, Xie et al. 2011), with default settings. MLE were averaged across runs and Bayes Factors were calculated following Hedin et al. (2015). 2lnBF > 10 indicate very strong evidence against a model as compared with the best (Kass & Raftery 1995).

In the second step, we evaluated how clear-cut validated species resulted subjecting the six-locus dataset to a Discriminant Analysis of Principal Components (DAPC; Jombart et al. 2010). This analysis was implemented using the package *adegenet* v.2.0.1 (Jombart 2008) in R v.3.2.5 (R Development Core Team 2014) and a multi-locus matrix of haplotype numbers obtained after collapsing sequence data with PGDSPIDER v.2.0.7.2 (Lischer & Excoffier 2012). Analyses were run with different numbers of retained axes, which preserved between 50–90% of the total variance, and all discriminant functions. Additionally, a NEIGHBORNET multi-locus network including only individuals with all markers available was generated in SPLITSTREE v.4.13.1 as described above.

2.5. Population assignment and admixture

Population stratification was assessed by using three complementary approaches that assume alternative population models. First, we conducted single and multi-locus mixture analyses under a Bayesian framework in Baps v.6 (Corander & Marttinen 2006; Corander et al. 2008). This method uses a stochastic-greedy algorithm that minimizes Hardy-Weinberg (HW) and linkage disequilibrium (LD) within *k* identified clusters. Analyses were run with single nucleotide polymorphism (SNP) data files, "clustering with linked loci" and codon linkage models, and *k* values ranging from 2 to 15, with 8 replicates for each value.

Secondly, because vegetative multiplication may play an important role in the propagation strategy of *Pseudephebe*, we used discriminant analysis of principal components (DAPC, Jombart et al. 2010), a simple parametric approach to estimate genetic clusters that does not imply strong prior assumptions on population dynamics. The method is implemented in the wrapper functions *optim.a.score* and *find.clusters* of R package *adegenet* (Jombart 2008), and it makes use of function *dudi.pca* to compress a matrix of haplotype numbers to its orthogonal components which are later used to infer individual clusters using *k-means* clustering. A preliminary run using function *optim.a.score* is used to choose the number of retained components and a maximum number of clusters, using 30 simulations. The retained number of components is later processed using function *find.clusters* to automatically infer the optimum number of genetic clusters (Jombart et al. 2010) and the individual adscription per sample.

Finally, the program STRUCTURE v.2.3.4 (Falush et al. 2003; Pritchard et al. 2000) was used to estimate adscription to populations under an admixture model based on a multi-locus matrix of haplotype numbers. Ten replicate runs were used for each level of stratification (*K)* ranging between 1 and 15 populations, each run consisting of 80.000 burn-in generations, followed by 800.000 iterations. The analysis used a model allowing admixture, no prior population information, a uniform alpha prior, whereas allele frequencies were kept independent among gene pools in order to avoid overestimating the number of gene pools (Falush et al. 2003). To estimate the optimum number of clusters (best *k*) we used the criteria of Evanno et al. (2005) as implemented in the *POPHELPER* R package (Francis 2016).

2.6. Polymorphism statistics, haplotype networks, and neutrality tests

We first calculated genetic diversity estimators for each marker to discuss their suitability for inter- and intraspecific studies. DNASP v.5.10 (Librado & Rozas 2009) was used to compute the number of segregating sites (*s*), number of haplotypes (*h*), haplotype diversity (*Hd*), average number of nucleotide differences (*k*), nucleotide diversity (π) either using the Jukes & Cantor (1969) correction or not, and parsimony informative sites. Next, DNA polymorphism was evaluated for each marker according to: a) candidate species delineated by species discovery-validation analyses and b) major geographical regions. Gaps were not considered in calculations. The three Chinese individuals were removed from these analyses. Statistical parsimony using the method TCS (Clement et al. 2002) as implemented in POPART v.1.7 (Leigh & Bryant 2015) was used to infer relationships among haplotypes. This approach does not take gaps into consideration, and therefore the total number of haplotypes can differ from those used in phylogenetic inference (see below). For the *nrITS*, we used both the extended and non-extended datasets. Finally, deviations from neutrality, which are useful for inferring past population size changes, were tested with Tajima's *D* and Fu's *Fs* statistics in DNASP v.5.10 using the number of segregating sites. The significance of these tests was assessed based on 10^4 coalescent simulations.

2.7. Quantifying genetic divergence and differentiation

The average number of nucleotide substitutions per site (Dxy, Nei 1987) and the allele-based estimator Θ for Wright's fixation index Fst (Weir & Cockerham 1984) were used as proxies to measure the extent of genetic divergence and differentiation between six major geographical regions: Northern Europe, Central-Southern Europe, North America, South America, New Zealand and Antarctica. Dxy and Fst values were estimated in ARLEQUIN v.3.5 (Excoffier & Lischer, 2010) and results were graphically represented with a collection of R functions (R Development Core Team 2014) implemented in *r-lequin* (http://heidi.chnebu.ch/doku.php?id=r-lequin). Haplotype input files were initially constructed with DNASP v.5.10, including gaps and invariable sites. China and Greenland were excluded from these analyses due to the small number of individuals.

2.8. Dating analyses

To set divergence and diversification of validated species into a temporal context, we used *BEAST and BEAST. Two alternative parmelioid *nrITS* average mutation rates were imposed on the multi-locus dataset: 2.4×10^{-3} s/s/MA (*Oropogon*, Leavitt et al. 2012a) and 3.41×10^{-3} s/s/MA (*Melanohalea*, Leavitt et al. 2012b). These rates are expected to accommodate the bias derived from the different calibration strategies used for their estimation as well as the likely variability in substitution rates within family *Parmeliaceae*. In *BEAST, multi-locus haplotypes were sorted into: (1) candidate species; (2) BAPS clusters; and (3) the previous six major geographical regions. Only individuals for which all markers were available were considered in all analyses. Convergence issues detected in more richly parameterized, preliminary analyses were overcome by imposing a strict clock and single partitions on each dataset. Clocks and trees were inferred independently for each locus. As starting tree, we used a ML topology obtained in RAxML which was transformed into an ultrametric tree using the *chronos* function in the *ape* R package (Paradis et al. 2004). The remaining parameters and prior distributions were set as in the species validation analyses. Subsequently, single-locus haplotype chronograms were calculated in BEAST v.1.8.1. We used average substitution rates for each marker inferred in previous candidate species dating analyses (Supplementary Table 4), and a relaxed (*nrITS*, *Mcm7*, *GAPDH*, *EF-1α*, *PGK*) or strict (*L1*) clock and a Yule tree prior for each marker according to preliminary Bayes Factor comparisons (data not shown). Overall running instructions included variable chain lengths ranging from 2.5×10^8 steps (multi-locus analyses) or 7.5×10^7 (single-locus analyses), saving always 10.000 trees. After selecting an adequate burn-in, and checking for convergence in TRACER v.1.5 (http://tree.bio.ed.ac.uk/software/tracer/), the mean heights of the post-burn-in tree samples were annotated in TREEANNOTATOR v.1.8.1 (Drummond et al. 2012). FIGTREE v.1.4.0 (http://tree.bio.ed.ac.uk/software/figtree/) was used to construct 50% majority rule consensus trees, which were then edited in ADOBE ILLUSTRATOR CS5.

3. Results

3.1. Molecular datasets

We obtained 2.107 sequences for 356 specimens of *Pseudephebe*: 352 *nrITS*, 355 *Mcm7*, 346 *GAPDH*, 353 *EF-1α*, 355 *L1*, and 346 *PGK*. The six loci were available for three hundred and thirty-seven individuals (including the outgroup). The two-loci dataset used in the first step of the species delimitation analysis included 48 *nrITS* and 38 *Mcm7* additional sequences downloaded from GENBANK (Appendix 2). Newly generated primers for *L1* and *PGK* proved also useful for amplification in other parmelioid and non-parmelioid lichenized fungi (data not shown). *GAPDH*, *EF-1α* and *L1* amplicons combined exonic and intronic regions, the last being more polymorphic. The *nrITS*, *EF-1α*, and *PGK* alignments showed the highest values of polymorphic and parsimony informative sites, haplotype diversity and average number of nucleotide differences, whereas nucleotide diversity was higher in the

nrITS and *L1* alignments. These and other genetic diversity statistics are summarized in Supplementary Table 5. The MAXCHI and GENECONV methods found non-statistically significant signals of intragenic recombination for *nrITS*, *EF-1α*, *L1* and *PGK*. The PHI test also detected recombination in *Mcm7* and *PGK* close to the 95% significance threshold, but this signal was lost when the data sets were analysed separately for each BFD validated species (see below). The high polymorphism shown by the former four loci coupled with the fact that *Pseudephebe* rarely reproduces sexually points to recombination signal to be the result of homoplasy. Data on alignments and estimated substitution models used in different analyses are in Supplementary Table 6.

3.2. Species delimitation

ABGD analyses of the *nrITS* dataset rendered either biologically unrealistic (82 partitions or candidate species) or more credible (3 partitions) outcomes across variable prior thresholds (*X*) ranging from 0.5 to 2 (Figure 1A,B). Considering the three-species model, one candidate species accommodated 347 individuals distributed in all continents (amphitropical distribution), a second included 51 European individuals, while the third consisted of only two Alaskan specimens. One hundred and fifty-seven multi-locus haplotypes were used for the multi-locus network analysis. The trimmed *nrITS* and *Mcm7* datasets consisted in 491 bp and 457 bp, respectively. Figure 1C shows data split into two or three main clusters, with dense reticulation in the larger cluster, which includes specimens with an amphitropical distribution. The three-cluster interpretation of that graph agrees with the ABGD outcome, while considering two clusters implies to merge the former two smaller groupings (51 European and two Alaskan individuals) into one candidate species. Extraordinary long branches in the network should not be taken into consideration as they correspond with individuals showing still many missing nucleotides at sequence ends. The BFD method supported the three-species over the one- or two-species model (Supplementary Table 3). Marginal likelihood values for the considered models averaged over two runs and calculated through PS and SS are shown in Supplementary Table 3.

In the second step, only the DAPC analysis that used 90% of the total variance in the six-locus dataset could discriminate the third BFD-validated species, composed of one Alaskan individual, from the amphitropical *Pseudephebe* (Supplementary Figure 1). The amphitropical and the strictly European species were always revealed as separate species. Finally, the NEIGHBOURNET six-locus network showed a large, strongly reticulate cluster corresponding with the amphitropical species, and a clearly separate, minor cluster including the strictly European species (Figure 1D). This analysis did not include the Alaskan individual (third species) as it lacked data for *EF-1α*.

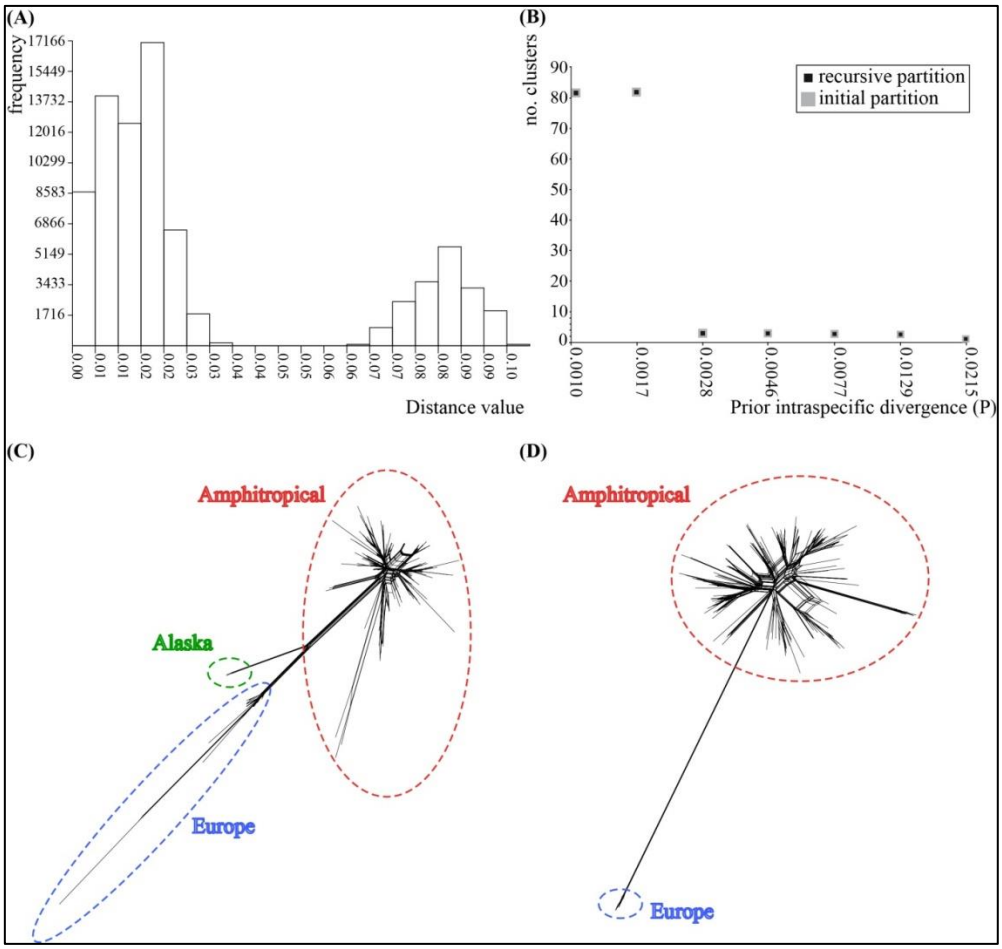

Figure 1. Species delimitation in *Pseudephebe*. (A–B) ABGD analysis output based on a *nrITS-Mcm7* dataset and using a prior threshold $X = 1.5$. (A) Histogram showing the distribution of pairwise genetic distances (Kimura 2-parameter) among all sequences and the major barcode gap. (B) Plot showing how different values of "prior intraspecific genetic divergences" affect the number of clusters or hypothetical species recovered by the ABGD method (note that recursive partitions are obtained by allowing the threshold to vary among species). (C) and (D) SPLITSTREE NEIGHBORNET diagrams obtained from two-locus or six-locus datasets, respectively. Delimited species are highlighted in different colours with an indication of their geographic distribution. In (C), the three delimited groups correspond with the three partitions or species inferred in *nrITS* ABGD analyses.

3.3. Phylogeographic structure and tokogenic relationships

According to the species delimitation results, our data was divided into three sets, or species, which shared no haplotypes. Only the amphitropical species was subjected to population assignment tests because it represents the main focus of the present work, i.e. it is amphitropically distributed and shows populations in Antarctica. The number of inferred SNP used in BAPS analyses were 62 (*nrITS*), 49 (*Mcm7*), 43 (*GAPDH*), 64 (*EF-1α*), 27 (*L1*) and 69 (*PGK*). Single-locus mixture clustering revealed neither a coherent number of clusters across markers, which ranged from six (*Mcm7*) to eight (*nrITS*, *L1*), nor geographically restricted

clusters supported by all loci (Figure 2). The assignment of individuals from widely distant localities in both hemispheres into the same cluster was common in all markers. This was especially true for *Mcm7*, *EF-1α* and *PGK*, in which several clusters were found to be widespread across continents. Noteworthy, the bulk of continental Antarctic individuals were usually included within a cluster of Northern Europe specimens (e.g. *nrITS*, *L1*), while the majority of maritime Antarctic specimens were allocated to a different cluster distributed in South America (Figure 2).

The BAPS analysis of the multi-locus dataset identified an optimum number of eleven mixture clusters (Figure 3, upper panel). Although not statistically tested, assignment of individuals mostly reflected specific combinations of *nrITS* and *L1* clusters (see Figure 2). Contrary to the single-locus clustering, the multi-locus clustering showed more geographically restricted assemblages of individuals, especially within Central-Southern Europe. Some clusters were shared among close geographic areas (e.g. between Northern and Central-Southern Europe, North and South America, or southern South America and Maritime Antarctica), but there were notable exceptions to it. For instance, the existence of a few South American (Bolivia) individuals within a predominantly Northern Europe cluster, a few Central-Southern Europe specimens in a prevalently South American-North American cluster, and the inclusion of all New Zealand samples together with a few ones from Alaska in a distinct cluster. Broadly, these three amphitropical clusters were also discriminated in STRUCTURE and DAPC analyses, despite the overall number of multi-locus clusters identified by these methods was slightly different: ten in STRUCTURE and nine in DAPC (Figure 3). STRUCTURE found several admixed populations which involved *Pseudephebe* specimens distributed in widely disjunct populations (Figure 3A, bottom panel). For example, the continental Antarctic and some individuals from Northern Europe, the North American and North European, or the New Zealand and some South American individuals. Particularly, all individuals from Bolivia, China, and some from Svalbard, Austria and Alaska showed significant admixed fractions. On the other hand, the DAPC analysis shed further light on the geographic extent of the inferred clusters (Figure 3B–C). Thus, clusters restricted to the Northern or Southern Hemisphere were five and one, respectively. A seventh cluster was found to be purely bipolar (Svalbard, Continental and Maritime Antarctica), and the remaining two were shown to be amphitropical in a broad sense (Figure 3B). Figure 3C shows a plot of the first seven PCs calculated from the data. Clusters II (blue dot) and V (light orange dot), and to a lesser extent cluster IV (red dot), were separated from the remaining six clusters, which lay close to each other. Cluster IV and V comprised specimens only from Central-Southern Europe, with cluster V made purely of Iberian Peninsula samples. Cluster II included Southern South American and maritime Antarctic specimens.

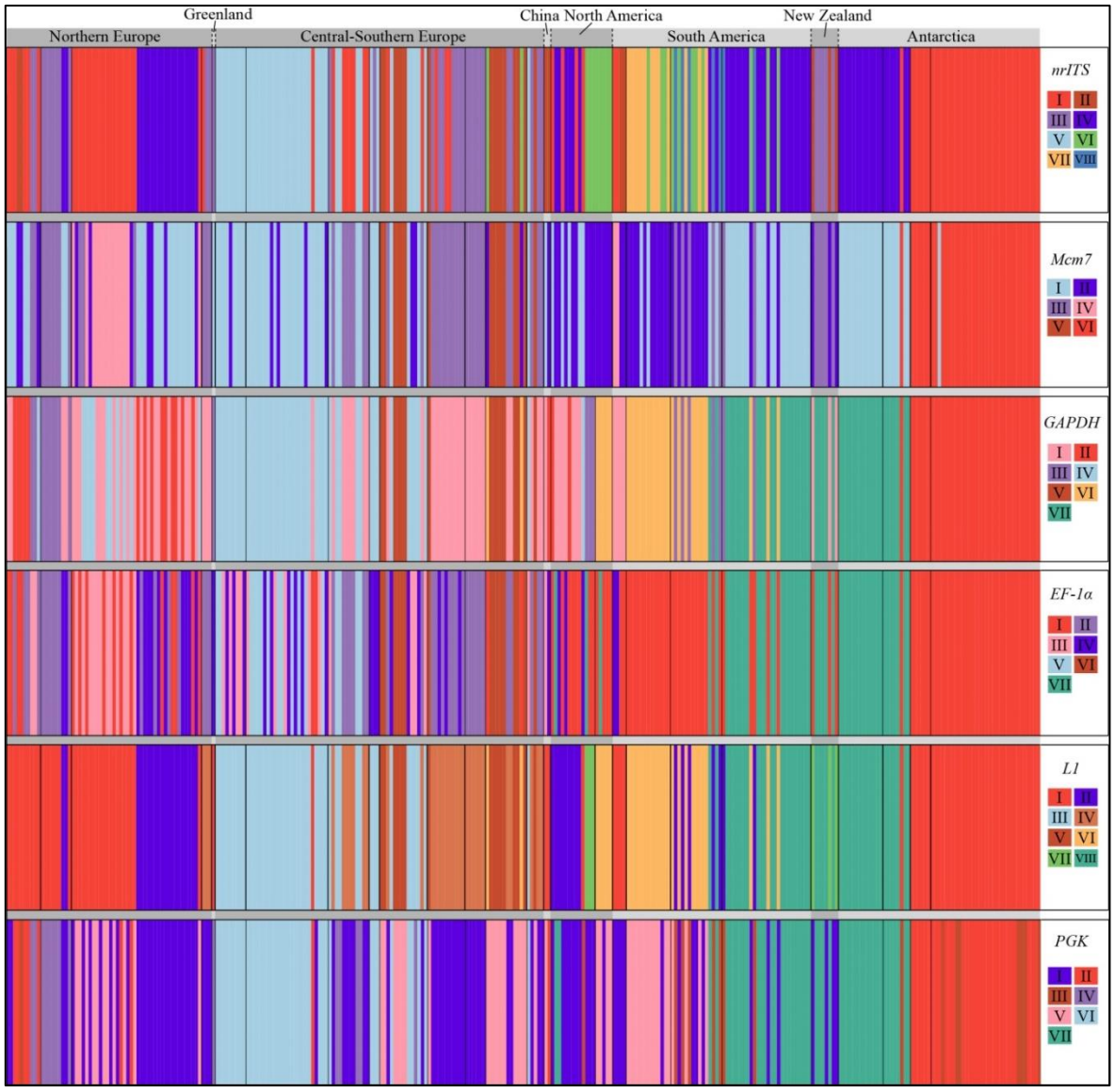

Figure 2. Mixture results from Bayesian clustering analyses conducted with BAPS using SNP data from six loci (*nrITS*, *Mcm7*, *GAPDH*, *EF-1α*, *L1* and *PGK*) from specimens of the amphitropical *Pseudephebe* species collected in Northern, Central and Southern Europe, Greenland, North and South America, China, New Zealand and Antarctica. Panels show individual population assignments based on single-locus data. Different genetic clusters are indicated with different colors and Roman numerals (on the right).

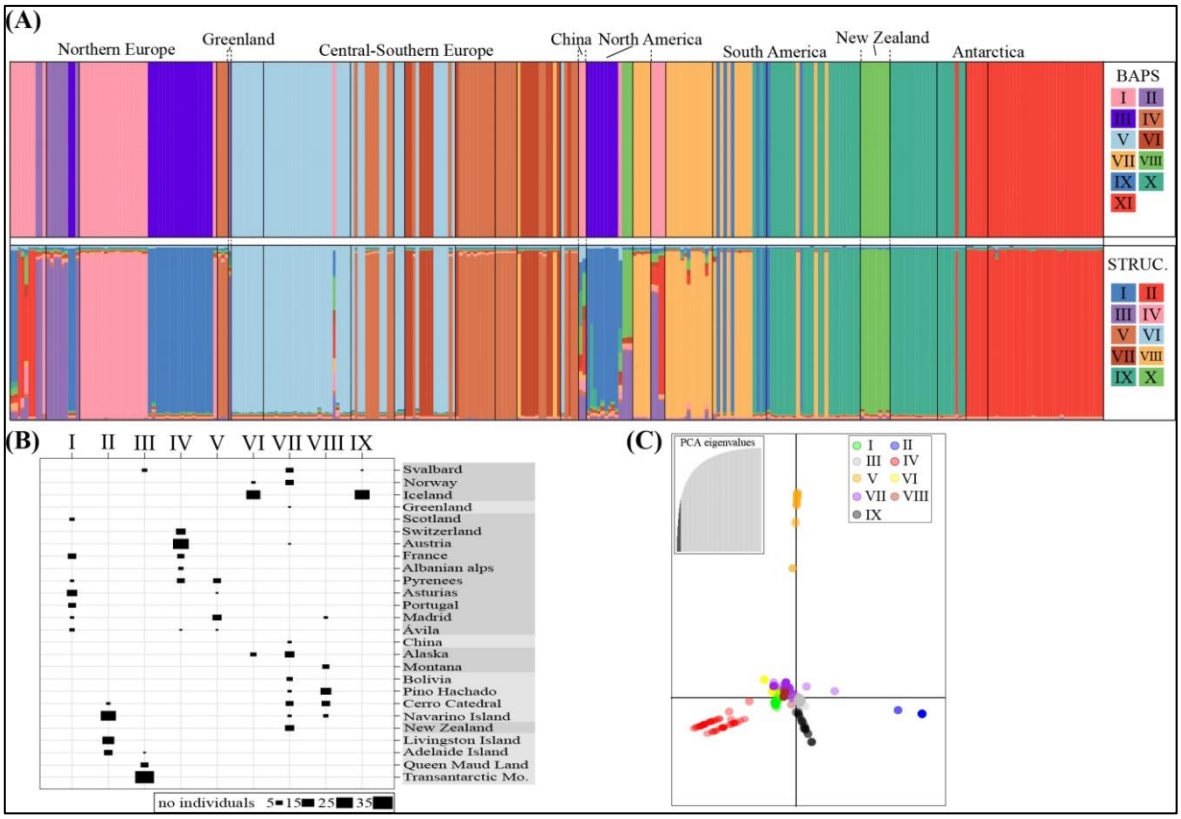

Figure 3. Phylogeographic structure of specimens of the amphitropical *Pseudephebe* species collected in Northern, Central and Southern Europe, Greenland, North and South America, China, New Zealand and Antarctica. (A) The top panel shows mixture results from a Bayesian clustering analysis conducted with BAPS using a combined matrix of SNP from the six loci (*nrITS*, *Mcm7*, *GAPDH*, *EF-1α*, *L1* and *PGK*); bottom panel shows the admixture results of a Bayesian clustering analysis with STRUCTURE using haplotype data under the K = 10 model; vertical bars represent individual assignment probabilities to different genetic clusters indicated with colors. Different genetic clusters are indicated with different colors. (B–C) Discriminant Analysis of Principal Components (DAPC) graphical outputs under K = 9. (B) The squares show the number of individuals assigned to the different clusters using the function *find.clusters* (R package: *adegenet*; Jombart et al. 2010). (C) Scatter plot of the amphitropical *Pseudephebe* grouped into 9 clusters on the first two axes (discriminant function variables) of DAPC; colored circles represent individuals with colors corresponding to assigned clusters; inset on the upper left corner shows the selected PCA eigenvalues (seven). Note that Roman numerals used in each analysis do not correspond to the same individual groupings.

Data of all three *Pseudephebe* species was used for calculating haplotype networks (Supplementary Figure 2–8). In all cases, the three species were well-resolved as separate. The extended and non-extend *nrITS* datasets comprised 78 (Supplementary Figure 2) and 64 (Supplementary Figure 3) haplotypes, respectively. The network for the amphitropical species

showed a complex pattern. Haplotypes from Northern and Central-Southern Europe were well-distributed across the entire network, while those from North America, South America, New Zealand and Antarctica were independently connected to different parts of the network. Some star-like sub-networks were also found, in which the central haplotype was usually one from Northern Europe (often shared by some North American specimens) or Central-Southern Europe.

The *Mcm7*, *GAPDH*, *EF-1α*, *L1* and *PGK* datasets comprised 43, 35, 48, 26 and 57 haplotypes, respectively (Supplementary Figure 4–8). Although the overall genealogical patterns depicted in the networks of the amphitropical species were also complex, some biogeographically relevant points could be distinguished. First, the existence of one or two star-like subnetworks with a central haplotype which was either amphitropically distributed or restricted to the Northern Hemisphere. For instance, in the *Mcm7*, *EF-1α* and *L1*, the central haplotype was shared at least by individuals from Northern Europe, South America and Antarctica; oppositely, the central haplotype in the star-like sub-network of *GAPDH* was from North America, while that of the *PGK* was shared by Northern Europe and Central-Southern Europe specimens. And second, the different haplotypes inferred from localities with few individuals, such as New Zealand and China, were connected to different parts of the network, as observed also in the *nrITS*, which suggests different origins for them.

3.4. Genetic polymorphism, population differentiation, and neutrality tests

Genetic diversity indices, genetic differentiation and divergence, and neutrality tests were again calculated only in the amphitropical species (Supplementary Figure 9; Supplementary Table 7). Values for number of haplotypes (*h*) and haplotype diversity (*Hd*) were greater for the three Northern Hemisphere regions than the Southern Hemisphere ones. The nucleotide diversity (π) followed the same trend as the previous indices for some markers, while in others the reversed situation was true. On the other hand, only New Zealand and to a lesser extent Central-Southern Europe and Antarctica showed some level of population differentiation (Fst) and distance-based (Dxy) divergence. The lowest values of Dxy were found between South America and Antarctica in five out of the six markers. High values of Dxy were observed between Northern Europe and Central-Southern Europe, in spite of their geographic proximity. Northern Europe and North America displayed low levels of Fst, indicating some level of population connectivity. Finally, neutrality tests for *nrITS*, *EF-1α* and *PGK* considering all geographic regions gave significant negative values of Tajima's *D* and Fu's *Fs*, which indicates population expansion, likely after a bottleneck. Oppositely, positive and significant values of *D* (*Mcm7*, *GAPDH*, *PGK*) and *Fs* (*nrITS*, *Mcm7*, *GAPDH*, *PGK*) were found for Antarctica, New Zealand and, more rarely South America. This finding could be congruent with a recent founder event or substantial population contraction scenario (Schneider & Excoffier 1999).

3.5. Estimation of divergence times

The use of a *Melanohalea nrITS* substitution rate produced younger estimates, but 95% highest posterior density (HPD) intervals largely overlapped to those obtained using the more slowly evolving *nrITS* rate of *Oropogon* (data not shown). For simplicity, only the mean age estimates deriving from using either an *Oropogon* or a *Melanohalea* substitution rate will be considered for discussion, while HPD intervals can be viewed at chronograms. The tMRCA of the amphitropical and strictly European species was estimated to be between 6.2–4.42 MA, during the late Miocene and Pliocene (Figure 4). The topology of the *BEAST tree of multi-locus BAPS clusters is not well resolved, particularly at recent nodes (Figure 5). Diversification of the amphitropical *Pseudephebe* species occurred between the late Pliocene and Pleistocene, 3.12–2.19 MA. Clusters VI and VII were placed at the root of the subtree and these were composed of individuals from Central-Southern Europe (VI) or Central-Southern Europe, North and South America (VII). This fact is coherent with DAPC results (Figure 3D) and the number of restricted and isolated haplotypes found in these regions in the haplotype networks (Supplementary Figure 2–8). Statistical support was given to the relationship of clusters III and X, and clusters I and XI. These two groups reflect independent acquisitions of a transequatorial distribution, including the origin of Antarctic populations, which likely took place in the late Pleistocene. On the other hand, when individuals of the amphitropical species were assembled in groups according to their geographic origin, the *BEAST reconstruction supported the basal placement of New Zealand individuals (Figure 6). This is also congruent with the isolated position of New Zealand haplotypes that was found in the haplotype networks (Supplementary Figure 2–8). Although the relative position of the remaining regions was not well-resolved, their specific association reflected the influence of geographic proximity. Thus, Northern and Central Southern Europe, and South America and Antarctica, lay closely related to each other.

Single-locus chronograms are depicted in Supplementary Figure 10–16. Phylogenetic relationships among haplotypes were largely unsupported and only very external and the recent-most nodes received some support. The two validated species referred above (the amphitropical and European) were well-resolved as separate across different markers, and their divergence was estimated to have occurred mainly between the mid-Miocene and Pliocene. Haplotype diversification occurred chiefly in the Pleistocene (*nrITS*, *Mcm7*, *EF-1α* and *PGK*) and also in the Pliocene (*GAPDH*, *L1*). In general, haplotypes from individuals collected in the Northern Hemisphere (i.e. Northern and Central-Southern Europe, and to a lesser extent North America) were evenly distributed along the phylogenetic trees. Oppositely, Southern Hemisphere haplotypes were placed in different branches along the tree that were mainly composed of Northern Hemisphere haplotypes. This latter observation agrees with the tokogenic relationships depicted in the haplotype networks (Supplementary Figure 2–8).

4. Discussion

4.1. Diversification in *Pseudephebe*

Lichen-forming fungi stand out among terrestrial organisms due to their extremely wide geographic ranges, although these patterns might sometimes be the result of very broad taxonomic concepts (Crespo et al. 2010a; Spribille et al. 2011; Amo de Paz et al. 2012). Here, we focused on two allegedly amphitropical species in the genus *Pseudephebe*, *P. minuscula* and *P. pubescens*, whose traditional circumscription based on morphological characters has been recently re-defined on the grounds of phylogenetic data by Boluda et al. (2016). We have found three lineages using the species discovery-validation approach and two of them could be ascribed to the phylogenetic species *P. minuscula* and *P. pubescens* (*sensu* Boluda et al. 2016). Our study further confirms the amphitropical distribution of the morphologically variable *P. minuscula*, which is here extended to include Antarctica, New Zealand, the Andean Cordillera and some Chinese localities. In contrast, the distribution of *P. pubescens* is so far restricted to the European continent. Our extensive individual sampling also allowed us to determine the existence of a third, undescribed species composed of only one Alaskan individual genetically and morphologically close to the strictly European *P. pubescens* (Supplementary Figure 17).

The fact that *P. minuscula* encompasses phenotypically variable individuals merits special attention (Supplementary Figure 17). In localities at high latitudes, such as Svalbard, Iceland and Antarctica, specimens showing the two morphological extremes coexist. These morphologies correspond with the former species concepts in the genus: a) *pubescens*-like thalli are decumbent to shrubby with more or less terete branches, and b) *minuscula*-like thalli are prostrate, sometimes subcrustose in the centre and have flattened branches closely attached to the substrate. In some regions, such as Iceland and Antarctica, individuals were sorted into two genetically-different clusters which match the morphological types. This is clear in BAPS *nrITS* and *L1* single- and multi-locus mixture clusters whereas alleles in the remaining markers were shared between morphotypes (Figure 2–3). This fact might indicate a genetic basis for the acquisition of certain morphotypes, despite an exclusive dependence on specific niche conditions, either abiotic (e.g. wind or sun exposure) or biotic (different associated microbiome or photobionts) cannot be discarded. Cases of intraspecific phenotypic variation with an incipient genetic basis have been documented in other lichen-forming fungi as well (Leavitt et al. 2011a,b). Pérez-Ortega et al. (2012b) found that vagrant forms of *Cetraria aculeata* occurring in steppe areas on the Iberian Peninsula were not a random genetic subset of the investigated populations. The distinct ecophysiological behaviour of each morphotype of vagrant *C. aculeata* suggested an adaptational background to environmentally harsh conditions, a scenario which might also stand for *P. minuscula*.

The phenotypic plasticity in *Pseudephebe* species, especially in *P. minuscula*, prevents from separating them on a morphological basis, and therefore only molecular tools can so far resolve with certainty species limits in this genus; in particular, the *nrITS* marker seems to

perform well as barcode (Figure 1A–B). When diagnosable phenotypic characters are lacking, contextualizing the temporal component of diversification may provide additional assistance for molecular-based species delimitation (Leavitt et al. 2016a). Our dating analyses showed that the three lineages diverged between the Miocene and Pliocene (Figure 4–6; Supplementary Figure 10). This time frame supports the hypothesis of three long-time molecularly differentiated species, and at the same time it overlaps with the proposed Neogene divergence of species in many other genera of lichen-forming fungi (Otálora et al. 2010; Amo de Paz et al. 2011; Leavitt et al. 2012b, 2013, 2015b; Garrido-Benavent et al. 2016). The phenotypical plasticity of *Pseudephebe* species contrasts with the morphological stasis shown at the genus level. The latter situation is common to several genera that also include cryptic lineages and for which diversification dated back into the Miocene and Plio/Pleistocene (Leavitt et al. 2012a,c, 2013). Phenotypic stasis in *Pseudephebe* may be explained by genetic and developmental constraints that limit the production of phenotypic variation (Gould 2002), or by stabilising selection promoting adaptation to an optimum that moves within an adaptive zone with stable boundaries (Estes & Arnold 2007). However, available genetic or ecological data for *Pseudephebe* does not allow for exploring these scenarios in further detail.

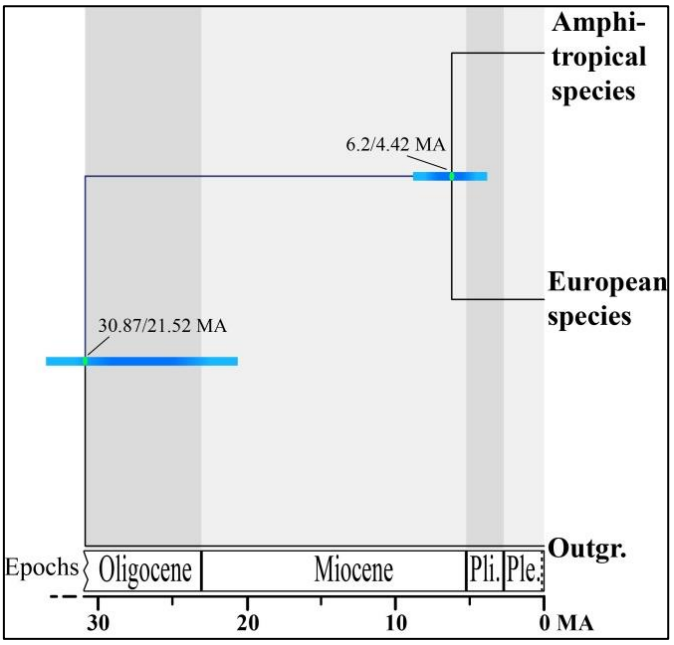

Figure 4. Chronogram depicting divergence times for the amphitropical (*Pseudephebe minuscula*) and the strictly European (*Pseudephebe pubescens*) species using multi-locus data and the *BEAST population/species tree reconstruction method. Dates on the left and right correspond with those inferred using an *Oropogon* (Leavitt et al. 2012a) or a *Melanohalea* (Leavitt et al. 2012b) *nrITS* fungal substitution rate, respectively. Bars show the 95% highest posterior density intervals (HPD) obtained in the analysis using an *Oropogon nrITS* substitution rate. The bar on the node connecting *Pseudephebe* spp. to the outgroup (*Bryoria*

bicolor) is trimmed for better visualization. Green ovals on nodes represent significant statistical support (PP ≥ 0.95). MA: million years ago.

Interspecific and intraspecific diversification in *Pseudephebe* was apparently modulated by different processes occurring at consecutive time frames. Our dating analyses indicates that speciation took place after the mid-Miocene Climatic Optimum (Figure 4–6; Supplementary Figure 10), when tundra-like ecosystems in polar and alpine regions started to expand, *c*. 7–5 MA (Mosbrugger et al. 2005; Graham 2010, 2011). It is reasonable to think that a fluctuating climate and geological events during this period (Zachos et al. 2001, 2008) promoted speciation in *Pseudephebe*, as has similarly proposed for other parmelioid lineages (Leavitt et al. 2012b,c). The fact that *P. minuscula* grows sympatrically with *P. pubescens* in Europe, and with the undescribed Alaskan species in North America may be explained by a combination of factors, including speciation-extinction events and contrasting patterns of historical migration among regions. Supplementary Figure 10 shows statistical support for the sister relationship of the Alaskan and the strictly European species (*P. pubescens*), suggesting an extinction of the European species in North America or, vice versa. Even though our sampling across North America was not as extensive as in other regions, the fact that only one specimen (plus another also from Alaska whose GENBANK *nrITS* accession is KJ947964; Supplementary Figure 10; Appendix 2) belonged to the third species while all other American individuals fall within *P. minuscula* supports the idea that this species has indeed a very restricted distribution. This specimen was found in Alaska, in a nearby region to the two proposed North American glacial refugia, Beringia and the Pacific Northwest (Shafer et al. 2010). Regarding *P. pubescens*, the highest genetic diversity is found in the Iberian Peninsula, also considered a refuge during Pleistocene glaciations (Taberlet et al. 1998; Petit et al. 2002; Feliner 2011). However, it is likely that Pleistocene glaciations had contrasting effects on each *Pseudephebe* species. In *P. pubescens*, it likely caused a reduction in genetic diversity (Supplementary Table 7), which is reflected in the shallow genetic clades (Supplementary Figure 10–16), a pattern that has been detected in other organisms that suffered range contractions in the last ice ages (Hewitt 1996). In the PGK dataset of *P. pubescens*, a statistically supported positive value of Fu's *Fs* test was indeed obtained (Supplementary Table 7) indicating a relatively recent bottleneck. On the contrary, population demographic statistics for *P. minuscula* suggest this species undergone recent population growth (Supplementary Table 7), probably in the last 3–2 MA, a period of time in which alpine versions of tundra ("páramo") formed in high altitude mountainous ranges across the New World (Graham 2010, 2011; Hoorn et al. 2010).

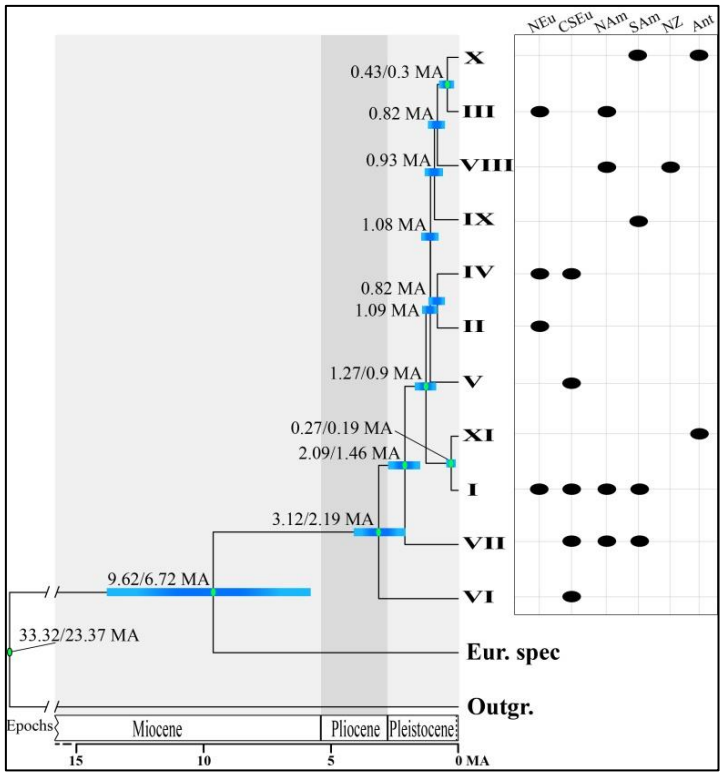

Figure 5. Chronogram depicting divergence times for the BAPS multi-locus clusters inferred for the amphitropical species (*Pseudephebe minuscula*) using multi-locus data and the *BEAST population/species tree reconstruction method. Roman numerals correspond with those in Figure 3A (upper panel). Right panel indicates the geographical origin of individuals belonging to each BAPS cluster. Dates on the left and right correspond with those inferred using an *Oropogon* (Leavitt et al. 2012a) or a *Melanohalea* (Leavitt et al. 2012b) *nrITS* fungal substitution rate, respectively. The two estimates are only given when a particular node receives significant statistical support (PP ≥ 0.95), which is indicated with a green oval on the node itself; otherwise, only the estimate based on the analysis using the *Oropogon nrITS* substitution rate is provided. Bars show the 95% highest posterior density intervals (HPD) obtained in the analysis using an *Oropogon nrITS* substitution rate. The strictly European *Pseudephebe pubescens* and the outgroup (*Bryoria bicolor*) are also included in the topology. The bar on the node connecting *Pseudephebe* spp. to the outgroup is trimmed for better visualization. NEu: Northern Europe; CSEu: Central-Southern Europe; NAm: North America; SAm: South America; NZ: New Zealand; Ant: Antarctica; MA: million years ago.

4.2. The amphitropical range distribution of *P. minuscula*

Although amphitropical distributions in lichens have been recognized since long (Du Rietz 1940; Lamb 1948; Galloway & Aptroot 1995; Øvstedal & Lewis Smith 2001; Galloway 2008), the questions on how and when these disjunctions were acquired remain largely unsolved, with contrasting evidence suggesting either a boreal or an austral origin (e.g. Crespo et al. 2002; Högnabba & Wedin 2003; Geml et al. 2012; Søcthing & Castello 2012; Fernández-Mendoza & Printzen 2013). The present study genetically analysed specimens of

P. minuscula from localities in the high Arctic and Continental Antarctica up to 83º S, providing substantial support for its transcontinental disjunct range. Strikingly, this species also shows high levels of genetic diversity (Supplementary Figure 2–8, Supplementary Table 7) despite structures for sexual reproduction are often absent in the thalli. We used two alternative approaches to determine genetic stratification in this species, BAPS and DAPC, which inferred slightly different numbers of clusters but agreed in overall structure. Thus, the number of strictly Northern Hemisphere and amphitropical clusters revealed by both methods were five and three, respectively. On the other hand, BAPS detected three clusters only occurring in the Southern Hemisphere and DAPC one. The higher levels of DNA polymorphism detected in most loci for Northern Hemisphere populations (Supplementary Table 7) and the fact that Northern Hemisphere haplotypes were the central ones in star-like subnetworks (Supplementary Figure 2–3,5–6) suggest a boreal origin for this *Pseudephebe* species. A similar pattern of higher genetic diversity in the Northern Hemisphere was used to support the boreal origin of another amphitropical species, *Cetraria aculeata* (Domaschke et al. 2012; Fernández-Mendoza & Printzen 2013). On the other hand, the levels of admixture found in the STRUCTURE analysis for some populations including specimens from the Northern and Southern Hemisphere may be due to allele sharing (see haplotype networks in Supplementary Figure 2–8) that might be explained by either historical or ongoing gene-flow and/or retained ancestral polymorphisms (Hudson & Coyne 2002; Rougeux et al. 2016; Sturge et al. 2016).

Long-distance dispersal and vicariance have traditionally been postulated as alternative mechanisms for generating amphitropical distributions in lichens (Du Rietz 1940; Lamb 1948, 1970; Galloway & Aptroot 1995; Castello & Nimis 1997; Bjerke & Elvebakk 2004). Our divergence estimates supported a more recent, Pleistocene acquisition of the extant geographic distribution of *P. minuscula* (Figure 5–6), therefore excluding the vicariant hypothesis, which implies more ancient time estimates (Scotese 2001; Mao et al. 2012). However, discerning whether such dispersal was through "mountain-hopping" along the American Cordilleras or directly across hemispheres is somewhat speculative. *Pseudephebe minuscula* is known from mountainous localities at lower latitudes in the Northern Hemisphere, including California and Mexico (Boluda et al. 2016; Herrera-Campos et al. 2016) and also from tropical sites in the northern Andes (e.g. Bolivia, this study). Pleistocene glaciations may have provided suitable habitat conditions at still lower latitudes, expanding suitable habitats at tropical and equatorial mountain ranges (van der Hammen 1974; Hoorn et al. 2010), and thus allowing species occurring at higher latitudes in both hemispheres to progressively approach and finally cross the equator ("Darwin's pump", Darwin 1872; Donoghue 2011). This hypothesis was advocated to explain the amphitropical distribution in several members of *Cladonia* (Stenroos 1993; Myllys et al. 2003), *Caloplaca* s.l. (Søchting & Olech 1995), neuropogonoid *Usnea* (Seymour et al. 2007; Wirtz et al. 2008, 2012) and *Lichenomphalia* (Geml et al. 2012). Nevertheless, most of these studies, as well as those focusing on the amphitropical distribution of *Parmelia saxatilis* (Crespo et al. 2002), the *Sphaerophorus globosus* complex (Högnabba and Wedin, 2003) and several teloschistacean

species (Lindblom & Søcthing 2008; Søcthing & Castello 2012), also pointed to direct long-distance dispersal as a plausible mechanism for the origin of their disjunct distribution pattern. Based on the results of gene flow analyses, Fernández-Mendoza & Printzen (2013) proposed that a series of colonisation from the Northern Hemisphere through both "mountain-hopping" and direct events could explain the dispersal of *Cetraria aculeata* into South America. This scenario is also the most plausible for *P. minuscula*, as the genetic imprints of South American populations reveal different connections with the Northern Hemisphere. For instance, the Bolivian specimens were allocated within a cluster with individuals from Arctic Europe, North America and China, whereas the Southern Andes populations showed a genetic affinity to either North American or Iberian Peninsula populations (Figure 3A, upper panel). Likewise, clustering analyses included New Zealand specimens together with some Alaskan specimens into a single cluster (Figure 2–3). Collectively, all these evidences suggest that the acquisition of the amphitropical range was not due to a single event. A denser sampling along the American Cordilleras, especially in high altitude localities at lower latitudes could help to elucidate specific patterns of connectivity among *P. minuscula* populations in boreal and austral landmasses.

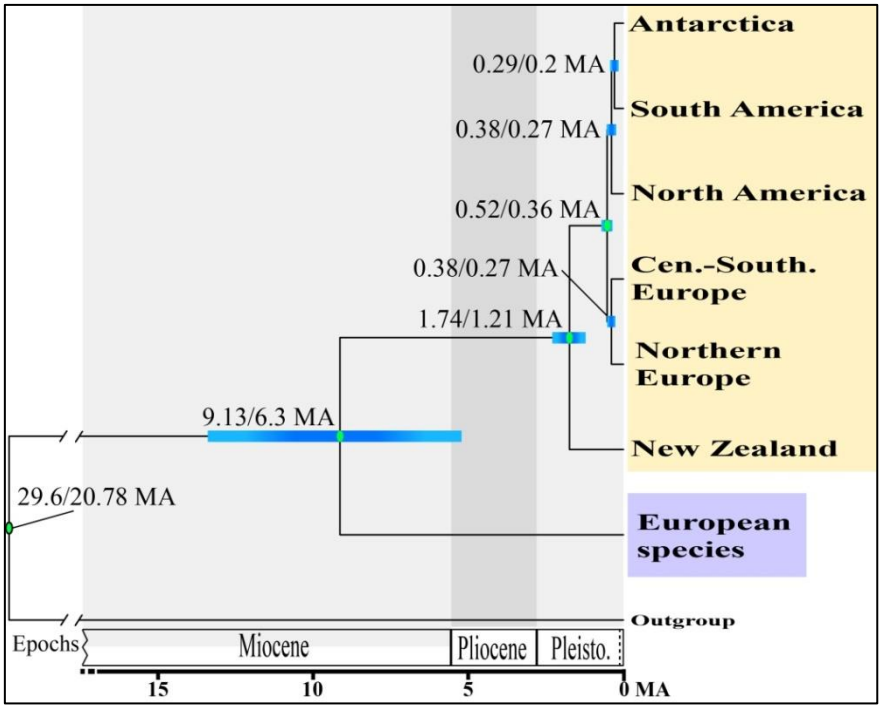

Figure 6. Chronogram depicting divergence times for the six geographical regions in which the amphitropical species (*Pseudephebe minuscula*) is distributed using multi-locus data and the *BEAST population/species tree reconstruction method. Dates on the left and right correspond with those inferred using an *Oropogon* (Leavitt et al. 2012a) or a *Melanohalea* (Leavitt et al. 2012b) *nrITS* fungal substitution rate, respectively. Bars show the 95% highest posterior density intervals (HPD) obtained in the analysis using an *Oropogon nrITS* substitution rate. The strictly European *Pseudephebe pubescens* and the outgroup (*Bryoria bicolor*) are also included in the topology. Branches connecting *Pseudephebe* spp. to

the outgroup are trimmed for better visualization. Green ovals on nodes represent significant statistical support (PP ≥ 0.95). MA: million years ago.

The absence of asexual propagules and the rare occurrence of spore-producing apothecia in *P. minuscula* call into question whether thallus fragmentation alone may be responsible for its broad distribution and the observed high genetic diversity. The ability of lichen sexual (spores) or asexual (conidia, soredia, isidia, thallus fragments) propagules to disperse *via* wind, water or animals over moderate to large distances is well-known (Bailey & James 1979; Armstrong 1981, 1994; Kappen & Straka 1988; Harmata & Olech 1991; Werth et al. 2006). However, thallus fragments are thought to be not well suited for long-distance dispersal mediated by wind or water (Heinken 1999) and its transport by birds or other animals over large distances remains speculative. Whatever the means of dispersal, the ability of *P. minuscula* species to disperse over thousands of kilometres is proved by its presence in the northern face of the inactive Hawaiian volcano Mauna Kea, at 3.300 m above sea level (Smith 1984). The estimated age of this volcano is *c.* 1 MA and it hosted glaciers during the latest glacial periods since 200 thousand years ago (Wolfe 1997). Wind-mediated dispersal of *Pseudephebe* propagules from any nearby continental landmass could be expected. Due to the trade winds blowing over the Hawaiian Islands from the NE to ENE (Leopold 1949), the most likely geographical origin would be North America.

4.3. Origin of Antarctic populations of *P. minuscula*

The inferred boreal origin and estimated time frame for the acquisition of the amphitropical distribution in *P. minuscula* point also to a recent, Pleistocene establishment of its Antarctic populations. This scenario will fit well expectations of earlier lichenologists about a recent origin for amphitropical (or subcosmopolitan) Antarctic lichens (e.g. Lamb 1948, 1970; Dodge 1964; Galloway 1991; Seppelt 1995). However, the topology of the tree containing the six major geographical regions (Figure 6), the clustering results (Figure 2–3) and the genealogical relationships of haplotypes (Supplementary Figure 2–8) suggest different origins for the Maritime and Continental Antarctic populations of this lichen, with limited connectivity among them (i.e. only one maritime individual belonging to a cluster including the bulk of continental specimens, Figure 2–3). The high level of allele sharing between specimens of southern South America and the Antarctic Peninsula (Supplementary Figure 2–8,10–16) coupled with the fact specimens in the second region are mostly clonal suggest that dispersal into Maritime Antarctica might have occurred from the former region. These results would go against the paradigm of Antarctica being an isolated continent due to the combined effect of its geographic position and strong winds and water currents flowing eastward, the latter hindering north-south dispersals (Fraser et al. 2012; Chown et al. 2015). Rather, it demonstrates that *de novo* establishment in Antarctica may be ultimately dependant on the environmental conditions (Clarke et al. 2005; Barnes et al. 2006). Neither climatic conditions nor other factors, such as photobiont availability, are expected to have posed a problem for the Antarctic establishment of *Pseudephebe*, as the former are similar between Tierra del Fuego and the Subantarctic regions (Rozzi et al. 2008) and the most plausible lichen propagules to

be dispersed are thallus fragments (containing both myco- and photobiont cells). Furthermore, the scarce genetic variability found in Maritime Antarctica populations is likely a result of a founder effect or a later bottleneck, as also supported by population demographic statistics (*Mcm7*, *GAPDH*, *PGK*; Supplementary Table 7). This scenario was also inferred for maritime Antarctic *Cetraria aculeata* populations (Fernández-Mendoza & Printzen 2013). On the other hand, a surprising genetic connexion was found in the present study between continental Antarctic (including specimens collected across the Transantarctic Mountains and the Queen Maud Land) and Arctic *P. minuscula* populations (Figure 3B, Supplementary Figure 2–8). The STRUCTURE analysis inferred a cluster with all continental Antarctic individuals together with partly admixed specimens from Svalbard, and to a lesser extent China and Bolivia (Figure 3A, bottom panel). As there are alleles shared between individuals at both poles it is reasonable to assume that there has not passed enough time to sort all ancestral polymorphism at sampled loci. At this moment, it is too tentative to propose an historical event of long-distance dispersal directly from the Northern Hemisphere into the Antarctic continent as long as other localities in, for example, Asia and other Subantarctic archipelagos (e.g. Kerguelen Is., New Zealand nearby islands) could have offered an alternative stepping-stone-like route in the colonisation of Antarctica.

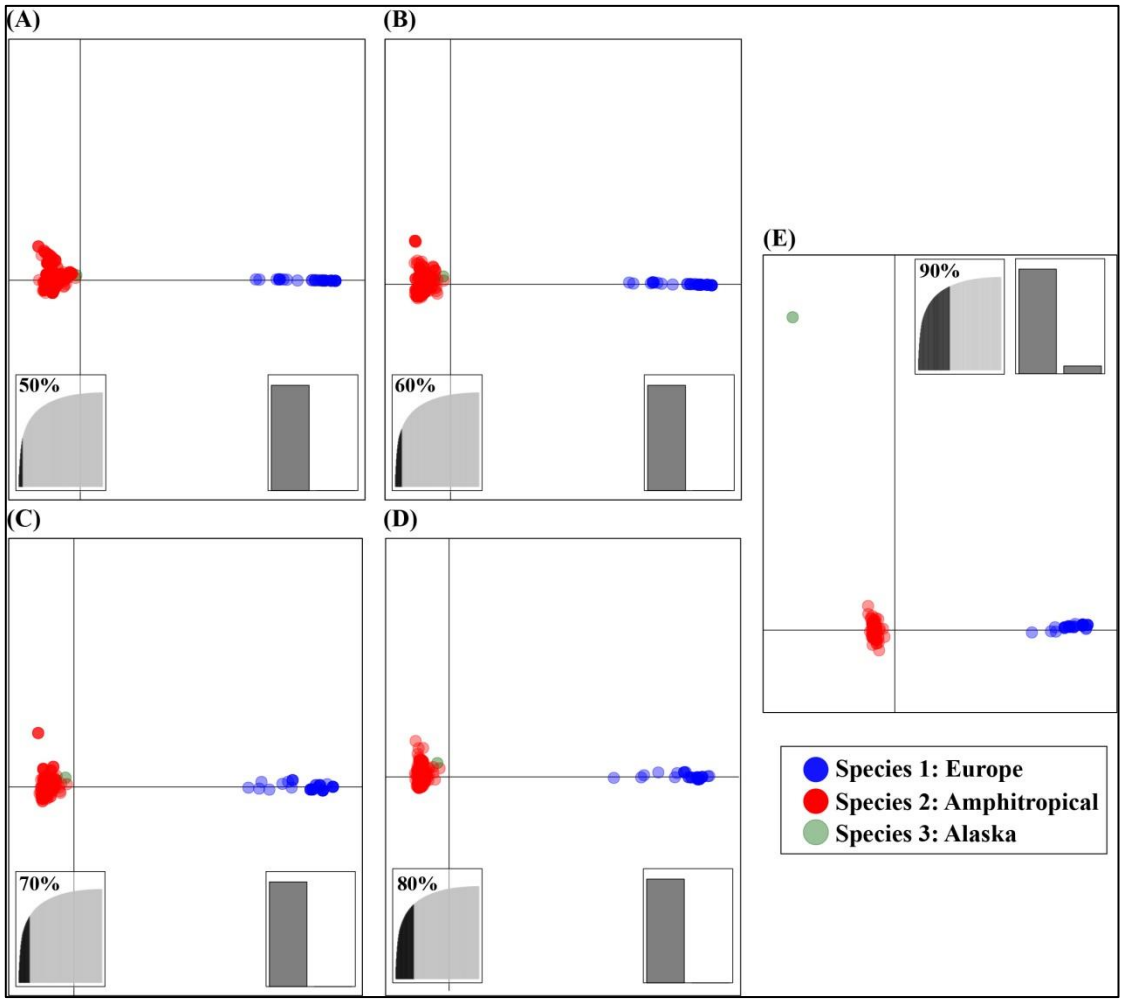

Supplementary Figure 1. Discriminant analysis of principal components (DAPC) scatter plots resulting from five analyses run with different numbers of retained axes, which preserved 50% (A), 60% (B), 70% (C), 80% (D) and 90% (E) of the total variance (inset on the left), and all discriminant functions (inset on the right). Only the DAPC analysis that used 90% of the total variance in the six-locus dataset could discriminate the third BFD-validated species, composed of one Alaskan individual, from the amphitropical *Pseudephebe* (see legend on the bottom right corner).

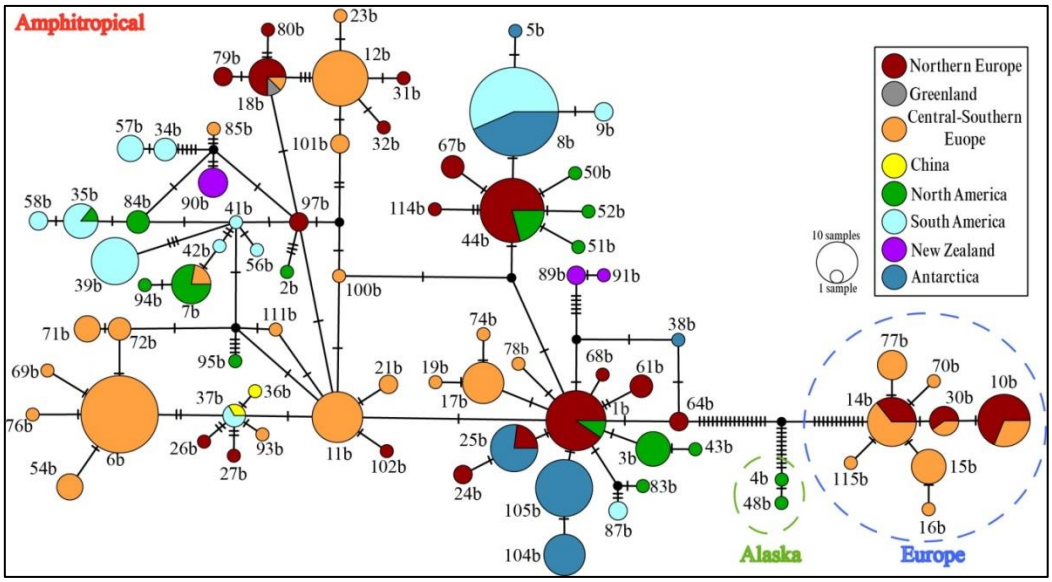

Supplementary Figure 2. Statistical parsimony network for haplotypes of *Pseudephebe* spp. based on the extended *nrITS* dataset (newly generated and GENBANK sequences). The three *Pseudephebe* species validated in the species delimitation approach are highlighted: amphitropical (*P. minuscula*), European (*P. pubescens*) and Alaskan (*Pseudephebe* sp.). Colors indicate the six major geographical regions where individuals were collected (see legend on the right). The sizes of the circles in the network are proportional to the numbers of individuals bearing the haplotype; black-filled circles indicate missing haplotypes. Mutations are shown as hatch marks. Haplotype codes are the same that those used in Supplementary Figure 10.

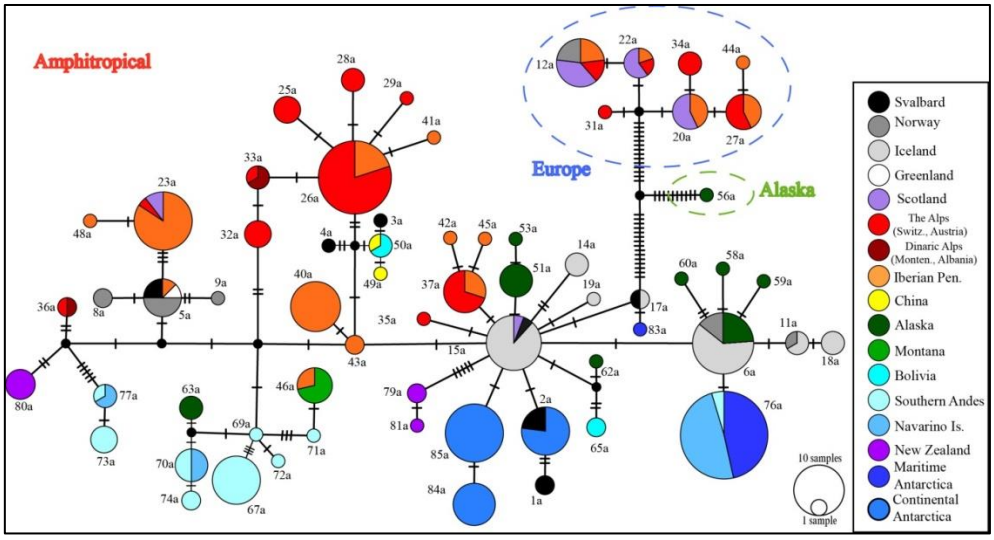

Supplementary Figure 3. Statistical parsimony network for haplotypes of *Pseudephebe* spp. based on the non-extended *nrITS* dataset (only newly generated sequences). The three *Pseudephebe* species validated in the species delimitation approach are highlighted: amphitropical (*P. minuscula*), European (*P. pubescens*) and Alaskan (*Pseudephebe* sp.). Colors indicate the localities where individuals were collected (see legend on the right). The

sizes of the circles in the network are proportional to the numbers of individuals bearing the haplotype; black-filled circles indicate missing haplotypes. Mutations are shown as hatch marks. Haplotype codes are the same that those used in Supplementary Figure 11.

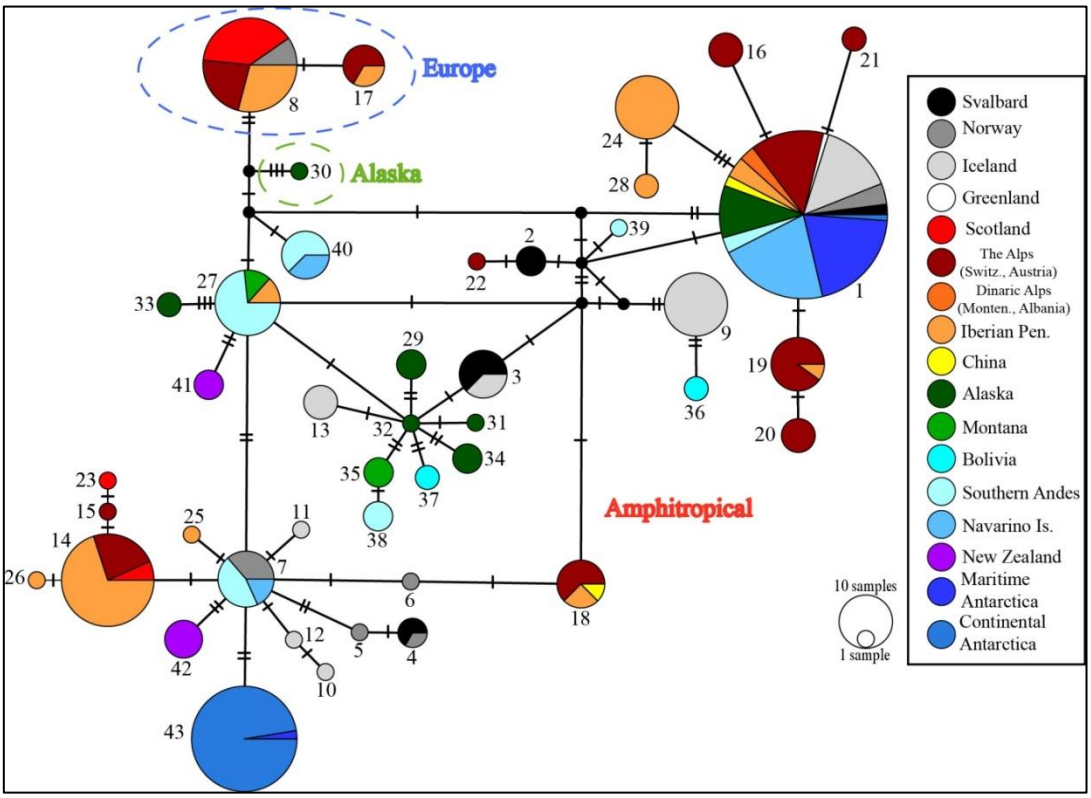

Supplementary Figure 4. Statistical parsimony network for haplotypes of *Pseudephebe* spp. based on the newly generated *Mcm7* dataset. The three *Pseudephebe* species validated in the species delimitation approach are highlighted: amphitropical (*P. minuscula*), European (*P. pubescens*) and Alaskan (*Pseudephebe* sp.). Colors indicate the localities where individuals were collected (see legend on the right). The sizes of the circles in the network are proportional to the numbers of individuals bearing the haplotype; black-filled circles indicate missing haplotypes. Mutations are shown as hatch marks. Haplotype codes are the same that those used in Supplementary Figure 12.

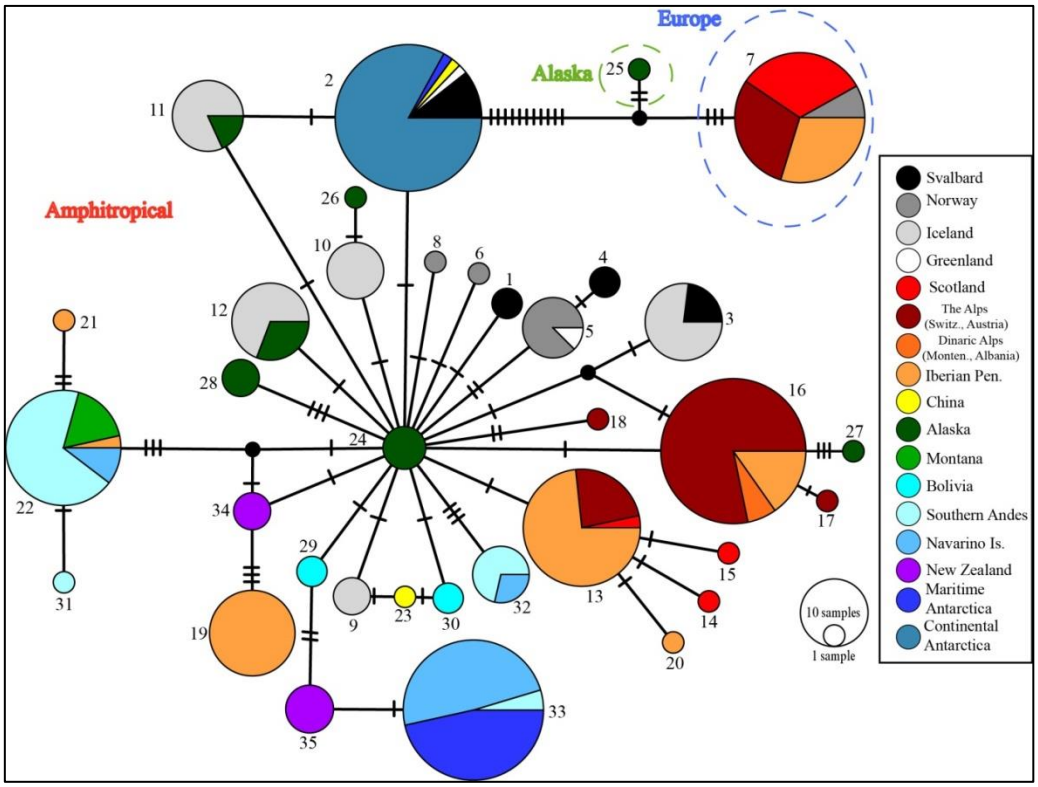

Supplementary Figure 5. Statistical parsimony network for haplotypes of *Pseudephebe* spp. based on the newly generated *GAPDH* dataset. The three *Pseudephebe* species validated in the species delimitation approach are highlighted: amphitropical (*P. minuscula*), European (*P. pubescens*) and Alaskan (*Pseudephebe* sp.). Colors indicate the localities where individuals were collected (see legend on the right). The sizes of the circles in the network are proportional to the numbers of individuals bearing the haplotype; black-filled circles indicate missing haplotypes. Mutations are shown as hatch marks. Haplotype codes are the same that those used in Supplementary Figure 13.

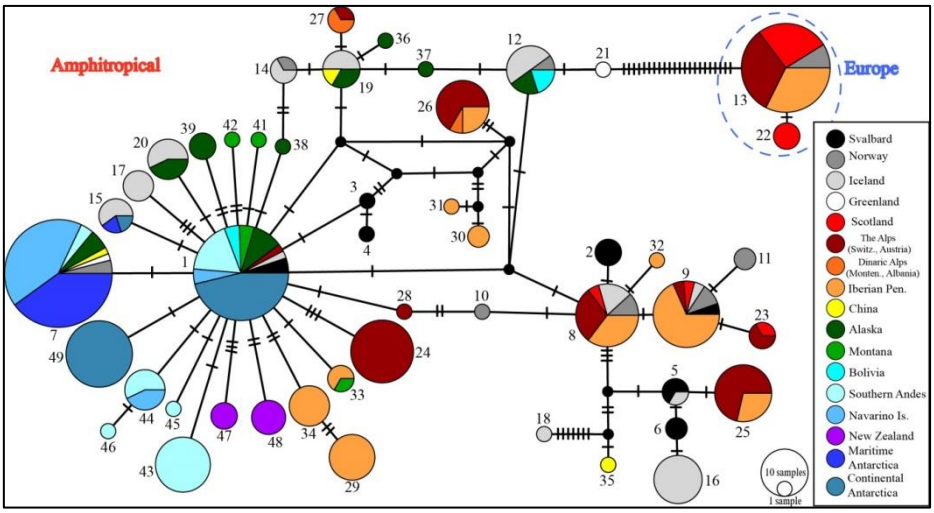

Supplementary Figure 6. Statistical parsimony network for haplotypes of *Pseudephebe* spp. based on the newly generated *EF-1α* dataset. Two out of the three *Pseudephebe* species validated in the species delimitation approach are highlighted: amphitropical (*P. minuscula*), and European (*P. pubescens*). Colors indicate the localities where individuals were collected (see legend on the right). The sizes of the circles in the network are proportional to the numbers of individuals bearing the haplotype; black-filled circles indicate missing haplotypes. Mutations are shown as hatch marks. Haplotype codes are the same that those used in Supplementary Figure 14.

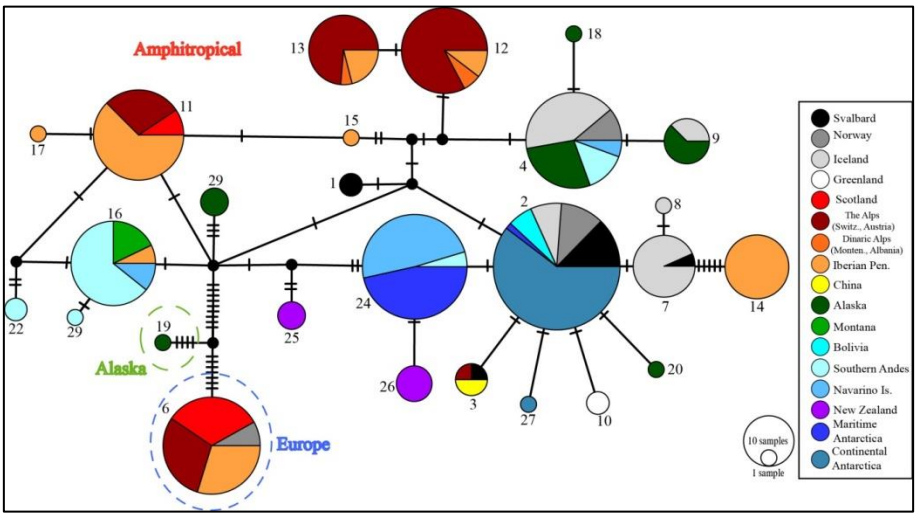

Supplementary Figure 7. Statistical parsimony network for haplotypes of *Pseudephebe* spp. based on the newly generated *L1* dataset. The three *Pseudephebe* species validated in the species delimitation approach are highlighted: amphitropical (*P. minuscula*), European (*P. pubescens*) and Alaskan (*Pseudephebe* sp.). Colors indicate the localities where individuals were collected (see legend on the right). The sizes of the circles in the network are proportional to the numbers of individuals bearing the haplotype; black-filled circles indicate missing haplotypes. Mutations are shown as hatch marks. Haplotype codes are the same that those used in Supplementary Figure 15.

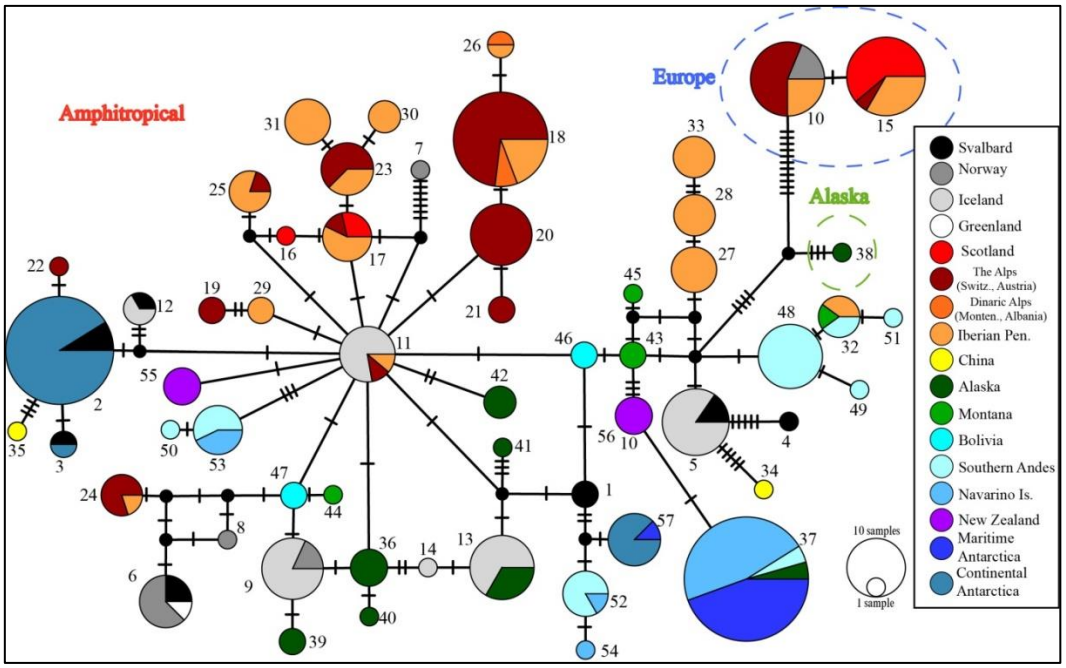

Supplementary Figure 8. Statistical parsimony network for haplotypes of *Pseudephebe* spp. based on the newly generated *PGK* dataset. The three *Pseudephebe* species validated in the species delimitation approach are highlighted: amphitropical (*P. minuscula*), European (*P. pubescens*) and Alaskan (*Pseudephebe* sp.). Colors indicate the localities where individuals were collected (see legend on the right). The sizes of the circles in the network are proportional to the numbers of individuals bearing the haplotype; black-filled circles indicate missing haplotypes. Mutations are shown as hatch marks. Haplotype codes are the same that those used in Supplementary Figure 16.

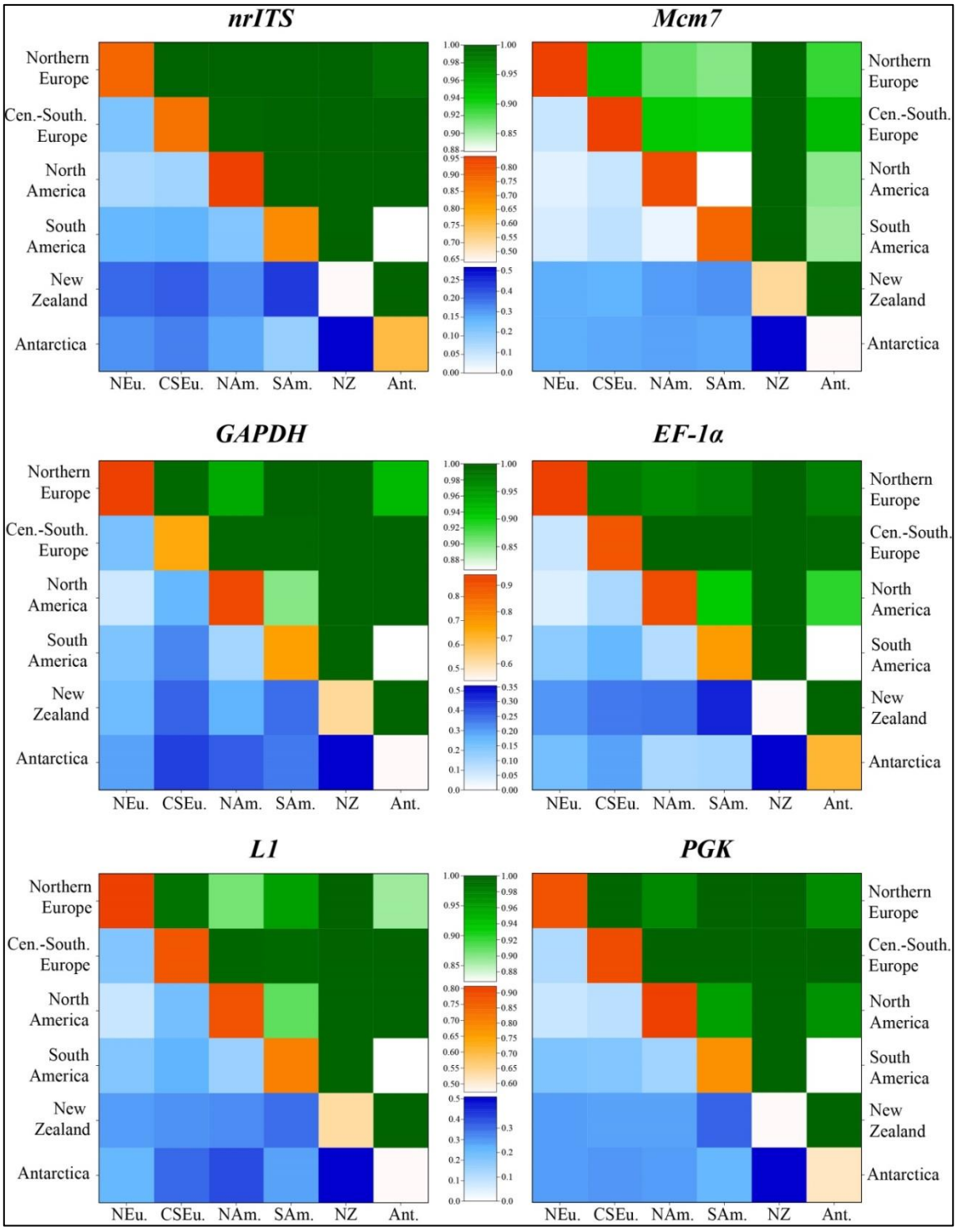

Supplementary Figure 9. Genetic divergence (Dxy, above diagonal, green shades), genetic differentiation (Fst, below diagonal, blue shades), and within group genetic diversity (π, diagonal, orange shades) between the six major geographical regions in the amphitropical species (*Pseudephebe minuscula*) based on data from the six loci (*nrITS*, *Mcm7*, *GAPDH*, *EF-1α*, *L1* and *PGK*). Scales on left- and right-hand sides of central bars correspond to graphs on left and right, respectively. NEu: Northern Europe; CSEu: Central-Southern Europe; NAm: North America; SAm: South America; NZ: New Zealand; Ant: Antarctica.

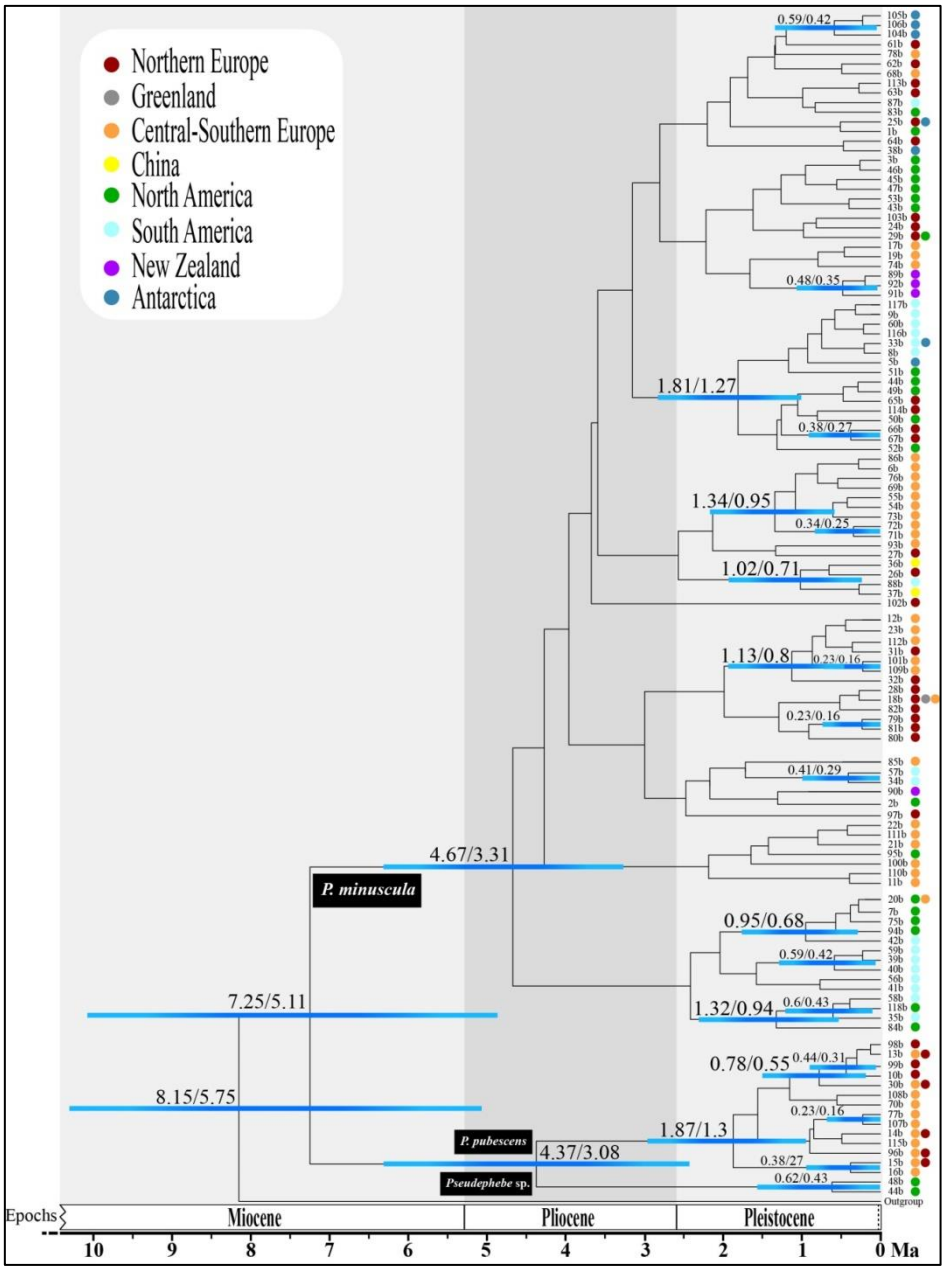

Supplementary Figure 10. Chronogram depicting divergence times for haplotypes of the three *Pseudephebe* species using the extended *nrITS* dataset (newly generated and GENBANK sequences) and the BEAST tree reconstruction method. The geographical distribution of each haplotype is indicated with a coloured circle (see legend on the upper left corner). Dates on the left and right correspond with those inferred using an *Oropogon* (Leavitt et al. 2012a) or a *Melanohalea* (Leavitt et al. 2012b) *nrITS* fungal substitution rate, respectively. Bars show the 95% highest posterior density intervals (HPD) obtained in the analysis using an *Oropogon* *nrITS* substitution rate only for those nodes with significant statistical support (PP ≥ 0.95). The bar on the node connecting *Pseudephebe* spp. to the outgroup (*Bryoria bicolor*) is trimmed for better visualization. Haplotype codes are the same that those used in Supplementary Figure 2. MA: million years ago.

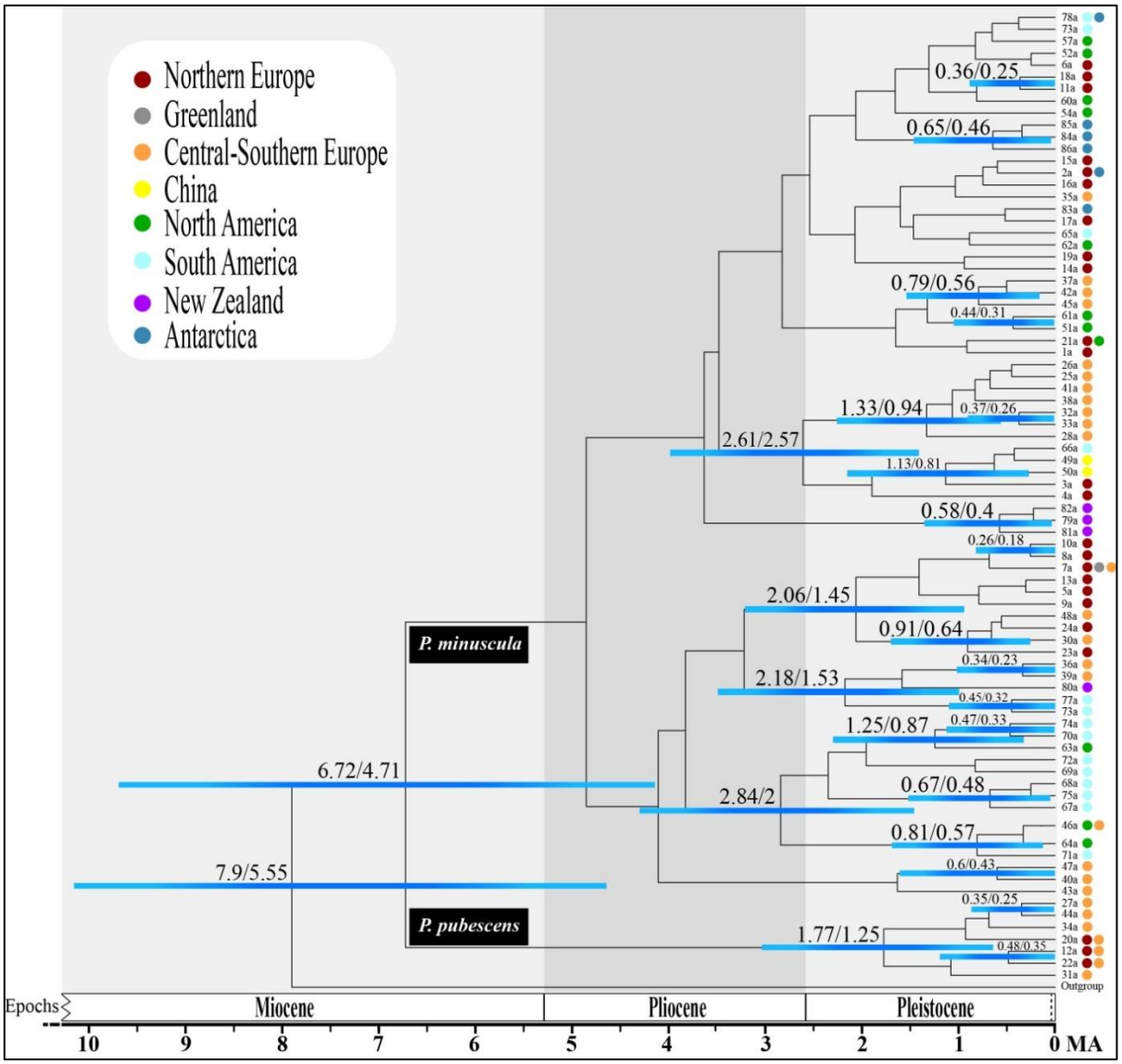

Supplementary Figure 11. Chronogram depicting divergence times for *Pseudephebe minuscula* and *P. pubescens* haplotypes using the non-extended *nrITS* dataset (only newly generated sequences) and the BEAST tree reconstruction method. The geographical distribution of each haplotype is indicated with a coloured circle (see legend on the upper left corner). Dates on the left and right correspond with those inferred using an *Oropogon* (Leavitt et al. 2012a) or a *Melanohalea* (Leavitt et al. 2012b) *nrITS* fungal substitution rate, respectively. Bars show the 95% highest posterior density intervals (HPD) obtained in the analysis using an *Oropogon nrITS* substitution rate only for those nodes with significant statistical support (PP ≥ 0.95). The bar on the node connecting *Pseudephebe* spp. to the outgroup (*Bryoria bicolor*) is trimmed for better visualization. Haplotype codes are the same that those used in Supplementary Figure 3. MA: million years ago.

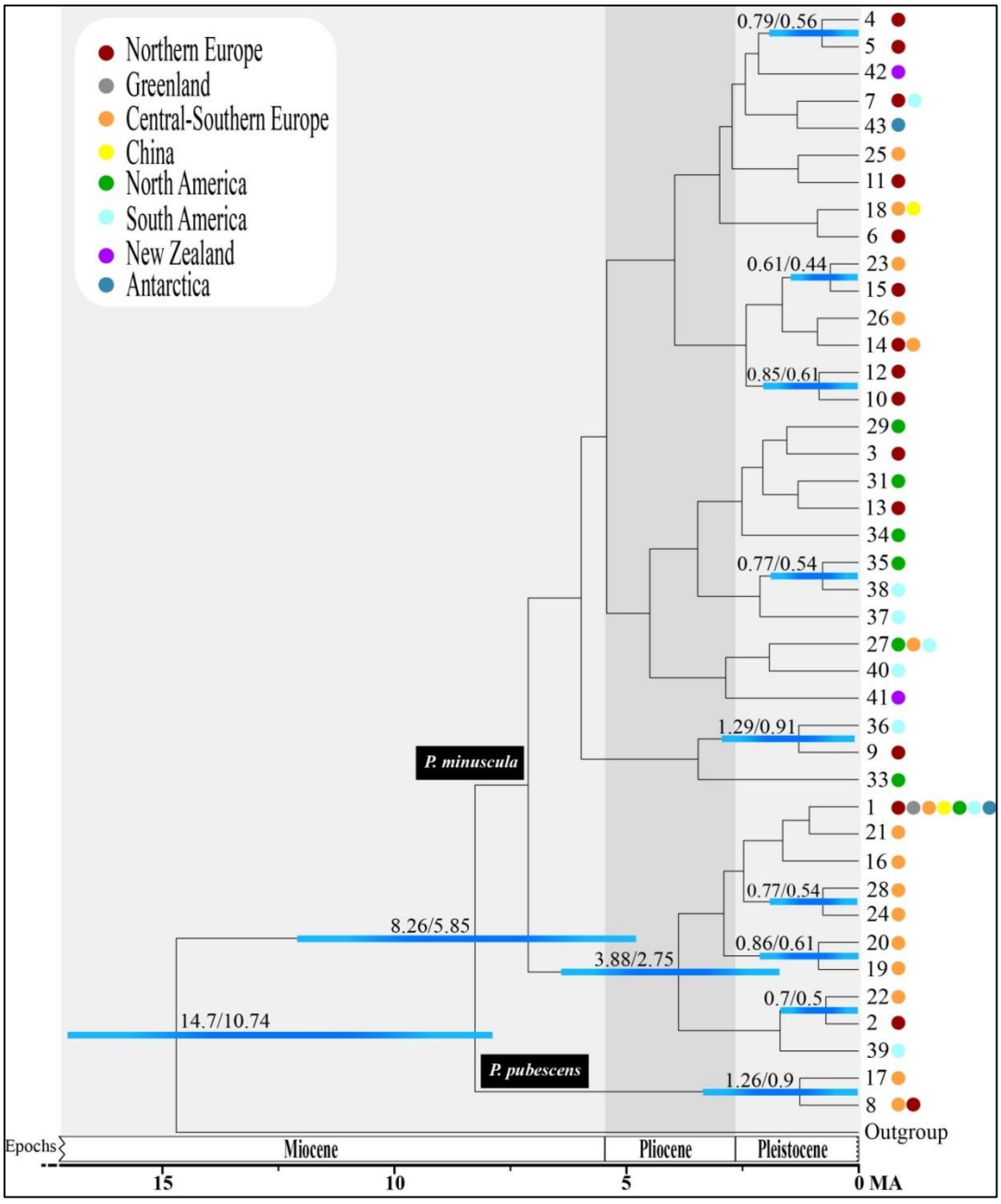

Supplementary Figure 12. Chronogram depicting divergence times for *Pseudephebe minuscula* and *P. pubescens Mcm7* haplotypes using the BEAST tree reconstruction method. The geographical distribution of each haplotype is indicated with a coloured circle (see legend on the upper left corner). Dates on the left and right correspond with those inferred using a co-estimated *Mcm7* substitution rate based on an *Oropogon* (Leavitt et al. 2012a) or a *Melanohalea* (Leavitt et al. 2012b) *nrITS* fungal substitution rate, respectively. Bars show the 95% highest posterior density intervals (HPD) obtained in the analysis using the former co-estimated *Mcm7* substitution rate only for those nodes with significant statistical support (PP ≥ 0.95). The bar on the node connecting *Pseudephebe* spp. to the outgroup (*Bryoria bicolor*) is trimmed for better visualization. Haplotype codes are the same that those used in Supplementary Figure 4. MA: million years ago.

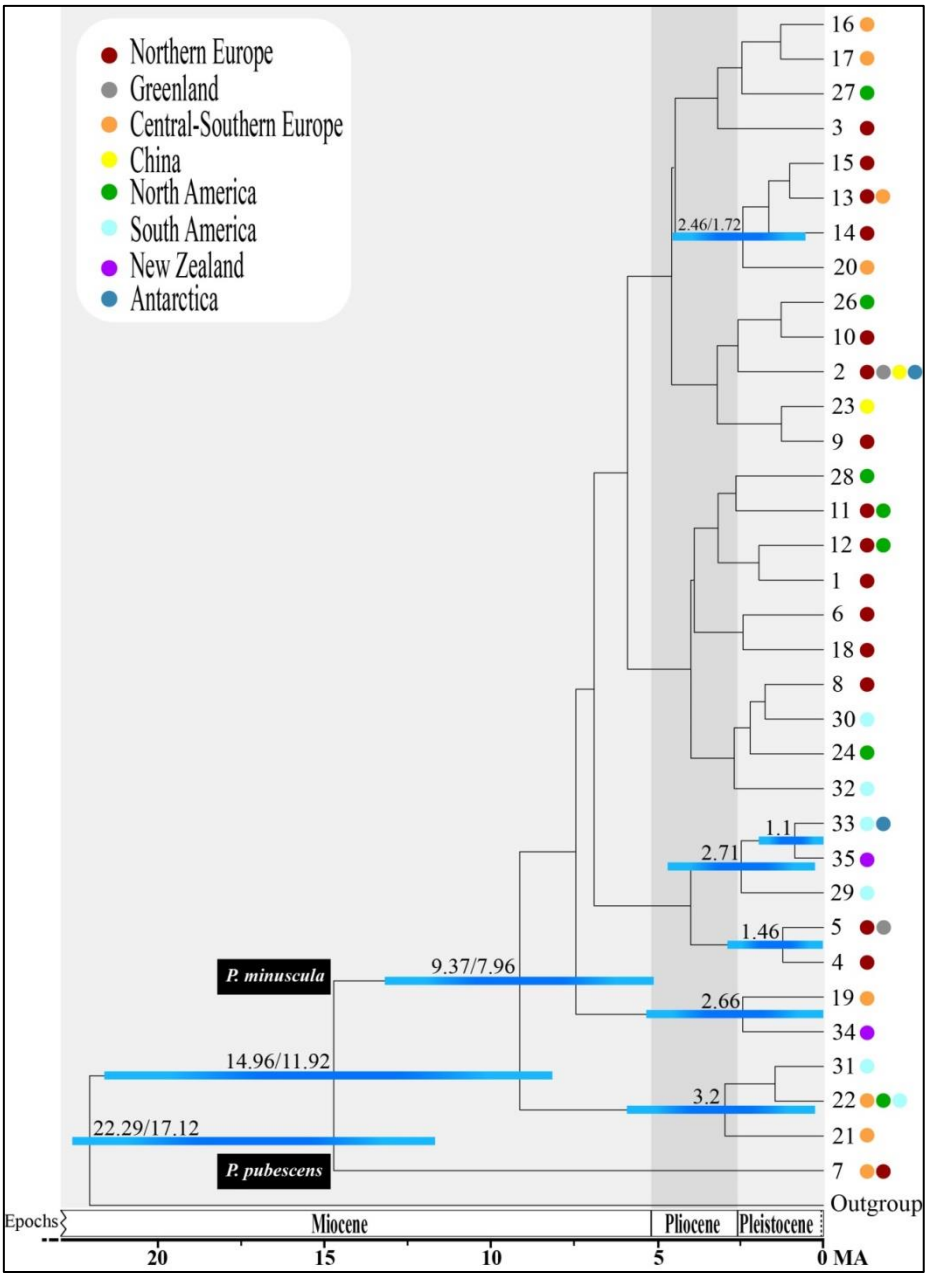

Supplementary Figure 13. Chronogram depicting divergence times for *Pseudephebe minuscula* and *P. pubescens GAPDH* haplotypes using the BEAST tree reconstruction method. The geographical distribution of each haplotype is indicated with a coloured circle (see legend on the upper left corner). Dates on the left and right correspond with those inferred using a co-estimated *GAPDH* substitution rate based on an *Oropogon* (Leavitt et al. 2012a) or a *Melanohalea* (Leavitt et al. 2012b) *nrITS* fungal substitution rate, respectively. Bars show the 95% highest posterior density intervals (HPD) obtained in the analysis using the former co-estimated *GAPDH* substitution rate only for those nodes with significant statistical support (PP ≥ 0.95). The bar on the node connecting *Pseudephebe* spp. to the outgroup (*Bryoria bicolor*) is trimmed for better visualization. Haplotype codes are the same that those used in Supplementary Figure 5. MA: million years ago.

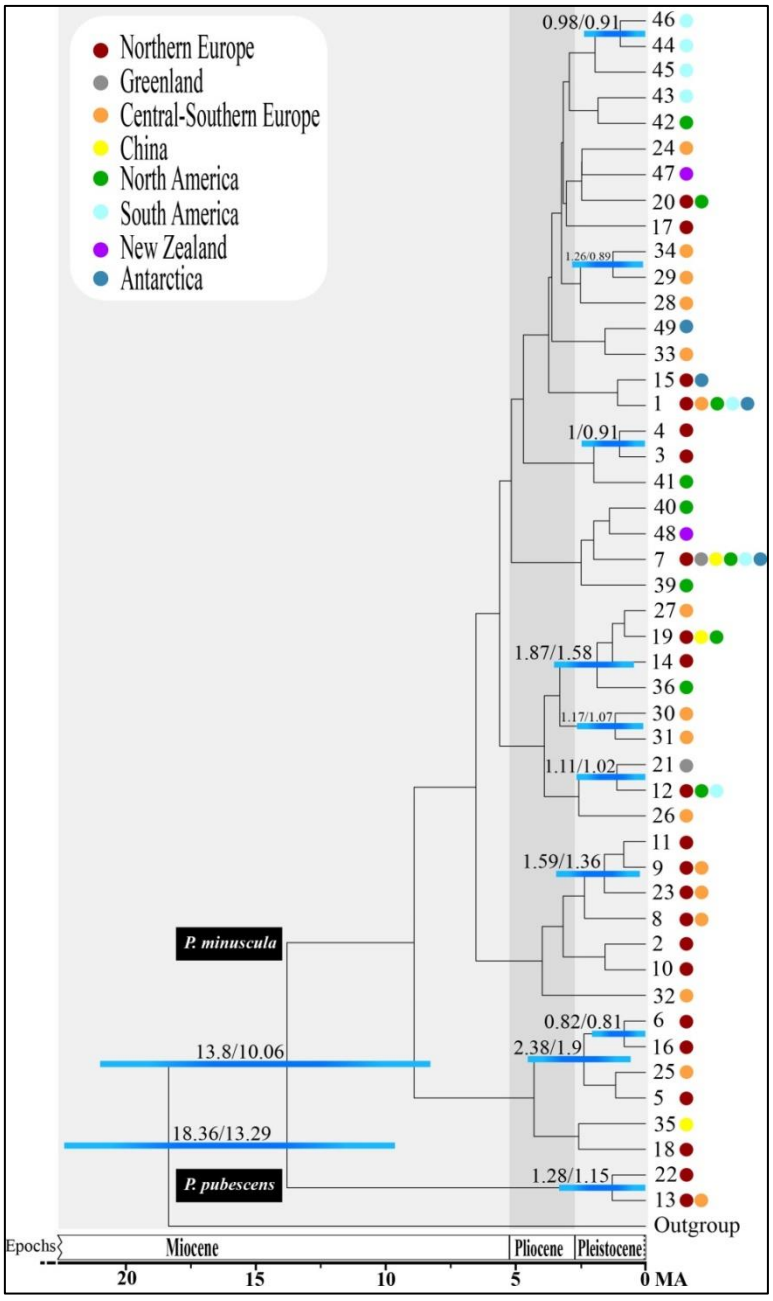

Supplementary Figure 14. Chronogram depicting divergence times for *Pseudephebe minuscula* and *P. pubescens EF-1α* haplotypes using the BEAST tree reconstruction method. The geographical distribution of each haplotype is indicated with a coloured circle (see legend on the upper left corner). Dates on the left and right correspond with those inferred using a co-estimated *EF-1α* substitution rate based on an *Oropogon* (Leavitt et al. 2012a) or a *Melanohalea* (Leavitt et al. 2012b) *nrITS* fungal substitution rate, respectively. Bars show the 95% highest posterior density intervals (HPD) obtained in the analysis using the former co-estimated *EF-1α* substitution rate only for those nodes with significant statistical support (PP ≥ 0.95). The bar on the node connecting *Pseudephebe* spp. to the outgroup (*Bryoria bicolor*) is trimmed for better visualization. Haplotype codes are the same that those used in Supplementary Figure 6. MA: million years ago.

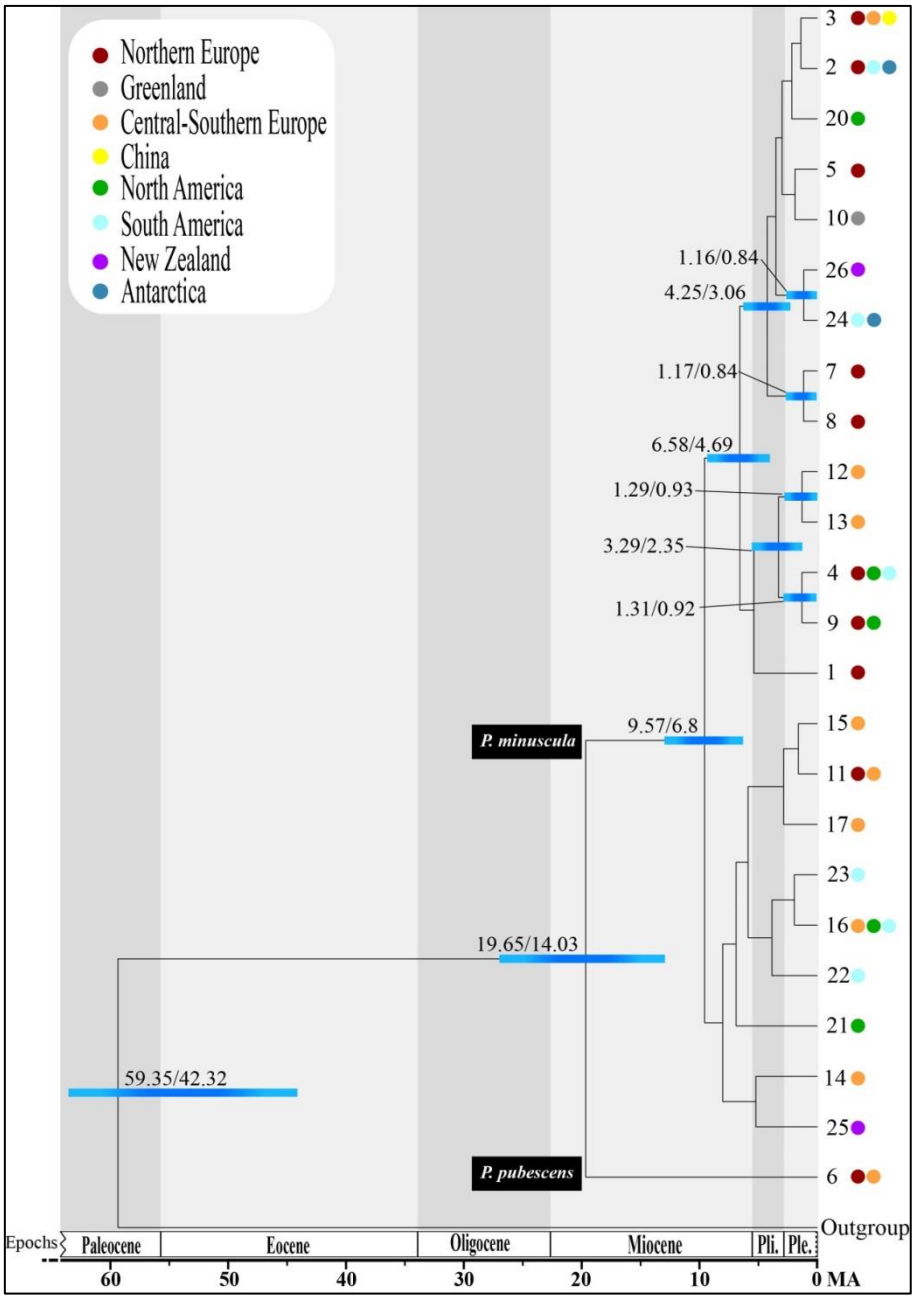

Supplementary Figure 15. Chronogram depicting divergence times for *Pseudephebe minuscula* and *P. pubescens L1* haplotypes using the BEAST tree reconstruction method. The geographical distribution of each haplotype is indicated with a coloured circle (see legend on the upper left corner). Dates on the left and right correspond with those inferred using a co-estimated *L1* substitution rate based on an *Oropogon* (Leavitt et al. 2012a) or a *Melanohalea* (Leavitt et al. 2012b) *nrITS* fungal substitution rate, respectively. Bars show the 95% highest posterior density intervals (HPD) obtained in the analysis using the former co-estimated *L1* substitution rate only for those nodes with significant statistical support (PP ≥ 0.95). The bar on the node connecting *Pseudephebe* spp. to the outgroup (*Bryoria bicolor*) is trimmed for better visualization. Haplotype codes are the same that those used in Supplementary Figure 7. MA: million years ago.

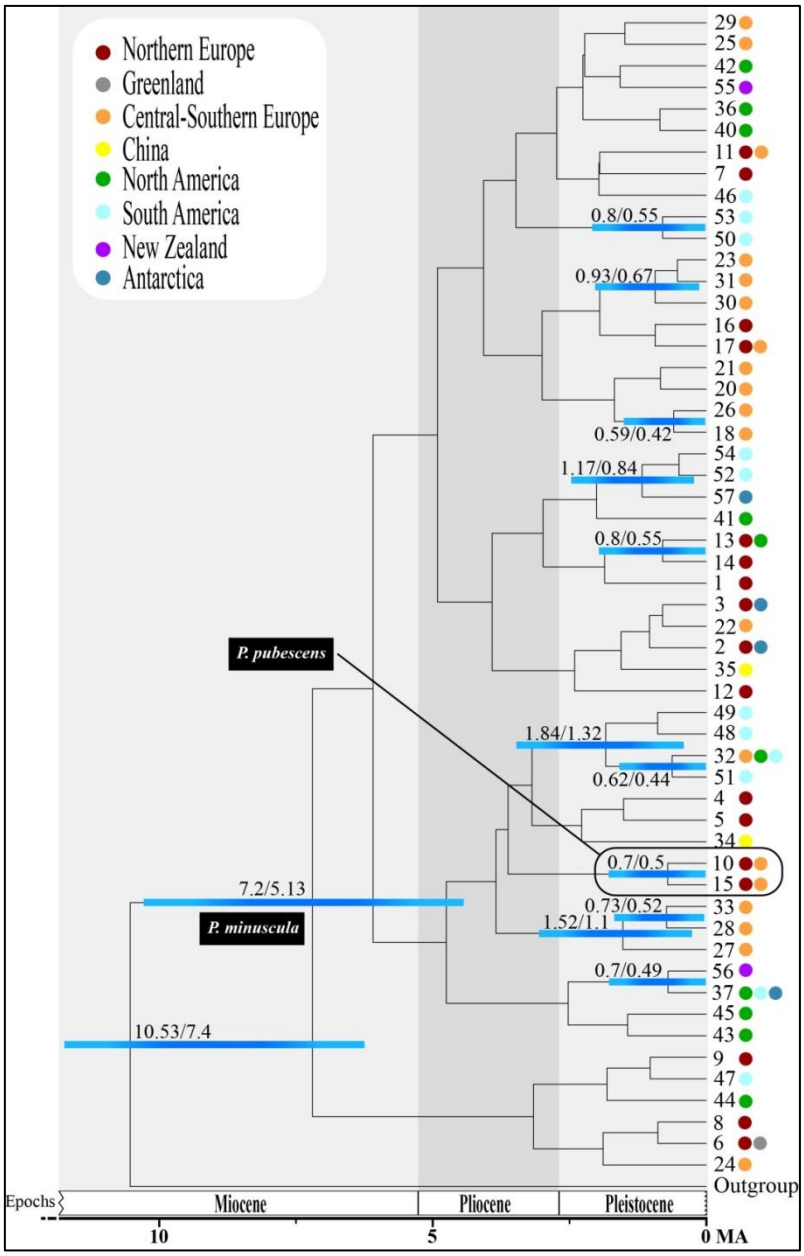

Supplementary Figure 16. Chronogram depicting divergence times for *Pseudephebe minuscula* and *P. pubescens PGK* haplotypes using the BEAST tree reconstruction method. The geographical distribution of each haplotype is indicated with a coloured circle (see legend on the upper left corner). Dates on the left and right correspond with those inferred using a co-estimated *PGK* substitution rate based on an *Oropogon* (Leavitt et al. 2012a) or a *Melanohalea* (Leavitt et al. 2012b) *nrITS* fungal substitution rate, respectively. Bars show the 95% highest posterior density intervals (HPD) obtained in the analysis using the former co-estimated *PGK* substitution rate only for those nodes with significant statistical support (PP ≥ 0.95). The bar on the node connecting *Pseudephebe* spp. to the outgroup (*Bryoria bicolor*) is trimmed for better visualization. Haplotype codes are the same that those used in Supplementary Figure 8. MA: million years ago.

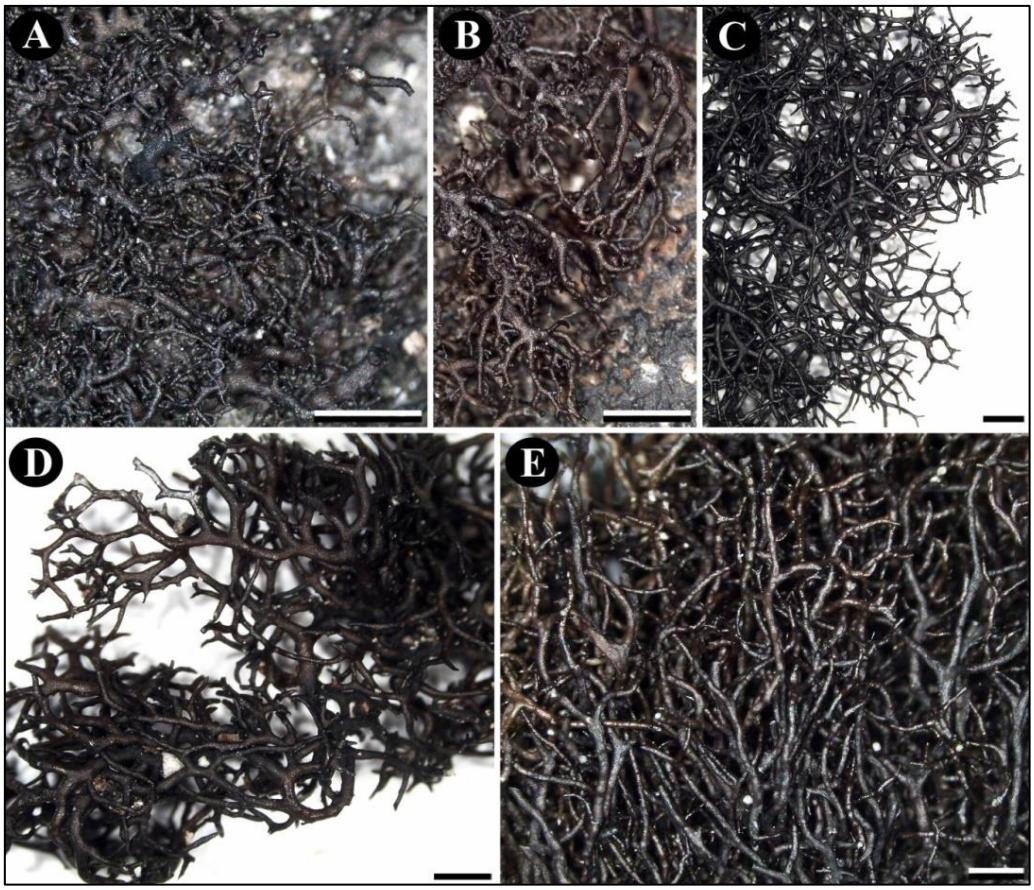

Supplementary Figure 17. *Pseudephebe* species. (A–B) Amphitropical *P. minuscula* (*minuscula*-like morphology; Iceland, specimens collected by *S. Pérez-Ortega* & *A. de los Ríos*). (C) Amphitropical *P. minuscula* (*pubescens*-like morphology; Livingston Island, Antarctica, specimen collected by *A. de los Ríos*). (D) The third, undescribed *Pseudephebe* species (*pubescens*-like morphology; Alaska, specimen collected by *S. Pérez-Ortega*). (E) European *Pseudephebe pubescens* (*pubescens*-like morphology; Asturias, specimen collected by *I. Garrido-Benavent*). Scales: 1 mm. (Photographs: IGB).

Supplementary Table 1. Loci and primers used in the current study. Newly designed primers are highlighted in bold.

Locus	Primer name	Orientation (F/R)	Primer sequence (5'–3')	Reference
nrITS	ITS1F	F	CTTGGTCATTTAGAGGAAGTAA	Gardes & Bruns (1993)
	ITS-Pse-F	**F**	**GCGGAAGGATCATTAYCGAGA**	**This study**
	ITS4	R	TCCTCCGCTTATTGATATGC	White et al. (1990)
	ITS-Pse-R	**R**	**GTTGGTTTCTTTTCCTCCGCT**	**This study**
Mcm7	Mcm7-709for	F	ACIMGIGTITCVGAYGTHAARCC	Schmitt et al. (2009)
	Mcm7-Pse-F	**F**	**ACCTGTGATCGATGTGGATG**	**This study**
	Mcm7-1348rev	R	GAYTTDGCIACICCIGGRTCWCCCAT	Schmitt et al. (2009)
	Mcm7-Pse-R	**R**	**TATGTCYCCACGTATTCGCA**	**This study**
GAPDH	Gpd1-LM	F	ATTGGCCGCATCGTCTTCCGCAA	Myllys et al. (2002)
	GPD-Pse-F	**F**	**TGAGCCTCACTATGCTGTAAG**	**This study**
	Gpd2-LM	R	CCCACTCGTTGTCGTACCA	Myllys et al. (2002)
	GPD-Pse-R	**R**	**TCAAATCGGTGGACACAAGC**	**This study**
EF-1α	EF1-1018-F	F	GAYTTCATCAAGAACATGAT	Stielow et al. (2015)
	EF1-Pse-F	**F**	**CTGCGCTATCCTCATCATCG**	**This study**
	EF1-1620-R	R	GACGTTGAADCCRACRTTGTC	Stielow et al. (2015)
	EF1-Pse-R	**R**	**GCATTTCGACGGACTTGACT**	**This study**
L1	60S-506-F	F	GHGACAAGCGTTTCTCNGG	Stielow et al. (2015)
	60S-Pse-F	**F**	**TCGCGTTCAGGTCTTCGTTA**	**This study**
	60S-908-R	R	CTTVAVYTGGAACTTGATGGT	Stielow et al. (2015)
	60S-Pse-R	**R**	**CGTTTCTCGGGCACTATCAAG**	**This study**
PGK	PGK-533-F	F	GTYGAYTTCAAYGTYCC	Stielow et al. (2015)
	PGK-Pse-F	**F**	**TGTCATCCTCATGTCGCATC**	**This study**
	PGK-533-R	R	ACACCDGGDGGRCCGTTCCA	Stielow et al. (2015)
	PGK-Pse-R	**R**	**ATACTCTTCTCSCCGCAATC**	**This study**

Supplementary Table 2. PCR settings.

Locus	Primer pair (F/R)	PCR protocol
nrITS	ITS-Pse-F/R	95° C (3 min), 7 cycles of 95° C (20 s) + 61° C (15 s, touchdown -1° C per cycle) + 72° C (28 s), 31 cycles of 95° C (20 s) + 54° C (15 s) + 72° C (28 s), 72° C (1 min 10 s), 4° C (∞)
Mcm7	Mcm7-Pse-F/R	95° C (3 min), 7 cycles of 95° C (20 s) + 59° C (15 s, touchdown -1° C per cycle) + 72° C (30 s), 32 cycles of 95° C (20 s) + 52° C (15 s) + 72° C (30 s), 72° C (1 min 10 s), 4° C (∞)
GAPDH	GPD-Pse-F/R	95° C (3 min), 5 cycles of 95° C (20 s) + 61° C (15 s, touchdown -1° C per cycle) + 72° C (30 s), 34 cycles of 95° C (20 s) + 56° C (15 s) + 72° C (30 s), 72° C (1 min 10 s), 4° C (∞)
EF-1α	EF1-Pse-F/R	95° C (3 min), 7 cycles of 95° C (20 s) + 60° C (15 s, touchdown -1° C per cycle) + 72° C (23 s), 31 cycles of 95° C (20 s) + 53° C (15 s) + 72° C (23 s), 72° C (1 min 10 s), 4° C (∞)
L1	L1-Pse-F/R	95° C (3 min), 7 cycles of 95° C (20 s) + 60° C (15 s, touchdown -1° C per cycle) + 72° C (23 s), 31 cycles of 95° C (20 s) + 53° C (15 s) + 72° C (23 s), 72° C (1 min 10 s), 4° C (∞)
PGK	PGK-Pse-F/R	95° C (3 min), 6 cycles of 95° C (20 s) + 59° C (15 s, touchdown -1° C per cycle) + 72° C (30 s), 32 cycles of 95° C (20 s) + 53° C (15 s) + 72° C (30 s), 72° C (1 min 10 s), 4° C (∞)

Supplementary Table 3. Marginal likelihood and Bayes Factor values for three alternative species delimitation hypotheses in *Pseudephebe* and their motivation. The best model is highlighted in bold.

Model	Distinct species	Motivation	Path Sampling		Stepping-Stone	
			Ln (Marginal Likelihood)	2ln (Bayes Factor)	Ln (Marginal Likelihood)	2ln (Bayes Factor)
Model 1 (1 spp.)	n/a	A morphologically variable lichen with a wide distribution	-6661.85	569.7	-6692.35	585.3
Model 2 (2 spp.)	sp1: all five continents[a] sp2: Europe and North America[b]	Two-cluster interpretation of multi-locus network, Boluda et al. (2016) results	-6381.45	8.9	-6407.5	15.6
Model 3 (3 spp.)	sp1: all five continents[a] sp2: Europe[c] sp3: North America[d]	ABGD *nrITS*, three-clusters interpretation of multi-locus network	**-6377**	**n/a**	**-6399.7**	**n/a**

[a]Individuals with *nrITS* haplotypes (from extended dataset): *hap1b–9b,11b–12b,17b–29b,31b–43b,45b–47b,49b–69b,71b–76b,78b–95b,97b,100b–106b,109b–114b,116b–118b*;

[b]Individuals with *nrITS* haplotypes (from extended dataset): *hap10b,13b–16b,30b,44b,48b,70b,77b,96b,98b–99b,107b–108b,115b*;

[c]Individuals with *nrITS* haplotypes (from extended dataset): *hap10b,13b–16b,30b,70b,77b,96b,98b–99b,107b–108b,115b*;

[d]Individuals with *nrITS* haplotypes (from extended dataset): *hap44b,48b*;

Supplementary Table 4. Results of *Pseudephebe* candidate species dating analyses (Section 2.8. in Material and Methods), with inferred average substitution rates for each marker used in subsequent single-locus dating analyses in bold. MA: million years ago.

Secondary calibration	Mean age spp. divergence	95% HPD	Geological time interval	*Mcm7* mean subs. rate (s/s/MA)	*GAPDH* mean subs. rate (s/s/MA)	*EF-1α* mean subs. rate (s/s/MA)	*L1* mean subs. rate (s/s/MA)	*PGK* mean subs. rate (s/s/MA)
Oropogon (2.4×10^{-3} s/s/MA, Leavitt et al. 2012a)	6.2	8.81–3.82	Miocene-Pliocene	**1.325×10^{-3}**	**7.974×10^{-4}**	**1.429×10^{-3}**	**1.225×10^{-3}**	**1.402×10^{-3}**
Melanohalea (3.41×10^{-3} s/s/MA, Leavitt et al. 2012b)	4.42	6.28–2.79	Miocene-Pliocene	1.864×10^{-3}	1.121×10^{-3}	2.017×10^{-3}	1.719×10^{-3}	1.971×10^{-3}

Supplementary Table 5. Summary of genetic diversity statistics of *nrITS*, *Mcm7*, *GAPDH*, *EF-1α*, *L1* and *PGK* markers for *Pseudephebe*.

	nrITS	*Mcm7*	*GAPDH*	*EF-1α*	*L1*	*PGK*
Number of sequences	352	355	346	353	355	346
Alignment length (bp)	525	514	797	600	400	768
Sites with alignment gaps or missing data	81	0	0	1	2	0
Number of polymorphic (segregating) sites, *s*	89	53	56	73	47	86
Parsimony informative sites	71	44	40	61	38	62
Number of haplotypes, *h*	64	43	35	48	26	57
Haplotype diversity, *Hd*	0.957	0.888	0.917	0.941	0.906	0.954
Average number of nucleotide differences, *k*	10.618	5.250	6.161	7.911	6.612	8.038
Nucleotide diversity, π	0.02391	0.01021	0.00773	0.01321	0.01661	0.01047
Nucleotide diversity (Jukes and Cantor), π(JC)	0.02480	0.01030	0.00780	0.01346	0.01698	0.01058

Supplementary Table 6. Substitution models used in different *BEAST and BEAST analyses for each dataset.

Analysis	Marker (dataset)	Alignment length (bp)	Partition	Inferred model	Less complex model used in *BEAST/BEAST
Section 2.4. Determination of species boundaries (*BEAST analyses)	*nrITS*	531	n/a	TrNef+I+Γ	n/a
	Mcm7	514	n/a	TrNef+I+Γ	n/a
Section 2.8. Dating analyses (*BEAST analyses using multi-locus data)	*nrITS*	529	n/a	TrNef+I+Γ	TrNef
	Mcm7	514	n/a	SYM+I+Γ	HKY
	GAPDH	798	n/a	K80+I+Γ	n/a
	EF-1α	602	n/a	SYM+I+Γ	HKY
	L1	402	n/a	TrNef+I+Γ	TrNef
	PGK	768	n/a	SYM+I+Γ	HKY
Section 2.8. Dating analyses (BEAST analyses using single-locus data)	*nrITS* (non-extended)[a]	529	*ITS1+ITS2*	TrNef+Γ	n/a
			5.8S	K80	n/a
	nrITS (extended)[b]	531	*ITS1+ITS2*	TrNef+Γ	n/a
			5.8S	K80	n/a
	Mcm7 (non-extended)[a]	514	exon (1st cod. pos.)	K80	n/a
			exon (2nd cod. pos.)	K80	n/a
			exon (3rd cod. pos.)	TrNef+Γ	n/a
	GAPDH	798	intron	K80	n/a
			exon	TrNef	n/a
	EF-1α	602	intron	K80	n/a
			exon	TrNef+Γ	n/a
	L1	402	intron	TrNef	n/a
			exon	TrNef	n/a
	PGK	768	exon (1st cod. pos.)	TrN+Γ	n/a
			exon (2nd cod. pos.)	HKY	n/a
			exon (3rd cod. pos.)	HKY+Γ	n/a

[a] using only newly generated data; [b] including sequences downloaded from GENBANK (Appendix 2)

Supplementary Table 7. Polymorphism statistics and neutrality tests results for each marker (*nrITS*, *Mcm7*, *GAPDH*, *EF-1α*, *L1* and *PGK*), species and geographic origin. (ns: not significant).

Dataset	n	bp	Gaps/ missing	*s*	*h*	*Hd*	*k*	π	π(JC)	Tajima's *D*	Fu's *Fs*
nrITS Pseudephebe bip N. Europe	63	525	33	24	17	0.866	3.535	0.00719	0.00724	-0.96314 (ns)	-3.8503 (ns)
nrITS Pseudephebe bip S-C. Europe	98	525	76	26	19	0.852	4.882	0.01087	0.01099	-0.09506 (ns)	-1.6378 (ns)
nrITS Pseudephebe bip N. America	25	525	56	17	11	0.890	5.223	0.01114	0.01127	0.56918 (ns)	-0.6926 (ns)
nrITS Pseudephebe bip S. America	58	525	66	25	11	0.783	6.039	0.01316	0.01332	0.37835 (ns)	2.5642 (ns)
nrITS Pseudephebe bip New Zeal.	8	525	31	14	3	0.607	7.214	0.01460	0.01487	1.71144 (ns)	5.2947 (**)
nrITS Pseudephebe bip Antarctica	60	525	31	8	5	0.745	2.495	0.00505	0.00508	1.19955 (ns)	3.3651 (ns)
nrITS Pseudephebe bip All regions	312	525	80	62	57	0.949	5.197	0.01168	0.01180	-1.37068 (ns)	-29.5470 (***)
nrITS Pseudephebe sp Europe	37	525	27	7	7	0.800	2.105	0.00423	0.00425	0.71923 (ns)	0.0534 (ns)
Mcm7 Pseudephebe bip N. Europe	65	514	0	21	14	0.833	4.917	0.00957	0.00965	0.34194 (ns)	-0.0273 (ns)
Mcm7 Pseudephebe bip S-C. Europe	98	514	0	20	14	0.840	4.738	0.00922	0.00930	0.64389 (ns)	0.7641 (ns)
Mcm7 Pseudephebe bip N. America	25	514	0	13	8	0.813	4.040	0.00786	0.00792	0.59610 (ns)	0.6688 (ns)
Mcm7 Pseudephebe bip S. America	58	514	0	17	8	0.767	3.609	0.00702	0.00707	-0.05257 (ns)	2.1711 (ns)
Mcm7 Pseudephebe bip New Zeal.	8	514	0	6	2	0.536	3.214	0.00625	0.00630	1.81343 (ns)	5.0114 (***)
Mcm7 Pseudephebe bip Antarctica	60	514	0	7	2	0.463	3.239	0.00630	0.00636	2.95888 (***)	11.2212 (***)
Mcm7 Pseudephebe bip All regions	314	514	0	49	40	0.871	4.929	0.00959	0.00967	-1.04055 (ns)	-11.280 (ns)
Mcm7 Pseudephebe sp Europe	37	514	0	1	2	0.279	0.279	0.00054	0.00054	0.24225 (ns)	0.7104 (ns)
GAPDH Pseudephebe bip N. Europe	64	797	0	15	14	0.891	2.458	0.00308	0.00309	-0.66421 (ns)	-3.6310 (ns)
GAPDH Pseudephebe bip S-C. Europe	96	797	0	15	8	0.658	2.345	0.00294	0.00295	-0.54830 (ns)	1.1126 (ns)
GAPDH Pseudephebe bip N. America	20	797	0	15	7	0.863	3.511	0.00440	0.00442	-0.62625 (ns)	0.4864 (ns)
GAPDH Pseudephebe bip S. America	58	797	0	13	6	0.680	4.685	0.00588	0.00591	1.95437 (ns)	5.9794 (**)
GAPDH Pseudephebe bip New Zeal.	8	797	0	4	2	0.536	2.143	0.00269	0.00270	1.69719 (ns)	3.7472 (**)
GAPDH Pseudephebe bip Antarctica	60	797	0	5	2	0.452	2.260	0.00284	0.00285	2.58676 (*)	8.3301 (***)
GAPDH Pseudephebe bip All regions	308	797	0	43	33	0.909	3.709	0.00465	0.00467	-1.29127 (ns)	-10.0263 (ns)
GAPDH Pseudephebe sp Europe	37	797	0	0	1	0	0	0	0	na	na
EF-1α Pseudephebe bip N. Europe	66	600	1	34	21	0.944	5.237	0.00874	0.00882	-0.86429 (ns)	-3.9261 (ns)
EF-1α Pseudephebe bip S-C. Europe	97	600	0	29	15	0.892	5.772	0.00962	0.00970	0.07436 (ns)	1.2653 (ns)
EF-1α Pseudephebe bip N. America	25	600	1	13	12	0.913	2.240	0.00374	0.00375	-1.20069 (ns)	-5.6692 (**)
EF-1α Pseudephebe bip S. America	58	600	0	8	7	0.753	1.774	0.00296	0.00297	0.07084 (ns)	0.1232 (ns)
EF-1α Pseudephebe bip New Zeal.	8	600	0	6	2	0.536	3.214	0.00536	0.00539	1.81343 (ns)	5.0114 (ns)
EF-1α Pseudephebe bip Antarctica	59	600	0	4	4	0.699	1.423	0.00237	0.00238	1.42910 (ns)	2.1371 (ns)
EF-1α Pseudephebe bip All regions	313	600	1	62	45	0.938	4.149	0.00693	0.00697	-1.68079 (ns)	-20.733 (***)

EF-1α Pseudephebe sp Europe	37	600	0	1	2	0.153	0.153	0.00026	0.00026	-0.52672 (ns)	-0.1484 (ns)
L1 Pseudephebe bip N. Europe	66	400	0	13	10	0.818	2.830	0.00707	0.00713	0.10315 (ns)	-0.0389 (ns)
L1Pseudephebe bip S-C. Europe	98	400	2	14	8	0.768	4.090	0.01028	0.01039	1.38877 (ns)	4.1875 (ns)
L1Pseudephebe bip N. America	25	400	0	12	6	0.773	3.460	0.00865	0.00873	0.30152 (ns)	1.8827 (ns)
L1Pseudephebe bip S. America	58	400	0	11	6	0.703	2.866	0.00717	0.00722	0.58518 (ns)	2.8820 (ns)
L1Pseudephebe bip New Zeal.	8	400	1	5	2	0.536	2.679	0.00671	0.00677	1.76414 (ns)	4.4131 (ns)
L1Pseudephebe bip Antarctica	60	400	0	2	3	0.474	0.485	0.00121	0.00122	0.22486 (ns)	0.4174 (ns)
L1Pseudephebe bip All regions	315	400	2	28	24	0.895	3.759	0.00944	0.00952	-0.40511 (ns)	-3.0504 (ns)
L1Pseudephebe sp Europe	37	400	0	0	1	0	0	0	0	na	na
PGK Pseudephebe bip N. Europe	63	768	0	29	15	0.888	4.457	0.00580	0.00583	-0.88542 (ns)	-1.1341 (ns)
PGK Pseudephebe bip S-C. Europe	98	768	0	29	18	0.895	4.495	0.00585	0.00589	-0.60955 (ns)	-1.5807 (ns)
PGK Pseudephebe bip N. America	22	768	0	21	11	0.922	4.446	0.00579	0.00582	-0.85216 (ns)	-1.7651 (ns)
PGK Pseudephebe bip S. America	58	768	0	19	11	0.783	5.204	0.00678	0.00682	0.82954 (ns)	1.7495 (ns)
PGK Pseudephebe bip New Zeal.	8	768	0	6	2	0.571	3.429	0.00446	0.00449	2.24509 (*)	5.2353 (***)
PGK Pseudephebe bip Antarctica	60	768	0	14	4	0.614	4.933	0.00642	0.00647	1.89408 (ns)	10.0872 (***)
PGK Pseudephebe bip All regions	309	768	0	65	52	0.948	5.593	0.00728	0.00733	-1.33733 (ns)	-20.9330 (***)
PGK Pseudephebe sp Europe	34	768	0	1	2	0.513	0.513	0.00067	0.00067	1.64657 (ns)	1.7695 (*)

* sig. $P < 0.05$, ** sig. $P < 0.02$, *** sig. $P < 0.01$

Appendix 1. Number of individuals collected in each locality and geographic region used in the present study.

Geographic Region	Locality	Latitude	Longitude	no. collected individuals
Northern Europe	Norway, Svalbard, Longyearbyen, Bolterdalen valley, E slope of Bolternosa, on siliceous rocks, 103 m a.s.l., 2014, leg. *S. Pérez-Ortega*	78º 10' 77" N	15º 50' 30" E	12
Northern Europe	Norway, Finnmark, Vardø, Bukkemoltangen, dolomites area, on siliceous rocks, 25 m a.s.l., 2014, leg. *A. Millanes* 1083–1084	70° 25.547' N	30° 45.315' E	2
Northern Europe	Norway, Finnmark, Vadsø, Itre Halsen, open area with small Betula and siliceous ricks, on granitic rocks, 27 m a.s.l., 2014, leg. *A. Millanes* 1077–1a-d	70° 5.770' N	29° 24.879' E	4
Northern Europe	Norway, Finnmark, Sør Varanger, Storsand hill, on granitic rocks, 26 m a.s.l., 2014, leg. *A. Millanes* 1132–a-f	70° 0.363' N	29° 22.306' E	6
Northern Europe	Norway, Troms, Tromsø, Kvaloya, SE slope of Tverrfjellet, 440 m a.s.l., 2004, leg. *J.W. Bjerke* 474/04, GZU41–2013	69° 38.73' N	18° 26.63' E	2
Northern Europe	Iceland, Breiðarmerkurjökull glacier forefield, on siliceous rocks, 34 m a.s.l., 2014, leg. *S. Pérez-Ortega* & *A. de los Ríos*	64º 3' 24" N	-16º 18' 13" E	38
Northern Europe	Greenland, SW, Alluitsup Paa (Sydproven), on rocks, 2008, leg. *E.S. Hansen*, GZU–69-2010	60° 28' N	-45° 35' E	1
Northern Europe	Greenland, S, Nanortalik, on gneissic gravel, 2004, leg. *E.S. Hansen*, GZU–57-2005	60° 09' N	-45° 15' E	1
Northern Europe	United Kingdom, Scotland, Caingorns National Park, on siliceous rocks, 836 m a.s.l., 2010, leg. *S. Pérez-Ortega*	57º 8' 1" N	-3º 39' 36" E	15
Central-Southern Europe	Switzerland, Alps, on siliceous rocks, 2011, leg. *S. Pérez-Ortega*	45° 59' 58.18" N	7º 4' 49.21" E	10
Central-Southern Europe	Switzerland, Alps, individuals collected in several localities stored in the GZU herbarium (Graz, Austria) under the following herbarium numbers: GZU–39–2011, GZU–37–2007 (leg. *J. Hafellner*)	46° 58' 10" N 46° 28' 15" N 46° 43' 10" N 46° 39' 20" N 46° 33' 35" N	9º 52' 35" E 9° 43' 35" E 8° 25' 45" E 8° 40' 15" E 8° 19' 40" E	6
Central-Southern Europe	Montenegro & Kosovo, Dinaric Alps, individuals collected in several localities stored in the GZU herbarium (Graz, Austria) under the following herbarium numbers: GZU–05–2013 (leg. *H. Mayrhofer & H. Zekaj*), GZU–31–2013 (leg. *D. Stesevic*)	42° 31' 58.2" N 42° 34' 26.76" N 42° 34' 19.5" N	20° 8' 26.3" E 20° 6' 30.42" E 20° 3' 28.9" E	3
Central-Southern Europe	Austria, Alps, individuals collected in several localities stored in the GZU herbarium (Graz, Austria) under the following herbarium numbers: GZU–18–2009, GZU–17–2010, GZU–38–2011, GZU–48–2012, GZU–15–2013 (leg. *J. Hafellner*), GZU–15–2011 (leg. *E. Feldner & H. Mayrhofer*)	47° 16' 11" N 47° 6' 50" N 47° 17' 15" N 47° 4' 15" N	14° 22' 46" E 14° 32' 50" E 14° 3' 5" E 9° 59' 00" E	13

		46° 55' 10" N 46° 55' 10" N 46° 54' 45" N 46° 54' 40" N 46° 53' 30" N 46° 52' 55" N 46° 50' 30" N 46° 50' 25" N	14° 40' 25" E 14° 40' 20" E 10° 5' 25" E 14° 40' 15" E 14° 39' 0" E 14° 39' 20" E 14° 40' 25" E 14° 38' 10" E	
Central-Southern Europe	Austria, Koralpe, on granitic rocks, 1800 m a.s.l., 2015, leg. *I. Garrido-Benavent & F. Fernández-Mendoza*	46° 50' 37.47" N	15° 1' 23.23" E	17
Central-Southern Europe	France, Mont Blanc, Plan de l'Aiguille, Aiguille du Midi, on granitic rocks, 2320 m a.s.l., 2015, leg. *A. Gómez-Bolea*	45° 54' 3.69" N	6° 53' 12.11" E	12
Central-Southern Europe	Spain, Huesca, Formigal, Spain-France border, on granitic rocks, 1790 m. a.s.l., 2015, leg. *I. Garrido-Benavent*	42° 47' 20.71" N	0° 24' 14.98" E	10
Central-Southern Europe	Spain, Huesca, Benasque, Gistaín, Pico de la Forqueta, Refugio de Biadós, on granitic rocks, 1768 m. a.s.l., 2015, leg. *A. Gómez-Bolea*	42.631253	0.426467	1
Central-Southern Europe	Spain, Huesca, Bielsa, on granitic rocks, 2340 m. a.s.l., 2015, leg. *A. Gómez-Bolea*	42.637150	0.284844	4
Central-Southern Europe	Spain, Huesca, Panticosa, on granitic rocks, 2015, leg. *Blanco-Moreno & E. Llop*	42.766218	-0.217004	1
Central-Southern Europe	Spain, Asturias, Caso, Lago Ubales, on granitic rocks, 1700 m. a.s.l., 2012, leg. *I. Garrido-Benavent & S. Pérez-Ortega*	43° 6' 12.39" N	-5° 21' 11.87" E	19
Central-Southern Europe	Portugal, Gerés, Cainheiras, on granitic rocks, 1040 m. a.s.l., 2014, leg. *I. Garrido-Benavent*	42° 1' 18.69" N	-8° 8' 26.59" E	7
Central-Southern Europe	Spain, Madrid, Peñalara, Refugio Zabala, on granitic rocks, 2085 m a.s.l., 2015, leg. *I. Garrido-Benavent*	40° 50' 14.57" N	-3° 57' 34.77" E	12
Central-Southern Europe	Spain, Ávila, Sierra de Gredos, subida a las lagunas, 2217 m a.s.l., 2011, leg. *S. Pérez-Ortega*	40º 16' 6.38" N	-5º 15' 42" E	5
China	China, Xizang, Naidong Co., leg. *L-S. Wang*, 07–28595, herb. KUN-L	28º 37' 808" N	92º 13' 293" E	1
China	China, Sichuan Prov., Xiangcheng Co. to Daocheng Co., leg. *L-S. Wang & X. Y. Wang*, 13–38395, herb. KUN-L	29º 9' 31" N	100º 4' 9.56" E	1
China	China, Xizang, Chayu Co., Demula col., leg. *L-S. Wang & H. Shi*, 14–46628, herb. KUN-L	29º 19.146' N	97º 1.755' E	1
North America	USA, Alaska, Klondike Historical National Park, White Pass, 1012 m a.s.l., 2012, leg. *S. Pérez-Ortega*	59º 37' 10.15" N	-135º 9' 34.93" E	5
North America	USA, Alaska, Klondike Historical National Park, Chilkoot Pass, 720 m a.s.l., 2012, leg. *S. Pérez-Ortega*	59º 41' 0.64" N	-135º 15' 00" E	12
North America	USA, Alaska, leg. *Toby Spribille*	65.396832	-145.981998	4

North America	USA, Montana, Deerlodge Co., Beaverhead-Deerlodge National Forest, vicinity of Four Mile Basin, on granitic boulders, 2438 m a.s.l., 2009, leg. *St. Clair* 16685, GZU–86–2010	46º 5.680' N	-113º 13.918' E	5
South America	Bolivia, Dept. La Paz., Prov. Murillo, below Potosí near Campamento de los Mineros, on the road to La Paz, Valle del Zongo, on rocks, 4335–4716 m a.s.l., 2011-2014, leg. *A. Flakus* 21852–26053, LPB herbarium	16º 17' 43" S 17º 16' 55" S	-68º 07' 42" E -65º 44' 14" E	4
South America	Chile, Paso de Pino Hachado, 1886 m a.sl., leg. *S. Pérez-Ortega*	-38.662050	-70.898447	13
South America	Argentina, Bariloche, Cerro Catedral, 2143 m a.s.l., leg. *S. Pérez-Ortega*	-41.246853	-71.344072	15
South America	Chile, Tierra del Fuego, Isla Navarino, Pico Estación, 2015, leg. *J. Raggio*	-55.031972	-67.644542	17
South America	Chile, Tierra del Fuego, Isla Navarino, Cerro Bandera, 2015, leg. *J. Raggio*	-55.031972	-67.644542	9
New Zealand	New Zealand, Otago, Old Man Range, 1640 m a.s.l., 2015, leg. *Allison Knight*, OTA herb.	-45.338411	169.179236	8
Antarctica	Antarctica, South Shetland Islands, Livingston Island, 2014, leg. *A. de los Ríos*	-62.665647	-60.394083	13
Antarctica	Antarctica, Adelaide Island, Loubet Coast, Rothera Point, 20 m a.s.l., 2011, leg. *U. Søchting* (US), C herb.	-67.499433	-68.208456	8
Antarctica	Antarctica, Dronning Maud Land, Vestfjella, nunatak, 550–678 m a.s.l., 2013, leg. *G. Thor*	-73.396392	-15.059531	6
Antarctica	Antarctica, Transantarctic Mountains: Massam Glacier (Garden Spur), Scott Glacier (Durham Point), Mt. Kyffin, The Gateway (Gateway Spur), Mt. Hope, Waldron Spur, Deception Hill, leg. *L. G. Sancho*	84º 32.129' S 85º 32.352' S 83º 46.485' S 83º 29.208' S	174º 57.249' E 151º 8.996' E 171º 49.655' E 170º 47.393' E	33
Outgroup (*Bryoria bicolor*)	Austria, Sölktal, Sankt Nikolai im Sölktal, on mosses on granitic rocks, 2015, leg. *I. Garrido-Benavent*	47º 18' 34.65" N	14° 2' 12.44" E	1

Appendix 2. *nrITS* and *Mcm7* sequences of *Pseudephebe* spp. downloaded from GENBANK and used in species delimitation analyses.

Species	Locality	Voucher specimen	*nrITS* accession no.	*Mcm7* accession no.
Pseudephebe minuscula	USA, Alaska	SRP L-0008791	KU647292	KU668487
P. pubescens	USA, Alaska	SRP L-0008806	KU647293	KU668489
P. minuscula	USA, Nevada	hb. *N. Noell* 1442	KU647294	KU668500
P. pubescens	USA, California	hb. *N. Noell* 1581	KU647295	-
P. pubescens	USA, Montana	S F175892	KU647296	KU668493
P. pubescens	USA, Montana	S F144171	KU647297	KU668491
P. pubescens	USA, Oregon	*Hollinger* 3971	KU647298	KU668492
			KX160147	-
P. pubescens	USA, Washington	hb. *N. Noell* 1557	KU647299	-
P. pubescens	Chile, Magallanes	MAF-Lich. 20105	KU647300	KU668481
P. pubescens	Chile, Magallanes	MAF-Lich. 20106	KU647301	KU668482
P. minuscula	Norway, South Nordland	MAF-Lich. 20107	KU647302	KU668496
P. minuscula	Norway, Sogn og Fjordane	MAF-Lich. 20102	KU647303	KU668497
P. minuscula	Sweden, Jämtland	S F149958	KU647304	KU668490
P. minuscula	Sweden, Jämtland	S F177970	KU647305	-
P. pubescens	Sweden, Västerbotten	S F240229	KU647306	KU668484
P. pubescens	Austria, Tirol	MAF-Lich. 17091	KU647307	KU668485
P. pubescens	Romania, Hunedoara	MAF-Lich. 19475	KU647308	KU668486
P. minuscula	Portugal, Beira Baixa	MAF-Lich. 19472	KU647309	KU668488
P. minuscula	Portugal, Minho	MAF-Lich. 19473	KU647310	KU668498
			KX160146	-
P. pubescens	Spain, Asturias	MAF-Lich. 17838	KU647311	KU668499
P. aff. *minuscula*	Spain, Segovia	MAF-Lich. 20103	KU647312	KU668494
P. aff. *minuscula*	Spain, Segovia	MAF-Lich. 20104	KU647313	KU668495
P. pubescens	Norway, Sogn og Fjordane	MAF-Lich. 20100	KU647314	KU668475
P. pubescens	Norway, Sogn og Fjordane	MAF-Lich. 20101	KU647315	KU668476
P. pubescens	Norway, South Nordland	MAF-Lich. 20108	KU647316	KU668479
P. pubescens	Sweden, Jämtland	S F149572	KU647317	KU668477
P. pubescens	Switzerland, Uri	MAF-Lich. 19476	KU647318	KU668474
P. pubescens	Spain, Asturias	MAF-Lich. 17907	KU647319	KU668470
P. pubescens	Spain, Asturias	MAF-Lich. 17915	KU647320	KU668472
P. pubescens	Spain, Asturias	MAF-Lich. 17930	KU647321	KU668478
P. pubescens	Spain, Asturias	MAF-Lich. 18112	KU647322	KU668471
P. pubescens	Spain, León	MAF-Lich. 19474	KU647323	KU668473
P. pubescens	Spain, Teruel	MAF-Lich. 16841	KU647324	-
P. pubescens	Spain, Zamora	MAF-Lich. 19470	KU647325	KU668469
P. pubescens	Spain, Zamora	MAF-Lich. 19471	KU647326	KU668468
P. aff. *pubescens*	Finland, Regio Aboensis	*T. Feuerer & A. Thell* (LD)	AF451737	-
P. aff. *pubescens*	Chile	*T. Feuerer* (HBG)	AF451738	-
P. aff. *minuscula*	Trentino-Alto-Adige	*T. Feuerer & A. Thell* (HBG)	AY251446	-
P. aff. *pubescens*	Spain, Zamora	MAF-Lich. 6774	AY611125	-
P. aff. *pubescens*	USA, Alaska	L221, *T. Ahti & S.S. Talbot* (H)	HQ402676	KJ948091
P. aff. *minuscula*	Russia, Franz Josef Land	L525, *S.S. Kholod*	KJ947962	KJ948090

		(H)		
P. aff. *pubescens*	USA, Alaska	L487 *T. Ahti & S.S. Talbot* (H)	KJ947963	KJ948092
P. aff. *pubescens*	USA, Alaska	L491 *T. Ahti & S.S. Talbot* (H)	KJ947964	KJ948093
P. aff. *pubescens*	Russia, Franz Josef Land	L524, *S.S. Kholod* (H)	KJ947965	KJ948094
P. minuscula	Falkland Islands	NMW.C.2015.004.8	KU647290	KU668483
P. minuscula	Falkland Islands	*Fryday* 10925	KU647291	KU668480

CAPÍTULO 7 (*CHAPTER 7*)

Pasado, presente y futuro en la investigación de hongos y algas liquenizados bipolares.

Título en inglés: “Past, present and future of research in bipolar lichen-forming fungi and their photobionts”

Abstract

Compared to vascular plants and mosses, lichen-forming fungi show a higher number of amphitropically-distributed species, i.e. those occurring in both hemispheres but largely absent from intermediate, tropical latitudes. For instance, *c*. 160 Antarctic lichens are also present in polar areas or mountainous temperate regions of the Northern Hemisphere. Early interpretations of this particular distribution pattern were made in terms of vicariance or long-distance dispersal. However, it was not until the emergence of phylogenetics and the possibility of dating past diversification events that these initial hypotheses started to be evaluated. The premise of a relatively recent, Pleistocene colonisation of the Southern Hemisphere of mainly boreal lichens through long-distance dispersal has gained wide acceptance in recent studies based on either the comparison of genetic affinities (i.e. tree topology) or more robust, statistical migratory models. Still, the scarcity of such studies and the growing concern of too wide taxonomic concepts for amphitropical lichens prevents from generating sound explanations on the mechanisms at the origin of such fascinating disjunct distribution.

The purpose of this review is to give a state-of-the-art overview of amphitropical distributions in lichen-forming fungi and their photobionts. Evidence provided by recent, molecular-based studies as well as data on the type of lichen reproduction, dispersal ability, photobiont availability and habitat preferences are brought together to discuss how and when these distributions originated and their genetic consequences. The concepts of amphitropical and bipolar distribution in lichens are also critically discussed, and a new analytical framework is proposed for their study.

1. Lichens and biogeography

Lichens represent a paradigmatic case of symbiosis involving a single heterotrophic fungus (mycobiont) and a population of compatible photoautotrophic microorganisms (photobionts), such as algae (phycobionts) and/or cyanobacteria (cyanobionts). Mycobionts belong mainly into Ascomycota (*c*. 90% of all species), lichenized green algae occur mostly in genera of classes *Trebouxiophyceae* and *Ulvophyceae* (e.g. *Trebouxia*, *Asterochloris*, and *Trentepohlia*) whereas cyanobionts are species of *Nostoc*, *Scytonema*, *Stigonema* and *Gloeocapsa* (Tschermak-Woess 1988; Friedl & Büdel 2008; Honegger 2012). The lichenized lifestyle has been adopted by *c*. 20% of all fungi, with nearly 15.000 species of lichen-forming fungi described so far (Kirk et al. 2008).

The phenotypical outcome of lichenization is the lichen thallus, which is generally composed of a network of mycobiont hyphae within which photobiont cells are distributed. The resulting external habit has been used traditionally to sort lichens into three main groups (crustose, foliose and fruticose) that represent different degrees of morphological and ultrastructural complexity. Yet, in all cases photobionts live protected from excessive exposure to solar radiation, changes in temperature and desiccation, while they provide carbohydrates and other nutrients to the fungal cells (Honegger 2012). The use of new techniques of molecular biology and microscopy has recently shown lichen thalli to represent small ecosystems which may include several myco- and photobiont strains, endolichenic fungi and bacteria (Hawksworth 1988; Hodkinson & Lutzoni 2009; Casano et al. 2011; U'Ren et al. 2010, 2012; Spribille et al. 2016).

Lichen symbioses display a high degree of morphological and functional diversity, being involved in a number of ecosystem-level processes (Cornelissen et al. 2007; Ellis 2012; Elbert et al. 2012). Traits as the growth form, type of photobiont, thallus pigmentation or the nature of the secondary metabolites have been shown to influence ecological processes as important as decomposition, accumulation and recycling of water and nutrients (C and N), the assemblage of invertebrate communities and even the rock weathering (Asplund & Wardle 2016). In addition, their longevity and ability to grow continuously over time have made them useful as bioindicators of air pollution, forest health, soil quality and climate change (McCune 2000).

The mycobiont often produces specialized sexual reproductive structures (apothecia and perithecia) in which meiotic spores are formed. Myco- and photobionts can be vegetatively co-dispersed through thallus fragments or specific structures developed on the thallus surface and/or margins, such as soredia, small groups of photobiont cells loosely surrounded by fungal hyphae which are formed in specialized areas named soralia, and isidia, which consist of easily-detachable, thallus outgrowths that are regularly larger and heavier than soredia. Lichen forming-fungi can also produce minute mitotic spores named conidia. Reproduction by either meiotic (sexual) or mitotic (asexual) spores has a major disadvantage as these have to find a new

photobiont partner prior to the formation of a new thallus. Nevertheless, in the absence of compatible photobionts, some lichen-forming fungi can momentarily engage in looser associations with other algae (Ott 1987) or even become saprophytes (Lawrey 1984, p. 407; Wedin et al. 2004).

Given their poikilohydric nature, i.e. they cannot modulate their own water content, and other physiological properties emerging from the mutualistic association, lichens are able to thrive in inhospitable terrestrial and subaquatic habitats where vascular plants fail (Kappen 2000; Sadowsky & Ott 2016). They occupy *c*. 8% of the planet surface (Nash 2008) and inhabit extreme environments as cold and hot deserts (McMurdo Dry Valleys in Antarctica, Øvstedal & Lewis Smith 2001, Pérez-Ortega et al. 2012a; Namib desert, Lalley & Viles 2005), the high Himalaya peaks up to 7.400 m (Hertel 1977) and those exposed to a high saline stress such as the intertidal zone of most oceans (Lamb 1948; Pérez-Ortega et al. 2016). Besides colonising hostile and remote habitats, many lichens show wider geographic distributions than vascular plants (Galloway 2008). Collectively, these features of lichens have since very long attracted the attention of many researchers (e.g. Santesson 1939; Du Rietz 1940; Lamb 1948), triggering biogeographic research which have roughly addressed three different topics. The first is based on the compilation and comparison of species lists. Several studies have used this method to study the biogeographic patterns in certain taxonomic groups (e.g. Otte et al. 2002, 2005; Lücking 2003; Martínez et al. 2003). At a worldwide scale, Feuerer & Hawksworth (2007) showed that lichens clustered into fewer but larger biogeographic regions than plants. Second, the exceptional distribution ranges of some lichens early stimulated researchers using DNA data to perform population genetic analyses on extensive individual datasets (Crespo et al. 2002; Printzen et al. 2003). In this context, recent phylogeographic surveys have also included formal tests of gene flow hypotheses (Buschbom 2007; Geml et al. 2010; Fernández-Mendoza & Printzen 2013; Sork & Werth 2014). Lately, new approaches have come up incorporating the comparison of phylogeographic patterns of myco- and photobionts as well as modelling species distributions under an ecological perspective (see Leavitt & Lumbsch 2016 for a review).

Although recent advancements in lichen biogeography have been made in the last years (Printzen 2008; Werth 2011), there are still numerous questions open. In this review we focus on the bipolar (amphitropical, antitropical) distribution, which already intrigued botanists and lichenologists since the early 19th century. In particular, we survey the lichenological literature that predates the molecular era, and then examine the main contribution of the phylogeography to the general discussion of bipolarity in lichens. We also provide a comprehensive examination of the origin of bipolar distributions in lichens under a dispersalist view. Finally, we discuss the concept "bipolar" in lichens as well as new approaches to address this topic from a molecular and ecological perspective.

2. Bipolarity in lichen-forming fungi: A "non-molecular" perspective

2.1. History of the bipolar lichen research

Early considerations on bipolar plants and mosses were done by eminent naturalists as Humboldt (1817), Darwin (1872), Wallace (1880), whereas Hooker & Taylor (1844) likely provided the first reference to bipolarity in lichens when pointing at morphological similarities between austral lichens collected by J. D. Hooker and those growing in northern latitudes. Later, the Swedish plant geographer G. Einar Du Rietz (1940) made one of the most remarkable contributions to the topic of bipolarity compiling and discussing historical evidences of bipolar austral taxa, including lichens. Such valuable work generated interest on both the numbers of bipolar lichens and the likely mechanisms explaining their disjunct distribution, especially in the context of Antarctic and New Zealand lichenology (Lamb 1948; Lindsay 1972, 1977; Galloway & Bartlett 1986). Lamb (1948) admitted the importance of the bipolar element in the Antarctic lichen biota, which he defined as those taxa being also present in the Arctic "with or without outlying occurrences at high altitudes in the temperate Northern Hemisphere". Hertel (1988) provided a preliminary checklist of bipolar (and also widespread) lichen species for Antarctica. Galloway (1991) and Seppelt (1995) highlighted the importance of the bipolar element in their phytogeographical works of austral landmasses. These early investigations ended up with the publication of a seminal work on bipolar lichens by Galloway & Aptroot (1995). Bipolar taxa have been recognized in many genera of lichen-forming fungi: e.g. *Caloplaca* (Søchting & Olech 1995), *Cladonia* (Stenroos 1993), *Collemopsidium* (Santesson 1939), *Neuropogon* (Walker 1985), *Pleopsidium* (Castello & Nimis 1994), *Protopannaria* (Jørgensen 2001), *Solorina* (Lewis Smith & Øvstedal 1994), *Sphaerophorus* (Wedin 1995), *Stereocaulon* (Lewis Smith & Øvstedal 1994), and *Verrucaria* (Santesson 1939; Lamb 1848).

2.2. On the numbers of bipolar lichens

Most of the information on the numbers of bipolar lichen-forming fungi is frequently found in the austral lichenological literature. One of the first figures was provided by Jørgensen (1983), who considered that approximately 25% of Antarctic lichens belonged to the bipolar element. Afterwards, Castello & Nimis (1997) updated the number of bipolar and cosmopolitan species in Antarctica which accounted for *c*. 41.5% of the total species diversity. Øvstedal & Lewis Smith (2001) in their reference work on the Antarctic lichen biota highlighted that 148 species occurring in Antarctica (> 60º S) were amphitropically distributed. Accordingly, *c*. 39.1% of the total diversity in Antarctica showed a bipolar distribution, while the proportion of Antarctic endemics was comparatively lower (*c*. 33.5%). These figures are repeated at local scales within the Antarctic and Subantarctic region. Nearly one third of the lichen-forming fungi found in Bouvetøya (Engelskjøn & Jørgensen, 1986), in the Hurd Peninsula (Livingston Island, South Shetland Islands) (Søchting et al. 2004) and the South Sandwich Islands (Convey et al. 2000) are bipolar or cosmopolitan. Likewise, Øvstedal & Lewis Smith (2001) reported that as much as 41% of lichens in the South Orkney Islands showed this

particular distribution pattern. Even extremely isolated places such as the Utsteinen Nunatak in the Sør Rondane Mountains (71–72º S, Continental Antarctica) have been recently shown to host considerable numbers of bipolar taxa (Ertz et al. 2014). Finally, Singh et al. (2015b) compared biogeographic patterns of the lichen biota in three Antarctic localities and found more bipolar taxa in Admiralty Bay in the Antarctic Peninsula (*c*. 41% of bipolar species) than in the Schirmacher Oasis and Victoria Land in Continental Antarctica (*c*. 29.8% and 35.6% of species, respectively).

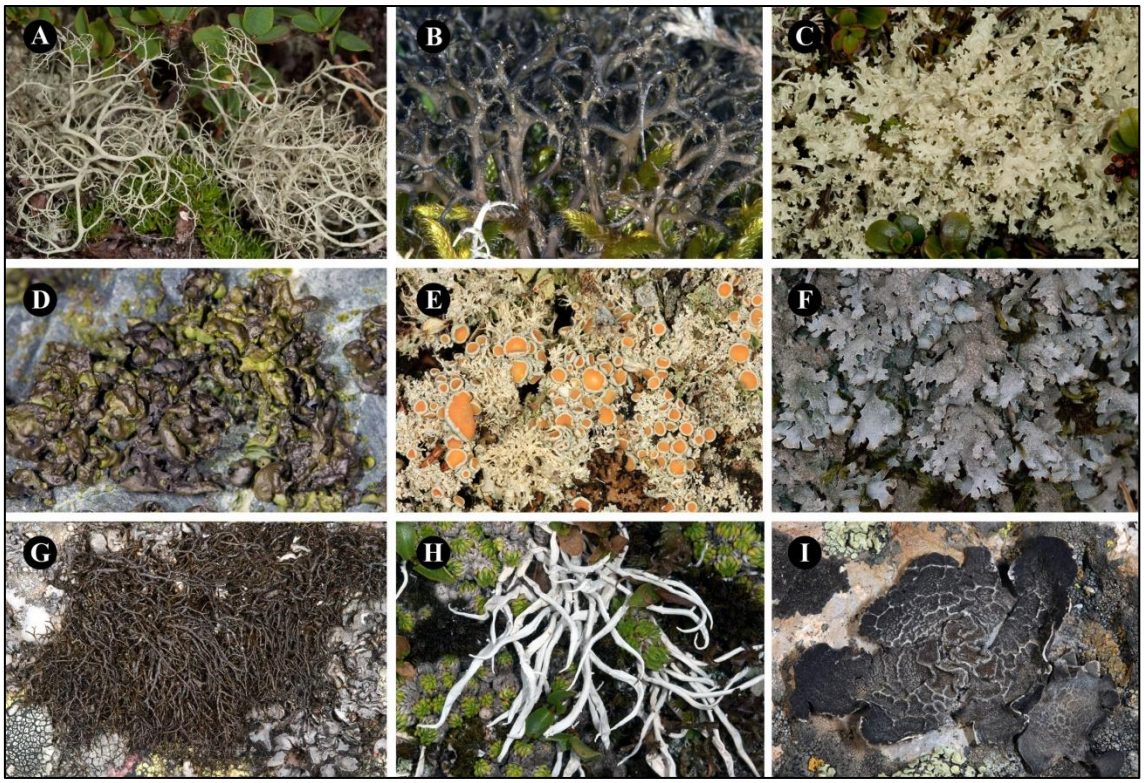

Figure 1. Species of bipolar lichen-forming fungi. (A) *Alectoria ochroleuca* ssp. *vexillifera* (Obergurgl, Austria). (B) *Cetraria aculeata* (Burgos, Spain). (C) *Flavocetraria nivalis* (Obergurgl, Austria). (D) *Mastodia tessellata* (Petersburg, Alaska, USA). (E) *Ochrolechia frigida* (Tierra del Fuego, Chile). (F) *Parmelia saxatilis* (Burgos, España). (G) *Pseudephebe* aff. *pubescens* (Soria, España). (H) *Thamnolia vermicularis* (Obergurgl, Austria). (I) *Umbilicaria decussata* (El Morado, Chile). (Photographs: SPO).

Compared to the Antarctic scenario, research on the bipolar element in the lichen biota of Australia, New Zealand and South America is scarce. In a preliminary lichen compilation of New Zealand (*c*. 34–47º S), up to 166 lichens were found to occur also in the Arctic (Galloway 1985). In Australia, Weber & Wetmore (1972) recorded 122 species that occurred also in the Arctic, and for the more southerly Tasmania, Wetmore (1963) listed 66 species of lichen-forming fungi in common also with the Arctic. Regarding Tasmania (40–43º S), species in *Alectoria*, *Arthrorhaphis*, *Candelariella*, *Thamnolia*, *Umbilicaria* and *Verrucaria* (see Figure 1) were also found to occur in other austral regions (e.g. South America and Antarctica) as well as in the Northern

Hemisphere (Kantvilas 1995; McCarthy & Kantvilas 2000; Kantvilas & Louwhoff 2007).

The occurrence of the bipolar element in the lichen biota of South America has also been highlighted (e.g. Messuti et al. 2003; Bjerke & Elvebakk 2004), and some relatively common Northern Hemisphere species in families *Cladoniaceae* (Stenroos & Ahti 1990; León et al. 2013), *Physciaceae* (Elvebakk & Moberg 2002) and *Parmeliaceae* (Stenroos 1991; Elvebakk et al. 2014) have been reported from southernmost South America. A regional study focused on the lichen mycobiota of Aysén (44–47º S, southern Chile) revealed that *c*. 13% of the total species belonged to the bipolar element and that most of these species occurred mainly in the steppe area in alpine habitats (Quilhot et al. 2012). Notably, the genus *Cladonia* shows a high incidence of bipolar species in the Falkland Islands, at 51–52º S (17 taxa, 59%, Stenroos & Ahti 1992) and the Navarino Island, at 54–55º S (15 taxa, 37%, Burgaz & Raggio 2007).

2.3. Early explanations of bipolarity

After the influential works of Du Rietz (1926, 1940) about bipolar distributions, many researchers discussed the origin of the bipolar distribution in lichens (Lamb 1948, 1970; Galloway & Aptroot 1995; Castello & Nimis 1997; Bjerke & Elvebakk 2004). Explanations for it were postulated in the context of either dispersal or vicariance, and can be summarized as follows:

1) "Stepping-stone" or "mountain-hopping" dispersal along the American Cordilleras. Pleistocene glaciations could have allowed species occurring at cold, higher latitudes in both hemispheres to progressively approach and finally cross the once warmer tropical belt, and establish in the opposite hemisphere. This is in agreement with the "Darwin's pump" hypothesis for plants (Darwin 1872; Donoghue 2011), which also predicted that most migrations occurred from north to south. A migration through the Andean Cordillera and the Rocky Mountains in bipolar lichens was suggested for several *Cladonia* (Stenroos 1993) and *Caloplaca* s.l. species (Søchting & Olech 1995) or, more generally, for members of the Antarctic lichen biota (Lamb 1948; Dodge 1964). Either Brodo (1973) or Castello & Nimis (1997) stated that this explanation was somewhat doubtful, as many bipolar species were not known from the northern Andes, or from the southernmost Rocky Mountains. The "mountain-hopping" hypothesis is in no case suitable for explaining bipolar distributions in marine lichens, such as *Mastodia tessellata* (Figure 1D), *Verrucaria* spp. and *Collemopsidium* spp. (Santesson 1939; Lamb 1948; Kohlmeyer et al. 2004).

2) Direct long-distance dispersal between hemispheres. This explanation implied a relatively recent time period for the colonisation of the opposite hemisphere. Seppelt (1995) suggested that a proportion of the Antarctic lichen biota, including the bipolar species, could have invaded Antarctica from the Northern Hemisphere or 'remote localities' during the Late Pleistocene or Holocene. Similarly, Castello & Nimis (2000) took the high incidence of bipolar and subcosmopolitan lichens in Terra Nova Bay area

(Victoria Land, Continental Antarctica) as an indication of a recent origin of the whole lichen biota in that area driven by long-distance dispersal in the Quaternary. Aptroot in Galloway & Aptroot (1995) adduced that 'lichen species are, in evolutionary terms, too young' for plate tectonics to have shaped their current disjunct distribution. In general, the long-distance dispersal has received ample support in the bipolar lichen literature (Culberson 1972; Walker 1985; Hertel 1987; Søchting et al. 2004). The high proportion of bipolar species recorded in Subantarctic islands, which had been subjected to heavy glaciations during the Pleistocene, such as Marion and Prince Edward islands and Bouvetøya (Hertel 1984; Engelskjøn & Jørgensen 1986), was alleged as remarkable evidence to support this hypothesis (Castello & Nimis 1997).

3) Bipolarity as a result of vicariant events. The fragmentation of Pangea and Gondwana would have brought once globally distributed species to higher latitudes at both hemispheres, thus giving rise to the extant bipolar distribution pattern (e.g. Du Rietz 1940). In this scenario, driven by an abiotic factor, population divergence would have started in the mid-Jurassic to Late Cretaceous, roughly 174–66 million years ago (Scotese 2001). Therefore, an old origin for bipolar species must be assumed. Seppelt (1995) suggested that a proportion of the Antarctic bipolar and widespread lichens could have an ancient origin. The amphitropical distribution of *Thamnolia* was suggested to have originated by vicariance due to 'continental rafting' (Sheard 1977; Platt & Spatafora 2000), as species in this genus not reproduce by spores and, therefore, thallus fragments could not be carried over vast distances by long-distance dispersal vectors. In fact, on the basis of the reproductive strategy of this lichen, Bjerke & Elvebakk (2004) suggested an old time frame for *Thamnolia* disjunction. In another vicariant scenario, the competition of once cosmopolitan taxa with recently evolved tropical biota in the Tertiary was proposed to have urged older species to the fringes of their original range (Briggs 1987). In lichens, vicariant hypotheses benefited from the earlier consideration of slow evolutionary rates in lichen-forming fungi (Kärnefelt 1990), which would explain the high morphologically similar specimens found at both poles.

3. A new momentum in the study of bipolar distributions in lichens

3.1. The molecular perspective

The emergence of the molecular era at the end of the past century has radically changed the fields of systematics and biogeography. The ease to produce large and cheap molecular data sets together with the availability of a plethora of analytical tools have led to an actual revolution in the field of biogeography. Lichen biogeography did not lag behind this transformation. The first molecular-based studies addressing questions of the origin of bipolar distributions focused on species of the *Parmeliaceae* (*Cetraria*, *Parmelia*, *Platismatia* and *Tuckermannopsis*). *nrITS*-based comparisons of individuals from both hemispheres usually revealed low levels of intraspecific variation among distant areas (Thell et al. 1998, 2000, 2002; Kärnefelt & Thell 2001), although

studies in *Cetraria aculeata* (Figure 1B) did show correlation between DNA data and geographic origin (Thell et al. 2000, 2002). Crespo et al. (2002) used *nrITS* and *β-tubulin* regions to infer phylogenetic relationships among 32 *Parmelia saxatilis* (Figure 1F) samples from Antarctica, Patagonia, the Arctic, boreal Europe, North America and some Mediterranean high elevation mountains. The low levels of intraspecific divergence found in the lichen-forming fungus, especially between Russian and Antarctic samples, were interpreted as evidence for a recent origin of the extant disjunct range, suggesting that migratory birds could have facilitated dispersal between hemispheres of asexual propagules (isidia).

On the other hand, Murtagh et al. (2002) studied the bipolar species *Rusavskia elegans* (= *Xanthoria elegans*) with RAPDs and *nrITS* data from 62 sampled thalli. The only one Antarctic isolate displayed different degrees of similarity to the remaining worldwide isolates depending on the type of marker, although a Mantel test on RAPD data showed that genetic similarity was negatively correlated with the geographical separation of samples. Myllys et al. (2003) used four loci and 42 specimens of the bipolar *Cladonia arbuscula* and *C. mitis* and showed no genetic differentiation between hemispheres. The disjunct distribution in these species was proposed to be due to relatively recent trans-tropical gene flow through either migrations along the American Cordilleras (see also Stenroos 1993) during or immediately after the Pleistocene, or a more recent, direct long-distance dispersal mediated by migratory birds. Likewise, long-distance dispersal was pointed out as the most plausible explanation for the multigene similarities found in 13 specimens from Europe, North America and southernmost South America in one lineage within the *Sphaerophorus globosus* complex (Högnabba & Wedin 2003).

Phylogenetic reconstructions in species belonging to *Pseudocyphellaria* (Summerfield & Eaton-Rye 2006) and *Pleopsidium* (Reeb et al. 2007) also revealed a close genetic relationship between specimens collected at both hemispheres. Seymour et al. (2007) in their study on the taxonomy of neuropogonoid *Usnea*, a group with a large diversity in southern South America and Antarctica, used *nrITS* and *RPB1* data from 68 specimens to show that *U. sphacelata* was made up of two different genetic lineages, one of them displaying a bipolar distribution. This disjunct distribution may have arisen from either pole-ward migration from common refugia after de-glaciations or transport of propagules between Antarctica and the Arctic in relatively recent times, likely by long-distance dispersal. Therefore, this could explain why specimens at both hemispheres were not significantly morphologically differentiated. Wirtz et al. (2008, 2012) used also these three loci to confirm the occurrence of this species in the Northern Hemisphere (Canada, Greenland, and Spitsbergen), the high Andes and Patagonia (but not in Antarctica) and found that individuals from the Northern Hemisphere were genetically almost uniform, with the most common northern haplotype also present in Ecuador. This was interpreted as an evidence of ongoing gene flow between the Andean and the more northerly populations. Wirtz et al. (2008) also showed the existence of a further species with bipolar disjunct range, *U. lambii*, present in Oregon (USA), South

America and Antarctica. Overall, although the results provided by these authors suggested an austral origin for both neuropogonoid species, their studies were more focused on the species delimitation problem in this difficult group than in providing a formal explanation for the acquisition of the bipolar distribution.

The *Teloschistaceae* is a family of lichenized fungi with a high diversity of species in polar regions that also harbors a substantial number of bipolar species (Søchting & Olech 1995). Lindblom & Søchting (2008) molecularly analysed the bipolar pattern in *Xanthomendoza borealis* (40 thalli, *nrITS* data) and used the fact that its most closely related species are mainly distributed in the Northern Hemisphere as an indication for its boreal origin. Later, Søchting & Castello (2012) used the same reasoning to propose an austral origin for the bipolar *Austroplaca soropelta* (= *Caloplaca soropelta*) using *nrITS* sequences from 5 samples of this species. In both studies, the acquisition of a bipolar distribution range was only marginally explained, and the authors appealed to the three mechanisms highlighted above. However, the fact that *A. soropelta* is largely absent from most Andean localities, the European Alps and most of North America was used by Søchting & Castello to favor the idea of direct long-distance dispersal from the Southern into the Northern Hemisphere. Finally, Vondrák et al. (2010) found a single specimen of the sorediate *Caloplaca phlogina* growing in a maritime site in the Chilean Navarino Island to have a nearly identical *nrITS* sequence to other specimens in Europe, which was interpreted as evidence for a young disjunction.

Geml et al. (2010, 2012) contributed to the growing body of bipolar lichen literature analysing in a coalescent framework phylogeographic patterns in the genera *Flavocetraria* and *Lichenomphalia*. Genetic similarity among South American and Northern Hemisphere populations of *Flavocetraria nivalis* (Figure 1C) and *F. cucullata* was explained by wind-mediated, long-distance dispersal (Geml et al. 2010) on the basis of a dataset consisting of *c*. 90 specimens and three markers (*nrITS, β-tubulin* and *EF-1α*). Likewise, using data of *nrITS, nuLSU* and *EF-1α*, Geml et al (2012) inferred high intercontinental gene flow among intraspecific populations of *Lichenomphalia* species in the Northern Hemisphere combined with rare transequatorial dispersals into the Southern Hemisphere leading to the establishment and subsequent origin of independent phylogenetic species. The presence of *Lichenomphalia* species in Ecuador, Colombia and Tierra del Fuego pointed also to the role of the "mountain hopping" mechanism of dispersal from north to south. In any case, these authors rejected vicariance as the driver of the spatial evolution of lineages in this basidiomycete genus of lichenized fungi. *Rhizoplaca melanophthalma* s.l. has been recently surveyed using a broad sampling including 240 specimens across five continents and seven loci (Leavitt et al. 2013). Shared *nrITS* haplotypes were observed between Chilean and North American and Eurasian specimens in at least two distinct phylogenetic clades. Results supported long-distance dispersal over vicariance as the most plausible mechanism shaping the intercontinental distribution of lineages in this lichen. Finally, Roca-Valiente (2013) examined bipolarity in *Rhizocarpon geographicum* with 237 specimens

and two loci (*nrITS* and *nuLSU*). Analyses on the mycobiont revealed two lineages with a broad bipolar distribution, and showed close genetic affinities between samples from Alaska, Tierra del Fuego and the Maritime Antarctica. These data were interpreted under the prism of long-distance dispersal.

Recent conceptual and analytical advances in phylogeography allow now to delve deeper into the population history of the species by reconstructing phylogeographic scenarios, estimating migration rates, demographic parameters and divergence times (Beerli & Palczewski 2010; Ronquist & Sanmartín 2011; Papadopoulou & Knowles 2016; Yang & Donoghue 2016). Lichenological research has greatly benefited from such advances (e.g. Werth 2010; Leavitt et al. 2015a). In particular, discussions on lichen bipolar distributions have shifted from comparing the relative position of bipolar specimens in a given topology (e.g. Crespo et al. 2002; Myllys et al. 2003; Högnabba & Wedin 2003) to a more inferential scenarios developed through a wide array of population genetics analyses. In the latter context, Fernández-Mendoza & Printzen (2013) addressed the historical and ecological processes that could have shaped the extant bipolar range of *Cetraria aculeata* using 356 thalli from all continents except Oceania and three molecular markers (*nrITS*, *mtLSU*, *GAPDH*). Some widely distributed haplotypes were detected in the low-copy nuclear protein-coding and mitochondrial markers, with some haplotypes shared between southernmost South America, Antarctica and several localities in Central and Northern Europe. Using a combined approach of a newly time-explicit stochastic character mapping and the comparison of migration models under a Bayesian coalescent framework, they inferred that *C. aculeata* originated in the Northern Hemisphere and dispersed into South America in a series of dispersal events during the Pleistocene, and it culminated in a more recent colonisation of Antarctica. Therefore, either direct long-distance dispersal or "mountain-hopping" along the Andes could have shaped the acquisition of the bipolar range in this lichen (Fernández-Mendoza & Printzen 2013).

3.2. Photobionts in bipolar lichens

Molecular appraisals of the photobionts associated with bipolar lichenized fungi have received comparatively little attention. On the one hand, most studies have focused on the patterns of specificity and selectivity (Beck et al. 2002; Yahr et al. 2004) shown by Antarctic specimens of bipolar lichenized fungi. Low mycobiont selectivity toward the photobionts may be analogously compared with a lack of specialized pollinators in flowering plants, a feature shown by most bipolar plants according to Raven (1963). Likewise, low selectivity toward their photobionts have indeed been found in the Antarctic bipolar mycobionts *Umbilicaria decussata* (Figure 1I), *Massalongia carnosa* and *Lepraria borealis* (Romeike et al. 2002; Wirtz et al. 2003; Engelen et al. 2010; but see Pérez-Ortega et al. 2012a and Engelen et al. 2016 for cases of differential specificity and selectivity), and authors interpreted these observations as the result of extreme climatic conditions selecting for more flexible mycobionts. On the other hand, biogeographic patterns in bipolar lichen photobionts have been rarely considered. Domaschke et al. (2012) and Lindblom & Søchting (2013) used *nrITS* data and found

that the genetic diversity of photobionts in the bipolar *Cetraria aculeata* and *Xanthomendoza borealis* was considerably larger in the Arctic-boreal zone than in Antarctica, a pattern that was explained by founder events during the colonisation of Antarctica (or a later bottleneck), or also by strong selective pressure favoring haplotypes well adapted to extreme climatic conditions. Furthermore, the existence of identical photobiont haplotypes in localities in both polar regions has been detected at specific (*C. aculeata*, Fernández-Mendoza et al. 2011; *Rhizocarpon geographicum*, Roca-Valiente 2013) and family-level (*Lecideaceae*, Ruprecht et al. 2012a) taxonomical ranges. Fernández-Mendoza et al. (2011) explained it by the existence of ancestral polymorphisms and slow genetic drift, or due to a high degree of photobiont dispersal, either jointly with the *C. aculeata* mycobiont (i.e. asexual propagules or thallus fragments) or independently with unrelated mycobionts. In fact, horizontal transmission of photobionts is common in lichens, even in those which reproduce purely in a vegetative (asexual) way (Piercey-Normore 2006; Nelsen & Gargas 2008; Wornik & Grube 2010). Similarly, the presence of compatible photobionts in the free-living state is largely accepted (e.g. Bubrick et al. 1984; Mukhtar et al. 1994), also in the climatically harshest regions on Earth, i.e. the McMurdo Dry Valleys in Antarctica (Yung et al. 2014). In general, explaining the mechanisms by which the bipolar pattern was acquired in microscopic photobionts is controversial, as either the mode of photobiont transmission or the impact of environmental conditions and historical co-dispersal may have shaped the patterns of mycobiont-photobiont association.

A very different scenario is posed by the photobiont of the bipolar *Mastodia tessellata* (Figure 1D) which belongs into the macroscopic, foliose green algae genus *Prasiola* (*Trebouxiophyceae*, Chlorophyta). This association has been reported as a paradigmatic case of one-to-one symbiotic relationship in which the photobiont, under certain biotic and/or abiotic conditions, is able to "escape" from the mycobiont (Pérez-Ortega et al. 2010). Recently, Garrido-Benavent et al. (2017) used three molecular markers (*nrITS*, *RPL10A*, *tufA*) from 140 specimens to address species delimitation and phylogeographic structure of the algal partner in this association. Results indicated that at least two photobiont species were involved: *Prasiola borealis*, which shows a bipolar distribution (Antarctica, Tierra del Fuego and Alaska), and a second, undescribed *Prasiola* species that is restricted to Antarctica. Furthermore, the genealogical relationships among haplotypes and the patterns of genetic diversity of *P. borealis* suggested a Southern to Northern Hemisphere migration. These data also argued against recurrent genetic exchange between localities at both poles, rather supporting a single historical event of trans-tropical dispersal. This agrees with the evolutionary history proposed for the mycobiont (Garrido-Benavent et al. in rev.).

3.3. Species delimitation, cryptic species, and bipolar phylogeography

Reliable species delimitations are critical for studies focusing on ecological and biogeographic patterns. Systematics of lichen-forming fungi has long been based on the comparison of morphological, chemical and ecological characters (Printzen 2009). The lack of diagnostic characters is, however, symptomatic in many groups, especially those

forming the so-called microlichens. Analyses based on DNA sequences and new conceptual frameworks to species delimitation have contributed to a better understanding of morphological variability and homoplasy in lichenized fungi, boosting the rate of newly published taxa (e.g. Arup et al. 2013; Lücking et al. 2014; Leavitt et al. 2016b). Numerous systematic studies over the last decades have revealed the presence of cryptic species in lichen mycobionts, i.e. two or more species-level lineages that would not likely be recognized using classical phenotypical characters (Bickford et al. 2007; Crespo & Pérez-Ortega 2009), or semi-cryptic when species are diagnosed mainly by ecological and/or chemical data and only by subtle morphological characters (Vondrák et al. 2009). Phylogeographic studies of allegedly bipolar or distantly disjunct lichenized fungi have played a significant role for discovering distinct allopatric, morphologically convergent, or even sympatric, species-level lineages hidden within traditionally circumscribed species (e.g. Crespo et al. 2010a; Amo de Paz et al. 2012; Boluda et al. 2016). Crespo et al. (2002) found two monophyletic lineages within the widely distributed *Parmelia saxatilis*. They match two different climatic regions: the first occurs in oceanic mild to cold environments, corresponding to the concept of *Parmelia saxatilis* s. str.; whereas the second is restricted to more continental areas within the Mediterranean, which was later described as *P. serrana* (Molina et al. 2004). Similarly, Högnabba & Wedin (2003) also revealed two phylogenetic species within the *Sphaerophorus globosus* complex, one restricted to hyperoceanic areas along the North American Pacific Northwest, subsequently described as *S. venerabilis* (Wedin et al. 2009), and the second displaying a wide distribution in both hemispheres. Data obtained by Murtagh et al. (2002) for *Xanthoria elegans* also suggested the presence of cryptic species. Lately, the phylogeographical appraisal of amphitropical *Lichenomphalia* also revealed two undescribed species-level lineages occurring in Campbell Island (New Zealand), one of these being closely related to the circumboreal *L. umbellifera*. The study of bipolar lineages has turned sometimes out in lumping disjunct species into a single widespread taxon. Summerfield & Eaton-Rye (2006) discussed the inclusion of *Pseudocyphellaria crocata, P. neglecta* and *P. perpetua* under a single phylogenetic species using an extensive sampling across Northern and Southern Pacific regions. Roca-Valiente (2013) proposed to lump a considerable number of *Rhizocarpon* species into only one species which would be then composed of two bipolar lineages. In other cases, the lack of diagnostic phenotypical characters prevented from describing new species in widely, amphitropically distributed lichenized fungi even when molecular data heavily supported their split (Muggia et al. 2014a). As well as in lichen-forming fungi, the use of DNA data has increased dramatically the description of new lineages in lichenized green algae (e.g. Moya et al. 2015; Vancurová et al. 2015; Kim et al. 2017), which are even more affected by morphological homoplasy and phenotypical plasticity than fungi (Verbruggen 2014; Leliaert et al. 2014). However, species limits in bipolar lichen photobionts have been rarely investigated and the only empirical evidence comes from the work of Garrido-Benavent et al. (2017) (see above).

4. Bipolar distribution under a dispersalist scenario

4.1. Lichen diaspores, vectors, and geographic range

Long-distance dispersal is often advocated as the main underlying mechanism for the acquisition of disjunct distributions in lichen-forming fungi and their photobionts (Högberg et al. 2002; Myllys et al. 2003; Fernández-Mendoza et al. 2011; Amo de Paz et al. 2012; Leavitt et al. 2012a; Magain et al. 2016), and the presence of lichens in isolated volcanic or de-glaciated islands provides undeniable evidence for its relevance (Jørgensen 1979; Smith 1984; Hertel 1987; Seppelt 1995). Lichenized fungi can disperse autonomously through meiotic spores (sexual reproduction), and/or by mitotic conidia, soredia, isidia and thallus fragmentation (asexual or vegetative propagation) (Figure 2). Meiotic spores range from a few microns in size up to a few hundred microns long (Pentecost 1981) and have been shown to withstand harsher environmental conditions than conidia (Seymour et al. 2005), such as high UV radiation (de Vera et al. 2003). On the contrary, the small size of conidia may allow a more effective means of intercontinental dispersal than vegetative propagules (Heinken 1999; Cassie & Piercey-Normore 2008) or even ascospores (Wilkinson et al. 2012). Lord et al. (2013) suggested a role for conidial dispersal in shaping the association of a single mycobiont genotype with a genetically diverse pool of photobionts in *Thamnolia vermicularis* (Figure 1H). In the dispersal of either sexual or asexual spores, the patterns of mycobiont re-lichenization will be ultimately dependent upon the spatial structure of suitable environmental conditions, the photobiont availability as well as the historical and contemporary patterns of gene flow among populations (Werth et al. 2006; Peksa & Škaloud 2011; Nadyeina et al. 2014; Werth & Sork 2014). In this sense, low selectivity of mycobionts toward the photobionts could allow spore-dispersed species to expand their ranges engaging with available, locally-adapted photobionts (Fernández-Mendoza et al. 2011).

The role of the three long-distance dispersal vectors (wind, water and animals) has been the focus of speculative debate since long. Muñoz et al. (2004) explained composition similarity in fern, bryophyte and lichen-forming fungi biotas across the Southern Ocean islands using “wind highways”. Spores and soredia are easily dispersed by wind over moderate distances up to a few hundred meters (Armstrong 1987, 1994; Werth et al. 2006). Soredia commonly appear in pollen traps (Tormo et al. 2001) and are the most abundant airborne propagules in Antarctica (Marshall 1996b). Water dispersal of lichen propagules has received comparatively less attention (Bailey 1968; Jahns et al. 1976; Armstrong, 1981, 1987). It has been shown to be key to many marine fungi (Kohlmeyer & Kohlmeyer 2013), and also in shaping lichen community composition (Giordani et al. 2014). Although dispersal by wind and water may shape the distribution of lichens at local, regional or even intracontinental scales, it seems unlikely that air- or waterborne lichen propagules could cross the equatorial belt (Wilkinson et al. 2012). In the context of lichen bipolar biogeography, the only evidence of long-distance dispersal of lichen propagules (soredia and thallus fragments) by wind was provided by Harmata & Olech (1991) who used traps for airborne

propagules along a transect between Antarctica and the Polish coast. However, these authors could not check the identity of the lichens producing the trapped propagules.

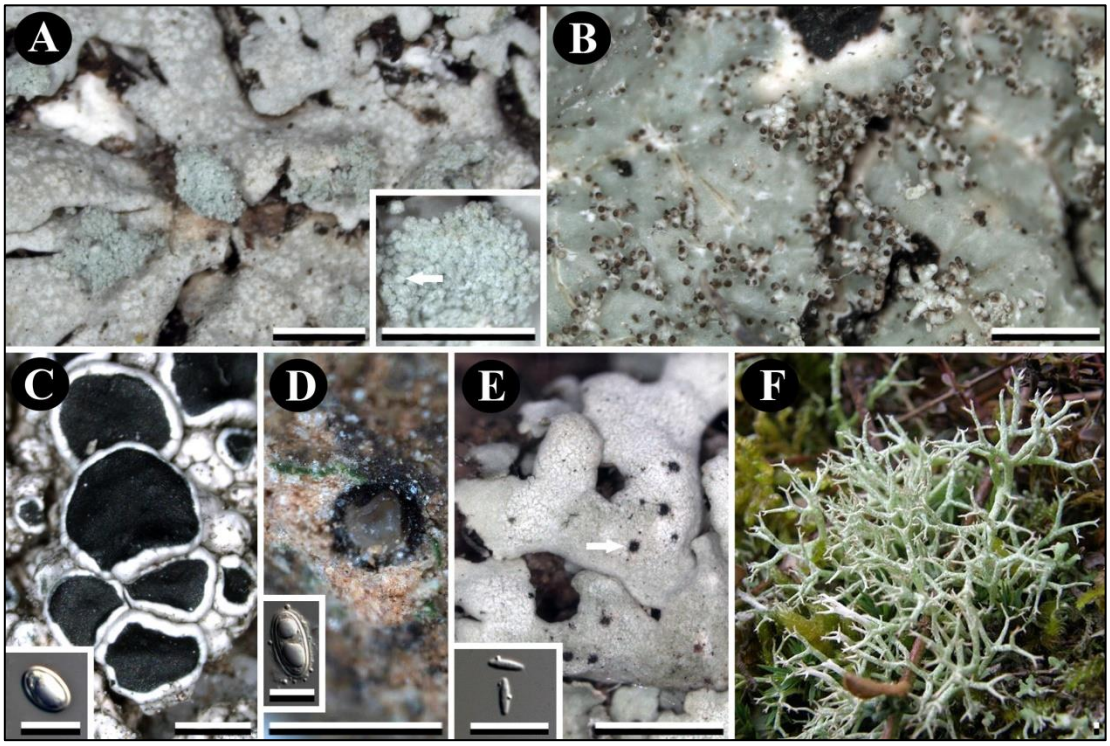

Figure 2. Lichen diaspores or propagules. (A) Soralia of *Physcia caesia*; inset with a white arrow indicating a soredium (Orihuela del Tremedal, Spain). (B) *Parmelia saxatilis* isidia (Orihuela del Tremedal, Spain). (C) *Tephromela atra* apothecia; inset with an ascospore (Orihuela del Tremedal, Spain). (D) Perithecium of *Verrucaria* sp.; inset with an ascospore (Quatretonda, Spain). (E) Conidiomata of *Physcia* sp. (white arrow); inset with conidia (Cerezo de Abajo, Spain). (F) Podetia of *Cladonia* sp. (Arròs, Spain). Scales: 1 mm (macroscopic photographs), 10 µm (microscopic photographs). (Photographs: IGB).

On the other hand, evidences for animals as dispersers of lichen diaspores are abundant. Small arthropods (mites, ants, booklice, and green lacewings) and gastropods (snails and slugs) can carry lichen propagules externally adhered to their bodies over short distances (Bailey 1970; Stubbs 1995; Lorentsson & Mattson 1999; Tauber et al. 2014). Endozoochorous dispersal by means of fecal pellets (Pyatt 1968; Fröberg et al. 2001; Meier et al. 2002; Boch et al. 2011) might also help to disperse both lichen partners over short and long distances, especially when those are transported by wind or vertebrates. However, it is expected that these small animals cannot account for trans-tropical dispersal of lichen propagules. Birds are then the most plausible animal agents for long-distance dispersal (see Viana et al. 2016 and Coughlan et al. 2017 for a review) and have indeed been suggested to generate bipolar distribution patterns in lichens (Crespo et al. 2002; Högnabba & Wedin 2003; Myllys et al. 2003; Lindblom & Søchting 2012; Geml et al. 2012; Garrido-Benavent et al. in rev.). These animals are usually in close contact with lichens (e.g. perching sites on tree branches or the top of

rocks), and even use them to construct their nests (Richardson & Young 1977). It is thus likely that lichen propagules get adhered to their feet or plumage (Bailey & James 1979), and carried along thousands of kilometers, even at trans-tropical scales (Lewis et al. 2014b). The sooty shearwater, the south polar skuas (Figure 3) or even Arctic terns and Wilson's storm petrels have been proposed as examples of bird species whose migration routes and nesting places overlap to a great extent with the distribution of extant bipolar lichens (Thomson 1984; Seymour et al. 2007; Garrido-Benavent et al., in. rev.). Moreover, some bipolar lichens are considered to be highly ornitocoprophilous, i.e. their growth is highly dependent upon the presence of nitrogen-rich spots caused by bird droppings (Figure 3A,E). For instance, the bipolar teloschistacean *Polycauliona candelaria* and *Xanthomendoza borealis* occur typically on rock ledges with a strong bird nutrient influence (Murtagh et al. 2002; Seppelt et al. 2010). Finally, it is worth to note that anthropogenic introductions are causing a major problem homogenizing biotas due to the introduction of species out of their natural ranges (Lodge 1993), including isolated and non-populated areas such as Antarctica (Tin et al. 2009). Reports on human induced introductions of lichen-forming fungi are still scarce (e.g. Aptroot 2011, 2016) but focus should be put on this likely source of diaspore dispersal.

4.2. Genetic consequences of the acquisition of a bipolar distribution

The higher frequency of self-compatible plants in remote islands has stand as a tenet in plant biogeography ("Baker's law", Baker 1955). Likewise, it is generally accepted that lichens showing vegetative propagation often have a larger geographic range than their fertile counterparts, at least in foliose and fruticose groups (Bowler & Rundel 1975), because co-dispersion of both symbionts increases the odds of a successful establishment in a new environment (Werth et al. 2006; Werth & Sork 2014). While some studies based on molecular data have supported this view (e.g. *Usnea ushuaiensis* vs. *U. lambii*, Wirtz et al. 2008), many other challenge it (*Sphaerophorus globosus* s. str. and *S. venerabilis*, Högnabba & Wedin 2003 and Wedin et al. 2009; *Pleopsidium chlorophanum* and *P. flavum*, Reeb et al. 2007; *Austroplaca soropelta* and *A. darbishirei*, Søchting & Castello 2012). On the other hand, the type of breeding system is likely to play a major role in permitting sexually-reproducing lichenized fungi to reproduce after effective establishment in distant regions outside their original ranges (Murtagh et al. 2000). Two breeding systems are described in Ascomycota: homothallism, in which individuals are self-fertile, and heterothallism, in which individuals are self-sterile and require for a compatible partner of different mating type for sexual reproduction to occur (Dyer et al. 1992). The latter system seems prevalent in lichen-forming fungi (Honegger & Zipler 2007; Singh et al. 2015a; Alors et al. 2017), even in species inhabiting climatically extreme habitats (Seymour et al. 2005). Oppositely, a higher incidence of homothallism would be expected in species showing wide disjunctions, such as the bipolar lichen mycobionts, allowing them to effectively reproduce in the newly colonised environment, yet there is so far no available study that has focused on this topic.

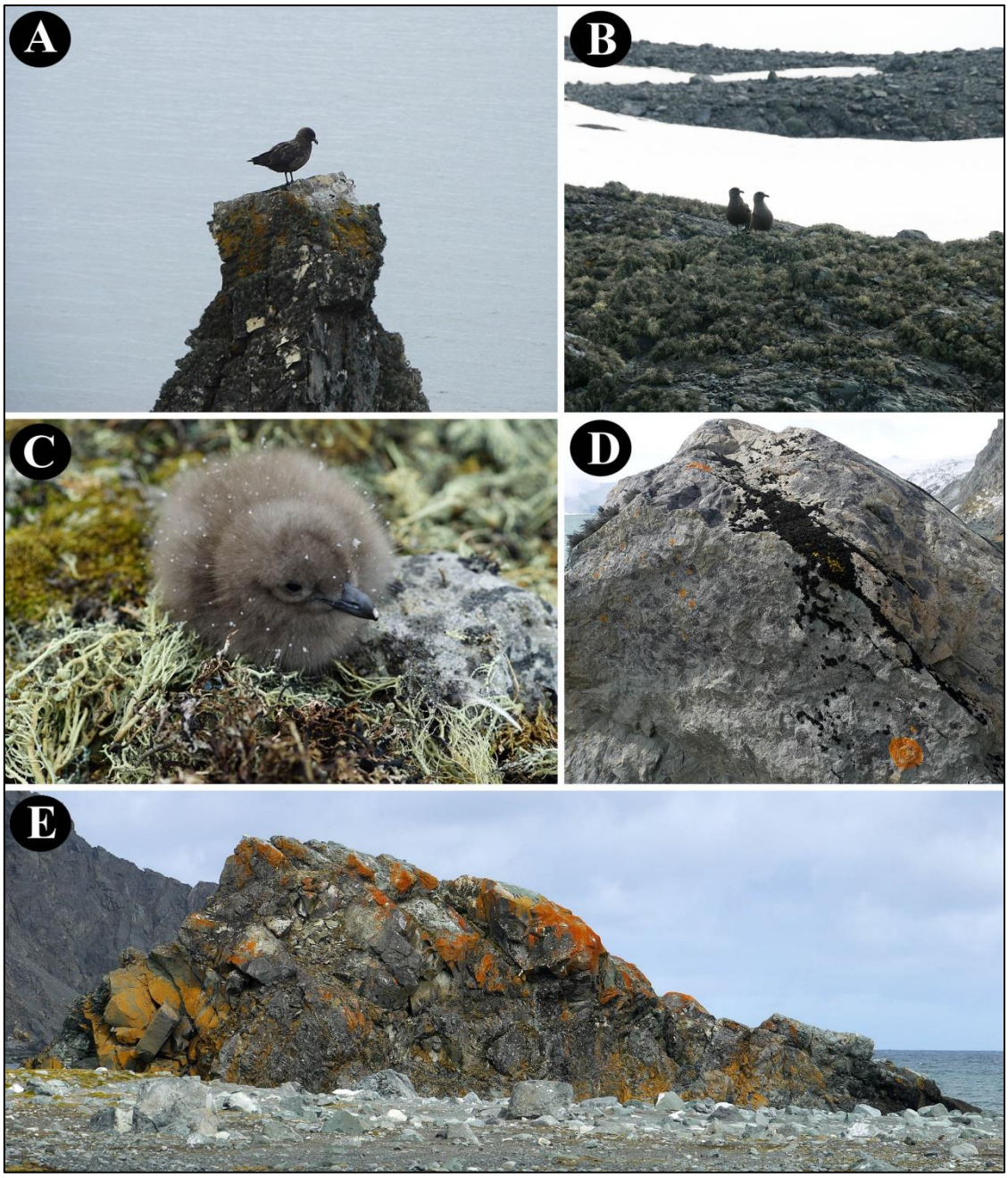

Figure 3. Skuas and lichen communities on rocks in Antarctica. (A) Perching site on the top of a rock with the presence of nitrogen-rich spots caused by bird droppings. (B) Two birds walking around a field of neuropogonoid *Usnea*. (C) Baby bird in a nest made of lichen thalli. (D) A population of the bipolar *Mastodia tessellata* on the top of a rock. (E) A diverse community of lichen species growing on rocks with a strong bird nutrient influence. (Photographs (A–B, D–E): AdR; (C): Jae Eun So).

Genetic variation in a species is influenced by several factors, such as the degree of randomness in matting patterns, the demographic history, the physical distribution of individuals, the patterns of migration among populations and natural selection (Nei 1975). In a biogeographic context, a pattern of reduced genetic variation has been inferred for leading edge populations in species that expanded their ranges after the last

ice age (Hewitt 2004), or in species invasions (Dlugosch & Parker 2008). A similar situation would be expected for bipolar mycobiont species which are widespread in one hemisphere and occur scarcely in the other, such as *Mastodia tessellata* (Kohlmeyer et al. 2004; Pérez-Ortega et al. 2010), *Arthrorhaphis citrinella* and *A. alpina* (Galloway & Bartlett 1986), *Flavocetraria cucullata* and *F. nivalis* (Bjerke & Elvebakk 2004; Geml et al. 2010), and *Austroplaca soropelta* (Søchting & Castello 2012). Assuming that isolated, disjunct populations of these species established recently after long-distance dispersal, probably during or after the last glacial times, and due to the scarcity of the dispersal events, a lower genetic diversity than in original areas continuously inhabited by the species is expected (Högberg et al. 2002; Lutsak et al. 2016). Accordingly, *C. aculeata* mycobiont showed reduced genetic diversity in Antarctica and to a lesser extent in South American populations, and it contrasted with the higher degree of genetic variability found in Arctic localities (Domaschke et al. 2012). Likewise, lower levels of DNA polymorphism were found in the myco- and photobiont of *M. tessellata* in the more recently colonised North American populations compared with those in Tierra del Fuego (Garrido-Benavent et al. 2017; Garrido-Benavent et al. in rev.). Overall, this pattern could be explained by genetic drift after a founder effect in a context of limited gene flow among disjunct populations (Fernández-Mendoza & Printzen 2013).

4.3. Ecological niches in bipolar lichens

Galloway & Aptroot (1995) highlighted the fact that the vast majority of bipolar lichens occurred in similar habitats in both hemispheres. In the Northern Hemisphere, they display an Arctic-alpine distribution (Stenroos et al. 2016), being common in coastal and more inland tundra areas in the Arctic (Kohlmeyer et al. 2004; Geml et al. 2010), and extending into the high mountain ranges at lower latitudes such as the Iberian Peninsula and Mexico (Sancho 1986; Herrera-Campos et al. 2016). In the Southern Hemisphere, bipolar species have been found growing in the steppe area on rocks and soil in alpine or subalpine grasslands in mountainous ranges of South America, Tasmania and New Zealand (Galloway & Bartlett 1986; Kantvilas 1995; Quilhot et al. 2012), in typically windy and dry, lichen-rich heaths in southernmost South America lowlands (Bjerke & Elvebakk 2004), and in cold-temperate marine habitats (Lamb 1948; McCarthy & Kantvilas 2000; Kohlmeyer et al. 2004). In Antarctica, many bipolar lichens inhabit nitrogen-rich areas affected by bird droppings (Øvstedal & Lewis Smith 2001; Seppelt et al. 2010). Although past distribution of biomes remains a matter of considerable debate (see Donoghue & Edwards 2014), tundra ecosystems are thought to have been widespread in the Northern Hemisphere after the mid-Miocene Climatic Optimum, *c.* 7–5 MA, while in the Southern Hemisphere their alpine version ("páramo") started to appear in the last 3–2 MA (Graham 2010, 2011; Hoorn et al. 2010). These habitats may have remained stable, open and isolated enough since then to have facilitated the range expansion of bipolar lichens (Galloway 2008), likely *via* habitat tracking. Even if some mountainous ranges were glaciated in the Pleistocene over the past 1–2 MA (Galloway & Aptroot 1995),

some extant bipolar species could have survived in glacial refugia (Fraser et al. 2012 and references therein). In fact, two bipolar species, *Pseudephebe minuscula* and *Umbilicaria decussata*, have been found growing abundantly in inland sites of the Antarctic continent like *nunataks* (Øvstedal & Lewis Smith 2001). So far, date estimates of population divergence and geographic range expansion support the hypothesis of recent long-distance dispersal over an old origin for bipolar populations (Fernández-Mendoza & Printzen 2013; Garrido-Benavent et al. in rev.). Nevertheless, the study of changes in size through time of suitable niches would help to model the chances of long-distance dispersal events.

5. Final remarks

5.1. Bipolarity in lichens re-defined

Most cited references used the terms "bipolar", "amphitropical" and "antitropical" (more rarely "biantitropical") to refer to species disjunctly distributed in both hemispheres but being largely absent from the tropics. The term "bipolar" refers, in our opinion, to a particular case of amphitropical (antitropical) distribution that may be vaguely defined as a geographic range restricted to high latitudes in both hemispheres. In other words, a bipolar species is also amphitropical, but an amphitropical species is not necessarily bipolar. The difficulty lies in how to establish the exact limits in the definition of "bipolar". Although a definition of that concept based on biome characterization would be the most desirable approach, considering lichens we are still far from such detailed delimitation. Thus, latitude is, for the time being, a more tractable criterion to circumscribe that term. We propose that "bipolar distributed species" would apply to species occurring at latitudes > 50º N in the Northern Hemisphere and > 46º S in the Southern Hemisphere. This delimitation includes polar and subpolar regions of both hemispheres, that is, the Arctic and Subarctic and Antarctica, Subantarctic islands and Southern South America. Lichenized fungi such as *Austroplaca soropelta* and *Mastodia tessellata* will fit well this renewed concept. In fact, Lamb (1948) already proposed *M. tessellata* as a paradigmatic example of strict bipolar lichen. On the contrary, traditionally allegedly bipolar species such as *Cetraria aculeata*, *Pseudephebe minuscula* and *Xanthoria elegans* would be considered merely as amphitropical. But even the existence of truly amphitropical distributions in lichens can be challenged because many supposedly amphitropical lichen species have been found growing in the alpine areas of the tropics, such as the Mt. Wilhelm which is located in tropical Papua New Guinea (Aptroot 2008). To circumvent this, we propose to resurrect the idea of "strictly" and "widely" bipolar distributions of Lamb (1948) to apply them instead to amphitropical (antitropical) distributions. Accordingly, *C. aculeata*, *P. minuscula* and *X. elegans* would be widely amphitropical, as they have populations in tropical areas such as Bolivia and Papua New Guinea.

5.2. Future perspectives in the study of bipolar and amphitropical lichens

The fact that some lichen-forming fungi and their photobionts show bipolar distributions is not in doubt now thanks to the use of molecular data and sound phylogeographic analyses. However, many questions remain unanswered and the onset of new technologies and the development of statistical methods now allow addressing previously unapproachable issues. In this section we try to summarize future challenges in the research of bipolarity in lichens.

First, most species of allegedly bipolar lichen-forming fungi have never been investigated under an adequate species delimitation scenario and therefore the figures of bipolar lichens given in this and previous reviews may be severely biased. A plethora of new methods for delimiting species *via* phylogenetics and population genetics using DNA sequences are currently available (Leavitt et al. 2015a; Choi 2016). However, special attention has to be put when delimiting species involving highly disjunct populations since the detection of population structure may lead to the recognition of spurious species (Sukumaran & Knowles 2017). A temporal framework may help in these cases to distinguish between species and populations within species (Leavitt et al. 2016a). Although the use of microsatellites has become popular in the last years in population studies of lichen-forming fungi (Dal Grande et al. 2013; Lindgren et al. 2016), the use of next-generation sequencing (NGS) technologies produces higher amounts of information across the whole genome and are currently used in population studies of lichen-forming fungi (Divakar & Crespo 2015; Werth et al. 2015). Genotype by sequencing methods (Narum et al. 2013; Andrews et al. 2016), including restriction-site associated DNA sequencing (RAD-seq; Baird et al. 2008), represent cost-effective means of improving population structure exploration, allowing the stochasticity of lineage sorting, the genetic footprint of founder effects, and the effects of natural selection and genetic drift on isolated populations to be accurately incorporated into analyses (Jeffery et al. 2017; Narum et al. 2017).

Second, although long-distance dispersal has received support over the vicariance hypothesis in phylogeographic studies of lichens, it has so far been not possible to distinguish between "mountain-hopping" migration and single, direct long-distance dispersal events (e.g. Myllys et al. 2003; Högnabba & Wedin 2003; Wirtz et al. 2008; Fernández-Mendoza & Printzen 2013). The existence of many sampling gaps along the Andean Cordillera and other regions such as Mexico and Central America prevents from elucidating the exact role of "mountain-hopping" migration. The current absence of certain amphitropical species in localities of the northern Andes in South America, or the southern Cordillera in North America was argued for rejecting transequatorial dispersion through that mechanism (Castello & Nimis 1997). Besides a comprehensive sampling in unsurveyed regions, the integration of ecological niche modelling (ENM) (Guisan et al. 2014; Cola et al. 2016) and phylogeography (Carstens & Richards 2007) may help to understand the role of American mountain ranges in hosting populations of amphitropical taxa by means of the reconstruction of ecological niches during the Last Glacial Maximum (LGM) (Dellicour et al. 2014, 2017). Further, ENM represents a

powerful set of tools that may contribute to answer important questions about the biology of amphitropical disjunctions such as whether disjunct populations share the same niche or isolated populations have undergone niche shifts (Guisan et al. 2014; Mainali et al. 2015). ENM may also provide additional insights into a more accurate definition of the term bipolar based on environmental envelopes rather than arbitrary latitudinal boundaries.

New technical NGS approaches such as environmental DNA (eDNA) (Bohman et al. 2014; Thomsen & Willerslev 2015) would now allow to address questions such as the role of certain animal vectors in the dispersal of lichen propagules and its geographic extent. The performance of studies using visual inspection of propagules (Lewis et al. 2014b) can be enhanced using eDNA techniques which may provide a more accurate picture of the actual cargo of transequatorial migrants. eDNA tools as well as other metagenomic techniques, including functional metagenomics (Bragg & Tyson 2014), may also shed light on the likely biotic niche shifts of the isolated populations regarding to the original metapopulation, these shifts including changes in the microbiome concerning both bacteria (Hodkinson & Lutzoni 2009; Grube et al. 2015) and endolichenic fungi (U'Ren et al. 2010, 2012), and also in the associated photobionts (Fernández-Mendoza et al. 2011). Finally, eDNA will, for sure, help to better understand the geographic ranges of many photobionts.

DISCUSIÓN

"*At a time when it's possible for thirty people to stand on the top of Everest in one day, Antarctica still remains a remote, lonely and desolate continent. A place where it's possible to see the splendours and immensities of the natural world at its most dramatic and, what's more, witness them almost exactly as they were, long, long before human beings ever arrived on the surface of this planet. Long may it remain so*". – David Attenborough

Los líquenes dominan los hábitats terrestres de la Antártida, no sólo en términos de diversidad, sino también en cobertura (Seppelt 1995; Kappen 2000; Green et al. 2015). Medran en las zonas costeras del continente, de condiciones climáticas más suaves, dónde algunas especies llegan a cubrir áreas extensas del territorio (Øvstedal y Lewis Smith 2001). En el interior, hongos y algas liquenizados sobreviven en áreas libres de hielo, como en los Valles Secos de McMurdo (Sancho et al. 2007; Green et al. 2011b; Pérez-Ortega et al. 2012a) y en *nunataks* (Engelskjøn 1986; Ertz et al. 2014), colonizando el substrato rocoso, donde ocupan posiciones tanto epilíticas como endolíticas, y sobre los pocos briófitos disponibles (Kappen et al. 1981; Friedmann 1982; de los Ríos et al. 2014). Tras casi dos siglos de investigación liquenológica antártica dedicados fundamentalmente al estudio de la diversidad, taxonomía y ecofisiología (Torrey 1823; Vainio 1903; Kappen 2000; Sancho et al. 2007; Schroeter et al. 2010; Green et al. 2011a), el estudio de la biota liquénica antártica ha sufrido recientemente un nuevo impulso gracias a la incorporación de técnicas moleculares. La secuenciación de fragmentos del ADN genómico y su posterior comparación ha permitido estimar de forma más precisa la diversidad de hongos liquenizados (p. ej. Dyer y Murtagh 2001; Poulsen et al. 2001; Lee et al. 2008; Ruprecht et al. 2010; Pérez-Ortega et al. 2012a; Garrido-Benavent et al. 2016), elevándose así a más de 500 las especies reconocidas en la Antártida e islas subantárticas (Øvstedal y Lewis Smith 2011). A pesar de este notable avance, es probable que exista todavía una elevada fracción de la diversidad liquénica por descubrir, como queda patente en los resultados de esta tesis doctoral. Además, aún quedan importantes cuestiones sin resolver, como el origen de la biota liquénica antártica, pregunta que esta tesis ha tratado de responder en la medida de lo posible.

Diversidad de líquenes antárticos

El peso del componente biogeográfico endémico y anfitropical en la biota liquénica antártica es bien conocido (Castello y Nimis 1997; Øvstedal y Lewis Smith 2001). La taxonomía integradora aplicada al estudio de taxones antárticos problemáticos implementada en esta tesis ha permitido describir nuevas especies, hasta el momento endémicas, de la familia de hongos liquenizados *Teloschistaceae* (Ascomycota), lo cual incrementa los niveles de diversidad conocida para esta familia en la Antártida (Søchting y Øvstedal 1992; Olech y Søchting 1993; Søchting y Olech 1995, 2000; Søchting et al. 2004; Lindblom y Søchting 2008; Søchting y Castello 2012). En esta tesis se asigna un nombre nuevo a *Austroplaca frigida*, y se describen como nuevas las especies *Charcotiana antarctica*, *Amundsenia austrocontinenalis* y *Shackletonia cryodesertorum* (Capítulos 1 y 3; Søchting et al. 2014a; Garrido-Benavent et al. 2016). Todas son endémicas del continente antártico y, además, *S. cryodesertorum* presenta aparentemente una distribución restringida a los Valles Secos de McMurdo. Este último descubrimiento se suma al de otras especies de *Teloschistaceae* descubiertas en dicha zona o, más general, en la Tierra de Victoria y que también parecen ser endemismos antártico-continentales (p. ej. *Caloplaca lewis-smithii* y *C. coeruleofrigida*, Søchting y

Øvstedal 1998; Søchting y Seppelt 2003; Seppelt et al. 2010). Por otra parte, se proponen los dos nuevos géneros *Charcotiana* y *Amundsenia* (*Teloschistaceae*) (Søchting et al. 2014a) para dos grupos de especies saxícolas, de biotipo crustáceo, con talos constituidos por pequeñas areolas anaranjadas, con apotecios más o menos abundantes y con disco anaranjado, presentando ambos un síndrome químico de tipo A (Søchting 1997). El género *Charcotiana* suele presentar de modo característico talos con aspecto fruticuloso, al igual que otras especies antárticas pertenecientes a géneros mayormente crustáceos (Lamb 1954, 1970; Øvstedal y Lewis Smith 2001). Por su parte, *Amundsenia* se caracteriza por sus ascosporas con septo comparativamente corto y se diferencia a nivel histológico de su grupo hermano, el género *Squamulea* (Søchting et al. 2014a). Mientras que *Charcotiana* parece tener una distribución endémica de la Antártida, *Amundsenia* presenta una distribución anfitropical de tipo bipolar, con las especies *A. austrocontinentalis* y *A. approximata* restringidas a la Antártida y al Ártico, respectivamente. Sin duda, los avances en el conocimiento de la diversidad de la familia *Teloschistaceae* en la Antártida en los últimos años, unidos al uso creciente de datos genéticos y al mayor número de colecciones disponibles, están contribuyendo a refinar aspectos evolutivos y biogeográficos de esta familia, la cual parece haber protagonizado una radiación adaptativa gracias a la adquisición del modo de vida saxícola y a la producción en talos y apotecios de antraquinonas, unos metabolitos secundarios que protegen a las células frente a la luz UV (Gaya et al. 2015).

Dentro de esta tesis también se describe un nuevo género de hongos liquenícolas, *Austrostigmidium* (Capítulo 2; Pérez-Ortega et al. 2015), contribuyendo así al escaso conocimiento de la diversidad y biogeografía de este grupo de hongos en la Antártida (Øvstedal y Lewis Smith 2001; Søchting et al. 2004; Hawksworth y Iturriaga 2006; Olech y Singh 2010; Halici et al. 2017). En particular, la nueva especie *A. mastodiae* infecta independientemente a las dos especies de *Mastodia tessellata* delimitadas en esta tesis (Capítulos 4 y 5; Garrido-Benavent et al. 2017; ver más abajo). Parasita talos de *Mastodia* sp. 2 en diversas localidades de la Antártida Marítima y de *Mastodia* sp. 1 en varias localidades de Tierra del Fuego. Su ausencia en talos de *Mastodia* sp. 1 en Norteamérica sugiere que *A. mastodiae* tiene una distribución restringida al Hemisferio Sur. Dada su baja incidencia en las poblaciones de *Mastodia* sp. 1 de Tierra del Fuego, es probable que los mecanismos de dispersión a larga distancia que facilitaron la migración de *Mastodia* sp. 1 a Norteamérica no actuasen igualmente sobre el parásito, es decir, el evento histórico de dispersión del liquen no incluyó propágulos del hongo liquenícola. Distribuciones disyuntas entre la Antártida, en especial las islas subantárticas, y Suramérica y Nueva Zealanda son muy comunes en especies de otros grupos de organismos, como plantas (Sanmartín y Ronquist 2004; Knapp et al. 2005), pero también en hongos liquenizados (Galloway 2008). *Austrostigmidium* representa un nuevo linaje de hongos liquenícolas dentro de la familia *Teratosphaeriaceae* (*Capnodiales*, Ascomycota), un grupo de hongos polifilético que alberga especialmente especies saprófitas y parásitas de plantas (Quaedvlieg et al. 2014), y que incluye otro linaje con modo de vida liquenícola, la especie *Xanthoriicola physciae* (Ruibal et al. 2009). El orden *Capnodiales* alberga numerosos ejemplos de hongos microcoloniales, o

levaduras negras ("*black yeasts*"), que habitan característicamente sustratos líticos y que han sido detectados frecuentemente en la Antártida (Selbmann et al. 2005; Egidi et al. 2014). Estos hongos también se han encontrado asociados a talos liquénicos en la Antártida (Selbmann et al. 2013), y parecen ser frecuentes en otros ambientes climáticamente extremos del planeta como por ejemplo el desierto de Atacama (Pérez-Ortega & de los Ríos, com. pers.). La presencia de hongos microcoloniales en talos liquénicos en ambientes extremos y superoligotróficos está probablemente relacionada con el fenómeno de la facilitación: los hongos que normalmente viven encima o inmersos en el sustrato lítico, aprovechan la presencia de una estructura biológica –el liquen– para nutrirse y para resguardarse. Esta proximidad en la asociación es probable que permita un cambio en el modo de vida a lo largo del tiempo evolutivo. Los cambios en el modo de vida son habituales a lo largo de la filogenia de muchos grupos de hongos (Hawksworth 2005, Divakar et al. 2015). Estos cambios no presentan direccionalidad y ningún modo de vida es favorecido a escalas macroevolutivas (Lutzoni et al. 2001; Arnold et al. 2009b).

La metodología de delimitación de especies implementada en esta tesis también ha revelado la existencia de especies crípticas en mico- y fotobiontes de la biota liquénica antártica conocida (Capítulos 4 y 6; Garrido-Benavent et al. 2017; Garrido-Benavent et al. in prep.). La especiación críptica, *i.e.* cuando dos especies distintas se incluyen erróneamente bajo el mismo epíteto generalmente por la incapacidad de encontrar evidencias fenotípicas que indiquen su separación (Bickford et al. 2007), es un fenómeno común en hongos liquenizados y sus fotobiontes (Crespo y Pérez-Ortega 2009; Crespo y Lumbsch 2010; Škaloud et al. 2016). En esta tesis doctoral se demuestra que el hongo liquenizado denominado *Mastodia tessellata* incluye dos especies crípticas cuya distribución geográfica prácticamente no se solapa: *Mastodia* sp. 1, distribuida mayormente en Tierra del Fuego y Norteamérica, y puntualmente en la Antártida Marítima (distribución bipolar), y *Mastodia* sp. 2, de distribución restringida a la Antártida Marítima (endemismo) (Capítulo 5). Todavía no se ha llevado a cabo un estudio profundo de las muestras disponibles para diagnosticar si existen caracteres morfológicos y/o anatómicos que permitan diferenciar ambas especies. Al estudio morfo-anatómico, que debería incluir también colecciones provenientes de todo el rango de distribución de este liquen (p. ej. Islas Kerguelen, Tasmania, Nueva Zelanda e islas adyacentes; Kohlmeyer et al. 2004; Pérez-Ortega et al. 2010), le seguiría un estudio nomenclatural. El lectotipo de *Mastodia tessellata* se designó en base a material recolectado en las Islas Kerguelen (Kohlmeyer et al. 2004), por lo que el estudio a nivel genético de muestras de dicha zona permitiría determinar su adscripción a la especie bipolar *Mastodia* sp. 1 o a la antártico-endémica *Mastodia* sp. 2. Si resultase ser *Mastodia* sp. 2, para *Mastodia* sp. 1 estaría disponible el nombre *Guignardia alaskana* (Reed 1902) que debería ser combinado al género *Mastodia*. Por otra parte, el fotobionte de este hongo liquenizado, *Prasiola* spp., también incluye en realidad a dos especies crípticas (Capítulo 4; Garrido-Benavent et al. 2017). Una de ellas pudo ser adscrita a *Prasiola borealis*, la cual se asocia a *Mastodia* sp. 1 en Antártida, Tierra del Fuego y Norteamérica, mientras que la segunda especie, todavía no descrita y endémica

de la Antártida, *Prasiola* sp., se asocia de forma restringida a *Mastodia* sp. 2. La presencia de especiación críptica en algas, resultando en la existencia de especies antártico-endémicas ha sido demostrada en otros grupos, por ejemplo, en el alga roja *Gigartina skottsbergii* (Billard et al. 2015). La existencia de taxones desconocidos pertenecientes a la familia *Prasiolaceae*, y en especial al género *Prasiola*, en el hemisferio austral ha sido revelada en estudios basados en secuencias de ADN en los últimos años (Heesch et al. 2012; Moniz et al. 2012a,b, 2014). En este contexto, los resultados aportados en esta tesis doctoral mejoran el conocimiento sobre este grupo de algas en la Antártida.

La presencia de especies crípticas también ha sido detectada en el género *Pseudephebe* (*Parmeliaceae*, Ascomycota), presente habitualmente tanto en la Antártida Continental como en la Marítima. A través del estudio de delimitación de especies basado en seis *loci*, con material proveniente de los cinco continentes, incluyendo localidades de ambas regiones antárticas (Capítulo 6) se ha confirmado la presencia de la especie *P. minuscula* en el continente y se descarta la presencia de *P. pubescens*, especie previamente citada en todo el territorio antártico (Ovstedal & Lewis-Smith 2001). Boluda et al. (2016), basándose en datos de tres *loci*, habían indicado la existencia de dos grandes clados filogenéticos que no podían ser atribuibles a las dos morfoespecies tradicionales, *P. pubescens* y *P. minuscula*, consideradas especies crípticas por ser imposible distinguirlas en base a caracteres morfológicos o químicos. La existencia de especies crípticas es recurrente en varios géneros de la familia *Parmeliaceae*, como en *Xanthoparmelia* (Leavitt et al. 2011a), *Oropogon* (Leavitt et al. 2012a) y *Melanelixia* (Leavitt et al. 2012c). En esta tesis se demuestra que las poblaciones antárticas de *Pseudephebe* corresponden a una única especie filogenética, *P. minuscula* (*sensu* Boluda et al. 2016) y son morfológicamente muy variables (Capítulo 6). Así, los individuos de la Antártida Marítima (p. ej. Isla Livingston) presentan talos desde decumbentes hasta arbustivos con ramas más o menos erectas, pudiendo alcanzar cerca de 5 cm de longitud (morfología tipo *pubescens*). Por el contrario, los individuos continentales provenientes de las Montañas Transantárticas y de la Reina Maud presentan talos con morfología tipo *minuscula*, es decir, postrados, con ramas de sección más aplanada y bastante adheridas al sustrato, y de tamaño menor, como máximo 2 cm. Diferenciación genética como la detectada entre individuos antárticos de *Pseudephebe* con morfología tan dispar (Capítulo 6) ha sido constatada también en otros grupos de hongos liquenizados (Leavitt et al. 2011a,b) y podría tener un trasfondo adaptativo (Pérez-Ortega et al. 2012b). Por otra parte, para *P. minuscula* se confirma el rango de distribución anfitropical amplio (Capítulos 6 y 7), puesto que posee poblaciones en latitudes tropicales (p. ej. Bolivia), y asimismo su presencia se confirma en Nueva Zelanda, la Cordillera de los Andes y algunas localidades de China. Este rango de distribución es similar al de otra especie de hongo liquenizado parmelioide, *Cetraria aculeata* (Fernández-Mendoza y Printzen 2013). Adicionalmente, el extenso muestreo molecular e individual realizado ha revelado la presencia de un tercer linaje críptico que posiblemente corresponda a una tercera especie, no descrita previamente, presente en Alaska (USA), y confirma el rango de distribución restringido

de *P. pubescens* al continente europeo, con poblaciones que van desde la Península Ibérica hasta Noruega. En la literatura existen otros estudios que han detectado la presencia de especies crípticas en taxones a los que tradicionalmente se les había atribuido una distribución muy amplia, en ambos hemisferios (Crespo et al. 2002; Molina et al. 2004; Högnabba y Wedin 2003; Wedin et al. 2009).

En conclusión, podemos afirmar que el conocimiento de la biota liquénica antártica dista mucho de estar completo, y que incluso especies aparentemente bien conocidas, como *M. tessellata* o *Pseudephebe pubescens*/*minuscula*, guardan sorpresas sólo desveladas tras un profundo estudio genético. La inaccesibilidad, que se traduce en falta de muestreos en muchas áreas antárticas, y el estado muchas veces alterado de los talos liquénicos debido a las condiciones climáticas adversas en donde crecen o a la falta de estructuras reproductivas (Hertel 1988; Pérez-Ortega et al. 2012a) ha hecho que el avance del conocimiento liquenológico antártico sea lento y a menudo, en direcciones erróneas (Almborn 1974; Castello & Nimis 1995). En este contexto, será interesante estudiar colecciones que se vayan realizando en expediciones venideras a la Antártida desde la perspectiva de la taxonomía integradora, es decir, aunando información proveniente de estudios morfológicos, anatómicos, químicos, ecológicos y filogenéticos (Dayrat 2005; Padial et al. 2010). Varias estrategias adicionales pueden también contribuir a mejorar dicho conocimiento, como sería el uso de técnicas de DNA *barcoding* (p. ej. Kelly et al. 2011; Divakar et al. 2016) aplicadas a colecciones antárticas con material alterado, así como la aplicación de nuevas tecnologías de secuenciación a material depositado en herbarios, lo que se ha denominado "museómica" (Guschanski et al. 2013; Chomicki y Renner 2015; Zedane et al. 2016).

Origen de los líquenes en la Antártida

Los resultados de los estudios filogeográficos llevados a cabo en mico- y fotobiontes de *Mastodia tessellata*, y micobiontes de *Pseudephebe* en los Capítulos 4, 5 y 6 (Garrido-Benavent et al. 2017), así como el marco temporal propuesto para la evolución de *Shackletonia cryodesertorum* en la Antártida (Capítulo 3; Garrido-Benavent et al. 2016) concilian las diferentes posturas propuestas por autores anteriores sobre el origen de la biota liquénica antártica (p. ej. Lamb 1948, 1949, 1970; Dodge 1964; Walker 1985; Hertel 1987; Seppelt 1995; Øvstedal y Lewis Smith 2001). El origen temporal de la biota liquénica antártica había sido interpretado como dual, basándose en los niveles relativos de especies antárticas endémicas, anfitropicales y cosmopolitas, y en su presencia en el continente o en la región subantártica. Asimismo, a lo largo del siglo XX e inicios del XXI, diferentes autores habían coincidido en señalar un origen relicto, posiblemente pre-pleistocénico, para las especies endémicas de la Antártida. El mismo origen temporal ha sido inferido para las especies *Mastodia* sp. 2, *Prasiola* sp. (Mioceno-Plio/Pleistoceno) y *Shackletonia cryodesertorum* (Oligoceno-Mioceno), todas ellas aparentemente antártico-endémicas, las dos primeras de la Antártida Marítima (Capítulo 4, Garrido-Benavent et al. 2017; Capitulo 5,

Garrido-Benavent et al., en rev.) y la tercera de los continentales Valles Secos de McMurdo (Capítulo 3, Garrido-Benavent et al. 2016). La estimación de tiempos de divergencia para distintos géneros y especies de *Xanthorioideae* incluida en Garrido-Benavent et al. (2016) ha permitido datar también el origen de las dos especies antártico-endémicas *Charcotiana antarctica* y *Amundsenia austrocontinentalis* (Capítulos 1y 3; Søchting et al. 2014a; Garrido-Benavent et al. 2016). La primera es característica porque, al igual que otras especies antárticas como *Catillaria corymbosa*, *Bacidia stipata* y *Lecania brialmontii*, suele formar talos con aspecto fruticuloso (Øvstedal y Lewis Smith 2001), lo que según Lamb (1954, 1970) constituiría un carácter indicativo de origen relicto. La divergencia de *C. antarctica* y *A. austrocontinentalis* respecto a sus especies próximas se estimó alrededor del Eoceno y Mioceno, respectivamente (Capítulo 3, Garrido-Benavent et al. 2016), lo cual apoya una vez más el origen más antiguo, pre-pleistocénico, de especies de hongos liquenizados endémicas.

Los trabajos de Jones et al. (2013, 2015) sobre *Buellia frigida* suponen los únicos estudios hasta el momento que han utilizado datos genéticos para investigar la estructura de las poblaciones de un liquen endémico de la Antártida. Estos autores explicaron la distribución antártica de genotipos del hongo y alga liquenizados por los patrones de vientos dominantes y a la existencia de barreras físicas que facilitarían o impedirían la dispersión de este liquen o sus simbiontes en la Antártida. Asimismo, Jones et al. (2013, 2015) propusieron la existencia de refugios glaciales históricos para justificar la presencia de alelos únicos del hongo y una mayor diversidad de genotipos algales en determinadas localidades del continente antártico. El marco temporal establecido para la divergencia de *Mastodia* sp. 2, *Prasiola* sp. y las tres especies de la familia *Teloschistaceae* descritas en esta tesis respecto a las especies próximas, en conjunto situado entre el Eoceno y Plio/Pleistoceno, apunta también a que estas especies han sobrevivido en la Antártida durante largos periodos de tiempo, sometidas a repetidos ciclos glaciales e interglaciares (Zachos et al. 2001; Lear y Lunt 2016). Dado que divergen respecto a su nicho ecológico, la supervivencia de estas especies tuvo que estar asociada a la existencia de refugios (áreas libres de hielo y *nunataks*), tanto costeros (*Mastodia* sp. 2, *Prasiola* sp.) como continentales (*S. cryodesertorum*, *C. antarctica*, *A. austrocontinentalis*). Estudios en otras criptógamas han inferido la existencia de tales refugios en áreas de la Península Antártica y en el interior del continente, como en la Tierra de Victoria, donde las especies de estudio de esta tesis habitan en la actualidad (Lamb 1970; Convey et al. 2008; Pugh y Convey 2008; Fraser et al. 2014). De hecho, en el caso de *S. cryodesertorum*, hasta ahora hallada solo en los Valles Secos de McMurdo, su origen coincide con las estimaciones del origen de *nunataks* en dicha zona que se remonta al Mioceno, hace unos 20–5.3 MA (Armienti y Baroni 1999; Oberholzer et al. 2003). No obstante, no se pueden descartar otras hipótesis que impliquen la existencia de poblaciones para estas tres especies a latitudes más bajas en la región insular subantártica, así como en Tierra del Fuego, Nueva Zelanda y Tasmania, desde donde pudieron recolonizar el continente antártico en periodos más recientes, por ejemplo después del Pleistoceno. De hecho, en otros grupos

de organismos se estima que el movimiento de taxones entre diferentes regiones subantárticas ha sido, y es, más común de lo esperado (Moon et al. 2017). En el caso de *M. tessellata* s.l., se conocen poblaciones en las Islas Kerguelen, isla sur de Nueva Zelanda e islas adyacentes y Tasmania (Kohlmeyer et al. 2004; Pérez-Ortega et al. 2010), cuyo estudio futuro a nivel genético no sólo permitiría ampliar el conocimiento sobre la diversidad genética de los simbiontes, sino también ahondar en la historia filogeográfica presentada en esta tesis y, en especial, determinar si *Mastodia* sp. 2 y *Prasiola* sp. son realmente endémicas de la Antártida. Más aún, un estudio filogeográfico que incluyera al hongo parásito, *Austrostigmidium mastodiae*, para el que se detectó cierta divergencia genética entre individuos de la Antártida Marítima y Tierra del Fuego (Capítulo 2; Pérez-Ortega et al. 2015), permitiría testear si la ha habido co-evolución entre los tres simbiontes: mico- y fotobionte, y parásito. Este tipo de estudios son escasos en la literatura liquenológica, y las evidencias disponibles sugieren que, aunque los huéspedes juegan un papel muy importante en la estructura de las poblaciones del parásito, creando un ambiente muy selectivo, la historia evolutiva y demografía de huéspedes y parásitos puede ser diferente (Werth et al. 2013; Millanes et al. 2014).

A las especies antárticas con distribución cosmopolita y anfitropical se les ha propuesto un origen reciente en la literatura, quizás post-pleistocénico (p. ej. Lamb 1948, 1949, 1970; Dodge 1964; Walker 1985; Hertel 1987; Seppelt 1995; Øvstedal y Lewis Smith 2001). Incluso con la introducción de análisis basados en datos de ADN, la respuesta a esta cuestión ha continuado siendo, en cierto modo, imprecisa tanto por lo que se refiere a si tienen un origen austral o boreal, como al marco temporal y los mecanismos que facilitaron la colonización de la Antártida (Crespo et al. 2002; Romeike et al. 2002; Lindblom y Søchting 2008; Wirtz et al. 2008, 2012; Søchting y Castello 2012). En el estudio filogeográfico de *P. minuscula* (Capítulo 6) se observó que las poblaciones de la Antártida Marítima y la Continental constituyen dos contingentes genéticos diferentes, con sólo un individuo de la Isla Adelaida (Antártida Marítima) genéticamente emparentado con los de la Antártida Continental. Además, los individuos de la Antártida Marítima se incluyen en el mismo contingente genético que gran parte de los de Suramérica, especialmente los de Tierra del Fuego, mientras que los de las Montañas Transantárticas (Antártida Continental) comparten el mismo contingente genético con individuos de varias localidades del Hemisferio Norte (p. ej. Svalbard, norte de Noruega e Islandia). Este escenario parece indicar poca conectividad entre las poblaciones marítimas y continentales antárticas de *P. minuscula* y, además, un origen distinto para las mismas. Así, las de la Antártida Marítima podrían haberse originado por colonización de propágulos desde el subcontinente suramericano, lo cual parece lógico dado la proximidad geográfica entre ambas regiones. Sin embargo, esta posibilidad iría en contra de considerar a la Antártida como paradigma de continente aislado debido, entre otros motivos, a los fuertes vientos y corrientes marinas que fluyen hacia el este impidiendo la dispersión norte-sur de propágulos (Fraser et al. 2012; Chown et al. 2015) El aparente flujo génico entre Tierra del Fuego y la Antártida Marítima en *P. minuscula* contrasta con lo observado en el otro liquen objeto de

estudio, *Mastodia tessellata* s.l., para el que las evidencias obtenidas en esta tesis sugieren que ha existido poca dispersión entre ambas regiones en los últimos millones de años (Capítulos 4 y 5; Garrido-Benavent et al. 2017). Por otro lado, el origen de las poblaciones continentales de *P. minuscula*, aunque más complicado de explicar, podría ser atribuido a la existencia de polimorfismos ancestrales o a dispersión a larga distancia directa entre ambos polos, sin descartar tampoco la posibilidad de que propágulos de esta especie hayan podido colonizar el continente antártico desde regiones que no han sido todavía muestreadas, por ejemplo, adheridos al plumaje y/o extremidades de aves migratorias (Lewis et al. 2014b). Sorprendentemente, los individuos de Nueva Zelanda analizados no mostraron proximidad genética alguna con los de Antártida (Capítulo 6). En cualquier caso, las estimas de tiempos de divergencia sitúan la adquisición de un rango de distribución austral y antártico en *P. minuscula* en el Pleistoceno (Capítulo 6). El único estudio comparable hasta la fecha es el realizado sobre del liquen anfitropical *Cetraria aculeata* (Fernández-Mendoza et al. 2011; Fernández-Mendoza y Printzen 2013). Así, tanto en *C. aculeata* como en *P. minuscula*, los mayores niveles de diversidad genética se encuentran en las localidades del Hemisferio Norte, mientras que los individuos antárticos son en muchos casos clonales (Domaschke et al. 2012; Capítulo 6). Además, el hecho de que individuos de Tierra del Fuego y Antártida Marítima compartan haplotipos en diferentes *loci* sugiere que estos líquenes colonizaron el continente antártico desde Suramérica, probablemente en el Pleistoceno (Fernández-Mendoza y Printzen 2013; Capítulo 6). Por tanto, la reducida diversidad genética de las poblaciones antárticas de *C. aculeata* y *P. minuscula* puede ser el resultado tanto de un efecto fundador y/o de un cuello de botella, a lo que contribuiría la reproducción mayormente vegetativa de estas especies. En general, niveles bajos de diversidad genética ocurren en especies tras un cuello de botella o por efecto fundador (Hewitt 1996; Schneider & Excoffier 1999). Para obtener evidencias más claras del origen de *P. minuscula* en las distintas localidades antárticas es necesario realizar análisis más robustos de flujo génico entre las distintas regiones estudiadas a nivel global.

Adquisición de la distribución anfitropical y bipolar

El hecho de que algunas especies estén presentes en regiones templadas y polares de ambos hemisferios y ausentes en localidades intermedias tropicales ya desafió el intelecto de eminentes naturalistas como Humboldt (1817), Darwin (1872) y Wallace (1880) en el siglo XIX. Aunque también presente en otros organismos como briófitos o plantas vasculares, son los hongos liquenizados los que muestran una mayor abundancia de especies con este patrón biogeográfico y por eso, su origen ha sido fuente de especulación en la literatura liquenológica (p. ej. Du Rietz 1940; Galloway y Aptroot 1995; Castello y Nimis 1997). La presente tesis doctoral supone una reseñable contribución al estudio de las especies de hongos liquenizados con distribución bipolar y/o anfitropical. Por un lado, se han compilado los resultados de los últimos veinte años basados en datos moleculares, y se redefine el concepto de distribución "bipolar" entendida como un tipo particular de distribución "anfitropical" que incluiría el de

aquellas especies distribuidas en latitudes > 50º N en el Hemisferio Norte (Ártico y región Subártica) y latitudes > 46º S en el Hemisferio Sur (Antártida, islas subantárticas y territorios más al sur de Suramérica) (Capítulo 7). Por otro lado se han estudiado dos taxones que muestran distribución bipolar y anfitropical utilizando marcadores moleculares y herramientas de análisis más avanzadas (*Mastodia tessellata* s.l., Garrido-Benavent et al. 2017, Capítulos 4 y 5; el género *Pseudephebe*, Capítulo 6). El estudio filogeográfico de *M. tessellata* s.l. demuestra con soporte estadístico y por primera vez un origen austral para organismos con distribución bipolar estricta (*Mastodia* sp. 1 y *Prasiola borealis*), reforzando la idea de Lamb (1948) de considerar a *M. tessellata* s.l. como ejemplo paradigmático de liquen bipolar. En base a la distribución de linajes bipolares en árboles filogenéticos, se ha inferido también un origen austral para otros líquenes anfitropicales como *Usnea sphacelata* y *U. lambii* (Wirtz et al. 2008, 2012) y *Austroplaca soropelta* (Søchting y Castello 2012), y para algunas especies de los géneros de plantas vasculares *Munroa* y *Lilaeopsis* (Spalik et al. 2010; Amarilla et al. 2015), aunque estos estudios no partían de un muestreo poblacional exhaustivo de individuos ni testeaban distintas hipótesis de flujo génico de manera estadística. Sin embargo, a diferencia de en *Mastodia* sp. 1 y *Prasiola borealis*, en la especie anfitropical *P. minuscula* se detectó un mayor número de contingentes genéticos y diversidad genética en el Hemisferio Norte en comparación al Sur, por lo que se le atribuye un origen boreal (Capítulo 6). En otros estudios de mico- y fotobiontes de líquenes anfitropicales los niveles de diversidad genética para la región Ártica han sido también mayores, como es el caso de *Cetraria aculeata* (Fernández-Mendoza et al. 2011; Domaschke et al. 2012) y *Xanthomendoza borealis* (Lindblom y Søchting 2008, 2013), indicando un origen boreal de estas especies (Lindblom y Søchting 2008; Fernández-Mendoza y Printzen 2013). El origen boreal de organismos que muestran una disyunción anfitropical ha sido también propuesto para varias especies de plantas vasculares (Popp et al. 2011; Villaverde et al. 2015a,b) y briófitos (Piñeiro et al. 2012; Lewis et al. 2014a). De hecho, los estudios de revisión de Raven (1963) y Wen y Ickert-Bond (2009) sugirieron una mayor frecuencia de especies de plantas anfitropicales de origen boreal, las cuales podrían haber migrado en dirección norte-sur, particularmente de Norteamérica a Suramérica, no antes del Mioceno. Este marco temporal, de migraciones transecuatoriales ocurridas a partir del Mioceno, ha sido avalado por la mayoría de estudios que han estimado tiempos de divergencia en especies anfitropicales de plantas y briófitos (Popp et al. 2011; Lewis et al. 2014a; Amarilla et al. 2015; Villaverde et al. 2015a,b) y también se cumple en el caso de *Mastodia* sp. 1, *Prasiola borealis* y *Pseudephebe minuscula*, que, independientemente de cual fuere su origen, todos los mico- y fotobiontes estudiados adquirieron su actual rango de distribución anfitropical en el Pleistoceno. En general, el contexto temporal en el que se adquirió la distribución anfitropical en plantas, briófitos y líquenes apoya la hipótesis de que el mecanismo responsable de la disyunción ha sido principalmente la dispersión a larga distancia y descarta la vicariancia debida a la fragmentación de los grandes supercontinentes Pangea y Gondwana, ya que esta última implicaría estimas de divergencia que fueran del Jurásico Medio al Cretácico tardío, aproximadamente hace 174–66 MA (Scotese 2001; Mao et al. 2012). Muchos autores ya habían intuido el papel

de la dispersión a larga distancia en el origen de distribuciones disyuntas anfitropicales en líquenes y plantas incluso antes de la irrupción de las métodos basados en el uso de secuencias de ADN (Van Steenis 1962; Moore y Chater 1971; Galloway y Aptroot 1995; Wen y Ickert-Bond 2009).

Otro aspecto a considerar es cómo ha tenido lugar la dispersión a larga distancia que, o bien puede ser directa, o bien por "*mountain-hopping*" a través de las principales cordilleras que recorren el continente americano. Wirtz et al. (2008, 2012) detectaron que el haplotipo más frecuente de *Usnea sphacelata* en el Hemisferio Norte estaba también presente en las montañas de Ecuador, lo cual parecía dar más apoyo a la existencia de flujo génico continuo entre ambos hemisferios a través de las cadenas montañosas. Sin embargo, en general, es complicado confirmar que sólo uno de los dos mecanismos fue el responsable del establecimiento de la disyunción anfitropical, y no los dos conjuntamente, y esta problemática se ha repetido a la hora de explicar la distribución bipolar tanto en líquenes (p. ej. Søchting y Olech 1995; Myllys et al. 2003; Geml et al. 2012) como en plantas vasculares (Escudero et al. 2010; Villaverde et al. 2015a,b). Ambos mecanismos de dispersión fueron también soportados por análisis estadísticos de flujo génico en *Cetraria aculeata* (Fernández-Mendoza y Printzen 2013). En el caso particular de *Pseudephebe minuscula*, que presenta una distribución similar a la de *C. aculeata* y para el que se observaron a nivel genético diferentes conexiones entre las poblaciones del Hemisferio Sur con las del Norte, ambos mecanismos de dispersión podrían haber influido igualmente en el establecimiento de su distribución anfitropical actual. De hecho, la capacidad de dispersión para esta especie está validada dado que existen referencias de su presencia en la cara norte del volcán hawaiano inactivo Mauna Kea, a más de 3.300 m de altura (Smith 1984). Este volcán tiene una edad aproximadamente de un millón de años y retuvo ocasionalmente glaciares en los últimos 200 mil años (Wolfe 1997). La presencia de *P. minuscula* en Hawái sugiere que su colonización fue mediada por dispersión a larga distancia directa desde alguna masa continental cercana, posiblemente Norteamérica, desde donde soplan vientos en dirección al archipiélago (Leopold 1949). Un mayor muestreo de especímenes en las cordilleras montañosas americanas podría permitir determinar la contribución de ambos tipos de dispersión a la hora de explicar la distribución espacial y temporal de los linajes de *P. minuscula* en la actualidad. En el caso de *Mastodia* sp. 1 y *Prasiola borealis*, el hecho de que éstas habiten en la región supralitoral y que aparentemente no crezcan en latitudes templadas ni tropicales (Galloway 2007; Rindi et al. 2007; Pérez-Ortega et al. 2010), apunta a que la adquisición de la distribución bipolar tuvo lugar necesariamente mediante dispersión a larga distancia directa. Por ello, un estudio genético de poblaciones de *M. tessellata* s.l. de Oceanía sería de gran interés porque permitiría dilucidar si la adquisición de la distribución bipolar ocurrió por dispersión de propágulos únicamente desde Tierra del Fuego u Oceanía, o desde ambas. Tanto en *P. minuscula* como en *Mastodia* sp. 1 y *Prasiola borealis*, el vector más probable que ha podido mediar en la dispersión a larga distancia son las aves migratorias, puesto que la probabilidad de que diásporas del tamaño de los propágulos liquénicos (esporas, conidios, isidios, soredios y fragmentos del talo) puedan atravesar el ecuador por viento

ha sido modelada como muy baja (Wilkinson et al. 2012). En cambio, las aves migratorias han sido propuestas como probables vectores de dispersión intercontinental en estudios de otras especies de líquenes anfitropicales (p. ej. Crespo et al. 2002; Högnabba y Wedin 2003; Myllys et al. 2003; Lindblom y Søchting 2012; Geml et al. 2012), y plantas y briófitos (Popp et al. 2011; Lewis et al. 2014a). De hecho, la presencia de propágulos transportados por aves migratorias ha sido recientemente confirmada en diversos estudios (p. ej. Lewis et al. 2014b; Viana et al. 2016).

La presente tesis doctoral aumenta el conocimiento de la biogeografía de líquenes y sienta las bases para futuras vías de investigación. Los estudios sobre el patrón de distribución anfitropical en hongos y algas liquenizados y el origen de la biota liquénica antártica se verán enriquecidos con el uso de nuevas aproximaciones metodológicas que integren un mayor conocimiento sobre la diversidad genética de los mico- y fotobiontes implicados así como de las propiedades del nicho ecológico que ocupan. En particular, tanto las nuevas técnicas de secuenciación masiva, en especial de ADN ambiental y la metagenómica (Bohmann et al. 2014; Werth et al. 2015; Andrews et al. 2016; Jeffrey et al. 2017) como las de modelado de nicho (Guisan et al. 2014; Cola et al. 2016) podrían contribuir a: i) evaluar la posibilidad de que poblaciones de líquenes anfitropicales existiesen en tiempos pasados en localidades montañosas a bajas latitudes permitiendo una dispersión entre ambos hemisferios por "*mountain-hopping*", como por ejemplo durante el Último Máximo Glacial (Dellicour et al. 2014, 2017); ii) determinar la presencia de propágulos liquénicos en muestras de aire, o asociadas al plumaje u otras partes de la anatomía de aves migratorias; iii) disponer de una mayor cantidad de datos genéticos para poder resolver patrones de flujo génico más específicos entre las diferentes localidades de muestreo; y iv) modelar los cambios en los rangos de distribución actuales de líquenes antárticos y anfitropicales en un contexto de cambio climático (Allen y Lendemer 2016; Kukwa y Kolanowska 2016; Matos et al. 2017).

CONCLUSIONS

PHYLOGEOGRAPHY AND BIOLOGY OF ANTARCTIC LICHENS

1. Using an integrative taxonomic approach, two genera of lichenized (*Charcotiana* and *Amundsenia*) and one genus of lichenicolous (*Austrostigmidium*) fungi as well as the four species *Charcotiana antarctica*, *Amundsenia austrocontinentalis*, *Austrostigmidium mastodiae* and *Shackletonia cryodesertorum* are described as new to science.

2. Statistical comparisons of competing hypotheses of species boundaries have allowed identification of cryptic species in the Antarctic lichenized fungi *Mastodia tessellata* and *Pseudephebe* spp., as well as in the photobiont of *M. tessellata*, the trebouxiophycean green alga *Prasiola* spp.

3. The study of the Antarctic biota by a combination of integrative taxonomy and DNA-based species delimitation approaches indicates that the diversity of lichenized fungi and algae in Antarctica is far from resolved. However, this combined approach has proved to be a useful tool for further progress in lichen diversity studies.

4. The existence of two *Mastodia tessellata* mycobiont species with contrasting geographical ranges has been demonstrated by means of a species delimitation approach combining data from three loci (*nrITS*, *Mcm7* y *EF-1α*). The results indicate a bipolar distribution for *Mastodia* sp.1, with localities in Tierra del Fuego, North America and more rarely in Maritime Antarctica, whereas *Mastodia* sp. 2 has a distribution restricted to Maritime Antarctica.

5. The photobiont of *Mastodia tessellata* has been shown to be composed of two species by using data from a combined dataset of four loci (*nrITS*, *tufA*, *rbcL* and *RPL10*). The bipolar *Prasiola borealis* associates with *Mastodia* sp. 1, while the endemic Antarctic *Prasiola* sp. associates with *Mastodia* sp. 2. It is also demonstrated the existence of a third photobiont, *P. delicata*, which associates with *Mastodia* sp. 1 in North America, and this represents an example of photobiont switch resulting from the geographical expansion of the mycobiont into a new region due to long-distance dispersal.

6. Divergence between *Mastodia* sp. 1 and *Mastodia* sp. 2 and their respective photobionts in the austral hemisphere is estimated to have occurred between the Miocene and Pliocene, thus favoring vicariant speciation due to a combined effect of geographic distance between Antarctica and South America, the intensification of the Antarctic Circumpolar Current, and the re-establishment of the Antarctic ice sheets since the mid-Miocene.

7. The inferred existence of *Mastodia* sp. 2 and *Prasiola* sp. in Antarctica since the Miocene suggests that these species survived through repeated glacial cycles likely taking refuge in ice-free coastal areas.

8. Cryptic speciation is confirmed in *Pseudephebe* spp. thanks to a species delimitation study based on a worldwide sampling of specimens and the sequencing of six loci (*nrITS*, *Mcm7*, *GAPDH*, *EF-1α*, *L1* y *PGK*). The highly phenotypically plastic *Pseudephebe minuscula* is amphitropically distributed, and the former known distribution is here extended to New Zealand, the Andean Cordillera and China. In Antarctica, the only *Pseudephebe* species present is *P. minuscula* and not *P. pubescens*. The latter species shows a limited distribution to the European continent, despite it is locally abundant in the Iberian, central European (the Alps) and Scottish mountainous ranges, and also present at more northerly latitudes (Norway). Finally, results reveal a third *Pseudephebe* species in Alaska (USA), which is morphologically and genetically close to *P. pubescens*.

9. The acquisition of a bipolar distribution in *Mastodia* sp. 1 and its photobiont, *Prasiola borealis*, was estimated to have occurred in the Pleistocene. Likewise, *Pseudephebe minuscula* colonization of the Southern Hemisphere took place during the same geological time period. Consequently, divergence time estimates favor the hypothesis of long-distance dispersal, likely *via* migratory birds, over the vicariant hypothesis as the mechanism responsible for the acquisition of their extant bipolar and/or amphitropical disjunct distribution.

10. While long-distance dispersal in *Mastodia* sp. 1 and *Prasiola borealis* likely occurred only once directly between both hemispheres, current genetic evidence for *Pseudephebe minuscula* suggests that austral populations of this species originated independently and this is particularly apparent when considering populations in Maritime and Continental Antarctica.

11. Contrasting evidence provided in this thesis points towards a mixed spatial origin for amphitropical distributions in lichens, with austral species such as *Mastodia* sp. 1 and *Prasiola borealis* probably migrating jointly to the Northern Hemisphere by direct long-distance dispersal, whereas other species such as the boreal *Pseudephebe minuscula* may have migrated southwards through "mountain-hopping" along the American Cordilleras and/or by direct long-distance dispersal.

12. The temporal framework set up for the origin of the Antarctic species of lichenized fungi and algae studied in this thesis supports the idea that endemic taxa such as *Mastodia* sp. 2, *Prasiola* sp. and *Shackletonia cryodesertorum* are old, dating back to pre-Pleistocene times, whereas amphitropical species as *Pseudephebe minuscula* are more recent colonisers, their populations establishing in relatively recent times (Pleistocene or later).

CONCLUSIONES

FILOGEOGRAFÍA Y BIOLOGÍA DE LÍQUENES ANTÁRTICOS

1. Se han descubierto y descrito dos géneros de hongos liquenizados (*Charcotiana* y *Amundsenia*) y uno de hongos liquenícolas (*Austrostigmidium*), así como cuatro especies, *Charcotiana antarctica*, *Amundsenia austrocontinentalis*, *Austrostigmidium mastodiae* y *Shackletonia cryodesertorum*, todos ellos nuevos para la ciencia, mediante un estudio taxonómico integrador.

2. La comparación estadística de hipótesis alternativas para la delimitación de especies ha permitido la identificación de especies crípticas en los hongos liquenizados antárticos *Mastodia tessellata* y *Pseudephebe* spp., así como en el alga trebouxiofícea *Prasiola* spp., fotobionte de *M. tessellata*.

3. En conjunto, los resultados obtenidos al aplicar la taxonomía integradora y la delimitación de especies basada en datos de ADN al estudio de la biota antártica indican que aún se está lejos de un conocimiento real de la diversidad de hongos y algas liquenizados en la Antártida pero que la combinación de ambos tipos de estudios es una estrategia apropiada para avanzar en esta línea.

4. Se demuestra la existencia de dos linajes en el hongo liquenizado *Mastodia tessellata* con distribución divergente por delimitación de especies usando tres *loci* (*nrITS*, *Mcm7* y *EF-1α*): *Mastodia* sp. 1, de distribución bipolar, con localidades en Tierra del Fuego, Norte América y muy rara en la Antártida Marítima; y *Mastodia* sp. 2, restringida a la Antártida Marítima.

5. Se han delimitado dos especies en el fotobionte de *Mastodia tessellata* en base a cuatro loci (*nrITS*, *tufA*, *rbcL* y *RPL10*). Así, *Prasiola borealis* se asociaría con *Mastodia* sp. 1 y presentaría igualmente una distribución bipolar, mientras que la especie *Prasiola* sp. sería endémica de la Antártida, donde se asocia con *Mastodia* sp. 2. Además, se demuestra la existencia de un tercer fotobionte en Norteamérica, *P. delicata*, asociado a *Mastodia* sp. 1., indicando un cambio de fotobionte ("*photobiont switch*") como consecuencia de la expansión geográfica de la especie de micobionte por dispersión a larga distancia.

6. La datación de la divergencia entre *Mastodia* sp. 1 y *Mastodia* sp. 2, así como la de sus respectivos fotobiontes, en el hemisferio austral entre el Mioceno y Plioceno apoya la especiación por vicarianza debida probablemente a un efecto combinado de la separación geográfica entre Antártida y Suramérica, la intensificación de la Corriente Circumpolar Antártica y el restablecimiento de las masas de hielo antárticas desde mediados del Mioceno.

7. La presencia de *Mastodia* sp. 2 y *Prasiola* sp. en la Antártida desde el Mioceno sugeriría que estas especies han sobrevivido a repetidos periodos glaciales en refugios costeros libres de hielo.

8. La delimitación de especies en el género *Pseudephebe* basada en un muestreo de especímenes a nivel mundial y seis *loci* (*nrITS*, *Mcm7*, *GAPDH*, *EF-1α*, *L1* y *PGK*) confirma la existencia de especiación críptica. *Pseudephebe minuscula* muestra un elevado grado de plasticidad fenotípica y una distribución anfitropical que en este estudio se amplía a Nueva Zelanda, la cordillera de los Andes y China. Por otro lado, se constata su presencia en el continente antártico y se descarta la de *P. pubescens*. Esta última presenta una distribución más discreta, relegada al continente europeo, a pesar de su relativa abundancia en las montañas ibéricas, centro-europeas (Alpes) y escocesas, y la presencia de poblaciones a elevadas latitudes (Noruega). Se demuestra, además, la existencia de una tercera especie de Alaska (EEUU), morfológica y genéticamente próxima a *P. pubescens*.

9. Los análisis de datación estimaron la adquisición de la distribución bipolar en *Mastodia* sp. 1 y su fotobionte, *Prasiola borealis*, en el Pleistoceno. Igualmente, *Pseudephebe minuscula* podría haber colonizado el Hemisferio Sur durante este periodo de tiempo, adquiriendo así una distribución anfitropical. Por consiguiente, estas estimas de tiempo de divergencia apoyan la hipótesis de dispersión a larga distancia, probablemente mediada por aves migratorias, y permiten rechazar la hipótesis de vicariancia como el mecanismo responsable de la distribución disyunta bipolar y/o anfitropical actual de estas especies.

10. Mientras que la dispersión a larga distancia en *Mastodia* sp. 1 y *Prasiola borealis* es probable que se debiera a un único evento directo de dispersión entre ambos hemisferios, las evidencias genéticas existentes para *Pseudephebe minuscula* apuntan a diferentes orígenes para las poblaciones australes de esta especie y, en particular, sugieren que la colonización de la Antártida Marítima y la Continental tuvo lugar de manera independiente.

11. El origen de la distribución anfitropical en las especies analizadas puede ser diferente, como demuestran los resultados de esta tesis doctoral. Las especies australes *Mastodia* sp. 1 y *Prasiola borealis* podrían haber migrado al Hemisferio Norte de forma conjunta, posiblemente de manera directa, mientras que *Pseudephebe minuscula*, de origen boreal, habría migrado en sentido reverso, norte-sur, probablemente mediante saltos entre las principales cordilleras americanas ("*mountain-hopping*") y/o por dispersión a larga distancia directa entre ambos hemisferios.

12. Los análisis filogeográficos y, en particular, las estimas de divergencia entre las diferentes especies de mico- y fotobiontes estudiadas en la presente tesis confirman un origen temporal dual para la biota liquénica antártica, siendo los taxones endémicos (*Mastodia* sp. 2, *Prasiola* sp., *Shackletonia cryodesertorum*) más antiguos (pre-pleistocénicos), y los de distribución anfitropical (*Pseudephebe minuscula*) datando de tiempos más recientes (a partir del Pleistoceno).

REFERENCIAS BIBLIOGRÁFICAS

Ahmadjian V (1970) Adaptations of Antarctic terrestrial plants. En MW Holdgate (ed.) Antarctic Ecology, 2ª ed., págs. 801–811. Academic Press, London, UK

Akaike H (1974) A new look at the statistical model identification. IEEE Transactions on Automatic Control AC 19: 716–723

Allen JL y Lendemer JC (2016) Climate change impacts on endemic, high-elevation lichens in a biodiversity hotspot. Biodiversity and Conservation 25: 555–568

Allen SJ, Bryant KA, Kraus RHS et al. (2016) Genetic isolation between coastal and fishery-impacted, offshore bottlenose dolphin (*Tursiops* spp.) populations. Molecular Ecology 25: 2735–2753

Almborn O (1974) Review of "Dodge Carroll W: Lichen Flora of the Antarctic continent and adjacent Islands". Botaniska Notiser 127: 454–455

Alors D, Dal Grande F, Cubas P et al. (2017) Panmixia and dispersal from the Mediterranean Basin to Macaronesian Islands of a macrolichen species. Scientific Reports 7: 40879

Altschul SF, Gish W, Miller W et al. (1990) Basic Local Alignment Search Tool. Journal of Molecular Biology 215: 403–410

Amarilla LD, Chiapella JO, Sosa V et al. (2015) A tale of North and South America: time and mode of dispersal of the amphitropical genus *Munroa* (*Poaceae*, *Chloridoideae*). Botanical Journal of the Linnean Society 179: 110–125

Amo de Paz G, Cubas P, Divakar PK et al. (2011) Origin and diversification of major clades in parmelioid lichens (*Parmeliaceae*, Ascomycota) during the Paleogene inferred by Bayesian analysis. PloS ONE 6: e28161

Amo de Paz G, Cubas P, Crespo A et al. (2012) Transoceanic dispersal and subsequent diversification on separate continents shaped diversity of the *Xanthoparmelia pulla* group (Ascomycota). PloS ONE 7: e39683

Andrews KR, Good JM, Miller MR et al. (2016) Harnessing the power of RADseq for ecological and evolutionary genomics. Nature Reviews Genetics 17: 81–92

Aoki M, Nakano T, Kanda H y Deguchi H (1998) Photobionts isolated from Antarctic lichens. Journal of Marine Biotechnology 6: 39–43

Aptroot A (2008) *Sticta alpinotropica*, a new saxicolous lichen species from the alpine zone of Mt Wilhelm, Papua New Guinea. Lichenologist 40: 419–422

Aptroot A (2011) A new species of *Arthonia* is a pest in an orchid nursery. Lichenologist 43: 199–201

Aptroot A (2016) The first European *Willeya* (*Verrucariaceae*) on limestone brought from China. Herzogia 29: 688–691

Aptroot A y van der Knaap WO (1993) The lichen flora of Deception Island, South Shetland Islands. Nova Hedwigia 56: 183–192

Armienti P y Baroni C (1999) Cenozoic climatic change in Antarctica recorded by volcanic activity and landscape evolution. Geology 27: 617–620

Armstrong RA (1981) Field experiments on the dispersal, establishment and colonization of lichens on a slate rock surface. Environmental and Experimental Botany 21: 115–120

Armstrong RA (1987) Dispersal in a population of the lichen *Hypogymnia physodes*. Environmental and Experimental Botany 27: 357–363

Armstrong RA (1994) Dispersal of soredia from individual soralia of the lichen *Hypogymnia physodes* (L.) Nyl. in a simple wind tunnel. Environmental and Experimental Botany 34: 39–45

Arnold AE, Miadlikowska J, Higgins KL et al. (2009a) Hyperdiverse fungal endophytes and endolichenic fungi elucidate the evolution of major ecological modes in the Ascomycota. Systematic Biology 58: 283–297

Arnold AE, Miadlikowska J, Higgins KL et al. (2009b) A phylogenetic estimation of trophic transition networks for ascomycetous fungi: are lichens cradles of symbiotrophic fungal diversification? Systematic Biology 58: 283–297

Arup U (2006) A new taxonomy of the *Caloplaca citrina* group in the Nordic countries, except Iceland. *Lichenologist* 38: 1–20

Arup U, Søchting U y Frödén P (2013) A new taxonomy of *Teloschistaceae*. Nordic Journal of Botany 31: 16–83

Asplund J y Wardle DA (2013) The impact of secondary compounds and functional characteristics on lichen palatability and decomposition. Journal of Ecology 101: 689–700

Asplund J y Wardle DA (2016) How lichens impact on terrestrial community and ecosystem properties. Biological Reviews doi: 10.1111/brv.12305

Avise JC (2000) Phylogeography: the history and formation of species. Harvard University Press, MA, USA

Baas Becking LGM (1934) Geobiologie of inleiding tot de milieukunde. W.P. Van Stockum & Zoon, The Hague, The Netherlands

Bachmann E (1890) Ueber nichtkrystalliserte Flechtenfarbstoff, ein Beitrag zur Chemie und Anatomie der Flechten. Jahrbücher für Wissenschaftliche Botanik 21: 1–61

Bagley JC, Matamoros WA, McMahan et al. (2016). Phylogeography and species delimitation in convict cichlids (*Cichlidae*: *Amatitlania*): implications for

taxonomy and Plio-Pleistocene evolutionary history in Central America. Biological Journal of the Linnean Society doi: 10.1111/bij.12845

Bailey RH (1968) *Lecanora conizaeoides* in Iceland. Lichenologist 4: 73

Bailey RH (1970) Animals and the dispersal of soredia from *Lecanora conizaeoides* Nyl. ex Cromb. Lichenologist 4: 256

Bailey RH y James PW (1979) Birds and the dispersal of lichen propagules. Lichenologist 11: 105–106

Baird NA, Etter PD, Atwood TS et al. (2008) Rapid SNP discovery and genetic mapping using sequenced RAD markers. PLoS ONE 3: e3376

Baker HG (1955) Self-compatibility and establishment after "long-distance" dispersal. Evolution 9: 347–349

Barker PF y Thomas E (2004) Origin, signature and palaeoclimatic influence of the Antarctic Circumpolar Current. Earth-Science Reviews 66: 143–162

Barnes DKA, Hodgson DA, Convey P et al. (2006) Incursion and excursion of Antarctic biota: past, present and future. Global Ecology and Biogeography 15: 121–142

de Bary A (1878) Ueber Symbiose. Tageblatt Versammlung Deutscher Naturforscher und Ärzte Cassel 1878: 121–126

Bass D, Richards TA, Matthai L et al. (2007) DNA evidence for global dispersal and probable endemicity of protozoa. BMC Evolutionary Biology 7: 162

Beck A, Kasalicky T y Rambold G (2002) Myco-photobiontal selection in a Mediterranean cryptogam community with *Fulgensia fulgida*. New Phytologist 153: 317–326

Beerli P (2006) Comparison of Bayesian and maximum-likelihood inference of population genetic parameters. Bioinformatics 22: 341–345

Beerli P (2010) Tutorial: comparison of gene flow models using Bayes Factors. MIGRATE-N. Disponible en http://popgen.sc.fsu.edu/Migrate/Tutorials.html

Beerli P y Palczewski M (2010) Unified framework to evaluate panmixia and migration direction among multiple sampling locations. Genetics 185: 313–326

Beimforde C, Feldberg K, Nylinder S et al. (2014) Estimating the Phanerozoic history of the Ascomycota lineages: combining fossil and molecular data. Molecular Phylogenetics and Evolution 78: 386–398

Bendiksby M, Mazzoni S, Jørgensen MH et al. (2014) Combining genetic analyses of archived specimens with distribution modelling to explain the anomalous

distribution of the rare lichen *Staurolemma omphalarioides*: long-distance dispersal o vicariance? Journal of Biogeography 41: 2020–2031

Berg LS (1933) Die Bipolare Verbreitung der Organismen und die Eiszeit. Zoogeographica 1: 449–484

Bergemann SE, Smith MA, Parrent JL et al. (2009) Genetic population structure and distribution of a fungal polypore, *Datronia caperata* (*Polyporaceae*), in mangrove forests of Central America. Journal of Biogeography 36: 266–279

Bickford D, Lohman DJ, Sodhi NS et al. (2007) Cryptic species as a window on diversity and conservation. Trends in Ecology and Evolution 22: 148–155

Billard E, Reyes J, Mansilla et al. (2015) Deep genetic divergence between austral populations of the red alga *Gigartina skottsbergii* reveals a cryptic species endemic to the Antarctic continent. Polar Biology 38: 2021–2034

BirdLife International (2015) *Ardenna grisea*. The IUCN Red List of Threatened Species 2015: e.T22698209A84999904. Disponible en http://birdlife.org

Birkenmajer K, Gaździcki A, Krajewski KP et al. (2005) First Cenozoic glaciers in West Antarctica. Polish Polar Research 26: 3–12

Bjerke JW y Elvebakk A (2004) Distribution of the lichen genus *Flavocetraria* (*Parmeliaceae*, Acomycota) in the Southern Hemisphere. New Zealand Journal of Botany 42: 647–656

Blaha J, Baloch E y Grube M (2006) High photobiont diversity associated with the euryoecious lichen-forming ascomycete *Lecanora rupicola* (*Lecanoraceae*, Ascomycota). Biological Journal of the Linnean Society 88: 283–293

Blume HP, Kuhn D y Bölter M (2002) Soils and soilscapes. En L Beyer y M. Bölter (eds.) Geoecology of Antarctic ice-free coastal landscapes, Ecological Studies vol. 154, págs. 91–113. Springer, Berlin, DE

Boch S, Prati D, Werth S et al. (2011) Lichen endozoochory by snails. PLoS ONE 6: e18770

Bohmann K, Evans A, Gilbert et al. (2014) Environmental DNA for wildlife biology and biodiversity monitoring. Trends in Ecology and Evolution 29: 358–367

Boluda CG, Hawksworth DL, Divakar PK et al. (2016) Microchemical and molecular investigations reveal *Pseudephebe* species as cryptic with an environmentally modified morphology. Lichenologist 48: 527–543

Bowler PA y Rundel PW (1975) Reproductive strategies in lichens. Botanical Journal of the Linnean Society 70: 325–340

Bowman JS y Deming JW (2017) Wind-driven distribution of bacteria in coastal Antarctica: evidence from the Ross Sea region. Polar Biology 40: 25–35

Bragg L y Tyson GW (2014) Metagenomics using next-generation sequencing. En T Paulsen y AJ Holmes (eds.) Environmental microbiology: methods and protocols, vol. 1096, págs. 183–201. Humana Press, Springer Science + Business Media, LLC

Bridge PD y Spooner BM (2012) Non-lichenized Antarctic fungi: transient visitors or members of a cryptic ecosystem? Fungal Ecology 5: 381–394

Briggs JC (1987) Antitropical distribution and evolution in the Indo-West Pacific Ocean. Systematic Zoology 36: 237–247

Brodo IM (1973) The lichen genus *Coccotrema* in North America. The Bryologist 76: 260–270

Brodo IM (1976) Lichenes Canadenses Exsciccati: Fascicle II. The Bryologist 79: 385–405

Brodo IM y Hawksworth DL (1977) *Alectoria* and allied genera in North America. Opera Botanica 42: 1–164

Brodo IM, Sharnoff SD y Sharnoff S (2001) Lichens of North America. Yale University Press, New Haven, USA

Bruen TC, Philippe H y Bryant D (2006) A simple and robust statistical test for detecting the presence of recombination. Genetics 172: 2665–2681

Bryant D y Moulton V (2004) NEIGHBORNET: an agglomerative method for the construction of phylogenetic networks. Molecular Biology and Evolution 21: 255–265

Bubrick P, Galun M y Frensdorff A (1984) Observations on free-living *Trebouxia* De Puymaly and *Pseudotrebouxia* Archibald, and evidence that both symbionts from *Xanthoria parietina* (L.) Th. Fr. can be found free-living in nature. New Phytologist 97: 455–462

Buckley TR, Arensburger P, Simon C y Chambers GK (2002) Combined data, Bayesian phylogenetics, and the origin of the New Zealand cicada genera. Systematic Biology 51: 4–18

Burgaz AR y Raggio J (2007) The *Cladoniaceae* of Navarino Island (Prov. Antártida Chilena, Chile). Mycotaxon 99: 103–116

Buschbom J (2007) Migration between continents: geographical structure and long-distance gene flow in *Porpidia flavicunda* (lichen-forming Ascomycota). Molecular Ecology 16: 1835–1846

Butterfield NJ, Knoll AH y Swett K (1994) Paleobiology of the Neoproterozoic Svanbergfjellet Formation, Spitsbergen. Fossils and Strata 34: 1–84

Calatayud V y Triebel D (2003) Three new species of *Stigmidium* s.l. (lichenicolous ascomycetes) on *Acarospora* and *Squamarina*. Lichenologist 35: 103–116

del Campo EM, Casano LM y Barreno E (2013) Evolutionary implications of intron-exon distribution and the properties and sequences of the *RPL10A* gene in eukaryotes. Molecular Phylogenetics and Evolution 66: 857–867

de Cárcer DA, López-Bueno A, Pearce DA y Alcamí A (2015) Biodiversity and distribution of polar freshwater DNA viruses. Science Advances 1: e1400127

Carstens BC y Richards CL (2007) Integrating coalescent and ecological niche modeling in comparative phylogeography. Evolution 61: 1439–1454

Carstens BC, Pelletier TA, Reid NM y Satler JD (2013) How to fail at species delimitation. Molecular Ecology 22: 4369–4383

Casano LM, del Campo EM, García-Breijo FJ et al. (2011) Two *Trebouxia* algae with different physiological performances are ever-present in lichen thalli of *Ramalina farinacea*. Coexistence versus competition? Environmental Microbiology 13: 806–818

Cassie DM y Piercey-Normore MD (2008) Dispersal in a sterile lichen-forming fungus, *Thamnolia subuliformis* (Ascomycotina, *Icmadophilaceae*). Botany 86: 751–762

Castello M (2010) Notes on the lichen genus *Rhizoplaca* from continental Antarctica and on some other species from northern Victoria Land. Lichenologist 42: 429–437

Castello M y Nimis PL (1994) Critical notes on Antarctic yellow *Acarosporaceae*. Lichenologist 26: 283–294

Castello M y Nimis PL (1995) A critical revision of Antarctic lichens described by C. W. Dodge. Bibliotheca Lichenologica 57: 71–92

Castello M y Nimis PL (1997) Diversity of lichens in Antarctica. En B Battaglia, J Valencia y DWH Walton (eds.) Antarctic communities: species, structure and survival, págs. 15–21. Cambridge University Press, Cambridge, UK

Castello M y Nimis PL (2000) The lichen vegetation of Terra Nova Bay (Victoria Land, Continental Antarctica). Bibliotheca Lichenologica 58: 43–55

Castresana J (2000) Selection of conserved blocks from multiple alignments for their use in phylogenetic analysis. Molecular Biology and Evolution 17: 540–552

Catalá S, del Campo EM, Barreno E et al. (2016) Coordinated ultrastructural and phylogenomic analyses shed light on the hidden phycobiont diversity of

Trebouxia microalgae in *Ramalina fraxinea*. Molecular Phylogenetics and Evolution 94: 765–777

Chapman MJ y Margulis L (1998) Morphogenesis by symbiogenesis. International Microbiology 1: 319–326

Chen X, Jiang K, Guo P et al. (2014) Assessing species boundaries and the phylogenetic position of the rare Szechwan ratsnake, *Euprepiophis perlaceus* (*Serpentes*: *Colubridae*), using coalescent-based methods. Molecular Phylogenetics and Evolution 70: 130–136

Chen J-M, Werth S y Sork VL (2016) Comparison of phylogeographical structures of a lichen-forming fungus and its green algal photobiont in western North America. Journal of Biogeography 43: 932–943

Choi SC (2016) Methods for delimiting species via population genetics and phylogenetics using genotype data. Genes and Genomics 38: 905–915

Chomicki G y Renner SS (2015) Watermelon origin solved with molecular phylogenetics including Linnaean material: another example of museomics. New Phytologist 205: 526–532

Chown SL, Clarke A, Fraser CI et al. (2015) The changing form of Antarctic biodiversity. Nature 522: 431–438

Clarke A, Barnes DK y Hodgson DA (2005) How isolated is Antarctica? Trends in Ecology and Evolution 20: 1–3

Clement M, Snell Q, Walke P et al. (2002) TCS: estimating gene genealogies. Proceedings of the 16th International Parallel and Distributed Processing Symposium 2: 184

Cocquyt E (2009) Phylogeny and molecular evolution of green algae. Tesis Doctoral, University of Gent, Gent, BE

Cola VD, Broennimann O, Petitpierre et al. (2016) *ecospat*: an R package to support spatial analyses and modeling of species niches and distributions. Ecography doi:10.1111/ecog.02671

Colesie C, Gommeaux M, Green TGA y Büdel B (2014) Biological soil crusts in Continental Antarctica: Garwood Valley, southern Victoria Land, and Diamond Hill, Darwin Mountains region. Antarctic Science 26: 115–123

Convey P, Lewis Smith RI, Hodgson DA y Peat HJ (2000) The flora of the South Sandwich Islands, with particular reference to the influence of geothermal heating. Journal of Biogeography 27: 1279–1295

Convey P, Gibson JAE, Hillenbrand CD et al. (2008) Antarctic terrestrial life – challenging the history of the frozen continent? Biological Reviews 83: 103–117

Corander J y Marttinen P (2006) Bayesian identification of admixture events using multi-locus molecular markers. Molecular Ecology 15: 2833–2843

Corander J y Tang J (2007) Bayesian analysis of population structure based on linked molecular information. Mathematical Biosciences 205: 19–31

Corander J, Marttinen P, Sirén J y Tang J (2008) Enhanced Bayesian modelling in BAPS software for learning genetic structures of populations. BMC Bioinformatics 9: 539

Cornelissen JHC, Lang SI, Soudzilovskaia NA y During HJ (2007) Comparative cryptogam ecology: a review of bryophyte and lichen traits that drive biogeochemistry. Annals of Botany 99: 987–1001

Coughlan NE, Kelly TC, Davenport J y Jansen MAK (2017) Up, up and away: bird-mediated ectozoochorous dispersal between aquatic enviroments. Freshwater Biology doi:10.1111/fwb.12894

Cox F, Newsham KK, Bol R et al. (2016) Not poles apart: Antarctic soil fungal communities show similarities to those of the distant Arctic. Ecology Letters 19: 528–536

Crane PR, Friis EM y Pedersen KR (1995) The origin and early diversification of angiosperms. Nature 374: 27–33

Crespo A y Pérez-Ortega S (2009) Cryptic species and species pairs in lichens: a discussion on the relationship between molecular phylogenies and morphological characters. Anales del Jardín Botánico de Madrid 66(S1): 71–81

Crespo A y Lumbsch HT (2010) Cryptic species in lichen-forming fungi. IMA Fungus 1: 167–170

Crespo A, Molina MC, Blanco O et al. (2002) rDNA *ITS* and *β-tubulin* gene sequences analyses reveal two monophyletic groups within the cosmopolitan lichen *Parmelia saxatilis*. Mycological Research 106: 788–795

Crespo A, Ferencova Z, Pérez-Ortega S et al. (2010a) *Austroparmelina*, a new Australasian lineage in parmelioid lichens (*Parmeliaceae*, Ascomycota). Systematics and Biodiversity 8: 209–221

Crespo A, Kauff F, Divakar PK et al. (2010b) Phylogenetic generic classification of parmelioid lichens (*Parmeliaceae*, Ascomycota) based on molecular, morphological and chemical evidence. Taxon 59: 1735–1753

Crous PW, Braun U y Groenewald JZ (2007) *Mycosphaerella* is polyphyletic. Studies in Mycology 58: 1–32

Cubero OF, Crespo A, Fatehi J y Bridge PD (1999) DNA extraction and PCR amplification method suitable for fresh, herbarium-stored, lichenized, and other fungi. Plant Systematics and Evolution 216: 243–249

Culberson WL (1972) Disjunctive distributions in the lichen-forming fungi. Annals of the Missouri Botanical Garden 59: 165–173

Dahl E (1946) On different types of unglaciated areas during the Ice Ages and their significance to phytogeography. New Phytologist 45: 225–42

Dalziel IWD, Lawver LA, Pearce JA et al. (2013) A potential barrier to deep Antarctic circumpolar flow until the late Miocene? Geology 41: 947–950

Darling KF, Wade CM, Steward IA et al. (2000) Molecular evidence for genetic mixing of Arctic and Antarctic subpolar populations of planktonic foraminifers. Nature 405: 43–47

Darriba D, Taboada GL, Doallo R y Posada D (2012) JMODELTEST 2: more models, new heuristics and parallel computing. Nature Methods 9: 772–772

Darwin C (1872) The origin of species. 6ª ed. John Murray, London, UK

Dayrat B (2005) Towards integrative taxonomy. Biological Journal of the Linnean Society 85: 407–415

Dellicour S y Flot J-F (2015) Delimiting species-poor datasets using single molecular markers: a study of barcode gaps, haplowebs and GMYC. Systematic Biology 64: 900–908

Dellicour S, Fearnley S, Lombal A et al. (2014) Inferring the past and present connectivity across the range of a North American leaf beetle: combining ecological niche modeling and a geographically explicit model of coalescence. Evolution 68: 2371–2385

Dellicour S, Kastally C, Varela S et al. (2017) Ecological niche modelling and coalescent simulations to explore the recent geographical range history of five widespread bumblebee species in Europe. Journal of Biogeography 44: 39–50

Diederich P, Ertz D, Lawrey JD et al. (2013) Molecular data place the hyphomycetous lichenicolous genus *Sclerococcum* close to *Dactylospora* (*Eurotiomycetes*) and *S. parmeliae* in *Cladophialophora* (*Chaetothyriales*). Fungal Diversity 58: 61–72

Divakar PK y Crespo A (2015) Molecular phylogenetic and phylogenomic approaches in studies of lichen systematics and evolution. En DK Upreti, PK Divakar, V Shukla y R Bajpai (eds.) Recent advances in lichenology, vol. 2, págs. 45–60. Springer India, IN

Divakar PK, Figueras G, Hladun NL y Crespo A (2010) Molecular phylogenetic studies reveal an undescribed species within the North American concept of *Melanelixia glabra* (*Parmeliaceae*). Fungal Diversity 42: 47–55

Divakar PK, Del-Prado R, Lumbsch HT et al. (2012) Diversification of the newly recognized lichen-forming fungal lineage *Montanelia* (*Parmeliaceae*, Ascomycota) and its relation to key geological and climatic events. American Journal of Botany 99: 2014–2026

Divakar PK, Crespo A, Wedin M et al. (2015) Evolution of complex symbiotic relationships in a morphologically derived family of lichen-forming fungi. New Phytologist 208: 1217–1226

Divakar PK, Leavitt SD, Molina MC et al. (2016) A DNA barcoding approach for identification of hidden diversity in *Parmeliaceae* (Ascomycota): *Parmelia sensu stricto* as a case study. Botanical Journal of the Linnean Society 180: 21–29

Döbbeler P (1978) Moosbewohnende Ascomyceten I. Die pyrenocarpen, den Gametophyten besiedelnden Arten. Mitteilungen der Botanischen Staatssammlung München 14: 1–360

Döbbeler P (1985) Moosbewohnende Ascomyceten VII. Neufunde einiger Arten der Gattung *Epibryon*. Mitteilungen der Botanischen Staatssammlung München 21: 757–773

Dodge CW (1948) Lichens and lichen parasites. British-Australian-New Zealand Antarctic Research Expedition 1929–1931, Report Series, B, Zoology-Botany 7: 1–276

Dodge CW (1964) Ecology and geographical distribution of Antarctic lichens. En R Carrick, MW Holdgate y J Prévost (eds.) Biologie Antarctique, págs. 165–171. Hermann et Cie, Paris, FR

Dodge CW (1973) Lichen Flora of the Antarctic continent and adjacent islands. Phoenix Publishing, Canaan, New Hampshire, USA

Domaschke S, Fernández-Mendoza F, García MA et al. (2012) Low genetic diversity in Antarctic populations of the lichen-forming ascomycete *Cetraria aculeata* and its photobiont. Polar Research 31 doi: 10.3402/polar.v31i0.17353

Donoghue MJ (2011) Bipolar biogeography. Proceedings of the National Academy of Sciences USA 108: 6341–6342

Donoghue MJ y Edwards EJ (2014) Biome shifts and niche evolution in plants. Annual Review of Ecology, Evolution, and Systematics 45: 547–572

Donohue KA, Tracey KL, Watts DR et al. (2016) Mean Antarctic Circumpolar Current transport measured in Drake Passage. Geophysical Research Letters 43: 11760–11767

Döring H, Clerc P, Grube M y Wedin M (2000) Mycobiont specific PCR primers for the amplification of nuclear *ITS* and *LSU* rDNA from lichenized ascomycetes. Lichenologist 32: 200–204

Drummond A, Ho S, Phillips M y Rambaut A (2006) Relaxed phylogenetics and dating with confidence. PloS Biology 4: e88

Drummond AJ, Suchard MA, Xie D y Rambaut A (2012) Bayesian phylogenetics with BEAUTI and BEAST 1.7. Molecular Biology and Evolution 29: 1969–1973

Dlugosch KM y Parker IM (2008) Founding events in species invasions: genetic variation, adaptive evolution, and the role of multiple introductions. Molecular Ecology 17: 431–449

Dyer PS y Murtagh GJ (2001) Variation in the ribosomal *ITS*-sequence of the lichens *Buellia frigida* and *Xanthoria elegans* from the Vestfold Hills, eastern Antarctica. Lichenologist 33: 151–159

Dyer PS, Ingram DS y Johnstone K (1992) The control of sexual morphogenesis in the Ascomycotina. Biological Reviews 67: 421–458

Edgar RC (2004) MUSCLE: multiple sequence alignment with high accuracy and high throughput. Nucleic Acids Research 32: 1792–1797

Egidi E, de Hoog G, Isola D et al. (2014) Phylogeny and taxonomy of meristematic rock-inhabiting black fungi in the *Dothideomycetes* based on multi-locus phylogenies. Fungal Diversity 65: 127–165

Eisinger DP, Dick FA y Trumpower BL (1997) *Qsr1p*, a 60S ribosomal subunit protein, is required for joining of 40S and 60S subunits. Molecular Cell Biology 17: 5136–5145

Ekman S (2001) Molecular phylogeny of the *Bacidiaceae* (*Lecanorales*, lichenized Ascomycota). Mycological Research 105: 783–797

Elbert W, Weber B y Burrows S (2012). Contribution of cryptogamic covers to the global cycles of carbon and nitrogen. Nature Geoscience 5: 459–462

Ellis CJ (2012) Lichen epiphyte diversity: a species, community and trait-based review. Perspectives in Plant Ecology, Evolution and Systematics 14: 131–152

Elvebakk A y Moberg R (2002) Foliose and placodioid species of the lichen family *Physciaceae* in southernmost Chile. Lichenologist 34: 311–320

Elvebakk A, Bjerke JW y Støvern LE (2014) Parmelioid lichens (*Parmeliaceae*) in southernmost South America. Phytotaxa 173: 1–30

Ence DD y Carstens BC (2011) SPEDESTEM: a rapid and accurate method for species delimitation. Molecular Ecology Resources 11: 473–480

Engel CR, Daguin C y Serrão EA (2005) Genetic entities and mating system in hermaphroditic *Fucus spiralis* and its close dioecious relative *F. vesiculosus* (*Fucaceae*, *Phaeophyceae*). Molecular Ecology 14: 2033–2046

Engelen A, Convey P y Ott S (2010) Life history strategy of *Lepraria borealis* at an Antarctic inland site, Coal Nunatak. Lichenologist 42: 339–346

Engelen A, Convey P, Popa O y Ott S (2016) Lichen photobiont diversity and selectivity at the southern limit of the maritime Antarctic region (Coal Nunatak, Alexander Island). Polar Biology 39: 2403–2410

Engelsksjøn T (1986) Botany of two Antarctic mountain ranges: Gjelsvikfjella and Mühlig-Hofmannfjella, Dronning Maud Land. I. General ecology and development of the Antarctic cold desert cryptogam formation. Polar Research 4: 205–224

Engelsksjøn T y Jørgensen PM (1986) Phytogeographical relations of the cryptogamic flora of Bouvetøya. Norsk Polarinstitutt Skrifter 185: 71–79

Ertz D, Lawrey JD, Common RS y Diederich P (2013) Molecular data resolve a new order of Arthoniomycetes sister to the primarily lichenized *Arthoniales* and composed of black yeasts, lichenicolous and rock-inhabiting species. Fungal Diversity 66: 113–137

Ertz D, Aptroot A, Van de Vijver B et al. (2014) Lichens from the Utsteinen Nunatak (Sør Rondane Mountains, Antarctica), with the description of one new species and the establishment of permanent plots. Phytotaxa 191: 99–114

Ertz D, Søchting U, Gadea A et al. (2017) *Ducatina umbilicata* gen. et sp. nov., a remarkable *Trapeliaceae* from the subantarctic islands in the Indian Ocean. Lichenologist 49: 127–140

Escudero M, Valcárcel V, Vargas P y Luceño M (2010) Bipolar disjunctions in *Carex*: long-distance dispersal, vicariance, or parallel evolution? Flora 205: 118–127

Estes S y Arnold SJ (2007) Resolving the paradox of stasis: models with stabilizing selection explain evolutionary divergence on all timescales. American Naturalist 169: 227–44

Etayo J y Sancho LG (2008) Hongos liquenícolas del sur de Sudamérica, especialmente de Isla Navarino (Chile). Bibliotheca Lichenologica 98: 1–302

Evanno G, Regnaut S y Goudet J (2005) Detecting the number of clusters of individuals using the software STRUCTURE: a simulation study. Molecular Ecology 14: 2611–2620

Excoffier L y Lischer HEL (2010) ARLEQUIN suite ver 3.5: a new series of programs to perform population genetics analyses under Linux and Windows. Molecular Ecology Resources 10: 564–567

Falush D, Stephens M y Pritchard JK (2003) Inference of population structure using multilocus genotype data, linked loci and correlated allele frequencies. Genetics 164: 1567–1587

Famà P, Wysor B, Kooistra WHCF y Zuccarello GC (2002) Molecular phylogeny of the genus *Caulerpa* (*Caulerpales*, *Chlorophyta*) inferred from chloroplast *tufA* gene. Journal of Phycology 38: 1040–1050

Feakins SJ, Warny S y Lee J-E (2012) Hydrologic cycling over Antarctica during the middle Miocene warming. Nature Geoscience 5: 557–560

Feliner GN (2011) Southern European glacial refugia: a tale of tales. Taxon 60: 365–372

Fernández-Martínez MA, de los Ríos A, Sancho LG y Pérez-Ortega S (2013) Diversity of endosymbiotic *Nostoc* in *Gunnera magellanica* Lam. from Tierra del Fuego, Chile. Microbial Ecology 66: 335–350

Fernández-Mendoza F (2013) Genetic diversity and geneflow between Arctic and Antarctic populations of the lichen *Cetraria aculeata* along the Andes and the Rocky Mountains. Tesis Doctoral, Johann Wolfgang Goethe-Universität, Frankfurt am Main, DE

Fernández-Mendoza F y Printzen C (2013) Pleistocene expansion of the bipolar lichen *Cetraria aculeata* into the Southern hemisphere. Molecular Ecology 22: 1961–1983

Fernández-Mendoza F, Domaschke S, García MA et al. (2011) Population structure of mycobionts and photobionts of the widespread lichen *Cetraria aculeata*. Molecular Ecology 20: 1208–1232

Feuerer T y Hawksworth DL (2007) Biodiversity of lichens, including a world-wide analysis of checklist data based on Takhtajan's floristic regions. Biodiversity and Conservation 16: 85–98

Filson RB (1982) Lichens of continental Antarctica. Journal of the Hattori Botanical Laboratory 53: 357–360

Fontaneto D, Barraclough TG, Chen K et al. (2008) Molecular evidence for broad-scale distributions in bdelloid rotifers: everything is not everywhere but most things are very widespread. Molecular Ecology 17: 3136–3146

Francis JE, Ashworth A, Cantrill DJ et al. (2008) 100 million years of Antarctic climate evolution: evidence from fossil plants. En AK Cooper, PJ Barrett, H Stagg et al. (eds.) Antarctica: a keystone in a changing world. Proceedings of the 10th International Symposium on Antarctic Earth Sciences, págs. 19–27. The National Academies Press, WA, USA

Francis RM (2016) *POPHELPER*: an R package and web app to analyse and visualize population structure. Molecular Ecology Resources http://dx.doi.org/10.1111/1755-0998.12509

Fraser CI, Hay CH, Spencer HG y Waters JM (2009a) Genetic and morphological analyses of the southern bull kelp *Durvillaea antarctica* (*Phaeophyceae*: *Durvillaeales*) in New Zealand reveal cryptic species. Journal of Phycology 45: 436–443

Fraser CI, Nikula R, Spencer H y Waters J (2009b) Kelp genes reveal effects of subantarctic sea during the Last Glacial Maximum. Proceedings of the National Academy of Science USA 106: 3249–3253

Fraser CI, Nikula R, Ruzzante DE y Waters JM (2012) Poleward bound: biological impacts of Southern Hemisphere glaciation. Trends in Ecology and Evolution 27: 462–471

Fraser CI, Terauds A, Smellie J et al. (2014) Geothermal activity helps life survive glacial cycles. Proceedings of the National Academy of Science USA 111: 5634–5639

Friedl T (1987) Aspects of thallus development in the parasitic lichen *Diploschistes muscorum*. Bibliotheca Lichenologica 25: 95–97

Friedl T (1989) Comparative ultrastructure of pyrenoids in *Trebouxia* (*Microthamniales*, *Chlorophyta*). Plant Systematics and Evolution 164: 145–159

Friedl T y Büdel B (2008) Photobionts. En TH Nash III (ed.) Lichen Biology, págs. 9–26. Cambridge University Press, Cambridge, UK

Friedmann EI (1982) Endolithic microorganisms in the Antarctic cold desert. Science 215: 1045–1053

Friis EM, Pedersen KR y Crane PR (2001) Fossil evidence of water lilies (*Nymphaeales*) in the Early Cretaceous. Nature 410: 357–360

Frisch A, Thor G, Ertz D y Grube M (2014) The Arthonialean challenge: restructuring *Arthoniaceae*. Taxon 63: 727–744

Fröberg L, Björn LO, Baur A y Baur B (2001) Viability of lichen photobionts after passing through the digestive tract of a land snail. Lichenologist 33: 543–545

Fujisawa T y Barraclough TG (2013) Delimiting species using single-locus data and the Generalized Mixed Yule Coalescent approach: a revised method and evaluation on simulated data sets. Systematic Biology 62: 707–724

Fujita MK, Leaché AD y Burbrink FT (2012) Coalescent based species delimitation in an integrative taxonomy. Trends in Ecology and Evolution 27: 480–488

Galloway DJ (1985) Flora of New Zealand: Lichens. Government Printer, Wellington, NZ

Galloway DJ (1987) Austral lichen genera: some biogeographical problems. Bibliotheca Lichenologica 25: 385–399

Galloway DJ (1991) Phytogeography of southern hemisphere lichens. En PL Nimis y TJ Crovello (eds.) Quantitative approaches to Phytogeography, págs. 233–262. Kluwer, Dordrecht, The Netherlands

Galloway DJ (2003) Additional lichen records from New Zealand 40. *Buellia aethalea* (Ach.) Th. Fr., *Catillaria contristans* (Nyl.) Zahlbr., *Frutidella caesioatra* (Schaer.) Kalb, *Placynthium rosulans* (Th. Fr.) Zahlbr. and *Pseudocyphellaria mallota* (Tuck.) H. Magn. Australasian Lichenology 53: 20–29

Galloway DJ (2007) Flora of New Zealand: Lichens, including lichen-forming and lichenicolous fungi. 2ª ed. Manaaki Whenua Press, Landcare Research Lincoln, NZ

Galloway DJ (2008) Lichen biogeography. En TH Nash III (ed.) Lichen Biology, 2ª ed., págs. 315–335. Cambridge University Press, Cambridge, UK

Galloway DJ y Bartlett JK (1986) *Arthrorhaphis* Th. Fr. (lichenised Ascomycotina) in New Zealand. New Zealand Journal of Botany 24: 393–402

Galloway DJ y Aptroot A (1995) Bipolar lichens: a review. Cryptogamic Botany 5: 184–189

Galloway DJ y Quilhot W (1998) Checklist of Chilean lichen-forming and lichenicolous fungi. Gayana Botanica 55: 111–185

Gardes M y Bruns TD (1993) *ITS* primers with enhanced specificity for basidiomycetes –application for the identification of mycorrhizae and rusts. Molecular Ecology 2: 113–118

Garrido-Benavent I, Søchting U, De los Ríos A y Pérez-Ortega S (2016) *Shackletonia cryodesertorum* (*Teloschistaceae*, Ascomycota), a new species from the McMurdo Dry Valleys (Antarctica) with notes on the biogeography of the genus *Shackletonia*. Mycological Progress doi:10.1007/s11557-016-1204-x

Garrido-Benavent I, Pérez-Ortega S y de los Ríos A (2017) From Alaska to Antarctica: species boundaries and genetic diversity of *Prasiola* (*Trebouxiophyceae*), a foliose chlorophyte associated with the bipolar lichen-forming fungus *Mastodia tessellata*. Molecular Phylogenetics and Evolution 107: 117–131

van der Gast CJ (2015) Microbial biogeography: the end of the ubiquitous dispersal hypothesis? Environmental Microbiology 17: 544–546

Gaya E, Fernández-Brime S, Vargas R et al. (2015) The adaptive radiation of lichen-forming *Teloschistaceae* is associated with sunscreening pigments and a bark-to-rock substrate shift. Proceedings of the National Academy of Science USA 112: 11600–11605

Geml J, Kauff F, Brochmann C y Taylor DL (2010) Surviving climate changes: high genetic diversity and transoceanic gene flow in two arctic-alpine lichens, *Flavocetraria cucullata* and *F. nivalis* (*Parmeliaceae*, Ascomycota). Journal of Biogeography 37: 1529–1542

Geml J, Kauff F, Brochmann C et al. (2012) Frequent circumarctic and rare transequatorial dispersals in the lichenised agaric genus *Lichenomphalia* (*Hygrophoraceae*, Basidiomycota). Fungal Biology 116: 388–400

Gillespie WH, Rothwell GW y Scheckler SE (1981) The earliest seeds. Nature 293: 462–464

Giordani P, Incerti G, Rizzi G et al. (2014) Functional traits of cryptogams in Mediterranean ecosystems are driven by water, light and substrate interactions. Journal of Vegetation Science 25: 778–792

Di Giuseppe G, Barbieri M, Vallesi A et al. (2013) Phylogeographical pattern of *Euplotes nobilii*, a protist ciliate with a bipolar biogeographical distribution. Molecular Ecology 22: 4029–4037

González-Wevar CA, Díaz A, Gerard K et al. (2012) Divergence time estimations and contrasting patterns of genetic diversity between Antarctic and southern South America benthic invertebrates. Revista Chilena de Historia Natural 85: 445–456

González-Wevar CA, Hüne M, Rosenfeld S et al. (2016) Patterns of genetic diversity and structure in Antarctic and sub-Antarctic *Nacella* (*Patellogastropoda*: *Nacellidae*) species. Biodiversity 17: 46–55

Gorbushina AA, Beck A y Schulte A (2005) Microcolonial rock inhabiting fungi and lichen photobionts: evidence for mutualistic interactions. Mycological Research 109: 1288–1296

Gould SJ (2002) The structure of evolutionary theory. Belknap Press, Cambridge, MA, USA

Goward T (1994) Living antiquities. Nature Canada, Summer 1994: 14–21

Graham A (2010) Late Cretaceous and Cenozoic history of Latin American vegetation and terrestrial environments. Missouri Botanical Garden Press, StLouis, MO, USA

Graham A (2011) The age and diversification of terrestrial New World ecosystems through Cretaceous and Cenozoic time. American Journal of Botany 98: 336–351

Dal Grande F, Widmer I, Wagner HH y Scheidegger C (2012) Vertical and horizontal photobiont transmission within populations of a lichen symbiosis. Molecular Ecology 21: 3159–3172

Dal Grande F, Beck A, Singh G y Schmitt I (2013) Microsatellite primers in the lichen symbiotic alga *Trebouxia decolorans* (*Trebouxiophyceae*). Applications in Plant Sciences 1: 1200400

Green TGA y Lange OL (1995) Photosynthesis in poikilohydric plants: a comparison of lichens and bryophytes. En ED Schulze y MM Caldwell (eds.) Ecophysiology of photosynthesis, págs. 319–341. Springer, Berlin, DE

Green TGA, Schroeter B y Sancho LG (2007) Plant life in Antarctica. En FL Pugnaire y F Valladares (eds.) Functional Plant Ecology, 2ª ed., págs. 389–433. CRC Press, Boca Raton, FL, USA

Green TGA, Sancho LG, Pintado A y Schroeter B (2011a) Functional and spatial pressures on terrestrial vegetation in Antarctica forced by global warming. Polar Biology 34: 1643–1656

Green TGA, Sancho LG, Türk R et al. (2011b) High diversity of lichens at 84º S, Queen Maud Mountains, suggests preglacial survival of species in the Ross Sea region Antarctica. Polar Biology 34: 1211–1220

Green TGA, Seppelt RD, Brabyn LR et al. (2015) Flora and vegetation of Cape Hallett and vicinity, northern Victoria Land, Antarctica. Polar Biology 38: 1825–1845

Grube M (2010) Die hard: lichens. En J Seckbach y M Grube (eds.) Symbioses and stress: joint ventures in biology (Cellular origin, life in extreme habitats and astrobiology), vol. 17, págs. 509–523. Springer, Dordrecht, The Netherlands

Grube M y Hafellner J (1990) Studien an Flechtenbewohnenden Pilzen der Sammelgattung *Didymella* (Ascomycetes, *Dothideales*). Nova Hedwigia 51: 283–360

Grube M y de los Ríos A (2001) Observations on *Biatoropsis usnearum*, a lichenicolous heterobasidiomycete, and other gall-forming lichenicolous fungi, using different microscopal techniques. Mycological Research 105: 1116–1122

Grube M, Cernava T, Soh J et al. (2015) Exploring functional contexts of symbiotic sustain within lichen-associated bacteria by comparative omics. The ISME Journal 9: 412–424

Grummer JA, Bryson Jr RW y Reeder TW (2014) Species delimitation using Bayes Factors: simulations and application to the *Sceloporus scalaris* species group (*Squamata*: *Phrynosomatidae*). Systematic Biology 63: 119–133

Gueidan C, Villaseñor CR, De Hoog, GS et al. (2008) A rock-inhabiting ancestor for mutualistic and pathogen-rich fungal lineages. Studies in Mycology 61: 111–119

Gueidan C, Aptroot A, da Silva Cáceres ME et al. (2014) A reappraisal of orders and families within the subclass *Chaetothyriomycetidae* (*Eurotiomycetes*, Ascomycota). Mycological Progress 13: 1027–1039

Guindon S y Gascuel O (2003) A simple, fast and accurate method to estimate large phylogenies by maximum likelihood. Systematic Biology 52: 696–704

Guindon S, Dufayard JF, Lefort V et al. (2010) New algorithms and methods to estimate maximum-likelihood phylogenies: assessing the performance of PhyML 3.0. Systematic Biology 59: 307–321

Guiry MD (2012) How many species of algae are there? Journal of Phycology 48: 1057–1063

Guiry MD y Guiry GM (2016, 2017) AlgaeBase. World-Wide Electronic Publication, National University of Ireland, Galway. Disponible en http://www.algaebase.org

Guisan A, Petitpierre B, Broennimann O et al. (2014) Unifying niche shift studies: insights from biological invasions. Trends in Ecology and Evolution 29: 260–269

Guschanski K, Krause J, Sawyer et al. (2013) Next-generation museomics disentangles one of the largest primate radiations. Systematic Biology 62: 539–554

Hale ME (1987) Epilithic lichens in the Beacon Sandstone Formation, Victoria Land, Antarctica. Lichenologist 19: 269–288

Halici MG, Güllü M y Parnikoza I (2017) *Sagediopsis bayozturkii* sp. nov. on the lichen *Acarospora macrocyclos* from Antarctica with a key to the known species of the genus (Ascomycota, *Adelococcaceae*). Polar Record doi:10.1017/S0032247417000043

Hall TA (1999) BioEdit: a user-friendly biological sequence alignment editor and analysis program for Windows 95/98/NT. Nucleic Acids Symposium Series 41: 95–98

Hamilton CA, Formanowicz DR y Bond JE (2011) Species delimitation and phylogeography of *Aphonopelma hentzi* (*Araneae*, *Mygalomorphae*,

Theraphosidae): cryptic diversity in North American Tarantulas. PLoS ONE 6: e26207

Hamilton CA, Hendrixson BE, Brewer MS y Bond JE (2014) An evaluation of sampling effects on multiple DNA barcoding methods leads to an integrative approach for delimiting species: a case study of the North American tarantula genus *Aphonopelma* (*Araneae*, *Mygalomorphae*, *Theraphosidae*). Molecular Phylogenetics and Evolution 71: 79–93

van der Hammen T (1974) The Pleistocene changes of vegetation and climate in tropical South America. Journal of Biogeography 1: 3–26

Hansen ES, Poelt J y Søchting U (1987) Die Flechtengattung *Caloplaca* in Grönland. Meddelelser om Gronland, Bioscience 25: 1–52

Harmata K y Olech M (1991) Transect for aerobiological studies from Antarctica to Poland. Grana 30: 458–463

Hawes TC (2015) Antarctica's geological arks of life. Journal of Biogeography 42: 207–208

Hawksworth DL (1982) Secondary fungi in lichen symbioses: parasites, saprophytes and parasymbionts. Journal of the Hattori Botanical Laboratory 52: 357–366

Hawksworth DL (1988) The variety of fungal-algal symbioses, their evolutionary significance, and the nature of lichens. Botanical Journal of the Linnean Society 96: 3–20

Hawksworth DL (2005) Life-style choices in lichen-forming and lichen-dwelling fungi. Mycological Research 109: 135–136

Hawksworth DL y Honegger R (1994) The lichen thallus: a symbiotic phenotype of nutritionally specialized fungi and its response to gall producers. En MAJ Williams (ed.) Plant Galls: organisms, interactions, populations, págs. 77–98. Clarendon Press, Oxford, UK

Hawksworth DL y Iturriaga T (2006) Lichenicolous fungi described from Antarctica and the sub-Antarctic islands by Carroll W. Dodge (1895–1988). Antarctic Science 18: 291–301

Hedenäs L (2009) Haplotype variation of relevance to global and European phylogeography in *Sarmentypnum exannulatum* (*Bryophyta*: *Calliergonaceae*). Journal of Bryology 31: 145–158

Hedges SB, Blair JE, Venturi ML y Shoe JL (2004) A molecular timescale of eukaryote evolution and the rise of complex multicellular life. BMC Evolutionary Biology 4: 2

Hedin M, Carlson D y Coyle F (2015) Sky island diversification meets the multispecies coalescent –divergence in the spruce-fir moss spider (*Microhexura montivaga*, *Araneae*, *Mygalomorphae*) on the highest peaks of southern Appalachia. Molecular Ecology 24: 3467–3484

Heesch S, Sutherland JE y Nelson W (2012) Marine *Prasiolales* (*Trebouxiophyceae*, *Chlorophyta*) from New Zealand and the Balleny Islands, with descriptions of *Prasiola novaezelandiae* sp. nov. and *Rosenvingiella australis* sp. nov. Phycologia 51: 217–227

Heesch S, Pažoutová M, Moniz MBJ y Rindi F (2016) *Prasiolales* (*Trebouxiophyceae*, *Chlorophyta*) of the Svalbard Archipelago: diversity, biogeography, and description of the new genera *Prasionella* and *Prasionema*. European Journal of Phycology 51: 1–17

Heinken T (1999) Dispersal patterns of terricolous lichens by thallus fragments. Lichenologist 31: 603–612

Heled J y Drummond AJ (2010) Bayesian inference of species trees from multilocus data. Molecular Biology and Evolution 27: 570–580

Henskens FL, Green TA y Wilkins A (2012) Cyanolichens can have both cyanobacteria and green algae in a common layer as major contributors to photosynthesis. Annals of Botany 110: 555–563

Herrera-Campos M, Pérez-Pérez RE y Nash III TH (2016) Lichens of Mexico. The *Parmeliaceae* –Keys, distribution and specimen descriptions. Bibliotheca Lichenologica 110, J. Cramer, DE

Herron MD, Hackett JD, Aylward FO y Michod RE (2009) Triassic origin and early radiation of multicellular volvocine algae. Proceedings of the National Academy of Sciences USA 106: 3254–3258

Hertel H (1977) Gesteinsbewohnende Arten der Sanmelgattung *Lecidea* (Lichenes) aus Zentral-Ost-und Sudostasien. Eine erste Ubersicht. Ergebnisse des Forschung Khumbu Himalaya Unternehmen Nepal 6: 145–378

Hertel H (1984) Über saxicole, lecideoide Flechten der Subantarktis. Nova Hedwigia 79: 399–499

Hertel H (1987) Progress and problems in taxonomy of Antarctic saxicolous lecideoid lichens. Bibliotheca Lichenologica 25: 219–242

Hertel H (1988) Problems in monographing Antarctic crustose lichens. Polarforschung 58: 65–76

Hewitt GM (1996) Some genetic consequences of ice ages, and their role in divergence and speciation. Biological Journal of the Linnean Society 58**:** 247–276

Hewitt GM (2004) Genetic consequences of climatic oscillations in the Quaternary. Philosophical Transactions of the Royal Society of London B: Biological Sciences 359: 183–195

Hey J (2010) Isolation with migration models for more than two populations. Molecular Biology and Evolution 27: 905–920

Hodkinson BP y Lutzoni F (2009) A microbiotic survey of lichen-associated bacteria reveals a new lineage from the *Rhizobiales*. Symbiosis 49: 163–180

Högberg N, Kroken S, Thor G y Taylor JW (2002) Reproductive mode and genetic variation suggest a North American origin of European *Letharia vulpina*. Molecular Ecology 11: 1191–1196

Högnabba F y Wedin M (2003) Molecular phylogeny of the *Sphaerophorus globosus* species complex. Cladistics 19: 224–232

Honegger R (2012) The symbiotic phenotype of lichen-forming ascomycetes and their endo- and epibionts. Chapter 15. En B Hock (ed.) Fungal associations. The Mycota IX, 2ª ed., págs. 287–339. Springer, Berlin, Germany

Honegger R y Zippler U (2007) Mating systems in representatives of *Parmeliaceae*, *Ramalinaceae* and *Physciaceae* (*Lecanoromycetes*, lichen-forming ascomycetes). Mycological Research 111: 424–432

Hooker JD (1853) Introductory essay to the Flora of New Zealand. Flora Novae Zelandiae, págs. 1–29. Reeve, London, UK

Hooker JD y Taylor T (1844) Lichenes Antarctici. London Journal of Botany 3: 634–658

Hoorn C, Wesselingh FP, Ter Steege H et al. (2010) Amazonia through time: Andean uplift, climate change, landscape evolution, and biodiversity. Science 330: 927–931

Hotaling S, Foley ME, Lawrence NM et al. (2016) Species discovery and validation in a cryptic radiation of endangered primates: coalescent-based species delimitation in Madagascar's mouse lemurs. Molecular Ecology 25: 2029–2045

Hubisz MJ, Falush D, Stephens M y Pritchard JK (2009) Inferring weak population structure with the assistance of sample group information. Molecular Ecology Resources 9: 1322–1332

Hudson RR y Coyne JA (2002) Mathematical consequences of the genealogical species concept. Evolution 56: 1557–1565

Humboldt FWHA (1817) De distributione geographica plantarum secundum coeli temperiem et altitudem montium, prolegomena. Libraria Graeco-Latino-Germanica, Paris, FR

Huson DH y Bryant D (2006) Application of phylogenetic networks in evolutionary studies. Molecular Biology and Evolution 23: 254–267

Jacobsen P y Kappen L (1988) Lichens from the Admiralty Bay region, King George Island (South Shetland Islands, Antarctica). Nova Hedwigia 46: 503–510

Jahns HM, Tuiz-Dubiel A y Blank L (1976) Hygroskopische bewegungen der sorale von *Hypogymnia physodes*. Herzogia 4: 15–23

Jeffery NW, DiBacco C, Van Wyngaarden M et al. (2017) RAD sequencing reveals genomewide divergence between independent invasions of the European green crab (*Carcinus maenas*) in the Northwest Atlantic. Ecology and Evolution doi.org/10.1002/ece3.2872

Johannesson HS, Johannesson KHP y Stenlid J (2000) Development of primer sets to amplify fragments of conserved genes for use in population studies of the fungus *Daldinia loculata*. Molecular Ecology 9: 375–377

Joly S y Bruneau A (2006) Incorporating allelic variation for reconstructing the evolutionary history of organisms from multiple genes: an example from *Rosa* in North America. Systematic Biology 55: 623–636

Jombart T (2008) *adegenet*: a R package for the multivariate analysis of genetic markers. Bioinformatics 24: 1403–1405

Jombart T, Devillard S y Balloux F (2010) Discriminant analysis of principal components: a new method for the analysis of genetically structured populations. BMC Genetics 11: 94

Jones TC, Wilkins RJ, Hogg ID y Green TGA (2013) Photobiont selectivity for lichens and evidence for a possible glacial refugium in the Ross Sea Region, Antarctica. Polar Biology 36: 767–774

Jones TC, Hogg ID, Wilkins RJ y Green TGA (2015) Microsatellite analyses of the Antarctic endemic lichen *Buellia frigida* Darb. (*Physciaceae*) suggest limited dispersal and the presence of glacial refugia in the Ross Sea region. Polar Biology 38: 941–949

Jørgensen PM (1979) The phytogeographical relationships of the lichen flora of Tristan da Cunha (excluding Gough Island). Canadian Journal of Botany 57: 2279–2282

Jørgensen PM (1983) Distribution patterns of lichens in the Pacific region. Australian Journal of Botany, Supplementary Series 10: 43–66

Jørgensen PM (2001) Studies in the lichen family *Pannariaceae* X. The lichen genus *Protopannaria* in the subantarctic islands. Cryptogamie Mycologie 22: 67–72

Jukes TH y Cantor CR (1969) Evolution of protein molecules. En HN Munro (ed.) Mammalian protein metabolism, págs. 21–132. Academic Press, NY, USA

Kantvilas G (1995) Alpine lichens of Tasmania's South West wilderness. Lichenologist 27: 433–449

Kantvilas G y Louwhoff HJJ (2007) The lichen genus *Umbilicaria* Hoffm. in Tasmania. Muelleria 25: 3–20

Kappen L (1982) Lichen oases in hot and cold deserts. Journal of the Hattori Botanical Laboratory 53: 325–330

Kappen L (1988) Ecophysiological relationships in different climatic regions. En M Galun (ed.) Handbook of Lichenology, vol. 2, págs. 37–99. CRC Press, Boca Ratón, FL, USA

Kappen L (1993) Lichens in the Antarctic region. En EI Friedmann (ed.) Antarctic Microbiology, págs. 433–490. Wiley-Liss, New York, NY, USA

Kappen L (2000) Some aspects of the great success of lichens in Antarctica. Antarctic Science 12: 314–324

Kappen L y Straka H (1988) Pollen and spores transport into Antarctica. Polar Biology 8: 173e180

Kappen L y Valladares F (2007) Opportunistic growth and desiccation tolerance: the ecological success of poikilohydrous autotrophs. En FI Pugnaire y F Valladares (eds.) Functional plant ecology, 2ª ed., págs. 7–67. CRC Press, Boca Ratón, FL, USA

Kappen L, Friedmann EI y Garty J (1981) Ecophysiology of lichens in the Dry Valleys of southern Victoria Land, Antarctica. I. Microclimate of the cryptoendolithic lichen habitat. Flora 171: 216–235

Kärnefelt I (1990) Evidence of a slow evolutionary change in the speciation of lichens. Bibliotheca Lichenologica 38: 291–306

Kärnefelt I y Thell A (2001) Delimitation of the lichen genus *Tuckermannopsis* Gyeln. (Ascomycotina, *Parmeliaceae*) based on morphology and DNA sequences. Bibliotheca Lichenologica 78: 193–209

Kass RE y Raftery AE (1995) Bayes Factors. Journal of the American Statistical Association 90: 773–795

Katoh K, Misawa K, Kuma KI y Miyata T (2002) MAFFT: a novel method for rapid multiple sequence alignment based on fast fourier transform. Nucleic Acids Research 30: 3059–3066

Katoh K y Toh H (2008) Recent developments in the MAFFT multiple sequence alignment program. Briefings in Bioinformatics 9: 286–298

Katoh K y Standley DM (2013) MAFFT Multiple sequence alignment software version 7: improvements in performance and usability. Molecular Biology and Evolution 30: 772–780

Kauff F y Lutzoni F (2002) Phylogeny of the *Gyalectales* and *Ostropales* (Ascomycota, Fungi): among and within order relationships based on nuclear ribosomal RNA small and large subunits. Molecular Phylogenetics and Evolution 25: 138–156

Kelly LJ, Hollingsworth PM, Coppins BJ et al. (2011) DNA barcoding of lichenized fungi demonstrates high identification success in a floristic context. New Phytologist 191: 288–300

Kenrick P y Crane PR (1997) The origin and early evolution of plants on land. Nature 389: 33–39

Kim MS, Jun M-S, Kim CA et al. (2015) Morphology and phylogenetic position of a freshwater *Prasiola* species (*Prasiolales*, *Chlorophyta*) in Korea. Algae 30: 197–205

Kim CS, Kim TW, Cho KH et al. (2016) Variability of the Antarctic Coastal Current in the Amundsen Sea. Estuarine, Coastal and Shelf Science. 181: 123-133

Kim JI, Nam SW, So JE et al. (2017) *Asterochloris sejongensis* sp. nov. (*Trebouxiophyceae*, *Chlorophyta*) from King George Island, Antarctica. Phytotaxa 295: 060–070

Kirk PM, Cannon PF, Minter DW y Stalpers JA (2008) Dictionary of the fungi, 10ª ed. CABI Europe, Oxford, UK

Knapp M, Stöckler K, Havell D et al. (2005) Relaxed molecular clock provides evidence for long-distance dispersal of *Nothofagus* (southern beech). PLoS Biology, 3: e14

Kohlmeyer J y Kohlmeyer E (2013) Marine mycology: the higher fungi. Elsevier

Kohlmeyer J, Hawksworth DL y Volkmann-Kohlmeyer B (2004) Observations on two marine and maritime ‘‘borderline” lichens: *Mastodia tessellata* and *Collemopsidium pelvetiae*. Mycological Progress 3: 51–56

Kopelman NM, Mayzel J, Jakobsson M et al. (2015) CLUMPAK: a program for identifying clustering modes and packaging population structure inferences across *K*. Molecular Ecology Resources http://dx.doi.org/10.1111/1755-0998.12387

Kovačik L y Pereira AB (2001) Green alga *Prasiola crispa* and its lichenized form *Mastodia tesselata* in Antarctic environment: general aspects. Nova Hedwigia 123: 465–478

Kroken S y Taylor JW (2000) Phylogenetic species, reproductive mode, and specificity of the green alga *Trebouxia* forming lichens with the fungal genus *Letharia*. The Bryologist 103: 645–660

Kukwa M y Kolanowska M (2016) Glacial refugia and the prediction of future habitat coverage of the South American lichen species *Ochrolechia austroamericana*. Scientific Reports 6: e38779

Lalley JS y Viles HA (2005) Terricolous lichens in the northern Namib Desert of Namibia: distribution and community composition. Lichenologist 37: 77–91

Lamb IM (1948) Antarctic pyrenocarp lichens. Discovery Reports 25: 1–30

Lamb IM (1949) La importancia de los líquenes como indicadores fitogeográficos en el Hemisferio Austral. Lilloa 20: 65–68

Lamb IM (1954) Studies in frutescent *Lecideaceae* (lichenized Discomycetes). Rhodora 36: 105–129, 137–153

Lamb IM (1968) Antarctic lichens II. The genera *Buellia* and *Rinodina*. British Antarctic Survey Scientific Reports 61: 1–129

Lamb IM (1970) Antarctic terrestrial plants and their ecology. En MW Holdgate (ed.) Antarctic Ecology, 2ª ed., págs. 733–751. Academic Press, London, UK

Lanfear R, Calcott B, Ho SYW y Guindon S (2012) PARTITIONFINDER: combined selection of partitioning schemes and substitution models for phylogenetic analyses. Molecular Biology and Evolution 29: 1695–1701

Lartillot N y Philippe H (2006) Computing Bayes Factors using thermodynamic integration. Systematic Biology 55: 195–207

Latch EK, Dharmarajan G, Glaubitz JC y Rhodes OE (2006) Relative performance of Bayesian clustering software for inferring population substructure and individual assignment at low levels of population differentiation. Conservation Genetics 7: 295–302

Lawrey JD (1984) Biology of lichenized fungi. Praeger Publishers, New York, NY, USA

Lawrey JD (1986) Biological role of lichen substances. The Bryologist 89: 111–122

Lawrey JD y Diederich P (2003) Lichenicolous fungi: interactions, evolution and biodiversity. The Bryologist 106: 80–120

Lawrey JD y Diederich P (2016) Lichenicolous fungi –worldwide checklist, including isolated cultures and sequences available. Disponible en http://www.lichenicolous.net

Lear CH y Lunt DJ (2016) How Antarctica got its ice. Science 352: 34–35

Leavitt SD, Johnson L y St. Clair LL (2011a) Species delimitation and evolution in morphologically and chemically diverse communities of the lichen-forming genus *Xanthoparmelia* (*Parmeliaceae*, Ascomycota) in Wester North America. American Journal of Botany 98: 1–14

Leavitt SD, Fankhauser JD, Leavitt DH et al. (2011b) Complex patterns of speciation in cosmopolitan "rock posy" lichens –discovering and delimiting cryptic fungal species in the lichen-forming *Rhizoplaca melanophthalma* species-complex (*Lecanoraceae*, Ascomycota). Molecular Phylogenetics and Evolution 59: 587–602

Leavitt SD, Esslinger TL y Lumbsch HT (2012a) Neogene-dominated diversification in Neotropical Montane lichens: dating divergence events in the lichen-forming fungal genus *Oropogon* (*Parmeliaceae*). American Journal of Botany 99: 1764–1777

Leavitt SD, Esslinger TL, Divakar PK y Lumbsch HT (2012b) Miocene and Pliocene dominated diversification of the lichen-forming fungal genus *Melanohalea* (*Parmeliaceae*, Ascomycota) and Pleistocene population expansions. BMC Evolutionary Biology 12: 176

Leavitt SD, Esslinger TL, Divakar PK y Lumbsch HT (2012c) Miocene divergence, phenotipically cryptic lineages, and contrasting distribution patterns in common lichen-forming fungi (Ascomycota: *Parmeliaceae*). Biological Journal of the Lineean Society 107: 920–937

Leavitt SD, Fernández-Mendoza F, Pérez-Ortega S et al. (2013) Local representation of global diversity in a cosmopolitan lichen-forming fungal species complex (*Rhizoplaca*, Ascomycota). Journal of Biogeography 40: 1792–1806

Leavitt SD, Moreau CS y Lumbsch HT (2015a) The dynamic discipline of species delimitation: progress toward effectively recognizing species boundaries in natural populations. En DK Upreti, PK Divakar, V Shukla y R Bajpai (eds.) Recent advances in lichenology, vol. 2, págs. 11–44. Springer India, IN

Leavitt SD, Divakar PK, Ohmura Y et al. (2015b) Who's getting around? Assessing species diversity and phylogeography in the widely distributed lichen-forming fungal genus *Montanelia* (*Parmeliaceae*, Ascomycota). Molecular Phylogenetics and Evolution 90: 85–96

Leavitt SD, Kraichak E, Nelsen MP et al. (2015c) Fungal specificity and selectivity for algae play a major role in determining lichen partnerships across diverse ecogeographic regions in the lichen-forming family *Parmeliaceae* (Ascomycota). Molecular Ecology 24: 3779–3797

Leavitt SD y Lumbsch HT (2016) Ecological biogeography of lichen-forming fungi. En IS Druzhinina y CP Kubicek (eds.) Environmental and microbial relationships, 3ª ed., The Mycota IV, págs. 15–37. Springer International Publishing, SUI

Leavitt SD, Divakar PK, Crespo A y Lumbsch HT (2016a) A matter of time – understanding the limits of the power of molecular data for delimiting species boundaries. Herzogia 29: 479–492

Leavitt SD, Esslinger TL, Divakar PK et al. (2016b) Hidden diversity before our eyes: delimiting and describing cryptic lichen-forming fungal species in camouflage lichens (*Parmeliaceae*, Ascomycota). Fungal Biology 120: 1374–1391

Leavitt SD, Kraichak E, Vondrak J et al. (2016c) Cryptic diversity and symbiont interactions in rock-posy lichens. Molecular Phylogenetics and Evolution 99: 261–274

Lee JS, Lee HK, Hur J-S et al. (2008) Diversity of the lichenized fungi in King George Island, Antarctica, revealed by phylogenetic analysis of partial large subunit rDNA sequences. Journal of Microbiology and Biotechnology 18: 10116–1023

Leigh JW y Bryant D (2015) POPART: full-feature software for haplotype network construction. Methods in Ecology and Evolution 6: 1110–1116

Leliaert F, Verbruggen H, Wysor B y De Clerck O (2009) DNA taxonomy in morphologically plastic taxa: algorithmic species delimitation in the *Boodlea* complex (*Chlorophyta*: *Cladophorales*). Molecular Phylogenetics and Evolution 53: 122–133

Leliaert F, Verbruggen H, Vanormelingen P et al. (2014) DNA-based species delimitation in algae. European Journal of Phycology 49: 179–196

León CA, Oliván G y Pino-Bodas R (2013) New distributional records for Chilean bryophyte and lichen flora. Gayana Botánica 70: 242–247

Leopold LB (1949) The interaction of trade wind and sea breeze, Hawaii. Journal of Meteorology 6: 312–320

Lewis LR, Rozzi R y Goffinet B (2014a) Direct long-distance dispersal shapes a New World amphitropical disjunction in the dispersal-limited dung moss *Tetraplodon* (*Bryopsida*: *Splachnaceae*). Journal of Biogeography 41: 2385–2395

Lewis LR, Behling E, Gousse H et al. (2014b) First evidence of bryophyte diaspores in the plumage of transequatorial migrant birds. PeerJ 2: 424

Lewis Smith RI (1984) Terrestrial plant biology of the Sub-Antarctic and Antarctic. En RM Laws (ed.) Antarctic ecology, págs. 61–162. Academic Press, London, UK

Lewis Smith RI (1988) Classification and ordination of cryptogamic communities in Wilkes Land, continental Antarctica. Vegetatio 76: 155–166

Lewis Smith RI (1991) Exotic sporomorpha as indicators of immigrant colonists in Antarctica. Grana 30: 313–324

Lewis Smith RI y Øvstedal DO (1994) *Solorina spongiosa* in Antarctica: an extremely disjunct bipolar lichen. Lichenologist 26: 209–215

Librado P y Rozas J (2009) DNASP v. 5: a software for comprehensive analysis of DNA polymorphism data. Bioinformatics 25: 1451–1452

Lindblom L y Sochting U (2008) Taxonomic revision of *Xanthomendoza borealis* and *Xanthoria mawsonii* (*Lecanoromycetes*, Ascomycota). Lichenologist 40 399–409

Lindblom L y Sochting U (2013) Genetic diversity of the photobiont of the bipolar lichen-forming ascomycete *Xanthomendoza borealis*. Herzogia 26: 307–322

Lindgren H, Leavitt SD y Lumbsch HT (2016) Characterization of microsatellite markers in the cosmopolitan lichen-forming fungus *Rhizoplaca melanophthalma* (*Lecanoraceae*). MycoKeys 14: 31

Lindsay DC (1972) Lichens from Vestfjella, Dronning Maud Land. Norsk Polarinstitutt Meddelelser 101: 1–21

Lindsay DC (1977) Lichens of cold deserts. En MRD Seward (ed.) Lichen ecology, págs. 183–209. Academic Press, London, UK

Linskens HF, Bargagli R, Cresti M y Focardi S (1993) Entrapment of long distance transported pollen grains by various moss species in coastal Victoria Land, Antarctica. Polar Biology 13: 81e87

Lischer HEL y Excoffier L (2012) PGDSPIDER: an automated data conversion tool for connecting population genetics and genomics programs. Bioinformatics 28: 298–299

Lodge DM (1993) Biological invasions: lessons for ecology. Trends in Ecology and Evolution 8: 133–137

Lord JM, Knight A, Bannister JM et al. (2013) Rediscovery of pycnidia in *Thamnolia vermicularis*: implications for chemotype occurrence and distribution 45: 394–411

Lorentsson S y Mattsson J-E (1999) New reports of soredia dispersed by ants, *Formica cunicularia*. Lichenologist 31: 204–207

Lücking R (2003) Takhtajan's floristic regions and foliicolous lichen biogeography: a compatibility analysis. Lichenologist 35: 33–53

Lücking R, Lawrey JD, Sikaroodi M et al. (2009) Do lichens domesticate photobionts like farmers domesticate crops? Evidence from a previously unrecognized

lineage of filamentous cyanobacteria. American Journal of Botany 96: 1409–1418

Lücking R, Dal Forno M, Sikaroodi M et al. (2014) A single macrolichen constitutes hundreds of unrecognized species. Proceedings of the National Academy of Sciences USA 111: 11091–11096

Lücking R, Dal Forno M, Moncada B et al. (2016) Turbo-taxonomy to assemble a megadiverse lichen genus: seventy new species of *Cora* (Basidiomycota: *Agaricales*: *Hygrophoraceae*), honouring David Leslie Hawksworth's seventieth birthday. Fungal Diversity doi:10.1007/s13225-016-0374-9

Lud D, Huiskes AHL y Ott S (2001) Morphological evidence for the symbiotic character of *Turgidosculum complicatulum* Kohlm. & Kohlm. (= *Mastodia tesselata* Hook. f. & Harvey). Symbiosis 31: 141–151

Lumbsch TH, Schmitt I y Messuti MI (2001) Utility of nuclear *SSU* and *LSU* rDNA data sets to discover the ordinal placement of the *Coccotremataceae* (Ascomycota). Organisms Diversity and Evolution 1: 99–112

Lutsak T, Fernández-Mendoza F, Kirika et al. (2016) Mycobiont-photobiont interactions of the lichen *Cetraria aculeata* in high alpine regions of East Africa and South America. Symbiosis 68: 25–37

Lutzoni F, Pagel M y Reeb V (2001) Major fungal lineages are derived from lichen symbiotic ancestors. Nature 411: 937–940

Maddison WP y Maddison DR (2014) Mesquite: a modular system for evolutionary analysis. Version 3.01. Disponible en http://mesquiteproject.org

Magain N, Miadlikowska J, Goffinet B et al. (2016) Macroevolution of specificity in cyanolichens of the genus *Peltigera* section *Polydactylon* (*Lecanoromycetes*, Ascomycota). Systematic Biology doi:10.1093/sysbio/syw065

Mainali KP, Warren DL, Dhileepan K et al. (2015) Projecting future expansion of invasive species: comparing and improving methodologies for species distribution modeling. Global Change Biology 21: 4464–4480

Malavasi V, Škaloud P, Rindi F et al. (2016) DNA-based taxonomy in ecologically versatile microalgae: a re-evaluation of the species concept within the coccoid green algal genus *Coccomyxa* (*Trebouxiophyceae*, *Chlorophyta*). PLoS ONE 11: e0151137

Mao K-S, Milne RI, Zhang L-B et al. (2012) Distribution of living *Cupressaceae* reflects the breakup of Pangea. Proceedings of the National Academy of Sciences USA 109: 7793–7798

Marchant DR y Head JW III (2007) Antarctic Dry Valleys: microclimate zonation, variable geomorphic processes, and implications for assessing climate change on Mars. Icarus 192: 187–222

Mark K, Saag L, Leavitt SD et al. (2016) Evaluation of traditionally circumscribed species in the lichen-forming genus *Usnea*, section *Usnea* (*Parmeliaceae*, Ascomycota) using a six-locus dataset. Organisms, Diversity and Evolution doi:10.1007/s13127-016-0273-7

Marshall WA (1996a) Biological particles over Antarctica. Nature 383: 680

Marshall WA (1996b) Aerial dispersal of lichen soredia in the maritime Antarctic. New Phytologist 134: 523–530

Martin DP, Lemey P, Lott M et al. (2010) RDP3: a flexible and fast computer program for analyzing recombination. Bioinformatics 26: 2462–2463

Martínez I, Burgaz AR, Vitikainen O y Escudero A (2003) Distribution patterns in the genus *Peltigera* Willd. Lichenologist 35: 301–323

Martiny JBH, Bohannan BJM, Brown JH et al. (2006) Microbial biogeography: putting microorganisms on the map. Nature Reviews Microbiology 4: 102–112

Mason-Gamer RJ y Kellogg EA (1996) Testing for phylogenetic conflict among molecular data sets in the tribe *Triticeae* (*Gramineae*). Systematic Biology 45: 524–545

Matos P, Geiser L, Hardman A et al. (2017) Tracking global change using lichen diversity: towards a global-scale ecological indicator. Methods in Ecology and Evolution doi:10.1111/2041-210X.12712

Mayer F, Piel FB, Cassel-Lundhagen A et al. (2015) Comparative multilocus phylogeography of two Palaearctic spruce bark beetles: influence of contrasting ecological strategies on genetic variation. Molecular Ecology 24: 1292–1310

McCarthy PM y Kantvilas G (2000) Additional lichen records from Australia 43. *Verrucaria fusconigrescens* and *V. prominula* in Tasmania, with notes on the habitats and biogeographical affinities of Tasmanian *Verrucariaceae*. Australasian Lichenology 46: 31–35

McCune B (2000) Lichen communities as indicators of forest health. The Bryologist 103: 353–356

McGaughran A, Stevens MI, Hogg ID y Carapelli A (2011) Extreme glacial legacies: a synthesis of the Antarctic springtail phylogeographic record. Insects 2: 62–82

Meier FA, Scherrer S y Honegger R (2002) Faecal pellets of lichenivorous mites contain viable cells of the lichen-forming ascomycete *Xanthoria parietina* and

its green algal photobiont *Trebouxia arboricola*. Biological Journal of the Linnean Society 76: 259–268

Messuti MI, Vobis G y Lumbsch HT (2003) Additions of the Lichen Flora of Tierra del Fuego. The Bryologist 106: 596–598

Millanes AM, Diederich P, Ekman S y Wedin M (2011) Phylogeny and character evolution in the jelly fungi (*Tremellomycetes*, Basidiomycota, Fungi). Molecular Phylogenetics and Evolution 61: 12–28

Millanes AM, Truong C, Westberg M et al. (2014). Host switching promotes diversity in host-specialized mycoparasitic fungi: uncoupled evolution in the *Biatoropsis-Usnea* system. Evolution 68: 1576–1593

Miller KG, Kominz MA, Browning JV et al. (2005) The Phanerozoic record of global sea-level change. Science 310: 1293–1298

Miller MA, Pfeiffer W y Schwartz T (2010) Creating the CIPRES Science Gateway for inference of large phylogenetic trees. Proceedings of the Gateway Computing Environments Workshop (GCE), 14 Nov. 2010, págs. 1–8. New Orleans, LA, USA

Miralles A y Vences M (2013) New metrics for comparison of taxonomies reveal striking discrepancies among species delimitation methods in *Madascincus* lizards. PLoS ONE 8: e68242

Molina MC, Crespo A, Blanco O et al. (2004) Phylogenetic relationships and species concepts in *Parmelia* s. str. (*Parmeliaceae*) inferred from nuclear *ITS* rDNA and *β-tubulin* sequences. Lichenologist 36: 37–54

Molina MC, Divakar PK, Goward T et al. (2017) Neogene diversification in the temperate lichen-forming fungal genus *Parmelia* (*Parmeliaceae*, Ascomycota) Systematics and Biodiversity 15: 166–181

Monaghan MT, Wild R, Elliot M et al. (2009) Accelerated species inventory on Madagascar using coalescent-based models of species delineation. Systematic Biology 58: 298–311

Moniz MBJ, Rindi F y Guiry MD (2012a) Phylogeny and taxonomy of *Prasiolales* (*Trebouxiophyceae*, *Chlorophyta*) from Tasmania, including *Rosenvingiella tasmanica* sp. nov. Phycologia 51: 86–97

Moniz MB, Rindi F, Novis PM et al. (2012b) Molecular phylogeny of Antarctic *Prasiola* (*Prasiolales*, *Trebouxiophyceae*) reveals extensive cryptic diversity. Journal of Phycology 48: 940−955

Moniz MBJ, Guiry MD y Rindi F (2014) *TufA* phylogeny and species boundaries in the green algal order *Prasiolales* (*Trebouxiophyceae*, *Chlorophyta*). Phycologia 53: 396–406

Montresor M, Lovejoy C, Orsini L et al. (2003) Bipolar distribution of the cyst-forming dinoflagellate *Polarella glacialis*. Polar Biology 26: 186–194

Moon KL, Chown SL y Fraser CI (2017) Reconsidering connectivity in the sub-Antarctic. Biological Reviews doi: 10.1111/brv.12327

Moore DM y Chater AO (1971) Studies on bipolar species. I. *Carex*. Botaniska Notiser 124: 317–334

Mosbrugger V, Utescher T y Dilcher DL (2005) Cenozoic continental climatic evolution of Central Europe. Proceedings of the National Academy of Sciences USA 102: 1496414969

Moya P, Škaloud P, Chiva S et al. (2015) Molecular phylogeny and ultrastructure of the lichen microalga *Asterochloris mediterranea* sp. nov. from Mediterranean and Canary Islands ecosystems. International Journal of Systematic and Evolutionary Microbiology 65: 1838–1854

Muggia L, Hafellner J, Wirtz N et al. (2008) The sterile microfilamentous lichenized fungi *Cystocoleus ebeneus* and *Racodium rupestre* are relatives of plant pathogens and clinically important dothidealean fungi. Mycological Research 112: 50–56

Muggia L, Pérez-Ortega S, Fryday A et al. (2014a) Global assessment of genetic variation and phenotypic plasticity in the lichen-forming species *Tephromela atra*. Fungal Diversity 64: 233–251

Muggia L, Pérez-Ortega S, Kopun T et al. (2014b) Photobiont selectivity leads to ecological tolerance and evolutionary divergence in a polymorphic complex of lichenized fungi. Annals of Botany 114: 463–475

Mukhtar A, Garty J y Galun M (1994) Does the lichen alga *Trebouxia* occur free-living in nature: further immunological evidence. Symbiosis 17: 247–253

Muñoz J, Felicísimo AM, Cabezas F et al. (2004) Wind as a long-distance dispersal vehicle in the Southern Hemisphere. Science 304: 1144e1147

Murray J (1963) Lichens from Cape Hallet area, Antarctica. Transactions of the Royal Society of New Zealand, Botany 2: 59–72

Murtagh GJ, Dyer PS y Crittenden PD (2000) Reproductive systems: sex and the single lichen. Nature 404: 564–564

Murtagh GJ, Dyer PS, Furneaux PA y Crittenden PD (2002) Molecular and physiological diversity in the bipolar lichen-forming fungus *Xanthoria elegans*. Mycological Research 106: 1277–1286

Myllys L, Lohtander K, Källersjö M y Tehler A (1999) Sequence insertions and *ITS* data provide congruent information on *Roccella canariensis* and *R. tuberculata* (*Arthoniales*, Euascomycetes) phylogeny. Molecular Phylogenetics and Evolution 12: 295–309

Myllys L, Stenroos S y Thell A (2002) New genes for phylogenetic studies of lichenized fungi: glyceraldehyde-3-phosphate dehydrogenase and beta-tubulin genes. Lichenologist 34: 237–246

Myllys L, Stenroos S, Thell A y Ahti T (2003) Phylogeny of bipolar *Cladonia arbuscula* and *Cladonia mitis* (*Lecanorales*, Euascomycetes). Molecular Phylogenetics and Evolution 27: 58–69

Nadyeina O, Dymytrova L, Naumovych A et al. (2014). Microclimatic differentiation of gene pools in the *Lobaria pulmonaria* symbiosis in a primeval forest landscape. Molecular Ecology 23: 5164–5178

Nagai M (1940) Marine algae of the Kurile Islands. I. Journal of the Faculty of Agriculture, Hokkaido Imperial University 46: 1–137

Narum SR, Buerkle CA, Davey JW et al. (2013) Genotyping-by-sequencing in ecological and conservation genomics. Molecular Ecology 22: 2841–2847

Narum SR, Gallardo P, Correa C et al. (2017) Genomic patterns of diversity and divergence of two introduced salmonid species in Patagonia, South America. Evolutionary Applications doi.org/10.1111/eva.12464

Nash III TH (2008) Lichen biology. Cambridge University Press, Cambridge, UK

Nathan R (2006) Long-distance dispersal of plants. Science 313: 786–788

Navarro-Rosinés P y Roux C (1996) Le *Clauzadella gordensis* gen. et sp. nov., ascomycète lichénicole non lichénisé (*Verrucariales*, *Verrucariaceae*). Canadian Journal of Botany 74: 1533−1538

Nei M (1975) Molecular population genetics and evolution. North-Holland Publishing Company, Amsterdam, The Netherlands

Nei M (1987) Molecular evolutionary genetics. Columbia University Press, New York, NY, USA

Nelsen MP y Gargas A (2008) Dissociation and horizontal transmission of co-dispersing lichen symbionts in the genus *Lepraria* (*Lecanorales*: *Stereocaulaceae*). New Phytologist 177: 264–275

Nelsen MP, Rivas Plata E, Andrew CJ et al. (2011) Phylogenetic diversity of trentepohlialean algae associated with lichen-forming fungi. Journal of Phycology 47: 282–290

Nylander W (1884) Lichenes novi e Freto Behringii. Flora 67: 211–223

Nylen TH, Fountain AG y Doran PT (2004) Climatology of katabatic winds in the McMurdo Dry Valleys, southern Victoria Land, Antarctica. Journal of Geophysical Research –Atmospheres 109: D03114

Oberholzer P, Baroni C, Schaefer JM et al. (2003) Limited Pliocene/Pleistocene glaciation in Deep Freeze Range, northern Victoria Land, Antarctica, derived from in situ cosmogenic nuclides. Antarctic Science 15: 493–502

Olech M (1990) Preliminary studies on ornithocoprophilous lichens of the Arctic and Antarctic regions. Proceedings of the NIPR Symposium on Polar Biology 3: 218–223

Olech M (2004) Lichens of King George Island, Antarctica. Institute of Botany of the Jagiellonian University, Kraków, PL

Olech M y Søchting U (1993) Four new species of *Caloplaca* from Antarctica. Lichenologist 25: 261–269

Olech M y Singh SM (2010) Lichens and lichenicolous fungi of Schirmacher Oasis, Antarctica. National Centre for Antarctic and Ocean Research, Ministry of Earth Sciences, Government of India, IN

Ortiz-Álvarez R, de los Ríos A, Fernández-Mendoza F et al. (2015) Ecological specialization of two photobiont-specific maritime cyanolichen species of the genus *Lichina*. PLoS ONE 10: e0132718

Otálora MAG, Aragón G, Molina MC et al. (2010) Disentangling the *Collema-Leptogium* complex through a molecular phylogenetic study of the *Collemataceae* (*Peltigerales*, lichen-forming Ascomycota). Mycologia 102: 279–290

Otálora MAG, Belinchón R, Prieto M et al. (2015) The threatened epiphytic lichen *Lobaria pulmonaria* in the Iberian Peninsula: genetic diversity and structure across a latitudinal gradient. Fungal Biology 119: 802–811

Ott S (1987) Reproductive strategies in lichens. Bibliotheca Lichenologica 25: 81–93

Ott S y Sancho LG (1993) Morphology and anatomy of *Caloplaca coralligera* (*Teloschistaceae*) as adaptation to extreme environmental conditions in the marine Antarctic. Plant Systematics and Evolution 185: 123–132

Otte V, Esslinger TL y Litterski B (2002) Biogeographical research on European species of the lichen genus *Physconia*. Journal of Biogeography 29: 1125–1141

Otte V, Esslinger TL y Litterski B (2005) Global distribution of the European species of the lichen genus *Melanelia* Essl. Journal of Biogeography 32: 1221–1241

Øvstedal DO y Lewis Smith RI (2001) Lichens of Antarctica and South Georgia. A guide to their identification and ecology. Cambridge University Press, Cambridge, UK

Øvstedal DO y Lewis Smith RI (2011) Four additional lichens from the Antarctic and South Georgia, including a new *Leciophysma* species. Folia Cryptogamica Estonica, Fascicle 48: 65–68

Padial JM, Miralles A, De la Riva I y Vences M (2010) The integrative future of taxonomy. Frontiers in Zoology 7: 16

Pante E, Puillandre N, Viricel A et al. (2015) Species are hypotheses: avoid connectivity assessments based on pillars of sand. Molecular Ecology 24: 525–544

Papadopoulou A y Knowles LL (2016) Towards a paradigm shift in comparative phylogeography driven by trait-based hypotheses. Proceedings of the National Academy of Sciences USA 113: 8018–8024

Parader S y Ahmadjian V (2000) Symbiosis: an introduction to biological associations. Oxford University Press, New York, NY, USA

Paradis E, Claude J y Strimmer K (2004) *ape*: analyses of phylogenetics and evolution in R language. Bioinformatics 20: 289–290

Pawlowski J, Fahrni J, Lecroq B et al. (2007) Bipolar gene flow in deep-sea benthic foraminifera. Molecular Ecology 16: 4089–4096

Pearce DA, Bridge PD, Hughes KA et al. (2009) Microorganisms in the atmosphere over Antarctica. FEMS Microbiology Ecology 69: 143–157

Peat HJ, Clarke A y Convey P (2007) Diversity and biogeography of the Antarctic flora. Journal of Biogeography 34: 132–146

Peksa O y Škaloud P (2011) Do photobionts influence the ecology of lichens? A case study of environmental preferences in symbiotic green alga *Asterochloris* (*Trebouxiophyceae*). Molecular Ecology 20: 3936–3948

Pentecost A (1981) Some observations on the size and shape of lichen ascospores in relation to ecology and taxonomy. New Phytologist 89: 667–678

Pérez-Ortega S, de los Ríos A, Crespo A y Sancho LG (2010) Symbiotic lifestyle and phylogenetic relationships of the bionts of *Mastodia tessellata* (Ascomycota, *incertae sedis*). American Journal of Botany 97: 738–752

Pérez-Ortega S, Ortiz-Álvarez R, Green TGA y de los Ríos A (2012a) Lichen myco- and photobiont diversity and their relationships at the edge of life (McMurdo Dry Valleys, Antarctica). FEMS Microbiology Ecology 82: 429–448

Pérez-Ortega S, Fernández-Mendoza F, Raggio J et al. (2012b) Extreme phenotypic variation in *Cetraria aculeata* (lichenized Ascomycota): adaptation or incidental modification? Annals of Botany 109: 1133–1148

Pérez-Ortega S, Suija A, Crespo A y de los Ríos A (2014) Lichenicolous fungi of the genus *Abrothallus* (*Dothideomycetes*: *Abrothallales* ordo nov.) are sister to the predominantly aquatic *Jahnulales*. Fungal Diversity 64: 295−304

Pérez-Ortega S, Garrido-Benavent I y de los Ríos A (2015) *Austrostigmidium*, a new austral genus of lichenicolous fungi close to rock-inhabiting meristematic fungi in *Teratosphaeriaceae*. Lichenologist 47: 143−156

Pérez-Ortega S, Garrido-Benavent I, Grube M et al. (2016) Hidden diversity of marine borderline lichens and a new order of fungi: *Collemopsidiales* (*Dothideomyceta*). Fungal Diversity 80: 285–300

Petit RJ, Brewer S, Bordács S et al. (2002) Identification of refugia and post-glacial colonisation routes of European white oaks based on chloroplast DNA and fossil pollen evidence. Forest Ecology and Management 156: 49–74

Piercey-Normore MD (2006) The lichen-forming ascomycete *Evernia mesomorpha* associates with multiple genotypes of *Trebouxia jamesii*. New Phytologist 169: 331–344

Piercey-Normore MD y DePriest PT (2001) Algal switching among lichen symbioses. American Journal of Botany 88: 1490–1498

Piñeiro R, Popp M, Hassel K et al. (2012) Circumarctic dispersal and long-distance colonization of South America: the moss genus *Cinclidium*. Journal of Biogeography 39: 2041–2051

Pisa S, Biersma EM, Convey P et al. (2014) The cosmopolitan moss *Bryum argenteum* in Antarctica: recent colonisation or in situ survival? Polar Biology 37: 1469–1477

Platt JM y Spatafora JW (2000) Evolutionary relationships of nonsexual lichenized fungi: molecular phylogenetic hypotheses for the genera *Siphula* and *Thamnolia* from *SSU* and *LSU* rDNA. Mycologia 92: 475–487

Poelt J y Pelleter U (1984) Zwergstrauchige Arten der Flechtengattung *Caloplaca*. Plant Systematics and Evolution 148: 51–88

Pointing SB, Chan Y, Lacap DC et al. (2009) Highly specialized microbial diversity in hyper-arid polar desert. Proceedings of the National Academy of Sciences USA 106: 19964–19969

Pointing SB, Büdel B, Convey P et al. (2015) Biogeography of photoautotrophs in the high polar biome. Frontiers in Plan Science 6: 692

Pons J, Barraclough TG, Gomez-Zurita J et al. (2006) Sequence-based species delimitation for the DNA taxonomy of undescribed insects. Systematic Biology 55: 595–609

Popp M, Mirré V, Brochmann C (2011) A single Mid-Pleistocene long-distance dispersal by a bird can explain the extreme bipolar disjunction in crowberries (*Empetrum*). Proceedings of the National Academy of Sciences USA 108: 6520–6525

Poulsen RS, Schmitt I, Søchting U y Lumbsch HT (2001) Molecular and morphological studies on the subantarctic genus *Orceolina* (*Agyriaceae*). Lichenologist 33: 323–329

Prieto M y Wedin M (2013) Dating the diversification of the major lineages of Ascomycota (Fungi). PLoS One 8: e65576

Printzen C (2008) Uncharted terrain: the phylogeography of arctic and boreal lichens. Plant Ecology and Diversity 1: 265–271

Printzen C (2009) Lichen systematics: the role of morphological and molecular data to reconstruct phylogenetic relationships. En U Lüttge, W Beyschlag, B Büdel y D Francis (eds.) Progress in botany, vol. 71, págs. 233–275. Springer, Berlin, DE

Printzen C, Ekman S y Tonsberg T (2003) Phylogeography of *Cavernularia hultenii*: evidence of slow genetic drift in a widely disjunct lichen. Molecular Ecology 12: 1473–1486

Printzen C, Domaschke S, Fernández-Mendoza F y Pérez-Ortega S (2013) Biogeography and ecology of *Cetraria aculeata*, a widely distributed lichen with a bipolar distribution. MycoKeys 6: 33–53

Pritchard JK, Stephens M y Donnelly P (2000) Inference of population structure using multi-locus genotype data. Genetics 155: 945–959

Pugh PJA y Convey P (2008) Surviving out in the cold: Antarctic endemic invertebrates and their refugia. Journal of Biogeography 35: 2176–2186

Puillandre N, Lambert A, Brouillet S y Achaz G (2012) ABGD, automatic barcode gap discovery for primary species delimitation. Molecular Ecology 21: 1864–1877

Pyatt FB (1968) The occurrence of a rotifer on the surfaces of apothecia of *Xanthoria parietina*. Lichenologist 4: 74–75

Quaedvlieg W, Binder M, Groenewald JZ et al. (2014) Introducing the Consolidated Species Concept to resolve species in the *Teratosphaeriaceae*. Persoonia 33: 1–40

Quilhot W, Cuellar M, Díaz R et al. (2012) Lichens of Aisen, Southern Chile. Gayana Botánica 69: 57−87

R Development Core Team (2013, 2014) R: A Language and Environment for Statistical Computing. The R Foundation for Statistical Computing, Vienna, Austria. ISBN: 3-900051-07-0. Disponible en http://www.R-project.org/

Raggio J, Green TGA y Sancho LG (2016) *In situ* monitoring of microclimate and metabolic activity in lichens from Antarctic extremes: a comparison between South Shetland Islands and the McMurdo Dry Valleys. Polar Biology 39: 113−122

Rambold G y Triebel D (1992) The inter-lecanoralean associations. Bibliotheca Lichenologica 48: 1−201

Rannala B (2015) The art and science of species delimitation. Current Zoology 61: 846–853

Raven PH (1963) Amphitropical relationships in the floras of North and South America. The Quarterly Review of Biology 38: 151–177

Reeb V, Haugen P, Bhattacharya D y Lutzoni F (2007) Evolution of *Pleopsidium* (lichenized Ascomycota) S943 Group I introns and the phylogeography of an intron-encoded putative homing endonuclease. Journal of Molecular Evolution 64: 285–298

Reed M (1902) Two new ascomycetous fungi parasitic on marine algae. I. University of California Publications in Botany 1: 141–164

Rehner SA y Samuels GJ (1994) Taxonomy and phylogeny of *Gliocladium* analysed from nuclear large subunit ribosomal DNA sequences. Mycological Research 98: 625−634

Reynolds ES (1963) The use of lead citrate at high pH as an electron-opaque stain in electron microscopy. Journal of Cell Biology 17: 208−212

Richardson DHS y Young CM (1977) Lichens and vertebrates. En MRD Seaward (ed.) Lichen ecology, págs. 121−144. Academic Press, London, UK

Du Rietz E (1926) Den subantarktiska florans bipolära element i lichenologisk belysning. Svenska Botanisk Tidskrift 20: 299–303

Du Rietz E (1940) Problems of bipolar plant distribution. Acta Phytogeographica Svecica 13: 215–282

Rikkinen J (2013) Molecular studies on cyanobacterial diversity in lichen symbioses. MycoKeys 6: 3–32

Rindi F (2010) Reproduction and life history of the green alga *Prasiola linearis* Jao (*Trebouxiophyceae, Chlorophyta*). Botanica Marina 53: 1–7

Rindi F, McIvor L y Guiry MD (2004) The *Prasiolales* (*Chlorophyta*) of Atlantic Europe: an assessment based on morphological, molecular and ecological data, including the characterization of *Rosenvingiella radicans* (Kützing) comb. nov. Journal of Phycology 40: 977–997

Rindi F, McIvor L, Sherwood AR et al. (2007) Molecular phylogeny of the green algal order *Prasiolales* (*Trebouxiophyceae*, *Chlorophyta*). Journal of Phycology 43: 811–822

Rindi F, Mikhailyuk TI, Sluiman HJ et al. (2011) Phylogenetic relationships in *Interfilum* and *Klebsormidium* (*Klebsormidiophyceae*, *Streptophyta*). Molecular Phylogenetics and Evolution 58: 218–231

de los Ríos A y Grube M (2000) Host-parasite interfaces of some lichenicolous fungi in the *Dacampiaceae* (*Dothideales*, Ascomycota). Mycological Research 11: 1348–1353

de los Ríos A y Ascaso C (2001) Preparative techniques for transmission electron microscopy and confocal laser scanning microscopy of lichens. En I Kranner, RP Beckett y AK Varma (eds.) Protocols in lichenology, págs 87–117. Springer-Verlag, Heidelberg, Berlin, DE

de los Ríos A, Ascaso C y Grube M (2002) Infection mechanisms of lichenicolous fungi studied by various microscopic techniques. Bibliotheca Lichenologica 82: 153–161

de los Ríos A, Sancho LG, Grube M et al. (2005) Endolithic growth of two *Lecidea* lichens in granite from continental Antarctica detected by molecular and microscopy techniques. New Phytologist 165: 181–190

de los Ríos A, Wierzchos J y Ascaso C (2014) The lithic microbial ecosystems of Antarctica's McMurdo Dry Valleys. Antarctic Science 26: 459–477

Roca-Valiente B (2013) Estudio filogenético del grupo de "*Rhizocarpon geographicum*" (líquenes, *Rhizocarpaceae*, Ascomycota). Análisis contrastado de los caracteres morfológicos y los patrones biogeográficos. Tesis Doctoral, Universidad Complutense de Madrid, Madrid, ES

Rodríguez R y Redman R (2008) More than 400 million years of evolution and some plants still can't make it on their own: plant stress tolerance via fungal symbiosis. Journal of Experimental Botany 59: 1109–1114

Romeike J, Friedl T, Helms G y Ott S (2002) Genetic diversity of algal and fungal partners in four species of *Umbilicaria* (lichenized ascomycetes) along a transect of the Antarctic Peninsula. Molecular Biology and Evolution 19: 1209–1217

Ronquist F y Sanmartín I (2011) Phylogenetic methods in biogeography. Annual Review of Ecology, Evolution, and Systematics 42: 441–464

Ronquist F, Teslenko M, van der Mark P et al. (2012) MRBAYES 3.2: Efficient Bayesian phylogenetic inference and model choice across a large model space. Systematic Biology 61: 539–542

Rougeux C, Bernatchez L y Gagnaire PA (2016). Modeling the multiple facets of speciation-with-gene-flow towards improving divergence history inference of a recent fish adaptive radiation. bioRxiv 068932

Roux C y Triebel D (1994) Révision des espèces de *Stigmidium* et de *Sphaerellothecium* (champignons lichénicoles non lichénisés, Ascomycetes) correspondant à *Pharcidia epicymatia* sensu Keissler ou à *Stigmidium schaereri* auct. Bulletin de la Société Linnéenne de Provence 45: 451–538

Rozzi R, Armesto JJ, Goffinet B et al. (2008) Changing lenses to assess biodiversity: patterns of species richness in sub-Antarctic plants and implications for global conservation. Frontiers in Ecology and the Environment 6: 131–137

Rudolph ED (1970) Local dissemination of plant propagules in Antarctica. En MW Holdgate (ed.) Antarctic ecology, 2ª ed., págs. 812–817. Academic Press, London, UK

Ruibal C, Gueidan C, Selbmann L et al. (2009) Phylogeny of rock-inhabiting fungi related to *Dothideomycetes*. Studies in Mycology 64: 123−133

Ruibal C, Millanes AM y Hawksworth DL (2011) Molecular phylogenetic studies on the lichenicolous *Xanthoriicola physciae* reveal Antarctic rock-inhabiting fungi and *Piedraia* species among closest relatives in the *Teratosphaeriaceae*. IMA Fungus 2: 97−103

Rundel PW (1978) The ecological role of secondary lichen substances. Biochemical Systematics and Ecology 6: 157–170

Ruprecht U, Lumbsch HT, Brunauer G et al. (2010) Diversity of *Lecidea* (*Lecideaceae*, Ascomycota) species revealed by molecular data and morphological characters. Antarctic Sciences 22: 727–741

Ruprecht U, Brunauer G y Printzen C (2012a) Genetic diversity of photobionts in Antarctic lecideoid lichens from an ecological view point. Lichenologist 44: 661–678

Ruprecht U, Lumbsch HT, Brunauer G et al. (2012b) Insights into the diversity of *Lecanoraceae* (*Lecanorales*, Ascomycota) in continental Antarctica (Ross Sea region). Nova Hedwigia 94: 287–306

Ryan PG, Watkins BP, Lewis Smith RI et al. (1989) Biological survey of Robertskollen, western Dronning Maud Land: area description and preliminary species lists. South African Journal of Antarctic Research 19: 10–20

Ryšánek D, Hrčková K y Škaloud P (2015) Global ubiquity and local endemism of free-living terrestrial protists: phylogeographic assessment of the streptophyte alga *Klebsormidium*. Environmental Microbiology 17: 689–698

Sadowska-Dés AD, Dal Grande F, Lumbsch HT et al. (2014) Integrating coalescent and phylogenetic approaches to delimit species in the lichen photobiont *Trebouxia*. Molecular Phylogenetics and Evolution 76: 202–210

Sadowsky A y Ott S (2016) Symbiosis as a successful strategy in continental Antarctica: performance and protection of *Trebouxia* photosystem II in relation to lichen pigmentation. Polar Biology 39: 139–151

Sancho LG (1986) Flora y vegetación liquénica saxícola de los pisos oro- y crioromediterraneo del Sistema Central español. Tesis Doctoral, Universidad Complutense de Madrid, Madrid, ES

Sancho LG, Green TGA y Pintado A (2007) Slowest to fastest: extreme range in lichen growth rates supports their use as an indicator of climate change in Antarctica. Flora 202: 667–673

Sanders W (2001) Lichens: the interface between mycology and plant morphology. BioScience 51: 1025–1034

Sanders W (2005) Observing microscopic phases of lichen life cycles on transparent substrata placed *in situ*. Lichenologist 37: 373–382

Sanders W y de los Ríos A (2017) Parenchymatous cell division characterizes the fungal cortex of some common foliose lichens. American Journal of Botany doi:10.3732/ajb.1600403

Sanmartín I y Ronquist F (2004) Southern Hemisphere biogeography inferred by event-based models: plant versus animal patterns. Systematic Biology 53: 216–243

Santesson R (1939) Amphibious pyrenolichens I. Arkiv för Botanik 29A 10: 1–67

Saunders GW y Kucera H (2010) An evaluation of *rbcL*, *tufA*, *UPA*, *LSU* and *ITS* as DNA barcode markers for the marine green macroalgae. Cryptogamie Algologie 31: 487–528

Scheidegger C, Bilovitz PO, Werth S et al. (2012) Hitchhiking with forests: population genetics of the epiphytic lichen *Lobaria pulmonaria* in primeval and managed forests in southeastern Europe. Ecology and Evolution 2: 2223–2240

Scher HD, Whittaker JM, Williams SE et al. (2015) Onset of Antarctic Circumpolar Current 30 million years ago as Tasmanian Gateway aligned with Westerlies. Nature 523: 580–583

Schlensog M, Schroeter B, Pannewitz S y Green TGA (2003) Adaptations of mosses and lichens to irradiance stress in maritime and continental habitats. En AHL Huiskes, WWC Gieskes, J Rozema et al. (eds.) Antarctic biology in a global context, págs. 161–166. Backhuys Publishers, Leiden, BE

Schmitt I, Crespo A, Divakar PK et al. (2009) New primers for promising single-copy genes in fungal phylogenetics and systematics. Persoonia 23: 35–40

Schneider S y Excoffier L (1999) Estimation of demographic parameters from the distribution of pairwise differences when the mutation rates vary among sites: application to human mitochondrial DNA. Genetics 152: 1079–1089

Schoch CL, Crous PW, Groenewald JZ et al. (2009) A class-wide phylogenetic assessment of *Dothideomycetes*. Studies in Micology 64: 1–15

Schoch CL, Seifert KA, Huhndorf A et al. (2012) Nuclear ribosomal internal transcribed spacer (*ITS*) region as a universal DNA barcode marker for Fungi. Proceedings of the National Academy of Sciences USA 109: 6241–6246

Schroeter B, Green TGA, Kappen L y Seppelt RD (1994) Carbon dioxide exchange at subzero temperatures: field measurements on *Umbilicaria aprina* in Antarctica. Cryptogamic Botany 4: 233–241

Schroeter B, Green TGA, Pannewitz S et al. (2010) Fourteen degrees of latitude and a continent apart: comparison of lichen activity over two years at continental and maritime Antarctic sites. *Antarctic Science* 22: 681–690

Schwarz G (1978) Estimating the dimension of a model. The Annals of Statistics 6: 461−464

Schwendener S (1869) Die algentypen der Flechtengonidien. Universitäts-Buchdruckerei von C. Schultze, Basel, SUI

Scotese CR (2001) Atlas of Earth history. University of Texas, Arlington, USA

Selbmann L, De Hoog GS, Mazzaglia A et al. (2005). Fungi at the edge of life: cryptoendolithic black fungi from Antarctic desert. Studies in Mycology 51: 1−32

Selbmann L, Grube M, Onofri S et al. (2013) Antarctic epilithic lichens as niches for black meristematic fungi. Biology 2: 784−797

Seppelt RD (1995) Phytogeography of continental Antarctic lichens. Lichenologist 27: 417–431

Seppelt RD, Green TGA y Schroeter B (1995) Lichens and mosses from the Kar Plateau, Southern Victoria Land, Antarctica. New Zealand Journal of Botany 33: 203–220

Seppelt RD, Türk R, Green TGA et al. (2010) Lichen and moss communities of Botany Bay, Granite Harbour, Ross Sea, Antarctica. Antarctic Sciences 22: 691–702

Seymour FA, Crittenden PD y Dyer PS (2005) Sex in the extremes: lichen-forming fungi. Mycologist 19: 51–58

Seymour FA, Crittenden PD, Wirtz N et al. (2007) Phylogenetic and morphological analysis of Antarctic lichen-forming *Usnea* species in the group *Neuropogon*. Antarctic Science 19: 71–82

Shafer A, Cullingham CI, Cote SD y Coltman DW (2010) Of glaciers and refugia: a decade of study sheds new light on the phylogeography of northwestern North America. Molecular Ecology 19: 4589–4621

Sheard JW (1977) Paleogeography, chemistry and taxonomy of the lichenized ascomycetes *Dimelaena* and *Thamnolia*. The Bryologist 80: 100–118

Singh G, Dal Grande F, Werth S y Scheidegger C (2015a) Long-term consequences of disturbances on reproductive strategies of the rare epiphytic lichen *Lobaria pulmonaria*: clonality a gift and a curse. FEMS Microbiology Ecology 91: 1–11

Singh SM, Olech M, Cannone N y Convey P (2015b) Contrasting patterns in lichen diversity in the continental and maritime Antarctic. Polar Science 9: 311–318

Singh G, Dal Grande F, Divakar PK et al. (2016) Fungal–algal association patterns in lichen symbiosis linked to macroclimate. New Phytologist 214: 317–329

Siple PA (1938) The Second Byrd Antarctic expedition –Botany. Annals of the Missouri Botanical Garden 25: 467–514

Škaloud P y Peksa O (2010) Evolutionary inferences based on *ITS* rDNA and actin sequences reveal extensive diversity of the common lichen alga *Asterochloris* (*Trebouxiophyceae*, *Chlorophyta*). Molecular Phylogenetics and Evolution 54: 36–46

Škaloud P y Rindi F (2013) Ecological differentiation of cryptic species within an asexual protist morphospecies: a case study of filamentous green alga *Klebsormidium* (*Streptophyta*). Journal of Eukaryotic Microbiology 60: 350–362

Škaloud P, Friedl T, Hallmann C et al. (2016) Taxonomic revision and species delimitation of coccoid green algae currently assigned to the genus

Dictyochloropsis (*Trebouxiophyceae*, *Chlorophyta*). Journal of Phycology 52: 599–617

Smith CW (1984) Hawaii's alectorioid lichens. Pacific Science 38: 3

Smith CW, Aptroot A, Coppins BJ et al. (2009) The Lichens of Great Britain and Ireland. 2ª ed. British Lichen Society, London, UK

Søchting U (1989) Lignicolous species of the lichen genus *Caloplaca* from Svalbard. Opera Botanica 100: 241–257

Søchting U (1997) Two major anthraquinone chemosyndromes in *Teloschistaceae*. Bibliotheca Lichenologica 68: 135–144

Søchting U y Olech M (1995) The lichen genus *Caloplaca* in polar regions. Lichenologist 27: 463–471

Søchting U y Olech M (2000) *Caloplaca scolecomarginata* spec. nov. and *Caloplaca frigida* spec. nov., two new lichen species from Antarctica. Bibliotheca Lichenologica 15: 19–26

Søchting U y Øvstedal DO (1992) Contributions to the *Caloplaca* flora of the western Antarctic region. Nordic Journal of Botany 12: 121–134

Søchting U y Øvstedal DO (1998) *Caloplaca lewis-smithii*, a new lichen species from continental Antarctica. Mycotaxon 69: 447–451

Søchting U y Seppelt RD (2003) *Caloplaca coeruleofrigida* sp. nova, a lichen from continental Antarctica. Mycotaxon 86: 163–168

Søchting U y Castello M (2012) The polar lichens *Caloplaca darbishirei* and *C. soropelta* highlight the direction of bipolar migration. Polar Biology 35: 1143–1149

Søchting U, Øvstedal DO y Sancho LG (2004) The lichens of Hurd Peninsula, Livingston Island, South Shetlands, Antarctica. Bibliotheca Lichenologica 88: 607–658

Søchting U, Lorentsen LB y Arup U (2008) The lichen genus *Caloplaca* (Ascomycota, *Lecanoromycetes*) on Svalbard. Notes and additions. Nova Hedwigia 87: 69–96

Søchting U, Garrido-Benavent I, Seppelt R et al. (2014a) *Charcotiana* and *Amundsenia*, two new genera in *Teloschistaceae* (lichenized Ascomycota, subfamily *Xanthorioideae*) hosting two new species from continental Antarctica, and *Austroplaca frigida*, a new name for a continental Antarctic species. Lichenologist 46: 763–782

Søchting U, Søgaard MZ, Elix JA et al. (2014b) *Catenarina* (*Teloschistaceae*, Ascomycota), a new Southern Hemisphere genus with 7-chlorocatenarin. Lichenologist 46: 175–187

Sojo F, Valladares F y Sancho LG (1997) Structural and physiological plasticity of the lichen *Catillaria corymbosa* in different microhabitats of the maritime Antarctica. The Bryologist 100: 171–179

Soltis PS, Soltis DE, Savolainen V et al. (2002) Rate heterogeneity among lineages of tracheophytes: integration of molecular and fossil data and evidence for molecular living fossils. Proceedings of the National Academy of Sciences USA, 99: 4430–4435

Sork VL y Werth S (2014) Phylogeography of *Ramalina menziesii*, a widely distributed lichen-forming fungus in western North America. Molecular Ecology 23: 2326–2339

Souza-Egipsy V, Valladares F y Ascaso C (2000) Water distribution in foliose lichen species: interactions between method of hydration, lichen substances and thallus anatomy. Annals of Botany 86: 595–601

Spalik K, Piwczyński M, Danderson CA et al. (2010) Amphitropic amphiantarctic disjunctions in *Apiaceae* subfamily *Apioideae*. Journal of Biogeography 37: 1977–1994

Spieth PT (1974) Gene flow and genetic differentiation. Genetics 78: 961–965

Spribille T (2011) Circumboreal lichen diversification: phylogenetic and phylogeographic studies in the genus *Mycoblastus*. Tesis Doctoral, Karl-Franzens-Universität Graz, Graz, AT

Spribille T, Klug B y Mayrhofer H (2011) A phylogenetic analysis of the boreal lichen *Mycoblastus sanguinarius* (*Mycoblastaceae*, lichenized Ascomycota) reveals cryptic clades correlated with fatty acid profiles. Molecular Phylogenetics and Evolution 59: 603–614

Spribille T, Tuovinen V, Resl P et al. (2016) Basidiomycete yeasts in the cortex of ascomycete macrolichens. Science 353: 488–492

Stamatakis A (2006) RAxML-VI-HPC: maximum likelihood-based phylogenetic analyses with thousands of taxa and mixed models. Bioinformatics 22: 2688−2690

Stamatakis A, Hoover P y Rougemont J (2008) A rapid bootstrap algorithm for the RAxML web servers. Systematic Biology 57: 758–771

Van Steenis CGGJ (1962) The mountain flora of the Malaysian tropics. Endeavour 21: 183–193

Steeves TE, Anderson DJ y Friesen VL (2005) The Isthmus of Panama: a major physical barrier to gene flow in a highly mobile pantropical seabird. Journal of Evolutionary Biology 18: 1000–1008

Stenroos S (1991) The lichen genera *Parmelia* and *Punctelia* in Tierra del Fuego. Annales Botanici Fennici 28: 241–245

Stenroos S (1993) Taxonomy and distribution of the lichen family *Cladoniaceae* in the Antarctic and peri-Antarctic regions. Cryptogamic Botany 3: 310–344

Stenroos S y Ahti T (1990) The lichen family *Cladoniaceae* in Tierra del Fuego: problematic or otherwise noteworthy taxa. Annales Botanici Fennici 27: 317–327

Stenroos S y Ahti T (1992) The lichen family *Cladoniaceae* in the Falkland Islands. Annales Botanici Fennici 29: 67–73

Stenroos S, Velmala S, Pykälä J y Ahti T (2016) Lichens of Finland. Norrlinia 30: 1–896

Sterflinger K (2006) Black yeasts and meristematic fungi: ecology, diversity and identification. En G Péter y C Rosa (eds.) Biodiversity and ecophysiology of yeasts, págs. 501−514. Springer Berlin, Heidelberg, DE

Stielow JB, Lévesque CA, Seifert KA et al. (2015) One fungus, which genes? Development and assessment of universal primers for potential secondary fungal DNA barcodes. Persoonia 35: 242

Stubbs CS (1995) Dispersal of soredia by the oribatid mite, *Humerobates arborea*. Mycologia 87: 454–458

Sturge RJ, Cortés-Rodríguez MN, Rojas-Soto OR y Omland KE (2016) Nuclear locus divergence at the early stages of speciation in the Orchard Oriole complex. Ecology and Evolution 6: 4307–4317

Suchard MA y Rambaut A (2009) Many-core algorithms for statistical phylogenetics. Bioinformatics 25: 1370–1376

Sugden DE, Bentley MJ y Cofaigh Ó (2006) Geological and geomorphological insights into Antarctic ice sheet evolution. Philosophical Transactions of the Royal Society A 364: 1607–1625

Suija A, Ertz D, Lawrey JD y Diederich P (2014) Multiple origin of the lichenicolous life habit in *Helotiales*, based on nuclear ribosomal sequences. Fungal Diversity 70: 55–72

Sukumaran J y Knowles LL (2017) Multispecies coalescent delimits structure, not species. Proceedings of the National Academy of Sciences USA 114: 1607–1612

Sul WJ, Oliver TA, Ducklow HW et al. (2013) Marine bacteria exhibit a bipolar distribution. Proceedings of the National Academy of Sciences USA 110: 2342–2347

Summerfield TC y Eaton-Rye JJ (2006) *Pseudocyphellaria crocata*, *P. neglecta* and *P. perpetua* from the Northern and Southern Hemispheres are a phylogenetic species and share cyanobionts. New Phytologist 170: 597–607

Swofford DL (2002) PAUP*: Phylogenetic Analysis Using Parsimony (*and Other Methods). Version 4.0b10. Sinauer Associates, Sunderland, MA, USA

Taberlet P, Fumagalli L, Wust-Saucy AG y Cosson JF (1998) Comparative phylogeography and postglacial colonization routes in Europe. Molecular Ecology 7: 453–464

Takamatsu S y Matsuda S (2004) Estimation of molecular clocks for *ITS* and *28S* rDNA in *Erysiphales*. Mycoscience 45: 340–344

Talavera G, Dinca V y Vila R (2013) Factors affecting species delimitations with the GMYC model: insights from a butterfly survey. Methods in Ecology and Evolution 4: 1101–1110

Tamura K, Peterson D, Peterson N et al. (2011) MEGA5: molecular evolutionary genetics analysis using maximum likelihood, evolutionary distance and maximum parsimony methods. Molecular Biology and Evolution 28: 2731–2739

Tauber CA, Tauber MJ y Albuquerque GS (2014) Debris-carrying in larval *Chrysopidae*: unraveling its evolutionary history. Annals of the Entomological Society of America 107: 295–314

Taylor JW y Berbee ML (2006) Dating divergences in the Fungal Tree of Life: review and new analyses. Mycologia 98: 838–849

Tedersoo L, Bahram M, Polme S et al. (2014) Global diversity and geography of soil fungi. Science 346: 1052–1053

Thell A, Berbee M y Miao V (1998) Phylogeny within the genus *Platismatia* based on rDNA *ITS* sequences (lichenized Ascomycota). Cryptogamie: Bryologie and Lichénologie 19: 307–319

Thell A, Stenroos S y Myllys L (2000) A DNA study of the *Cetraria aculeata* and *C. islandica* groups. Folia Cryptogamica Estonica 36: 85–106

Thell A, Stenroos S, Feuerer T et al. (2002) Phylogeny of cetrarioid lichens (*Parmeliaceae*) inferred from *ITS* and *β-tubulin* sequences, morphology, anatomy and secondary chemistry. Mycological Progress 1: 335–354

Thomsen PF y Willerslev E (2015) Environmental DNA –an emerging tool in conservation for monitoring past and present biodiversity. Biological Conservation 183: 4–18

Thomson JW (1984) American Arctic lichens. 1. Macrolichens. Columbia University Press, NY, USA

Thüs H, Muggia L, Pérez-Ortega S et al. (2011) Revisiting photobiont diversity in the lichen family *Verrucariaceae* (Ascomycota). European Journal of Phycology 46: 399–415

Tin T, Fleming ZL, Hughes KA et al. (2009) Impacts of local human activities on the Antarctic environment. Antarctic Science 21: 3–33

Tormo R, Recio D, Silva I y Muñoz AF (2001) A quantitative investigation of airborne algae and lichen soredia obtained from pollen traps in south-west Spain. European Journal of Phycology 36: 385–390

Torrey J (1823) Description of a new species of *Usnea*, from New South Shetland. The American Journal of Science and Arts 6: 104–106

Tschermak-Woess E (1988) The algal partner. En M Galun (ed.) Handbook of lichenology, vol. 1, págs. 39–92. CRC Press, Boca Raton, FL, USA

Turner J, Anderson P, Lachlan-Cope T et al. (2009) Record low surface air temperature at Vostok station, Antarctica. Journal of Geophysical Research 114: D24102

U'Ren JM, Lutzoni F, Miadlikowska J y Arnold AE (2010) Community analysis reveals close affinities between endophytic and endolichenic fungi in mosses and lichens. Microbial Ecology 60: 340–353

U'Ren JM, Lutzoni F, Miadlikowska J et al. (2012) Host and geographic structure of endophytic and endolichenic fungi at a continental scale. American Journal of Botany 99: 898–914

Vainio EA (1903) Lichens. Résultats du voyage du S.Y. Belgica en 1897-1898-1899: sous le commandement de A. de Gerlache de Gomery. Rapports scientifiques publiés aux frais du gouvernement belge, sous la direction de la Commission de la Belgica, págs. 1–46

Valladares F, Sancho LG y Ascaso C (1998) Water storage in the lichen family *Umbilicariaceae*. Botanica Acta 111: 99–107

Vančurová L, Peksa O, Němcová Y y Škaloud P (2015) *Vulcanochloris* (*Trebouxiales*, *Trebouxiophyceae*), a new genus of lichen photobiont from La Palma, Canary Islands, Spain. Phytotaxa 219: 118–132

de Vera J-P, Horneck G, Rettberg P y Ott S (2003) The potential of the lichen symbiosis to cope with extreme conditions of outer space –I. Influence of UV radiation and

space vaccum on the vitality of lichen symbiosis and germination capacity. International Journal of Astrobiology 1: 285–293

Verbruggen H (2014) Morphological complexity, plasticity, and species diagnosability in the application of old species names in DNA-based taxonomies. Journal of Phycology 50: 26–31

Viana DS, Gangoso L, Bouten W y Figuerola J (2016) Overseas seed dispersal by migratory birds. Proceedings of the Royal Society, Biological Sciences 283: 20152406

van de Vijver B, Gremmen NJM y Beyens L (2005) The genus *Stauroneis* (*Bacillariophyceae*) in the Antarctic region. Journal of Biogeography 32: 1791–1798

Vilgalys R y Hester M (1990) Rapid genetic identification and mapping of enzymatically amplified ribosomal DNA from several *Cryptococcus* species. Journal of Bacteriology 172: 4238−4246

Villaverde T, Martín-Bravo S, Escudero M y Luceño M (2012) Extreme phylogeography in *Carex* (*Cyperaceae*). Informatore Botanico Italiano 44: 58–61

Villaverde T, Escudero M, Luceño M y Martín-Bravo S (2015a) Long-distance dispersal during the middle-late Pleistocene explains the bipolar disjunction of *Carex maritima* (*Cyperaceae*). Journal of Biogeography 42: 1820–1831

Villaverde T, Escudero M, Martín-Bravo S et al. (2015b) Direct long-distance dispersal best explains the bipolar distribution of *Carex arctogena* (*Carex* sect. *Capituligerae*, *Cyperaceae*). Journal of Biogeography 42: 1514–1525

Villesen P (2007) FABOX: an online toolbox for fasta sequences. Molecular Ecology Notes 7: 965–968

Vondrák J, Pavel ŘÍHA, Arup U y Søchting, U (2009). The taxonomy of the *Caloplaca citrina* group (*Teloschistaceae*) in the Black Sea region; with contributions to the cryptic species concept in lichenology. Lichenologist 41: 571–604

Vondrák J, Šoun J, Søgaard MZ et al. (2010) *Caloplaca phlogina*, a lichen with two facies; an example of infraspecific variability resulting in the description of a redundant species. Lichenologist 42: 685–692

Vondrák J, Frolov I, Arup U y Khodosovtsev A (2013) Methods for phenotypic evaluation of crustose lichens with emphasis on *Teloschistaceae*. Chornomorski Botanical Journal 9: 382–405

Walker FJ (1985) The lichen genus *Usnea* subgenus *Neuropogon*. Bulletin of the British Museum (Natural History), Botany series 13: 1–130

Wallace AR (1880) Island Life. McMillan and Co, London, UK

Walser JC, Holderegger R, Gugerli F et al. (2005) Microsatellites reveal regional population differentiation and isolation in *Lobaria pulmonaria*, an epiphytic lichen. Molecular Ecology 14: 457–467

Weber WA y Wetmore CM (1972) Catalogue of the lichens of Australia. Beihefte Nova Hedwigia 41: 1–136

Wedin M, Döring H y Gilenstam G (2004) Saprotrophy and lichenization as options for the same fungal species on different substrata: environmental plasticity and fungal lifestyles in the *Stictis-Conotrema* complex. New Phytologist 164: 459–465.

Wedin M, Högnabba F y Goward T (2009) A new species of *Sphaerophorus*, and a key to the family *Sphaerophoraceae* in western North America. The Bryologist 112: 368–374

Wei X, McCune B, Lumbsch HT et al. (2016) Limitations of species delimitation based on phylogenetic analyses: a case study in the *Hypogymnia hypotrypa* group (*Parmeliaceae*, Ascomycota). PloS ONE 11: e0163664

Weir BS y Cockerham CC (1984) Estimating F-statistics for the analysis of population structure. Evolution 38: 1358–1370

Wen J (1999) Evolution of eastern Asian and eastern North American disjunct distributions in flowering plants. Annual Review of Ecology and Systematics 30: 421–455

Wen J y Ickert-Bond SM (2009) Evolution of the Madrean-Tethyan disjunctions and the North and South American amphitropical disjunctions in plants. Journal of Systematics and Evolution 47: 331–348

Werth S (2010) Population genetics of lichen-forming fungi –a review. Lichenologist 42: 499–519

Werth S (2011) Biogeography and phylogeography of lichen fungi and their photobionts. En D Fontaneto (ed.) Biogeography of microscopic organisms: is everything small everywhere? págs. 191–208. Cambridge University Press, Cambridge, UK

Werth S y Sork VL (2010) Identity and genetic structure of the photobiont of the epiphytic lichen *Ramalina menziesii* on three oak species in southern California. American Journal of Botany 97: 821–830

Werth S y Sork VL (2014). Ecological specialization in *Trebouxia* (*Trebouxiophyceae*) photobionts of *Ramalina menziesii* (*Ramalinaceae*) across six range-covering

ecoregions of western North America. American Journal of Botany 101: 1127–1140

Werth S, Millanes AM, Wedin M y Scheidegger C (2013) Lichenicolous fungi show population subdivision by host species but do not share population history with their hosts. Fungal Biology 117: 71–84

Werth S, Miao VPW, Jónsson ZO y Andrésson ÓS (2015) High-Throughput sequencing in studies of lichen population biology. En DK Upreti, PK Divakar, V Shukla y R Bajpai (eds.) Recent advances in lichenology, vol. 2, págs. 61–94. Springer India, IN

Werth S, Reynisdóttir S, Gudmundsson H y Andrésson ÓS (2016) A fast and inexpensive high-throughput protocol for isolating high molecular weight genomic DNA from lichens. Herzogia 29: 610–616

Wetmore CM (1963) Catalogue of the lichens of Tasmania. Revue Bryologique et Lichénologique 32: 223–264

Wetmore CM (1996) The *Caloplaca sideritis* group in North and Central America. The Bryologist 99: 292–314

De Wever A, Leliaert F, Verleyen E et al. (2009) Hidden levels of phylodiversity in Antarctic green algae: further evidence for the existence of glacial refugia. Proceedings of the Royal Society, Biological science 276: 3591–3599

White TJ, Bruns T, Lee S y Taylor J (1990) Amplification and direct sequencing of fungal ribosomal RNA genes for phylogenetics. En MA Innis, DH Gelfand, JJ Sninsky y TJ White (eds.) PCR Protocols: a guide to methods and applications, págs. 315–322. Academic Press, San Diego, CA, USA

Widmer I, Dal Grande F, Excoffier L et al. (2012) European phylogeography of the epiphytic lichen fungus *Lobaria pulmonaria* and its green algal symbiont. Molecular Ecology 21: 5827–5844

Wiens JJ (2007) Species delimitation: new approaches for discovering diversity. Systematic Biology 56: 875–878

Wilkinson DM, Koumoutsaris S, Mitchell EAD y Bey I (2012) Modelling the effect of size on the aerial dispersal of microorganisms. Journal of Biogeography 39: 89–97

Will KW, Mishler BD y Wheeler QD (2005) The perils of DNA barcoding and the need for integrative taxonomy. Systematic Biology 54: 844–851

Werth S, Wagner HH, Gugerli F et al. (2006) Quantifying dispersal and establishment limitation in a population of an epiphytic lichen. Ecology 87: 2037–2046

Winkworth RC, Hennion F, Prinzing A y Wagstaff SJ (2015) Explaining the disjunct distributions of austral plants: the roles of Antarctic and direct dispersal routes. Journal of Biogeography 42: 1197–1209

Wirtz N, Lumbsch HT, Green TGA et al. (2003) Lichen fungi have low cyanobiont selectivity in maritime Antarctica. New Phytologist 160: 177–183

Wirtz N, Printzen C y Lumbsch HT (2008) The delimitation of Antarctic and bipolar species of neuropogonoid *Usnea* (Ascomycota, *Lecanorales*): a cohesion approach of species recognition for the *Usnea perpusilla* complex. Mycological Research 112: 472–484

Wirtz N, Printzen C y Lumbsch HT (2012) Using haplotype networks, estimation of gene flow and phenotypic characters to understand species delimitation in fungi of a predominantly Antarctic *Usnea* group (Ascomycota, *Parmeliaceae*). Organisms, Diversity and Evolution 12: 17–37

Wolfe EW, Wise SW y Dalrymple B (1997) The geology and petrology of Mauna Kea Volcano, Hawaii –a study of post-shield volcanism. U.S. Geological Survey Professional Paper 1557: 129

Wornik S y Grube M (2010) Joint dispersal does not imply maintenance of partnerships in lichen symbioses. Microbial Ecology 59: 150–157

Xie W, Lewis PO, Fan Y et al. (2011) Improving marginal likelihood estimation for Bayesian phylogenetic model selection. Systematic Biology 60: 150–160

Yahr R, Vilgalys R y Depriest PT (2004) Strong fungal specificity and selectivity for algal symbionts in Florida scrub *Cladonia* lichens. Molecular Ecology 13: 3367–3378

Yahr R, Vilgalys R y DePriest PT (2006) Geographic variation in algal partners of *Cladonia subtenuis* (*Cladoniaceae*) highlights the dynamic nature of a lichen symbiosis. New Phytologist 171: 847–860

Yang Z y Rannala B (2010) Bayesian species delimitation using multi-locus sequence data. Proceedings of the National Academy of Sciences USA 107: 9264–9269

Yang Z y Donoghue PCJ (2016) Dating species divergences using rocks and clocks. Philosophical Transactions of the Royal Society B 371: 20150126

Ye J, Coulouris G, Zaretskaya I et al. (2012) PRIMER-BLAST: a tool to design target-specific primers for polymerase chain reaction. BMC Bioinformatics 13: 134

Yung CC, Chan Y, Lacap DC et al.(2014) Characterization of chasmoendolithic community in Miers Valley, McMurdo Dry Valleys, Antarctica. Microbial Ecology 68: 351–359

Zachos J, Pagani M, Sloan L et al. (2001) Trends, rhythms, and aberrations in global climate 65 MA to present. Science 292: 686–693

Zachos J, Dickens GR y Zeebe RE (2008) An early Cenozoic perspective on greenhouse warming and carbon-cycle dynamics. Nature 451: 279–283

Zedane L, Hong-Wa C, Murienne J et al. (2016) Museomics illuminate the history of an extinct, paleoendemic plant lineage (*Hesperelaea, Oleaceae*) known from an 1875 collection from Guadalupe Island, Mexico. Biological Journal of the Linnean Society 117: 44–57

Zhang J (2015) Species Delimitation Server. The Exelixis Lab, Scientific Computing Group, Heidelberg Institute for Theoretical Studies. Disponible en http://species.h-its.org/

Zhang J, Kapli P, Pavlidis P y Stamatakis A (2013) A general species delimitation method with applications to phylogenetic placements. Bioinformatics 29: 2869–2876

Zhou S y Stanosz GR (2001) Primers for amplification of *mtSSU* rDNA, and a phylogenetic study of *Botryosphaeria* and associated anamorphic fungi. Mycological Research 105: 1033–1044

Zhurbenko MP (2009a) Arctic lichenicolous mycota: an invisible diversity. Species and communities in extreme environments. En SI Golovatch, OL Makarova, AB Babenko y Penev LD (eds.) Festschrift towards the 75th anniversary and a Laudatio in honour of academician Yuri Ivanovich Chernov, págs. 225−233. Pensoft Publishers & KMK Scientific Press, Sofia-Moscow, RUS

Zhurbenko MP (2009b) Lichenicolous fungi and some lichens from the Holarctic. Opuscula Philolichenum 6: 87−120

Zhurbenko MP (2010) Lichenicolous fungi and lichens growing on *Stereocaulon* from the Holarctic, with a key to the known species. Opuscula Philolichenum 8: 9−39

Zhurbenko MP y Laursen G (2003) Lichenicolous fungi from Central Alaska: new records and range extensions. The Bryologist 106: 460−464

Zimmer A, Lang D, Richardt S et al. (2007) Dating the early evolution of plants: detection and molecular clock analyses of orthologs. Molecular Genetics and Genomics 278: 393–402

Zoller S, Lutzoni F y Scheidegger C (1999) Genetic variation within and among populations of the threatened lichen *Lobaria pulmonaria* in Switzerland and implications for its conservation. Molecular Ecology 8: 2049–2059

Zúñiga C, Leiva D, Carú M y Orlando J (2017) Substrates of *Peltigera* lichens as a potential source of cyanobionts. Microbial Ecology doi:10.1007/s00248-017-0969-z

FIGURAS, TABLAS Y ANEXOS

INTRODUCCIÓN

METODOLOGÍA

CAPÍTULO 1 (*CHAPTER 1*)

CAPÍTULO 2 (*CHAPTER 2*)

CAPÍTULO 3 (*CHAPTER 3*)

CAPÍTULO 4 (*CHAPTER 4*)

CAPÍTULO 5 (*CHAPTER 5*)

CAPÍTULO 6 (*CHAPTER 6*)

CAPÍTULO 7 (*CHAPTER 7*)

ANEXO I

Autores de los nombres científicos

Acarospora macrocyclos Vain.

Alectoria Ach.

Alectoria ochroleuca subsp. *vexillifera* Nyl.

Amandinea punctata (Hoffm.) Coppins & Scheid.

Amundsenia Søchting, Garrido-Benavent, Arup & Frödén

Amundsenia approximata (Lynge) Søchting, Arup & Frödén

Amundsenia austrocontinentalis Garrido-Benavent, Søchting, Pérez-Ortega & Seppelt

Ardenna grisea Gmelin

Arthoniales Henssen ex D. Hawksw. & O.E. Erikss.

Arthrorhaphis Th. Fr.

Arthrorhaphis alpina (Schaer.) R. Sant.

Arthrorhaphis citrinella (Ach.) Poelt

Ascomycota Caval.-Sm.

Asterochloris Tschermak-Woess

Asterochloris sejongensis J.I. Kim & W. Shin

Austrolecia Hertel

Austroplaca Søchting, Frödén & Arup

Austroplaca darbishirei (Dodge & Baker) Søchting, Frödén & Arup

Austroplaca frigida Søchting & Garrido-Benavent

Austroplaca soropelta (Hansen, Poelt & Søchting) Søchting, Frödén & Arup

Austrostigmidium Pérez-Ortega & Garrido-Benavent

Austrostigmidium mastodiae Pérez-Ortega & Garrido-Benavent

Bacidia De Not.

Bacidia stipata I.M. Lamb

Bryoria bicolor (Ehrh.) Brodo & D. Hawksw

Bryum argenteum Hedw.

Buellia De Not.

Buellia anisomera Vain.

Buellia frigida Darb.

Calogaya Arup, Frödén & Søchting

Caloplaca Th. Fr.

Caloplaca agrata (Vain.) Zahlbr.

Caloplaca approximata (Lynge) H.Magn.

Caloplaca cacuminum Poelt

Caloplaca cladodes (Tuck.) Zahlbr.

Caloplaca coeruleofrigida Søchting & Seppelt

Caloplaca darbishirei (Dodge & Baker) Cretz.

Caloplaca erecta Arup & H. Mayrhofer

Caloplaca exsecuta (Nyl.) Dalla Torre & Sarnth.

Caloplaca frigida Søchting

Caloplaca hueana de Lesd.

Caloplaca lewis-smithii Søchting & Øvstedal

Caloplaca magni-filii Poelt

Caloplaca pellodella (Nyl.) Hasse

Caloplaca phlogina (Ach.) Flagey

Caloplaca psoromatis Olech & Søchting

Caloplaca scolecomarginata Søchting & Olech

Caloplaca sideritis (Tuck.) Zahlbr.

Caloplaca sonorae Wetmore

Caloplaca soropelta (Hansen, Poelt & Søchting) Søchting

Caloplacoideae Arup, Søchting & Frödén

Candelariella Müll. Arg.

Capnodiales Woron.

Capnodium coffeae Pat.

Carex L.

Catillaria corymbosa (Hue) I.M. Lamb

Cavernularia hultenii Degel.

Cerothallia Arup, Frödén & Søchting

Cetraria Ach.

Cetraria aculeata (Schreb.) Fr.

Chaetothyriales M.E. Barr

Charadriiformes Huxley

Charcotiana Søchting, Garrido-Benavent & Arup

Charcotiana antarctica Søchting, Garrido-Benavent, Pérez -Ortega, Seppelt & Castello

Chlorellaceae Brunnthaler

Chlorophyceae Wille

Chlorophyta Reichenbach

Cinclidium Sw.

Cladonia Hill ex Browne

Cladonia arbuscula (Wallr.) Flot.

Cladonia mitis Sandst.

Cladoniaceae Zenker

Clauzadella Nav.−Ros. & Cl. Roux

Coccomyxa Schmidle

Coenogonium Ehrenb.

Collemopsidium Nyl.

Colobanthus quitensis (Humboldt, Bonpland & Kunth) Bartl.

Conotrema Tuck.

Constantinomyces Egidi & Onofri

Cyanophora paradoxa Korshikov

Cystocoleus Thwaites

Deschampsia antarctica Desvaux

Desmococcus F. Brand

Dictyochloropsis Geitler

Diplosphaera M.W. Bialosuknia

Dothideomycetes O.E. Erikss. & Winka

Dufourea Ach. in Luyken

Durvillaea antarctica (Chamisso) Hariot

Elasticomyces Zucconi & Selbmann

Elasticomyces elasticus Zucconi & Selbmann

Elliptochloris bilobata Tschermak-Woess

Empetrum L.

Ephebe Fr.

Epibryaceae S. Stenroos & C. Gueidan

Epibryon Döbbeler

Erysiphales E. Warming

Eurotiomycetes O.E. Erikss. & Winka

Flavocetraria Kärnefelt & A. Thell

Flavocetraria cucullata (Bellardi) Kärnefelt & A. Thell

Flavocetraria nivalis (L.) Kärnefelt & A. Thell

Friedmanniomyces Onofri

Friedmanniomyces endolithicus Onofri

Friedmanniomyces simplex Selbmann, de Hoog, Mazzaglia, Friedmann & Onofri

Gigartina skottsbergii Setchell & N. L. Gardner

Gloeocapsa Kützing

Gondwania Søchting, Frödén & Arup

Guignardia alaskana Reed

Gunnera magellanica Lam.

Gyalolechia stipitata (Wetmore) Søchting, Frödén & Arup

Huea C.W. Dodge & G.E. Baker

Huea coralligera (Hue) C.W. Dodge & G.E. Baker

Lecania Massal.

Lecania brialmontii (Vain.) Zahlbr.

Lecanora Ach.

Lecanora fuscobrunnea C.W. Dodge & G.E. Baker

Lecanora mons-nivis Darb.

Lecanora physciella (Darb.) Hertel

Lecanora polytropa (Ehrh.) Rabenh.

Lecanoraceae Körb.

Lecidea Ach.

Lecidea atrobrunnea (DC.) Schaer.

Lecidea cancriformis C. W. Dodge & G. E. Baker

Lecideaceae Chevall.

Lepraria borealis Loht. & Tønsberg

Leproplaca xantholyta (Nyl.) Nyl.

Leptoxyphium fumago (Woron.) R.C. Srivast.

Lichenomphalia Redhead, Lutzoni, Moncalvo & Vilgalys

Lichenomphalia umbellifera (L.) Redhead, Lutzoni, Moncalvo & Vilgalys

Lichenostigmatales Ertz, Diederich & Lawrey

Lilaeopsis Greene

Lobaria pulmonaria (L.) Hoffm.

Massalongia carnosa (Dicks.) Körb.

Mastodia Hook. f. & Harv.

Mastodia tessellata (Hook. f. & Harv.) Hook. f. & Harv

Melanelixia O. Blanco, A. Crespo, Divakar, Essl., D. Hawksw. & Lumbsch

Melanohalea O. Blanco, A. Crespo, Divakar, Essl., D. Hawksw. & Lumbsch

Montanelia Divakar, A. Crespo, Wedin & Essl.

Monticola Selbmann & Egidi

Monticola elongata Selbmann & Egidi

Muellerella pygmaea (Körb.) D. Hawksw.

Munroa Torr.

Nannochloris normandinae Tschermak-Woess

Neuropogon Nees & Flotow

Nostoc Vaucher ex Bornet & Flahault

Nothofagus Blume

Ochrolechia frigida (Sw.) Lynge

Ostropales Nannf.

Pachypeltis Søchting, Arup & Frödén

Pannaria hookeri (Borrer) Nyl.

Parmelia Ach.

Parmelia saxatilis (L.) Ach.

Parmelia serrana A. Crespo, M.C. Molina & D. Hawksw.

Parmeliaceae Zenker

Parmelina carporrhizans (Taylor) Poelt & Vězda

Parvoplaca tiroliensis (Zahlbruckner) Arup, Søchting & Frödén

Peltigera Willd.

Peltigerales Watson

Pertusaria corallophora Vain.

Physcia (Schreb.) Michx.

Physcia aipolia (Ehrh. ex Humb.) Fürnr.

Physcia caesia (Hoffm.) Hampe ex Fürnr.

Physciaceae Zahlbr.

Placopsis (Nyl.) Linds.

Platismatia W.L. Culb. & C.F. Culb.

Pleopsidium Körb.

Pleopsidium chlorophanum (Wahlenb.) Zopf

Pleopsidium flavum Körb.

Pleurosticta acetabulum (Neck.) Elix & Lumbsch

Polycauliona candelaria (L.) Frödén, Arup & Søchting

Polychaeton citri (Pers.) Lév.

Prasiola (C. Agardh) Meneghini

Prasiola antarctica Kützing

Prasiola borealis M. Reed

Prasiola crispa (Lightfoot) Kützing

Prasiola crispa ssp. *antarctica* (Kützing) Knebel

Prasiola delicata Setchell & N.L. Gardner

Prasiola furfuracea (Mertens ex Hornemann) Trevisan

Prasiola glacialis M.B.J. Moniz, Rindi, Novis, Broady & Guiry

Prasiola linearis C.-C. Jao

Prasiola meridionalis Setchell & N.L. Gardner

Prasiola novaezelandiae S. Heesch & W. A. Nelson

Prasiola stipitata Suhr ex Jessen

Prasiolaceae F. F. Blackman & A. G. Tansley

Prasiolales F. E. Fritsch

Prasiolopsis ramosa Vischer

Procellariidae Leach

Protopannaria (Gyeln.) P.M. Jørg. & S. Ekman

Pseudephebe M. Choisy

Pseudephebe minuscula (Arnold) Brodo & D. Hawksw.

Pseudephebe pubescens (L.) M. Choisy

Pseudocyphellaria Vain.

Pseudocyphellaria crocata (L.) Vain.

Pseudocyphellaria neglecta (Müll. Arg.) H. Magn.

Pseudocyphellaria perpetua McCune & Miadl.

Pseudostigmidium Etayo

Pseudostigmidium biseptatum Etayo

Pseudostigmidium nephromiarium (Linds.) Etayo

Pyrenodesmia A. Massal.

Racodium Pers.: Fr.

Rhizocarpon geographicum (L.) DC.

Rhizoplaca Zopf

Rhizoplaca melanophthalma (DC.) Leuckert

Rinodina olivaceobrunnea C.W. Dodge & G.E. Baker

Rosenvingiella P.C. Silva

Rosenvingiellopsis Heesch, M. Pazoutová & Rindi

Rusavskia elegans (Link) S. Y. Kondr. & Kärnefelt

Sarmentypnum Tuom. & T. J. Kop.

Shackletonia Søchting, Frödén & Arup

Shackletonia buelliae (Olech & Søchting) Søchting, Frödén & Arup

Shackletonia cryodesertorum Garrido-Benavent, Søchting & Pérez-Ortega

Shackletonia hertelii (Søchting, Øvstedal & Sancho) Søchting, Frödén & Arup

Shackletonia insignis (Søchting & Øvstedal) Søchting, Frödén & Arup

Shackletonia sauronii (Søchting & Øvstedal) Søchting, Frödén & Arup

Shackletonia siphonospora (Olech & Søchting) Søchting, Frödén & Arup

Scytonema Agardh ex Bornet & Flahault

Solorina Ach.

Sphaerellothecium Zopf

Sphaerophorus Pers.

Sphaerophorus globosus (Huds.) Vain.

Sphaerophorus venerabilis Wedin, Högnabba & Goward

Squamulea Arup, Søchting & Frödén

Staurolemma omphalarioides (Anzi) Jørg. & Henssen

Staurothele Norman

Stercorariidae Gray

Stereocaulon Hoffm.

Stichococcus Nägeli

Stictis Pers.

Stigmidium Trevis

Stigmidium acetabuli Calat. & Triebel

Stigmidium placynthii Cl. Roux & Nav.-Ros.

Stigmidium psorae (Anzi) Hafellner

Stigonema Agardh ex Bornet & Flahault

Streptophyta Jeffrey

Syntrichia sarconeurum Ochyra & R. H. Zander

Teloschistaceae Zahlbr.

Teloschistoideae Arup, Søchting & Frödén

Tephromela atra (Huds.) Hafellner

Teratosphaeriaceae Crous & U. Braun

Tetraplodon Bruch & Schimp.

Thamnolia Ach. ex Schaer.

Thamnolia vermicularis (Sw.) Schaer.

Trebouxia Puymaly

Trebouxia arboricola Puymaly

Trebouxia decolorans Ahmadjian

Trebouxia incrustata Ahmadjian ex Gärtner

Trebouxia cf. *impressa* Ahmadjian

Trebouxiophyceae Friedl

Trentepohlia Martius

Trentepohliales Chadefaud ex Thompson & Wujek

Tuckermannopsis Gyeln

Ulvophyceae Mattox & Stewart

Umbilicaria Hoffm.

Umbilicaria aprina Nyl.

Umbilicaria decussata (Vill.) Zahlbr.

Usnea Dill. ex Adans.

Usnea antarctica Du Rietz

Usnea lambii (Imshaug) Wirtz & Lumbsch

Usnea sphacelata R. Br.

Usnea ushuaiensis (I.M. Lamb) Wirtz, Printzen & Lumbsch

Verrucaria Schrad.

Verrucaria tessellatula Nyl.

Verrucariaceae Zenker

Verrucariales Mattick ex D. Hawksw. & O.E. Erikss.

Viridiplantae Cavalier-Sm.

Xanthocarpia A. Massal. & De Not.

Xanthomendoza Kondr. & Kärnefelt

Xanthomendoza borealis (Sant. & Poelt) Søchting

Xanthopeltis Sant.

Xanthoria (Fr.) Th. Fr.

Xanthoria elegans (Link) Th. Fr.

Xanthoria parietina (L.) Beltr.

Xanthoriicola D. Hawksw.

Xanthoriicola physciae (Kalchbr.) D. Hawksw.

Xanthorioideae Arup, Søchting & Frödén

Zea mays L.

Zwackhiomyces coepulonus (Norman) Grube & R. Sant.

ANEXO II

Glosario

Biogeografía ("*biogeography*", en inglés): constituye un campo multidisciplinar de la biología enfocado principalmente al estudio de los patrones de distribución actuales e históricos de los organismos, y que propone y compara hipótesis para explicarlos.

Biotipo ("*growth form*", en inglés): se refiere a la forma de vida o apariencia externa del talo liquénico, que es determinada principalmente por el micobionte. Raramente es el fotobionte quien la determina (p. ej. en los géneros filamentosos *Coenogonium, Ephebe, Cystocoleus* y *Racodium*). Tradicionalmente se han establecido tres biotipos liquénicos: crustáceo, foliáceo y fruticuloso. Existen otros biotipos adicionales, como por ejemplo el gelatinoso, que se presenta en muchos líquenes que tienen como fotobionte a cianobacterias.

Coalescencia, Teoría de la ("*Coalescence Theory*", en inglés): es un marco conceptual dentro de la genética de poblaciones que analiza las propiedades actuales de las poblaciones y permite inferir los procesos históricos que han tenido un efecto sobre ellas a partir de las genealogías de genes. Está basada en un modelo matemático de divergencia de linajes y deriva genética que concibe la variación genética como un proceso estocástico y permite reconstruir en el tiempo los eventos genéticos poblacionales hasta el ancestro común.

Corriente Circumpolar Antártica, ACC ("*Antarctic Circumpolar Current, CCA*", en inglés): es la corriente oceánica más potente del mundo que envuelve al continente antártico, fluyendo en dirección Este.

Dispersión ("*dispersal*" o "*dispersion*", en inglés): es un mecanismo mediante el cual se produce una extensión del rango geográfico de una especie al atravesar una barrera geográfica preexistente, como por ejemplo una montaña u océano. Si dicha barrera impide el flujo génico entre la población original y la resultante del evento de dispersión, ello puede conllevar a la especiación alopátrida.

Disyunción, o distribución disyunta ("*disjunct distribution*", en inglés): distribución discontinua en el espacio debido a la existencia de barreras geográficas o climáticas.

Efecto fundador ("*founder effect*", en inglés): se refiere a las consecuencias genéticas, morfológicas y de distribución derivadas del establecimiento de una nueva población de individuos de una especie a partir de un número muy reducido de propágulos o diásporas.

Endemismo ("*endemism*", en inglés): es la condición de un taxón cuya distribución queda restringida a una única región o área geográfica.

Especiación alopátrida ("*allopatric speciation*", en inglés): formación de dos o más especies en regiones geográficas separadas de una misma especie ancestral.

Filogeografía ("*phylogeography*", en inglés): disciplina enfocada al estudio de la distribución espacial de los linajes de una genealogía, derive ésta de una única especie (estudios dentro y entre poblaciones), o de dos o más especies estrechamente emparentadas. La filogeografía pretende trasladar el razonamiento filogenético al estudio de los niveles de diversidad intraespecífica, de manera que es un campo que tiende puentes empíricos y conceptuales entre la genética de poblaciones, interesada en los procesos de microevolución, y la filogenética, centrada en la macroevolución.

Flujo génico ("*gene flow*", en inglés): se refiere a cualquier movimiento de individuos y/o de su carga genética de una población a otra. El flujo génico puede constituir una fuente muy importante de variación genética en el caso de que algunas variantes del ADN sean transportadas a una población donde antes eran ausentes. En la literatura, los conceptos de "flujo génico" y "migración" se usan indistintamente en el sentido propuesto en la anterior definición. En esta tesis, sin embargo, el término "migración" se emplea más bien para describir el proceso de ampliación del rango de distribución geográfica de un taxón por dispersión a larga distancia, ya sea ésta directa o por "*mountain-hopping*".

Gondwana: supercontinente hipotético del Hemisferio Sur que hace alrededor de 200 millones de años contenía a las masas terrestres que hoy en día constituyen, entre otros, Suramérica y la Antártida.

Haplotipo ("*haplotype*", en inglés): un genotipo haploide, es decir, una variante del ADN que difiere de otras variantes pertenecientes al mismo fragmento del genoma por la presencia de uno o varios nucleótidos diferentes.

Microbioma ("*microbiome*", en inglés): en líquenes, se refiere al conjunto de organismos procariotas, especialmente bacterias, que habitan el talo liquénico y que parecen tener un papel clave en la ecología y fisiología de los mismos. En esta tesis, sin embargo, este concepto abarca también a otros linajes de eucariotas, también microscópicos, como los hongos endoliquénicos, los cuales suelen ser componentes habituales de los talos liquénicos y cuya presencia, al igual que la de las bacterias, suele revelarse mediante la aplicación de tecnologías de secuenciación masiva.

Mioceno ("*Miocene*", en inglés): época geológica que duró desde *ca*. 23.03 hasta hace 5.3 millones de años y que se caracterizó por un clima por lo general cálido. El movimiento de los continentes produjo, por una parte, cambios en la circulación global de las corrientes oceánicas, así como la elevación de cordilleras montañosas tan importantes como los Andes. En conjunto, estos cambios produjeron, a su vez, cambios en los regímenes de precipitaciones globales con un efecto muy importante sobre el tipo y la distribución de la flora y la fauna.

Modelado de nicho ecológico ("*Ecological niche modelling*", en inglés): se refiere a un conjunto de herramientas que permiten generar información sobre las preferencias abióticas y tolerancia de las especies y, por tanto, estimar la distribución geográfica actual, pasada y potencial de las especies. Los datos generados pueden ser usados para

evaluar o desarrollar hipótesis filogeográficas sobre los procesos que generan los patrones de variación genética en diversos taxones y a diferentes escalas espaciales.

Nunatak: área libre de hielo (p. ej. una roca, un montículo o elevación) que sobresale del hielo de un glaciar; o el pico expuesto de una montaña.

Pangea: supercontinente hipotético que data de finales de la era Paleozoica e inicios de la Mesozoica (300–200 millones de años) y que agrupaba a todas las masas continentales existentes.

Pleistoceno ("*Pleistocene*", en inglés): época geológica que comienza hace alrededor de 2.59 millones de años y finaliza aproximadamente en el 10.000 a. C. Durante el Pleistoceno se sucedieron períodos de glaciación, en donde se formaron enormes capas de hielo que cubrieron grandes extensiones de tierra, y períodos interglaciales, donde se reducía el tamaño de las capas de hielo y el clima era más cálido.

Plioceno ("*Pliocene*", en inglés): época geológica que abarcó desde *ca*. 5.3 hasta hace 2.6 millones de años y en la que se produjo un enfriamiento paulatino del clima global, lo cual contrastaba con la época anterior, el Mioceno, más cálido. El clima también se hizo más árido. Gran parte de las cadenas montañosas de Norte América y Eurasia tuvieron su origen en esta época.

Poiquilohidria ("*poikilohydry*", en inglés): condición de hongos y algas liquenizados por la que son incapaces de regular su contenido hídrico celular, lo que implica para ellos una dependencia directa del agua y, consecuentemente, su desecación ante la ausencia de la misma.

Polimorfismo ancestral ("*ancestral polymorphism*", en inglés): se define como el conjunto de variantes genéticas que surgieron por mutación antes del evento de especiación que dio lugar a las especies en donde éstas segregaron. Su presencia puede complicar la interpretación de los datos genéticos e inducir a la inferencia errónea de relaciones filogenéticas.

Propágulo ("*propagulum*", en inglés): parte de un liquen que es capaz de originar vegetativamente otro individuo. En líquenes se pueden distinguir dos tipos de propágulos, los simbióticos y los aposimbióticos. Los primeros permiten la dispersión conjunta de mico- y fotobionte, como por ejemplo isidios, filidios, esquizidios, bulbilos, soredios, blastidios, goniocistos y fragmentos del talo. Por su parte, los propágulos aposimbióticos sólo permiten propagar uno de los dos simbiontes, como es el caso de conidios (mitósporas) y talósporas fúngicos, y los hormogonios de cianobacterias. Aunque el término "propágulo" parece estar relegado al contexto de la reproducción asexual o vegetativa en algunos tratados de liquenología (ver Nash 2008), en la presente tesis doctoral los términos "propágulo" y "diáspora" pretenden abarcar también a las estructuras de reproducción sexual, principalmente esporas meióticas, que producen exclusivamente los hongos liquenizados.

Refugio ("*refugium*", en inglés): área geográfica en la que las poblaciones de organismos susceptibles de ser afectados por las glaciaciones persistieron a lo largo de todo el período de tiempo que duró la glaciación (p. ej. valles o regiones costeras libres de hielo).

Saltos entre cadenas montañosas ("*mountain-hopping*", en inglés): proceso de dispersión a larga distancia por el cual diferentes organismos adaptados a ambientes polares (p. ej. tundra) pudieron extender su rango de distribución y colonizar latitudes de condiciones ambientales similares en el continente opuesto gracias a la colonización sucesiva de picos montañosos situados en latitudes intermedias pero que igualmente presentaban dichas condiciones ambientales.

Talo liquénico ("*lichen thallus*", en inglés): estructura compleja que resulta de la asociación estable entre el micobionte y fotobionte que, generalmente, difiere en gran medida de cualquiera de los simbiontes en estado de vida libre, y cuya morfología y anatomía pueden ser interpretadas como el resultado de la adaptación a las características ecofisiológicas de la simbiosis. Las características morfológicas, anatómicas y químicas del talo liquénico son empleadas en la taxonomía tradicional de hongos liquenizados.

Tierra del Fuego: es un archipiélago situado en el extremo meridional de Suramérica, entre los océanos Atlántico, Pacífico y Antártico, y que comprende tierras pertenecientes a Chile y Argentina (52–56º S). Se compone de una isla principal, la isla Grande de Tierra del Fuego, y una infinidad de islas de diferentes tamaños separadas por una complicada red de canales.

Último Máximo Glacial ("*Last Glacial Maximum, LGM*", en inglés): se refiere a la época de máxima extensión de las capas de hielo durante el último período glacial, que tuvo lugar hace entre 18.000 y 20.000 años.

Vicarianza ("*vicariance*", en inglés): proceso o mecanismo biogeográfico por el cual el rango geográfico ancestral de una especie o población original se divide en dos o más fragmentos debido a la aparición de una barrera climática o geográfica (p. ej. la formación de nuevos océanos tras la fragmentación continental, o la formación de una cadena montañosa) a lo que le sigue la especiación alopátrida. Esto puede conllevar a que cada descendiente sea endémico de un continente o de una vertiente de la montaña.

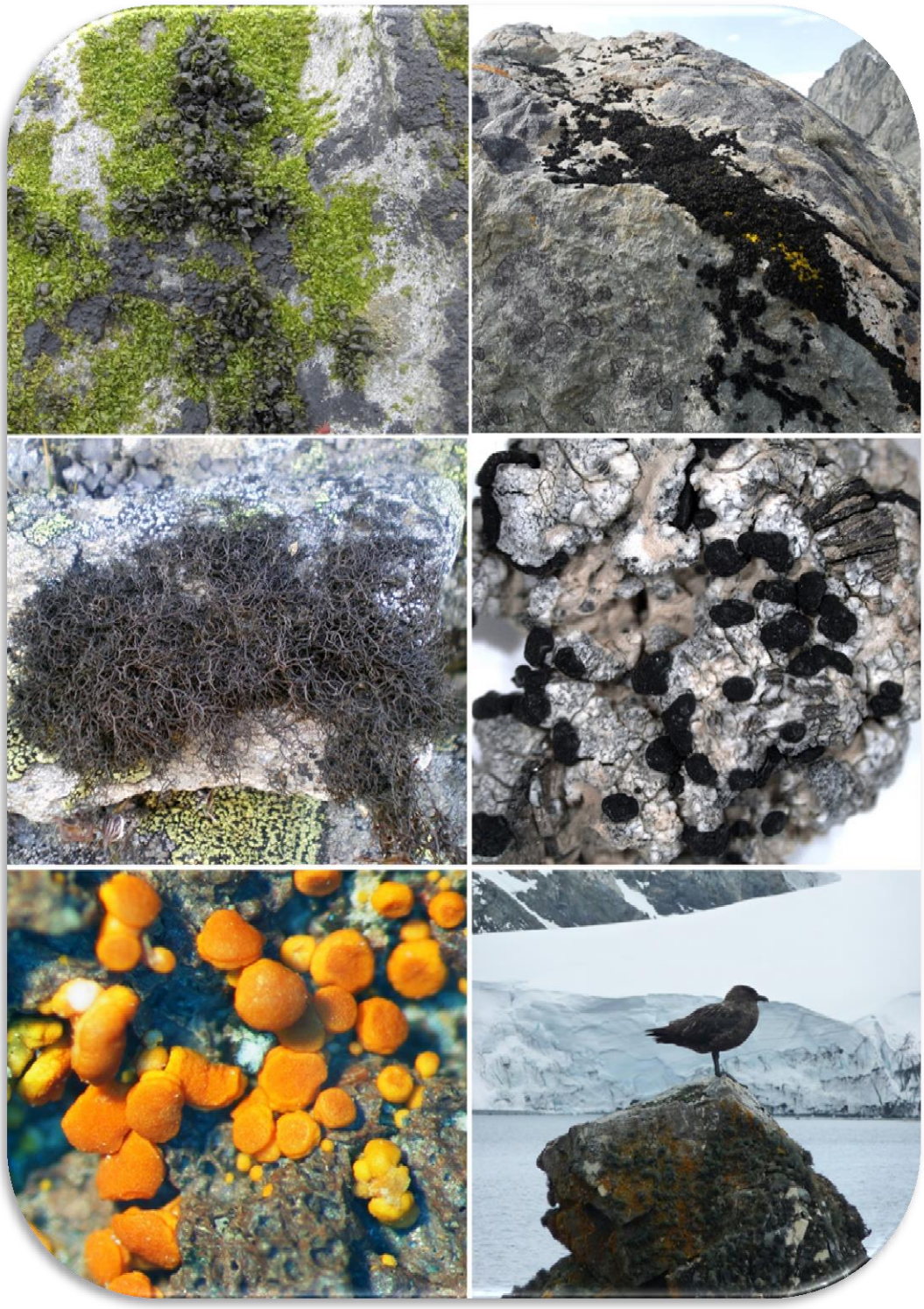

FILOGEOGRAFÍA Y BIOLOGÍA DE LÍQUENES ANTÁRTICOS

ISAAC GARRIDO BENAVENT

CSIC
CONSEJO SUPERIOR DE INVESTIGACIONES CIENTÍFICAS
mncn
museonacionaldecienciasnaturales